♻EPA Environmental Assessment

Deep Sea Fisheries Shore Plant and Cumulative Effects of Seafood Processing Activities in Akutan Harbor, Alaska

ENVIRONMENTAL ASSESSMENT

*Deep Sea Fisheries Shore Plant
and Cumulative Effects
of Seafood Processing Activities
in Akutan Harbor, Alaska*

Prepared by:

**U.S. Environmental Protection Agency
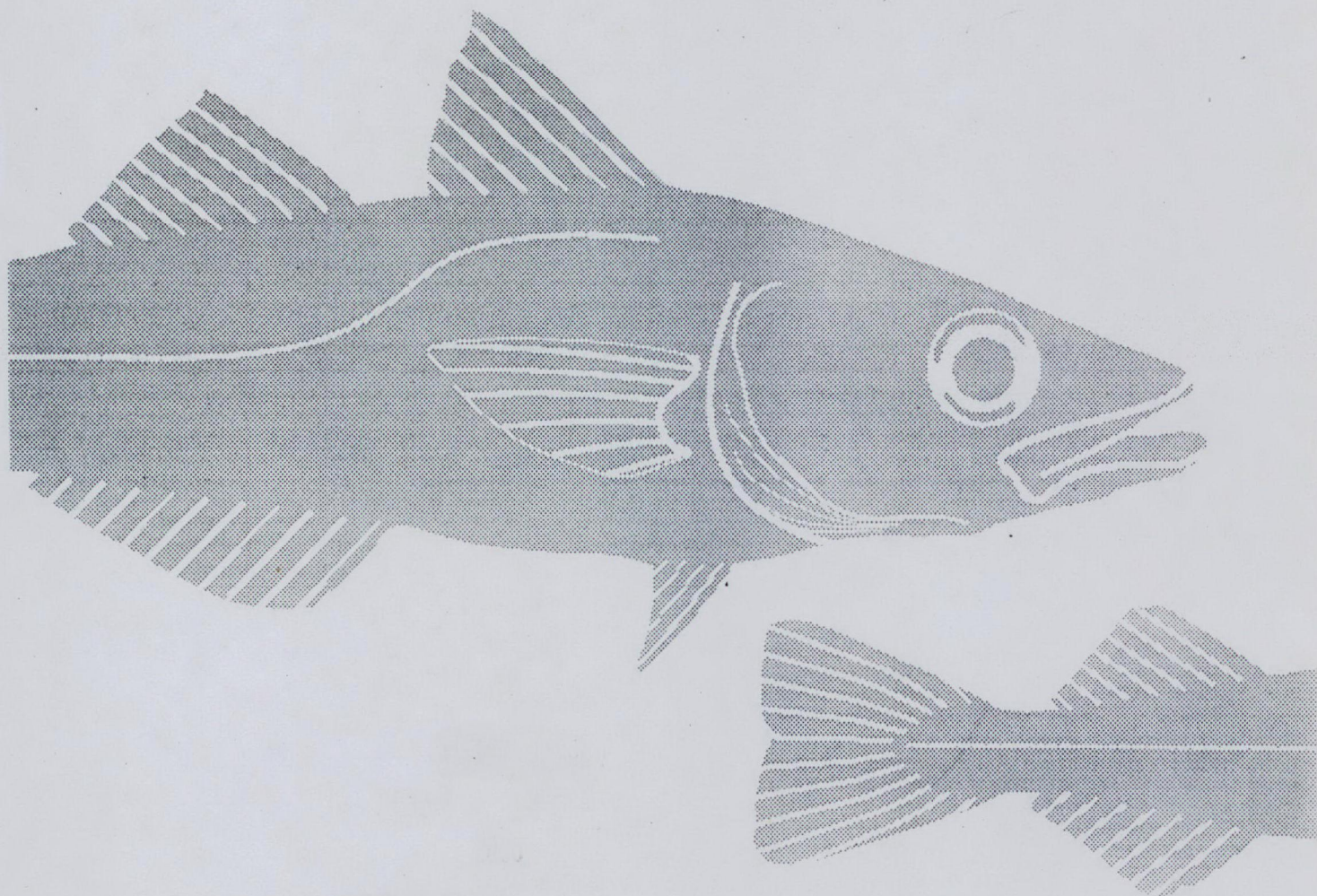Region 10
1200 Sixth Avenue
Seattle, WA 98101**

In association with:

**Jones & Stokes Associates, Inc.
2820 Northup Way, Suite 100
Bellevue, WA 98004
(206) 822-1077**

June 1993

This document should be cited as:

U.S. Environmental Protection Agency, Region 10. 1993. Deep Sea Fisheries shore plant and cumulative effects of seafood processing activities in Akutan Harbor, Alaska. Environmental assessment. June. (JSA 92-228.) Seattle, WA. In association with Jones & Stokes Associates, Inc., Bellevue, WA.

Table of Contents

i

List of Tables

List of Figures

List of Acronyms

ADT: Alaska Daylight Time
BOD: biological oxygen demand; see glossary
BOD_5: 5-day biological oxygen demand; see glossary
cfs: cubic feet per second
cm: centimeter
cm/s: centimeter per second
Corps: U.S. Army Corps of Engineers
DMRs: discharge monitoring reports
DO: dissolved oxygen
EA: environmental assessment
EHI: Evans-Hamilton, Inc.
EPA: U.S. Environmental Protection Agency
FONSI: Finding of No Significant Impact
ft: foot
gal: gallon
GIS: Geographic Information System
gpd: gallons per day
GPS: geographical positioning system
hr: hour
IDOD: immediate dissolved oxygen demand
in: inch
kg: kilogram
km: kilometer
kW: kilowatt
l: liter
lbs: pounds
m: meter
m^2:   square meter
m^3:   cubic meter
m/s: meter per second
m^2/s: square meter per second
m^3/s: cubic meter per second
mg/l: milligram per liter
ml: milliliter
MLLW: mean lower low water
mm: millimeter
MR4:   Motorola Miniranger IV
mt: metric ton
M/V: marine vessel
$\mu g/g$: microgram per gram

μs/cm:	microsiemen per centimeter
NEPA:	National Environmental Policy Act
N-N:	nitrate + nitrite nitrogen
NPDES:	National Pollutant Discharge Elimination System
QA/QC:	quality assurance/quality control
ROV:	remotely operated vehicle
SAIC:	Scientific Applications International Corporation
SPCC:	Spill Prevention Control and Countermeasure
SSS:	side-scan sonar
t:	ton
TKN:	total Kjeldahl nitrogen
TOC:	total organic carbon
UM:	Updated Merge

Glossary

Anoxia:	Conditions in which there is an abnormally low amount of oxygen.
Bailwater:	Water pumped from the holds of fishing vessels during the fish unloading process.
BOD:	Biological oxygen demand. The oxygen utilized by microorganisms in nutrient-rich water; often measured over a period of 5 days (see BOD_5).
BOD_5:	Five day biological oxygen demand. The oxygen utilized by microorganisms in nutrient-rich water over a period of 5 days.
Coefficient of Eddy Diffusivity:	The exchange coefficient for the diffusion of a substance by eddies in a turbulent flow.
Depth-Averaged Velocity:	The total transport of water across a grid boundary in a computer model divided by the water depth at the grid boundary.
Fecal Coliforms:	Bacteria found in the intestines of humans and animals that are used as indicators of the degree of sewage contamination in a body of water.
Maximum-Rated Capacity:	Production scenarios based on the maximum throughput of processing equipment.
Maximum Seasonal Production:	Production scenario based on 1992 crab production and annual production estimates. Seasonal production is assumed to mimic that of Trident Seafoods.
Overlap Depth:	In computer modeling, the depth at which the plume element can no longer be consistently defined due to geometric constraints of the PLUMES model. This condition has been associated with anvil-shaped plumes.
Plume Centerline:	The physical center of the discharge plume.
Presswater:	Waste liquor, which still contains solids and light oils, produced in dehydrating fish meal. After solids and oils are removed, the remaining liquor is termed stickwater.

Process Water: A mix of fresh and marine waters used to process fish.

Richardson Number: A comparison of the stabilizing forces of the density stratification to the destabilizing forces of the velocity shear. The larger the value of the Richardson number, the higher the resistance of a fluid medium to vertical mixing. The mathematical definition of the Richardson number is included in Appendix B. See Velocity Shear.

Scrubber Water: Seawater spray used as an odor control measure for fish meal process emissions.

Seiche: A local, periodic rise or fall of water level.

Sigma t: A measure of water density determined primarily by the water's salinity and temperature. Density is generally expressed as grams per cubic centimeter. Sigma t = 1000 x (density - 1).

Stickwater: Waste liquor produced during fish meal processing. See Presswater.

Velocity Shear: The rate of change in the speed of currents with changes in water depth. The velocity shear is larger at the boundary of two layers with greatly different velocities.

Executive Summary

Executive Summary

Deep Sea Fisheries, Inc., is proposing to build a shore-based crab and finfish processing facility in Akutan Harbor (Akutan Island, Alaska). Deep Sea Fisheries has applied for the issuance, by the U.S. Environmental Protection Agency (EPA), of a National Pollutant Discharge Elimination System (NPDES) permit. EPA has determined that this action is subject to the provisions of the National Environmental Policy Act (NEPA) under 40 CFR Part 122.29 and 40 CFR Part 6, Subpart F. Pursuant to NEPA, this environmental assessment (EA) will provide the basis for EPA's decision on whether to issue a Finding of No Significant Impact (FONSI) or require the preparation of an environmental impact statement on the proposed action. Because of the high level of seafood processing activity presently occurring in the harbor, this EA includes an extensive analysis of potential cumulative impacts associated with seafood processing activities in the harbor. As part of this analysis, oceanographic and biological field studies were conducted in Akutan Harbor during April 1992.

The 1992 field studies indicated that there has been a cumulative effect from seafood processing waste discharges in Akutan Harbor. Between 1983 and 1992, the concentration of total organic carbon in sediments; the abundance, species composition, and diversity of benthic communities; and the area impacted by waste piles generated by existing seafood activities in the harbor have all increased. Although these changes are not considered significant impacts at this time, they do indicate that Akutan Harbor could be at risk.

The EA evaluates Deep Sea Fisheries' proposed action based on its annual estimated production, maximum-rated daily production capacity, historical production records, and potential maximum seasonal production. Three computer simulation models were used to evaluate potential water quality impacts (dissolved oxygen violations) from the proposed action, alternatives to the proposed action (outfall locations), and cumulative seafood processing in the harbor. The results of the PLUMES model indicated that there is a potential for Deep Sea Fisheries to impact water quality during peak summer processing periods. No impacts were indicated during the winter processing season. The circulation model and the WASP model also demonstrated that there is a potential for water quality impacts from the proposed action during the peak summer processing periods. In addition, these two models indicated the potential for cumulative impacts from the combined discharges of Deep Sea Fisheries' proposed facility and other seafood waste dischargers in the harbor.

1

Environmental Assessment

Environmental Assessment

INTRODUCTION

Proposed Action

The proposed action is the issuance by the U.S. Environmental Protection Agency (EPA) of a National Pollutant Discharge Elimination System (NPDES) permit to Deep Sea Fisheries, Inc. The NPDES permit would authorize, subject to its stated effluent limitations, conditions, and monitoring requirements, the discharge of seafood processing and sanitary wastewater from a land-based seafood processing plant owned by Deep Sea Fisheries to Akutan Harbor, Alaska. EPA has determined that this action is subject to the provisions of the National Environmental Policy Act (NEPA) under 40 CFR Part 122.29 and 40 CFR Part 6, Subpart F. Pursuant to NEPA, this environmental assessment (EA) will provide the basis for EPA's decision on whether to issue a Finding of No Significant Impact (FONSI) or require preparation of an environmental impact statement for the proposed action.

PROJECT DESCRIPTION

Deep Sea Fisheries is proposing to build a shore-based crab and finfish processing facility on Akutan Island, Alaska (Figure 1). The proposed location for the facility is on the south shore of Akutan Harbor, between the abandoned whaling station and the head of the harbor (Figure 2).

Existing Facilities

Deep Sea Fisheries began crab and finfish processing operations in Akutan Harbor in 1975. Its existing facilities, the floating processor marine vessel (M/V) Deep Sea, the refrigeration barge TNT, and the support vessel M/V Hemlock, have been located along the south shore of Akutan Harbor (northwest of the abandoned whaling station) since 1979 (see Figure 2). The M/V Deep Sea is anchored at the stern and bow and discharges waste through an outfall located just below the water surface.

The existing facilities have primarily produced sectioned king crab (*Paralithodes camtschatica*), Tanner crab (*Chionoecetes bairdi* and *C. opilio*), and glazed bottomfish. Crab

2

North
Head

Lava
Point

Akutan
Bay

**AKUN
ISLAND**

*Hot Springs
Bay*

Reef
Bight

**AKUTAN
ISLAND**

Akutan
Point

Akutan Harbor

N

Cape
Morgan

Battery
Point
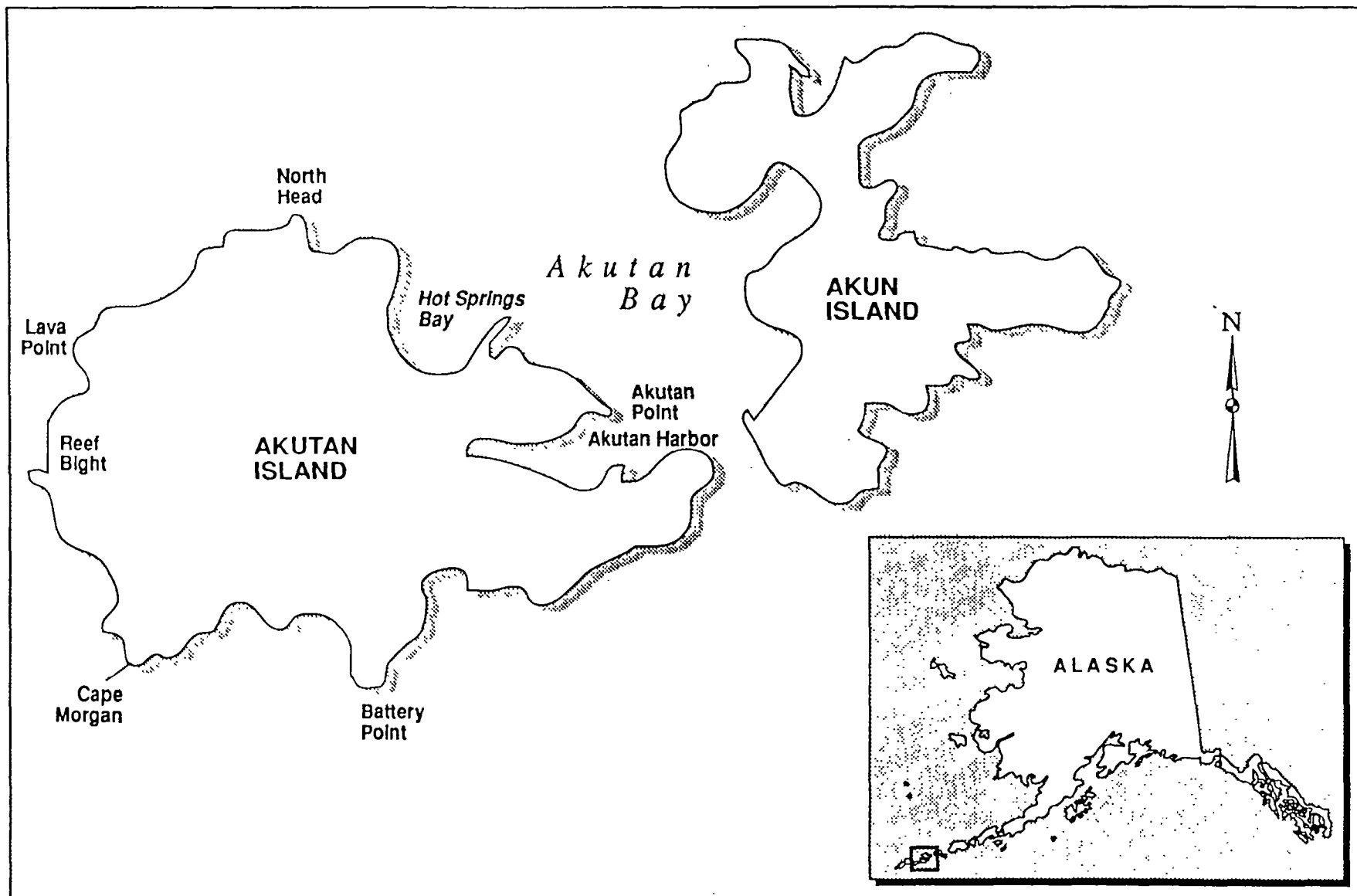
ALASKA

Figure 1. Location of Akutan Harbor, Alaska
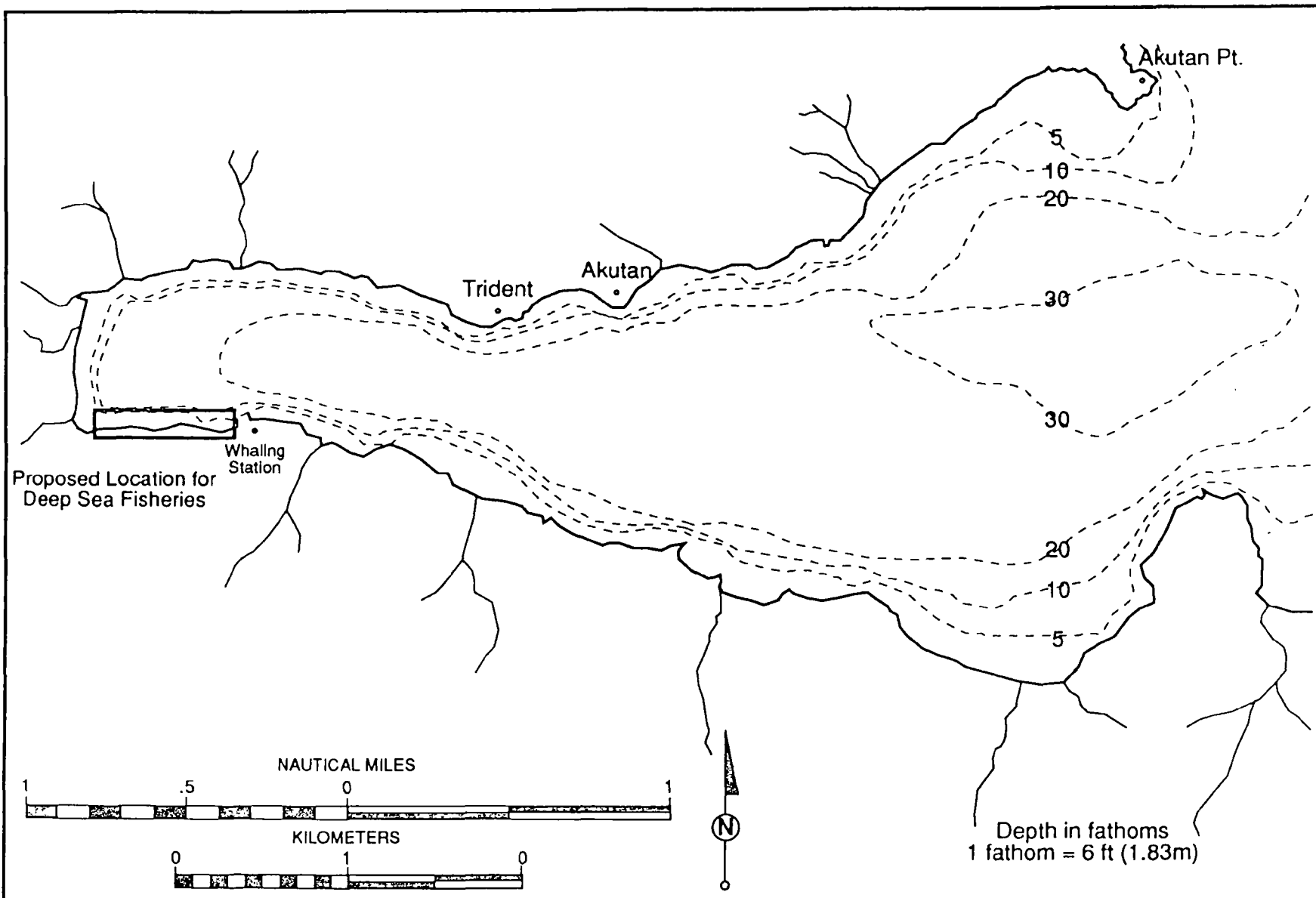
Figure 2. Proposed Location of Deep Sea Fisheries Shore-Based Seafood Processing Facility in Akutan Harbor, Alaska

waste, the primary component of the effluent, has been ground to 0.5 inch (in), or 1.27 centimeters (cm), diameter and discharged to Akutan Harbor. Discharges associated with the bottomfish glazing process have been minimal, and have consisted primarily of washwater and bailwater (water pumped from the hold of the vessels). Deep Sea Fisheries' peak processing period has been between November and May (during the crabbing season). During the 1991/1992 crabbing season, Deep Sea Fisheries discharged an estimated 655 tons (t) or 594 metric tons (mt) of ground crab waste to the harbor.

Under the last individual NPDES permit issued to the M/V Deep Sea (AK-002904-1), the total permitted seafood discharge was 540,000 pounds (lbs), or 245 mt per month. This individual permit expired in March 1991. Deep Sea Fisheries is currently operating under the general NPDES permit for Akutan Harbor recently reissued by EPA (September 1989) which allows floating processors operating in the harbor to discharge up to 310,000 lbs (140,613 kilograms [kg]) of seafood waste solids per month.

The existing facility normally employs approximately 45 people during the peak of the crab processing season; however, there were about 90 employees during the 1991/1992 crab season. The employees are housed and fed on the three vessels. Sanitary wastes from the vessels are treated with approved marine sanitary devices (primary treatment with chlorination). In addition to the seafood processing and sanitary wastes identified above, other wastes discharged from the facility include cooling water, boiler water, freshwater pressure relief, refrigeration condensate, bailwater, and live-tank water. Solid refuse is either transported to a private landfill or incinerated on shore.

In addition to Deep Sea Fisheries, there are a number of other seafood processors operating in Akutan Harbor. Trident Seafoods Corporation currently operates a shore-based seafood processing plant on the north shore of the harbor, just west of the village of Akutan. The Trident Seafoods facility consists of a crab processing plant, a fish processing line, a surimi line, and a fish meal plant.

A number of floating processors also operate in Akutan Harbor seasonally. Under the general NPDES permit, these floating processors may operate east of longitude 165°46′ in the harbor and discharge up to 310,000 lbs (140,613 kg) of seafood waste solids per month. The number of floating processors operating in the harbor varies seasonally and annually, with the peak number of floating processors in the harbor during the crab and early pollock (*Theragra chalcogramma*) seasons (November to about May) and a lesser number during the second pollock season (beginning in June and lasting until the quota is reached). The number of floating processors has increased since the reissuance of the general NPDES permit for Akutan Harbor, particularly during the winters of 1990/1991 and 1991/1992. During the winter of 1990/1991, a total of 14 floating processors operated in the harbor (4 crab processors and 10 finfish processors). Eighteen floating processors (9 crab processors and 9 finfish processors) reportedly operated in the harbor during the winter of 1991/1992 (Griffin, Cronauer pers. comms.).

Proposed Facilities

Deep Sea Fisheries has applied for an individual NPDES permit for discharge of wastewater from a proposed shore-based seafood processing plant in Akutan Harbor. The proposed site lies on the south shore of the harbor, between the abandoned whaling station and the head of the harbor (Figure 2). The shore-based facilities are expected to replace the existing floating processor which Deep Sea Fisheries currently operates in the harbor. During periods of peak operation, the new facility is expected to employ approximately 200 people.

The proposed facility site will encompass approximately 23.4 acres and will include crab and finfish processing buildings, a fish meal plant, a cold storage building, a dry storage area, a powerhouse, a machine shop, an incinerator, offices, employee housing, food services, and recreational facilities (Figure 3). In addition to processing activities, the facility will provide support for the fishing fleet (fuel, supplies, and gear storage).

Deep Sea Fisheries conducted an extensive siting evaluation for the proposed facility (Reid Middleton 1991). Based on economics, land availability, and location in relation to the fishery, Deep Sea Fisheries concluded that there were no reasonable alternatives to the proposed site in Akutan Harbor.

The proposed site is composed of a steep, rocky shoreline and will require extensive excavation and filling to meet the area requirements for the facility. The construction plan calls for the removal of 672,000 cubic yards (513,778 cubic meters [m^3]) of earth from the hillside which will be used to create an 18-acre aquatic fill. The fill will eliminate 2,400 lineal feet, or 732 meters (m), of intertidal and subtidal habitat to an average depth of -25 feet (ft), -7.6 m, mean lower low water (MLLW).

Deep Sea Fisheries proposes to use a combination of sheet pile and riprap to contain the fill. Riprap with a slope of 1.5:1 (horizontal to vertical) will be used across most of the face of the wharf. Sheet pile will be used along the face of the crab processing building (the landed TNT barge) only. Berthing space will be provided by installing 27 piers between the crab processing building and the western boundary of the facility. These piers will have pilings approximately every 12 ft along their length.

Electrical power for the facility will be supplied by up to four 2,000-kilowatt (kW) diesel generators producing up to 8,000 kW of power. Approximately 1.5 million gallons (5.7 million liters) of diesel fuel will be stored in new storage tanks located within a bermed containment basin. In addition to supplying fuel for the generators, the diesel fuel will be used to fuel the fishing vessels associated with the operation. In all, Deep Sea Fisheries estimates that approximately 10 million gallons (38 million liters) of diesel fuel will either be consumed at the facility (3.5 million gallons) or used to fuel the fleet (6.5 million gallons) each year. Fish oil (recovered from the fish meal process) will be used in combination with diesel to fuel the generators, as well as to fuel the boilers in the meal plant.
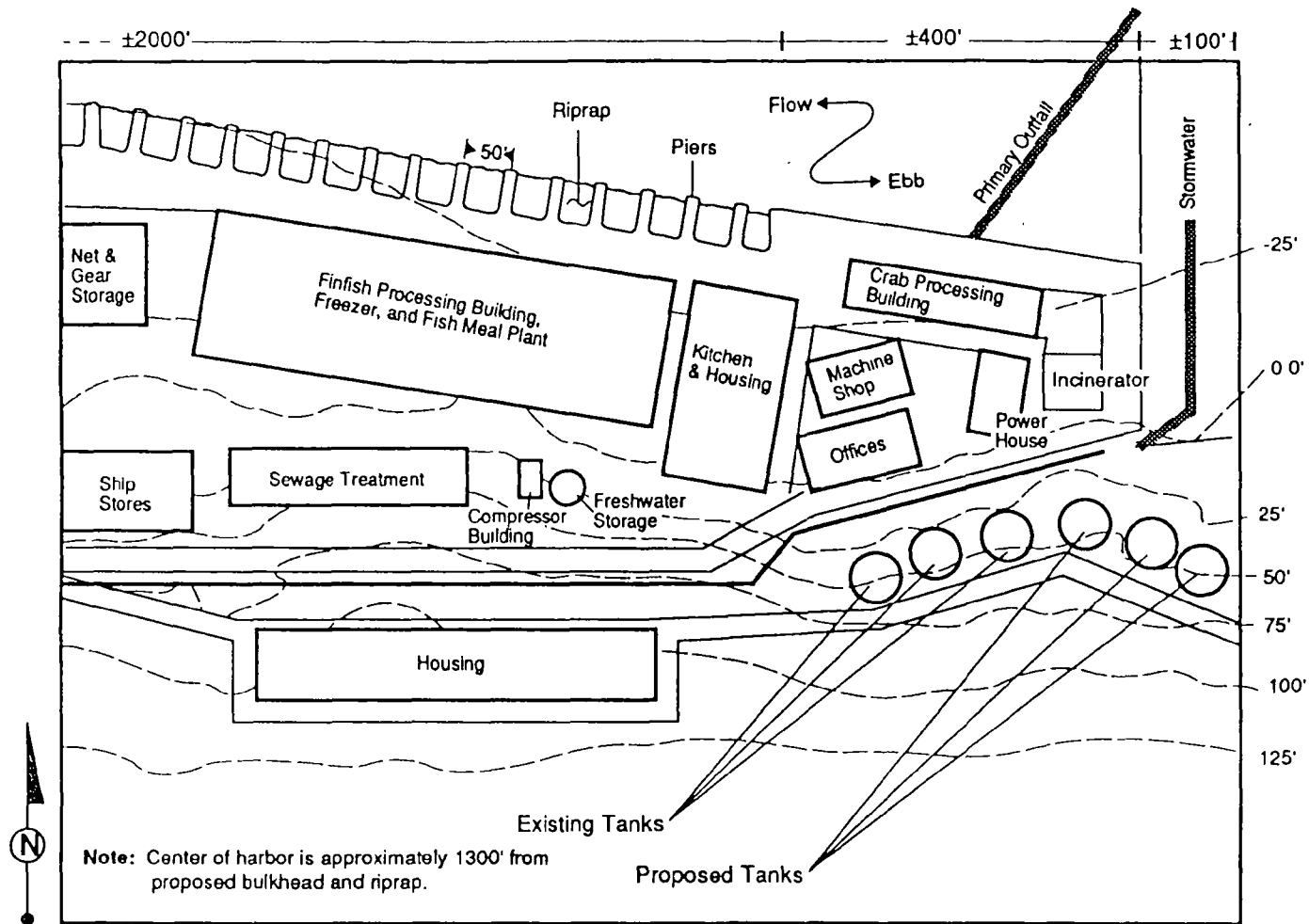
Figure 3. Site Plan for Deep Sea Fisheries' Proposed Shore-Based Processing Plant (Eastern Portion)
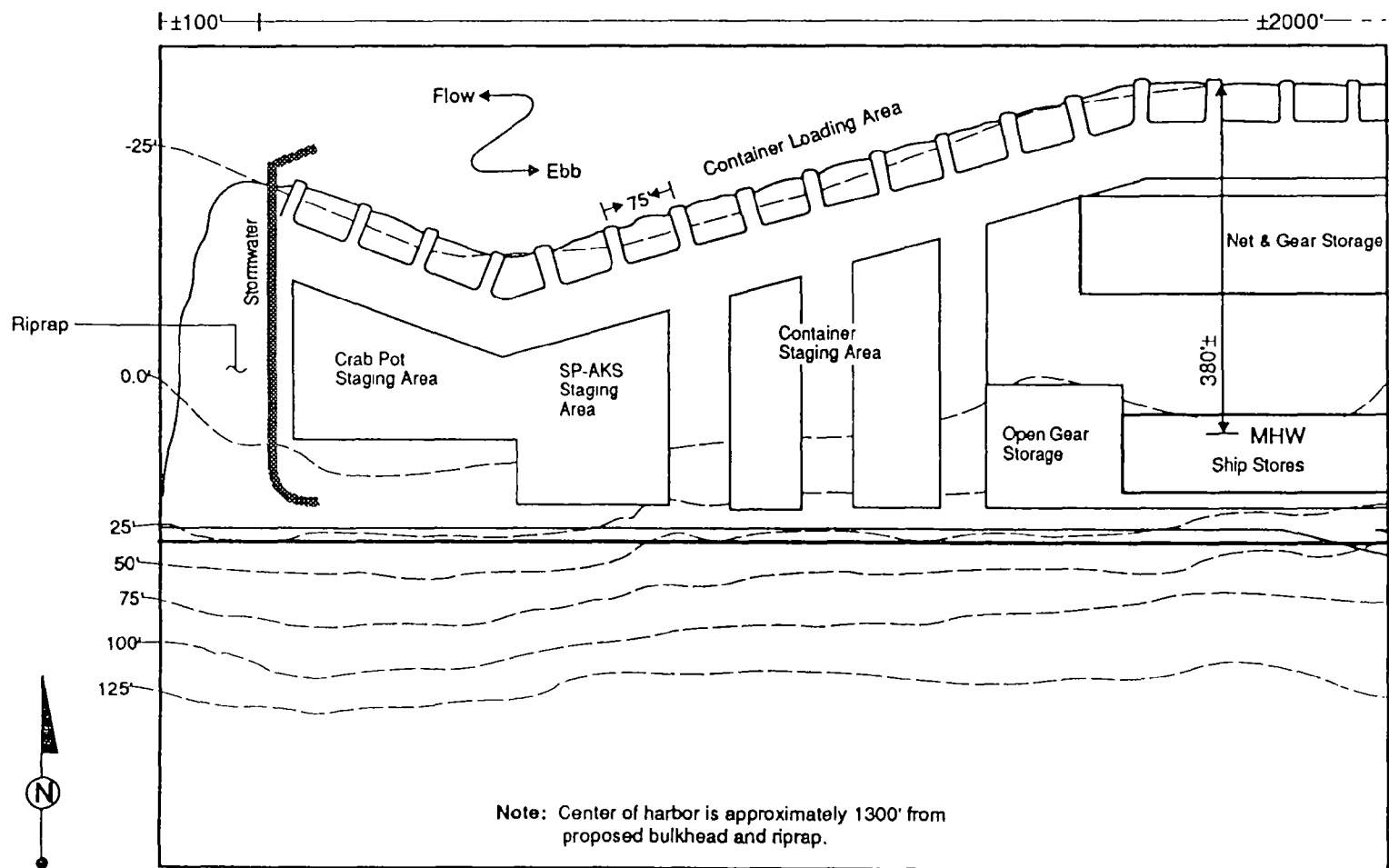
Figure 3 (continued). Site Plan for Deep Sea Fisheries' Proposed Shore-Based Processing Plant (Western Portion)

Both fresh water and saltwater will be required for processing operations. A proposed water flow diagram is presented in Figure 4. The estimated total fresh water required for operations at capacity is 720,000 gallons per day (gpd) (2.73 million liters). Deep Sea Fisheries proposes to obtain fresh water from a previously impounded stream near the site and chlorinate it prior to use. Deep Sea Fisheries is presently trying to obtain water rights to a second previously impounded stream adjacent to its existing water source. A 150,000-gallon (gal), or 567,812-liter (l), freshwater tank will provide onsite storage. Saltwater requirements at capacity are estimated to be about 10 million gpd (38 million liters). Saltwater will be pumped from Akutan Harbor. Saltwater used in processing operations will be chlorinated.

Deep Sea Fisheries is proposing to process several species of crab, pollock, cod, halibut (*Hippoglossus stenolepis*), and salmon at its proposed facility. The approximate annual raw quantities and method of processing include (in round weights):

- Tanner and king crab (sectioned): 9,000 t (8,165 mt),
- cod (filleted): 2,000 t (1,814 mt),
- pollock (filleted): 24,000 t (21,772 mt),
- halibut (headed/gutted): 100 t (91 mt),
- salmon (headed/gutted): 500 t (454 mt), and
- salmon (slimed): 100 t (91 mt).

At capacity, the plant would be capable of producing 24,250 t (22,000 mt) of finished seafood product annually and would have a product storage capacity of 2,756 t (2,500 mt). In addition to fisheries products processed at the plant, Deep Sea Fisheries may act as a transshipment and cold storage facility for part of the Eastern European fleet as part of a proposed joint venture. Transshipment would include loading and unloading foreign vessels with block or case frozen products which have been processed on the high seas.

Waste Streams

Deep Sea Fisheries is proposing to discharge all processing, sewage, and domestic wastewaters through a single outfall to a new discharge site. The new outfall site is located approximately 150 ft (46 m) northeast of the proposed facility site and about 2,000 ft (609 m) east of the existing discharge. The main 12 or 18 in (30 or 46 cm [inside diameter]) outfall will be located in about 90 to 110 ft (28 to 34 m) of water and will terminate in a 20 ft (6.1 m) standpipe configuration. Stormwater discharges will consist of two separate surface discharges to the harbor located on either side of the facility. Bailwater (water from vessel refrigeration systems used to transport fish from vessel holds to the dock) will be discharged off the dock. The anticipated volumes and sources of the discharges based on maximum-rated capacity of the proposed facility are shown in Table 1.

9
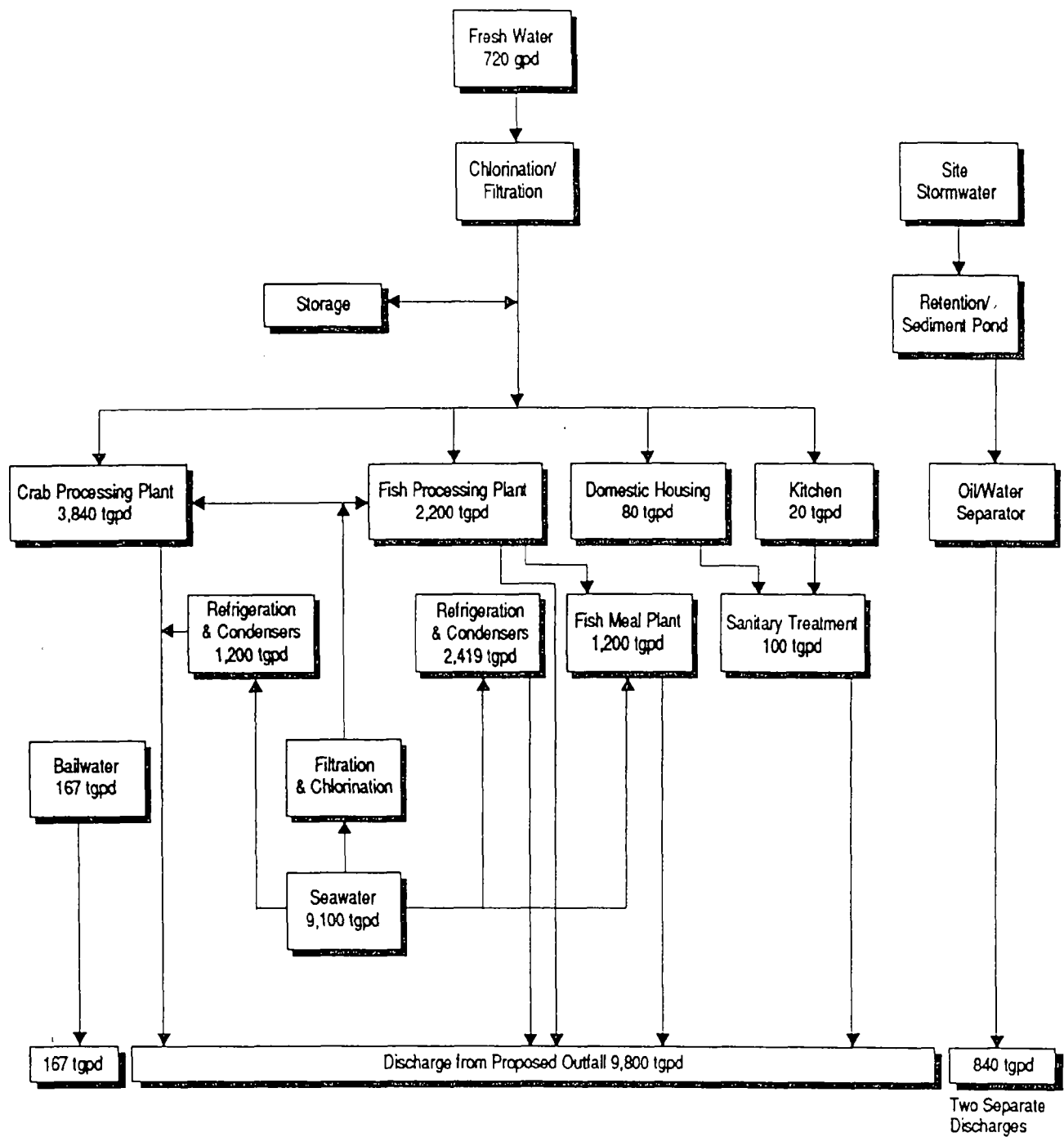
Figure 4. Proposed Water Flow

tgpd = gallons per day in 1,000s

10

Table 1. Estimated Daily Flow and BOD$_5$ Loading of Wastes Discharged from Deep Sea Fisheries at Maximum-Rated Production Capacity[a]

Outfall	Estimated Flow		BOD$_5$ Loading[b]	
	(gpd)	(l/day)	(lbs/day)	(kg/day)
Bailwater	167,400	633,678	7,150	3,243
Crab processing plant	5,040,000	19,078,475	3,485	1,581
Finfish processing plant	3,419,000	12,942,323	10,231	4,641
Fish meal plant	1,242,833	4,704,635	22,223	10,080
Sewage treatment plant	100,000	378,541	25	11
Stormwater	840,000	3,179,746	0	0
Total	10,809,233	40,917,398	43,114	19,556

[a] Maximum-rated production equal to 405 mt pollock (filleted) and 110 mt crab (sectioned).

[b] See text for BOD loading calculations.

BOD$_5$ = 5-day biological oxygen demand
gpd = gallons per day
l/day = liters per day
lbs/day = pounds per day
kg/day = kilograms per day

Deep Sea Fisheries proposes to grind (to 0.5 in [1.27 cm] diameter) and discharge solid crab waste through the proposed outfall site. Nearly all solid waste produced by finfish processing will be conveyed to the fish meal plant for processing. However, some fine solids which flow through the 0.2 in (5-millimeter [mm]) screens in the plant drainage systems would be discharged through the proposed outfall.

There are several essentially liquid waste streams from the proposed processing operations which contain varying amounts of fine solids. These include bailwater, process water collected in the crab and finfish processing building drainage systems, stickwater (waste liquor from the fish meal plant), and water used for the air scrubbing system in the fish meal plant. Deep Sea Fisheries is proposing to recirculate coolant water from the powerhouse. In addition to the effluents directly related to processing operations, Deep Sea Fisheries is proposing to discharge secondarily treated sanitary wastewater and stormwater to the harbor.

The total daily loading and concentration of solids in liquid waste streams from the proposed processing operations will depend on the amount of crab and fish processed each day. Two methods were used to estimate production and consequent discharges from the proposed facility: maximum-rated capacity and maximum seasonal production. Maximum-rated capacity (Table 1) is based on the rated capacity of the processing equipment. Under this production scenario, crab production was based on the rated capacity of the crab line. Maximum daily finfish production was based on the maximum-rated capacity of the fish meal plant.

Due to the seasonal nature of the fisheries, the volume and composition of wastes discharged to Akutan Harbor from Deep Sea Fisheries' proposed operations will vary through the year. The seasonality of production is primarily driven by the two dominant fisheries in the Bering Sea/Gulf of Alaska region, crab and pollock. Table 2 illustrates the maximum seasonal production of the proposed facility. These production rates are based on several factors. Crab production is based on Deep Sea Fisheries' 1992 discharge monitoring reports (DMRs) (Carroll pers. comm.). Crab data for 1992 were used in the analysis because they represent the greatest crab production levels since the decline of the king crab fishery.

Since Deep Sea Fisheries does not currently process finfish, the maximum seasonal production rates for pollock and other finfish species were based on the anticipated yearly production of the proposed facility and the seasonality of the fisheries. To account for seasonality, the maximum seasonal production values were based on the percent of annual production achieved by Trident Seafoods each month in 1992.

The estimated daily loading of 5-day biological oxygen demand (BOD$_5$) from the proposed facility is also presented in Tables 1 and 2. The projected BOD$_5$ loading is calculated to be extremely variable on an annual basis. Peak BOD$_5$ loading occurs during two periods coinciding with the peaks of the crab and pollock fisheries in the winter, and the peak of the pollock fishery in the summer. The basis of the Table 2 calculations, and calculated worst-case conditions for the individual processes, are presented below.

12

Table 2. Maximum Seasonal Production and Associated BOD$_5$ Loading for Deep Sea Fisheries Proposed Discharge

Month	Daily Production Estimates			Daily BOD Loading Estimates					Total Projected Daily BOD Loading (lbs/day)
	1992 Crab Production (lbs/day)	Projected Pollock Production (lbs/day)	Projected Other Fish Production (lbs/day)	Bailwater (lbs/day)	Crab Process (lbs/day)	Fish Processing (lbs/day)	Fishmeal Plant Pollock (lbs/day)	Fishmeal Plant Other Species (lbs/day)	
January	108,636	275,044	26,541	2,413	1,173	3,383	7,189	657	14,814
February	248,563	979,725	0	7,838	2,684	12,051	25,606	0	48,179
March	133,934	270,426	35,726	2,449	1,446	3,326	7,068	884	15,174
April	68,754	0	51,497	412	743	0	0	1,275	2,429
May	0	0	21,058	168	0	0	0	521	690
June	0	129,958	4,852	1,078	0	1,598	3,397	120	6,194
July	0	615,773	1,246	4,936	0	7,574	16,094	31	28,635
August	0	1,117,501	1,788	8,954	0	13,745	29,207	44	51,951
September	0	860,681	149	6,887	0	10,586	22,495	4	39,971
October	0	0	0	0	0	0	0	0	0
November	38,744	0	0	0	418	0	0	0	418
December	25,031	551,962	0	4,416	270	6,789	14,426	0	25,901

Note: Data are based on Deep Sea Fisheries' 1992 crab data, Trident Seafoods' seasonal production for 1992, and Deep Seas Fisheries' projected production.

13

The fish meal plant Deep Sea Fisheries proposes to use has a maximum-rated capacity of 331 t (300 mt) per day raw input (Johnson pers. comm.). The calculated waste yield for the pollock filleting process ranges between 64 and 78% (Crapo et al. 1988). Based on a waste yield of 74% (Trident Seafoods' estimated yield), Deep Sea Fisheries could process a maximum of 446 t (405 mt) round weight of pollock per day and still remain within the maximum-rated capacity of the meal plant.

Based on the calculations in Table 2, Deep Sea Fisheries could exceed the rated capacity of its meal plant during the peak months of pollock processing (February and August). Since meal plant capacity can be modified, it will be assumed that Deep Sea Fisheries can increase the capacity of the plant to process maximum seasonal production quantities. This assumption will allow the analysis of worst-case conditions because it accounts for maximum waste discharge. If Deep Sea Fisheries cannot increase the production capacity of the meal plant, and fish processing wastes do exceed the capacity of the plant, Deep Sea Fisheries would be required to obtain an ocean dumping permit to dispose of the excess solid waste offshore.

The maximum amount of crab which can be processed in a day is estimated to be 110 t (100 mt) based on cooking capacity (Cronauer pers. comm.). However, based on the 1992 DMR, Deep Sea Fisheries did achieve an average daily processing rate of 124 t (113 mt) in February 1992 (Carroll pers. comm.). The February 1992 value was used as the maximum seasonal production estimate.

Bailwater. Fish will be unloaded from boats at the Deep Sea Fisheries dock by pumps. The pumps will transport fish from the boat holds directly into the processing building. Bailwater will either be recycled back to the boats, or will be discharged directly into Akutan Harbor. As a worst case, this analysis assumes that bailwater is discharged to the harbor. The daily volume of water necessary to offload fish is approximately 1 cubic foot (.03 m^3) of water per 40 lbs (18 kg) of fish. No specific bailwater characteristics are available for pollock; however, typical bailwater characteristics reported by EPA (1975) are:

- BOD$_5$: 16 lbs/ton (8 kg/mt),
- suspended solids: 10 lbs/ton (5 kg/mt), and
- oil and grease: 6 lbs/ton (3 kg/mt).

Based on the maximum-rated capacity of the pollock line, there would be an estimated BOD$_5$ loading of approximately 7,136 lbs per day (3,237 kg). The estimated daily discharge of suspended solids and oil and grease would be 4,460 lbs (2,023 kg) and 2,676 lbs (1,214 kg), respectively.

Based on the maximum seasonal production rate calculated for pollock (August), the maximum BOD$_5$ loading from bailwater would be approximately 8,954 lbs per day (4,061 kg). The estimated maximum seasonal discharge of suspended solids and oil and grease from bailwater is 5,588 lbs (2,534 kg) and 3,353 lbs (1,521 kg) per day, respectively. Bailwater also contains solids, such as scales, which would be deposited on the harbor bottom.

14

Crab Processing Waste. The waste streams from the crab processing facility will consist of both liquid fraction wastes (from the washing and cooking processes) and solid fraction wastes (carapace, gills, offal). The solid wastes are ground prior to discharge. The crab is processed in sections. Crapo et al. (1988) estimated that the waste yield of Tanner crab processed for cooked sections ranges from 34 to 42% and averages 40% of the raw weight. However, according to the 1991 and 1992 DMRs submitted to EPA by Deep Sea Fisheries and Trident Seafoods, waste yields for crab at the existing facilities are approximately 30% of the raw weight. Based on this waste yield, Deep Sea Fisheries would discharge 33 t (30 mt) of crab waste per day when the facility is operating at maximum-rated capacity, or 37.2 t (33.7 mt) at maximum seasonal production levels. The annual cumulative discharges of crab waste for Deep Sea Fisheries for 1991 and 1992 were estimated to be 482 t (437 mt) and 655 t (594 mt), respectively.

Typical unscreened waste loads for whole Alaskan crab and sections reported in EPA (1974, 1975) are:

- BOD_5: 72 lbs/ton (36 kg/mt),
- suspended solids: 44 lbs/ton (22 kg/mt), and
- oil and grease: 16 lbs/ton (7 kg/mt).

Based on the maximum-rated capacity for crab, there would be an estimated BOD_5 loading of approximately 2,376 lbs per day (1,078 kg). The estimated daily discharge of suspended solids and oil and grease would be 1,452 lbs (659 kg) and 528 lbs (239 kg), respectively, at the maximum-rated capacity.

Based on maximum seasonal production values for crab (Table 2), the BOD_5 loading is estimated to be approximately 2,864 lbs (1,300 kg) per day. The estimated maximum seasonal discharge of suspended solids and oil and grease is 1,637 lbs (742 kg) and 595 lbs (270 kg) per day, respectively.

Finfish Process Wastes. The waste stream from the fish processing facility will consist primarily of liquid fraction wastes from the washing and rinsing processes. The liquids will flow into the building drainage system and will be conveyed to the main outfall. Prior to entering the outfall, the waste liquids will pass through a 0.2 in (5 mm) screen to remove solids. Solids from the screens and other solid wastes from processing will be ground and conveyed to the meal plant.

At maximum-rated capacity, Deep Sea Fisheries can process 446 t (405 mt) of finfish per day. The largest amounts of waste are generated in the filleting processes for pollock and cod. In the analysis of waste streams of other seafood processors, the concentration of BOD_5 in the fillet process effluent ranged from 1,047 to 1,226 milligrams per liter (mg/l) and 746 to 1,145 mg/l for pollock and cod, respectively (University of Alaska 1988). Using a discharge flow of 1,000,000 gpd (3,785,412 l) from the finfish processing plant with a BOD_5 concentration of 1,226 mg/l, the total BOD_5 loading from the finfish processing operation at maximum-rated capacity would be 5.1 t (4.6 mt) per day. Based on maximum seasonal production during a peak month such as August (Table 2), Deep Sea Fisheries could process

15

as much as 559 t (507 mt) of pollock per day. Assuming Deep Sea Fisheries can process this amount of fish, projected average daily BOD_5 loading for the month of August could be as high as 6.9 t (6.2 mt) per day.

Fish Meal Process Wastes. The primary waste streams which will be produced by the fish meal process are stickwater and the discharges from the air scrubbing system. Fish waste from the finfish processing operations (including solids collected from 0.2 in [5 mm] screens in the building's drainage system) will be ground and conveyed to the fish meal plant. The meal is cooked, then dehydrated with a mechanical press. Presswater is the waste liquor produced in dehydrating the fish meal. The presswater (which is a slurry of hot liquor and fine solids) is decanted to remove the solids. The solids are returned to the meal process. The remaining liquid fraction is centrifuged to remove light oils. These oils can be used as fuel for the boilers and generators. The remaining waste liquor is termed stickwater. Deep Sea Fisheries proposes to recycle 17% of the stickwater to the meal plant. This will allow Deep Sea Fisheries to maintain product salt content within a range acceptable to the market. Stickwater not recycled to the meal plant will be discharged to Akutan Harbor through the primary outfall.

Riley (pers. comm.) reported that the amount of stickwater produced by the Trident Seafoods fish meal plant is approximately equal to 70% of the amount of fish processed into meal. Based on this proportion, at a maximum-rated capacity (331 t [300 mt] of raw input per day), the Deep Sea Fisheries fish meal plant would produce approximately 231 t (210 mt) or 55,476 gal (210,000 l) of stickwater per day. Based on estimates made by the manufacturer of the fish meal plant (Johnson pers. comm.), the BOD_5 loading of the stickwater, after 17% of the stickwater is recycled, would be approximately 8.8 t (8 mt) per day (38,000 mg/l). Reported BOD_5 values for stickwater vary greatly. Trident Seafoods (Donegan pers. comm.) reported that the BOD_5 concentration of stickwater from its facility varies in relation to the amount of fish meal being produced in its plant (batch loaded process), with lower BOD_5 concentrations in stickwater when the plant is operating near capacity. The BOD_5 concentration estimated for the Trident Seafoods stickwater is 48,000 mg/l (Riley pers. comm.). Independent testing of Trident Seafoods' stickwater discharge by Jones & Stokes Associates in June 1992 found BOD_5 concentrations of 48,000 and 60,750 mg/l. When these samples were collected, the fish meal plant was operating at reduced capacity. Donegan (pers. comm.) indicated that the meal plant process is less efficient when run at reduced capacity. Though the BOD_5 concentrations of the stickwater are higher during periods of reduced production, the actual loading of BOD_5 would be lower than when the plant is running at full capacity. Since the analysis of worst-case conditions coincides with periods when the fish meal plant is operating at full capacity, a BOD_5 concentration of 48,000 mg/l will be used in this analysis. At the maximum-rated capacity of the meal plant (331 t [300 mt]), the daily BOD_5 loading from the meal plant would be 11.1 t (10.1 mt).

Based on maximum seasonal production during a peak production month such as August (Table 2), Deep Sea Fisheries could generate as much as 443 t (402 mt) of pollock waste per day. Assuming Deep Sea Fisheries can process this amount of fish in its meal plant, the stickwater discharge volume would be 74,472 gal (281,908 l). Based on a BOD_5

concentration of 48,000 mg/l in stickwater, the average daily BOD_5 loading from the meal plant for a peak summer month could be as high as 14.6 t (13.2 mt) per day.

As an odor control measure, vapors from the meal plant will be channeled through a spray of seawater. The spray functions to scrub aromatic organic compounds from the vented meal plant air prior to release to the atmosphere. The system at Deep Sea Fisheries will use about 1.2 million gallons (4.5 million liters) of seawater per day, which will be discharged through the main outfall. There is currently no information on the character of this discharge. Odorous chemicals are often detected by humans at concentrations measured in a few parts per billion. For the purposes of impact assessment, it is assumed that the concentration of aromatic compounds in the scrubber water will be in the range of a few parts per billion. The BOD_5 exerted by this loading in 1.2 million gallons (4.5 million liters) per day is expected to be almost zero.

Sanitary Wastewater. The BOD_5 content of the sanitary wastewater from the Deep Sea Fisheries facility is expected to be low. In the absence of information, it is assumed that the BOD_5 concentration would be comparable to the 30 mg/l limit typically placed on effluent from secondary treatment facilities. At a reported volume of 100,000 gpd (378,541 l), this would result in an estimated BOD_5 loading of 7 lbs per day (3 kg) from sanitary wastewater.

Stormwater. Deep Sea Fisheries proposes to divert stormwater to two surface discharges to Akutan Harbor. The expected characteristics of stormwater discharge from the site are not known. Stormwater running through the site would be expected to contain some hydrocarbons (fuels), associated with the machine shop and fuel storage areas, and sediments. The proposed stormwater recovery and treatment system includes retention/ detention ponds and oil/water separators on each of the two stormwater discharges, which should minimize hydrocarbon and sediment loading to the harbor. BOD_5 loading is expected to be minimal.

Solid Waste Accumulation

Deep Sea Fisheries is proposing to construct a new crab processing facility. Based on processing efficiencies during the 1991/1992 processing season, Deep Sea Fisheries expects to increase its maximum-rated capacity for production of crab from 62.5 t (56.7 mt) to 110 t (100 mt). The maximum seasonal production in 1992 was 124 t (113 mt) per day. The NPDES permit application indicated that the annual production of crab would remain unchanged at 9,000 t (8,165 mt). Estimates of crab pile dimensions are discussed later in the Marine Benthic Environments Section of Operational Impacts.

EXISTING ENVIRONMENT

The existing environment section was compiled from literature sources, personal communications, and information gathered during a field study conducted in Akutan Harbor during April 1992. Field methodologies are included with the following sections. The chronological report of the field study is presented in Appendix A.

Climate and Air Quality

The eastern Aleutian Islands are characterized by a maritime climate. Low-lying fog, overcast skies, and rain and drizzle dominate weather conditions along the archipelago because air masses over the warmer Pacific Ocean encounter chilled air over the colder Bering Sea. The nearest weather station is located at Dutch Harbor on Unalaska Island (approximately 40 miles west of Akutan Harbor). Mean maximum and minimum temperatures in Dutch Harbor are 56°F (13°C) and 25°F (-3.8°C) respectively, with little diurnal variation (City of Akutan 1982).

Topography

Akutan Harbor is a glacially-formed fjord approximately 3.9 miles (6.3 kilometers [km]) long. The harbor is approximately 1.8 miles (3 km) wide at its mouth and narrows to approximately 0.6 mile (1 km) wide at its head. The northern and southern shorelines are generally rocky and steep. Elevations of 1,082 ft (330 m) are reached in under 0.6 mile (1 km) along both sides of the fjord. The head of the fjord is a flat valley with a gradually increasing slope as it curves around to a high ridge to the northeast. The community of Akutan, the Trident Seafoods facility, and the abandoned whaling station are located on the only other relatively flat ground (terraces) near sea level.

Bathymetry

The submarine slopes along the sides of the fjord are steep with water depths of 60 ft (18 m) reached within 480 ft (146 m) from shore (8:1 slope). The harbor bottom is relatively flat and gradually deepens from 88 ft (27 m) at the head of the harbor, to 200 ft (61 m) at the mouth of the harbor. The harbor does not have an outer barrier sill that might act to inhibit the exchange of deeper waters between the harbor and the Bering Sea.

General Overview of Physical Processes

This section includes a discussion of measurements of winds and currents, as well as a discussion of a numerical model of the wind-driven circulation developed for Akutan Harbor. Using the measurements and the numerical calculations, assessments were made concerning the effects of fish waste discharged into the harbor. A more detailed description of field measurements and circulation modeling can be found in Appendix B.

Stratification. Since Akutan Harbor is an arm off the Bering Sea, density stratification within the harbor is determined by the stratification of the Bering Sea waters. During the winter, Bering Sea waters in the vicinity of the Aleutians are well mixed to depths in excess of the depths in Akutan Harbor (Kinder and Schumacher 1981). Based on the studies conducted as part of this assessment, there is insufficient freshwater flow into Akutan Harbor to measurably stratify the homogeneous Bering Sea waters of the harbor in the winter. A weak stratification at the head of the harbor was noted in the summer of 1983 (EPA 1984b). The stratification was measurable seaward to about the location of the Trident Seafoods facilities. Because of this weak stratification, density is not considered to be an important factor in determining the circulation in Akutan Harbor.

Wind and Currents. Wind speed and direction have been continually monitored since September 1991 at a meteorological station located on top of the old processing building at the Trident Seafoods facility. Quarterly wind roses for 1992 are presented in Figure 5. The dominant winds during the study period were north-east-north to west-north-west but also demonstrated a strong east-south-east component.

Three Aanderra current meters were deployed in Akutan Harbor on April 6, 1992. These current meters collected data on current speed and direction, pressure, and temperature continuously until their recovery on June 4, 1992, a period of 60 days. Two of the current meters were deployed at depths of 72 ft (22 m) and 82 ft (25 m) at the proposed outfall location for the Deep Sea Fisheries facility (Figure 6). The third current meter was deployed at a depth of 141 ft (43 m) and located in midchannel, offshore from the Trident Seafoods facility. Data collected from the current meters are included as Appendix C. Table 3 shows the average current velocities observed at each of the three moorings.

Based on the current meter records, tidal currents were found to be weak (1 to 2 centimeters per second [cm/s]). The tides accounted for less than 10% of the observed current velocities. The dominant currents observed were primarily generated by wind events. A display of the relationships between winds and currents is contained in Appendix B, Figures B-2 to B-4.

Severe storm activity (sustained winds in excess of 40 knots) did not occur during the spring of 1992. The winds generally blew either into the harbor (from the east) or out of the harbor (from the west). Westerly winds occurred about 70% of the time and the winds seldom exceeded 20 knots (10 meters per second [m/s]) in sustained hourly wind speed. Currents related to these winds were generally in the 5 to 20 cm/s range, with the stronger

Trident Windrose - 1992 1st Quarter
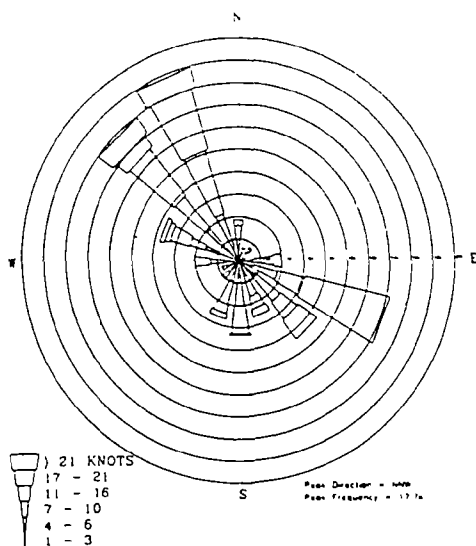
**January to March
1992**

Trident Windrose - 3rd Qtr 1992 (per.)
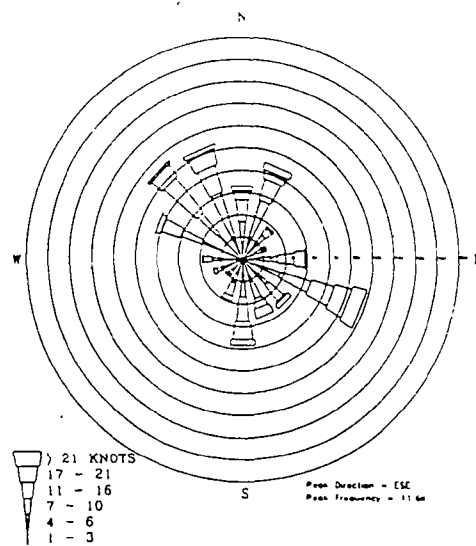
**April to June
1992**

Trident Windrose - 3rd Qtr 1992
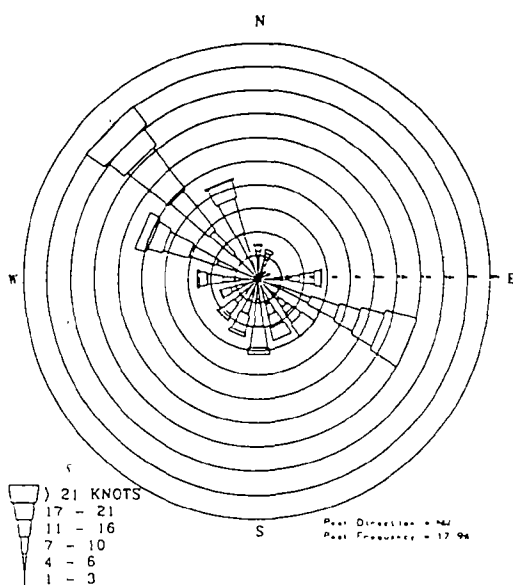
**July to September
1992**

Trident Windrose - 4th Qtr 1992
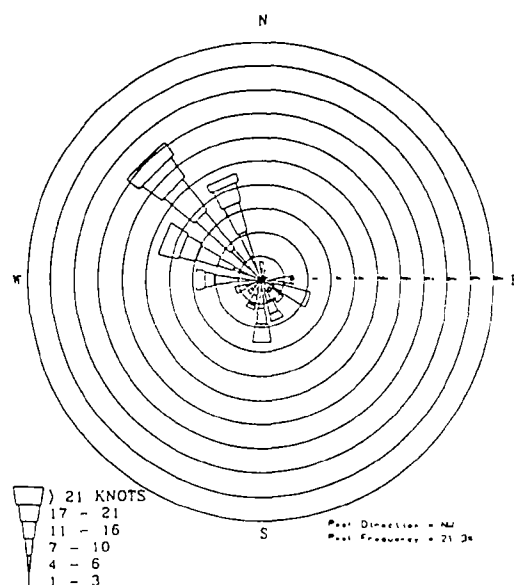
**October to December
1992**

Source: Winges pers. comm.

Figure 5. Wind Roses Depicting Quarterly Summaries of Wind Direction and Magnitude in Akutan Harbor, Alaska, January to December 1992

20
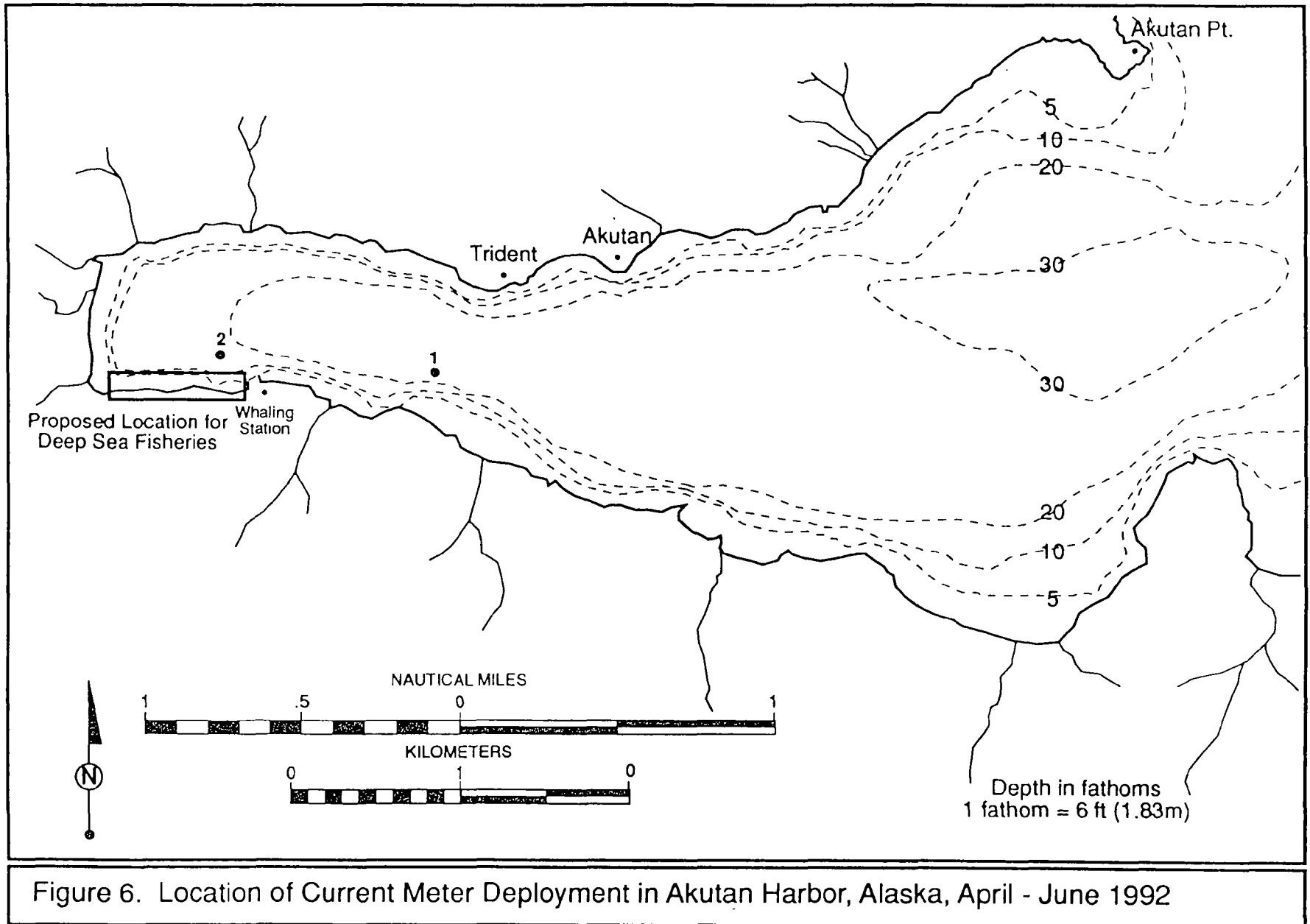
Figure 6. Location of Current Meter Deployment in Akutan Harbor, Alaska, April - June 1992

Table 3. Average Current Velocities Recorded by
Three Current Meters Located in Akutan Harbor

Meter Location	Average Currents*	
	u(cm/s)	v(cm/s)
Near Trident (43 m)	1.177	-2.66
Deep Sea (22 m)	1.305	-7.60
Deep Sea (25 m)	0.844	-6.81

* u = east-west directional component
  v = south-north directional component
  cm/s = centimeters per second

15 to 20 cm/s currents occurring following and during easterly wind storms. The current speeds were greater at the midchannel mooring near the Trident Seafoods facility (Mooring 1) than at either of the instruments at the site of the proposed Deep Sea Fisheries outfall (Mooring 2).

Modeling Wind-Driven Circulation

Wind-driven circulation refers to estuarine currents created by wind stress on surface waters of the estuary. This stress causes two responses: (1) surface waters are pulled in the same direction as the winds, piling up against any boundary (shoreline) impeding the flow, and (2) a deep recirculating countercurrent (opposite to the wind direction) develops to offset water transport near the sea surface.

The model chosen to analyze the wind-driven circulation in Akutan Harbor predicts the depth-averaged velocities and the sea level. The model is described in detail in Appendix B, and it generally follows the calculations for a 2-1/2 dimensional circulation model developed by Koutitas (1988). The Koutitas calculations and program coding used for modeling Akutan Harbor are presented in Appendices D and E, respectively.

Model results are presented here for short-term storm events (40-knot [20 m/s] winds) and longer quiescent periods (10-knot [5 m/s] winds). Four cases are presented. Figures 7 and 8 illustrate the model-predicted currents in the harbor 4 hours (hr) following the onset of 40-knot easterly winds (Figure 7) and 40-knot westerly winds (Figure 8). Figures 9 and 10 illustrate the currents in the harbor following 32 hr of weak wind (10 knots) from the east and west, respectively. Each arrow in the figures represents the magnitude and direction of the predicted depth-averaged currents. The current flow is toward the bold head on the arrows. Under short-term strong wind conditions (Figures 7 and 8), the circulation model predicted incomplete mixing between the inner harbor (west of Trident Seafoods) and the outer harbor. This suggests a higher potential for effluents discharged to the inner harbor to concentrate and settle in this area. Under longer-term, weak wind conditions (Figures 9 and 10), predicted currents 32 hr after the onset of the winds were slow (generally less than 10 cm/s), with very little apparent net transport of water between the inner and outer harbor.

To evaluate the potential for dispersion of effluent from the proposed outfall site, the hydrodynamic models were modified to illustrate the effect of predicted currents on the movement of a tracer. The modeling methods and the results of these model simulations are discussed in detail as part of the alternative outfall location analysis (under Alternatives and their Environmental Effects below). As expected, the storm event scenarios showed a much wider dispersion pattern than the quiescent scenarios. In all cases, more dispersion was realized for the east wind scenarios as compared to the west wind scenarios.
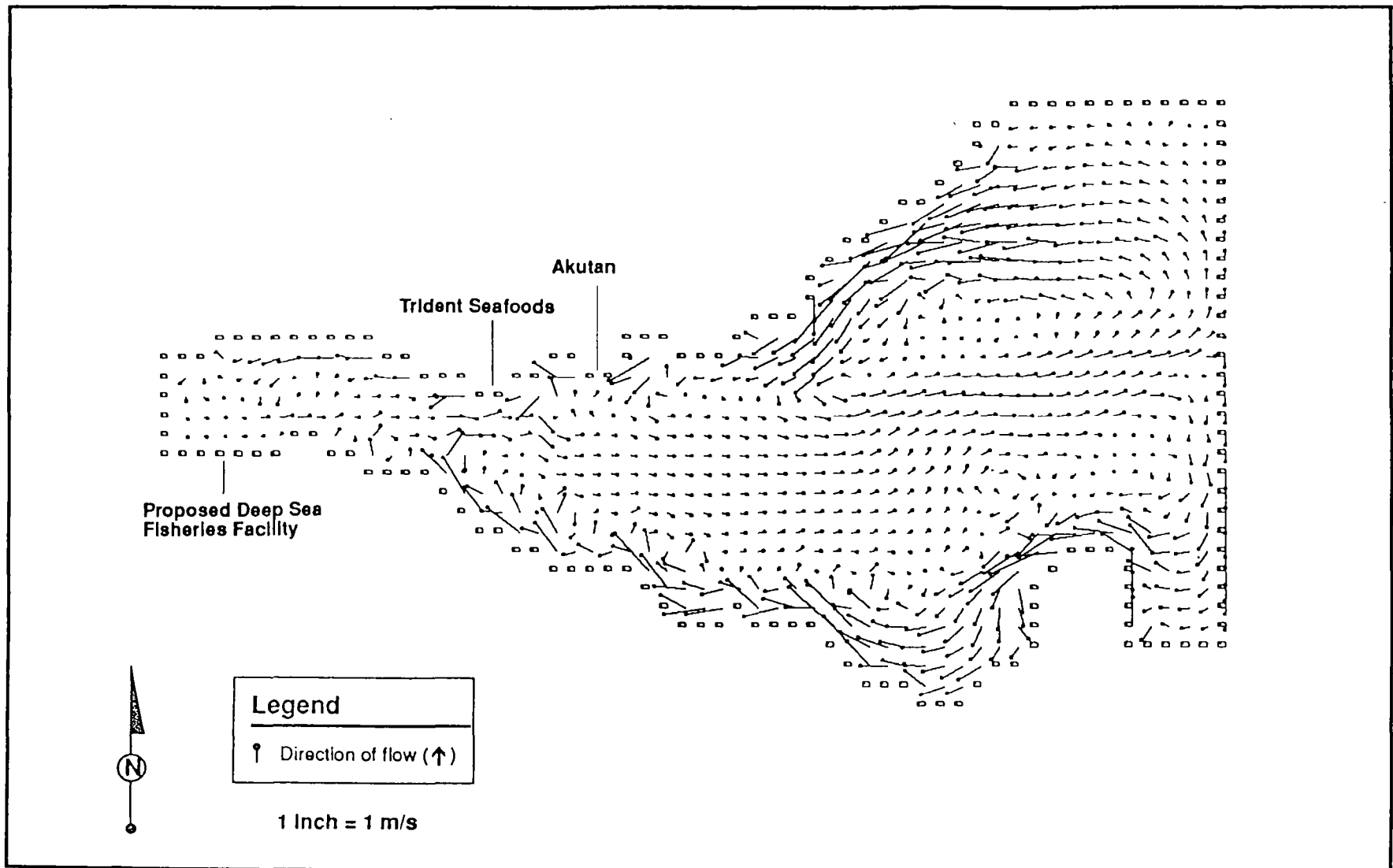
Figure 7. Predicted Circulation Pattern in Akutan Harbor, Alaska, 4 Hours after the Onset of a 20 m/s East Wind

Akutan

Trident Seafoods

Proposed Deep Sea
Fisheries Facility

N

Legend

↑   Direction of flow (↑)

1 Inch = 1 m/s
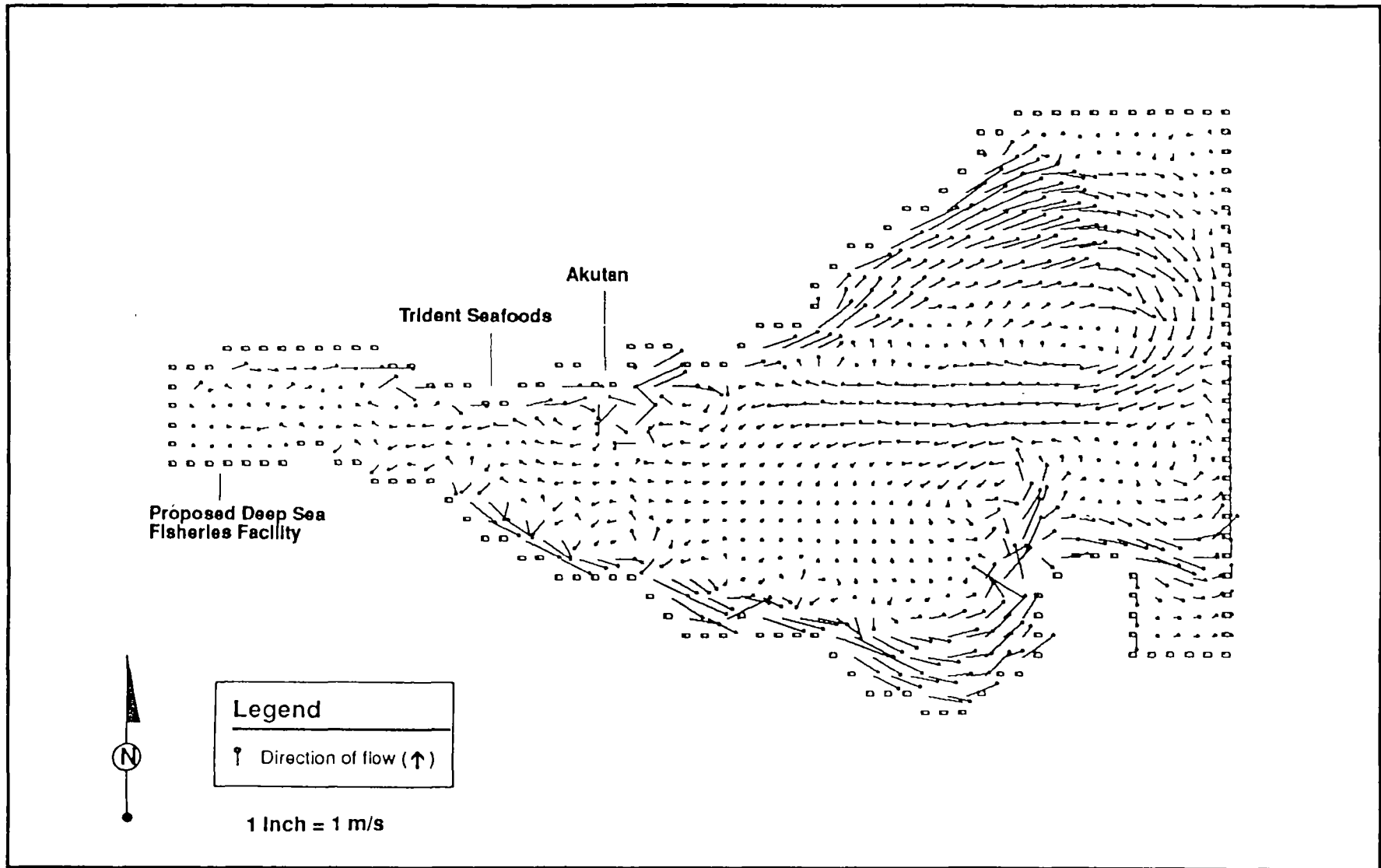
Figure 8.   Predicted Circulation Pattern in Akutan Harbor, Alaska, 4 Hours after the Onset of a 20 m/s
West Wind

Akutan

Trident Seafoods

Proposed Deep Sea
Fisheries Facility

Legend

ʃ Direction of flow (↑)

1 inch = 1 m/s

N
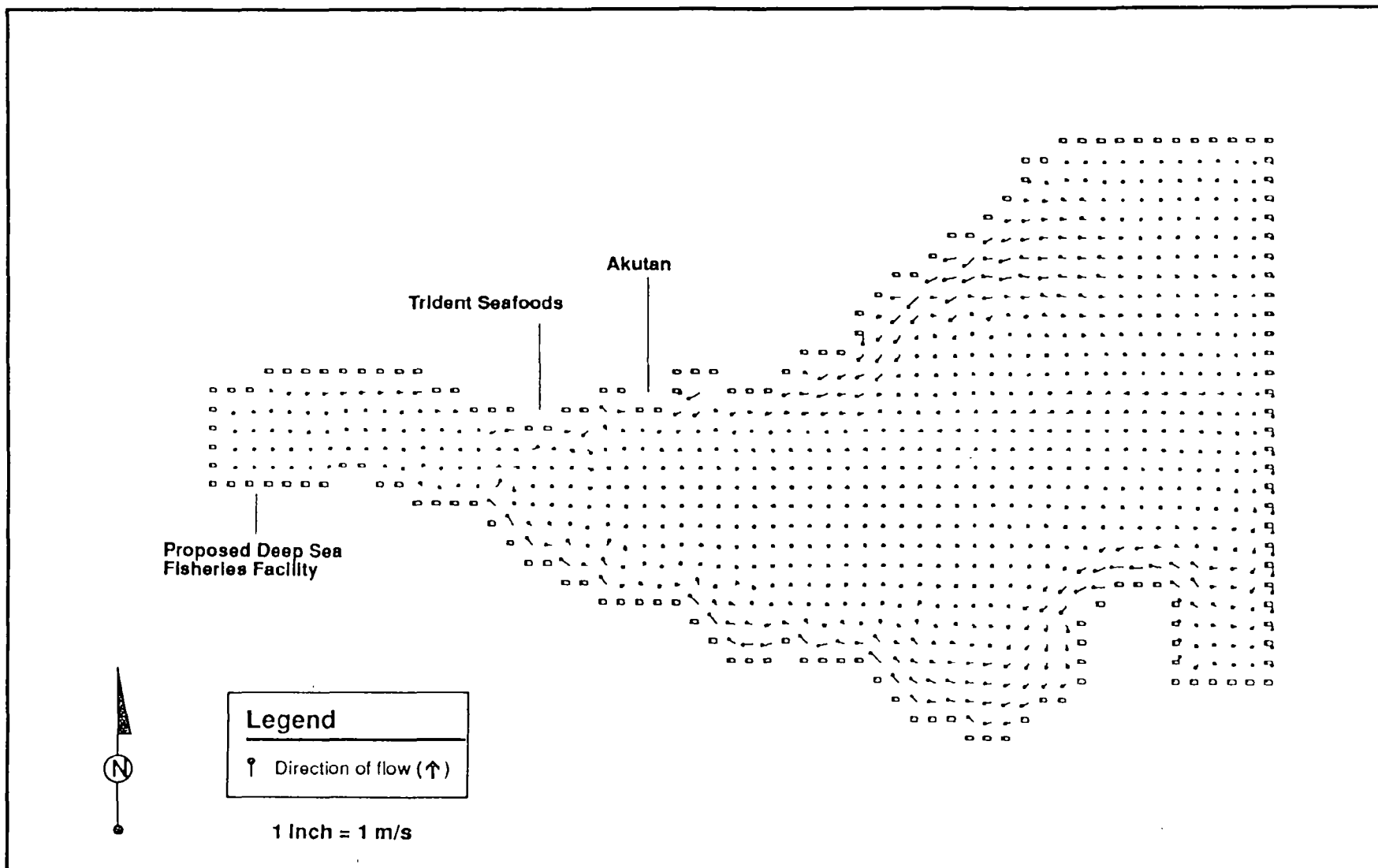
Figure 9. Predicted Circulation Pattern in Akutan Harbor, Alaska, 32 Hours after the Onset of a 5 m/s
East Wind
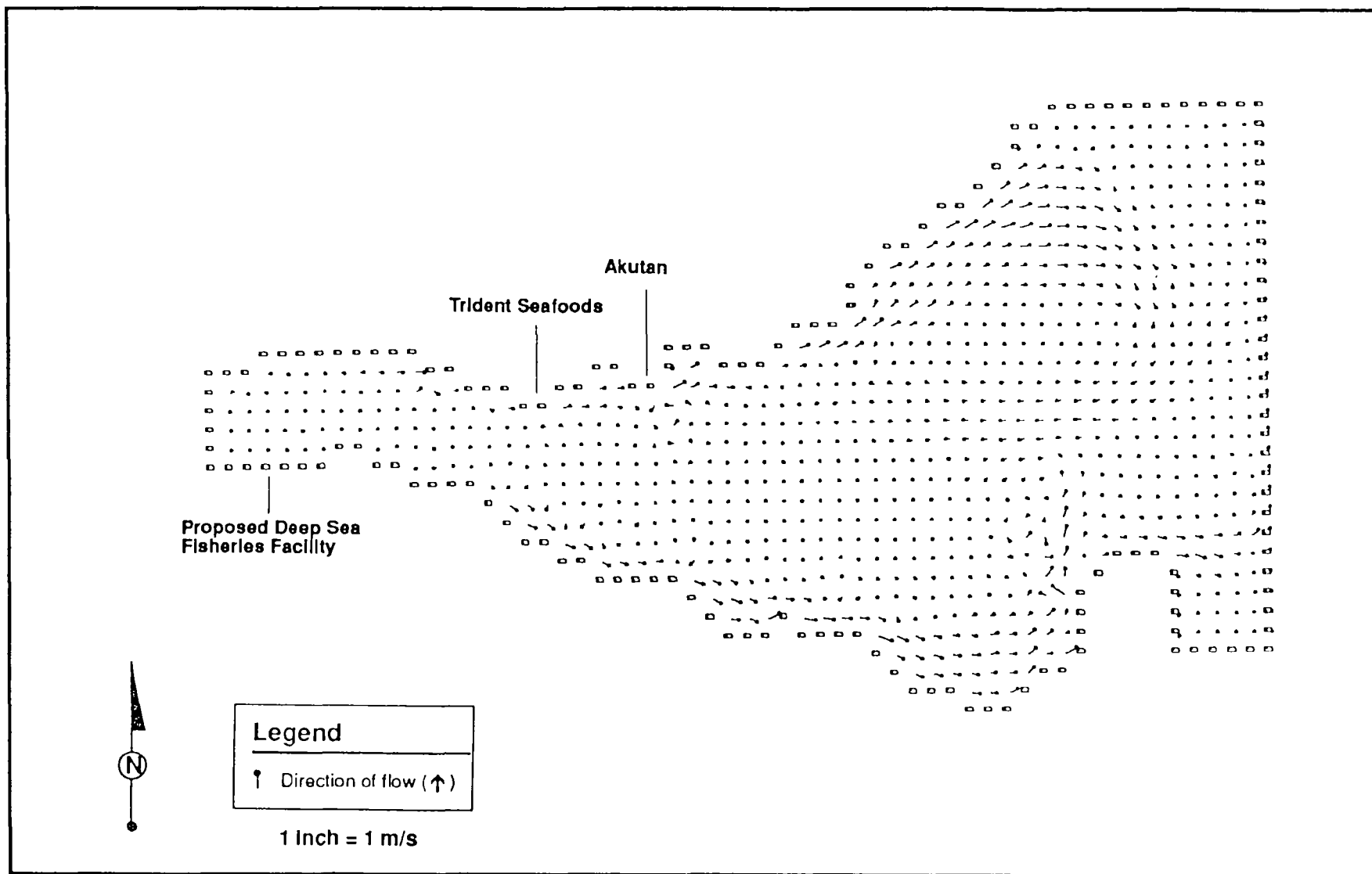
Figure 10. Predicted Circulation Pattern in Akutan Harbor, Alaska, 32 Hours after the Onset of a 5 m/s West Wind

Water Quality

Ambient water quality conditions within Akutan Harbor were characterized to assess potential impacts of seafood processing activities on receiving waters. Water quality studies were also performed to determine the potential for Deep Sea Fisheries and other shore-based and floating processors to cause cumulative impacts to the harbor. Water quality parameters were selected to identify harbor stratification and evaluate impacts known to be associated with processing activities such as anoxia, nutrient loading, and the presence of fecal coliforms.

More crab were landed and processed in Akutan Harbor during the 1991/1992 crab season than in the preceding four seasons (Table 4). Over 30,700 t (27,850 mt) of crab were processed in the harbor between the weeks of November 17, 1991, and April 26, 1992. At the peak of the 1991/1992 season, 3,956 t (3,589 mt) of crab were processed in a week (Appendix F). During the 4 weeks prior to the study, between 1,732 t (1,571 mt) and 2,325 t (2,110 mt) of crab were processed each week. However, very limited processing activity was occurring in the harbor during the field study. Most of the transient floating processors had left the harbor about a week prior to the study. Trident Seafoods, the M/V Clipperton, and the M/V Deep Sea processed only small quantities of crab at different times during the study period. Unfortunately, water quality samples could not be obtained from the outfall plumes of these processors while they were actively discharging. However, some water samples were collected from waters immediately above the waste piles at the Trident Seafood outfall and above the M/V Deep Sea crab waste pile. During the week of the study, 627 t (569 mt) of crab were processed in the harbor.

Water Quality Profiles

A variety of sampling methods were used during the water quality sampling effort. Data on physical parameters were gathered using a Hydro Lab Model 4001. The Hydro Lab was used to determine conductivity, temperature, and dissolved oxygen concentrations throughout the water column. These data were used to calculate water density and determine if waters were stratified within the harbor. Profile data were collected at 11 stations throughout the harbor (Figure 11). Figure 12 illustrates several typical harbor profiles.

Near-bottom temperature ranged from 36.5°F to 37°F (2.5°C to 2.7°C) (Table 5). Surface temperatures showed more variability and ranged from 35.8°F to 39.4°F (2.1°C to 4.1°C). Conductivity at all stations, except the Trident Seafoods outfall station, remained relatively constant throughout the water column with a range of 503 to 510 microsiemens per centimeter (µs/cm). At the Trident Seafoods outfall station (H-9), the conductivity profiles showed a decrease from 504 µs/cm at the surface to 329 µs/cm in near-bottom waters. Dissolved oxygen concentrations were above 100% saturation (12.1 to 15.5 mg/l) in surface waters at all stations except the Trident Seafoods outfall station, which contained

28

Table 4. Annual Crab Landings in Akutan Harbor
between 1987 and 1992*

Season	Pounds
1987/1988	21,850,100
1988/1989	19,241,150
1989/1990	14,030,000
1990/1991	33,883,000
1991/1992	61,406,000

Source: Griffin pers. comm.

* Crab seasons generally occur between November and May.
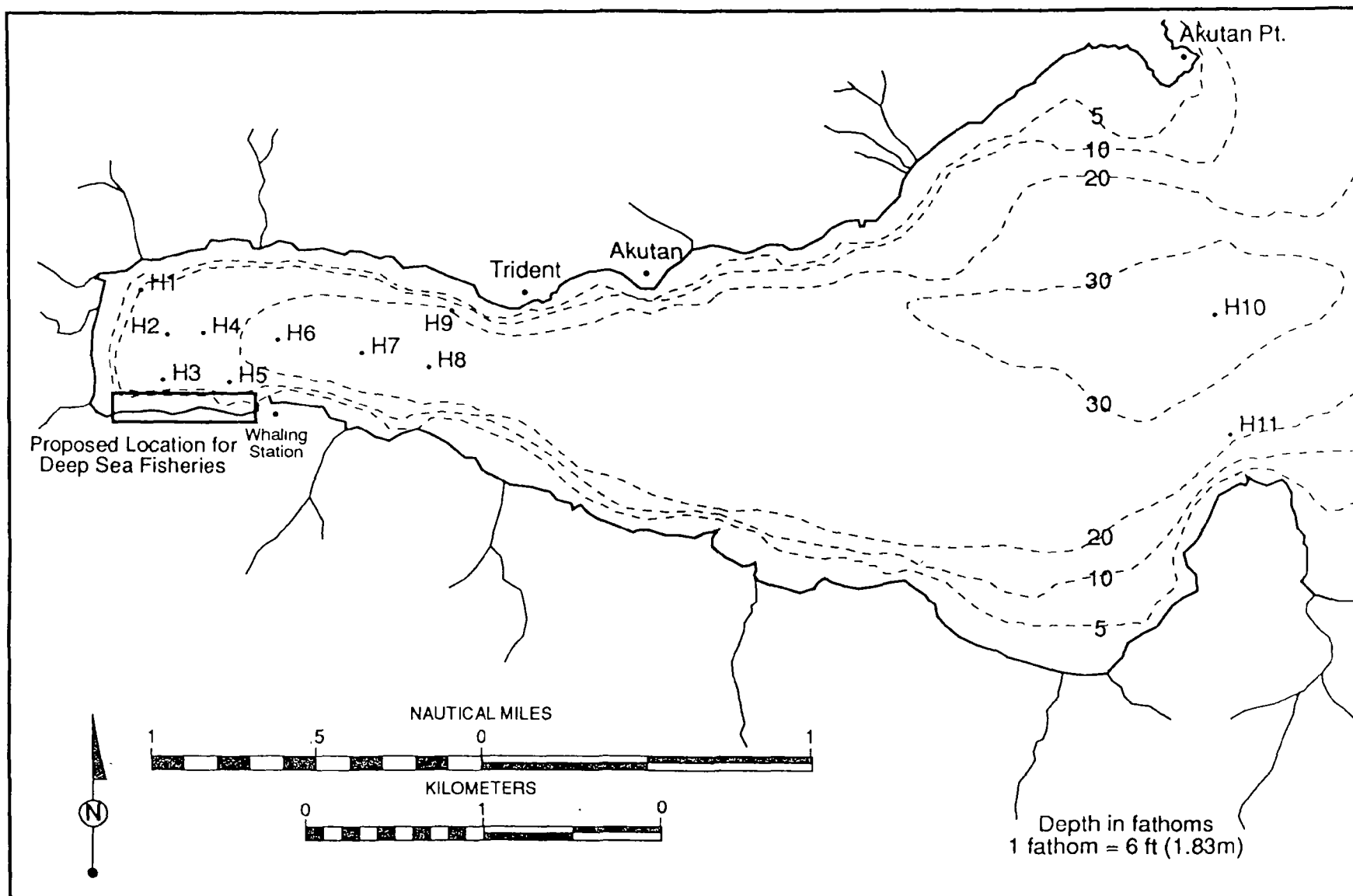
Figure 11.   Location of Water Quality Profile Stations in 1992, Akutan Harbor, Alaska
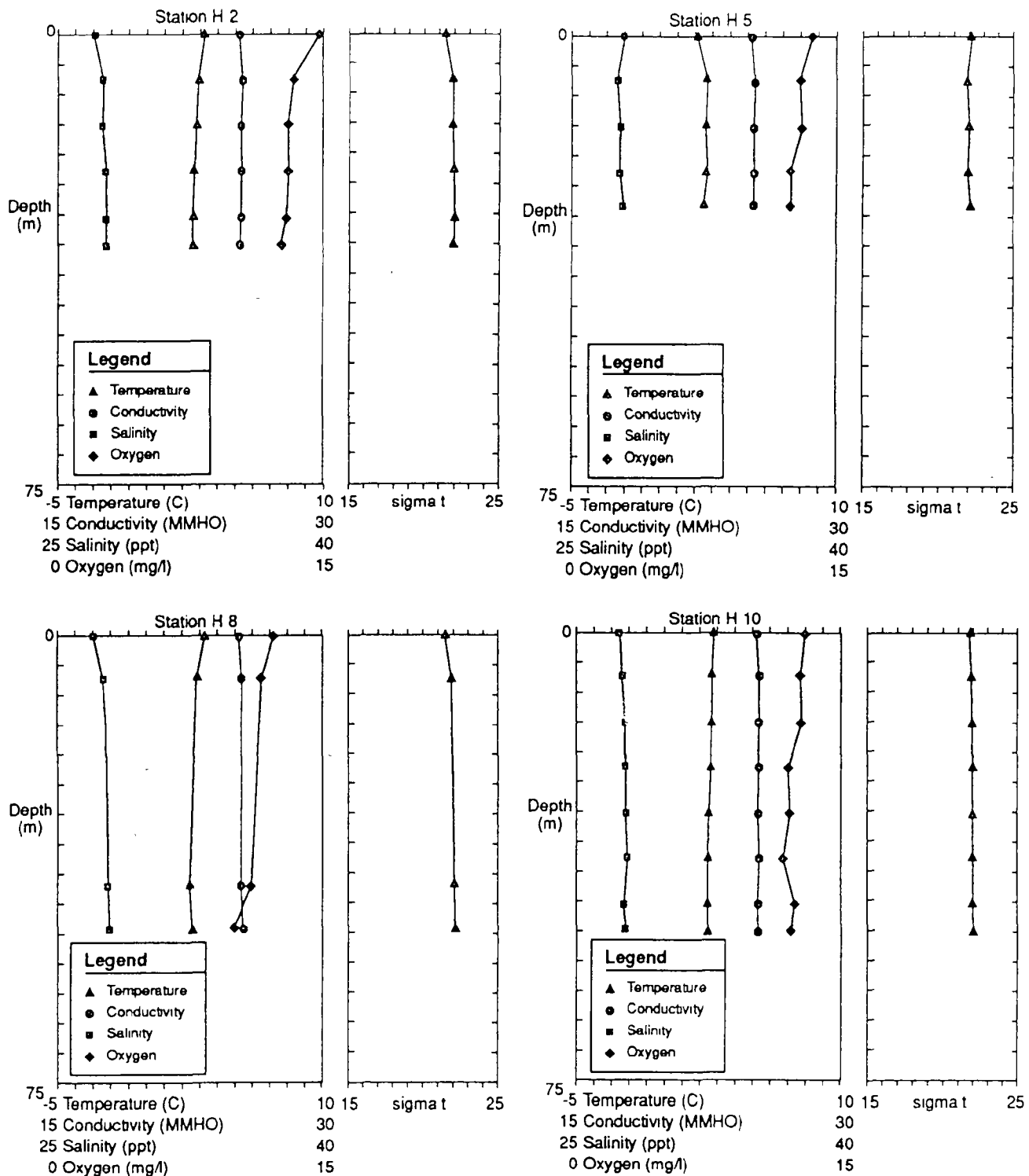
Figure 12. Typical Water Quality Profiles of Akutan Harbor, April 1992

Table 5. Water Quality Data Collected during Hydrocast Surveys of
Akutan Harbor 1992

Station	Depth (ft)	Temp. (°C)	Conduct. (µs/cm)	Salinity (o/oo)	Density (sigma t)	DO (mg/l)	Secchi Disk (m)
H-1, S	0	3.0	506	27.34	21.69	15.5	6.5
H-1, B	69	2.7	507	27.71	21.95	12.7	--
H-2, S	0	3.2	505	27.11	21.49	14.8	7.0
H-2, B	115	2.6	507	27.74	22.03	12.7	--
H-3, S	0	3.0	506	27.34	21.69	14.5	5.5
H-3, B	85	2.6	508	27.80	22.08	13.0	--
H-4, S	0	3.4	507	27.06	21.44	13.4	--
H-4, B	97	2.7	508	27.71	22.08	12.5	--
H-5, S	0	2.1	503	27.94	22.21	13.8	5.0
H-5, B	93	2.5	508	27.89	22.15	12.5	--
H-6, S	0	3.5	506	26.92	21.32	12.6	--
H-6, B	127	2.5	508	27.89	22.15	11.6	--
H-7, S	0	4.0	505	26.45	20.92	12.6	--
H-7, B	147	2.5	509	27.95	22.20	10.3	--
H-8, S	0	3.3	506	27.08	21.47	12.2	--
H-8, B	162	2.6	510	27.92	22.17	10.0	--
H-9, S	0	4.1	504	26.31	20.80	11.2	--
H-9, B	122	2.5	329	17.34	13.86	6.2	--
H-10, S	0	2.8	506	27.51	21.83	13.0	>15
H-10, B	165	2.5	508	27.89	22.15	12.3	--
H-11, S	0	2.7	506	27.59	21.91	12.1	>15
H-11, B	160	2.5	509	27.95	22.20	11.5	--

S = surface   ft = feet   mg/l = milligrams per liter
B = bottom   µs/cm = microsiemens per   m = meters
                     centimeter   o/oo = parts per thousand

11.2 mg/l. Near-bottom waters at all but the Trident Seafoods outfall station contained oxygen concentrations between 10.0 and 13.0 mg/l. Dissolved oxygen in near-bottom waters at the Trident Seafoods outfall station was 6.2 mg/l.

Based on calculated densities, the harbor was not stratified at the time of the 1992 study. Profile data collected in June and September of 1983 also showed no signs of stratification in the harbor.

Discrete Water Samples

Discrete depth water samples for chemical analysis were collected from fixed stations with a 4-liter Van Dorn bottle (Figure 13). Water column profile data indicated the harbor was not stratified; therefore, samples for chemical analysis were collected only from surface and near-bottom waters at each station. Water quality sampling Stations WQ-1 to WQ-11 were located as close as possible to water quality Stations 1 through 11 used during the September 1983 surveys. These were considered background water quality stations. Stations WQ-12 to WQ-15 were located approximately 800 ft offshore from the Trident Seafoods facility, in the vicinity of the proposed Deep Sea Fisheries outfall site, over the M/V Deep Sea waste pile, and near the mouth of the harbor, respectively.

Samples were placed into bottles containing appropriate chemical preservatives. The samples were transported on ice from Akutan Harbor to Seattle, Washington, where analysis was performed by an accredited laboratory. The water quality samples were analyzed for total Kjeldahl nitrogen (TKN), nitrate + nitrite nitrogen (N-N), oil and grease, and hydrogen sulfide. All sampling procedures followed the guidelines outlined by EPA.

Water quality data indicated that waters in the harbor contained very low concentrations of TKN, N-N, hydrogen sulfide, and oil and grease at the time of the study (Table 6). TKN concentrations ranged from below detectable levels (0.25 mg/l) to 0.64 mg/l in surface waters, and from below detectable levels to 0.92 mg/l in the near-bottom samples. N-N concentrations remained low throughout the harbor and ranged from below detectable levels (0.01 mg/l) to 0.079 mg/l in surface waters, and from below detectable levels to 0.070 mg/l in near-bottom waters at all stations except Station WQ-13. Near-bottom N-N concentrations at this site (near the Deep Sea Fisheries outfall) were greater (0.20 mg/l) than at other areas in the harbor. Hydrogen sulfide concentrations were below detectable levels (1.0 mg/l) at 13 of the 15 sampling stations, but hydrogen sulfide was detected in surface waters at Station WQ-6 (2.4 mg/l) and Station WQ-8 (1.2 mg/l). Total oil and grease concentrations were below detectable levels (1.0 mg/l) at all 15 sampling locations.
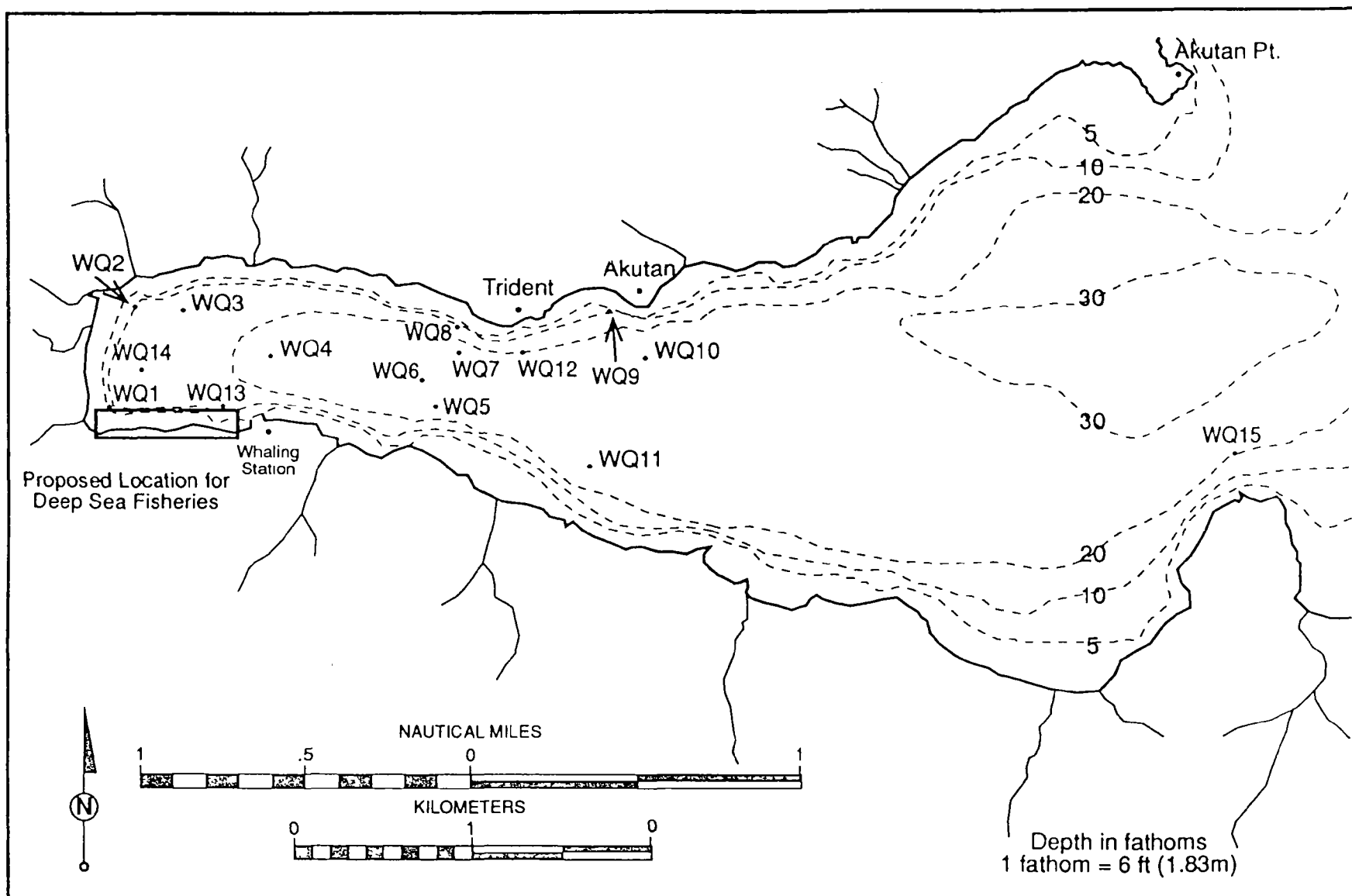
Figure 13. Location of Water Quality Sampling Stations in 1992, Akutan Harbor, Alaska

Table 6. Surface and Near-Bottom Water Quality Parameters
Measured in Akutan Harbor, April 1992

Station	Total Nitrogen (mg/l)	Nitrate and Nitrite (mg/l)	Total Oil and Grease (mg/l)	Sulfide (mg/l)
Surface				
WQ-1	<0.25	<0.01	<1	<1
WQ-2	<0.25	<0.01	<1	<1
WQ-3	<0.25	<0.01	<1	<1
WQ-4	<0.25	<0.01	N/C	<1
WQ-5	<0.25	<0.01	<1	<1
WQ-6	<0.25	<0.01	<1	2.4
WQ-7	<0.25	0.012	<1	<1
WQ-8	<0.25	0.052	<1	1.2
WQ-9	<0.25	0.048	<1	<1
WQ-10	<0.25	0.076	<1	<1
WQ-11	<0.25	<0.01	<1	<1
WQ-12	0.27	<0.01	<1	<1
WQ-13	0.29	<0.01	<1	<1
WQ-14	<0.25	0.024	<1	<1
WQ-15	<0.25	0.079	<1	<1
Near-Bottom				
WQ-1	<0.25	0.055	<1	<1
WQ-2	<0.25	0.030	<1	<1
WQ-3	0.27	0.033	<1	<1
WQ-4	<0.25	0.018	N/C	<1
WQ-5	<0.25	0.067	<1	<1
WQ-6	0.26	0.050	<1	<1
WQ-7	<0.25	0.061	<1	<1

Table 6. Continued

Station	Total Nitrogen (mg/l)	Nitrate and Nitrite (mg/l)	Total Oil and Grease (mg/l)	Sulfide (mg/l)
WQ-8	0.41	0.045	< 1	< 1
WQ-9	0.64	0.055	< 1	< 1
WQ-10	< 0.25	0.021	< 1	< 1
WQ-11	0.92	0.064	< 1	< 1
WQ-12	< 0.25	0.042	< 1	< 1
WQ-13	< 0.25	0.20	< 1	< 1
WQ-14	0.31	0.061	< 1	< 1
WQ-15	< 0.25	0.070	< 1	< 1

mg/l = milligrams per liter
N/C = not collected

Samples for the biological parameters, BOD$_5$ and fecal coliform bacteria, were collected on the final day of water quality testing. Samples were collected from surface waters at eight sites near areas where contamination from marine sanitary or seafood processing discharges were possible. Sample locations within the harbor included:

(1) off the Trident Seafoods dock,
(2) at the Trident Seafoods surface water outfall,
(3) at the docking site along the Trident Seafoods dock,
(4) at a reference ("clean") site in the central harbor,
(5) off the dock in Akutan Village,
(6) at the site of the proposed Deep Sea Fisheries outfall,
(7) off the bow of the M/V Clipperton, and
(8) off the bow of the M/V Deep Sea.

These samples were put on ice and hand-carried to Dutch Harbor, Alaska, where they were analyzed by an accredited laboratory. This procedure was necessary to ensure that the samples reached the testing laboratory within 24 hr.

Data for BOD$_5$ and fecal coliform bacteria are presented in Table 7. BOD$_5$ in the surface waters ranged from 0.88 to 2.07 mg/l. These levels of BOD$_5$ seemed low considering the amount of crab processing which had occurred in the harbor during the preceding 2-month period (Appendix F). Processing activities did decrease dramatically a week before the study from a peak of 3,956 t (3,589 mt) during the last week in February, to 627 t (569 mt) during the week of the study.

Fecal coliform bacteria concentrations ranged from 2 to 55 fecal coliforms per 100 milliliter (ml). The highest concentrations of bacteria were found at the three stations near the Trident Seafoods facility (Stations 1, 2, and 3). The mean bacterial concentration from these three samples was 44 fecal coliforms per 100 ml.

Existing Seafood Waste Deposits

Historical Information

There has been a relatively long history of seafood processing in Akutan Harbor. Several substantial seafood processing waste piles have been located with the aid of side-scan sonar (SSS) and diver surveys. The largest waste pile lies off the Trident Seafoods dock at a depth of 88 ft (27 m) and is composed of both crab and finfish waste. Using SSS data collected in May 1989, the pile was estimated to cover 7.75 acres (31,800 square meters [m^2]) and to have a maximum height of 26 to 33 ft (8 to 10 m).

A waste pile was also identified beneath the M/V Deep Sea. Diver measurements collected in 1990 indicated that the waste pile covered an area of 0.27 acre (1,107 m^2) and had a maximum height of 10 ft (3 m). There has been a continuous discharge (during the winter months) at this location since 1979.

Table 7. Fecal Coliform, Total Coliform, and BOD$_5$ Data
Collected from Akutan Harbor, April 1992

Station	Fecal Coliform (#/100 ml)	Total Coliform (#/100 ml)	BOD$_5$ (mg/l)
1	32	118	N/D
2	45	120	1.09
3	55	137	2.70
4	0	9	1.06
5	2	4	1.22
6	0	0	0.88
7	12	14	1.20
8	5	14	--

ml = millileter
mg/l = milligrams per liter
N/D = not detectable
-- = no data

Results of Side-Scan Sonar Surveys in 1992

Scientific Applications International Corporation (SAIC) conducted an SSS survey of Akutan Harbor in April 1992 as part of a separate EPA contract (Appendix G). The SSS survey was used to delineate the location of seafood processing waste piles in Akutan Harbor. The SSS survey was conducted using an EG&G Model 260 Digital Image Correcting Side-Scan Sonar system mounted on a 24 ft fishing boat. Because permanent survey monuments were unavailable in the area, a rectilinear coordinate system was established in the harbor by DOWL Engineers, Anchorage. A Motorola Miniranger IV (MR4) positioning system was used to fix the location of the vessel carrying the SSS system and determine its position with respect to the rectilinear coordinate system.

The SSS survey was conducted in two phases and included 19 survey tracklines. The first phase was a reconnaissance survey of the harbor that included 9 tracklines which ran east to west down the length of the harbor. Overlap of tracklines ensured complete coverage of the harbor during this phase of the survey. The SSS system was equipped with a printer which supplied an output of bottom features found during the survey of each trackline. The survey logs were evaluated in the field to establish the position of suspect waste piles to be further delineated during the second phase of the survey.

Preliminary assessment of the reconnaissance survey data indicated that three areas warranted a more detailed survey. These included waste piles near the Trident Seafoods shore-based facility; the permanently moored floating crab processor, M/V Deep Sea; and the temporarily moored floating crab processor, M/V Clipperton. Two additional tracklines each were surveyed at the M/V Deep Sea and M/V Clipperton sites. The Trident Seafoods pile was delineated by running two additional north-to-south transects and four additional east-to-west transects.

Twelve grab samples were collected using a 0.1 m^2 Van Veen sampler to substantiate findings of the SSS survey data (Figure 14). The vessel carrying the side-scan equipment was inadequate for benthic sampling; therefore, the MR4 navigation system was transferred to the M/V Flying D, a 90 ft converted landing craft, to locate and collect grab samples.

The SSS data analysis revealed significant waste piles associated with the Trident Seafoods plant outfall and the M/V Deep Sea. Although several temporarily moored floating processors, including the M/V Clipperton, were currently or recently operating in Akutan Harbor, waste piles from temporary processors were not substantial enough to be detected using the SSS alone. Apparently, many of the temporarily moored processors use a single-point moorage arrangement, allowing them to swing on their moorage points in response to the wind and thereby disperse their processing wastes over a broad area. The SSS survey did not detect significant waste piles associated with the temporarily moored floating processors. However, grab samples VSSS2 and VSSS3, taken from the outer harbor, had a strong hydrogen sulfide smell. Additional surveys were conducted near the M/V Clipperton because it was moored with both a fore and aft anchor and remained in the same location throughout the 1991/1992 crab season. Evidence of wastes was found in grab samples taken near the M/V Clipperton; however, waste accumulations were not substantial enough for detection using the SSS.
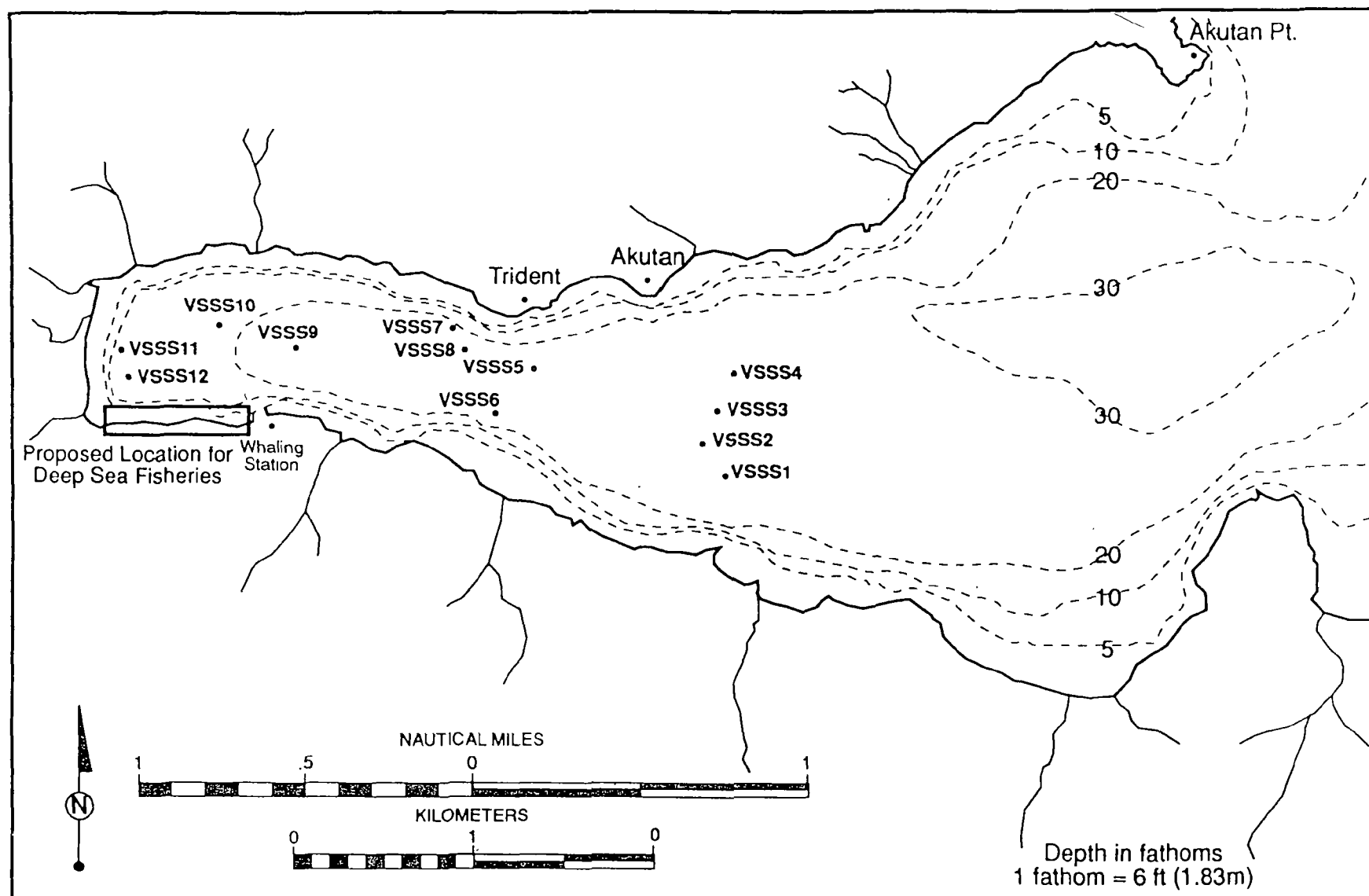
Figure 14. Locations of Benthic Samples Collected to Evaluate Side-Scan Sonar Surveys in 1992, Akutan Harbor, Alaska

The results of the SSS survey in April 1992 indicate that the waste piles near the M/V Deep Sea and the Trident Seafoods outfall are much larger than was indicated by the diver surveys or the earlier SSS surveys. The waste pile associated with the M/V Deep Sea had been estimated to cover 0.27 acre (1,093 m²) during diver surveys conducted in 1990. Based on SSS surveys in April 1992, SAIC estimated that the M/V Deep Sea waste pile covered 2.5 acres (10,117 m²). Distribution of the waste pile was quite patchy based on the SSS survey data. The patchiness of the M/V Deep Sea pile was further confirmed by grab sample data. A total of six piles were found. Because precise positioning for the collection of benthic samples could not be achieved, confirmation of each pile as a waste pile was not possible. Therefore, estimated acreage of the waste piles under the M/V Deep Sea was assigned an error of ±25%. It is possible that the ancillary piles located near the main M/V Deep Sea waste pile may not have been included in earlier surveys.

Earlier SSS surveys in 1989 estimated the total areal coverage of the Trident Seafoods waste pile to be 7.5 acres (31,352 m²). The SAIC SSS surveys indicated that the Trident Seafoods waste pile covered 11.2 acres (45,325 m²). The primary portion of the pile was estimated at 1.2 acres (4,047 m²). It appeared that wastes had spread downslope in a southerly direction and had spread in both an easterly and westerly direction from the point of origin. Difficulty in determining the waste boundary near the Trident Seafoods dock warranted an estimated error of ±15%.

Marine Benthic Environments

The conditions of benthic habitats and the community structure of benthic organisms can be used to assess the potential for impacts from the proposed project, and they can act as an indicator of cumulative impacts associated with seafood processing in Akutan Harbor. Data collected from the harbor during 1983 (EPA 1984b and other studies) on benthic community structure, chemical quality of sediments, and location and size of crab waste piles provide a baseline for the determination of cumulative impacts on subtidal environments.

Several methods were used to identify benthic habitat conditions within the harbor in April 1992. In addition to the SSS surveys, Van Veen grab samples were used to quantitatively characterize sediment quality and benthic community structure; gravity cores were used to qualitatively characterize a broader area of sediments within the harbor; and a remotely operated vehicle (ROV) with a VCR camera was use to document conditions on the natural bottom and those areas affected by seafood processing activities. The following describes methodologies and results of marine benthic habitat studies conducted in Akutan Harbor during April 1992.

Sediment Quality. Sediment samples for chemical analysis were collected at 17 stations within the inner harbor in April 1992 (Figure 15). Twelve of the stations were located as close as possible to harbor background Stations 1 through 3 and 5 through 13 used during the June 1983 studies (EPA 1984b). These stations duplicated the 1983 survey
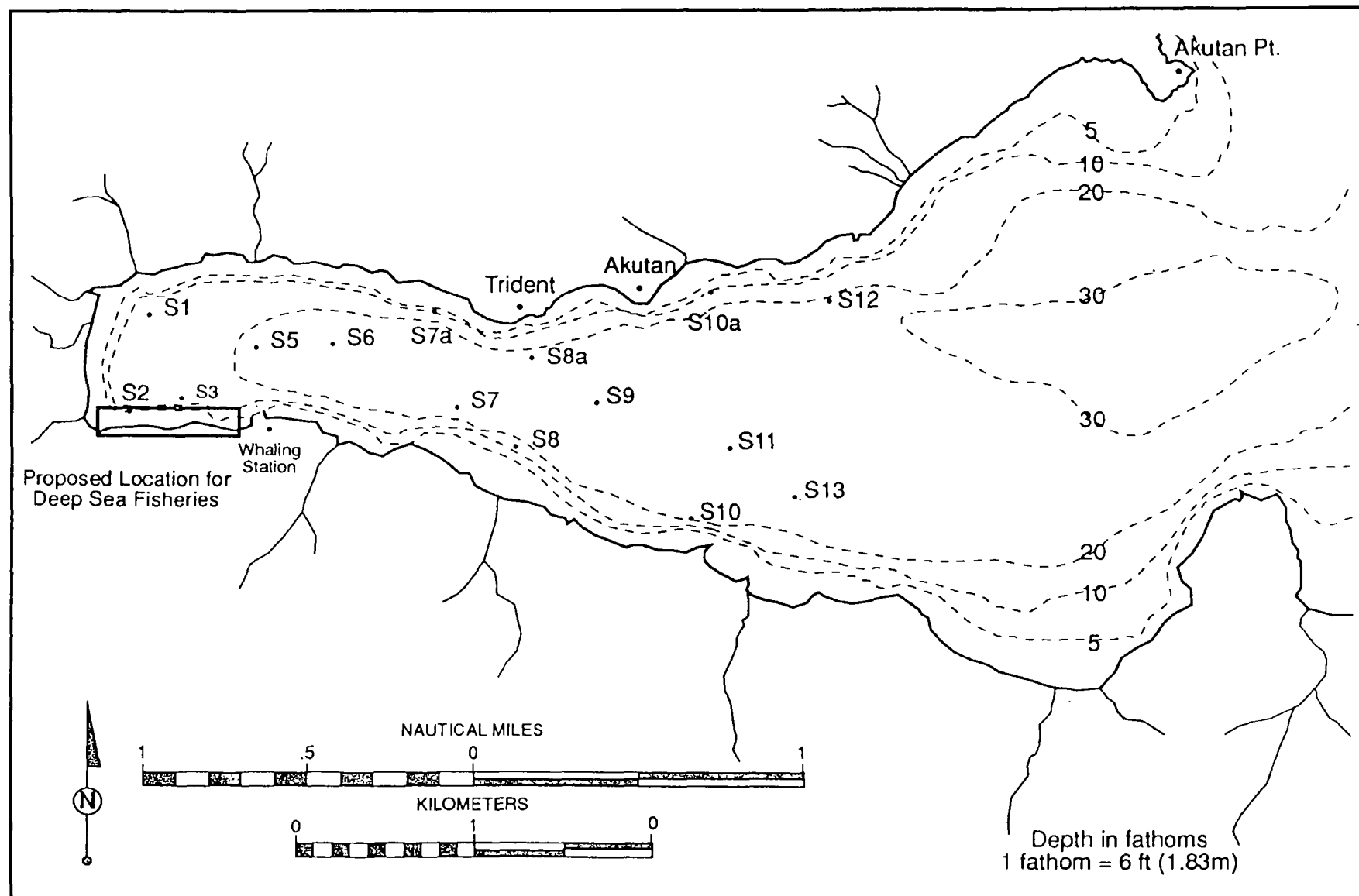
Figure 15. Location of Sediment Sampling Stations in 1992, Akutan Harbor, Alaska

locations in an attempt to provide an accurate comparison with samples collected during earlier studies. Five additional sediment stations were added in 1992; one station east (S-8A) and one station west (S-7A) of the Trident Seafoods facility, one station east of the Akutan city dock (S-10A), and two stations (S-PO3 and S-BPO) near the proposed Deep Sea Fisheries outfall location. The sediment sampling effort concentrated on determining harborwide effects of seafood processing activities on sediments, characterizing sediments underlying areas exposed to discharges from floating seafood processors, and characterizing areas expected to be impacted by crab waste discharges caused by the proposed action. The sampling effort was not specifically concentrated on the existing Trident Seafoods or Deep Sea Fisheries waste piles. The main focus of the sediment surveys was to determine if cumulative impacts have occurred within the inner harbor. However, several samples were collected in the near vicinity of these piles.

All sediment samples were collected using a 0.1 m^2 Van Veen grab. The grabs were subsampled to characterize sediment chemistry, and they were collected as close as possible to samples collected for benthic community analysis. Only samples with at least a 5 in (12 cm) penetration depth and an undisturbed sediment-water interface were retained for analysis. In the field, notes were taken to describe basic substrate character, smell, and presence or absence of seafood waste debris. A subsample of the top 1 in (2 cm) of sediment was collected and analyzed in the laboratory for grain size, total organic carbon (TOC), N-N, TKN, oil and grease, and sulfides. In addition to quantitative samples, approximately 32 qualitative sediment samples were collected with either the Van Veen grab or a 3 in diameter gravity corer (Appendix H). These qualitative samples were inspected in the field, the character (texture, smell, color, presence of seafood waste, or presence of organisms) of the substrates was noted, and the sample was discarded. The locations of the sites were determined with a geographical positioning system (GPS).

Benthic sediment samples collected from the harbor in 1983 (EPA 1984b) and 1992 consisted typically of brown, stiff silts. Sediment chemistry data collected during 1992 are presented in Table 8. Sediments at Station S-7A, the station closest to and directly west of the Trident Seafoods outfall, contained the highest concentrations of TOC, TKN, oil and grease, and sulfides. Sediments collected at Station S-2, the station closest to the M/V Deep Sea, contained the second highest concentrations of these sediment constituents. The concentrations of TOC and sulfide at Station S-7A were nearly double the concentrations at Station S-2, and 3 times and 10 times greater than TOC and sulfide concentrations found at other background stations, respectively. The concentration of oil and grease was more than 8 times greater at Station S-7A than at Station S-2, and nearly 9 times greater than at other background stations (except Station S-6, where concentrations were 5 times less than at Station S-7A). It is apparent from these data that discharges from these two facilities have influenced the sediment chemistry in surrounding areas.

The scope of the April 1992 field studies included opportunistic sampling of sediments in the vicinity of transient floating processors in the harbor. However, when the study team arrived in Akutan, most of the floating processors, with the exception of the M/V Deep Sea and the M/V Clipperton, had either left or were preparing to leave the harbor. The general area where some of the processors operated was known, but specific

Table 8. Sediment Quality Parameters for Akutan Harbor, April 1992

Station	Total Organic Carbon (%)	Total Kjeldahl Nitrogen (μg/g)	Nitrate and Nitrite (μg/g)	Total Oil and Grease (μg/g)	Total Sulfides (mg/kg)
S-1	1.2	960	<0.08	20	55
S-2	1.7	1,400	0.54	48	220
S-3	0.97	1,100	0.26	77	34
S-5	0.92	860	0.16	47	14
S-6	1.2	920	0.22	160	20
S-7	0.74	1,100	<0.05	<5	23
S-7A	3.9	1,900	<0.09	910	570
S-8	0.74	1,100	<0.05	50	27
S-8A	1.7	810	0.18	<5	64
S-9	0.82	1,000	0.15	22	14
S-10	0.82	970	0.08	42	12
S-10A	0.65	580	0.08	35	10
S-11	0.68	950	0.17	110	16
S-12	0.30	550	0.05	33	8
S-13	0.59	450	0.07	90	36
S-PO1	1.2	350	<0.06	35	17
S-PO2	3.8	1,300	1.5	120	18

μg/g = micrograms per gram
mg/kg = milligrams per kilogram

sites could not be identified, and additional quantitative sediment samples were not collected. The M/V Clipperton had been operating at the same location in the harbor for most of the 1991/1992 crab season. The M/V Clipperton had been anchored at the bow and stern, and therefore discharged to the same immediate area throughout the season, similar to the M/V Deep Sea. The closest station to the M/V Clipperton was Station S-6. Sediments from this station contained elevated levels of TOC and oil and grease. However, other indicators of organic pollution such as TKN and sulfides were within the range of other background stations.

The concentration of TOC increased from a mean of 0.21% (June 1983, background station data) to a mean of 0.88% (April 1992, data from Stations 1 to 13). However, September 1983 data for the same background stations were not significantly different from the 1992 observations. The organic carbon enrichment reported in 1983 from the inner harbor background stations was also apparent in 1992. In 1992, the TOC was 1.07% in the inner harbor (Stations 1 to 8) and 0.64% in the outer harbor (Stations 9 to 13).

Sediment quality data were collected at Stations S-BPO and S-PO3 to characterize sediment near the location of the proposed Deep Sea Fisheries outfall site. Sediments from these two stations were quite different in character. Station S-BPO contained substantially higher concentrations of TOC, TKN, and oil and grease. It is possible that the sample at Station S-BPO may have been collected at the site of an old waste pile or an area affected by activities at the whaling station.

Benthic Community Structure. A 0.1 m² Van Veen grab was used to sample benthic invertebrates in Akutan Harbor. The benthic samples were collected as close as possible to the locations of the sediment chemistry samples and the inner harbor sites (Stations 1 through 3 and Stations 5 through 13) sampled in 1983 (Figure 16).

The locations of all stations were determined with a GPS. The benthic invertebrate stations were within 50 to 300 ft (15 to 91 m) of the corresponding sediment sampling stations (with the exception of Station B-5, which was located approximately 500 ft [152 m] from Station S-5). All infaunal samples were washed through 0.2 in (5 mm) and 0.04 in (1 mm) screens to collect organisms. When practical, infaunal organisms collected on the screens were sorted into major taxonomic categories (Polychaeta, Mollusca, Crustacea, Echinodermata, and miscellaneous taxa) in the field, and preserved in a 10% buffered formalin solution.

Infaunal samples were identified to the lowest practical taxonomic level and enumerated by Marine Taxonomic Services. In addition, an outside taxonomic expert (Dr. Jerry Kudenov, University of Alaska) performed the quality assurance/quality control (QA/QC) by recounting 20% of the samples and verifying species identification. Dr. Kudenov also conducted the taxonomic work on polychaetes during the 1983 studies.
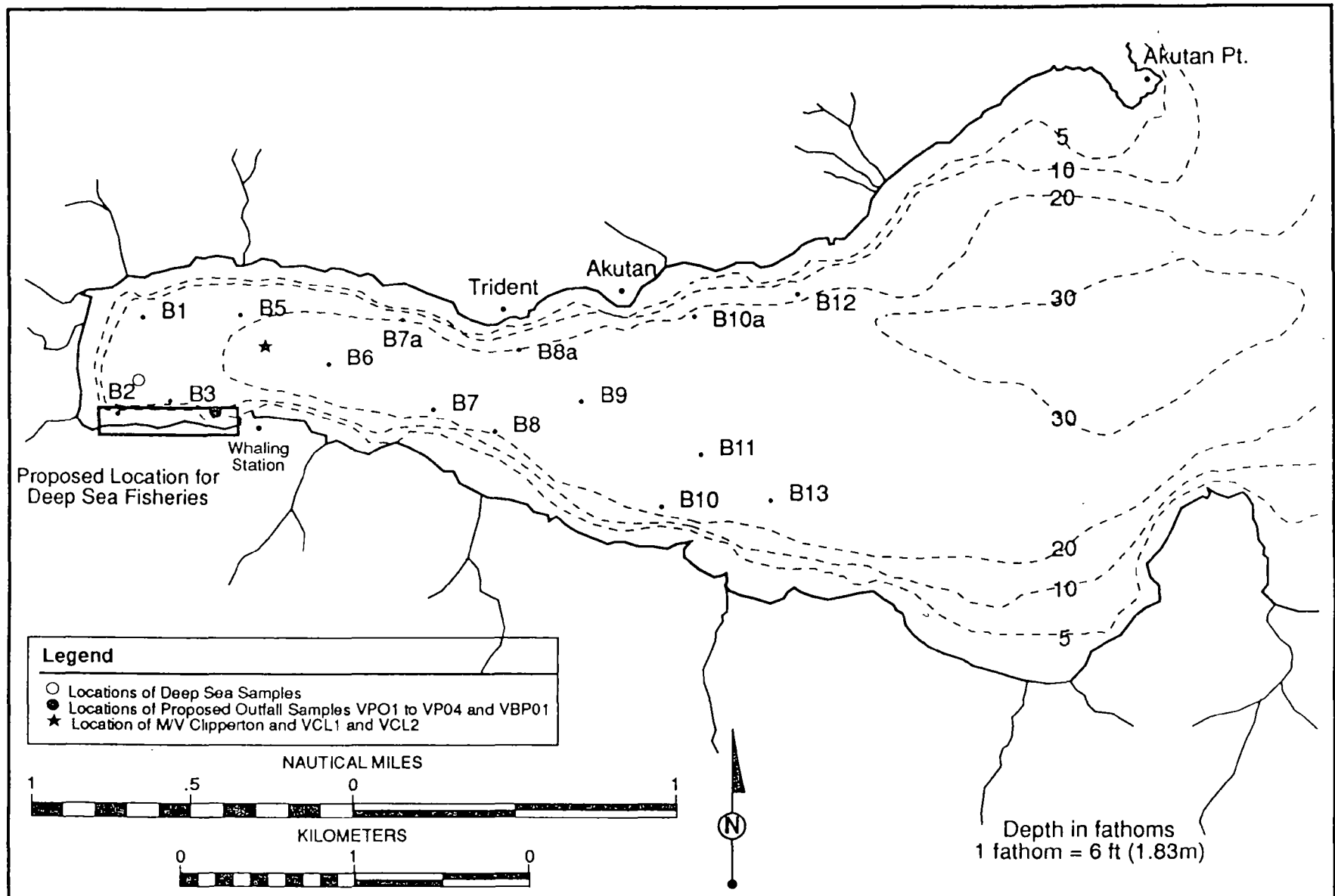
Figure 16. Location of Benthic Biological Community Sampling Stations in 1992, Akutan Harbor, Alaska

The 1992 benthic sampling studies revealed significant changes in the composition, diversity, and abundance of benthic organisms in Akutan Harbor since 1983. The numerically dominant benthic species in 1992 included the lumbrinerid polychaete *Lumbrineris luti*, the sigalionid polychaete *Pholoe minuta*, the ampharetid polychaete *Glyphanostomum* nr. *pallescens*, a capitellid polychaete of the *Capitella capitata* species complex, and the thyasirid bivalve *Axinopsida serricata* (Appendix I). In contrast, a spionid polychaete (*Boccardia* nr. *polybranchia*) was the most numerically abundant organism in the inner harbor benthic community in 1983. Other common species found in 1983 included *Lumbrineris luti*, a scalibregmid polychaete (*Scalibregma inflatum*), and a tellinid bivalve (*Macoma moesta*) (EPA 1984b). The dominant lumbrinerid polychaete found in 1983 was tentatively identified as *Ninoe simpla* in the 1983 survey report (EPA 1984b), but has since been definitely identified as *Lumbrineris luti* (Kudenov pers. comm.).

The abundance, number of species, and diversity of polychaetes in samples increased dramatically between 1983 and 1992 (Table 9). The average number of polychaetes per sample increased from 608/m² in 1983, to an average density of 2,395/m² in 1992 (Figure 17). The average number of species per sample increased from 8.9 in 1983 to 23.5 in 1992. The Shannon-Wiener diversity index (H') increased from an average of 1.214 in 1983 to 2.219 in 1992. The abundance and diversity of benthic organisms at all stations except Stations B-7A and B-PO2 were similar. These two stations were located near the Trident Seafoods outfall and the proposed Deep Sea Fisheries outfall location, respectively, and were represented by two species and only three individuals. However, two other stations located near the proposed outfall (B-PO1 and B-BPO) were similar in terms of abundance and diversity to other background sites in the harbor.

The cause of such a dramatic increase in the abundance and diversity of benthic organisms between 1983 and 1992 cannot be defined with certainty. However, Pearson and Rosenberg (1978) and Pearson et al. (1986) considered fluctuations in organic input to be one of the principal causes of faunal change in nearshore benthic environments. Their work has shown that a succession of benthic macrofaunal species occurs along a gradient of organic enrichment. In areas of high organic enrichment, the populations are composed of rapidly breeding, short-lived and opportunistic species. As enrichment decreases, the fauna shifts toward a more complex group of species adapted to maintaining themselves in a competitive, biologically controlled community.

The changes seen between 1983 and 1992 in Akutan Harbor suggest the benthic community is responding to the harborwide increase in organic loading (described earlier) with increases in species number and densities of benthic fauna. Some of these increases may be attributable to the recruitment of opportunistic species, which were either not present or were present in low numbers in 1983 (for example, *Capitella capitata*). The increased abundance of these species and of *Glyphanostomum* in the inner harbor indicates organic enrichment has had a modifying influence on the benthic community. When enrichment is extreme, such as on the waste piles and surrounding areas of fine particle deposition (see ROV observations, below), benthic diversity and density are greatly reduced. Elsewhere, benthic recruitment and production in the inner harbor appear to be stimulated by organic enrichment, without, as yet, a decline in diversity.

47

Table 9. Shannon-Wiener Diversity Indices (H'), Number of Species, and Number of Individual Polychaetes Found in Akutan Harbor, 1983 and 1992

Station	H' 1983	H' 1992	Number of Species 1983	Number of Species 1992	Number of Individuals 1983	Number of Individuals 1992
Background						
B-1	1.329	2.666	11	34	67	391
B-2	1.020	1.607	10	16	104	199
B-3	1.362	1.626	9	15	66	129
B-5	0.990	2.159	4	26	52	368
B-6	0	2.162	1	17	38	162
B-7	1.279	2.008	9	14	48	62
B-8	1.347	2.294	8	24	73	309
B-9	1.339	2.683	8	26	41	134
B-10	1.445	1.756	14	26	76	258
B-11	1.088	2.580	10	25	63	149
B-12	1.656	2.338	15	37	82	412
B-13	1.708	2.746	8	23	20	301
Proposed Outfall Site						
B-BP0	--	2.230	--	30	--	225
B-PO1	--	2.174	--	31	--	339
B-PO2	--	0	--	2	--	3
Other						
B-7A	--	0	--	2	--	3
B-8A	--	2.028	--	20	--	179
B-10A	--	2.580	--	33	--	251

-- = station not sampled in 1983
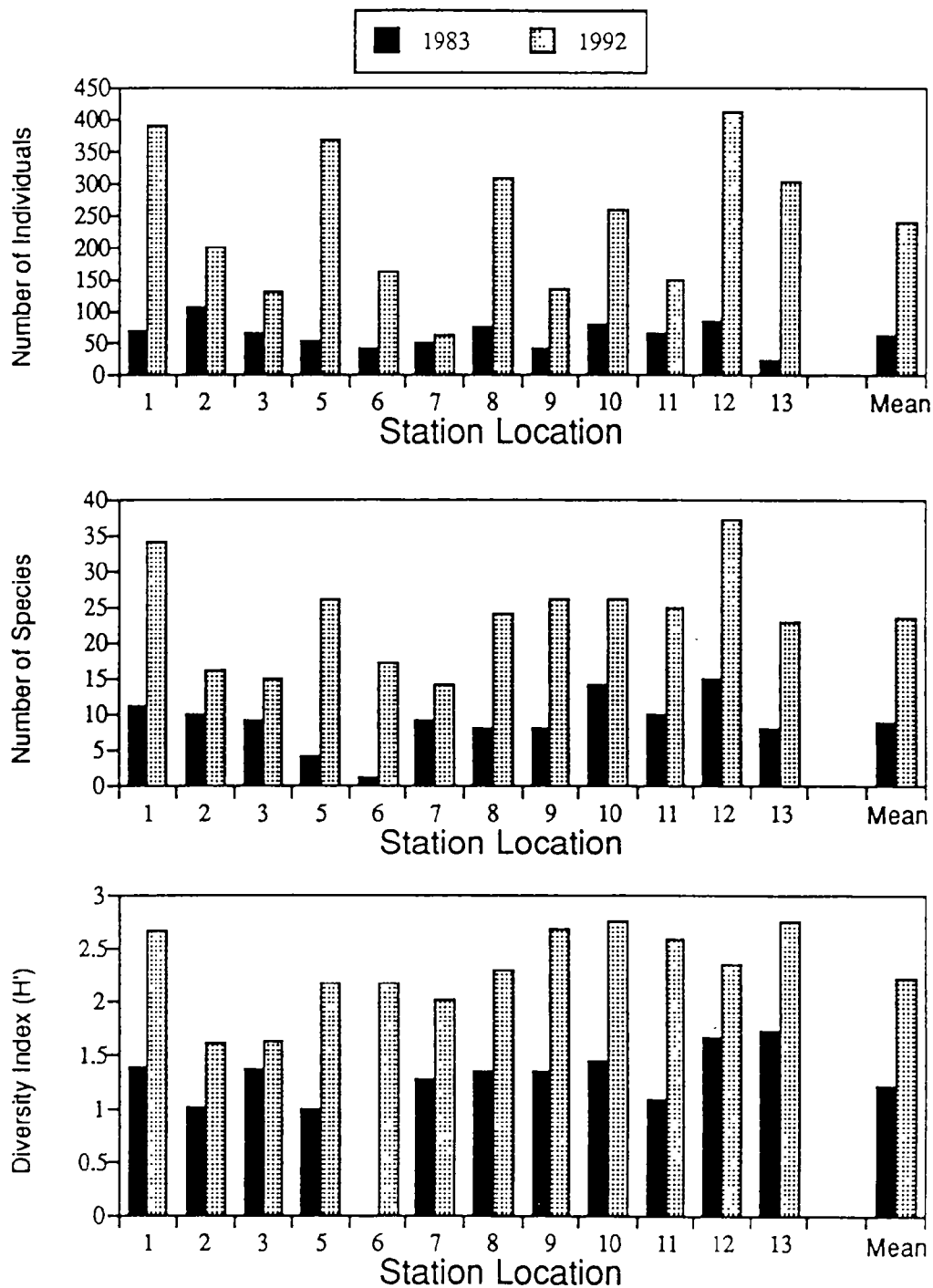
Figure 17. Comparison of Number of Individuals, Number of Species, and Shannon-Wiener Diversity Indices for Polychaetes Found in Akutan Harbor, Alaska

Remotely Operated Vehicle Video Observations. ROV transects were completed at 10 locations in Akutan Harbor (Figure 18). A variety of bottom types and depths were surveyed, ranging from outer harbor, deep water sites with soft sediments (ROV-1) to shallow water sites with crab waste piles (ROV-3 and ROV-7). A detailed summary of the ROV observations is provided in Appendix J.

The ROV surveys were completed using a Deep Ocean Engineering Model Phantom 300, with video observations recorded on 8 mm and VHS format tapes. Also taped were the comments of a narrator on key bottom features, depth, timing, etc. The quality of the underwater video was generally very good and the wide-angle lens of the camera produced sharp color images from a distance of a few inches to 5 to 10 ft (1.5 to 3 m).

Each transect was completed by holding the boat at a fixed location and swimming or "flying" the ROV over a 1 to 10 ft (0.3 to 3 m) wide by 100 to 300 ft (30 to 91 m) long area of the bottom. Initially it was planned to swim the machine over a marked leadline on the bottom. However, a combination of high surface winds, sometimes extremely turbid conditions on the bottom, and burial of the leadline in the sediments made it impossible to follow the line. All transects were subsequently completed by maintaining a fixed compass heading at the ROV and tracking the location of the machine by observing the location of buoys attached to the ROV power cord. More detailed information on video timing and transect coordinates and a qualitative report of the ROV observations are given in Appendix J.

Evidence of human disturbance was visible at all transects. There was scattered crab waste and litter in the outer harbor, with little or no impact on the benthos. Nearshore portions of the inner harbor (i.e., near the whaling station and inshore from the M/V Deep Sea [Stations ROV-3, ROV-4, and ROV-5]) had the most diverse benthic macrofauna, and they were the only areas where any benthic algae were seen. The whaling station transect (ROV-5) was heavily littered with the debris of past commercial and military activities. Localized disruption and elimination of benthic fauna and broader changes to the benthic community were associated with the crab waste piles near the M/V Deep Sea and M/V Clipperton. Fish waste and large-scale discharges of crab waste from the Trident Seafoods processing plant appeared to have the greatest impact on the benthos. These significant effects extended for a considerable distance beyond the immediate area of Trident Seafoods' outfall.

Pelagic and Surface Environments

Akutan Island is located near the center of one of the most productive fishing grounds in the world. Vast resources of demersal fish (e.g., pollock, cod) occur in the southeastern Bering Sea. Salmon, halibut, crab, and shrimp are or have been historically abundant in the nearshore zone. Marine mammals, waterfowl, and pelagic birds are abundant, with large colonies of nesting birds occurring on many of the smaller islands in the region.
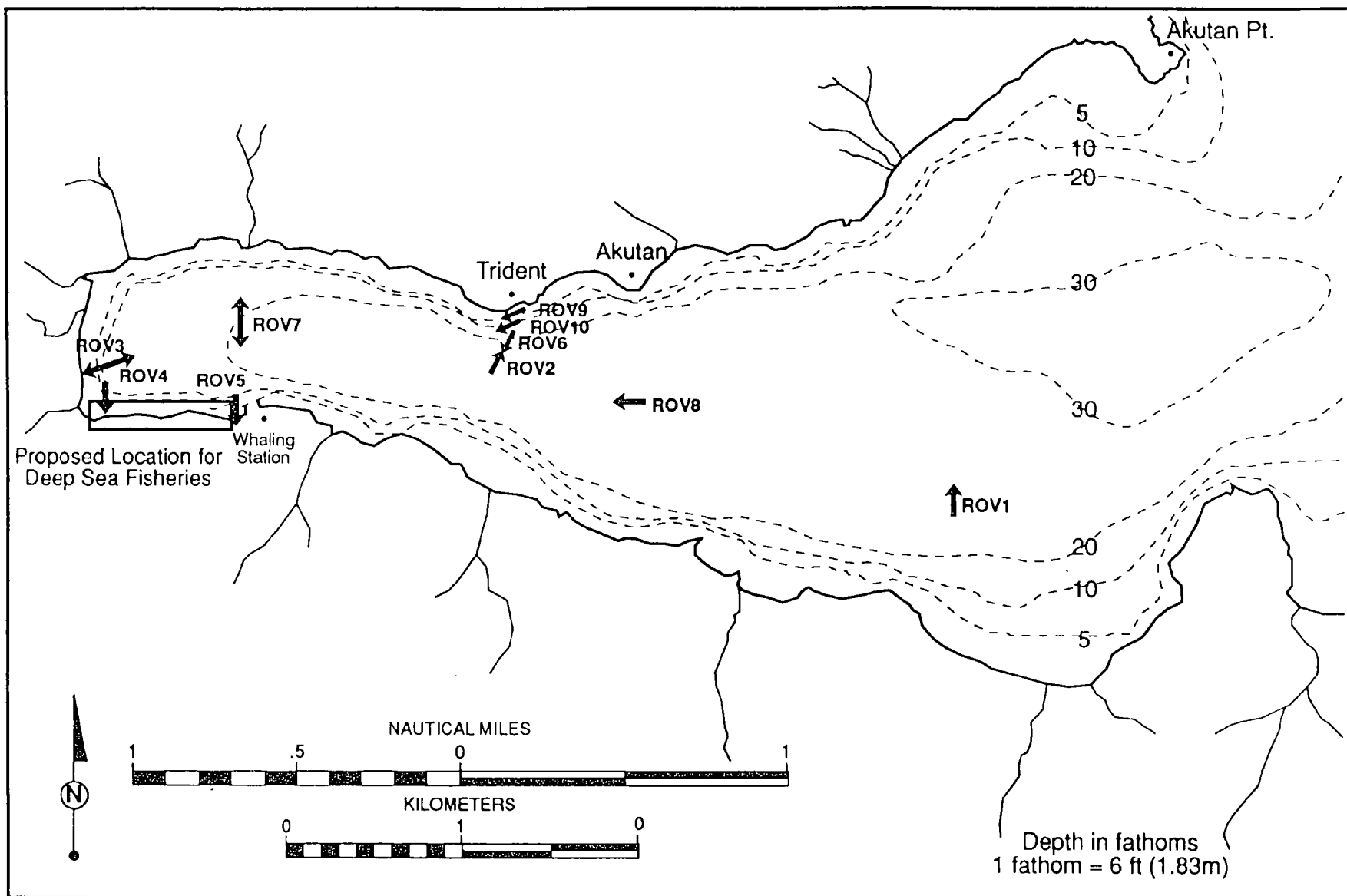
Figure 18. Locations of Remotely Operated Vehicle Survey Transects in 1992, Akutan Harbor, Alaska

The great fisheries of the Bering Sea and Gulf of Alaska, and the biological productivity of Akutan Harbor, stem from the high production of phytoplankton and zooplankton. While sampling for phytoplankton and zooplankton was not included in the 1992 survey, a wide variety of these organisms are known to be seasonally important in the waters surrounding the Aleutian Islands. Upwelling associated with the Alaska Coastal Current and local upwelling produced by water movement through the Aleutian passes play an important role in maintaining phytoplankton production, especially during summer months (Sambrotto and Lorenzen 1987). Zooplankton, which are largely supported by the phytoplankton populations, are dominated by small crustaceans; fish, bivalve, and echinoderm larvae; and jellyfish. These animals are important in the production of adult stocks (i.e., for shrimp and finfish) and serve as forage for fishes, shellfishes, marine birds, and mammals (Cooney 1987).

Fish sampling in Akutan Harbor in 1983 was limited to the shallow littoral zone. During July 1983, juvenile pink salmon (*Oncorhynchus gorbuscha*) and sand lance (*Ammodytes hexapterus*) were the major species captured in beach seines (EPA 1984a). Other fishes included coho salmon (*Oncorhynchus kisutch*), Pacific tomcod (*Microgadus proximus*), flatfishes, sculpins, and Dolly Varden (*Salvelinus malma*). In the deeper areas of the harbor, daubed shanny (*Lumpenus maculatus*) were observed to be abundant by underwater video camera. Based on subsistence harvests, herring (*Clupea harengus pallasi*) and Pacific cod (*Gadus macrocephalus*) inhabit the harbor area. Rock sole (*Lepidopsetta bilineata*), arrowtooth flounder (*Atheresthes stomias*), and pollock are expected to be abundant in the outer harbor.

Marine mammals common in or near Akutan Harbor are primarily harbor seals (*Phoca vitulina*), Steller sea lions (*Eumetopias jubatus*), and sea otters (*Enhydra lutris*). Sea lion haulout areas near Akutan Harbor include an islet off the north coast of Rootok Island; Akun Head on the north shore of Akun Island; and North Head, the shore from Reef Bight to Lava Point, and Cape Morgan on Akutan Island (see Figure 1). Sea otters and sea lions were frequently observed in Akutan Harbor during the 1992 survey.

Intertidal and Shallow Subtidal Environments

The intertidal and nearshore shallow subtidal bottom areas in Akutan Harbor may be impacted by floating or drift materials driven shoreward by waves and winds. These areas were surveyed, in part, by the U.S. Fish and Wildlife Service in July 1983 (U.S. Fish and Wildlife Service 1983). Floating debris, oil, fish waste, and other pollutants have been identified as being of concern to the Akutan community and EPA.

Qualitative epifaunal and semi-quantitative infaunal intertidal and shallow subtidal surveys were performed in Akutan Harbor during an ebbing -0.55 ft (-1.7 m) MLLW tide on April 10, 1992. The surveys were conducted to visually assess physical conditions, habitats, biological communities, and anthropogenic impacts on beach habitats and communities. During the survey, the upper (2 to 4 ft [0.6 to 1.2 m] MLLW) and

middle/lower (0 to 2 ft [0 to 0.6 m] MLLW) intertidal areas were exposed and assessments were made while walking through the study area. Extreme lower intertidal and shallow subtidal areas were surveyed by wading.

Nine survey stations were examined during the 1992 survey (Figure 19). Five stations (Stations IT-1 to IT-5) were located along the southern shore, Station IT-9 was located on the northern shore near the mouth of the harbor, and Stations IT-6 to IT-8 were located along the eastern shore at the head of the harbor. Survey Stations IT-1, IT-2, IT-3, IT-6, IT-8, and IT-9 were beaches located at the mouths of streams. Station IT-4 was located at the site of the abandoned whaling station, which is currently being used as a materials storage area. Station IT-5 was located near the proposed Deep Sea Fisheries site, and Station IT-7 was located at the apex of the harbor.

Infaunal organisms were sampled from beaches containing primarily small substrates (i.e., gravel, sand, and silt). Infaunal samples were collected by randomly placing a 2.7-square-foot (0.25 m^2) quadrat on the ground and using a shovel to excavate the substrate down approximately 1 ft (0.3 m). Excavated substrates were collected and separated from organisms by sieving them through a 0.25 in (6.3 mm) sieve. Areas sampled included upper to middle/lower intertidal areas. Extreme lower intertidal areas were inundated during the survey.

It was noted during previous studies in Akutan Harbor (Crayton pers. comm.) that oil residues were found within the intertidal zone on the sand/gravel beaches at the head of the harbor. Five sediment samples (IT7-A through IT7-E) were collected along the continuous sand/gravel beach that encompasses survey Stations IT-6, IT-7, and IT-8 on April 10, 1992 (Figure 20). Samples were stored in glass jars lined with freon and analyzed for total petroleum hydrocarbons.

In addition to chemical analysis, sediments from each hydrocarbon sample were sieved to determine grain size distribution. Sediments were sorted into three size classes: gravel or larger (>2 mm), sand (0.063 mm to 2 mm), and silt or smaller (<0.063 mm).

Physical Conditions and Habitats

Stations IT-1, IT-6, IT-7, and IT-8 consisted of sand/gravel beaches located at or near the mouths of relatively low gradient streams (Figure 19). Scattered cobbles were also found at Stations IT-1 and IT-6. Stations IT-3, IT-4, and IT-5 contained primarily cobble substrates with some gravel at Station IT-3. Substrates at Stations IT-2 and IT-9 consisted of bedrock and boulders at lower elevations and cobbles and boulders in the upper and middle intertidal zones. Bedrock was also found at Stations IT-1 and IT-8 where the streams had cut against the valley wall. Former channels, now dry, were evident near the mouths of both of these streams.

Beach slopes were very shallow at the head of the harbor, especially at Station IT-6 (1 to 2%), but became progressively steeper toward the most eastern sampling locations. Beach angles were approximately 10% at Stations IT-1 and IT-9.
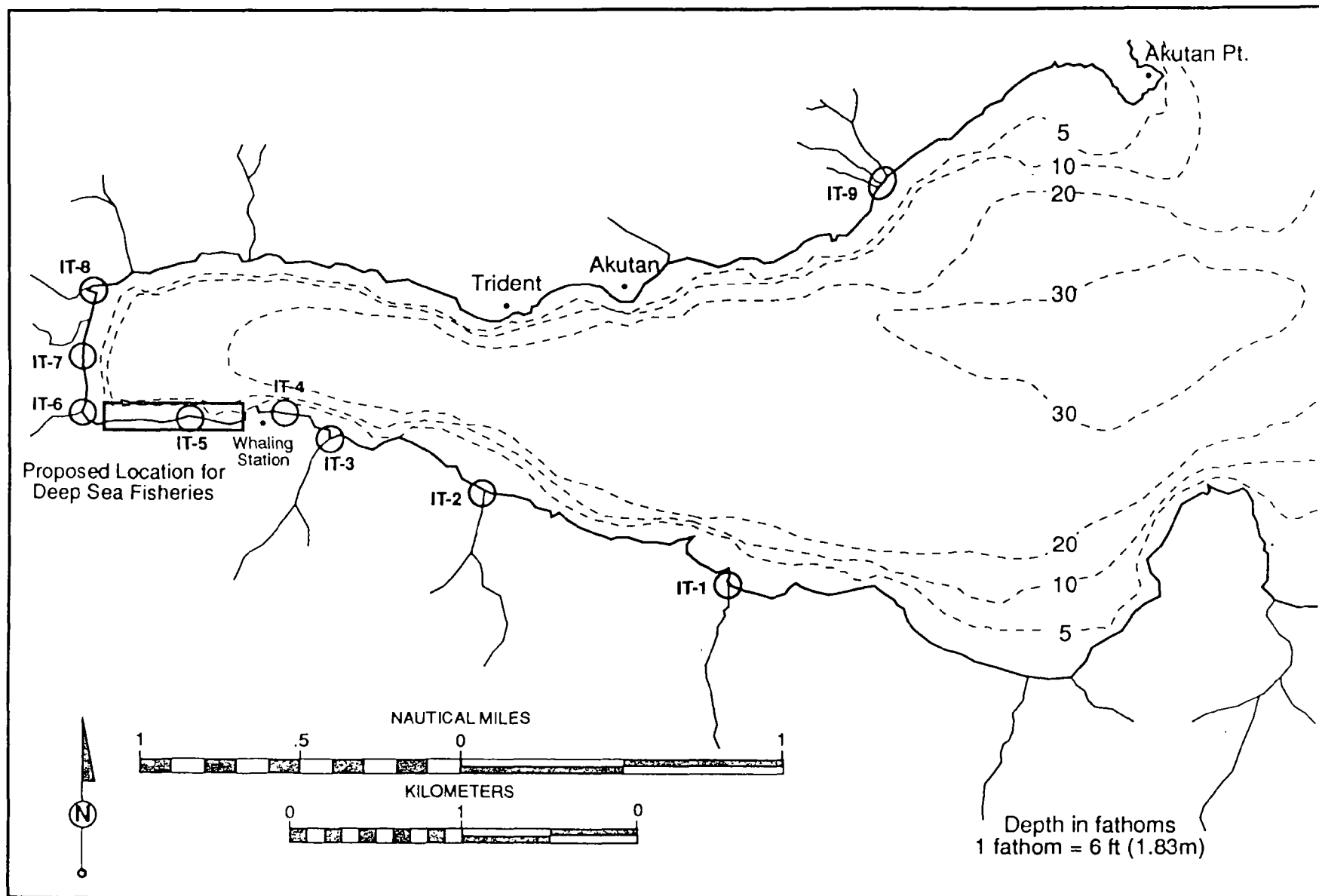
Figure 19. Location of Intertidal and Shallow Subtidal Survey Transects in 1992, Akutan Harbor, Alaska
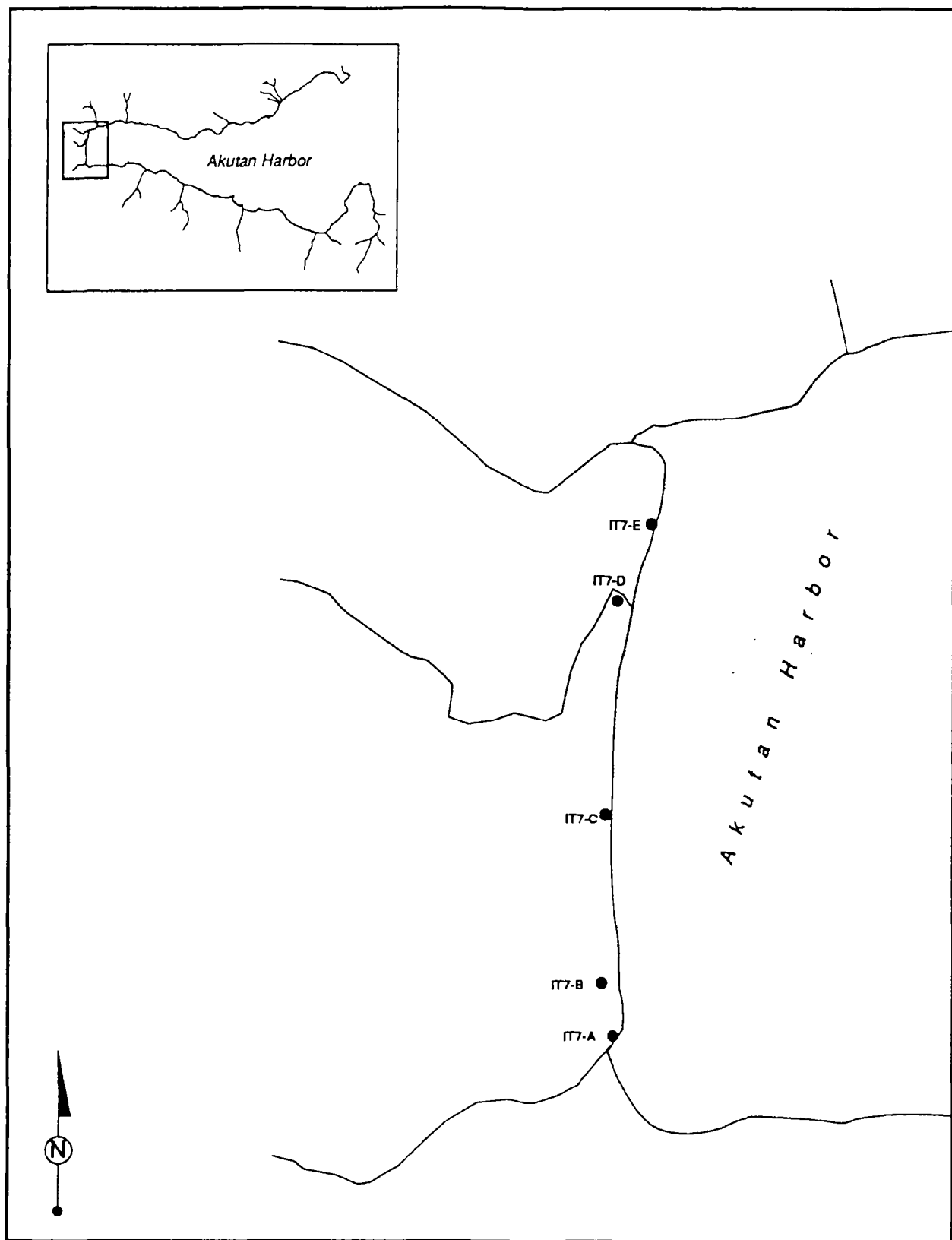
Figure 20. Location of Intertidal Sediment Sampling Stations in 1992, Akutan Harbor, Alaska

The surrounding uplands rapidly gained elevation from most of the sample sites. Upland slopes ranged from approximately 40° to 45° at Stations IT-1 to IT-5. Slopes appeared stable and well vegetated, with native grasses along the southern shoreline, and probably contribute little material to the beaches. The upland at Station IT-4 was the site of the abandoned whaling station and is currently used as a storage area for crab harvesting gear. The site was graded level at approximately +20 ft (+6.1 m) MLLW. The upland slope at Station IT-9 was approximately 80°. A cutbank was formed at the extreme upper supralittoral zone where erosion has occurred, probably during strong winter storms from the south. Above the cutbank, slopes were well vegetated.

Uplands sloped back at gentle gradients from sample stations at the head of the harbor (IT-6 to IT-8). Upland slopes ranged from approximately 2° to 6°. Uplands were well vegetated with low growing shrubs and native grasses at this site.

Sediment grain size analysis from samples taken at Stations IT-6, IT-7, and IT-8 revealed beach sediments to be composed primarily of sand. The sand component of each sample ranged from 60.6 to 85.7% by weight (Table 10). Gravel or larger sized substrates ranged from 8.4 to 34.2% of the weight of each sample. Silt/clay accounted for 1.1 to 7.7% of the sample weight, with the largest portion of the silt/clay group always between 0.033 and 0.063 mm in size.

Epibenthic Communities

Sand/gravel beaches (Stations IT-1, IT-6, IT-7, and IT-8) appeared nearly devoid of epibenthic macroinvertebrates and plants. Station IT-6, however, had a few mussels growing on the cobble-sized rocks scattered on the beach. Beach debris at all stations included crab and shrimp exoskeletons and shell debris. Rocky beaches were much more productive. Dense colonies of brown alga (*Alaria* sp.), to 100% coverage, dominated the upper subtidal/lower intertidal zones. Other brown algae and a green alga (*Ulva* sp.) were also present. Algal density decreased with increased elevation. The extreme upper intertidal zone was inhabited by only occasional filamentous green algae. Mid-intertidal areas were dominated by a mixture of *Fucus* sp. (to 100% coverage) and other brown algae. Red algae were also observed occasionally on rocky beaches.

Yellow encrusting sponges were found ubiquitously in the lower intertidal/shallow subtidal zones on rocky substrates. Other animals inhabiting this zone included juvenile shrimp, mussels, isopods, limpets, snails, and barnacles. Mussels were more abundant in the mid-intertidal zone than in lower zones. Snails, limpets, and barnacles were also found in the mid-intertidal zone in all rocky habitats.

Table 10. Beach Sediment Grain Size Distribution by Percent Weight from
Samples Taken at the Head of Akutan Harbor

Seive Opening (mm)	Sample Station Grain Size Distribution (% retention)				
	IT7-A	IT7-B	IT7-C	IT7-D	IT7-E
4.75	14.0	3.40	5.20	8.30	2.60
4.00	2.00	2.90	3.60	2.40	0.40
2.00	18.2	13.8	22.2	20.6	5.40
1.00	25.7	32.9	30.0	39.3	27.2
0.50	26.6	15.5	18.8	18.3	44.5
0.25	7.60	20.3	15.2	3.60	12.6
0.125	0.50	9.60	3.60	0.30	1.40
0.063	0.20	0.50	<0.1	<0.1	<0.1
0.032	5.00	0.90	1.30	7.10	5.80
0.016	<0.1	<0.1	<0.1	<0.1	<0.1
0.008	<0.1	<0.1	<0.1	<0.1	<0.1
0.004	<0.1	<0.1	<0.1	<0.1	<0.1
0.002	<0.1	<0.1	<0.1	<0.1	<0.1
0.001	<0.1	<0.1	<0.1	<0.1	<0.1
<0.001	<0.1	<0.1	<0.1	<0.1	<0.1

mm = millimeter

Stratification of the mid-intertidal zone was more pronounced at Station IT-4 (the whaling station) than at other stations. This zone was stratified into two distinct communities. The upper mid-intertidal zone was dominated by *Fucus* sp. (to 100% coverage). The lower mid-intertidal zone contained dense beds of mussels that covered approximately 80% of the substrate. Snails and limpets were also found with the mussel colony. In addition, many polychaete worms were found interstitially among the mussels at this site, but were not observed in other intertidal areas surveyed.

Infauna Communities

Infaunal organisms were found at only one of the nine stations sampled. Three juvenile mussels were found after taking two samples at Station IT-6. Samples taken at other locations were barren. It can be speculated that low densities of infaunal organisms were a result of the harsh intertidal environment on the sand/sand-gravel beaches. Substrates are probably alternately degraded and aggraded during and following severe storm events, especially at Station IT-1. A constantly changing beach morphology provides poor habitat for sustained colonization and growth by infaunal organisms.

Station IT-6 appeared to provide the best habitat for infaunal species. Deposition of materials from the stream flowing through the site formed a shallow, sloping alluvial fan. The relatively high silt component (>5% by weight) and freshwater intrusion were conducive to colonization by bivalves. Although sampling at this station revealed a density of 1.5 mussels per sample, habitat conditions warranted a higher abundance of organisms. It is possible that the lack of infaunal organisms at this site was pollution-related. An oily sheen was observed during sampling, and subsequent testing revealed that surficial sediments contain fairly high levels of petroleum hydrocarbons (see Hydrocarbon Analysis, below).

Hydrocarbon Analysis

Total petroleum hydrocarbons in five beach sediment samples collected at the head of the harbor ranged from 47 to 120 micrograms per gram (μg/g) (Figure 20). Samples IT7-B and IT7-D were collected in the upper intertidal zone. Samples IT7-A, IT7-C, and IT7-E were collected in the middle to lower intertidal zones. No background or reference stations were sampled for petroleum hydrocarbons. Distribution of petroleum hydrocarbons among sampling locations did not result in a definable pattern (Table 11). It appeared, however, that petroleum hydrocarbons were more likely to wash ashore at the south and north ends of the beach than at the center. In addition, because of the close proximity of Sample IT7-D to IT7-E and the higher petroleum hydrocarbon concentration found in the former, it could be hypothesized that petroleum hydrocarbons are continually lifted out of lower intertidal sections of the beach and transported higher in the intertidal zone, resulting in higher levels therein.

Table 11. Total Petroleum Hydrocarbon Levels Found
at Intertidal Sediment Sampling Stations
in 1992, Akutan Harbor, Alaska

Station Number	Total Petroleum Hydrocarbon (μg/g)
IT7-A	93
IT7-B	75
IT7-C	47
IT7-D	120
IT7-E	73

μg/g = micrograms per gram

Freshwater Environments

Discharge levels of six streams entering Akutan Harbor were measured with a Marsh-McBirney Model 201D electromagnetic flow meter on April 9 and 11, 1992 (Figure 21).

All freshwater streams flowing into the harbor were small. Stream discharge levels ranged from approximately 0.012 to 2.63 cubic feet per second (cfs), or 0.0004 to 0.08 cubic meter per second (m^3/s). The discharge within each stream and the relative discharge levels between streams were quite different from previous measurements taken in July 1983 (EPA 1984b). The largest stream, draining to the northwest corner of the head of the harbor (Stream 4), had an estimated flow of 27 cfs (0.8 m^3/s) in June 1983. Most of the upland areas were covered with snow during the 1992 survey, resulting in a much lower discharge pattern than previously measured.

There are 15 streams which empty to Akutan Harbor. Of these, only one stream is known to support fish. The stream at the northwest corner of the harbor (Stream 4) is cataloged by the Alaska Department of Fish and Game as an anadromous fish stream. The stream is small, with a base flow at the time of the survey of 2 cfs, and highly sinuous. In August 1982, approximately 10,500 adult pink salmon were observed in the stream (EPA 1984a). Coho salmon and Dolly Varden are also reported to spawn in the stream. Based on pre-emergence studies in the Shumagin Islands, pink salmon fry probably begin to emerge from the gravel and enter the harbor in early April. Pink salmon may also spawn in the stream at the southeast corner of the harbor (Stream 2); however, pink salmon use of Stream 2 is unconfirmed.

Terrestrial Environments

Soils

Akutan Island is volcanic in origin, and the soils in the vicinity of the proposed facilities are derived from weathered volcanic rock and ash. The slopes above the proposed Deep Sea Fisheries site are primarily exposed rock or reddish, sandy soil deeply incised by small, swift streams.

Vegetation

Akutan Island is treeless. The valley at the head of the fjord is occupied by tundra and riparian vegetation. Vegetation in the vicinity of the proposed Deep Sea Fisheries site is composed of a thick mat of heath (*Ericaceae* sp.) or dry tundra. Wetland vegetation is not present on the proposed site.
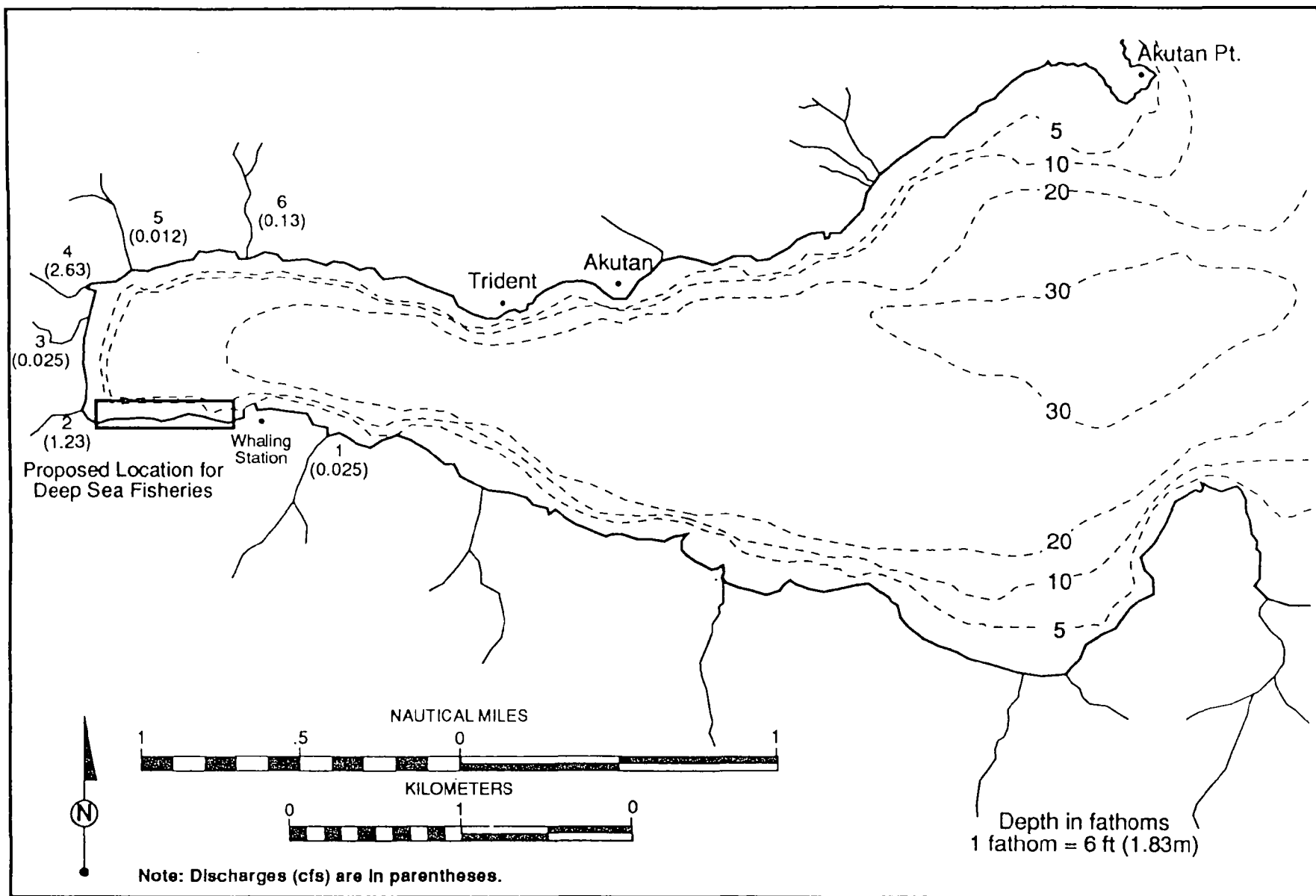
Figure 21. Location of Stream Flow Measurement Stations and Associated Discharge Levels Found in April 1992, Akutan Harbor, Alaska

Akutan Pt.

5
10
20

Trident   Akutan

30

3
(0.025)

30

4
(2.63)

5
(0.012)

6
(0.13)

2
(1.23)

Whaling
Station

1
(0.025)

Proposed Location for
Deep Sea Fisheries

20
10
5

NAUTICAL MILES

1   .5   0   1

KILOMETERS

0   1   0

Depth in fathoms
1 fathom = 6 ft (1.83m)

N

Note: Discharges (cfs) are in parentheses.

61

Wildlife

Wildlife on the island is composed primarily of birds and small mammals (e.g., voles, shrews, and foxes). Wildlife most commonly observed on Akutan Island includes eagles, ptarmigans, various songbird species, and foxes (City of Akutan 1982).

Approximately 50% of the Alaskan population of whiskered auklet (*Aethia pygmaea*) and about 45% of the Alaskan population of tufted puffin (*Fratercula cirrhata*) occur in the Fox Island group. No major nesting colonies are located along the shores of Akutan Harbor, but a small nesting colony of cormorants (*Phalacrocorax* spp.) and tufted puffins occupies Akutan Point, and a high-density tufted puffin colony occurs on "North Island" in Akun Strait.

Threatened and Endangered Species

The two listed bird species that occur in the Aleutian Islands are the threatened Aleutian Canada goose (*Branta canadensis leucopareia*) and the endangered short-tailed albatross (*Diomeda albatross*) (Anderson pers. comm.). The Aleutian Canada goose nests in the Aleutian Islands, but sightings east of the Islands of the Four Mountains are not common, and migrations do not appear to occur in the vicinity of Akutan. The short-tailed albatross has been making a slow comeback, but sightings have been primarily in the western Aleutians (U.S. Department of Interior 1985). Bald eagles (*Haliaeetus leucocephalus*) are common on Akutan Island and reportedly nest near Akutan Point (Crayton 1983). This species, however, is not designated as an endangered species in Alaska. Nonmigratory Peale's peregrine falcons (*Falco peregrinus pealei*) are relatively abundant in the Aleutian Islands, but this subspecies is not considered endangered.

Steller sea lions (*Eumetopias jubatus*), a species listed as threatened under the Endangered Species Act, are common in the harbor and surrounding waters (Smith pers. comm.). During the surveys in 1992, sea lions were observed in the harbor, but no haulout areas were noted. Harbor seals (*Phoca vitulina*) are also present in the harbor, but they are not presently listed as threatened or endangered.

Large numbers of sea otters (*Enhydra lutris*) were observed feeding on crab in Akutan Harbor during the April 1992 studies. Sea otters, however, are not considered threatened or endangered in Alaska.

The bowhead whale (*Balaena mysticetus*), right whale (*Balaena glacialis*), fin whale (*Balaenoptera physalus*), sei whale (*Balaenoptera borealis*), blue whale (*Balaenoptera musculus*), humpback whale (*Megaptera novaeangliae*), gray whale (*Eschrichtius robustus*), and sperm whale (*Physeter macrocephalus*) are listed as endangered species and may occur in the region. With the possible exception of the gray and humpback whales, most of these species are typically found offshore, and therefore are not likely to be found in Akutan Harbor. Gray whale migration corridors generally are found in more easterly passages through the

Aleutian Islands. Both gray and humpback whales may remain in the vicinity of Akutan Harbor throughout the summer, but they are unlikely to enter the harbor.

Thus, the only threatened or endangered species expected to be found in the vicinity of the proposed Deep Sea Fisheries site is the Steller sea lion.

Land Use

In 1878/1879, several Aleut families and groups moved from other islands in the area and established the community of Akutan. The community occupies approximately 5.5 acres (2.2 hectares) of relatively flat land lying between the harbor and steep slopes along the northern shore. In response to rapid expansion of the seafood processing industry's use of Akutan Harbor, the village of Akutan was incorporated as a second class city in late 1979.

In 1912, the Pacific Whaling Company built a processing station near the head of the harbor along the southern shore and operated it until 1942. The gently rising slopes on which the station stood are now used by fishermen for storage of crab pots during the off-season. A small marine bench, located across the harbor from the Trident Seafoods plant, is also used to store crab pots.

Floating seafood processors began using Akutan Harbor in the late 1940s. Permanent mooring buoys are located in the inner harbor. The M/V Deep Sea has been permanently moored in the southwest corner of the harbor for over a decade. In 1981, Trident Seafoods began construction of a shore-based seafood processing facility on its present site, about 0.5 mile (0.8 km) west of the community of Akutan. The present site is privately owned and leased to Trident Seafoods.

Approximately 50 acres (20 hectares) of lowlands at the head of the harbor are under the city's jurisdiction. These lowlands are approximately 2 miles (3.2 km) west of the City of Akutan and immediately adjacent to the proposed facility site. The city's 1982 comprehensive plan designated this area for future community growth and development. Currently, the head of the harbor is accessible only by skiff, by foot over rough, steep terrain, or along exposed beachline at low tide. Development of the proposed Deep Sea Fisheries facility would allow immediate access to this area.

A seaplane ramp was recently constructed west of the City of Akutan. The community has also recently replaced the city dock.

The site for the Deep Sea Fisheries facilities would be leased from the Akutan Village Corporation. Construction and operation of the proposed facilities would not result in significant change to allowable land use.

63

Socioeconomics

The municipal boundary of Akutan includes the Aleut Native community that inhabits the village and the transient workers associated with the seafood processing industry. Of the latter, workers at the Trident Seafoods facility and the M/V Deep Sea are the least transient. Historically, the policy has been to discourage frequent social interaction between the two communities (City of Akutan 1982).

Between 1890 and 1980, the population of the City of Akutan has ranged from 60 to 107, indicating a fairly stable community. The 1980 census showed 17 households in Akutan and a population of 69 (City of Akutan 1982). A population of 589 was reported in 1992 (Alaska Municipal League 1992). This figure included the seasonal work force at Trident Seafoods. The economy of the community is mixed cash and subsistence; incomes are derived from work on seafood processors and fishing vessels and indirectly from a fish tax assessed by the city on business in the harbor.

Public Services

Primary and secondary education for the residents of the City of Akutan is funded by the State of Alaska. The city and the state (through the Aleutian Pribilof Island Association) fund a full-time village public safety officer. Alascom provides phone service for general public use, and federal funds support infrequent visits by a physician from the Alaska Native Hospital. The traditional council method of government has existed in Akutan since the community was established.

Archaeological and Cultural Resources

Although few archaeological surveys have occurred near Akutan Harbor, seven historic sites and an apparent prehistoric site have been identified (Lobdell pers. comm.). These include several village sites, the Russian Orthodox church, and the shore-based whaling station. The Trident Seafoods facility has occupied and modified essentially all available flat land on the marine terrace on which it is located. The existing topography at the proposed Deep Sea Fisheries site is located in an area with steep slopes which were historically less habitable than other areas in the harbor. Thus, undisturbed archaeological or historical resources are not expected to be encountered on the proposed Deep Sea Fisheries site.

ENVIRONMENTAL EFFECTS OF THE PROPOSED ACTION

The Deep Sea Fisheries shore-based facilities proposal includes the construction and operation of crab and finfish processing facilities, a fish meal plant, cold storage, dry storage, and fuel docks. Support facilities would include a powerhouse, maintenance shop, incinerator, gear storage, ship stores, offices, housing, and recreation and food service facilities. The facilities will be built in phases. The crab processing line is expected to be operational by the 1993/1994 crabbing season. Other facilities are expected to be completed and operational in an additional 1 to 2 years.

The construction of the facility will necessitate a 672,000-cubic-yard excavation of a previously undisturbed site and filling approximately 18 acres of previously undisturbed intertidal and subtidal habitats. The operation of the facility will include the discharge of crab and finfish processing wastewater, solid waste from crab processing, stickwater and scrubber water from the fish meal plant, bailwater, sanitary wastewater, and stormwater.

Potential construction phase and operational impacts of the proposed action on the environment are discussed below.

Construction Phase Impacts

Air Quality and Noise

During the construction of the facility, heavy construction equipment will be operating in the harbor. Operation of this equipment could temporarily impact air quality in the harbor; however, because of the prevailing winds in the area and the temporary nature of the work, these impacts are considered to be less than significant.

Some blasting will be required to regrade the slopes. A light concussion will occur, and a short-term, high level of dust may occur after each blast. An experienced explosives specialist will be retained to perform the blasting and to minimize hazards. In addition, Deep Sea Fisheries is required under the U.S. Army Corps of Engineers (Corps) Section 404 Permit to prepare a blasting plan to ensure no disturbance occurs to bald eagles or marine mammals. The effects of blasting are not expected to be significant outside the immediate construction area.

Water Quality

The construction of the facility will involve filling approximately 18 acres of intertidal and subtidal areas. Turbidity associated with filling operations and runoff from exposed slopes could cause significant temporary impacts on the water quality in the head of the

harbor. However, Deep Sea Fisheries will employ proper construction and stormwater control methods to minimize turbidity impacts on Akutan Harbor, and no significant water quality impacts are anticipated.

Deep Sea Fisheries' Corps 404 Permit stipulates the following additional mitigation measures to minimize construction impacts on water quality:

- A silt curtain or similar device must be installed between the riprap dike and the mainland during fill placement to trap silt-laden water.

- All water containing silts as a result of upland construction activities must be collected and filtered or the silts allowed to settle prior to its discharge to marine waters.

- If overburden is to be buried within the fill area, it must be encapsulated within a filter fiber liner. Bedding material consisting of smooth gravel or sand must be placed between the rock fill and the filter fabric to maintain the integrity of the fabric.

In addition, Deep Sea Fisheries will be required to obtain an NPDES general permit for stormwater discharges during the construction phase, which stipulates the preparation and implementation of a stormwater pollution prevention plan.

Heightened vessel activity in the inner harbor, and the presence of construction equipment, would increase the potential for fuel spills in the harbor. To mitigate this potential, stipulations to Deep Sea Fisheries' Corps 404 Permit require that:

- All fuels, petroleum, and other toxic products stored onsite shall be stored so as to prevent a spill from entering any ground or surface waters. Any spills shall be promptly and appropriately mopped up.

- Absorbent materials in sufficient quantity to handle operational spills shall be on hand at all times for use in the event of a spill.

Marine Pelagic Environments

Short-term impacts on salmon could occur during the construction phase of the project. Increased turbidity could affect the health of salmonids and their food supply during the construction phase. Assuming that proper methods are used to contain fine sediments (Corps 404 Permit stipulations) during the filling operation, and appropriate construction windows are used (no construction during periods of juvenile outmigration), impacts on salmonids should be less than significant.

Construction of the facility will significantly alter the shoreline in the vicinity of the salmon stream at the head of the harbor. However, the placement of riprap and piers should provide juvenile salmon with cover during outmigration periods and should not

impair the movement of adult salmon returning to the stream to spawn. In addition, partial mitigation for the loss of habitat was included in the Corps 404 Permit. Mitigation included the enhancement of the salmon-bearing stream (Stream 4) at the head of the harbor.

Intertidal Environments

A total of approximately 18 acres of natural intertidal and subtidal habitats will be eliminated by the planned filling activity in the harbor. Mitigation for unavoidable adverse impacts on intertidal and subtidal habitats has been addressed in Deep Sea Fisheries' Corps 404 Permit, which has authorized Deep Sea Fisheries to proceed with the construction of the facility. Negotiation between Deep Sea Fisheries and the Corps led to changes in the facility design to minimize impacts where possible. This included reduction in sheet pile construction and placement of riprap slopes under the slips and around the facility to provide rocky habitat and cover for fish. Mitigation stipulations in the Corps 404 Permit included monetary and in-kind contributions totaling $100,000 for both water quality studies and a stream enhancement project in the harbor.

Sedimentation associated with filling activities could impact surrounding benthic habitats. However, these impacts would be less than significant because of requirements to minimize turbidity.

Terrestrial Environments

Construction of the facility will include blasting and excavating 672,000 cubic yards of earth from the hillside. This would impact approximately 5 acres of terrestrial habitat. The existing slope is vegetated, but provides little habitat for wildlife. The loss of this area is not considered significant.

Noise and activity associated with the construction of the facility could temporarily cause terrestrial and avian wildlife to move from the inner harbor. This impact is considered temporary and less than significant. Because of the ongoing processing activities in the harbor, the wildlife appear tolerant of high levels of human activity.

Operational Impacts

The following section describes potential impacts which would be attributable solely to operation of the proposed Deep Sea Fisheries shore-based seafood processing plant. The potential for Deep Sea Fisheries to add to cumulative impacts in the harbor is discussed in the Cumulative Impacts Section.

Air Quality and Noise

Deep Sea Fisheries is proposing to install and operate a total of four approximately 2,000 kW diesel generators to provide power to the facility. Boilers, fueled by fish oil (process by-product) and diesel fuel, will be operated as part of the fish meal production plant. The facilities will include an incinerator to burn waste oil and combustible refuse, and various types of machinery will load and unload vessels and move equipment and materials on and around the site.

Some deterioration of air quality is likely in the vicinity of Deep Sea Fisheries; however, because of the prevailing winds in the area, the impacts are not expected to be significant. Deep Sea Fisheries will, however, be required to conduct air quality modeling of emissions prior to attaining permits from the Alaska Department of Environmental Conservation, to ensure compliance with state air quality regulations.

Noise emissions from the generators and other fixed machinery, including refrigeration equipment, will be limited with mufflers in conformance with state and federal regulations, and equipment will be enclosed.

Water Quality

Wastewater Discharges. Under the proposed action, several waste streams will be discharged from the facility to Akutan Harbor. These include solid wastes from crab processing operations; liquid wastes from crab and finfish processing; bailwater; stickwater and scrubber water from the fish meal plant; sanitary wastewater; and stormwater. Deep Sea Fisheries proposes to discharge all wastes through a single outfall (primary discharge), except stormwater and bailwater. Stormwater will be discharged through two separate surface outfalls located on either side of the facility. Bailwater will be discharged from a surface outfall on the dock.

Based on the projected production schedule of the proposed facility (see Table 2), there are two operational periods which warrant evaluation. During the winter, Deep Sea Fisheries will primarily process crab and pollock with smaller amounts of cod. During the summer, the facility will process pollock and smaller quantities of salmon, halibut, and cod. Seasonal differences in harbor conditions and biotic production in the harbor warrant the evaluation of both periods.

Discharges common to both periods are stormwater and bailwater. Because fish are transported by pump directly inside the processing building, stormwater should exert relatively little biological oxygen demand (BOD). BOD_5 loading of bailwater is expected to consist primarily of fish feces and urine, mucus, scales, and small quantities of tissue fluids. If bailwater is discharged at the water surface during unloading, it would be expected to rapidly aerate, dilute, and disperse the organic load. Surface foam can be created by these bailwater discharges; however, this can be mitigated by discharging beneath the water surface. Windy conditions in the harbor are also expected to maintain oxygen concentrations in the surface waters. Water quality impacts from the discharge of bailwater

68

are not expected to be significant. However, a zone of deposit will likely be formed below the outfall. If Deep Sea Fisheries opts to shunt bailwater to the outfall, any potential impact at the waterfront would be eliminated. However, shunting bailwater to the outfall would contribute solids, oil and grease, and BOD to the primary discharge (see Alternatives Section).

Winter Discharge Scenario. The greatest volumes of waste will be discharged during the winter, when Deep Sea Fisheries proposes to discharge crab, pollock, and fish meal processing wastes from the facility simultaneously. The quantities of wastes discharged for the maximum-rated capacity scenario are based on the facilities' maximum-rated daily processing capacity for crab (110 t; 100 mt round weight) and pollock (446 t; 405 mt round weight) (Table 1). This case also assumes that the fish meal plant is operating at maximum-rated capacity (331 t; 300 mt raw input). Based on these conditions, the daily volume of the primary discharge would be 9,801,333 gal (37,103,974 l), including sanitary discharges. The total BOD_5 loading to the inner harbor from the primary discharge would be 35,964 lbs (16,313 kg) per day (439 mg/l). Bailwater, a secondary surface discharge, would also contribute 167,400 gal (663,678 l) of water and 7,150 lbs (3,243 kg) of BOD_5 per day. Thus, Deep Sea Fisheries' total BOD_5 loading to the inner harbor for the winter scenario would be 43,114 lbs (19,556 kg) per day. These calculations assume that stormwater discharges contain relatively insignificant amounts of BOD_5.

To determine the potential for water quality impacts of discharges associated with Deep Sea Fisheries, the Updated Merge (UM) model (Baumgartner et al. 1992) was used to estimate near-field dilution (initial dilution), trapping depth, and far-field dilution of effluent parameters. The focus of this modeling effort was to determine the potential effects of effluent BOD on ambient dissolved oxygen, and to apply the results to Alaska state water quality standards as a measure of impact significance. It is assumed in this analysis that the plant is operating at its maximum-rated capacity (Table 1).

This modeling effort was conducted conservatively. Table 12 describes the assumptions used to model winter discharges. The model assumes that all solids remain entrained throughout the simulation. In reality, the bulk of the solids likely settle out of the effluent plume rather rapidly. The model, therefore, gives the most conservative estimate of BOD_5 contained in the effluent after initial dilution. The following equation (Mills et al. 1985) is used to determine the resulting dissolved oxygen (DO) concentration of the effluent plume after initial dilution:

$$DO_f = \overline{DO_a} + \left[\frac{DO_e - IDOD - \overline{DO_a}}{S_a} \right]$$

where

DO_f = final DO concentration (mg/l) of receiving water at the plume's trapping level;

DO_a = average ambient DO concentration (mg/l), diffuser depth to the trapping depth;

69

Table 12. Assumptions Used to Model Winter Discharges from
Deep Sea Fisheries' Proposed Outfall

Parameter	Assumption
Effluent	
Flow	9.8 MGD
BOD_5 concentration	439 mg/l
DO content	0 mg/l
BOD decay rate	0
Density	1.030 g/cm^3
Outfall	
Depth above bottom	20 ft (6.1 m)
Depth below surface	80 ft (24.4 m)
Vertical angle	90°
Diameter	12 in (0.305 m)
Receiving Waters	
Stratification	none
DO concentration (surface)	13.4 mg/l
DO concentration (outfall depth)	11.9 mg/l
Average DO concentration (outfall to surface)	12.6 mg/l
Temperature (surface)	4°C
Temperature (outfall depth)	2.5°C
Currents (surface)	0.1 m/s
Currents (outfall depth)	0.05 m/s
Density (surface)	1.021 g/cm^3
Density (outfall depth)	1.022 g/cm^3

DO_c = DO of effluent (mg/l);
$\underline{IDOD}$ = immediate DO demand (mg/l); and
S_a = initial dilution.

The immediate dissolved oxygen demand (IDOD) represents the oxygen demand of reduced substances which are rapidly oxidized during initial dilution. The IDODs of stickwater and crab and fish waste are not known. As a conservative approach, this analysis will use 10% and 20% of the effluent BOD_5 as values for IDOD. For the winter analysis, this would equate to IDODs of 43.9 and 87.8 mg/l. The model simulation also assumes that the effluent contains no DO.

Appendix K contains the modeling results. Table K-1 contains the result of the UM model simulation for the winter discharge conditions. The results indicate that initial dilution of the plume would occur at an overlap depth of 9.7 m, and at that depth the plume would be diluted approximately 26:1. The resulting plume centerline concentration of BOD_5 at the overlap depth would be 16.9 mg/l. Based on the previous equation (IDOD = 43.9 and 87.8 mg/l), the receiving water DO within the plume at the overlap depth would be approximately:

$$12.65 + ([0 - 43.9 - 12.65]/26.17) = 10.5 \text{ mg/l}$$

or

$$12.65 + ([0 - 87.8 - 12.65]/26.17) = 8.9 \text{ mg/l}.$$

The far-field models indicate that, once the effluent reached the overlap depth, the BOD_5 concentration would dilute rapidly to less than 6 mg/l within 2 hr. Based on these simulations, it does not appear that winter discharges from Deep Sea Fisheries' proposed outfall would violate Alaska state water quality standards for DO (which state that DO shall be greater than or equal to 6 mg/l) when the facility is operating at its maximum-rated capacity. Significant impacts on water quality during winter conditions are not anticipated based on this modeling effort.

It is possible that the wastes generated by the Deep Sea Fisheries fish processing facility could exceed the maximum-rated capacity of the fish meal plant. If this were to occur, Deep Sea Fisheries would be required to increase the capacity of its meal plant or obtain an ocean dumping permit to dispose of excess solid wastes. If Deep Sea Fisheries' meal plant can process quantities in excess of its maximum-rated capacity, additional wastes generated would be discharged through the proposed outfall. To evaluate this possibility, it was assumed that Deep Sea Fisheries was operating at a level equivalent to production levels projected for February in Table 2 (124 t [113 mt] of crab and 490 t [444 mt] of pollock per day). This is considered the maximum seasonal production for winter. Assuming that there would need to be a proportional increase in water usage, the BOD_5 concentration of the effluent discharged from the outfall would be the same as the maximum-rated capacity scenario, 439 mg/l. However, the volume and resulting discharge velocities would increase slightly. Results of outfall modeling are presented in Table K-2. Results indicate that the dilution at the overlap depth would be 28:1, slightly greater than that resulting from the operation scenario presented above. This analysis indicates that the additional BOD loading incurred from operating the fish plant at the maximum seasonal

71

production levels presented in Table 2 would not create additional impacts on water quality in the winter. Even though total BOD$_5$ loading is higher for this second case, the velocity associated with increased volumes would allow greater dilution at the overlap depth.

Summer Discharge Scenario. During the summer months, Deep Sea Fisheries proposes to discharge pollock and fish meal processing wastes from the facility simultaneously. The quantity of wastes discharged at the maximum-rated capacity is based on the facilities' maximum-rated daily capacity for pollock (446 t; 405 mt round weight) and assumes that the fish meal plant is operating at full rated capacity (331 t; 300 mt raw input) (Table 1). Based on these conditions, the daily volume of the primary discharge would be 4,761,833 gal (18,025,499 l), including sanitary discharges. The total BOD$_5$ loading to the inner harbor from the primary discharge would be 32,479 lbs (14,732 kg) per day (817 mg/l). Bailwater, a secondary surface discharge, would also contribute 167,400 gal (663,678 l) of water and 7,150 lbs (3,243 kg) of BOD$_5$ per day. Thus, Deep Sea Fisheries' total BOD$_5$ loading to the inner harbor for the summer scenario would be 39,629 lbs (17,975 kg) per day at maximum-rated capacity. These calculations assume that stormwater discharges contain relatively insignificant amounts of BOD$_5$.

The UM model (Baumgartner et al. 1992) was also used to model the summer discharge scenario. Because the crab plant would not be operational, the volume of the discharge would be much less (approximately 4.76 million gallons per day). The BOD content of crab waste is small relative to fish processing and meal plant BOD. During summer operation, the concentration of BOD$_5$ in the effluent is estimated to be 817 mg/l. Receiving water conditions are also different during summer. Most notably, temperatures are greater, and DO concentrations are lower. Data used to determine the ambient conditions were estimated from data collected during June and September 1983 (EPA 1984b). However, only near-bottom DO values are available for June 1983, and only surface values are available for September 1983. Reasonable and conservative values for late summer DO were selected for this simulation (9 mg/l and 8 mg/l for surface and near-bottom waters, respectively). Table 13 outlines other parameters used during modeling of the summer scenario. The IDODs of stickwater and fish waste are not known. As a conservative approach, this analysis uses 10% and 20% of the effluent BOD$_5$ as values for IDOD. For the summer analysis, this would equate to IDODs of 81.7 and 163.4 mg/l. The model simulation also assumes that the effluent contains no DO.

The model results are presented in Table K-3. Initial dilution of the plume will occur at an overlap depth of 17.11 m. At that depth, the effluent will have been diluted approximately 13:1. The BOD$_5$ concentration at the plume centerline is estimated to be 63.1 mg/l at the overlap depth. Based on the Mills et al. (1985) equation (IDOD = 81.7 and 163.4 mg/l), the receiving water DO within the plume at the overlap depth would be approximately:

$$8.5 + ([0 - 81.7 - 8.5]/13) = 1.6 \text{ mg/l}$$

or

$$8.5 + ([0 - 163.4 - 8.5]/13) = -4.7 \text{ mg/l}.$$

Table 13. Assumptions Used to Model Summer Discharges from
Deep Sea Fisheries' Proposed Outfall

Parameter	Assumption
Effluent	
Flow	4.76 MGD
BOD_5 concentration	817 mg/l
DO content	0 mg/l
BOD decay rate	0
Density	1.030 g/cm^3
Outfall	
Depth above bottom	20 ft (6.1 m)
Depth below surface	80 ft (24.4 m)
Vertical angle	90°
Diameter	12 in (0.305 m)
Receiving Waters	
Stratification	none
DO concentration (surface)	9 mg/l
DO concentration (outfall depth)	8 mg/l
Average DO concentration (outfall to surface)	8.5 mg/l
Temperature (surface)	8.2°C
Temperature (outfall depth)	8°C
Currents (surface)	0.1 m/s
Currents (outfall depth)	0.05 m/s
Density (surface)	1.022 g/cm^3
Density (outfall depth)	1.023 g/cm^3

Based on this simulation, it appears that summer discharges from Deep Sea Fisheries' proposed outfall would violate Alaska state water quality standards for DO (which state that DO shall be greater than or equal to 6 mg/l). Significant localized impacts on water quality would be expected based on this modeling effort.

Additional analyses were conducted to determine if impacts would result from discharges associated with maximum seasonal production from the fish processing plant during the summer. The analyses were similar to those discussed for the winter scenario. To evaluate increased production, it was assumed that Deep Sea Fisheries would operate at a level equivalent to the production level projected for August in Table 2 (559 t [507 mt] of pollock and 0.9 t [0.8 mt] of other fish species). Assuming that there would need to be a proportional increase in water usage, the BOD_5 concentration of the effluent discharged from the outfall would be the same as the maximum-rated capacity scenario, 817 mg/l. Results of outfall modeling are presented in Table K-4. Results indicate that the dilution at the overlap depth would be somewhat greater than the above analysis, 16:1, but would still result in impacts on water quality in the summer.

To further evaluate the potential for localized water quality violations for the summer discharge scenario, additional model simulations (WASP model; Baumgartner et al. 1992) were performed. The WASP modeling techniques are discussed as part of the alternatives analysis. However, for this analysis, Deep Sea Fisheries' estimated BOD_5 load for the maximum seasonal production scenario (primary outfall and bailwater; see Table 2) was used because of the close proximity of the two sources. Since this set of simulations was used to evaluate the effect of Deep Sea Fisheries' discharge only, no other pollutant sources were included in the model. The results of this analysis (Figure 22) also indicate that there is a potential for water quality violations under the summer discharge scenario. The concentration of DO near the proposed outfall site is predicted to be 4 mg/l, assuming the higher projected production levels.

Fuel Storage and Handling. Diesel fuel for operating equipment, the electrical power generators, and fleet supply will be stored in six 247,000 gal tanks. These tanks will be located in a lined containment basin. Deep Sea Fisheries will be required by 40 CFR Part 112 to prepare a Spill Prevention Control and Countermeasure (SPCC) Plan for its facility operations. The plan will define guidelines and procedures for spill prevention, containment, and control. Full compliance with the SPCC Plan by Deep Sea Fisheries will minimize the potential for significant impacts from fuel handling activities. Additional measures, such as requiring vessels to be boomed with oil absorbent materials during refueling and establishing guidelines and responsibility incentives for fuel handlers, would further minimize the potential for fuel-related impacts to the environment.

Vessel Operation. Minor spills of waste products and hydrocarbons from vessels associated with the operation of the facility may occur. The likelihood of such spills would increase in relation to existing conditions as vessel traffic and use of the fueling facility expand. There will be an at-dock no-discharge policy for visiting vessels. Signs and notices will be posted on and around the facility to alert both visitors and plant staff to the importance of spill prevention, reporting, and cleanup. Trash receptacles will be placed on and around the moorage area for vessel solid wastes.

Proposed Outfall Site

```
                                              9 9
                                            9 9 9 9 0
                                          9 9 9 9 9 9 0
                                          9 9 9 9 9 0
                  8 8 9           9 9 9 9 9 9 9 9 9 9 0
      8 8 8 7 8 8 9 9 9   9 9 9 9 9 9 9 9 9 9 9 9 0
      8 8 7 6 7 8 9 9 9 9 9 9 9 9 9 9 9 9 9 9 9 9 9 0
      8 7 5 4 6 7 9 9 9 9 9 9 9 9 9 9 9 9 9 9 9 9 9 0
              9 9 9 9 9 9 9 9 9 9 9 9 9 9 9 9 9 0
                  9 9 9 9 9 9 9 9 9 9 9 9 9 9 0
       Proposed Outfall Site   9 9 9 9 9 9 9 9 9 9 9 9 0
                          9 9 9 9 9 9 9 9 9 9 9 0
                            9 9 9 9 9
                            9 9 9
```

Alternative Outfall Site A-1

```
                                              9 9
                                            9 9 9 9 0
                                          9 9 9 9 9 9 0
                                          9 9 9 9 9 0
                  7 7 8           9 9 9 9 9 9 9 9 9 9 0
      8 8 7 6 7 8 9 9 9   9 9 9 9 9 9 9 9 9 9 9 9 0
      8 8 6 5 7 8 9 9 9 9 9 9 9 9 9 9 9 9 9 9 9 9 9 0
      8 8 6 5 7 8 9 9.9 9 9 9 9 9 9 9 9 9 9 9 9 9 0
              9 9 9 9 9 9 9 9 9 9 9 9 9 9 9 9 9 0
                  9 9 9 9 9 9 9 9 9 9 9 9 9 9 0
     Alternative Outfall Site A-1   9 9 9 9 9 9 9 9 9 9 9 9 0
                          9 9 9 9 9 9 9 9 9 9 9 0
                            9 9 9 9 9
                            9 9 9
```

Alternative Outfall Site A-2

```
                                              9 9
                                            9 9 9 9 0
                                          9 9 9 9 9 9 0
                                          9 9 9 9 9 0
                  8 8 8           9 9 9 9 9 9 9 9 9 9 0
      9 9 9 8 8 8 8 8 9   9 9 9 9 9 9 9 9 9 9 9 9 0
      9 9 8 8 7 6 7 8 9 9 9 9 9 9 9 9 9 9 9 9 9 9 9 0
      9 9 8 7 6 4 7 8 9 9 9 9 9 9 9 9 9 9 9 9 9 9 0
              7 8 9 9 9 9 9 9 9 9 9 9 9 9 9 9 9 0
                  9 9 9 9 9 9 9 9 9 9 9 9 9 9 0
     Alternative Outfall Site A-2   9 9 9 9 9 9 9 9 9 9 9 0
                          9 9 9 9 9 9 9 9 9 9 9 0
                            9 9 9 9 9
                            9 9 9
```

Alternative Outfall Site A-3

```
                                              9 9
                                            9 9 9 9 0
                                          9 9 9 9 9 0
                                          9 9 9 9 9 0
                  9 9 9           9 9 9 9 9 9 9 9 9 0
      9 9 9 9 9 9 8 8 8   9 9 9 9 9 9 9 9 9 9 9 9 0
      9 9 9 9 9 9 8 8 7 7 8 9 9 9 9 9 9 9 9 9 9 9 9 0
      9 9 9 8 8 8 8 7 6 7 8 9 9 9 9 9 9 9 9 9 9 9 9 0
              7 7 5 7 8 9 9 9 9 9 9 9 9 9 9 9 9 9 0
                  9 9 9 9 9 9 9 9 9 9 9 9 9 0
     Alternative Outfall Site A-3   9 9 9 9 9 9 9 9 9 9 9 0
                        9 9 9 9 .9 9 9 9 9 9 0
                            9 9 9 9 9
                            9 9 9
```

N

Note:

Numbers represent
Deep Sea Fisheries
maximum projected
Summer discharge
only.

Figure 22. Predicted Dissolved Oxygen Concentration (mg/l) in Surface
Waters of Akutan Harbor Based on WASP Model Simulations
for the Proposed and Alternative Outfall Sites

75

Intertidal Environments

Potential operational impacts to intertidal and shallow subtidal environments are primarily restricted to contact with light fraction wastes and debris which drifts or is blown ashore by the wind. These wastes may include, but are not limited to, fish oil, fish waste, crab shells, petroleum hydrocarbons, detergents, and litter. The proposed action will include discharges along the south shore of the harbor, and will result in higher concentrations of fishing and other support vessels in the inner harbor. Under east wind conditions, floating material would tend to disperse along the southern and western shore in the inner harbor. The proposed activities could result in higher levels of petroleum hydrocarbons and fish oil in sediments in the inner harbor. Sediments at the head of the harbor were found to have elevated levels of petroleum hydrocarbons during the surveys conducted in April 1992.

Habitats in this area support low abundances of both epibenthic and infaunal organisms. The cause of lower abundance is thought to be a combination of disturbance caused by storms and sediment contamination. Increased activities which generate light fraction wastes could result in increased sediment contamination in the inner harbor. Determining the magnitude of this increase would be speculative. Accidental discharge of petroleum hydrocarbons has the greatest potential for impacting intertidal and shallow subtidal areas near the proposed site. Strict adherence to the company's SPCC Plan, and the use of oil absorbent booms and employee guidelines and incentives during refueling operations, would minimize potential impacts from fuel spills.

Marine Benthic Environments

Deep Sea Fisheries is proposing to discharge liquid and solid fraction wastes to a new outfall location. New accumulations of seafood waste will occur as a result of the discharge of solid crab waste and, to a lesser extent, from the discharge of screened fish processing waste and of bailwater. Waste from crab processing will be ground (0.5 in [1.27 cm] or smaller) and discharged from the primary outfall. Under the proposed project conditions, the maximum annual crab production would be 9,000 t (8,165 mt). If Deep Sea Fisheries were to process its maximum projected annual crab production, waste crab discharges would amount to 2,700 t (2,450 mt) assuming a 30% waste yield. Deep Sea Fisheries estimated its crab waste discharge to be 482 t (437 mt) and 655 t (594 mt) for 1991 and 1992, respectively.

Estimates of crab waste pile volume and area were made numerically assuming the maximum annual production of crab (9,000 tons per year) indicated by Deep Sea Fisheries in its NPDES permit. It was assumed that the density of the crab waste is 1.024 kilograms per liter. The hypothetical crab pile is described by the following equations:

$$h = \gamma \ Z \exp(- \ \alpha \ Z_1)$$

$$Z = (x^2 + y^2)^{1/2}$$

$$Z_1 = (x^2 + \beta y^2)^{1/2}$$

where α, β, and γ are constants and h = pile depth.

These equations were chosen because they model a relatively flat-topped pile that decays exponentially in depth at large distances from the source.

Estimates of pile volume for a 15-year period are illustrated in Figure 23. The two curves on this figure represent different pile dispersal and decomposition rates. The curves depict conditions under which either 25% or 10% of the annual waste discharge volume remains each year.

The coverage of the pile is delineated by showing the calculated depth contours of the waste pile in a 100 m^2 (330-square-foot) area (Figures 24 and 25). The discharge is assumed to occur 7.6 m (25 ft) in from one side of the boundary. The pile origin is located asymmetrically because there is often a dominant direction to the flow of waste imparted by the mean ambient water currents and the orientation of the discharge pipe. The thinnest contour depicted in each figure is 15 cm (6 in). A layer of waste this thick would likely cause anoxic conditions in the surficial sediments. The pile height is cropped in the illustrations at 10 ft to allow better resolution in the depiction of the outer reaches of the crab waste pile.

Based on the discharge volume associated with the maximum projected annual production, the pile is calculated to cover approximately 1.92 acres (0.77 hectare) after the first year, and 3.65 acres (1.48 hectares) after 15 years of discharge, assuming 25% of the volume remains. If 10% of the discharge volume remains annually, the model indicates that the pile will cover approximately 1.59 acres (0.64 hectare) after the first year of discharge, and 2.98 acres (1.21 hectares) after the 15th year of discharge. Based on the findings of the April 1992 survey by Jones & Stokes Associates and previous surveys (EPA 1984b), the infaunal benthic community beneath the waste pile will be eliminated and replaced with anaerobic bacteria, filamentous and sulfide-reducing bacteria *Beggiatoa*, and perhaps oligochaete worms.

Figure 23. Estimated Crab Waste Pile Volume Assuming Annual Waste Discharges of 2,450 mt with 10% and 25% Annual Pile Retention
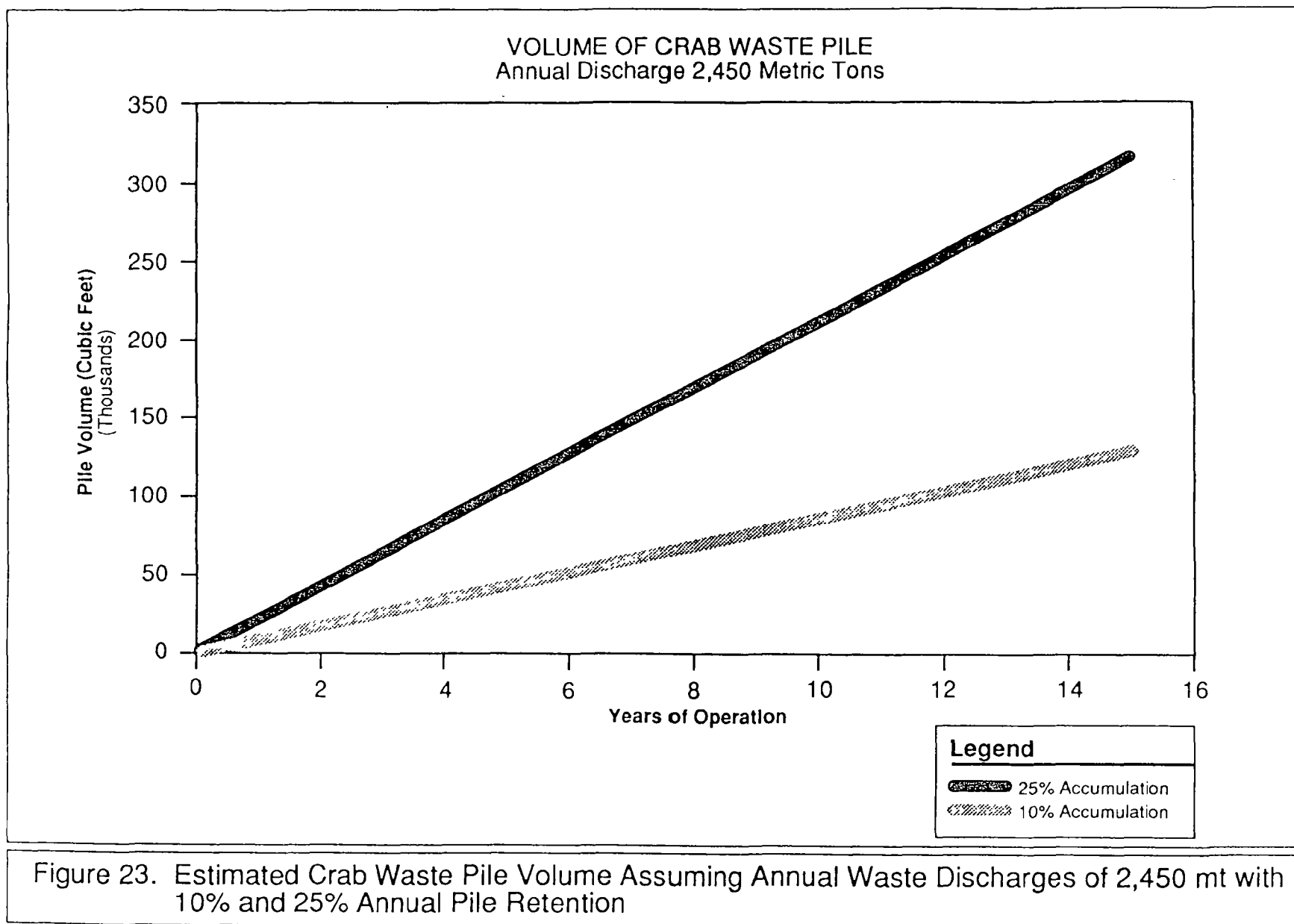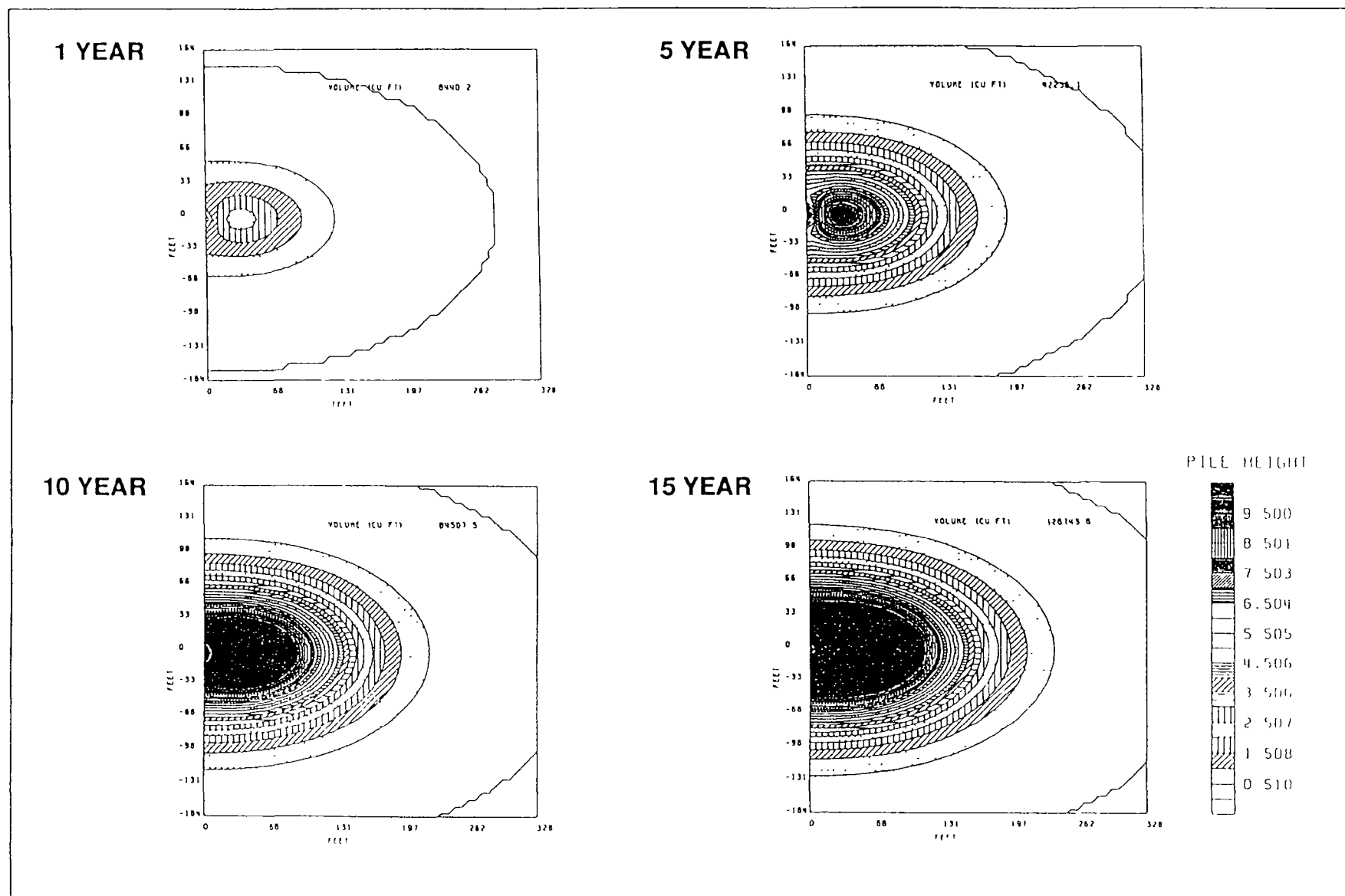
Figure 24. Calculated Depth and Area of Crab Waste Discharges Assuming Annual Discharges of 2,450 mt of Waste Annually and a 10% Annual Retention
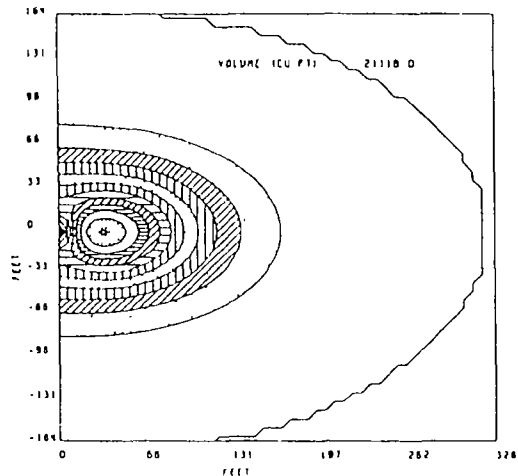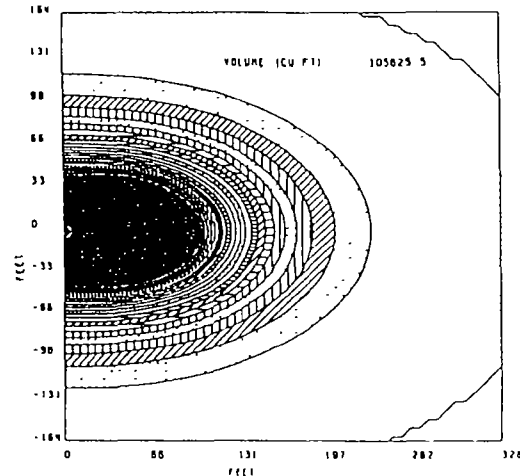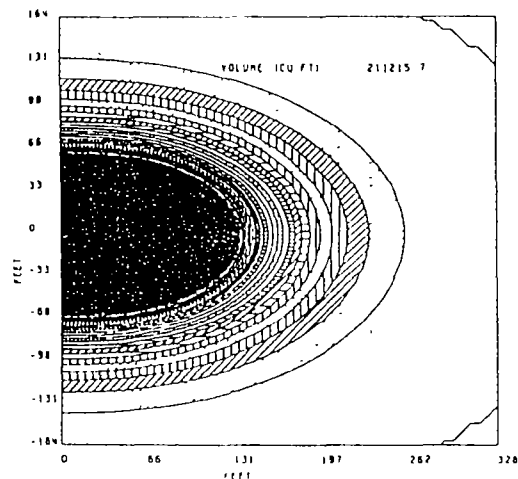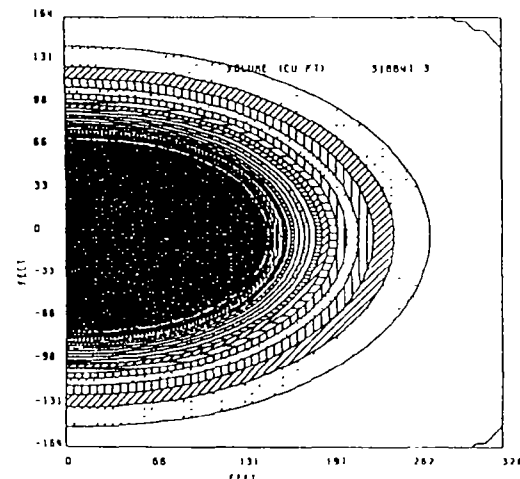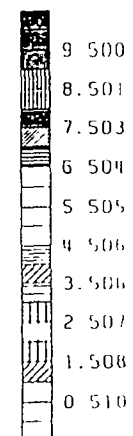
Figure 25. Calculated Depth and Area of Crab Waste Discharges Assuming Annual Discharges of 2,450 mt of Waste Annually and a 25% Annual Retention

A liquid waste from fish processing will be discharged with the crab waste. Screening (to 5 mm or less) and processing of the fish solids in the fish meal plant will significantly reduce the volume of settleable materials in the discharge. The larger and heavier particles will settle on the crab waste pile. Some of the finer and/or lighter waste particles will be carried down-current from the outfall. A small fraction of the material will reach the surface (as was seen over the Trident Seafoods outfall). These finer particles will settle in a zone down-current from the waste pile.

The characteristics of the bottom sediments and benthic community in the fine particle settlement zone around the pile would be altered. Immediately adjacent to the waste pile, both species richness and diversity would probably be significantly reduced in relation to similar unimpacted communities. Mounds and burrows typical of animal activity in undisturbed sediments would disappear. The sediments in areas of heavier deposition may become colonized with mats of *Beggiatoa*. Anemones would probably be abundant wherever rocks and debris provide a solid substrate for attachment above the sediments.

The effects of seafood wastes on infauna would become less visible further down-current from the outfall. There may continue to be higher numbers of anemones (and perhaps polychaete worms, bivalves, and other filter-feeding infauna) in response to the increased suspended particle loading. These biota would tend to consume the suspended waste particles, decreasing waste accumulation.

With the exception of an increase in settleable particles down-current from the crab waste pile, the impacts of crab and fish processing wastes on benthic communities under the proposed action should not differ markedly from existing conditions for Deep Sea Fisheries. Impacts would include elimination of the benthos under the pile and modification of the surrounding benthic community to one characteristic of organic enrichment. Because Deep Sea Fisheries is not proposing to increase its annual production, the crab waste pile created by the proposed facility should increase incrementally in size at a rate similar to pile expansion under the existing operation. Some impact outside the immediate area of the crab waste deposits would occur. The most severe effect should be limited to a zone of fine particle deposition surrounding the crab waste pile. The width of this zone would depend on the distance suspended solids are entrained in the water column before sedimentation occurs. Significant accumulations of seafood wastes in this area could result in anoxic conditions in the sediments and severely affect benthic communities. Beyond the deposition zone there should be a transition zone with features similar to those seen at Deep Sea Fisheries' existing waste pile. Community changes similar to those described by Pearson and Rosenberg (1978) would occur in this transition zone. Opportunistic species such as detrital-feeding polychaetes would increase in response to organic enrichment. The transition zone would cover a much larger area than the zone of direct impact. For example, effects of the Deep Sea Fisheries waste discharge (increased numbers of anemones and tube worms) were apparent in ROV surveys at least 200 ft from the outfall.

Recovery of the affected benthic community beneath the existing Deep Sea Fisheries crab waste pile may take months or years. The rate of recovery would depend on bottom current velocities at the existing site, microbial decomposition, and macrofaunal activity. Currents at the existing pile site were weak and would not be expected to contribute to pile

dispersion. Therefore, biological processes would be more important in biological recovery. The benthic community in the transition zone surrounding the waste pile should return rapidly to the conditions found in the less impacted portions of the harbor. The rate of biological recovery will depend on the condition and degree of organic enrichment of the bottom sediments and successional colonization by different species.

Marine Pelagic Environments

Plankton (such as the larvae of mussels and clams) could become entrained in the effluent plume and be carried down-current. Because there are no toxic substances in the discharge, and any localized decrease in DO is not expected to be detrimental, the discharge would not be expected to have significant adverse impacts on plankton. However, nutrients in the discharge may stimulate the growth of certain algal species during the spring and summer months. The effect of Deep Sea Fisheries' discharge is not likely to adversely affect phytoplankton dynamics. However, the discharge may contribute to cumulative nutrient loading to the harbor (see the Cumulative Impacts Section).

Juvenile and adult salmon and plankton may migrate or drift along the shoreline and encounter wastewater plumes. Salmon orient to nearshore areas in the vicinity of their home streams. Once in the nearshore environment, olfaction plays an important role in the discrimination between streams. Based on studies of adult sockeye salmon (*Oncorhynchus nerka*) in the vicinity of Bristol Bay (Straty 1969), it is expected that adult salmon bound for the streams at the head of Akutan Bay would begin to travel more directly and actively toward the mouths of the streams once they reach those portions of the harbor influenced by the streams' flow. The path would likely keep them from entering the main core of Deep Sea Fisheries' effluent plume. These fish are very sensitive to temperature and oxygen gradients when in saltwater and should instinctively avoid the more concentrated portions of the plume.

A similar condition would exist for juvenile salmon. While these fish are shoreline-dependent, they may actively avoid the wastewater plumes. A wastewater discharge in the intertidal zone (for example, cooling plant waters) may force the fish to swim farther offshore and expose them to open water predators, such as larger salmonids. Juvenile salmonids are expected to migrate through Akutan Harbor between April and June. This period in spring is normally a period of minimal processing activities in the harbor. Because of the relatively small discharge anticipated, migrating juvenile salmonids should not be significantly impacted by Deep Sea Fisheries' discharge during this period.

Adverse water quality impacts are anticipated under the summer discharge scenarios. These impacts would be associated with production levels occurring during peak processing periods, which most likely occur in July or August. Juvenile salmonids may rear in Akutan Harbor for some time during their first summer at sea. Because fish are highly mobile and can avoid localized DO depressions, fish should not be significantly affected as a direct result of Deep Sea Fisheries' proposed discharge. However, the proposed discharge may contribute to cumulative water quality impacts on the harbor (see the Cumulative Impacts Section).

Freshwater Environments

Operation of the proposed facility would result in increased access to the three streams at the head of Akutan Harbor. Stream 4 at the north end of the valley is known to contain runs of pink salmon which provide an important fishery for the residents of the City of Akutan. Access to this stream could result in increased subsistence and sport fishing on pink salmon populations, disturbance of salmon spawning activities, and disturbance of salmon redds during egg incubation. The potential for impacts on fisheries resources could be minimized by limiting access to Stream 4.

Operation of the facility could result in increased gull (*Larus* spp.) activity in the area. An increase in the gull population in the area could result in higher levels of predation on pink salmon fry during the March to June period of fry emigration. However, because of the existing processing activities in the harbor, gull populations and consequent increases in predation should not increase enough to significantly affect fisheries resources.

Terrestrial Environments

The heath grasses on the hillside at the proposed construction site will be removed during site preparation. No wetland vegetation will be affected. Because of the relatively small and typical nature of the area affected by the construction and operation of the proposed project, significant impacts on terrestrial wildlife species are not anticipated.

Threatened and Endangered Species

The only threatened or endangered species expected to be found in the vicinity of the proposed project site is the Steller sea lion (Smith pers. comm.). This species presently co-exists in the harbor with existing seafood processing operations. The proposed project will not impact sea lion haulout or rookery areas; therefore, significant adverse impacts on threatened and endangered species are not anticipated.

Land Use

Deep Sea Fisheries is proposing to lease the project site from the Akutan Village Corporation. Since this project is not in conflict with land use policies of the corporation, the City of Akutan, or the Aleutians East Borough, significant adverse impacts on land use are not anticipated.

Socioeconomics

The processing operations and marketing of fish meal are expected to expand tax revenues for the City of Akutan. The city receives a portion of a 1.5% fish tax provided by

processors to the Aleutians East Borough. The processing and marketing of seafood products and fish meal by Deep Sea Fisheries will increase tax revenues payable to the city. There would be significant economic impacts on the city due to these increased revenues. City staff would, therefore, be concerned about the long-term economic viability of the fish processing business in the region (Juettner, Pelkey, and Tritremmel pers. comms.). The potential for social interaction between the community of Akutan and the workers in the harbor is expected to increase with the increased work force, but the socioeconomic impacts of this increase are expected to be less than significant. There are few opportunities for workers to become involved in local government or similar activities.

Public Services

Expansion of the work force at the Deep Sea Fisheries facility is not expected to have an adverse impact on public services because of the nature of the work force and the low opportunity for community interaction. Most of the work force will be composed of local residents and young transient adults. Demands on schools or utilities in the community of Akutan are not expected, and Deep Sea Fisheries will likely provide telephone service and medical care as needed.

CUMULATIVE IMPACTS

Seafood processing activities in Akutan Harbor have increased dramatically in the last decade. In the past 5 years alone crab landings have tripled, from approximately 20 million pounds annually to 60 million pounds (Figure 26). Unfortunately there are no historical processing data for pollock in Akutan Harbor because of the confidentiality of fish production quantities for individual facilities.

The identification of potential cumulative impacts was a major focus of the field studies, analysis, and modeling. The following section describes cumulative impacts of fish and shellfish processing in Akutan Harbor and discusses the potential for Deep Sea Fisheries to add to those impacts.

Because Trident Seafoods and several transient floating processors operate in Akutan Harbor, there is the potential for Deep Sea Fisheries' proposed facility to contribute to cumulative impacts in the harbor. Where possible, an incremental assessment method is used to judge the significance of Deep Sea Fisheries' contribution to potential cumulative impacts.

Air Quality and Noise

Some incremental deterioration of air quality and increased noise levels will occur in Akutan Harbor as processing and vessel activity expand. Air quality impacts would primarily be sustained during periods of calm winds. The two primary sources of air
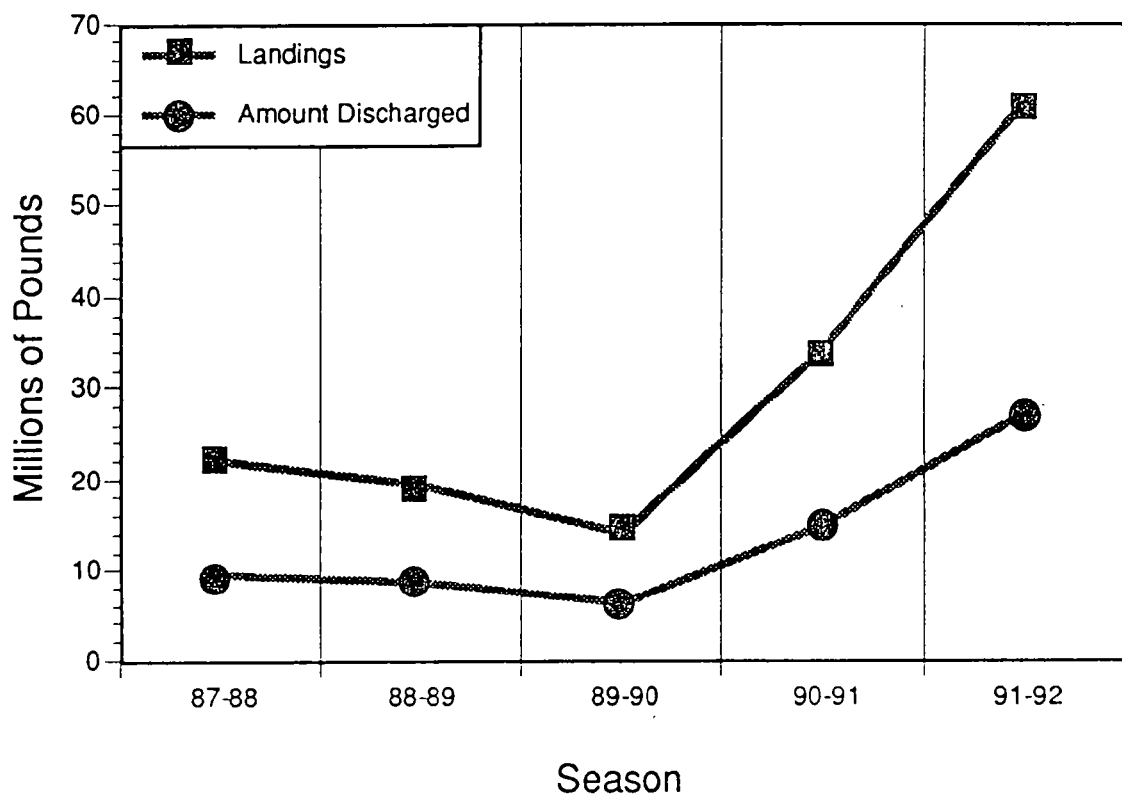
Figure 26. Annual Crab Landings and Approximate Annual Crab Waste
Discharge in Akutan Harbor, 1987 - 1992

emissions would be Deep Sea Fisheries and Trident Seafoods. Improved methods of odor control (seawater spray air scrubbers) during fish meal drying were recently adopted by Trident Seafoods. This has eliminated a significant air quality problem in the harbor. Air quality may also be affected in the vicinity of power generation and machinery emissions; however, the impacts are not expected to be significant because quiescent periods are short and infrequent.

Water Quality

Deep Sea Fisheries' proposed shore-based plant will contribute organic loading to the harbor. Since existing seafood processors, including the shore-based Trident Seafoods facility and several floating processors, currently discharge large quantities of fish and crab processing wastes, it is necessary to characterize the cumulative impacts of existing and proposed discharges. Given the oxygen-demanding nature of these discharges, there is particular concern about the cumulative impacts of seafood processors on DO in Akutan Harbor. For Akutan Harbor, the State of Alaska water quality standard regulations (Alaska Department of Environmental Conservation 1989) require:

> Surface dissolved oxygen (DO) concentrations in coastal waters shall not be less than 6.0 mg/l for a depth of one meter except when natural conditions cause this value to be depressed. DO shall not be reduced below 4 mg/l at any point beneath the surface.

Environmental Conditions Favorable for Oxygen Depletion. The BOD of the effluent will have the greatest impact on the water column during those intermittent times when the circulation is weak and relatively little new water is available to disperse the effluent. These are the times of lulls in windy weather, such as the 10-day period from day 112 to day 124 shown in Figure B-2. During these times of low winds (< 5 m/s), there may be bursts of current activity unrelated to the local winds as seen in Figure B-2; however, most of the time there will be only a weak circulation driven by the weak winds.

Four simulations of the modified circulation model were used to illustrate dispersion during weak wind events. Two of the simulations used the model to simulate discharge from Deep Sea Fisheries' proposed outfall. Two of the simulations follow discharges from the Trident Seafoods facility. The graphical results are presented in Appendix L (Figures L-9, L-10, L-17, and L-18). For each facility, simulations are for both east and west winds of 5 m/s. Each model run is for 32 hr of real time.

The simulations show localization of the effluent, with only a small fraction of the discharges moving any appreciable distance (1,000 m) from the discharge location during the 32 hr simulated.

Tidal velocities were evaluated from the current meter observations (Table B-2). The two main constituents (K1 and O1) have amplitudes (the combined magnitude of the u and v components) of 0.585 and 0.595 cm/s, respectively. The semidiurnal (half-period)

displacements associated with the K1 tide (period 23.934 hr) and the O1 tide (period 25.819 hr) are 252 and 276 m. These displacements are smaller than the wind-driven advection. The tide contribution to effluent dispersion would be smaller during neap tides and somewhat larger during spring tides than the displacements indicated. However, the tidal component is too small in either case to be the dominant force driving circulation in the harbor.

Oxygen Deficits. The hydrodynamic model and tide calculations suggest that effluents could be confined to relatively small areas (1 km square or less) of the inner harbor for extended periods. The periods are sufficiently long that the BOD of the effluents would locally affect the ambient DO concentration.

The conceptual model for estimating cumulative impacts of seafood processing on the DO in Akutan Harbor is derived from the equations of mass balance for dissolved constituents as described in the manual for WASP4 (Ambrose et al. 1991). More specifically, it assumes that the oxygen-demanding properties of the seafood waste can be described in terms of BOD and the important physical processes.

Appendix M contains details of the WASP model evaluations conducted by EPA. Some of the important assumptions and the resulting conclusions are summarized here.

The discussion of the hydrodynamics during lull conditions suggests that the dispersion of the effluent can be modeled by a purely diffusive system, neglecting ambient advection of the plume. There is some uncertainty associated with a few of the parameters used in the model due to limited data availability. These include loading rates, deoxygenation rate, reaeration rate, effluent density, and coefficient of eddy diffusivity. The rationale for selecting particular parameter values is discussed in Appendix M.

One of the more critical parameters is the diffusivity coefficient. Because the mean currents predicted by the circulation model were weak during calm wind conditions, the WASP model was employed without using mean currents in the calculations. Given the random small and directionally variable effects of winds expected during calm conditions, it would be impossible to predict precise water displacement. Instead, a range of diffusivity coefficients was used in the model (0.03 square meter per second [m^2/s] to 89 m^2/s). This range of coefficients represents all conceivable natural occurrences, and it was estimated from observed daily displacements derived from the current meter deployments in 1992.

An eddy diffusivity coefficient value of 0.5 m^2/s was used for most of the WASP model simulations to evaluate the proposed project (Appendix M). Using the calculations defined in Appendix M, 75% of the observations from the upper current meter at the proposed Deep Sea Fisheries outfall site would support a lower estimate of the dispersion coefficient (0.03 m^2/s). Only 25% of the observations from the current meter mooring near the Trident Seafoods facility would support the use of the lower coefficient estimate. This indicates that coefficient value of 0.5 m^2/s used in the analysis is a true intermediate value and not a worst-case estimate.

The analysis presented in Appendix M is conservative in several respects. The analysis assumes that:

- all wastes are discharged to the surface waters of Akutan Harbor;

- the amount of discharged materials is equivalent to maximum seasonal production discharge volumes from all processors in the harbor (Tables M-2, M-3, and M-4 in Appendix M); and

- materials are discharged during quiescent wind periods.

Table 14 illustrates the potential for water quality violations from existing and proposed discharges. Since low and intermediate values of dispersion are possible during any given season of processing, this table shows that the harbor is at a high risk for cumulative impacts on water quality.

Model Results. The WASP model results (Figures M-10, M-11, and M-12) predict that combined discharge to the harbor under the proposed action will result in water quality violations for DO during peak summer processing periods. Surface DO concentrations near the Deep Sea Fisheries and Trident Seafoods outfalls would be lowered to 3 mg/l based on model simulations. The plumes of the two shore-based facilities do not appear to commingle under the proposed action. The effect of floating processors would be minor when compared to the effects of discharges from the shore-based facilities.

There may also be indirect effects on summer DO levels due to stimulation of phytoplankton and benthic algae by increased inorganic nutrients originating from the discharge of fish and crab wastes. These effects are discussed in greater detail under Marine Pelagic Environments below.

The analysis conducted for winter maximum seasonal production indicated that no significant cumulative impacts on water quality are expected in winter from the combination of the proposed action and existing discharges (Figures M-19, M-20, and M-21 in Appendix M).

Fuel Storage and Handling. Both Trident Seafoods and Deep Sea Fisheries are required by 40 CFR Part 112 to prepare SPCC Plans for their facility operations. These plans specify fuel handling procedures, spill prevention, and systematic responses to spill events. Potential cumulative impacts due to increased fuel storage and handling in Akutan Harbor could be minimized by implementing several additional measures, including placing booms around vessels during fueling and developing guidelines and responsibility incentives for fuel handlers.

Vessel Operation. Most of the spillage of waste products and hydrocarbons into Akutan Harbor probably originates from fishing vessels and floating processors. Motor vessels undoubtedly pump oily bilge water and wastes into the harbor. Oil sheens and slicks were encountered several times during the field surveys.

Table 14. Violations of Water Quality Standards
in Any of 30 Scenarios

Season	Dispersion		
	Low	Intermediate	High
Summer	yes	yes	no
Winter	yes	no*	no

*   No violations projected except for Alternative
Outfall Site A-3.

Deep Sea Fisheries will increase its processing activities and operate more actively in both seasons. Therefore, there could be substantially more vessel activity and more potential for spills in the inner harbor.

Procedures to minimize these discharges to the harbor from the proposed action should be applied to all users of the harbor. All processors should strictly comply with SPCC Plans and encourage their fishing fleets to avoid oily discharges to the harbor. This would minimize the incremental increases in spill events in Akutan Harbor and minimize the accumulations of petroleum hydrocarbons in the intertidal areas of the inner harbor. Additional measures to minimize potential cumulative impacts were discussed as part of the Fuel Storage and Handling Section.

Intertidal Environments

Epibenthic and infaunal organisms in the intertidal and shallow subtidal environments are exposed to light fraction wastes which come ashore. Increased activity in the inner harbor under the proposed action will likely increase the exposure of these organisms to these light fraction wastes, including petroleum hydrocarbons. The extent of cumulative impacts associated with present and proposed processing activities is not quantitatively known.

As discussed above, procedures to minimize the impact of accidental spills should be applied to all users of the harbor.

Marine Benthic Environments

Cumulative impacts on the marine benthos in Akutan Harbor from the proposed action can include local effects, such as those described for Deep Sea Fisheries and Trident Seafoods, and cumulative impacts on a harborwide scale. The picture is complicated by the presence of both shore-based processors, which have a mix of waste streams and treatment processes, and floating processors, which have limited waste treatment (grinding solid wastes to 0.5 in [1.27 cm]).

Effluent from shore-based processors can be considered as well-defined point sources. Most floating processors are diffuse point sources. Floating processors anchor at various locations in the harbor and are constantly swinging on their anchors in response to changing winds and tides. A few floating processors (the M/V Clipperton, M/V Deep Sea, and M/V Northland) have semi-permanent, multianchor moorages and move very little in relation to the bottom. Treatment of both crab and fish waste by all floating processors is limited, at best, to grinding.

The point-source discharges of the shore-based and semi-permanent, ship-based processors result in the accumulation of seafood waste on the bottom. All or most of the benthos beneath the waste piles is eliminated. There is a zone of deposition surrounding the main waste piles that is enriched by the deposition of finer organic particles. The

composition of benthic communities surrounding the waste piles appears to be altered by this organic enrichment, from mixed-species communities to communities dominated by a reduced assemblage of species. For example, anemones and the small deposit-feeding polychaete worm *Capitella capitata*, which is indicative of organic enrichment, are typically abundant in these zones.

Impacts on the benthic community resulting from the operation of floating processors are not as easy to distinguish because of the diffuse nature of their waste streams. Nevertheless, some effects were clearly noted in the ROV transects (Appendix J) and bottom samples (Appendix H). The semi-permanent, ship-based processor M/V Clipperton was moored in the same location during the 1991/1992 crab season. A relatively thin layer of crab waste was deposited from this vessel. This relatively short duration of discharge was sufficient to eliminate most tube worms in the affected area (ROV video transect 7). Scattered crab waste outside the zone of heavy deposition appeared to have little or no impact on existing animal life. Crab waste observed in the central portions of Akutan Harbor (ROV video transect 8) was colonized with the filamentous bacteria *Beggiatoa*, which is also indicative of excessive organic deposition.

The benthic community in Akutan Harbor in 1992 was significantly different than communities observed in 1983. In 1983, the opportunistic polychaete worm *C. capitata* was rare or absent from samples. In 1992, *C. capitata* occurred commonly in samples collected in the northern and western portions of the inner harbor, west of Akutan village. *Glyphanostomum pallescens*, a small tube-dwelling polychaete not reported in 1983, was common in 1992 in all areas of Akutan Harbor which were not directly impacted by crab or fish waste. The total abundance of polychaetes, such as *Lumbrineris* sp., increased markedly between 1983 and 1992.

It appears obvious from the sediment and benthic community data collected in 1983 and 1992 that seafood processing has had a cumulative impact on the benthic environment. The most likely cause of this impact is enrichment of the sediment through dispersed settlement of fine organic particles from both shore-based and floating processors. At present, the benthic communities not affected directly by waste piles appear relatively healthy and robust. However, there is evidence (in the increased presence of opportunistic species such as *C. capitata*) that communities in the harbor are being altered and in some areas degraded by continued enrichment.

Deep Sea Fisheries is not proposing to increase its annual discharge of crab waste to the harbor. However, Deep Sea Fisheries is proposing to discharge wastes to a new location. Discharged crab wastes contribute the largest fraction of solids to the waste pile. The direct impacts on benthic habitats (alteration of substrate and anoxic sediments) associated with the remnant waste pile at the present discharge site will decrease over the next 10 to 15 years. Simultaneously, the area of benthic habitat directly impacted by the proposed outfall will increase at a rate similar to accretion of the former waste pile. There will be a net increase in benthic habitat directly impacted by the proposed project. This net increase will contribute a cumulative increase in the acreage of benthic habitat affected by

waste accumulation in the harbor. However, the net increase of waste pile acreage occurring as a result of the proposed project is not expected to cause a significant cumulative impact on the benthos.

Another aspect of waste discharge to the harbor is organic enrichment of sediments throughout the harbor, and a consequent impact on benthic community structure and abundance. This question was discussed for the existing condition with reference to work by Pearson and Rosenberg (1978) and Pearson et al. (1986). Those authors found that increases in organic input to embayments enriched the organic content of sediments and resulted in relatively predictable changes in the species composition, abundance, and biomass of benthic taxa. These changes in the benthic fauna of Akutan Harbor appear to have already occurred between the 1983 and 1992 sample periods. Some of the changes are consistent with the "transitional" conditions described by Pearson and Rosenberg (1978). The changes include an increase in species richness or diversity and abundance of certain opportunistic species. Benthic populations will be more likely to shift rapidly in species composition or abundance than communities with a lower level of organic enrichment. With the exception of those areas directly impacted by deposits of crab wastes, benthic communities in the harbor will not be eliminated. However, the "transitional" condition is expected to at least continue in the harbor with the operation of the two shore-based processors and floating processors.

Marine Pelagic Environments

Based on the analysis in Appendix M, the combined discharges from floating and shore-based processors can potentially impact water quality in the harbor during the summer processing season. This may affect pelagic species which use the inner harbor nearshore environments. Short-term and localized effects (i.e., lowered DO and increased turbidity) do occur, especially in and adjacent to effluent plumes. Juvenile and adult salmon, as well as herring and other fish species, probably would not be susceptible to the plume effects because of their mobility. As discussed earlier, juvenile salmonids would migrate through Akutan Harbor between April and June when processing activities are limited. Larval fish and crustaceans, and other smaller organisms, could be entrained in the plumes. Losses or displacement of the zooplankton community would be of a relatively small scale and probably not significant.

Phytoplankton dynamics are controlled by a number of factors including light, nutrients, temperature, hydrodynamics, and zooplankton grazing. During the winter months, light availability limits phytoplankton production. Therefore, nutrient loading from seafood processor discharges is not expected to impact phytoplankton in winter. However, nutrient deposition on the harbor bottom may recycle to the water column through the year as the wind-driven circulation causes upwelling at the head of the harbor.

During the early spring and summer, nutrient availability tends to be the primary limiting factor for phytoplankton production. When light is not limiting, nutrient loading from seafood processing discharges will very likely affect phytoplankton production, biomass, and species composition. This could have several different effects.

Changes in phytoplankton species composition and biomass will have a direct effect on herbivorous zooplankton dynamics, and an indirect effect on higher trophic levels such as predatory zooplankton and fish. Often phytoplankton blooms are composed primarily of dinoflagellates. Dinoflagellate blooms have been associated with red tide events, which cause toxic conditions and often affect a wide variety of marine organisms. In addition, when blooms die, decomposition of the algal cells consumes oxygen in the water.

Nitrogen is typically the limiting nutrient in cold water marine environments. Nitrogen is not typically measured as a characteristic of seafood processing waste, so an estimate of nitrogen loading to the harbor is not available at this time. Increases in plankton production due to nutrient loading are possible during spring and summer. However, no documented adverse effects of algal blooms associated with human-caused activities have been reported for Alaskan waters.

Terrestrial Environments

Impacts on the terrestrial environment from the proposed project are considered less than significant. Therefore, cumulative impacts on the terrestrial environment with the addition of the Deep Sea Fisheries processing facility are not anticipated.

Threatened and Endangered Species

Steller sea lions are the only threatened or endangered species known to occur in the vicinity of the proposed project site. The sea lions presently co-exist with processing activities in the harbor, and there will be no impacts to sea lion haulout areas or rookeries. Therefore, no cumulative impacts on threatened or endangered species are likely within Akutan Harbor.

Land Use

No cumulative changes in land use are expected as a consequence of the proposed project. The proposed project is consistent with existing land uses.

Socioeconomics

Because of an increase in taxable revenue, the proposed action will result in a net positive cumulative impact on the socioeconomics of Akutan Harbor.

Public Services

No cumulative changes in public services are expected other than those public services provided directly by Deep Sea Fisheries.

ALTERNATIVES AND THEIR ENVIRONMENTAL EFFECTS

A variety of alternatives to the proposed action have been considered. Operational alternatives include:

- The No Action Alternative: NPDES permit not issued.

Several discharge alternatives were considered for the determination of impacts, as well as economic implications for Deep Sea Fisheries. These include:

- alternative bailwater disposal;
- recycling of stickwater;
- placement of the outfall at an alternative site within the harbor;
- reduction of production levels during critical periods; and
- removal and disposal of crab waste solids by means of
  - barging,
  - landfilling,
  - incineration,
  - chitin and chitosan production, or
  - crab meal production.

Operational Alternatives

No Action Alternative: NPDES Permit Not Issued

If EPA determines that an individual NPDES permit should not be issued, the proposed shore-based Deep Sea Fisheries facility for Akutan Harbor would have to be either abandoned or relocated. The company would be permitted to continue its existing operation.

Environmental Consequences. There would be no additional impacts on the waters or shoreline of Akutan Harbor from the proposed project if EPA decides not to issue an NPDES permit to Deep Sea Fisheries. Deep Sea Fisheries, however, would likely continue to operate under the general NPDES permit, which would allow the discharge of 310,000 lbs (140,614 kg) of seafood waste per month.

Economic Consequences. Abandonment or relocation of the proposed project would pose severe economic impacts on Deep Sea Fisheries. The capital investment made by Deep Sea Fisheries would be lost or, at best, greatly diminished. The City of Akutan and the Aleutians East Borough would lose a significant income base from taxes on 70 to 90 million dollars expected to be earned annually by the proposed facility (Reid Middleton 1991).

Discharge Alternatives

Alternative Discharge of Bailwater

Deep Sea Fisheries proposes to discharge bailwater through a surface discharge at the loading dock. It is estimated that up to 167,400 gpd (633,600 l) of bailwater will be discharged off-dock at maximum production levels. This discharge can create substantial deposition piles, primarily fish scales, and add to BOD_5 loading in the vicinity of the discharge.

Most trawlers expected to off-load raw fish at the Deep Sea Fisheries dock will use chilled refrigeration systems. The fish pump removes all of the fish and associated water and waste from the system while off-loading the catch. The fish/water mixture is run over a dewatering conveyor; the water is captured in another plumbing system, and the fish are transported to the processing facilities. This provides the opportunity for three alternatives to the proposed discharge method:

- recycling of bailwater to the trawler;

- discharge of bailwater through the fish processing plant's drainage system, where it can be screened, ground, and discharged through the outfall; or

- removal of solids from the bailwater; solids can then be reduced in the meal plant, and the liquid fraction can be discharged through the finfish processing building outfall.

The first two alternatives could be easily implemented; however, a bailwater collection and conveyance system would have to be built. A two-way valve could be installed in the plumbing system close to the point of bailwater collection (after the catch is dewatered). The valve would allow operators to shunt bailwater directly back to the trawler, or to the finfish processing plant drainage system.

In some cases, Deep Sea Fisheries expects to off-load vessels which use ice to chill fish, rather than a chilling system. In this case, bailwater cannot be recycled to the trawler. However, by resetting the valve, the bailwater could be easily shunted to the finfish processing plant drainage system and discharged through the outfall.

The third alternative, removal and transport of solids to the meal plant, would be more difficult to implement. Solids in the finfish processing plant drainage system would be screened through a 0.2 in (5 mm) screen, which would not retain smaller particles such as fish scales. The technology to remove solids from bailwater has not been fully developed; however, there are several potential options such as:

- hydroscreens,
- decanters,
- centrifuges,

95

- rotating drum screens, or
- sand filtration.

Environmental Consequences. Recycling bailwater back to the trawler could eliminate most of the impacts of bailwater discharge into Akutan Harbor. The bailwater would eventually be dumped outside the harbor, but at a much lower rate (greater dilution) and over a wider area, resulting in less accumulation of solids on benthic habitats. A stipulation could also be implemented restricting trawlers from exchanging water from chilled seawater systems at the dock or within Akutan Harbor, further decreasing potential water quality impacts. By restricting all vessels from dumping recycled bailwater in the harbor, the cumulative BOD loading in the harbor could be reduced by approximately 21,000 lbs (9,505 kg) per day during the peak summer production periods (based on projected bailwater produced by Deep Sea Fisheries and Trident Seafoods in August).

Shunting bailwater through the finfish processing plant drainage would eliminate the impacts of bailwater in the vicinity of the dock; however, bailwater solids (less than 1-inch diameter) would be deposited from the outfall. The relative contribution of solids and BOD_5 loading from bailwater to the outfall could contribute as much as 21,000 lbs (9,505 kg) of additional BOD_5 per day during peak summer processing periods to that being contributed by other proposed processes. Additional BOD_5 loading to the proposed or alternative outfall sites could result in further degradation of water quality during peak summer processing periods.

Removal and transport of solids to the meal plant would eliminate impacts of solid deposition; however, the liquid fraction, and its associated BOD_5, would still need to be discharged. Depending on the solids removal technique used, the potential BOD_5 loading from the bailwater could be considerably reduced.

Economic Consequences. Minimal capital funding would be required to implement the first two alternatives. Some small additional operational cost would be incurred in pumping bailwater; however, this would be extremely small compared to the total costs of the proposed operation. Returning the bailwater to the trawler would be a benefit to the trawler. If bailwater was dumped, the trawler would have to take on a fresh supply of water and expend time and energy chilling the system to the desired temperature. By recycling the bailwater back to the trawler, cooler system temperatures can be maintained, saving the trawler operator time and money.

The third option is also considered economically feasible, with some small increase in capital and operational costs. However, specific details and economic assessments would have to be evaluated.

Stickwater Recycling

Recycling the stickwater produced during the production of fish meal involves evaporating the stickwater. Some of the solids remaining after evaporation can be added back to the fish meal. Approximately 5.7% (by weight) of stickwater is solids (Plesha pers.

96

comm.). With 100% recycling of stickwater, the amount of solid wastes requiring disposal would decrease by approximately 13.2 t (12 mt) per day, with a subsequent decrease in BOD_5 loading of 11 t (10 mt) per day. However, addition of these solids to the meal results in a product with higher salt content. The upper limit of salt content in fish meal is 7%. According to Plesha's assessment in 1989, fish meal with a salt content above 3% is of much lower economic value than fish meal with a salt content of less than 2%, and there is currently no market for meal with a salt content of 3% or higher. However, the fish meal market was not evaluated as part of this assessment, and production of meal with higher salt content may now be more economically viable.

A second alternative is to completely evaporate the stickwater separately to recover the solids. The excess solids might be used in another market, or disposed outside of Akutan Harbor, rather than adding them to the meal plant. Landfilling residual solids is not considered a viable option because of limited land disposal sites and health concerns. If barging of crab waste is required (see below), residual stickwater solids could be barged and dumped at a deep water site as well.

Environmental Consequences. The evaporation of stickwater and the drying of the resulting solubles into the meal requires that additional heat be generated for the process. As an example, Trident Seafoods quantified the air and water discharges that would result from the evaporation processes for its proposed facility in Akutan Harbor using diesel generators. For every ton of water-soluble protein (solids in stickwater) not discharged into the harbor, an additional 1.1 t (1 mt) of carbon dioxide and 19 lbs (8.7 kg) of sulfur dioxide would be produced and discharged into the atmosphere (Bundrant pers. comm.).

Recycling stickwater, disposing of residual solids through an alternative market, or barging and dumping the solids would significantly reduce the amount of BOD_5 loading to Akutan Harbor. The BOD_5 of the stickwater comprises approximately 50 to 55% of the total loading under the Deep Sea Fisheries proposed operations.

Economic Consequences. It is beyond the scope of this EA to evaluate the current economics of fish meal recycling alternatives. As an example of the potential economic consequences to Deep Sea Fisheries from recycling stickwater, the following describes an analysis conducted by Trident Seafoods during its permitting process in 1989 (Bundrant pers. comm.). It should be noted that the market for fish meal and feasible processing technology may have changed since the analyses by Bundrant in 1989. The following assumptions were used in the Bundrant analysis:

- A salt content of 1.52%, determined from chemical analysis of stickwater produced at the Unisea Dutch Harbor plant, was used for stickwater generated by the Trident Seafoods fish meal plant.

- The market price for cake meal (i.e., meal with less than 50% of the water-soluble proteins added back into the product) is $600 per metric ton.

97

- The market price for whole meal (i.e., meal with more than 50% of the water-soluble proteins added back into the product) with 3% or less salt is also $600 per metric ton.

- Although there is probably not a market for meal with over 7% salt, meal with 7.4% was assumed to have a market value of $200 per metric ton.

- The maximum production rate at the Trident Seafoods proposed facility would be 440 t (400 mt) of raw pollock per day.

The following four production scenarios were used in the economic analysis performed by Trident Seafoods:

- Discharge all stickwater produced by the plant.

- Recycle all stickwater produced by the plant.

- Recycle 17% of the stickwater to yield fish meal with 3% salt.

- Reduce the salt content of the stickwater to a level permitting evaporation of the entire product into the meal and remain under 3% salt content.

According to the economic analysis, the recycling of all stickwater produced by the Trident Seafoods fish meal plant would result in a net loss of income of approximately $2,200 per day (in 1989 dollars). The results also indicate that discharging all stickwater would save Trident Seafoods $15,905 per day (in 1989 dollars). However, according to the analysis, it would be more profitable to recycle 17% of the stickwater, which would produce a savings of $17,132 per day (1989 dollars).

From this it can be inferred that it would be in Deep Sea Fisheries' economic interest to recycle some percentage of the stickwater. Optimally, the seafood industry needs to develop the technology to reduce the salt content of the stickwater and evaporate as much water-soluble protein back into the meal as possible without exceeding 3% salt content; this could result in a daily income of $21,377 (in 1989 dollars).

Outfall Location Alternatives

Three outfall locations were considered as alternatives to the proposed outfall location. Two methods were used to evaluate the outfall location alternatives for the Deep Sea Fisheries facility:

- A modified version of the circulation model was used to illustrate dispersion at different locations in the harbor under differing environmental conditions.

- WASP model simulations were used to determine the potential for alternative discharge scenarios to violate Alaska state water quality standards.

The circulation model of the harbor was modified to determine if other reasonable, alternative outfall locations were feasible. The modified model was used to assess the relative dispersion of liquid fraction wastes from continuous discharge sources located at the proposed outfall site, and three alternative sites in the harbor. Diffusion is based on depth-averaged velocities predicted by the circulation model and parameterized by a random walk process. This process is described below.

In the modified model, one unit of a tracer (density equal to seawater) is discharged every 0.45 second (one time step in the numerical model). This unit tracer is added to the center of the 128 m by 128 m grid in which the outfall terminates (source grid). With each addition of a unit of tracer, the grid accumulates a displacement vector of a magnitude and direction dictated by the simulated currents. This displacement vector increases incrementally with each new unit addition of tracer. The amount of this increase is equivalent to the depth-averaged current velocity occurring in the grid at the time of the addition, times the incremental time step (0.45 second).

When the magnitude of the vector reaches 70 m (the average distance from the center of the grid to the grid boundary), some of the tracer in the grid is displaced to adjoining grids (Figure 27). The average distance is defined as $\ell/2(\int 1/\cos[t])$ between the limits $t=0$ and $t=\pi/4$, where ℓ is the length of the grid boundary. The dispersion model depicts the effluent as contained in a circle whose radius is that of its center of mass displacement from the center of the grid. On average, the center of mass leaves the grid when the displacement is 70 m. The size of the circle reflects both that the currents waver in direction with time, and that there is lateral diffusion. When the center of mass reaches the average grid boundary, about 50% of the circle will be out of the host grid. It will be 40% in the primary receiving grid, and 10% in the grid adjacent to the primary receiving grid. The direction of the displacement is determined by the direction of the vector. After this displacement, the grid which initially received the discharge (source grid) contains 50% of its original amount of tracer, and its displacement vector is set equal to zero. In this way the tracer moves through grids at velocities given by the time development of the numerical model and has a component of lateral dispersion.

The resulting graphics are intended to assess the relative diffusion characteristics of liquid fraction wastes at each chosen discharge location in the harbor, rather than being a quantitative assessment of dispersion. Because current velocities are relatively small, larger fraction solid wastes are expected to settle in the near vicinity of each outfall site.

The source grids in the following analyses are positioned at the location of the proposed outfall, an alternative site midchannel in the inner harbor (Alternative Outfall Site A-1), an alternative site just east of the abandoned whaling station (Alternative Outfall Site A-2), and a site just east of the headlands which lie directly south of the Trident Seafoods facility (Alternative Outfall Site A-3) (Figure 28). The results of the model simulations are presented in Appendix L.

40% of tracer

10% of tracer

Vector

50% of tracer remains

Source grid
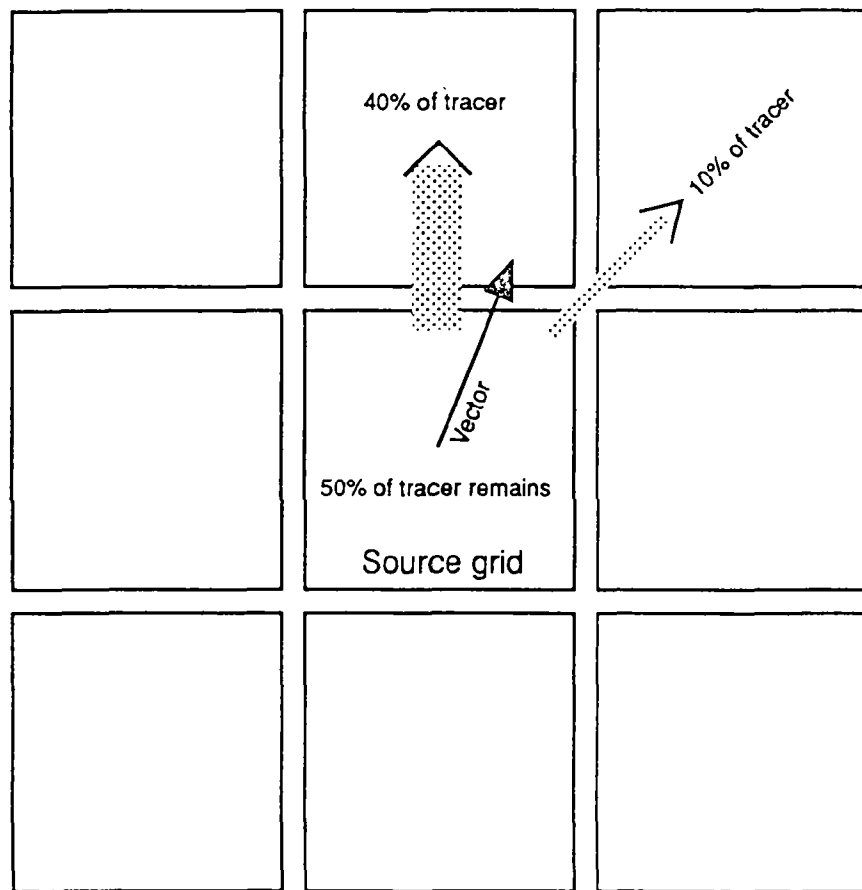
Figure 27. Illustration of Tracer Displacement when a Vector Reaches a Threshold Magnitude of 70 Meters
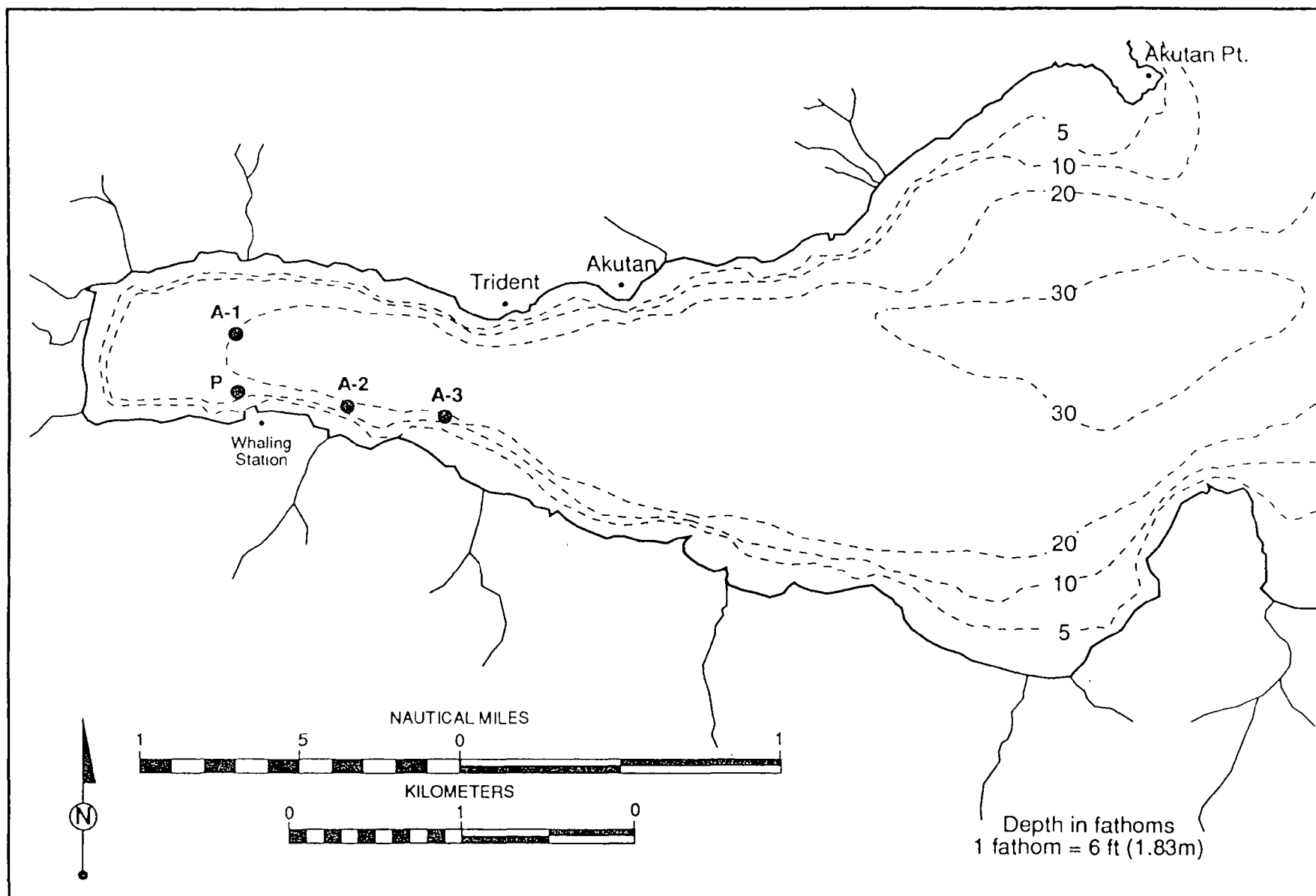
Figure 28. Approximate Location of the Proposed (P) and Three Alternative (A-1 to A-3) Locations for the Deep Sea Fisheries Outfall

The concentration of the tracer at each location, and within adjacent grids as the tracer disperses, is depicted by an asterisk that increases linearly in size with increased amounts of tracer within the grid. An asterisk 0.5 inch in diameter would contain 40,000 units of tracer.

Several possible environmental scenarios are presented in Appendix L, including:

- simulated dispersion from the proposed outfall site and the three alternative outfall sites during a short-term (4 hr) storm event with winds from the west at 20 m/s (Figures L-1, L-3, L-5, and L-7);

- simulated dispersion from the proposed outfall site and the three alternative outfall sites during a short-term (4 hr) storm event with winds from the east at 20 m/s (Figures L-2, L-4, L-6, and L-8);

- simulated dispersion from the proposed outfall site and the three alternative outfall sites during longer (32 hr) quiescent periods with winds from the west at 5 m/s (Figures L-9, L-11, L-13, and L-15); and

- simulated dispersion from the proposed outfall site and the three alternative outfall sites during longer (32 hr) quiescent periods with winds from the east at 5 m/s (Figures L-10, L-12, L-14, and L-16).

In addition to the modified circulation model, a WASP model was used to evaluate each alternative. EPA conducted a cumulative effects evaluation for the proposed and alternative outfall sites (Appendix M). WASP model simulations were run for both summer and winter conditions for each site alternative. The model included discharges from Deep Sea Fisheries (projected), Trident Seafoods (1992 DMRs), and floating processors (estimated from tax data) in the harbor. For each site and season, the contribution of floating processors was analyzed using three different assumptions: floating processors located randomly throughout the harbor; floating processors located east of longitude 165° 46' only; or no floating processors located in the harbor. The analysis presented in Appendix M is conservative in several respects. The analysis assumes that:

- All wastes are discharged to the surface waters of Akutan Harbor.

- The amount of discharged materials is equivalent to the maximum seasonal production discharge volumes from all processors in the harbor (Tables M-2, M-3, and M-4 in Appendix M).

- All wastes except bailwater and stormwater are discharged through Deep Sea Fisheries' primary outfall.

- Bailwater discharges from Deep Sea Fisheries enter the harbor in the model cell located nearest to the facilities dock.

- Materials are discharged during quiescent wind periods.

102

Uncertainties associated with the model simulations were discussed earlier (see the Cumulative Impacts Section).

The following sections discuss the results of the modeling analysis for the proposed outfall location and the three outfall location alternatives. A summary of the WASP model simulation results is presented in Table 15.

Proposed Outfall Site. Figures L-1 and L-2 illustrate the effect of 20 m/s west and east wind events, respectively, on dispersion from the Proposed Outfall Site. As illustrated in the figures, very little dispersion was realized under west wind conditions and all of the tracer accumulated in the inner harbor. Under east wind conditions, the net dispersion was to the east; however, most of tracer still accumulated in the inner harbor.

A similar dispersion pattern was obtained when the 32 hr, 5 m/s model was used to evaluate the Proposed Outfall Site (Figures L-9 and L-10). Under west wind conditions, the tracer accumulated at the head of the harbor. Under east wind conditions, the tracer generally dispersed to the east; however, most of the tracer was still within the inner harbor after 32 hr.

The WASP model analysis indicated there would be no cumulative impact on water quality in the harbor during the winter discharge scenarios for the Proposed Outfall Site (Figures M-25, M-26, and M-27 in Appendix M). However, there were localized impacts on water quality from Deep Sea Fisheries' discharge from the Proposed Outfall Site under the summer scenario (Figures M-10, M-11, and M-12 in Appendix M; see also Figure 22 in main text). The WASP model indicated that the bailwater and primary discharges would commingle under the proposed action, resulting in water quality violations near the facility. The model also indicated that a minor commingling of the Deep Sea Fisheries and Trident Seafoods discharges would occur. The effect of the commingling of the two discharges would be relatively minor.

Alternative Outfall Site A-1. Figures L-3 and L-4 illustrate the effects of 20 m/s west and east wind events, respectively, on dispersion from Alternative Outfall Site A-1, which is located midchannel in the inner harbor at about the 20-fathom contour. Under west wind conditions, the net dispersion was to the east/northeast; however, very little of the tracer left the inner harbor after 4 hr. Under east wind conditions, dispersion was slightly greater than west wind conditions, with net transport to the east/southeast.

A similar dispersion pattern was obtained when the 32 hr, 5 m/s model was used to evaluate Alternative Outfall Site A-1 (Figures L-11 and L-12). Under west wind conditions, the tracer accumulated immediately east of the discharge site within the inner harbor. Under east wind conditions, the tracer also tended to concentrate greatly at the mouth of the inner harbor after 32 hr. Under east wind conditions, the model indicated that discharges from Deep Sea Fisheries and Trident Seafoods could commingle near the mouth of the inner harbor (see Figure L-17).

103

Table 15. Potential for Water Quality Violations at the Proposed and Alternative Sites for Deep Sea Fisheries

Season	Dispersion		
	Low	Intermediate	High
Proposed Outfall			
Summer	yes	yes	no
Winter	yes	no	no
Alternative A-1			
Summer	*	yes	*
Winter	*	no	*
Alternative A-2			
Summer	*	no	*
Winter	*	no	*
Alternative A-3			
Summer	*	yes	*
Winter	*	yes	*

* Model run not available.

The WASP model analysis indicated that there would be no cumulative impact on water quality in the harbor during the winter discharge scenarios for Alternative Outfall Site A-1 (Figures M-28, M-29, and M-30 in Appendix M). However, there were localized impacts on water quality from Deep Sea Fisheries' discharge from Alternative Outfall Site A-1 under the summer scenario (Figures M-13, M-14, and M-15 in Appendix M). The WASP model indicated that the bailwater and primary discharges would commingle if Alternative Outfall Site A-1 were selected, resulting in water quality violations near the facility. However, the effect of the commingling would result in less pronounced water quality deterioration than that which would be expected under the proposed action. The model also indicated that a minor commingling of the Deep Sea Fisheries and Trident Seafoods discharges would occur. The effect of the commingling of these two discharges would be no greater than that expected under the proposed action.

Alternative Outfall Site A-2. Figures L-5 and L-6 illustrate the effects of west and east wind events, respectively, on dispersion from Alternative Outfall Site A-2, which is located just east of the whaling station at about the 15-fathom contour. Under west wind conditions, tracer dispersed from this alternative site along the southern shore; however, it still tended to concentrate at the outfall site. Under east wind conditions, the tracer dispersed rather rapidly to the north/northeast toward the Trident Seafoods facility.

A similar dispersion pattern was obtained when the 32 hr, 5 m/s model was used to evaluate Alternative Outfall Site A-2 (Figures L-13 and L-14). Under west wind conditions, the tracer demonstrated some dispersion eastward along the south shore. Under east wind conditions, the tracer tended to disperse along the north shore in the vicinity of the Trident Seafoods facility. Under east wind conditions, the model also indicated that discharges from Deep Sea Fisheries and Trident Seafoods could commingle (see Figure L-17).

The WASP model analysis indicated no cumulative impact on water quality in the harbor during the winter discharge scenarios for Alternative Outfall Site A-2 (Figures M-31, M-32, and M-33 in Appendix M). However, impacts on water quality were apparent from discharges under this alternative (Figures M-16, M-17, and M-18 in Appendix M) in the summer scenarios. The WASP model also indicated that a commingling of the Deep Sea Fisheries and Trident Seafoods discharges would occur. Based on the model simulations, this commingling would result in a decrease in DO concentration between the two outfalls; however, additional water quality violations as a result of the commingling were not evident.

Alternative Outfall Site A-3. Figures L-7 and L-8 illustrate the effects of west and east wind events, respectively, on dispersion from Alternative Outfall Site A-3, which is located just east of the headlands, directly south of the Trident Seafoods facility. Under both west and east wind conditions, the tracer dissipated rather rapidly toward the mouth of the harbor. Under west wind conditions, the tracer dispersed along the southern shore. A relatively small accumulation of tracer occurred at the outfall site, which may be related to the eddies which the model developed near the headlands. Under east wind conditions, the tracer dispersed to the east/northeast.

The dispersion pattern obtained when the 32 hr, 5 m/s circulation model was used to evaluate Alternative Outfall Site A-3 is presented as Figures L-15 and L-16. Under west

wind conditions the tracer dispersed and accumulated along the south shore of the harbor. Under east wind conditions the tracer accumulated in the vicinity of Alternative Outfall Site A-3. The model indicated that there is a potential for these discharges to commingle with discharges from Trident Seafoods.

The WASP model indicated a significant commingling of the Deep Sea Fisheries and Trident Seafoods discharges with Alternative Outfall Site A-3 (Figures M-19, M-20, M-21, M-34, M-35, and M-36 in Appendix M). The commingling would result in water quality violations during the peak processing periods in both summer and winter.

Environmental Consequences. The tracer model simulations for both the strong and weak wind conditions indicated that effluent discharged from the Proposed Outfall Site and Alternative Outfall Site A-1 would tend to concentrate in the inner harbor. Discharge from Alternative Outfall Sites A-2 and A-3 was predicted to disperse to the east and commingle with Trident Seafoods' effluent plume.

Both the PLUMES and the WASP model simulations indicated that maximum discharges occurring in the winter months would not result in individual or cumulative impacts in most cases. The exception was discharges from Alternative Outfall Site A-3. Discharges from this site in the winter were predicted to interact with Trident Seafoods' discharges and result in water quality violations for DO in the vicinity of Trident Seafoods' outfall.

Both the PLUMES and the WASP model simulations indicated that maximum discharges occurring in summer would result in water quality violations for DO for the proposed and all alternative discharge sites. However, the sources of these violations varied for the different alternatives. For the Proposed Outfall Site or Alternative Outfall Site A-1, violations occurred near the Deep Sea Fisheries outfall and near the Trident Seafoods outfall. These two separate areas of violations did not appear to be related. When Alternative Outfall Sites A-2 or A-3 were selected, the two discharges (Deep Sea Fisheries and Trident Seafoods) appeared to commingle and affect a broader area. Use of Alternative Outfall Site A-3 resulted in the most widespread area of water quality impact. Based on the WASP model results of proposed and alternative outfall sites, Alternative Outfall Site A-1 is considered the environmentally preferred site.

Economic Consequences. The alternative outfall sites are located farther from Deep Sea Fisheries than the proposed site. Selection of one of the alternative discharge locations would require lengthening the outfall and upgrading pumps and associated equipment. The alternative sites are located approximately 1,500 ft (Alternative Outfall Site A-1), 2,000 ft (Alternative Outfall Site A-2), and 4,000 ft (Alternative Outfall Site A-3) from the Proposed Outfall Site. The cost of these outfalls could be as high as $1,000 per foot for deeper sections of the outfall (Cronauer pers. comm.). Additional costs associated with the use of the preferred alternative site (A-1) would be approximately $1.5 million.

106

In addition to the installation of additional outfall pipe, Deep Sea Fisheries would have to upgrade the pumping facilities for the discharge. The approximate capital costs for resizing the pump would be approximately $2,500. The pump would require additional maintenance and would be much less fuel efficient than the pump for the proposed facility.

BOD$_5$ Effluent Limitations

The WASP model simulations indicated that the cumulative BOD$_5$ loading (Appendix M) and the BOD$_5$ loading solely attributable to Deep Sea Fisheries (Figure 22) would cause DO water quality violations during the peak of the summer processing season. Effluent water quality limitations for BOD$_5$ could be used to alleviate the potential water quality impacts during peak processing periods.

The WASP model was used to determine the maximum BOD$_5$ loading which would not result in water quality violations for DO for the proposed and alternative outfall sites. Because of differing current regimes, and the presence of the Trident Seafoods discharge, each site would require different limitations. At the two inner harbor sites, which did not significantly commingle with the Trident Seafoods discharge (the Proposed Outfall Site and Alternative Outfall Site A-1), the maximum BOD$_5$ loadings would be 34,000 and 45,000 lbs (15,422 and 20,412 kg) per day, respectively. This limitation would reflect total loading from the facility due to the commingling of the primary and bailwater discharges under these alternatives. For the two alternative sites which commingled with the Trident Seafoods discharge (Alternative Outfall Sites A-2 and A-3), the maximum permissible BOD$_5$ loading from the primary outfall would be 32,000 and 10,000 lbs (14,515 and 4,536 kg) per day, respectively.

Environmental Consequences. Limiting Deep Sea Fisheries' permissible BOD$_5$ loading to Akutan Harbor would result in minimizing the potential for its discharge to violate water quality standards for DO.

Economic Consequences. A limitation of BOD$_5$ loading to Akutan Harbor from the proposed facility can be achieved by two primary means: reductions in production, or incorporation of pollution prevention strategies which would decrease the BOD content of the effluent. Pollution prevention and waste recovery strategies applicable in the summer are discussed elsewhere (see the Stickwater Recycling and Alternative Discharge of Bailwater Sections).

The peak summer processing season consists primarily of pollock and consequent fish meal production. The quantity of fish processed and the price of pollock and fish meal products are extremely variable. To evaluate the potential economic consequences of placing limitations on BOD$_5$ loading, both the maximum-rated capacity (Table 1) and the maximum seasonal production (Table 2) of pollock by Deep Sea Fisheries will be used. Table 16 summarizes the changes in production which would be required under this alternative.

107

Table 16. Effect of the BOD_5 Limitation Alternative on Daily Production of Pollock at Deep Sea Fisheries Proposed Shore-Based Facility

Outfall Site	Projected BOD_5 Loading (lbs)	Recommended BOD_5 Limitation (lbs)	Percent Reduction in Production Required	Daily Reduction in Production Required[a] (lbs)	Daily Loss of Finished Product (lbs)	Daily Loss of Revenue[b] ($)	Number of Months Affected[c]
Maximum-Rated Capacity (Table 1)							
Proposed	39,629[d]	34,000	14	126,664	32,933	34,580	--
A-1	39,629[d]	45,000	0	0	0	0	--
A-2	32,479	32,000	1.5	13,155	3,420	3,591	--
A-3	32,479	10,000	69	617,361	160,514	168,540	--
Maximum Seasonal Production (Table 2)							
Proposed	51,951[d]	34,000	35	387,274	100,690	105,726	2
A-1	51,951[d]	45,000	13	149,760	38,938	40,885	1
A-2	42,997	32,000	26	286,271	74,430	78,152	2
A-3	42,997	10,000	77	858,971	223,332	234,500	3

[a]   Raw input.
[b]   Based on approximate wholesale price of single frozen, skinless, boneless fillet in 1993 ($1.05/lb).
[c]   Number of summer months in which the recommended BOD_5 limitation is exceeded each year assuming maximum projected production.
[d]   Combined BOD_5 loading due to commingling of primary and bailwater discharges.

108

The maximum-rated capacity of the proposed Deep Sea Fisheries facility for pollock was estimated to be 446 t (405 mt) of raw input per day based on the capacity of the meal plant. The BOD_5 loading associated with this rate of production in summer is 39,629 lbs (17,975 kg) per day (7,150 lbs and 32,479 lbs of BOD_5 per day associated with bailwater and the primary discharge, respectively; no crab processing occurs during the summer).

Based on the maximum seasonal production values in Table 2 (August), the total effluent BOD_5 loading associated with processing is approximately 51,951 lbs (23,645 kg) per day (8,954 lbs and 42,997 lbs of BOD_5 per day associated with bailwater and the primary discharge, respectively; no crab processing during the summer).

Table 16 presents the daily production and revenue loss associated with implementing the effluent limitation alternative for the proposed and alternative outfall sites. The table illustrates that effluent limitations for BOD_5 would have the greatest economic effect if Alternative Outfall Site A-3 or the Proposed Outfall Site is selected. A lesser economic impact would be associated with Alternative Outfall Site A-2. It is apparent from the analysis that the least economic impact would be associated with the selection of Alternative Outfall Site A-1. There would be no loss in revenue associated with production at maximum-rated capacity, and only the highest seasonal production periods in summer (less than 1 month) would be affected by effluent limitations if Alternative Outfall Site A-1 is selected.

Barging of Crab Wastes for Ocean Disposal

Disposal of crab waste only is considered in this alternative. A deep water disposal site for seafood waste has been designated outside Akutan Harbor in Akutan Bay. However, screening and barging the solids for ocean disposal by an individual processor results in significant costs. At the Trident Seafoods facility on Akutan Island, solids separation through screening was estimated to require a capital expenditure of approximately $370,000 (in 1989 dollars) (Riley pers. comm.). In addition, storm conditions in the area may at times prevent barging of wastes to an adequate dump site.

Environmental Consequences. Barging of crab waste to an ocean disposal site would minimize the deposition of solid waste at the Deep Sea Fisheries proposed outfall site. Other fine solids would still accumulate in the vicinity of the outfall; however, impacts on benthic organisms would be vastly reduced. In addition, BOD and nutrient loading to Akutan Harbor would be reduced.

The loading of BOD and nutrients to the harbor could be further reduced if a system can be developed to evaporate stickwater and dispose of the solids with the crab waste. It may also be possible to collect and dispose of solids from the bailwater. BOD loading from these three sources (crab processing, stickwater, and bailwater) comprises nearly 75% of the total BOD loading expected from Deep Sea Fisheries during the winter processing season.

Depending on the ocean disposal site chosen, the impacts on the disposal site are not expected to be significant. Wastes would be expected to disperse over a wide area, with little or no accumulation. Because waters are vigorously mixed in open waters, no significant impacts on water quality are anticipated.

Economic Consequences. In 1992, the estimated cost for disposal of the crab wastes generated by Deep Sea Fisheries through barging and dumping to the ocean was estimated by Foss Maritime Company, using the following assumptions (McElroy pers. comm.):

- equipment and crews are supplied by Foss Maritime;

- contract duration is approximately 250 days (crab processing during October through May);

- two dump barges are used;

- a 2,000 to 2,200 horsepower tugboat suitable for winter use in Unalaska Bay is used;

- a trip out to sea to dump wastes is required every day;

- the distance from the plant to the dump site is approximately 5 miles; and

- safe and free moorage for the tug and barge is available.

Based on these assumptions, the total annual cost for a single facility to dispose of crab wastes through barging is approximately $1.5 million. This cost estimate includes barge rental, maintenance, labor, insurance, and all other associated expenses, but it does not include fuel costs (McElroy pers. comm.). Annual costs could be reduced by purchase and operation of a tug and barge by Deep Sea Fisheries; however, capital costs would be higher. Costs of purchasing a tug and barge could range between $3 and $6 million depending on the specifications. Annual costs for fuel, crew, and maintenance would also have to be considered.

Another alternative would be a cooperative lease or purchase of a tug and a barge between Deep Sea Fisheries and other processors in the harbor. The costs to Deep Sea Fisheries would vary depending on the number of processors involved and whether a lease or purchase option was used.

Disposal of Crab Wastes at a Landfill

The disposal of crab wastes by landfill burial would require solids separation, collection, and transport, and landfill operation and maintenance. Wastes could be transported by barge, vessel, truck, or possibly pipeline. In addition, vehicles for moving and covering the wastes would be required at the landfill. The disadvantages of this alternative are the lack of land for landfills, the potential for groundwater and surface water

110

contamination, odor, aesthetic degradation, and attraction of vermin. The advantage is the cessation of the discharge of crab wastes to Akutan Harbor.

A detailed cost estimate was not prepared for this alternative because of the disadvantages. This alternative would likely have relatively high costs due to:

- capital expenditures for screens, holding tanks, and conveyance systems;
- transport costs;
- siting and land acquisition;
- landfill design; and
- construction, control, and monitoring of the landfill.

In addition, landfilling of seafood waste is not generally encouraged by the Alaska Department of Environmental Conservation (Dolan pers. comm.).

Incineration of Crab Wastes

This alternative would require the crab wastes to be screened and centrifuged prior to combustion in a furnace. Incineration is not viewed as a viable disposal alternative for seafood wastes because of their high moisture content and low British thermal unit content (Environmental Associates 1974). Disadvantages of this alternative include high energy consumption, potential air pollution, and odor problems.

A detailed cost estimate was not prepared for this alternative. The EPA (1984c) estimate for annual fuel costs alone to incinerate wastes generated at Akutan seafood processing facilities was approximately $240,000 (1984 dollars). Additional costs would be incurred for purchase of the centrifuge, screening system, incineration facility, skilled labor, and ash transport and disposal. These costs have probably risen significantly since 1984.

Processing of Crab Wastes to Produce Chitin and Chitosan

Chitin and chitosan production remains a viable option, at least for a portion of the crab waste. The only domestic producer is Protan Laboratories, Inc., located in Raymond, Washington. Protan experiences shortages of waste crab and shrimp shells during the winter and must truck in dried crab meal from Louisiana. While there is good demand for the product, the supply shortages prevent any significant expansion of the facility. Protan would, therefore, be very interested in securing other sources of crab shell in container-load quantities. Protan feels it can expand its market if a dependable, year-round source of shell can be secured. Protan could utilize about 25 t (22.7 mt) wet weight of crab shell per day. The shell would have to be dried for shipment (Protan can use about 5 t [4 mt] per day dry weight). Protan would be willing to pay about $150 per ton and pay for shipment to its facility. If markets can be expanded, Protan would prefer to locate a facility near the source. (Sargent pers. comm.)

111

Environmental Consequences. By-product recovery from crab shell would decrease the amount of shell discharged to Akutan Harbor by only 9%. The accretion of the crab waste pile would be slightly reduced. The consequent decrease in the impact on benthic communities would be small. A by-product recovery facility located in Akutan Harbor would contribute additional chemical and biological oxygen demand to the harbor. The BOD content of these discharges is thought to be about 1,000 to 2,000 mg/l. Caustic chemicals are used in the process and must be neutralized prior to discharge. The process also bleaches the shell, resulting in discoloration of the discharge (red color).

Economic Consequences. Deep Sea Fisheries could benefit financially from the sale of crab waste, if capital and annual costs of storing and drying shell do not exceed sales. Also, Deep Sea Fisheries might require additional land space to dry shell. If a by-product recovery facility can be located near Akutan Harbor, shell could be delivered to the facility without drying and the associated costs of that process. However, a recent economic evaluation indicated that the costs of chemicals to process and neutralize process wastes are high enough to offset any potential profit in today's market (Frasier pers. comm.).

Converting Solid Crab Waste to Crab Meal or Fish/Crab Meal

Seafood processors in Unalaska are currently evaluating a variety of methods for crab waste recovery which may be applicable to Akutan Harbor processors (Frasier pers. comm.). One potential method involves producing crab meal or supplementing fish meal production with crab waste. This alternative use of crab waste could potentially decrease crab waste discharges, decrease benthic habitat impacts associated with seafood processing, and provide additional income to processors. The logistics, markets, and economics for crab meal and fish meal supplemented with crab waste are currently being evaluated.

Environmental Consequences. If markets accept the addition of crab waste to fish meal, this alternative could result in decreased crab waste discharges to Akutan Harbor. Assuming all crab waste could be shunted to the fish meal plant, solid waste discharges from crab processing could be eliminated. This would result in decreased BOD loading from the primary outfall, and it would significantly decrease benthic impacts associated with solid waste discharges from the facility. Reductions in BOD loading would be small compared to other BOD sources operating in the winter, but would have no effect on BOD loading during the more critical summer processing season. Elimination of the solid waste discharge would minimize impacts to benthic invertebrates from smothering and decrease the effects of sediment nutrient enrichment.

Economic Consequences. Assuming market acceptance of the mixed meal product, Deep Sea Fisheries could increase revenue slightly once additional capital and operational expenses were recovered. A feasibility and cost/benefit analysis is currently being prepared.

CITATIONS

Printed References

Akutan, City of. 1982. City of Akutan Comprehensive Plan. Akutan, AK.

Alaska Department of Environmental Conservation. 1989. Water quality standard regulations 18 AAC 70. 30 pp.

Alaska Municipal League. 1992. Alaska Municipal Officials Directory 1992. Alaska Municipal League. Juneau, AK.

Ambrose, R. B., T. A. Wool, J. L. Martin, J. P. Connolly, and R. W. Schanz. 1991. WASP4, a hydrodynamic and water quality model--model theory, user's manual, and programmer's guide. Environmental Research Laboratory, ORD, EPA, Athens, Georgia. 324 pp.

Baumgartner, D. J., W. E. Frick, P. J. W. Roberts, and C. A. Bodeen. 1992. Dilution models for effluent discharges. U.S. Environmental Protection Agency, Pacific Ecosystems Branch. Newport, OR.

Bloomfield, P. I. 1976. Fourier analysis of time series: an introduction. John Wiley and Sons. New York, NY.

Brown and Caldwell. 1983. Seafood waste management study - Unalaska/Dutch Harbor, Alaska. Pacific Seafood Processors Association.

Cooney, R. T. 1987. Zooplankton. Pages 285-303 in D. W. Hood and S. T. Zimmerman (eds.), The Gulf of Alaska, physical environment and biological resources. (Pub. No. MMS 86-0095.) U.S. Minerals Management Service, Ocean Assessments Division. Anchorage, AK.

Crapo, C., B. Paust, and J. Babbitt. 1988. Recoveries and yields from Pacific fish and shellfish. (Marine Advisory Bulletin No. 37.) Alaska Sea Grant College Program. Fairbanks, AK.

Crayton, W. M. 1983. Akutan, Alaska bottomfish harbor study planning aid report. Western Alaska Ecological Field Services Field Office. Anchorage, AK.

Dyer, K. 1973. Estuaries, a physical introduction. John Wiley and Sons. New York, NY.

Environmental Associates, Inc. 1974. Upgrading seafood processing facilities to reduce pollution; waste treatment systems. Prepared for U. S. Environmental Protection Agency Region 10, Corvallis, OR.

EPA. See "U.S. Environmental Protection Agency".

Ippen, A. 1966. Estuary and coastline hydrodynamics. McGraw-Hill. New York, NY.

Jones & Stokes Associates, Inc. and Tetra Tech, Inc. 1989. Trident shore-based seafood processing plant, WA #25. Final environmental assessment. Bellevue, WA. Prepared for U.S. Environmental Protection Agency, Region 10, Seattle, WA.

Kinder, T. H., and J. D. Schumacher. 1981. Hydrograph structure over the continental shelf of the southeastern Bering Sea. Pages 31-52 in D. W. Hood and J. A. Calder (eds.), The eastern Bering Sea shelf: Oceanography and resources, Volume One.

Koutitas, C. G. 1988. Mathematical models of coastal circulation. Pages 49-103 in Mathematical models in coastal engineering. Pentech Press. London, England.

Mills, W. B., D. B. Porcella, M. J. Ungs, S. A. Gherini, K. V. Summers, L. Mok, G. L. Bowie, and D. A. Haith. 1985. Water quality assessment: A screening procedure for toxic and conventional pollutants. Part II. (EPA/600/6-85/002b.) U.S. Environmental Protection Agency. Athens, GA.

Pearson, T. H., G. Duncan, and J. Nuttall. 1986. Long term changes in the benthic communities of Loch Linnhe and Loch Eil (Scotland). Hydrobiologia 142:113-119.

Pearson, T. H., and R. Rosenberg. 1978. Macrobenthic succession in relation to organic enrichment and pollution of the marine environment. Oceanography and Marine Biology Annual Review 16:229-311.

Reid Middleton, Inc. 1991. Deep Sea Fisheries, Inc., Akutan, Alaska, shore processing plant, project description and environmental review. Anchorage, AK. Prepared for Deep Sea Fisheries, Inc., Akutan, AK.

Sambrotto, R. N., and C. J. Lorenzen. 1987. Phytoplankton and primary production. Pages 249-282 in D. W. Hood and S. T. Zimmerman (eds.), The Gulf of Alaska, physical environment and biological resources. (Pub. No. MMS 86-0095.) U.S. Minerals Management Service, Ocean Assessments Division. Anchorage, AK.

Straty, R.S. 1969. The migration pattern of adult sockeye salmon (*Oncorhynchus nerka*) in Bristol Bay as related to the distribution of their home-river waters. Ph.D. thesis Oregon State University, Corvallis, OR.

Tetra Tech. 1986. Evaluation of seafood processing waste disposal - Akutan Harbor, Alaska. Final report. Prepared for Trident Seafoods Corporation and Deep Sea Fisheries, Inc. Akutan, AK.

University of Alaska. 1988. Final report on the characterization of Alaska seafood wastes. Prepared for the Alaska Fisheries Department Foundation Fisheries Industrial Technology Center. Kodiak, AK.

U.S. Department of Interior. 1985. St. George Basin sale 89 final environmental impact statement. OCS EIS, MMS 85-0029. Prepared by Minerals Management Service. Anchorage, AK.

U.S. Environmental Protection Agency. 1974. Development document for proposed effluent limitations guidelines and new source performance standards for the catfish, crab, shrimp, and tuna segments of the canned and preserved seafood processing point source category. EPA-440/1-74-020. Washington, DC.

_____. 1975. Development document for effluent limitations guidelines and new source performance standards for the fish meal, salmon, bottom fish, clam, oyster, sardine, scallop, herring and abalone segment of the canned and preserved fish and seafood processing industry point source category. EPA 440/1-75/041a. Washington, DC.

_____. 1984a. Draft environmental impact statement for ocean dumping permit, City of Akutan, Alaska. Seattle, WA.

_____. 1984b. Effects of seafood waste deposits on water quality and benthos, Akutan Harbor, Alaska. EPA 910/9-83-114. Seattle, WA.

_____. 1984c. Fact sheet for Trident Seafoods Corporation NPDES permit dated June 8, 1984. Akutan, AK.

_____. 1990. Westward Seafoods, Inc., seafood processing, WA #40. Environmental assessment. Seattle, WA.

U.S. Fish and Wildlife Service. 1983. Bottomfish harbor study, Akutan, Alaska. Prepared for U.S. Army Corps of Engineers, Alaska District, Anchorage, AK.

Personal Communications

Anderson, Brian. Endangered species coordinator. U.S. Fish and Wildlife Service, Anchorage, AK. June 23, 1993 - Section 7 consultation letter.

Bundrant, C. Trident Seafoods Corporation, Seattle, WA. May 30, 1989 - letter to Mr. Harold E. Geren, U.S. Environmental Protection Agency Region 10, concerning supplementary information on costs to recycle stickwater.

Carroll, Florence. Water compliance specialist. U.S. Environmental Protection Agency, Region 10, Seattle, WA. Multiple contacts.

Crayton, Wayne M. Fish and wildlife biologist. U.S. Fish and Wildlife Service, Anchorage, AK. August 25, 1983 - letter to Mr. Harvey Van Veldhuizen, Jones & Stokes Associates, Inc.

Cronauer, Paul. Agent for Deep Sea Fisheries, CITICO, Port Angeles, WA. June through August 1991 - multiple contacts.

Donegan, Doug. Environmental specialist. Trident Seafoods, Akutan, AK. Multiple telephone conversations.

Dolan, Robert. Environmental engineer. Alaska Department of Environmental Conservation, Anchorage, AK. June 1993 - multiple telephone conversations.

Frasier, Joe. Manager. Unisea, Inc., Redmond, WA. June 1993 - telephone conversation.

Fuller, Frank. Fisheries biologist. Alaska Department of Fish and Game, Juneau, AK. September 8, 1992 - telephone conversation.

Griffin, Ken. Area shellfish biologist. Alaska Department of Fish and Game, Dutch Harbor, AK. February 25 and May 12, 1992 - letters.

Johnson, Brett. Atlas Industries, Bellevue, WA. August 1991 - telephone conversations.

Juettner, Robert S. Aleutians East Borough, Anchorage, AK. April 8, 1992 - meeting.

Kudenov, Dr. J. Benthic ecologist. University of Alaska, Anchorage, AK. Multiple telephone conversations.

Lobdell, J.E. Environmental archaeologist, Anchorage, AK. 1983 - letter report prepared for Jones & Stokes Associates. Sacramento, CA.

McElroy, D. Foss Maritime Company, Seattle, WA. June 9, 1989 - telephone conversation.

Pelkey, Darryl. City of Akutan, Akutan, AK. April 13, 1992 - meeting.

Plesha, J. Trident Seafoods Corporation, Seattle, WA. February through April 1989 - correspondence to U.S. Environmental Protection Agency Region 10.

Riley, C. Trident Seafoods Corporation, Seattle, WA. Multiple contacts.

Sargent, Gordon. Manager. Protan Laboratories, Inc., Redmond, WA. June 15, 1989 and July 14 and September 18, 1992 - telephone conversations.

Smith, Brad. Fisheries biologist. National Marine Fisheries Service, Anchorage, AK. July 1, 1993 - Section 7 consultation letter.

Tritremmel, Erika. City of Akutan, Akutan, AK. April 15, 1992 - meeting.

Winges, Kirk D. Vice president and manager. Northwest Regional Office, TRC Environmental Consultants, Mountlake Terrace, WA. June 30, 1992 - letter regarding meteorological data.

116

Appendix A. Chronological Report of Field Studies
Conducted in Akutan Harbor, April 1992

CHRONOLOGICAL REPORT OF FIELD STUDIES
CONDUCTED IN AKUTAN HARBOR

A project team consisting of personnel from Jones & Stokes Associates and Evans-Hamilton, Inc., (EHI) conducted field studies in Akutan Harbor, Alaska, between April 6 and 13, 1992. The field studies were conducted jointly with personnel from Scientific Applications International Corporation (SAIC), who conducted side-scan sonar surveys of the harbor under a separate EPA contract.

This is a nontechnical chronology of the April 1992 fieldwork. It documents contacts made, general fieldwork accomplished, and logistical problems encountered.

Logistics

The project team included the following personnel:

Jones & Stokes Associates

Rick Oestman	Project Manager, Aquatic Ecologist
Dan Cheney	Marine Biologist
Larry Larsen	Oceanographer, Computer Modeler
Greg Volkhardt	Fisheries Biologist
Jenna Getz	Water Quality Specialist

EHI

Keith Kurrus	Oceanographic Instrumentation Specialist

SAIC

Tony Petrillo	Oceanographer, Side-Scan Sonar and ROV Operator
Peter Jepsen	Navigator

The work was successfully completed with a minimum of logistical problems. Timely and safe arrival of the scientific equipment was accomplished by packing all equipment in one aircraft cargo container and shipping it as priority cargo between Seattle and Dutch Harbor. Although this method was relatively expensive, it ensured all of the equipment arrived on time.

The weather was unusually mild throughout the study period, with relatively light winds (0 to 30 knots) blowing from the northeast. A weather system that moved over the Aleutians on April 12 prevented a number of flights between Dutch Harbor and Akutan. The study team was able to fly to Dutch Harbor; however, if we had been solely dependent on air transport, the cargo may have been delayed for days. Fortunately, we were able to ship the equipment from Akutan to Dutch Harbor by boat upon our departure.

Deep Sea Fisheries supplied the study team with a 90 ft landing craft (the M/V Flying D) as a research vessel. SAIC personnel decided the vessel was not suitable for their side-scan work and requested that Deep Sea Fisheries find a suitable vessel. Arrangements were made to rent a smaller (20 ft) covered skiff for the side-scan and ROV work. However, the boat needed some engine work, and a generator had to be flown to Akutan to provide a power source for the equipment. The change of boats and delays in receiving the generator delayed the start of the side-scan studies by one and a half days. Once the boat was operational, it provided a good working platform for the side-scan and ROV studies.

The M/V Flying D had to be modified to operate bottom sampling equipment. The modifications delayed starting the benthic surveys by half a day. However, the system did operate adequately after the modification.

When the study team arrived in Akutan, we found that all but a few floating processors had left the harbor. In addition, very little seafood processing occurred during the study period. This prevented the study team from conducting extensive sampling of process waste discharges. There were some short periods when Deep Sea Fisheries, Trident Seafoods, the M/V Clipperton, and the M/V Northlander were processing crab. The fish meal plant at Trident Seafoods was not operating during the study period.

All scientific equipment functioned adequately except for the ammonia and oxidation-reduction probes. These probes were received late from the vendor and would not stabilize in the field for accurate measurement of these parameters.

Chronology

April 6 - Monday

Study team members tested all the rented equipment including radios, side-scan sonar, ROV, miniranger navigation system, and water quality equipment. Field gear was delivered to the Alaska Airlines cargo terminal in Seattle by 1630 hrs and was flown to Anchorage early Tuesday morning. Jones & Stokes Associates crew members flew to Anchorage and arrived at 2200 hrs Alaska Daylight Time (ADT).

April 7 - Tuesday

I checked with Mark Air in the morning (0800 hrs ADT) and found that the cargo arrived in Anchorage on time. Mark Air transferred the cargo container to its facilities for shipment to Dutch Harbor later in the day. Though the cargo was shipped priority, the container was bumped to the second flight Tuesday because of the mail. Jones & Stokes Associates personnel met Tony, Peter, and Keith at the Anchorage airport. Everyone except Dan and I flew to Dutch Harbor on the midmorning flight.

Tony, Peter, Jenna, and Larry flew to Akutan on the earliest available Peninsula Airlines flight. Greg and Keith remained in Dutch Harbor until the cargo arrived at 1700 hrs ADT. The cargo was transferred to Akutan by two chartered amphibious aircraft and arrived at 2000 hrs ADT. All equipment arrived except two buoys for the current meters. These buoys were too large for the doors on the Peninsula Airlines Goose, and had to be transferred on a Mark Air flight the following day.

Dan and I remained in Anchorage and attended a meeting with several agency staff including Valerie Haney (EPA), Brad Smith (National Marine Fisheries Service), Sandy Tucker (U.S. Fish and Wildlife Service), and Bob Dolan (Alaska Department of Environmental Quality). Wayne Dozel and Kim Sundburg (Alaska Department of Fish and Game) were unable to attend. All those attending the meeting expressed a mutual desire to use monitoring to acquire more adequate baseline data.

April 8 - Wednesday

Akutan weather was partly cloudy with light wind and temperatures in the upper 30s.

The current meters were deployed by 1730 hrs ADT following the arrival of the buoys from Dutch Harbor. Keith returned to Dutch Harbor Wednesday evening, but could not make connections to Anchorage/Seattle until Thursday morning.

Deep Sea Fisheries had secured a 90 ft landing barge (the M/V Flying D) for our use. Peter and Tony determined that the side-scan sonar studies could not be performed from this vessel. Rick Hastings (Deep Sea Fisheries) arranged to borrow Daryll Pelkey's (the mayor of Akutan) boat, an enclosed 20 ft skiff, for the side-scan and ROV portions of the study. The boat had engine and electrical power problems. Tony and Peter worked on the boat, but could not begin their side-scan sonar work until the generator arrived (April 9). Peter installed the shore stations for the navigation gear. These sites were surveyed the previous day by Dowl Engineering (Deep Sea Fisheries' contracted surveyors).

Larry, Greg, and Jenna unpacked the gear and calibrated the water quality equipment, then conducted preliminary water quality sampling from the M/V Flying D. A number of sites were sampled with the Hydrolab to determine vertical and spatial homogeneity of the harbor. The harbor showed no signs of stratification, and there was very little difference in water quality parameters between stations.

Dan and I met with Bob Juettner (administrator of the Aleutians East Borough) on the morning of April 8 to discuss the project and future plans for Akutan Harbor. After the meeting, we left Anchorage and arrived in Akutan in the late afternoon.

April 9 - Thursday

Akutan weather had some clouds, but was mostly sunny with light northeast winds and temperatures in the mid-40s.

Several problems were encountered in setting up the M/V Flying D for collection of van Veen and core samples. The vessel was not equipped with a crab block or other device to raise or lower the equipment. By midmorning, a system using the hydraulic capstan at the bow of the vessel and several blocks was put together. This method proved to be an effective means of collecting benthic samples. Dan, Larry, and I collected the first set of 15 benthic infaunal and sediment chemistry samples from Akutan Harbor. We used a Magellan geographic positioning system to locate sample sites.

Greg collected flow measurements from the larger stream at the head of the bay; then he and Jenna collected most of the water quality samples and additional hydrocast data. All but one hydrocast indicated that harbor waters were well oxygenated. A sample taken just above the Trident Seafoods outfall indicated depressed oxygen in the bottom waters (6.2 mg/l). Surface waters at this site were similar to surface waters in other areas of the harbor (10 to 13 mg/l).

Tony and Peter continued to work on the side-scan skiff. The generator arrived midafternoon, and side-scan surveys began about 1500 hrs ADT. Rick Hastings acted as skipper on the side-scan skiff. The side-scan crew managed to complete the three major low resolution east-west transects that evening.

Dan toured the Trident Seafoods facility with Valerie Haney and Bob Dolan. During the tour, Dan recorded processing operations and systems with his video camera. Afterward, he joined us on the M/V Flying D to collect and sort benthic infaunal samples.

April 10 - Friday

Akutan weather was mostly cloudy with light northeast winds and temperatures in the upper 30s.

Tony and Peter continued side-scan sonar surveys, conducting higher resolution east-west transects through the harbor.

Greg and Jenna continued to collect water quality data and samples in the morning. Dan, Larry, and I began core sampling at 15 stations in the harbor.

In the afternoon, Dan, Greg, and Jenna conducted intertidal beach surveys. Surveys were conducted on nine of the 13 beach sites identified in the work plan. Tidal conditions and daylight limited the number of beaches that could be sampled on Friday. The tide height was approximately -0.5 at 1900 hrs ADT. Infaunal samples were collected from sand/silt and gravel beaches on the southern shore and near the head of the harbor. Samples revealed no intertidal organisms on the gravel beaches along the southern shore, and few organisms in the intertidal areas at the head of the harbor. Several other beaches along the south shore consisted of bedrock or were rocky, but supported diverse flora and fauna populations, particularly in the mid- and lower intertidal areas. Notes and photographs were taken of each site. Five sediment samples for hydrocarbon analysis were collected at the head of the harbor.

Larry and I conducted a number of coring transects to determine the extent of processing wastes near the M/V Deep Sea. We could not collect a core sample 40 ft due north of the Deep Sea Fisheries discharge. Instead, we used the van Veen grab to collect a bottom sample. The sample contained a number of whole crab carapaces and about a dozen crab leg sections 6 to 8 in long. The crab pieces were relatively fresh, indicating that Deep Sea Fisheries had discharged unground crab waste sometime during the last few weeks.

While conducting core sampling in the outer harbor, we noted a large oil sheen. The sheen probably covered several acres, was restricted to the mouth of the harbor, and may have been concentrated by the gyre effect noted in the 1983 surveys. A sample of surface water was collected for hydrocarbon analysis. We could not identify the source of the spill.

April 11 - Saturday

Akutan weather was cloudy with northeast winds increasing with gusts 20 to 30 knots, temperatures in the mid-30s, and light snowfall beginning in the evening with approximately 8 in of snow accumulated by Sunday morning.

Tony and Peter completed side-scan sonar surveys at about 1100 hrs ADT after performing higher resolution transects in the vicinity of the Trident Seafoods and Deep Sea Fisheries piles. Tony and I met to review side-scan records and determine where additional ROV and grab samples should be collected. Tony and Peter packed the side-scan and set up the ROV gear on the mayor's skiff. Dan, Tony, and Peter performed ROV transects midharbor near the south shore in an area that showed some abnormal features on the side-scan. The images were in the vicinity of where two floating processors had been operating during the crab season. However, core samples and the ROV transects indicated these side-scan images were the result of geological features rather than crab waste.

The first transect took some time as we worked the bugs out of the system. Also, the wind had picked up and kept blowing the survey boat off-station, causing the ROV tether to become entangled with the marker buoy lines. Later in the evening, ROV transects were performed at the old Trident Seafoods outfall pile.

Larry and I began collecting van Veen and core samples associated with the side-scan work. Greg and Jenna collected additional water quality data and helped position the ROV marker buoys.

April 12 - Sunday

Akutan weather was low overcast. Snow persisted throughout the day, with northeast winds gusting to 25 knots and temperatures in the mid-30s.

Peter moved the navigation system from the sonar skiff to the M/V Flying D so we could accurately locate dredge sites for side-scan verification. Larry and I inspected 20 to 25 Van Veen grab samples on this day.

Dan, Tony, and Greg conducted ROV transects all day. The transects were conducted under the M/V Clipperton and the M/V Deep Sea at the proposed location for the new outfall and at the old Trident Seafoods waste pile.

Jenna collected water samples for analysis of BOD and fecal coliform bacteria at the Trident Seafoods facility, near the site of the proposed outfall, in the central harbor, and over the Deep Sea Fisheries pile. Jenna also met with one of the laboratory technicians at the Trident Seafoods facility. In the late afternoon, all samples were packed and logged on the chain of custody forms.

April 13 - Monday

Akutan weather was low clouds with diminishing snowfall, winds northeast-east and variable with gusts to 20 knots, and temperatures in the mid-30s.

Tony, Dan, and Greg completed the remaining ROV transects in the central harbor and offshore from Akutan, and several transects at the new Trident Seafoods outfall. Peter collected the shore stations for the miniranger. Because of the wind, one shore station could not be retrieved. Deep Sea Fisheries personnel picked it up on April 14 and mailed it back to Seattle.

Later in the day, Dan, Larry, and Greg met with Mayor Pelkey to discuss the study and get additional information about the harbor.

The rest of the crew packed up the gear to prepare it for transport. Because of the weather, there had been no flights into Akutan Harbor since April 11. Arrangements were made to transport the gear and personnel to Dutch Harbor on the M/V Flying D. The equipment was stored below deck to prevent water damage. In the late afternoon, the cloud cover lifted just enough to permit two flights between Dutch Harbor and Akutan. All the crew except Larry were able to fly to Dutch Harbor in the late afternoon. Larry opted to travel to Dutch Harbor on the M/V Flying D.

Jenna and I flew directly to Anchorage because I had contracted an infection that required medical attention. The rest of the team remained in Dutch Harbor for the night. The M/V Flying D arrived in Dutch Harbor about 2300 hrs ADT. A flatbed truck was used to transport the equipment to the airport. The gear was loaded in a Mark Air cargo container that night for shipment to Seattle.

April 14 - Tuesday

Jenna and I flew from Anchorage to Seattle in the early morning. Greg, Larry, Tony, and Peter flew from Dutch Harbor to Seattle later in the day. Dan flew to Anchorage, where he later met with Erika Tritremmel (administrator for the City of Akutan) to discuss the project and future plans for Akutan Harbor. Dan returned to Seattle on April 15. The cargo from Anchorage also arrived in Seattle the morning of April 15. All rented equipment, with the exception of the radios, was returned by the evening of April 15.

Appendix B.   Circulation Modeling

Appendix B. Circulation Modeling

This section describes the approach and findings of field measurements and modeling of water circulation in Akutan Harbor. These modeling results and results of plume modeling are integrated to assess possible site-specific and cumulative impacts of seafood processing on Akutan Harbor.

In general, circulation in Akutan Harbor is driven by five mechanisms:

● freshwater influxes to the marine waters,

● responses to larger scale (regional) wind stresses that modify ocean circulation patterns,

● responses to seasonal oceanic conditions,

● local wind stresses acting over the specific area, and

● local responses to open ocean tides.

The importance of each mechanism is dependent on the region in which a site is located, the geometry and bathymetry of the site, and the time scale (minutes to months) which is used for the inquiry. However, it is possible to separate these physical processes and discuss their influences on circulation individually.

General Overview of Physical Processes

Freshwater Inputs to Akutan Harbor. Akutan Harbor does not have appreciable freshwater influx, and freshwater inflow represents about 0.01% of the mean harbor volume (EPA 1984b).

Regional Effects. On a regional scale, the winds over the Bering Sea and the position and strength of the Alaska Current can cause temporary changes in the sea level in the region. For instance, a relaxation of westerly winds can result in a release of pent-up waters along the western coast of Alaska and result in a subsequent temporary rise in sea level in embayments along the north coast of the Aleutians. Sea level changes associated with these regional effects could be on the order of a meter. During the observation, we did not document any such large sea-level changes. Accordingly, this discussion focuses on local winds and how they influence the circulation in Akutan Harbor.

Seasonal Effects. During the observation period (typical of winter months), the waters in Akutan Harbor were unstratified. In the 1983 studies (summer), a weak stratification was observed measuring 0.00025 g/cm^3 at the Trident Seafoods facility and lesser amounts over the main reaches of the estuary.

When a fluid is stratified, the density gradient resists the exchange of energy by the turbulence and a velocity shear is necessary to cause mixing. The Richardson number (Dyer 1973) is a comparison of the stabilizing forces of the density stratification to the destabilizing influences of velocity shear, and is defined:

$$\frac{g}{\rho}\left(\frac{\Delta\rho}{\Delta Z}\right) / \left(\frac{\Delta u}{\Delta Z}\right)^2 = \frac{9.8}{1}\left(\frac{0.00025}{20}\right) / \left(\frac{0.25}{20}\right)^2 = 0.784$$

The numerical model of the circulation predicts velocity changes of 25 cm/s over 20 m in the vertical. At these shears the Richardson number is less than 1.0, which means the waters mix readily in the vertical and, thus, stratification does not have an important influence on isolating upper waters from the deeper waters of the estuary. In this discussion we will treat Akutan Harbor waters as unstratified.

Local Wind and Current Observations. Wind speed and direction have been continually monitored since September 1991 at a meteorological station located on top of the old processing building at the Trident Seafoods facility (see Figure 5 in main text). For the purposes of this analysis, we used 15 min averaged wind speed and direction data which were collected at the Trident Seafoods station coincident with the deployment period of the current meters.

Three Aanderaa current meters were deployed in Akutan Harbor on April 6, 1992. These current meters collected data on current speed and direction, pressure, and temperature continuously until their recovery on June 4, 1992, a period of 60 days. Two of the current meters were deployed at depths of 72 ft (22 m) and 82 ft (25 m) at the proposed outfall location for the Deep Sea Fisheries facility (Figure B-1). The third current meter was deployed at a depth of 141 ft (43 m) and located in midchannel, offshore from the Trident Seafoods facility. Data collected from the current meters are included as Appendix C. Table B-1 shows the average currents observed at each of the three moorings.

The u and v components represent the east-west and south-north directional components of the currents, respectively. Because Akutan Harbor has an almost east-to-west orientation, a positive velocity u indicates a flow toward the head of the bay, and a negative value u indicates a flow toward the mouth of the bay. A positive v indicates a northerly flow, and a negative v indicates a southerly flow. The data collected from all three current meters during the 2-month deployment period demonstrate that the predominate flow pattern at the depth of the instruments was to the west (toward the head of the bay), with a smaller southerly component.
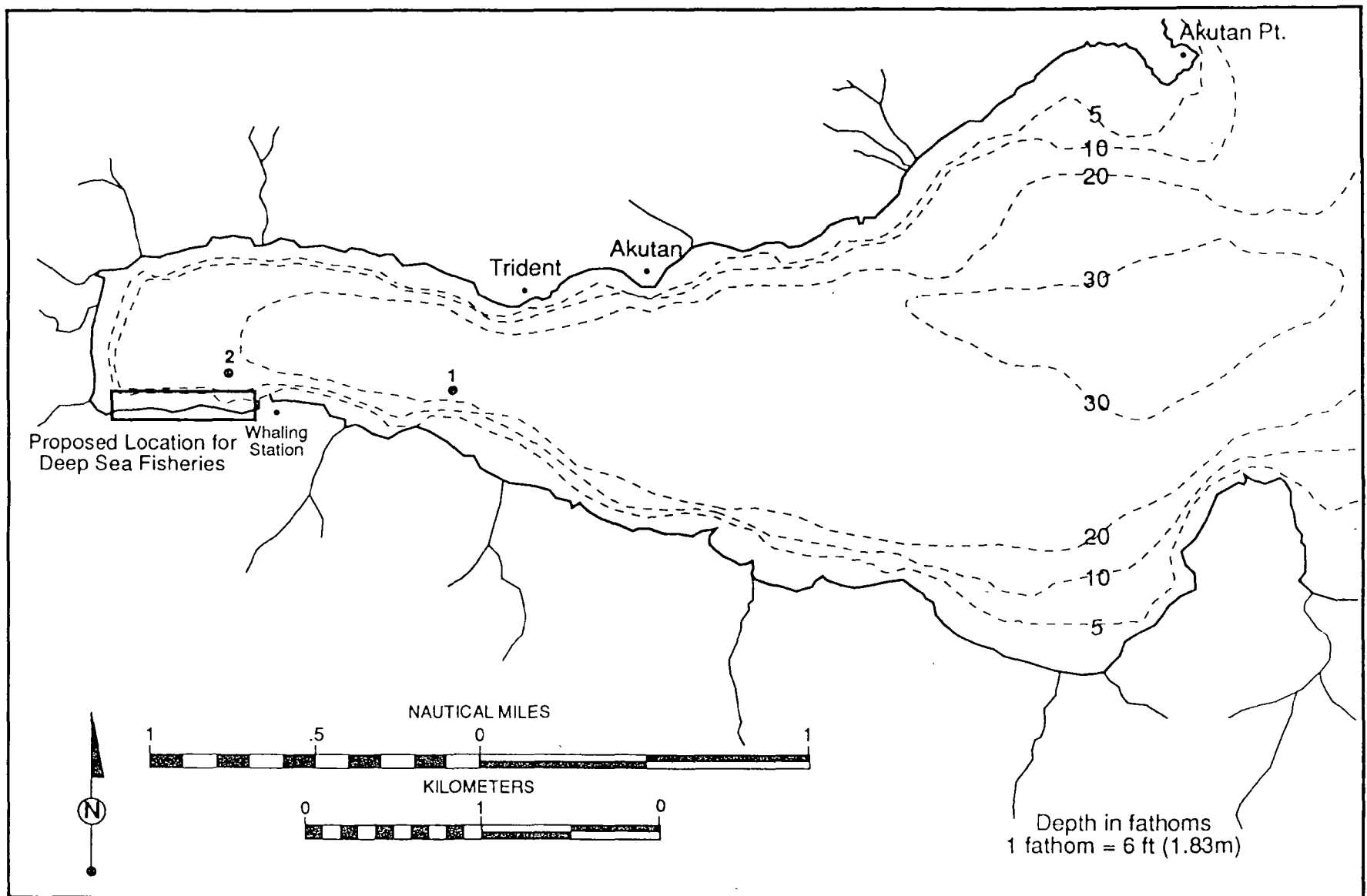
Figure B-1. Location of Current Meter Deployment in Akutan Harbor, Alaska, April - June 1992

Table B-1. Average Current Velocities Recorded by
Three Current Meters Located in Akutan Harbor

Meter Location	Average Currents*	
	u(cm/s)	v(cm/s)
Near Trident (43 m)	1.177	-2.66
Deep Sea (22 m)	1.305	-7.60
Deep Sea (25 m)	0.844	-6.81

* u = east-west directional component
  v = south-north directional component
  cm/s = centimeters per second

Figures B-2, B-3, and B-4 show the relationship between the wind and current data collected in the harbor. The current sticks are oriented such that flow into the bay is represented by vertical lines projecting upward from the centerline of the graph. Northward flows deflect these lines in a clockwise direction, and southerly flows deflect the lines in a counterclockwise direction. To facilitate visual comparisons, the recorded winds are presented in the same coordinate system as the current data. It should be noted that this is the reverse of the usual meteorological definition of winds, in which the direction refers to the compass point from which the wind originates.

In these figures, the lines represent the direction toward which the winds are blowing. The lengths of the lines reflect wind speed. The units are m/s for wind speed and cm/s for currents. The greatest average current speeds were recorded at the 22 m deep current meter at the proposed Deep Sea Fisheries outfall (Table B-1); however, the midchannel current meter near the Trident Seafoods facility recorded much larger fluctuations in current speed and direction than the two current meters near the proposed outfall. The mean wind velocity during the period of investigation (in the current data coordinate system) had a u value of 0.418 m/s and a v value of -0.963 m/s, indicating that on average the winds blew into the bay and to the south.

Figures B-2 through B-4 suggest that outbreaks of strong currents are associated with wind events. The correlation is not perfect, and there are current events not obviously associated with the winds as measured at the Trident Seafoods facility. However, the three major easterly wind events (days 104, 126, and 144) are each followed by an outgoing (negative) current which would be expected from theory. When a wind event blows into the harbor from the east, it drives the surface waters toward the head of the bay, which sets up a deeper water recirculation pattern, driving bottom waters seaward. Easterly winds appear to enhance the flow of water in the bay. They cause downwelling at the head of the bay and upwelling at the mouth of the harbor as the surface waters are driven toward the head of the harbor.

Progressive vector diagrams for each of the current meter recordings are shown in Figure B-5. A progressive vector diagram is constructed by graphing the cumulative displacement a water particle would attain if, at each instant of time, it had the velocity observed by the moored current meter. Because a water parcel advected from the location of the current meter need not experience the same time history of currents seen by the current meter, a progressive vector diagram is not a trajectory of a real drifter. However, the progressive vector diagram does illustrate the relation between mean drift currents and the fluctuating currents which show as departures from a straight line.

The Trident Seafoods mooring (Mooring 1) showed more fluctuations than either of the instruments at the Deep Sea Fisheries mooring (Mooring 2). Of the two instruments at the Deep Sea Fisheries location, the deeper meter (82 ft [25 m]) recorded the slowest velocities. Note that the scale was changed to accommodate the reduced velocities at this depth. The curves are labeled at 5-day intervals. There are a number of time periods when the advective displacement is less than 1,000 m/day. These lulls in the advection indicate times when the BOD in the effluent may impact ambient dissolved oxygen concentrations.
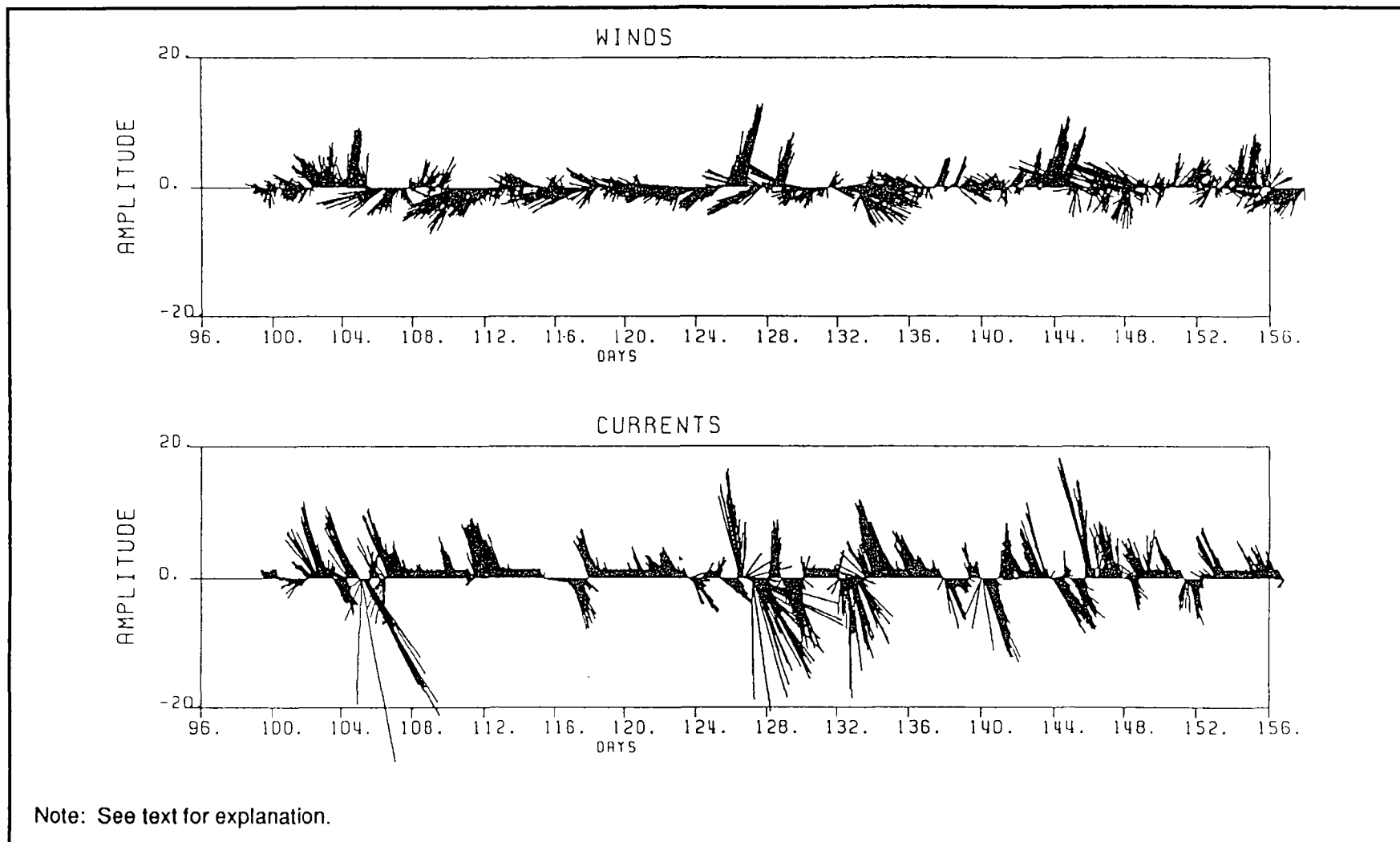
Figure B-2.   Comparison of Wind Data Collected at Trident Seafoods to Current Data Collected from the Current Meter Mooring near Trident Seafoods
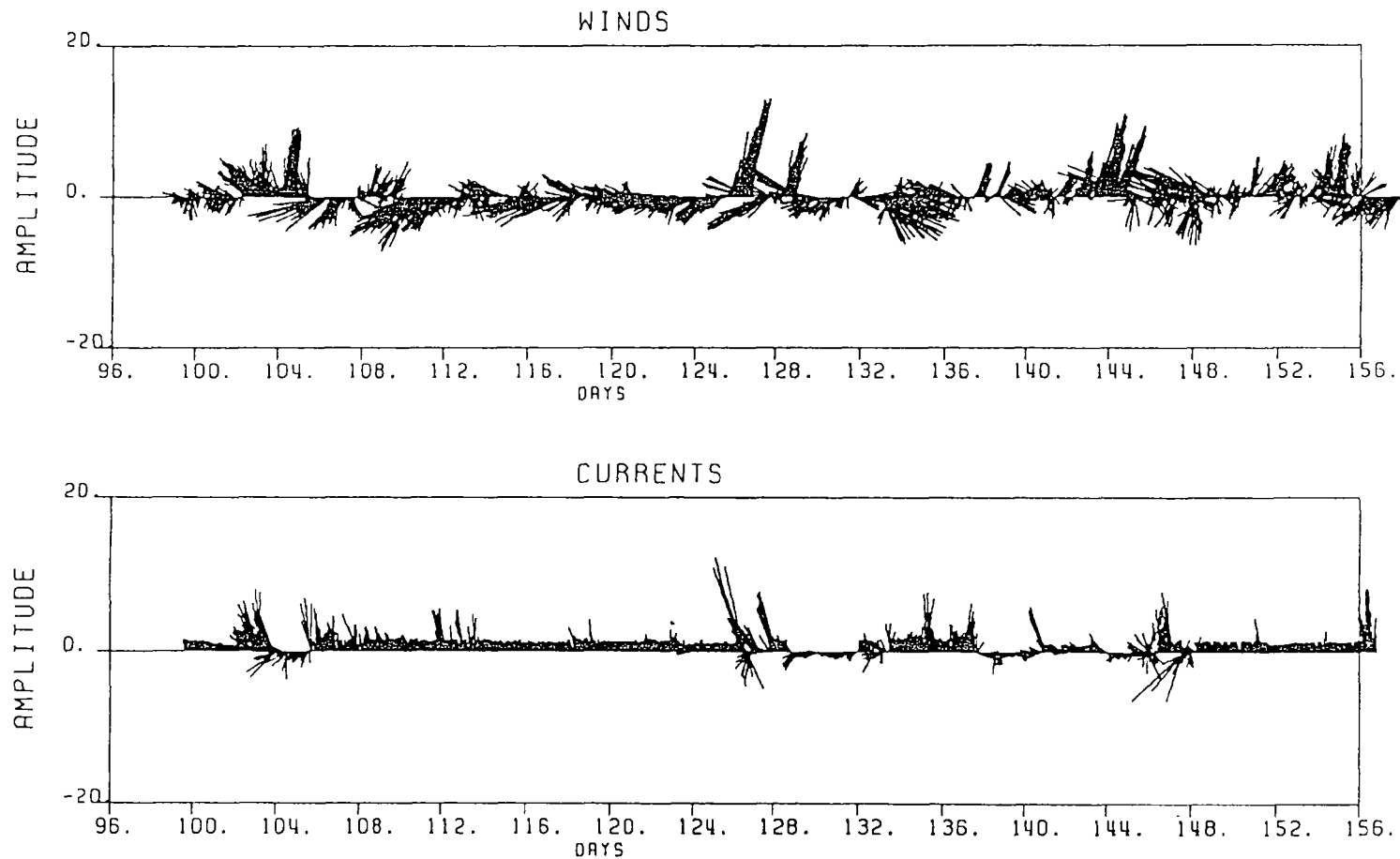
Figure B-3. Comparison of Wind Data Collected at Trident Seafoods to Current Data Collected from the Upper (22 m) Current Meter Mooring near Deep Sea Fisheries' Proposed Outfall
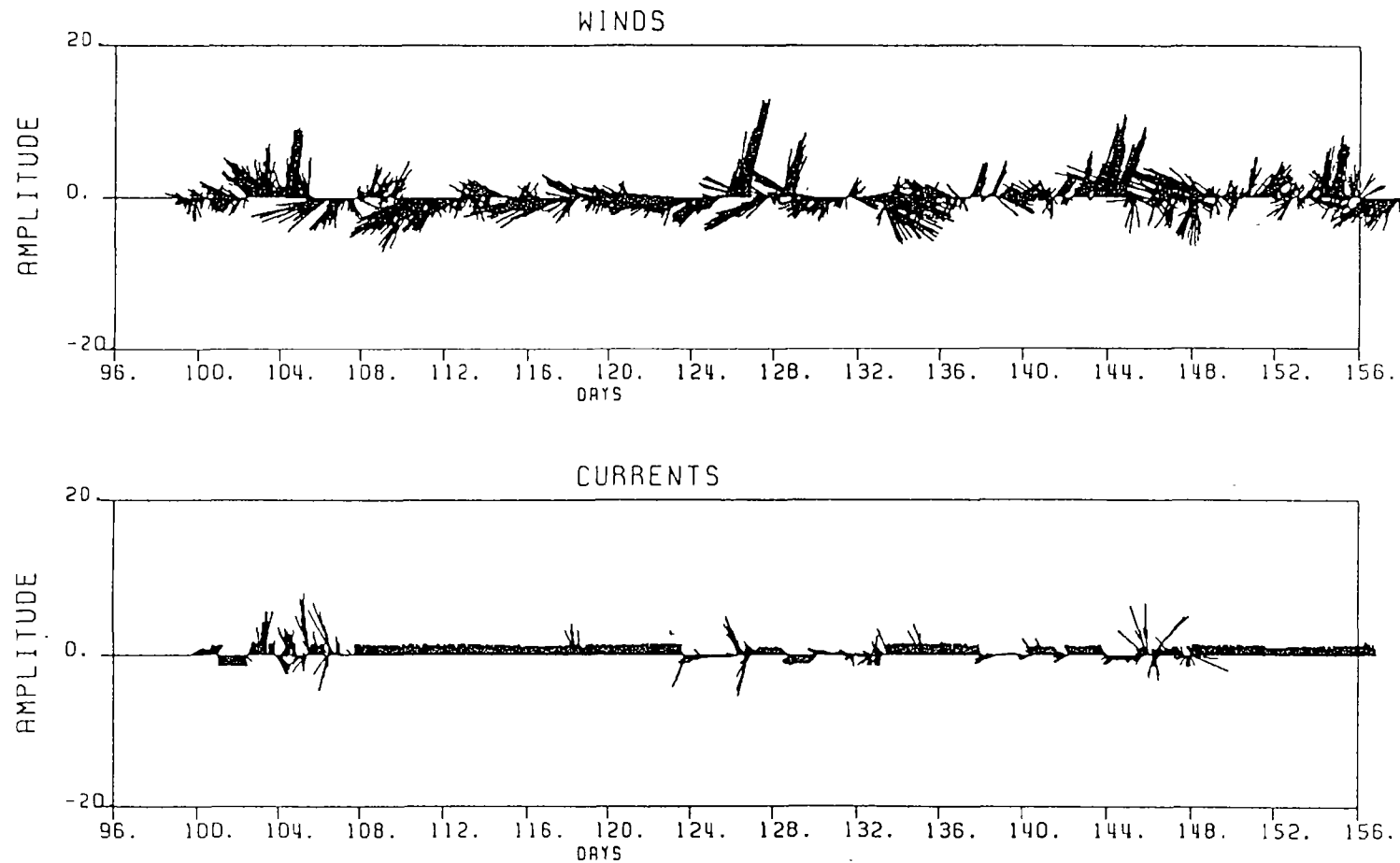
Figure B-4. Comparison of Wind Data Collected at Trident Seafoods to Current Data Collected from the Lower (25 m) Current Meter Mooring near Deep Sea Fisheries' Proposed Outfall

Mooring 1
Depth: 43m

Mooring 2
Depth: 22m

Mooring 2
Depth: 25m

1" = 10,000 meters
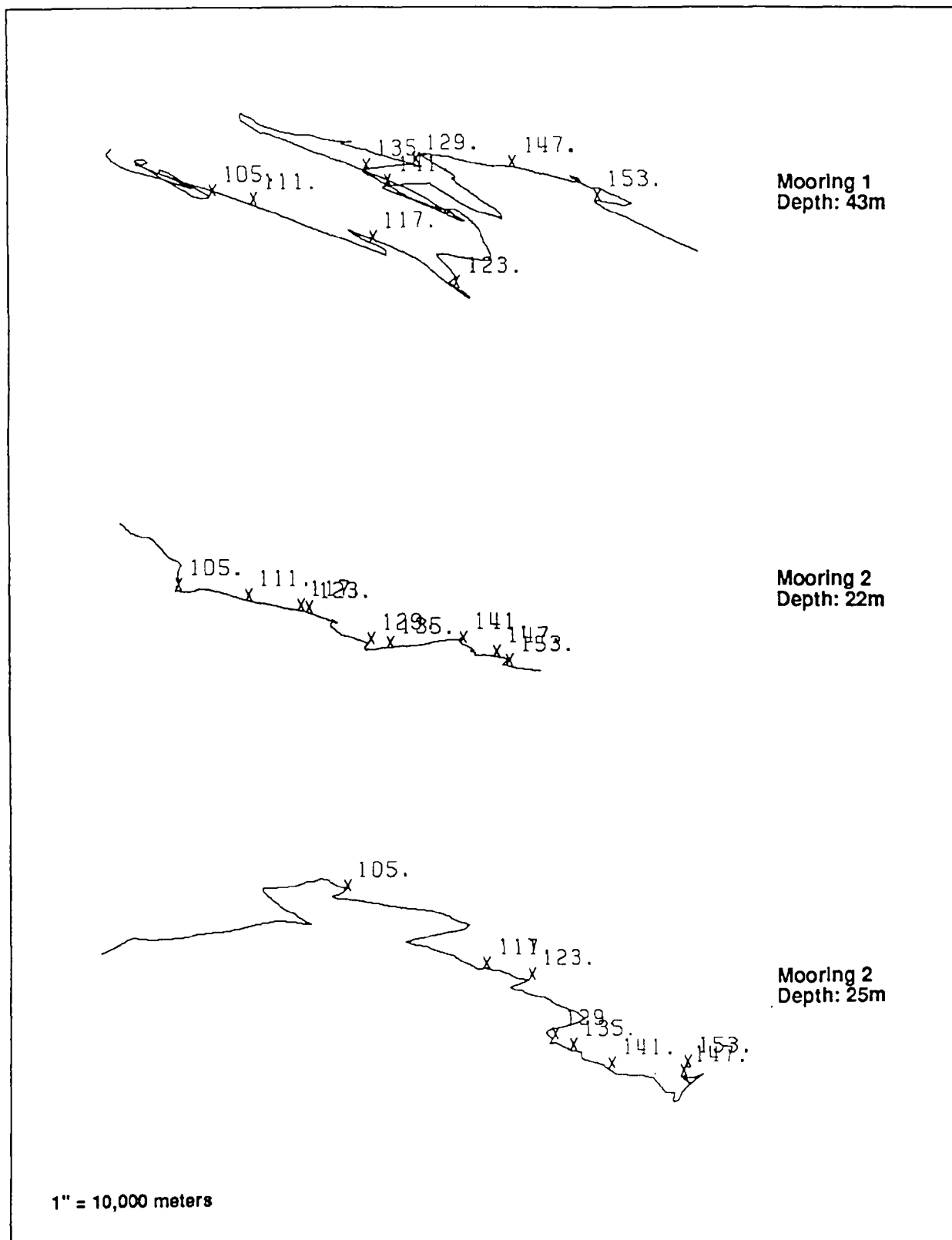
Figure B-5. Progressive Vector Diagrams for Three Current Meter
Deployments in Akutan Harbor, April 6 to June 4, 1992

Tides. The current meter and pressure records were examined to determine the tidal components of flow in the harbor. Tidal currents recorded in the harbor were extremely weak (Table B-2). The K1 and O1 values were the strongest tidal constituents, with periods of 23.934 and 25.819 hr, respectively. Based on this data, the tidal currents only account for 1.5 cm/s of the observed current flow. Therefore, the tides account for 10% of the variance of the observed currents. This indicates that the influence of the tides on currents in the harbor is relatively small when compared to other physical processes.

The overall tidal range or amplitude at Akutan Harbor is small, with a range of 4 ft (1.2 m) between MLLW and MHHW. The maximum (spring) tidal exchange is less than 5% of the mean harbor volume (estimated to be 7.5×10^{11} l).

Modeling Wind-Driven Circulation

Wind-driven circulation refers to estuarine currents created by wind stress on surface waters of the estuary. This stress causes two responses: (1) surface waters are pulled in the same direction as the winds, piling up against any boundary (shoreline) impeding the flow, and (2) a deep recirculating counter current develops to offset the water transport near the sea surface. The amount of recirculation that occurs depends on the water depth. In shallow estuaries, energy exerted on surface waters by the wind is transmitted through the water column to the bottom.

Numerical models of wind-driven circulation must predict the sea level changes caused by the winds and evaluate the currents at all positions within the estuary. Numerical models are classified according to the completeness with which they address horizontal coordinates (east to west and south to north) and the vertical coordinate, which is perpendicular to earth's surface. Horizontal and vertical coordinates must be treated differently in modeling hydrodynamics. The wind and bottom friction act primarily in the horizontal plane. The aspect ratio (ratio of vertical to horizontal scales) for estuaries is very small, usually of the order of meters in the vertical direction to kilometers in the horizontal plane. Gravity acts to restrain vertical movements but not horizontal movements.

An estuary model which completely neglects the vertical component is called a two-dimensional model. Such a model for an estuary cannot predict recirculation of waters. A model completely solving the hydrodynamics equations for the horizontal and vertical directions would be considered a three-dimensional model. Because of mathematical complexities, the use of a three-dimensional model on an estuarine scale is prohibitive. However, circulation models which can compute recirculation but simplify the vertical component of the calculations are available (Koutitas 1988) and are termed 2-1/2 dimensional models. The alternative to using 2-1/2 dimensional models is to use models composed of superimposed two-dimensional models (layered models). The choice between the layered and 2-1/2 dimensional model approaches depends on the importance of stratification in the embayment. Layered models are more appropriate when the embayment in question stratifies. Observations of Akutan Harbor in early spring and summer indicated that the harbor has minimal stratification. Thus the 2-1/2 dimensional model is the most efficient.

Table B-2. Values for Tidal Constituents in Akutan Harbor Based on Data Collected from Current Meters[a]

Tidal Constituent	Trident		Deep Sea, 22 m		Deep Sea, 25 m[b]	
	Height	KAPPA	Height	KAPPA	Height	KAPPA
Tide Heights						
M2	.0940	152.6917	.1627	141.5999	.0250	127.5664
K1	.1666	178.6087	.2680	172.1273	.0326	160.8326
S2	.0224	275.3664	.0175	267.9690	.0102	300.8354
M4	.0199	327.6917	.0254	283.7758	.0037	72.0103
O1	.1239	153.3743	.1882	145.5049	.0241	134.5474
MS4	.0118	42.7621	.0099	350.9474	.0032	224.4072
u Velocity (cm/s)						
M2	.3603	161.6752	.1226	201.1959	.0527	125.3883
K1	.5434	341.0895	.1127	220.3048	.1181	315.9909
S2	.2163	17.0157	.1218	0.5381	.0671	29.7529
M4	.0872	165.7401	.0316	231.3107	.0203	41.0051
O1	.5348	235.7854	.0920	245.0312	.0621	203.7997
MS4	.0904	63.6891	.0516	273.9102	.0073	250.1531

Table B-2. Continued

Tidal Constituent	Trident		Deep Sea, 22 m		Deep Sea, 25 m[b]	
	Height	KAPPA	Height	KAPPA	Height	KAPPA
v Velocity (cm/s)						
M2	.1201	18.3193	.0695	77.5648	.0059	239.3019
K1	.2170	157.8784	.0506	334.8546	.0539	90.1269
S2	.1349	217.0813	.0179	99.5678	.0275	236.3204
M4	.0739	47.4321	.0304	136.0063	.0215	295.1946
O1	.2573	32.5555	.0380	286.4638	.0485	297.0258
MS4	.0568	214.2430	.0109	301.7322	.0135	196.1509

cm/s = centimeters per second
m = meters

[a] Each tidal variable, sea level, u, and v, is defined by an equation of the form $H = F \times AMP \times \cos(A \times T + [VO+U] - KAPPA)$ where H is the tide height; F is the 19-year correction factor; AMP is the amplitude; A is the tidal frequency; T is time; VO and U are tabulated constants; and KAPPA is the phase angle. The amplitude and KAPPA differ for each of the variables.

[b] Data suspect because of insufficient pressure gauge resolution.

Modeling Approach for Akutan Harbor. The model we have chosen for this analysis predicts the depth-averaged velocities and the sea level at specific points within the harbor given the assigned wind stress distribution. The surface currents, intermediate depth currents, and bottom friction can be derived from the mean velocities. The model calculations assume that the estuary is initially at rest. The calculations begin when the wind starts to blow. For the model simulations generated for Akutan Harbor, the wind field was considered constant over the entire estuary.

The bathymetry and geometry of Akutan Harbor were input to the model by digitizing the navigation chart of Akutan Harbor (National Oceanic and Atmospheric Administration chart 16532) using a UNIX-based Geographic Information System (GIS). The GIS system produced a grid map contoured in 5-fathom increments to depths of 20 fathoms and 10-fathom intervals for the greater depths. The data were organized into a 40- by 60-unit grid configuration, with each side of a grid unit equal to 420 ft (128 m). With such a finely spaced grid pattern, numerical stability considerations dictate that the time step (or the unit of time increase in each iteration) can be no greater than 0.5 second.

To describe the wind-driven circulation in Akutan Harbor, we used a numerical model described by Koutitas (1988). This document, which is attached as Appendix D, contains details of the equations and their solutions, taking into account bathymetry and estuarine geometry.

The coding in the Koutitas paper is written in BASIC. This coding has been translated into FORTRAN for this study. A listing of the program code is provided in Appendix E.

Results of the Akutan Numerical Model. Model results are discussed for four cases:

- a 20 m/s wind blowing from the east,
- a 20 m/s wind blowing from the west,
- a 5 m/s wind blowing from the east, and
- a 5 m/s wind blowing from the west.

The predicted circulation patterns illustrated in Figures B-6 and B-7 represent currents expected to be present 4 hr after the onset of the 20 m/s winds. Figures B-8 and B-9 represent currents expected 32 hr following the onset of 5 m/s winds. At each grid point, the computer used an arrow to depict the depth-averaged velocity and depth-averaged direction of the currents. The head of the arrow is bold to help visualize the directionality of the flow. The flow is toward the bold end of the arrow.

Moderately Strong Easterly Winds. Under the 20 m/s east wind conditions, the model predicts that the developing circulation east of the town of Akutan would have a net seaward flux of water over most of the central basin (Figure B-6). The inflowing waters are confined to the north and south shores. The inner bay, west of the Trident Seafoods facility, is predicted to have a circulation somewhat isolated from that in the outer

B-13

Akutan

Trident Seafoods

**Proposed Deep Sea
Fisheries Facility**

Legend

↑ Direction of flow (↑)

1 inch = 1 m/s

N
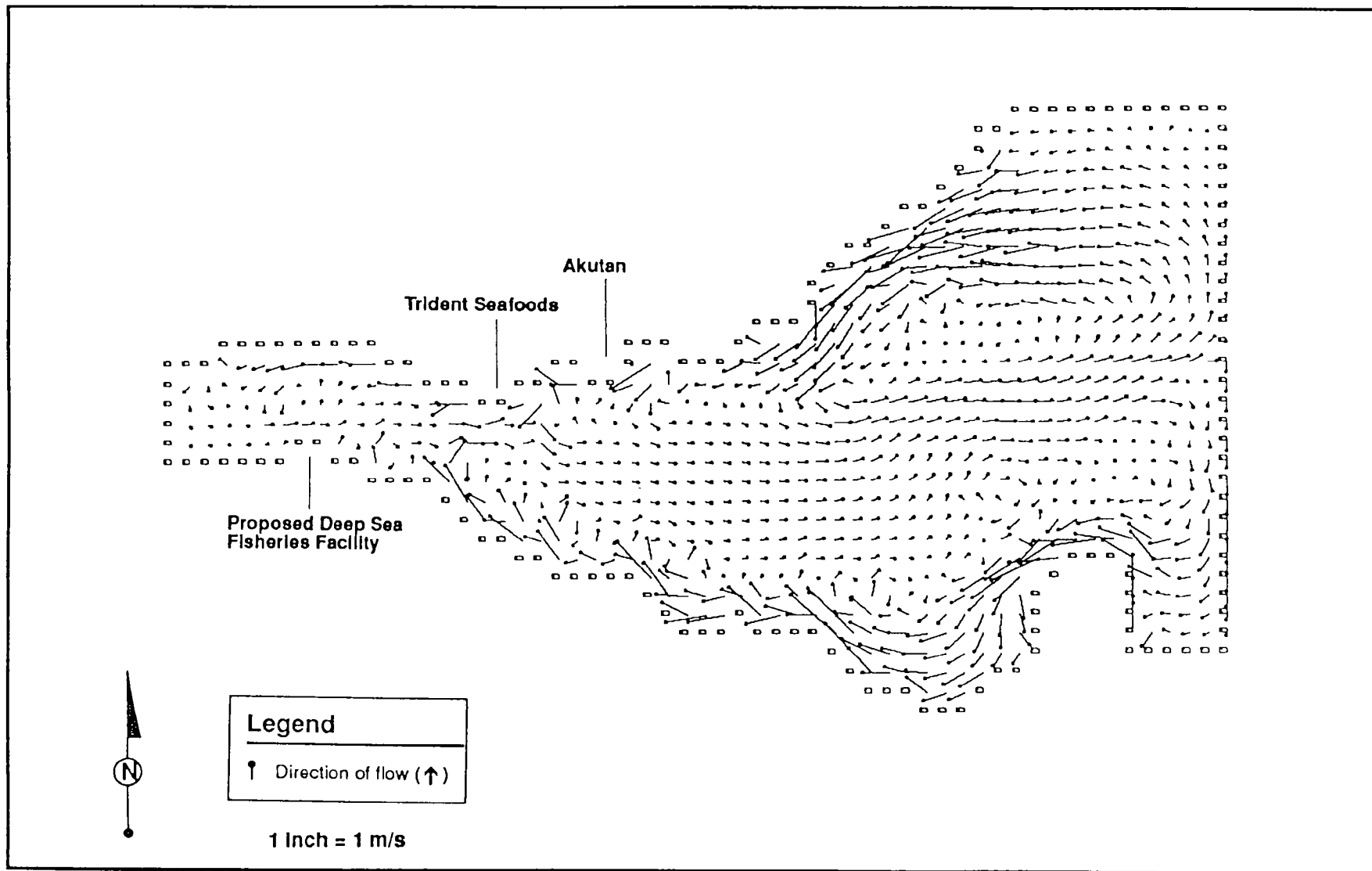
Figure B-6. Predicted Circulation Pattern in Akutan Harbor, Alaska, 4 Hours after the Onset of a 20 m/s East Wind
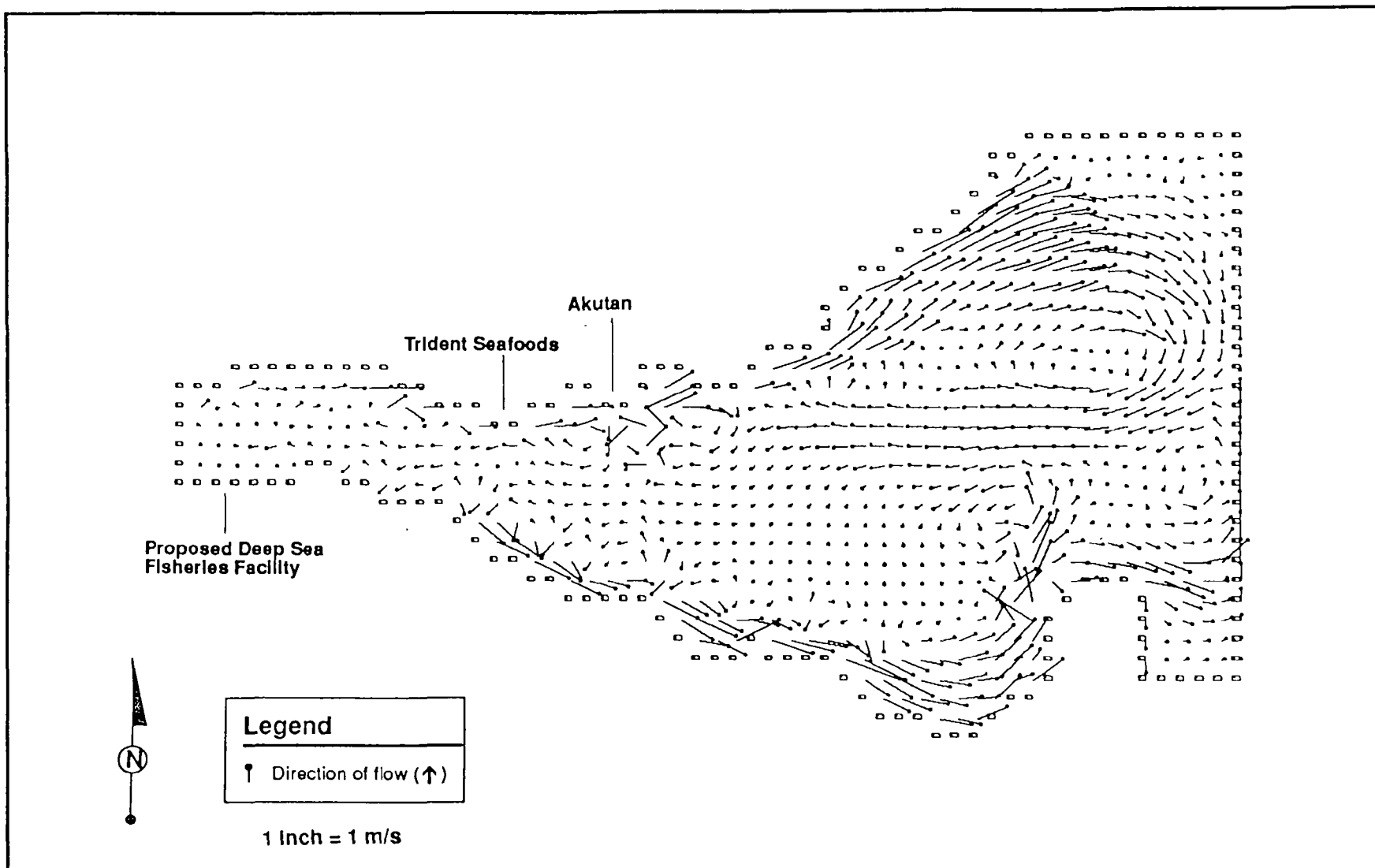
Figure B-7. Predicted Circulation Pattern in Akutan Harbor, Alaska, 4 Hours after the Onset of a 20 m/s West Wind
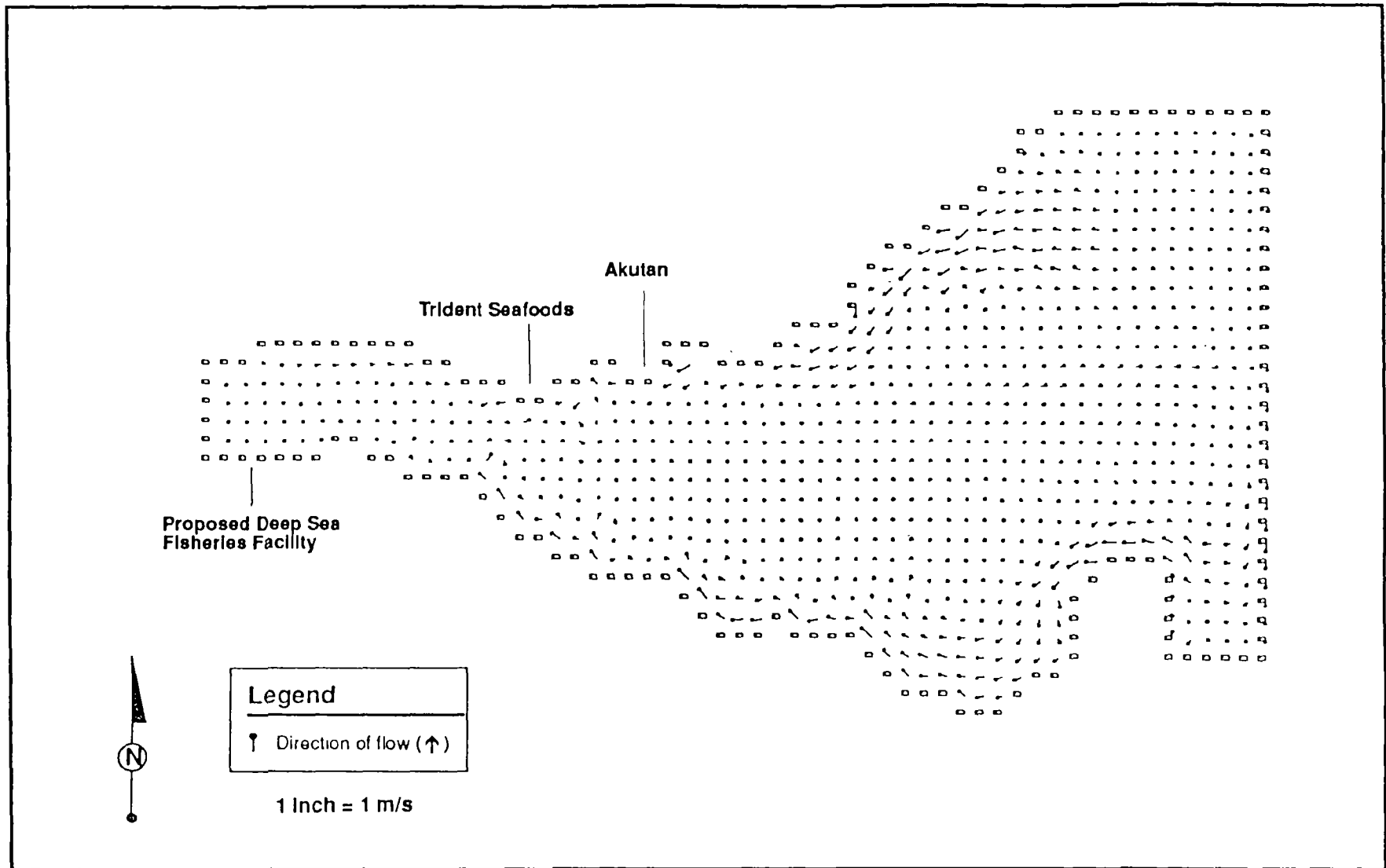
Figure B-8. Predicted Circulation Pattern in Akutan Harbor, Alaska, 32 Hours after the Onset of a 5 m/s East Wind
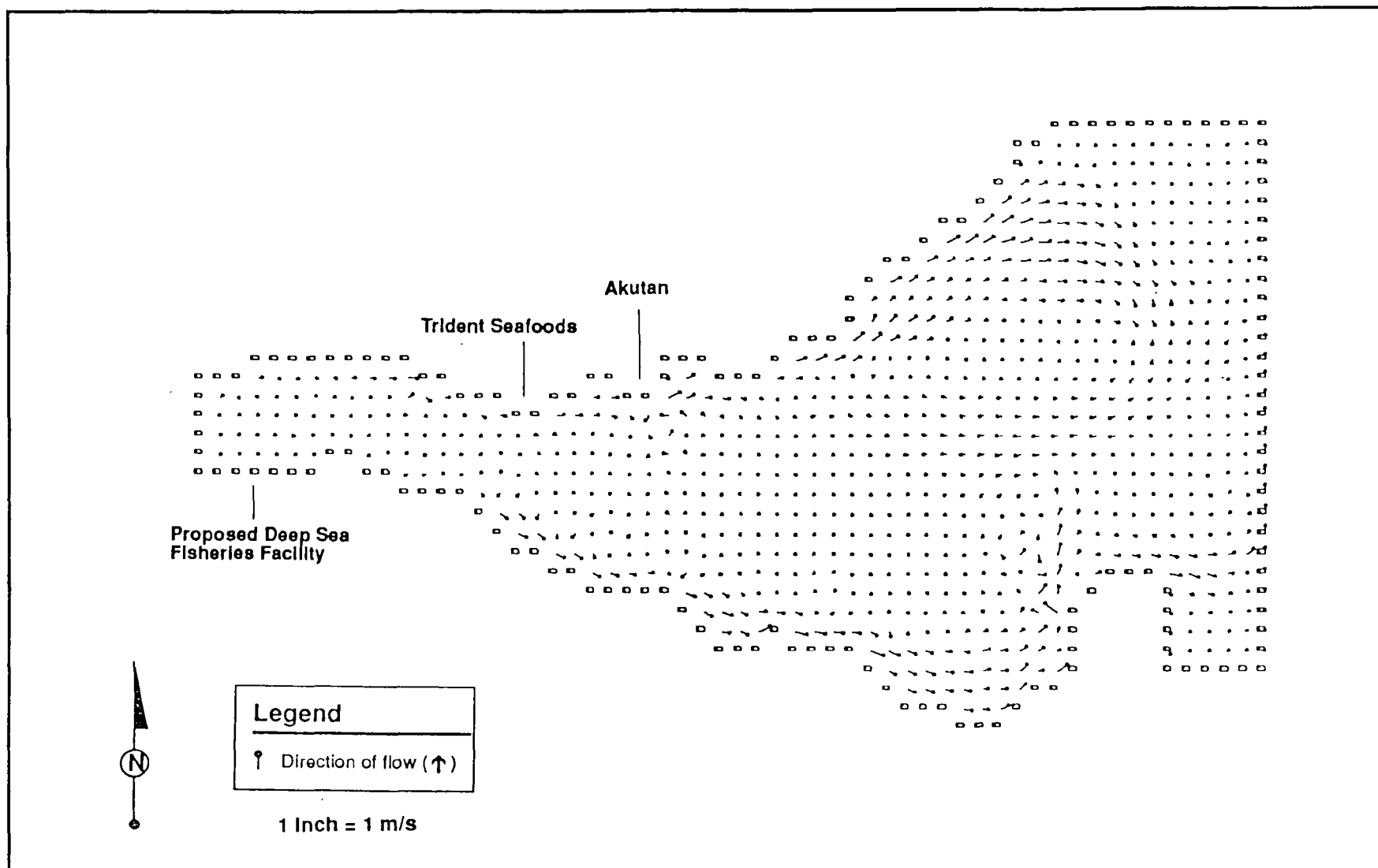
Figure B-9. Predicted Circulation Pattern in Akutan Harbor, Alaska, 32 Hours after the Onset of a 5 m/s West Wind

harbor. The model predicted that this cell would have a counterclockwise circulation pattern with inflowing waters occurring along the north shore between Trident Seafoods and the head of the harbor. The flows tend to be eastward near the old whaling station.

The expected increase in sea level resulting from east winds is shown in Figure B-10. The changes in the slope in the figure, which represent differences in sea level increases from east to west in the harbor, occur at constricting points in the harbor geometry (i.e., near the Trident Seafoods facility where the north-south width of the harbor is reduced). This figure also indicates a separation between inner and outer harbor circulation patterns as shown by the difference in the slopes of the sea level curves in the inner and outer harbor.

Figure B-10 also illustrates the theoretical solution expected from the model if the basin were of constant depth and rectangular in shape. In this case the equations can be solved analytically. The slope is:

$$\frac{\partial \eta}{\partial \chi} = 0.5 * C_w * W_s{}^2/gh$$

where C_w is the wind stress coefficient, W_s is the wind speed, g is gravity, and h is the constant water depth. To calculate the slope for the rectangular basin, a wind stress coefficient of 0.000005, a wind speed of 20 m/s, and a depth of 50 m were used. Because Akutan Harbor has a funnel shape, the sea surface has a greater slope in the model based on the actual geometry than it would have for a rectangular basin.

Figure B-6 illustrates the predicted depth-averaged currents in Akutan Harbor for 20 m/s east wind conditions. To interpret these averaged currents in terms of surface and bottom currents, it is necessary to examine individual velocity profiles as they relate to the depth-averaged currents generated by the model. The vertical distribution of currents for three values of the depth-averaged currents are shown in Figures B-11, B-12, and B-13. The velocity profiles are calculated for a 20 m/s easterly wind. A near zero velocity has a peak negative current (opposite to the wind direction) of about -6.0 cm/s. A mean current of -3.0 cm/s (opposite to the wind direction) has a peak negative current of -8.5 cm/s, and a mean current of 3 cm/s in the direction of the wind has a peak negative current of -4 cm/s.

Although not constituting a full verification of the model, these currents are of the magnitudes indicated in Figures B-2 through B-4. The current meters were located about 10 to 15 m off the bottom. In the nondimensional depth coordinates used in Figures B-2 through B-4, this puts the current meters near the depths of maximum reverse flows.

Moderately Strong Westerly Winds. Under moderately strong west wind conditions, the model predicts that the developing circulation east of the town of Akutan would have a net (depth averaged) westward flux of water in most of the central basin (Figure B-7). The net outflowing (easterly) waters are confined to the north and south shores within the outer harbor. The model also predicted, as with the east wind simulations,
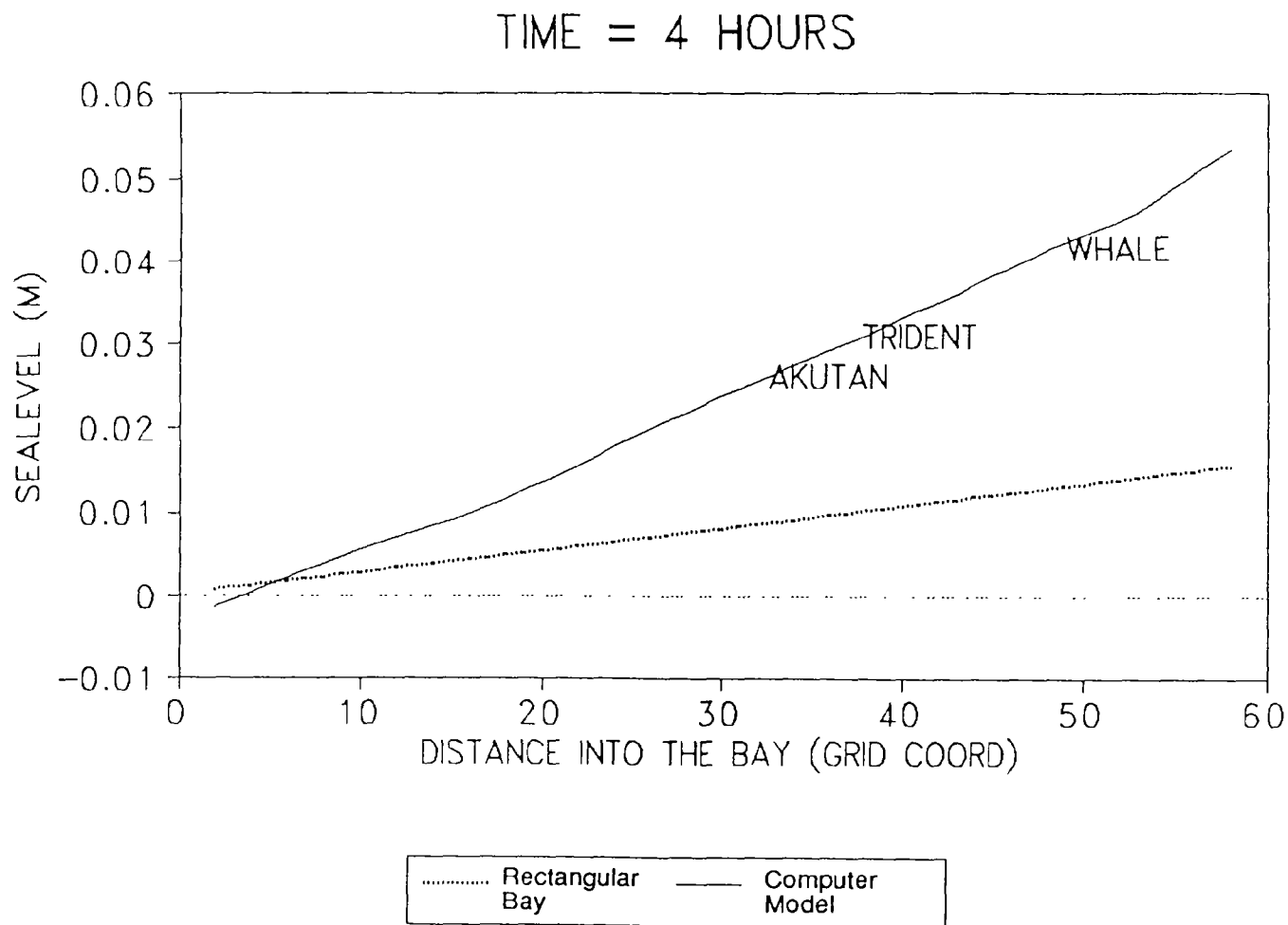
Figure B-10. Predicted Sea Levels Resulting from a 20 m/s East Wind along a Midchannel Transect in Akutan Harbor, Alaska
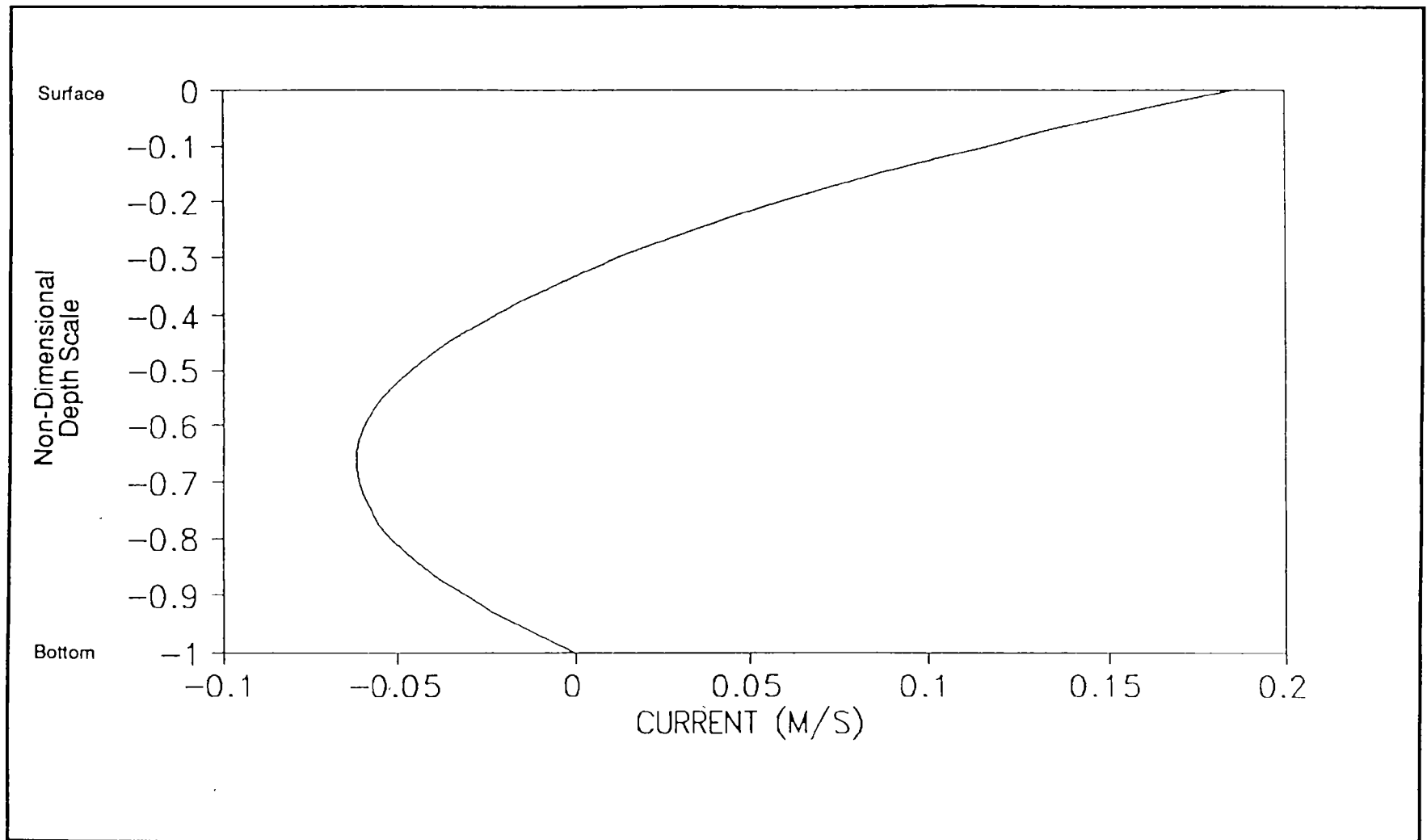
Figure B-11. Predicted Vertical Current Distribution in Akutan Harbor with a Mean Current Velocity of Near 0.0 cm/s

Note: Flow opposite of wind direction.
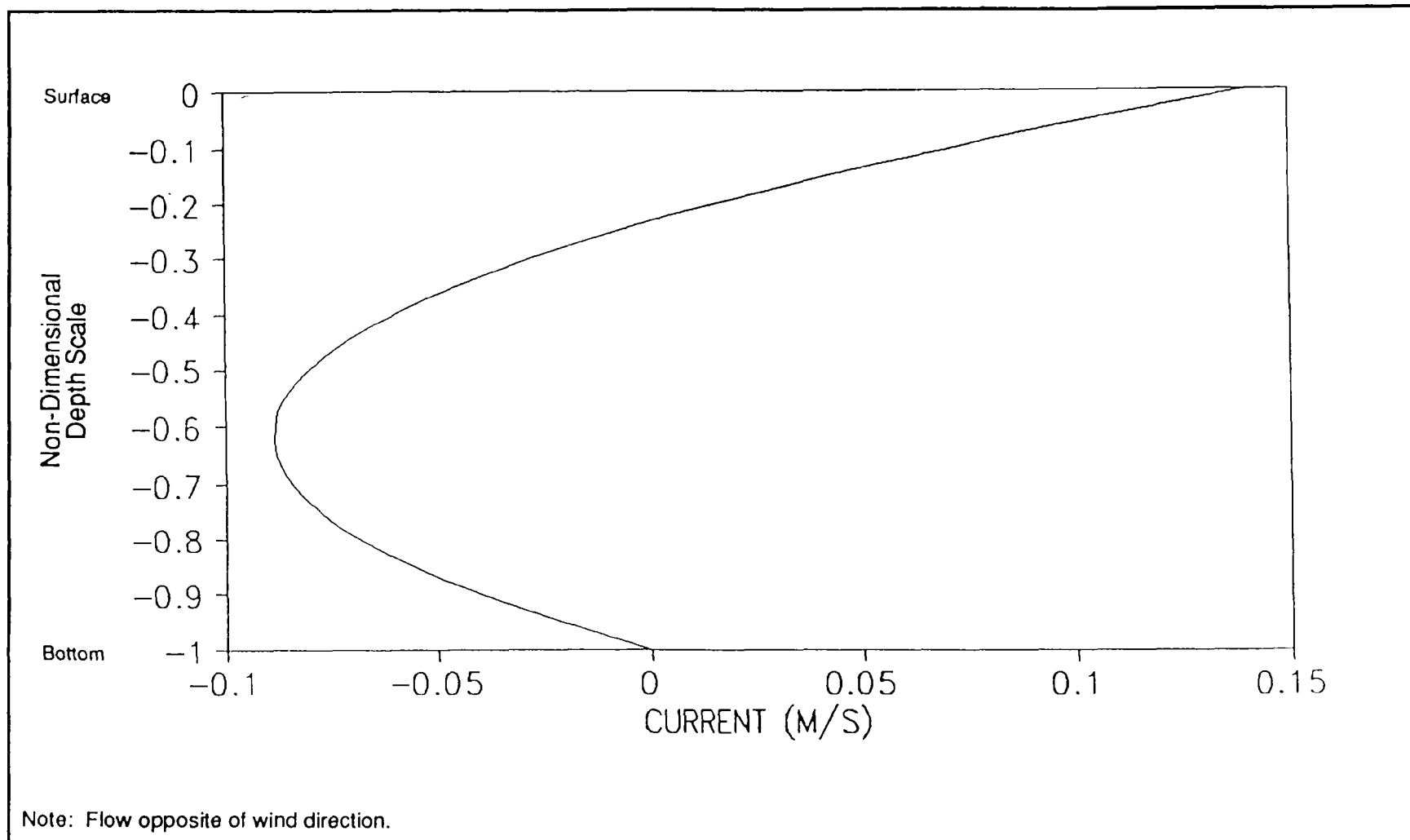
Figure B-12. Predicted Vertical Current Distribution in Akutan Harbor with a Mean Current Velocity of -0.3 cm/s
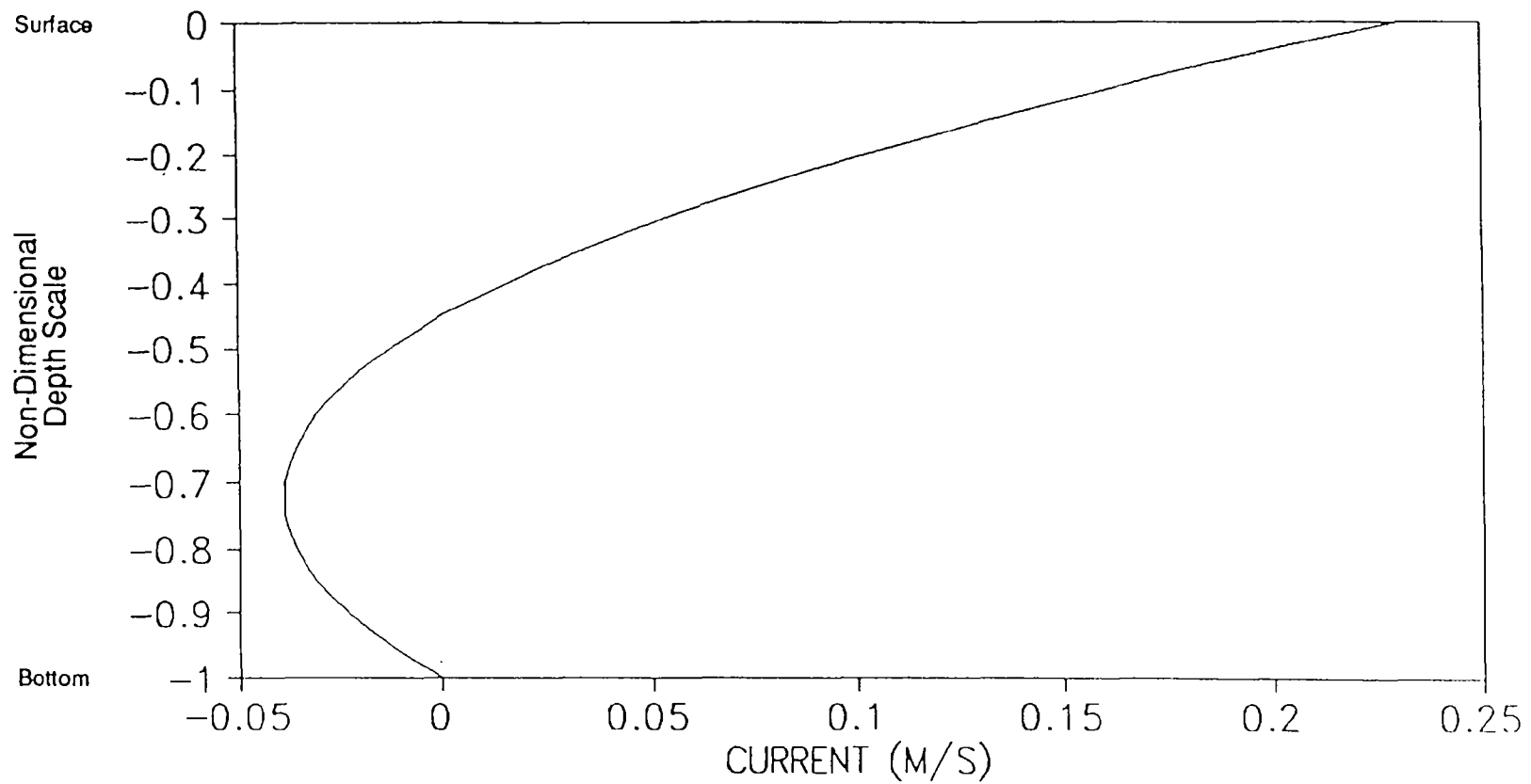
Figure B-13. Predicted Vertical Current Distribution in Akutan Harbor with a Mean Current Velocity of 0.3 cm/s

that the circulation in the inner bay, west of Trident Seafoods, would be somewhat isolated from the outer harbor circulation. With a west wind, the inner harbor cell is predicted to have a clockwise circulation pattern with net outflowing waters along the north shore between Trident Seafoods and the head of the harbor. Under these wind conditions, the net westerly flows tend to be near the proposed Deep Sea Fisheries outfall.

The expected changes in sea level resulting from west winds are shown in Figure B-14. As with the east wind condition, the changes in the slope on the figure occur at constricting points in the bay. However, in contrast to the east wind condition, the sea levels decrease toward the head of the harbor. The figure also indicates a separation between inner and outer harbor circulations. As with the easterly wind simulation, the separation is indicated by the difference in the slopes of the sea level curves between the inner and outer harbor.

Figure B-14 also illustrates the theoretical solution expected from the model if the basin were of constant depth and rectangular in shape. In this case the equations can be solved analytically. The slope is:

$$\frac{\partial \eta}{\partial \chi} = -0.5 * C_w * W_s{}^2/gh$$

where C_w is the wind stress coefficient, W_s is the wind speed, g is gravity, and h is the constant water depth. To calculate the slope for the rectangular basin, a wind stress coefficient of 0.000005, a wind speed of 20 m/s, and a depth of 50 m were used. Because the geometry of Akutan Harbor fans out toward the mouth of the harbor, the sea surface has a greater slope in the model based on the actual geometry than it would have for a rectangular basin.

Model Discussion. The following discussions are based on model simulations using a 20 m/s wind from the east. The model predicts depth-averaged currents within the harbor. Model calculations are carried out for a period of 4 hr from the onset of the wind. The development of the depth-averaged velocities over time at the two current meter stations is shown in Figures B-15 and B-16. The figures show that, immediately after the onset of the winds, there is a wave-like oscillation in the currents. This "wave" has a period of about 20 min.

We hypothesize that this periodicity results from oscillations caused when a wind event is impulsively initiated at the wind velocity being evaluated, rather than building in strength to that velocity over some period of time. To test this hypothesis, the model was run with the wind speed rising linearly from zero to its maximum speed (20 m/s) over a period of 20 min. This analysis revealed that the gradually developing winds resulted in reduced amplitudes in the oscillations. The calculations for the gradually developing winds are used in this analysis.
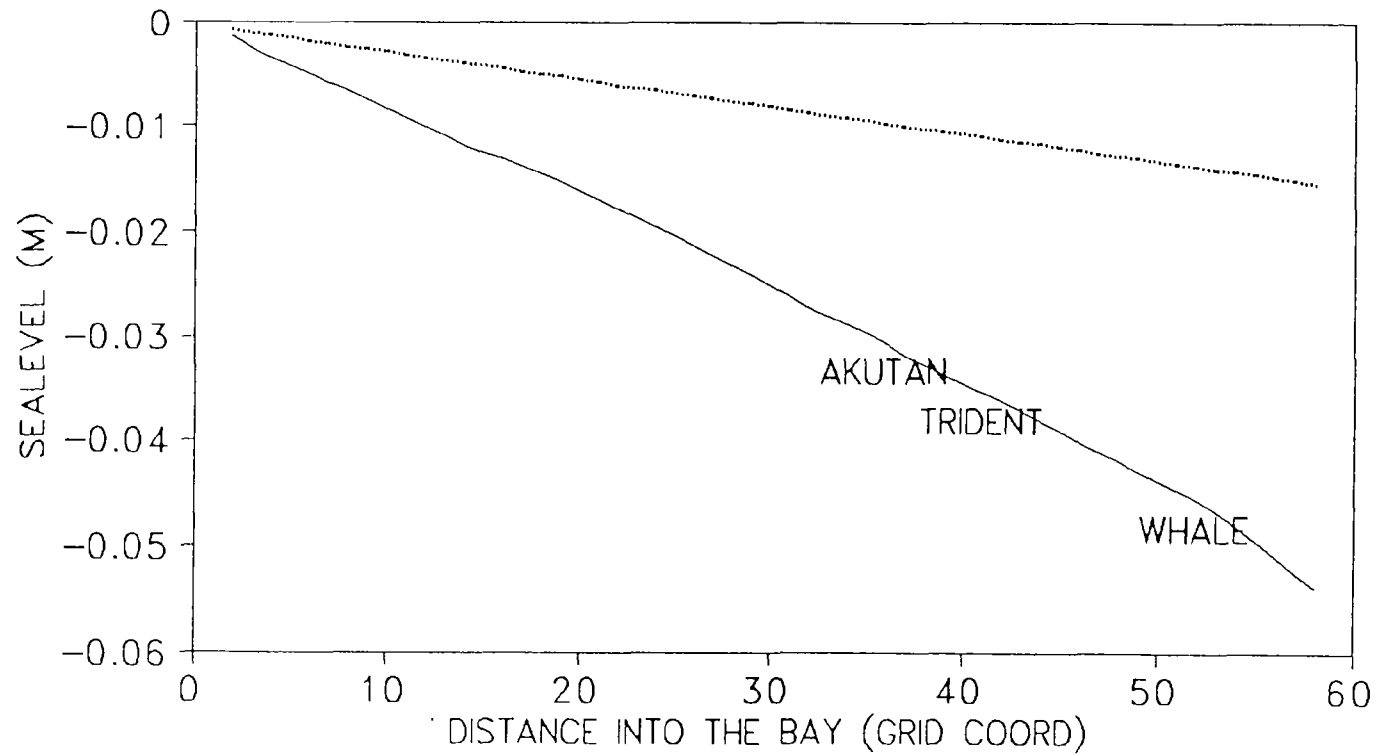
Figure B-14. Predicted Sea Levels Resulting from a 20 m/s West Wind along a Midchannel Transect in Akutan Harbor, Alaska
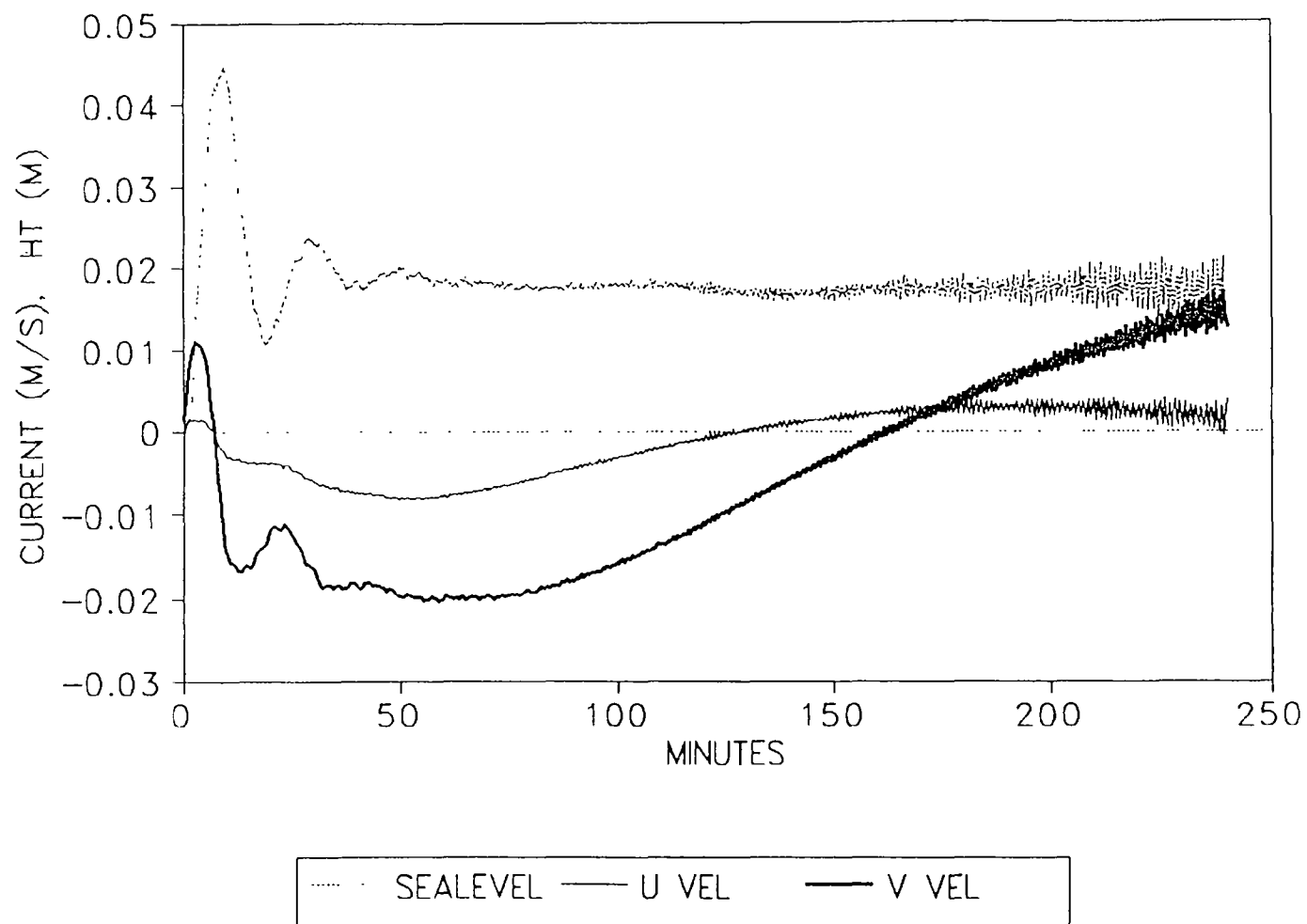
Figure B-15. Predicted Depth-Averaged Velocities Resulting from a 20 m/s East Wind at the Current Meter Mooring Near Trident Seafoods in Akutan Harbor
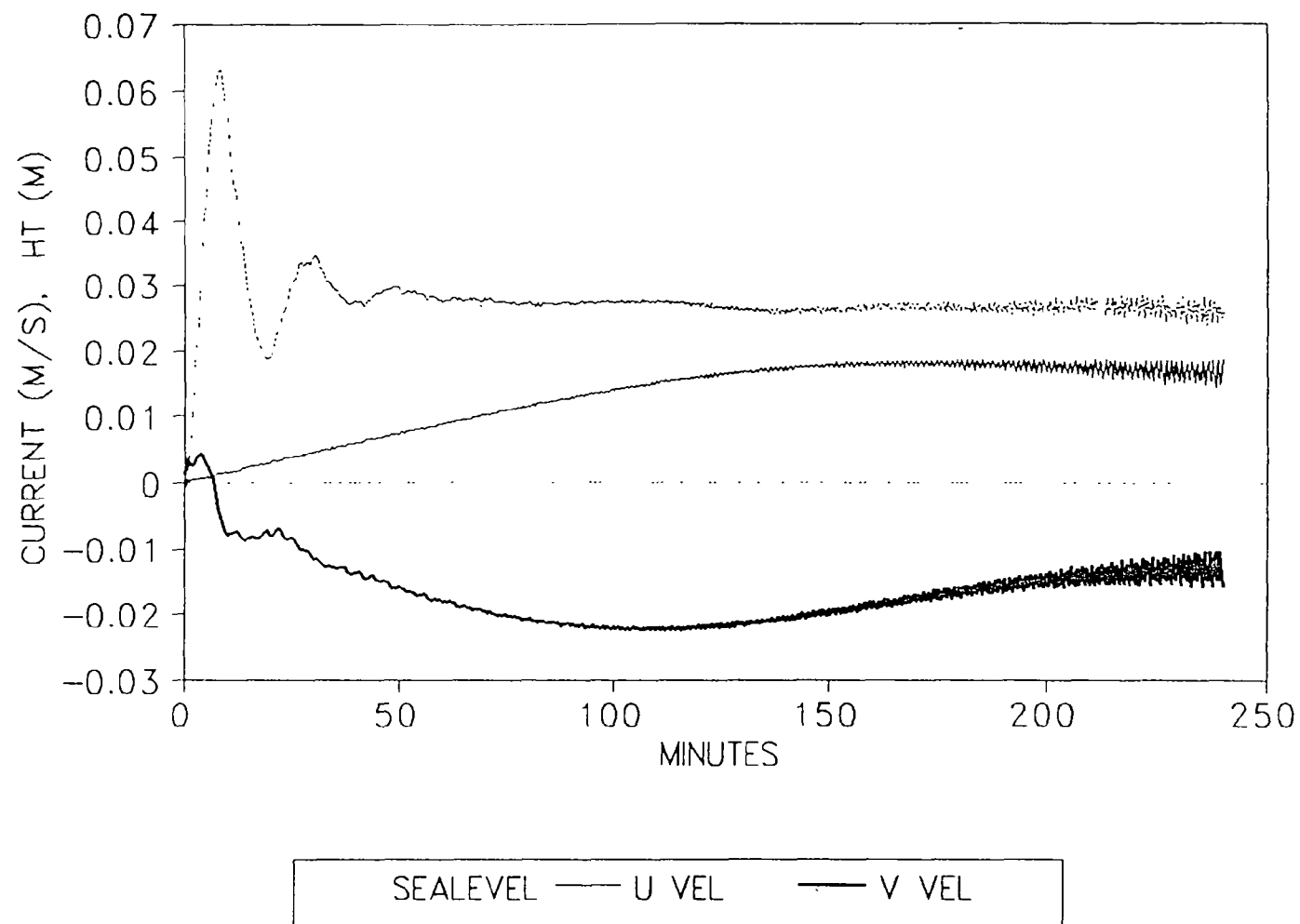
Figure B-16. Predicted Depth-Averaged Velocities Resulting from a 20 m/s East Wind at the Current Meter Mooring Near the Proposed Deep Sea Fisheries Outfall in Akutan Harbor

The natural seiche period for a long narrow basin is given by Meriam's formula as $2l/(gh)^{1/2}$, where l is the length of the estuary, g is a gravitational constant, and h is the mean depth of the water (Ippen 1966). For Akutan Harbor, this period is about 11.3 min. This is less than the 20 min signal observed in the numerical model; however, Meriam's formula is known to underestimate the resonant periods of harbors open to the ocean (Ippen 1966).

Figure B-17 shows the spectrum of the observed east and west currents for the current meter near Trident Seafoods. The time period is for days 102 to 105. The spectrum shows peaks at frequencies between 1 and 1.5 cycles/hr. The sampling rate for the currents was every 15 min. Therefore, a 22 min signal would be aliased (Bloomfield 1976). It would be expected to show up at an aliased frequency of 1.28 Hz. This is the frequency at which we see energy in the spectrum illustrated in the figure. This demonstrates that the seiching predicted by the model is consistent with the observed seiching in the harbor. However, because the magnitudes of the currents associated with the seiching are small (< 1.0 cm/s), seiching would be an unimportant factor in the design of the proposed outfall.

At high wind speeds, the model develops a numerical instability as it is run for time periods in excess of 4 hr. As time progresses, the model tries to create eddies (i.e., the winds drive the model system to turbulence) near the headlands on the south shore (south of the Trident Seafoods facility). The horizontal scale of the turbulence is, at least initially, the size of the headlands. The numerical resolution of the model (128 m) is insufficient for flows on these small scales; therefore, an instability develops. We have no direct knowledge of whether headland eddies form in Akutan Harbor during storm events. If headland eddies do develop in Akutan Harbor, their effect would be to diminish the nearshore transports by diffusing wind energy as turbulence rather than contributing energy to long-shore currents. As a practical matter, we have no choice but to terminate the calculations before the instabilities dominate the solutions. One way to cure the instability is to decrease the resolution with which the harbor is defined (smoother boundaries). Because this option removes some of the important headland features, we chose instead to truncate the run time of high wind speed models to 4 hr. This time is sufficient to evaluate the effects of moderate storms on currents in the harbor.

Effects of Quiescent Wind Conditions on Circulation

When the winds are weak, the development and strength of eddy patterns in the circulation is reduced (Figures B-8 and B-9). Under these conditions, the model is numerically stable for long periods. Runs of 32 hr are used to describe the quiescent flows in Akutan Harbor. As expected, the model simulations indicated very little net water transport within the harbor. These model runs were used in conjunction with the WASP model for predicting dissolved oxygen concentrations (see Appendices L and M).
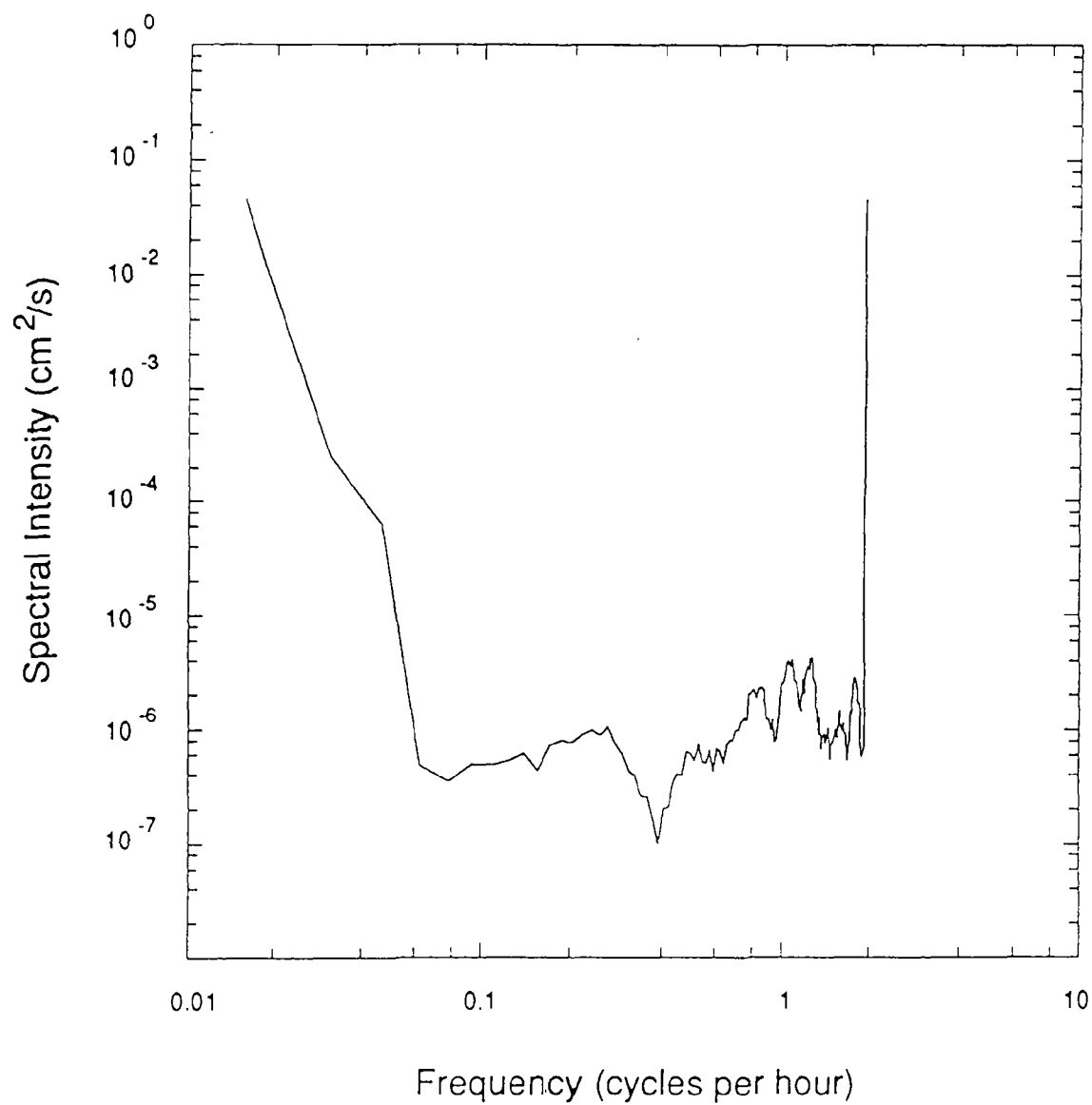
Figure B-17. Spectrum of the Observed East and West Currents in Akutan Harbor, Alaska

Appendix C.   Current Meter Data Supplied by Evans-Hamilton, Inc.
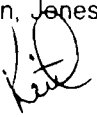
DATE.   June 11, 1992

TO.   Rick Oestman, Jones & Stokes Associates, Inc

FROM: Keith Kurrus

SUBJECT.   Akutan Current Meter Data

EHI JOB FILE: 289

Rick:

Enclosed are two sets of data files on IBM 3.5 HD floppies File names 718.dat, 3180 dat, and 7315.dat are the data from each current meter directly from the tape dump, these files are still in "Aanderaa" units. File name 718.fin, 3180.fin, and 7315.fin are the final data files for each current meter in engineering units. These files have been edited to remove the data before and after the deployment when the current meters were not in the water. The *.fin files are ASCII, sequential data files with each line containing the following parameters.

PARAMETER	UNITS
Year	
Julian Day	
Hour	Alaska Local Time
Minute	Alaska Local Time
Pressure	PSIG
Depth	Meters
Temperature	Degrees Celsius
Conductivity	mmho/cm
Salinity	PPT
Density	Sigma-t
X Component	cm/sec
Y Component	cm/sec
Direction	Degrees True
Speed	cm/sec
Vr	
Tilt	
Hdg	

The last three parameters do not apply to Aanderaa current meters and just contain zeros for place holders

I have included the pre-deployment calibration sheets, the field logs for each current meter, and the data plots for each current meter Meter number 718 was on mooring #1 off of Trident, and meter numbers 3180 and 7315 were on mooring #2 off the proposed Deep Sea outfall (3180 was the top meter on the mooring and 7315 the bottom meter)

It looks like I will be going to China this weekend for approximately two weeks. If you have any

questions or need further help while I am gone, please contact Carol Coomes and she will be available to help you   Thanks for the work

Cheers!
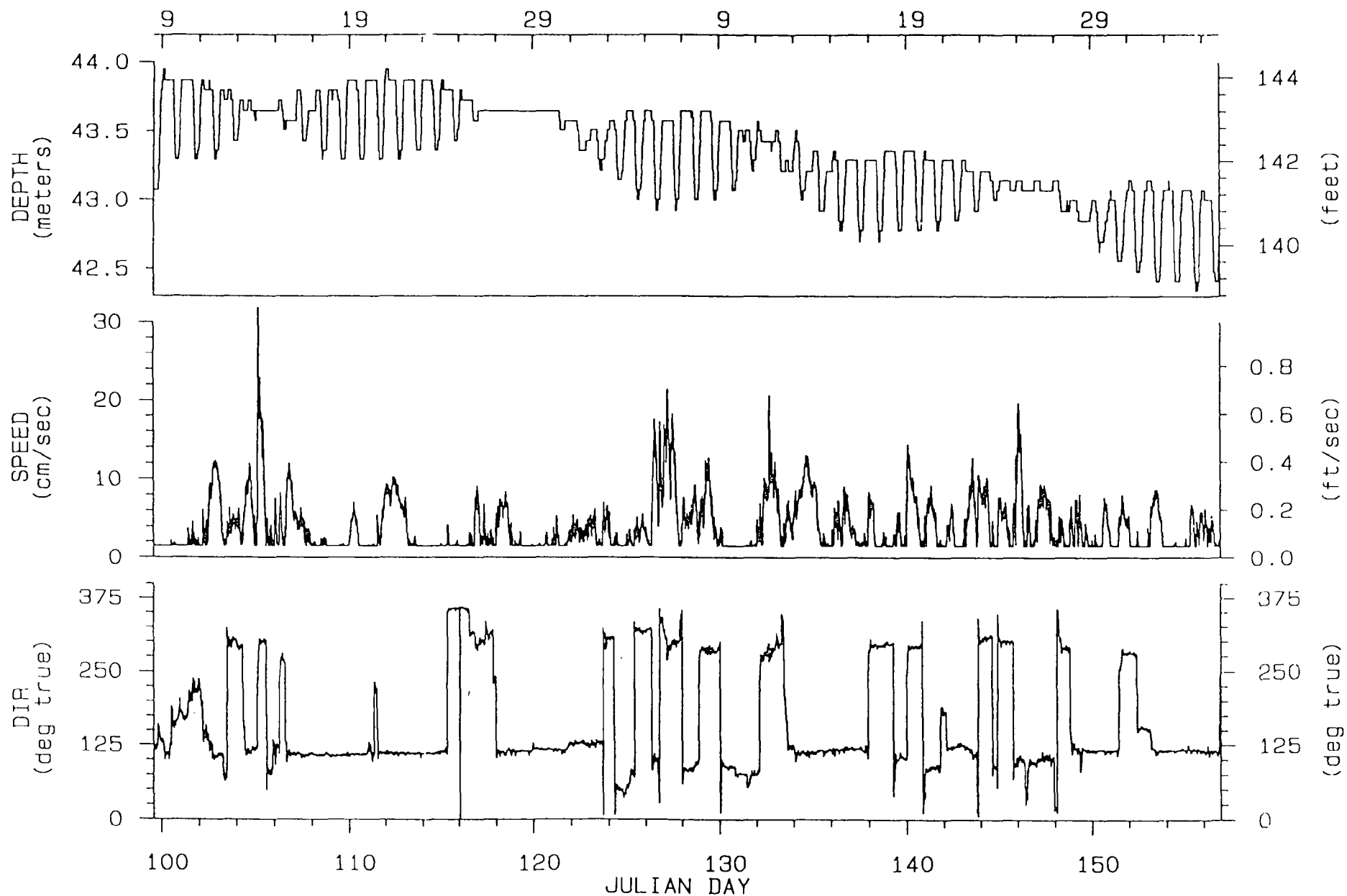
57 DAY SERIES BEGINNING APRIL 9, 1992

Mooring #1 (Trident) - S/N 718
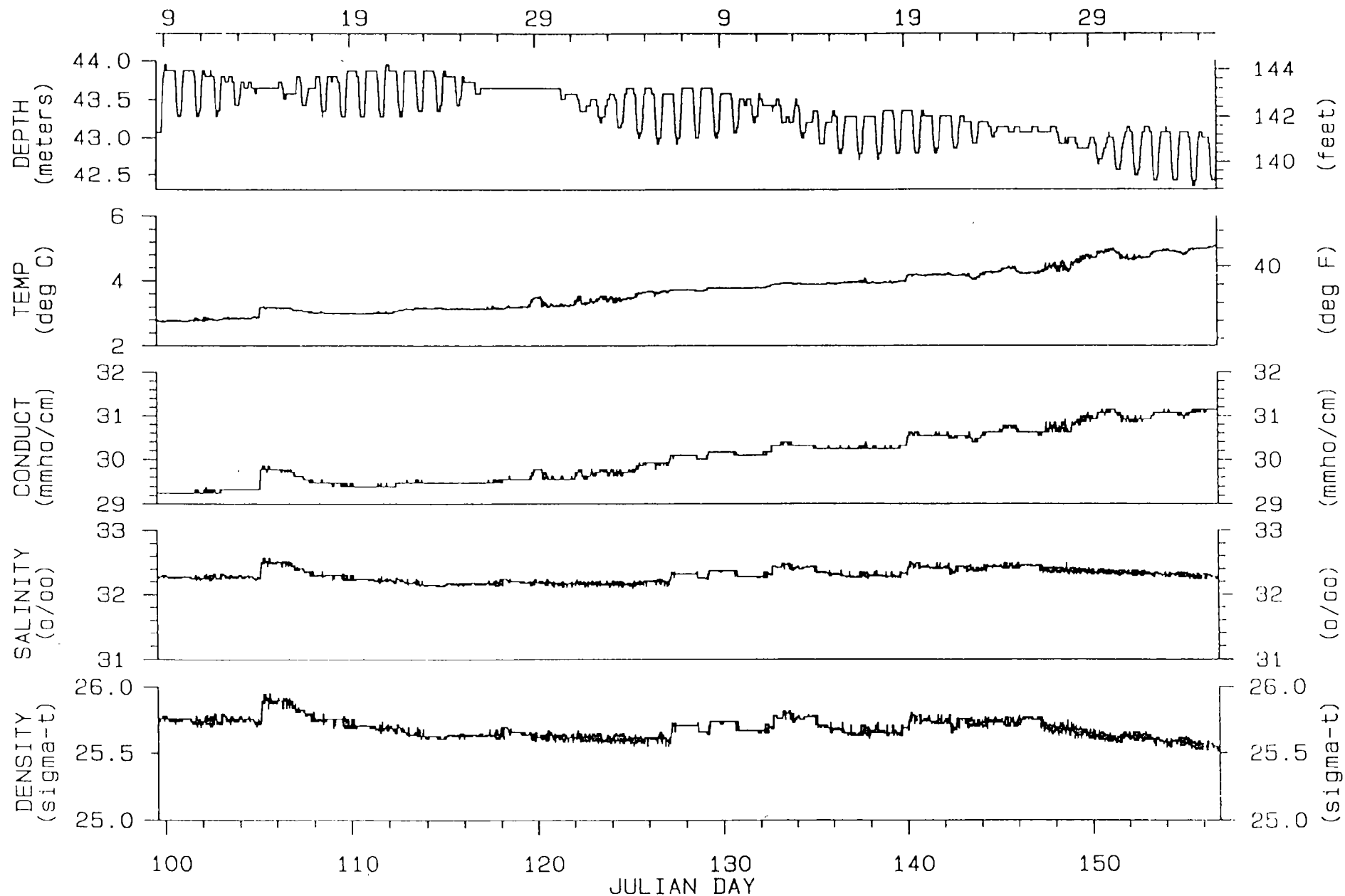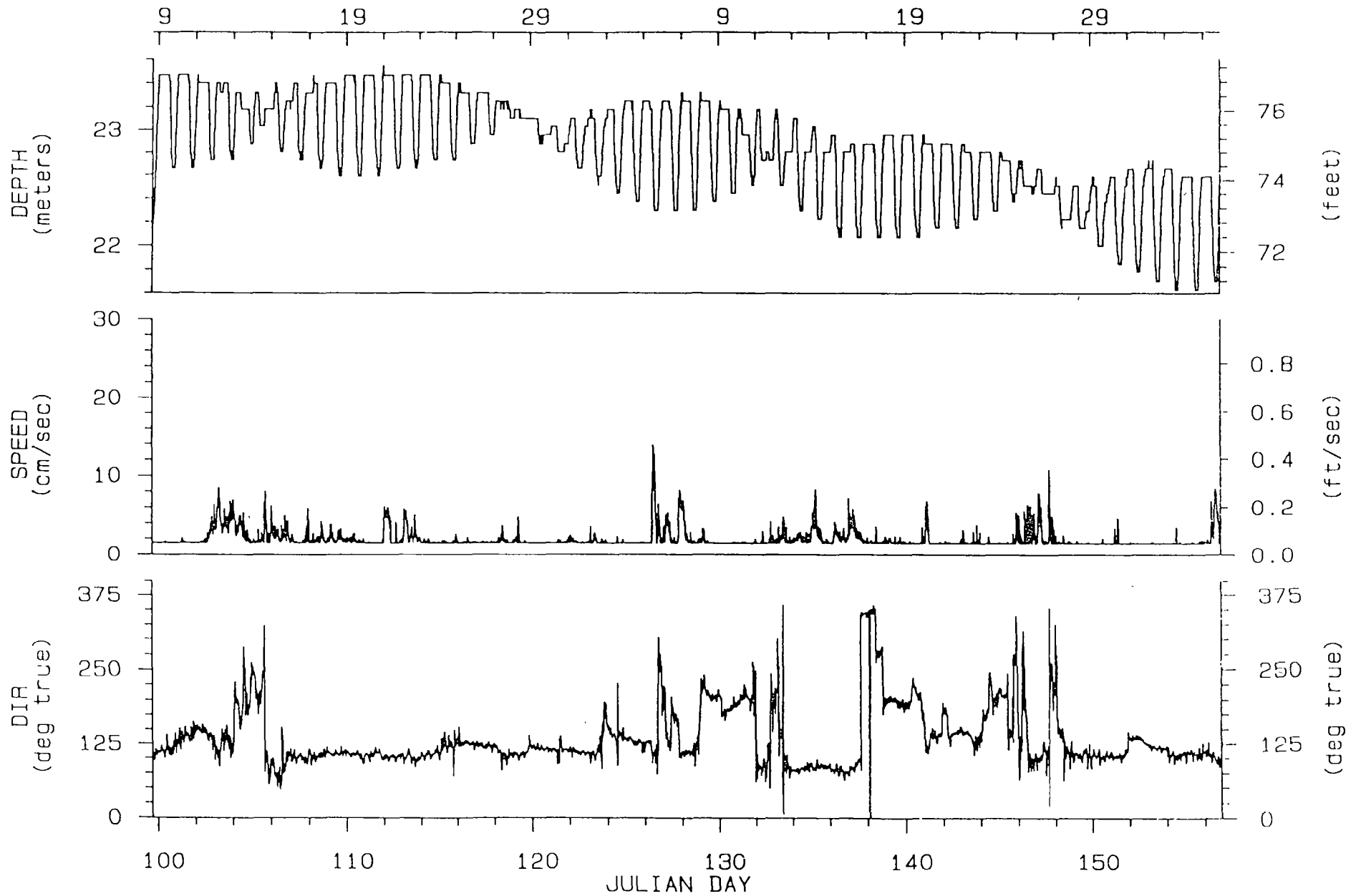
57 DAY SERIES BEGINNING APRIL 9, 1992

JULIAN DAY

Mooring #1 (Trident) - S/N 718

57 DAY SERIES BEGINNING APRIL 9, 1992

Mooring #2 (Deep Sea Fisheries) – S/N 3180

57 DAY SERIES BEGINNING APRIL 9, 1992
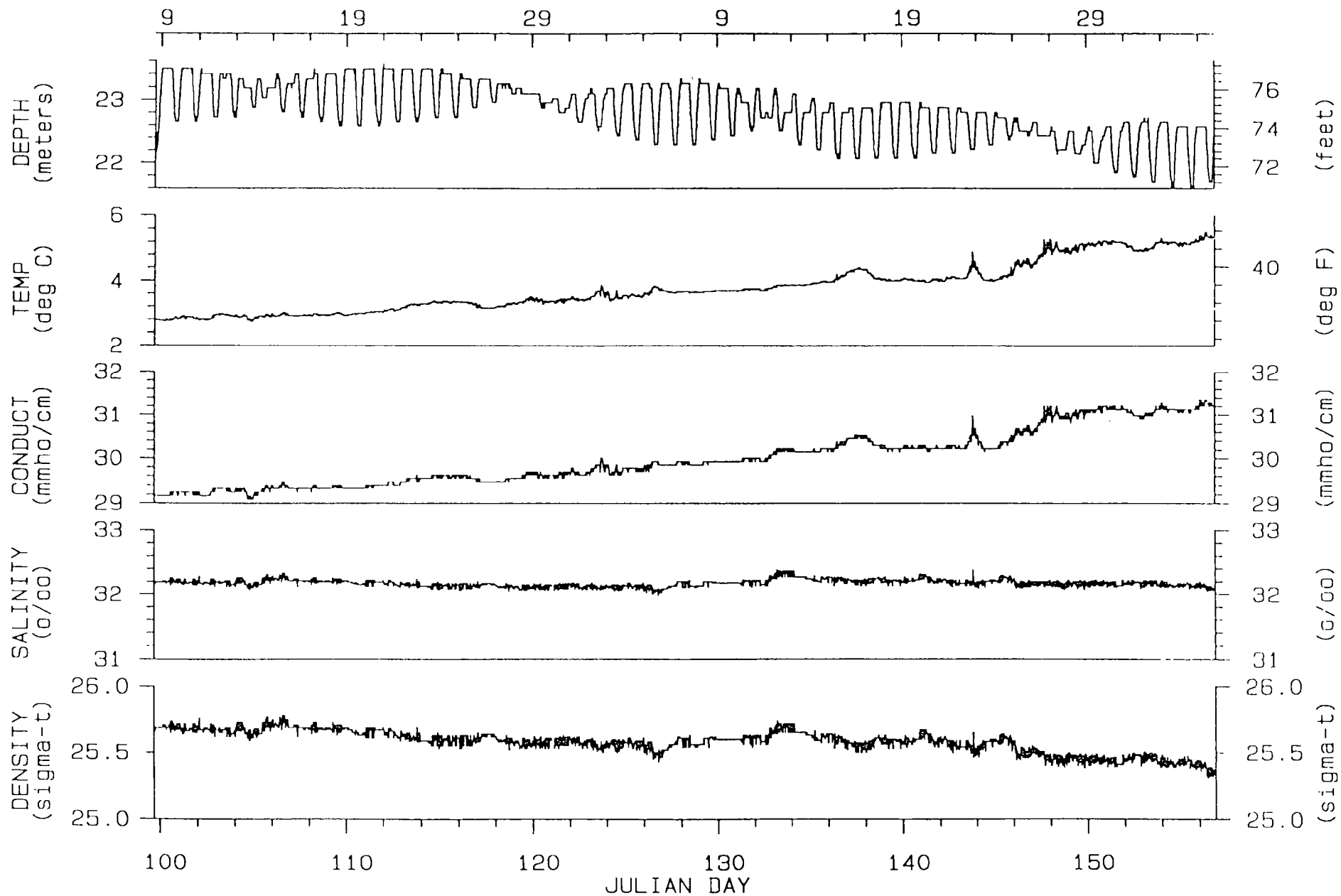
Mooring #2 (Deep Sea Fisheries) - S/N 3180

57 DAY SERIES BEGINNING APRIL 9, 1992
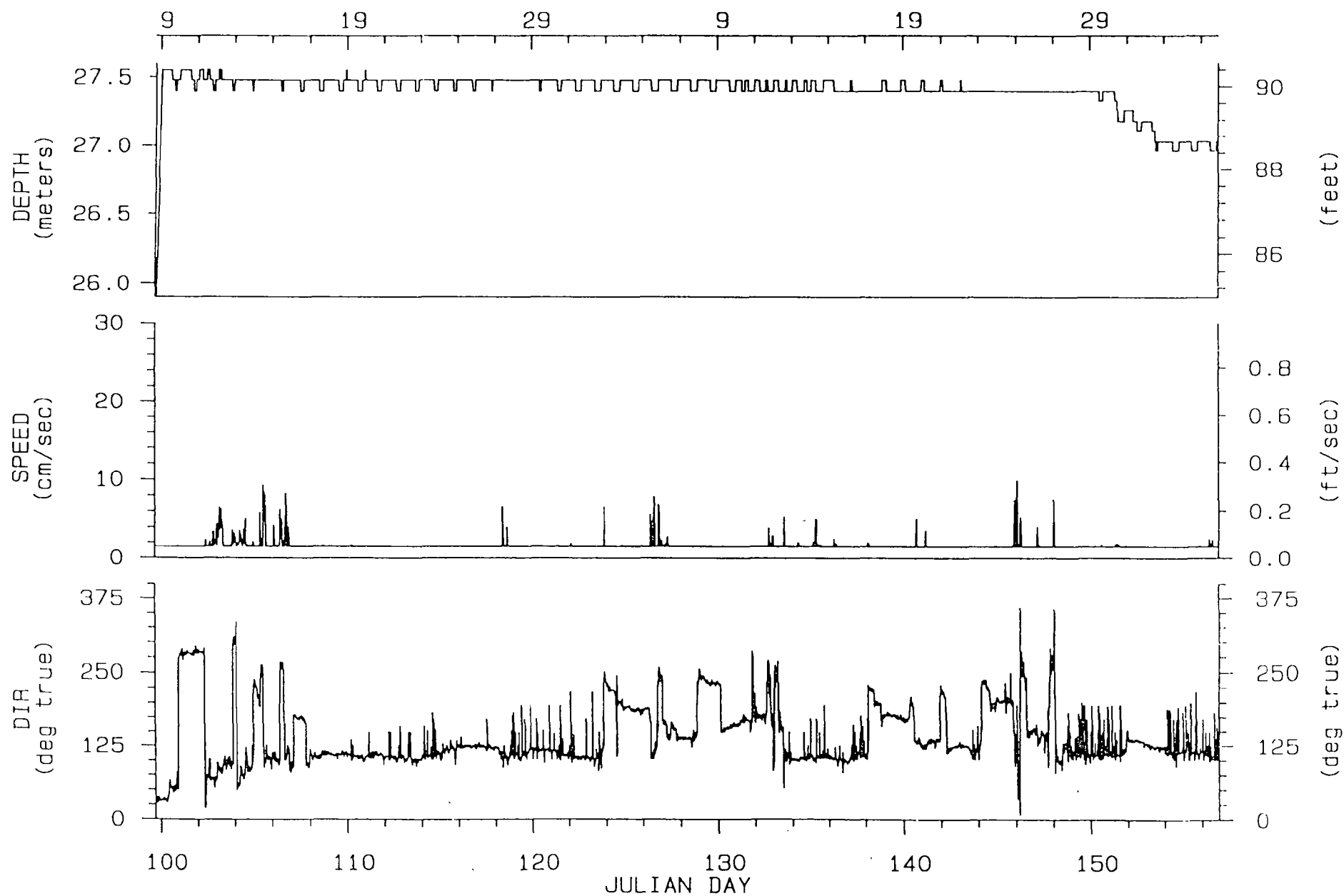
Mooring #2 (Deep Sea Fisheries) – S/N 7315

57 DAY SERIES BEGINNING APRIL 9, 1992
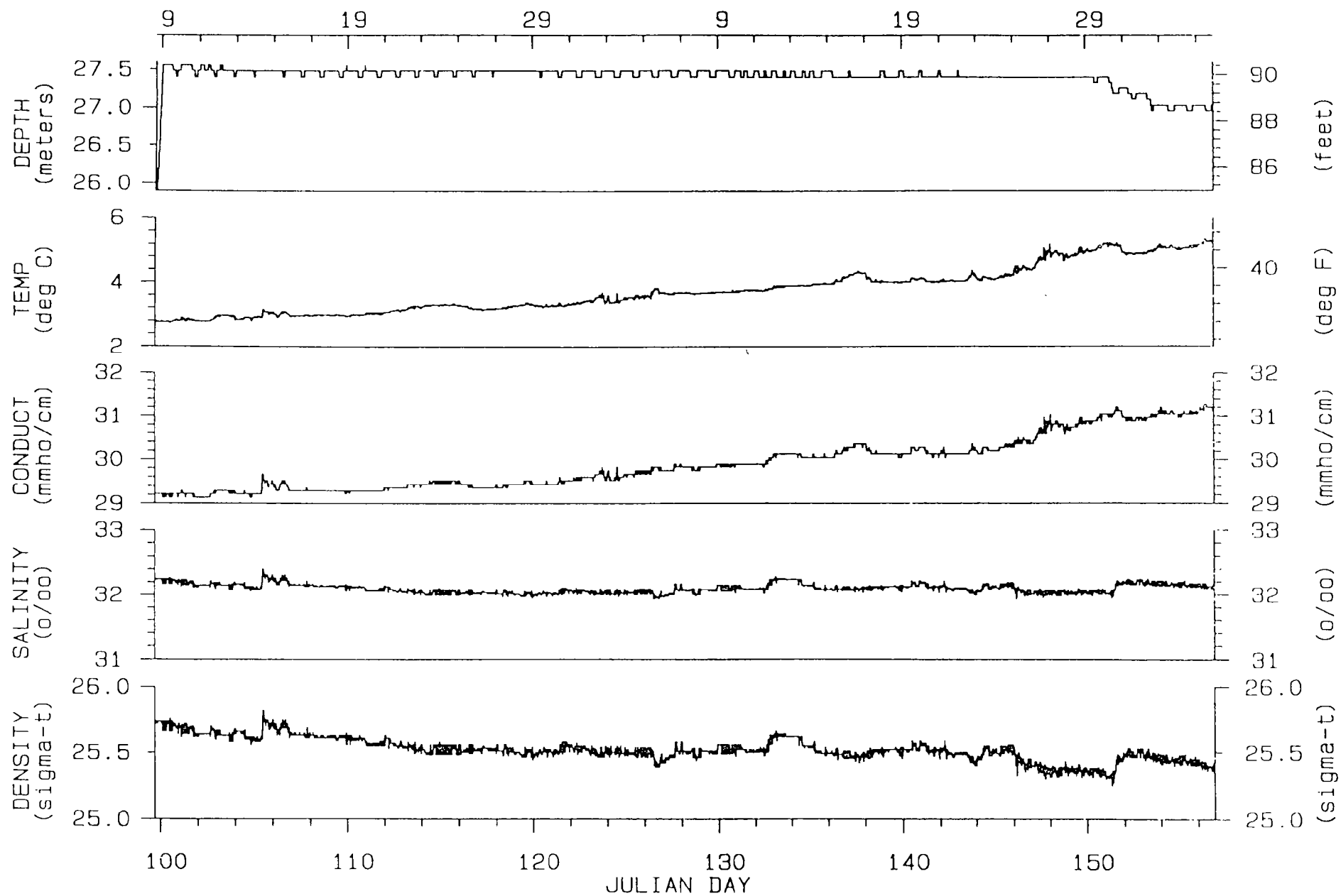
Mooring #2 (Deep Sea Fisheries) - S/N 7315

PERCENT OCCURRENCE OF CURRENT SPEED VERSUS CURRENT DIRECTION
LOCATION: Mooring #1 (Trident) - S/N 718
DATE: 4/8 - 6/4/92
DEPTH: 44 Meters
NUMBER OF OBSERVATIONS: 5504

DIRECTION (DEGREES TRUE)

SPEED CM/SEC	0-20	20-40	40-60	60-80	80-100	100-120	120-140	140-160	160-180	180-200	200-220	220-240	240-260	260-280	280-300	300-320	320-340	340-360	TOTAL
0 - 5	0.49	0.47	1.73	3.27	4.74	30.90	7.59	2.31	1.40	1.07	0.96	0.96	0.38	1.54	5.60	4.69	1.11	2.45	71.68
5 - 10	0.00	0.05	0.00	0.15	2.82	11.50	1.02	0.07	0.00	0.00	0.00	0.02	0.16	0.65	3.96	1.94	0.18	0.07	22.60
10 - 15	0.00	0.00	0.00	0.00	0.40	1.98	0.00	0.00	0.00	0.00	0.00	0.00	0.02	0.22	1.29	0.31	0.07	0.02	4.31
15 - 20	0.00	0.00	0.00	0.00	0.13	0.15	0.00	0.00	0.00	0.00	0.00	0.00	0.00	0.13	0.40	0.29	0.11	0.02	1.22
20 - 25	0.00	0.00	0.00	0.00	0.00	0.00	0.00	0.00	0.00	0.00	0.00	0.00	0.00	0.05	0.04	0.04	0.00	0.00	0.13
25 - 30	0.00	0.00	0.00	0.00	0.00	0.00	0.00	0.00	0.00	0.00	0.00	0.00	0.00	0.02	0.02	0.02	0.00	0.00	0.05
30 - 35	0.00	0.00	0.00	0.00	0.00	0.00	0.00	0.00	0.00	0.00	0.00	0.00	0.00	0.00	0.02	0.00	0.00	0.00	0.02
35 - 40	0.00	0.00	0.00	0.00	0.00	0.00	0.00	0.00	0.00	0.00	0.00	0.00	0.00	0.00	0.00	0.00	0.00	0.00	0.00
40 - >	0.00	0.00	0.00	0.00	0.00	0.00	0.00	0.00	0.00	0.00	0.00	0.00	0.00	0.00	0.00	0.00	0.00	0.00	0.00
TOTAL	0.49	0.53	1.73	3.42	8.09	44.53	8.61	2.38	1.40	1.07	0.96	0.98	0.56	2.62	11.32	7.29	1.47	2.56	100.00

PERCENT OCCURRENCE OF CURRENT SPEED VERSUS CURRENT DIRECTION

LOCATION: Mooring #2 (Deep Sea Fisheries) - S/N 3180

DATE: 4/8 - 6/4/92

DEPTH: 22 Meters

NUMBER OF OBSERVATIONS: 5495

DIRECTION (DEGREES TRUE)

SPEED CM/SEC	0- 20	20- 40	40- 60	60- 80	80- 100	100- 120	120- 140	140- 160	160- 180	180- 200	200- 220	220- 240	240- 260	260- 280	280- 300	300- 320	320- 340	340- 360	TOTAL
0 - 5	0.09	0.04	0.33	3.48	12.59	35.85	15.83	7.42	2.42	6.30	6.15	1.71	1.13	0.91	0.31	0.16	0.22	1.16	96.11
5 - 10	0.00	0.00	0.00	0.09	1.49	1.64	0.25	0.02	0.00	0.02	0.02	0.04	0.02	0.04	0.07	0.00	0.00	0.00	3.69
10 - 15	0.00	0.00	0.00	0.00	0.02	0.16	0.00	0.00	0.00	0.00	0.00	0.02	0.00	0.00	0.00	0.00	0.00	0.00	0.20
15 - 20	0.00	0.00	0.00	0.00	0.00	0.00	0.00	0.00	0.00	0.00	0.00	0.00	0.00	0.00	0.00	0.00	0.00	0.00	0.00
20 - 25	0.00	0.00	0.00	0.00	0.00	0.00	0.00	0.00	0.00	0.00	0.00	0.00	0.00	0.00	0.00	0.00	0.00	0.00	0.00
25 - 30	0.00	0.00	0.00	0.00	0.00	0.00	0.00	0.00	0.00	0.00	0.00	0.00	0.00	0.00	0.00	0.00	0.00	0.00	0.00
30 - 35	0.00	0.00	0.00	0.00	0.00	0.00	0.00	0.00	0.00	0.00	0.00	0.00	0.00	0.00	0.00	0.00	0.00	0.00	0.00
35 - 40	0.00	0.00	0.00	0.00	0.00	0.00	0.00	0.00	0.00	0.00	0.00	0.00	0.00	0.00	0.00	0.00	0.00	0.00	0.00
40 - >	0.00	0.00	0.00	0.00	0.00	0.00	0.00	0.00	0.00	0.00	0.00	0.00	0.00	0.00	0.00	0.00	0.00	0.00	0.00
TOTAL	0.09	0.04	0.33	3.57	14.10	37.65	16.09	7.44	2.42	6.31	6.17	1.77	1.15	0.95	0.38	0.16	0.22	1.16	100.00

PERCENT OCCURRENCE OF CURRENT SPEED VERSUS CURRENT DIRECTION
LOCATION: Mooring #2 (Deep Sea Fisheries) - S/N 7315
DATE: 4/8 - 6/4/92
DEPTH: 27 Meters
NUMBER OF OBSERVATIONS: 5495

DIRECTION (DEGREES TRUE)

SPEED CM/SEC	0- 20	20- 40	40- 60	60- 80	80- 100	100- 120	120- 140	140- 160	160- 180	180- 200	200- 220	220- 240	240- 260	260- 280	280- 300	300- 320	320- 340	340- 360	TOTAL
0 - 5	0.07	1.36	1.31	1.62	5.51	40.09	16.65	5.13	7.77	5.81	3.37	4.57	1.97	1.26	2.13	0.25	0.04	0.05	98.96
5 - 10	0.00	0.02	0.04	0.07	0.31	0.29	0.07	0.02	0.00	0.02	0.00	0.02	0.15	0.00	0.00	0.00	0.02	0.02	1.04
10 - 15	0.00	0.00	0.00	0.00	0.00	0.00	0.00	0.00	0.00	0.00	0.00	0.00	0.00	0.00	0.00	0.00	0.00	0.00	0.00
15 - 20	0.00	0.00	0.00	0.00	0.00	0.00	0.00	0.00	0.00	0.00	0.00	0.00	0.00	0.00	0.00	0.00	0.00	0.00	0.00
20 - 25	0.00	0.00	0.00	0.00	0.00	0.00	0.00	0.00	0.00	0.00	0.00	0.00	0.00	0.00	0.00	0.00	0.00	0.00	0.00
25 - 30	0.00	0.00	0.00	0.00	0.00	0.00	0.00	0.00	0.00	0.00	0.00	0.00	0.00	0.00	0.00	0.00	0.00	0.00	0.00
30 - 35	0.00	0.00	0.00	0.00	0.00	0.00	0.00	0.00	0.00	0.00	0.00	0.00	0.00	0.00	0.00	0.00	0.00	0.00	0.00
35 - 40	0.00	0.00	0.00	0.00	0.00	0.00	0.00	0.00	0.00	0.00	0.00	0.00	0.00	0.00	0.00	0.00	0.00	0.00	0.00
40 - >	0.00	0.00	0.00	0.00	0.00	0.00	0.00	0.00	0.00	0.00	0.00	0.00	0.00	0.00	0.00	0.00	0.00	0.00	0.00
TOTAL	0.07	1.38	1.35	1.69	5.82	40.38	16.72	5.15	7.77	5.82	3.37	4.59	2.11	1.26	2.13	0.25	0.05	0.07	100.00

AANDERAA INSTRUMENTS
Bergen, Norway, Tel. 05/132500

Visual and Mechanical Checks

Check		Comments
Epoxy coating intact (especially near conductivity cell)	☑	chips in epoxy coating
No corrosion, O-ring groove pressure case	☑	
No corrosion, other parts	☑	
No marine fouling (especially in bore of conductivity cell)	☑	
Zinc anode installed	☑	
Rotor end play (0.1 – 0.5 mm)	☑	
Rotor threshold check	☑	
Pressure sensor oil filled	☑	
Upper spool brake, normal	☑	
Pinch roller pressure, normal	☑	Date 4-7-92 Signature KAK

Performance Tests (to be carried out with test battery and *Printer 2152* connected)

First run, with 100Ω in sea water loop and orientation block facing east. *Second run,* with 1000Ω in sea water loop, orientation block facing west and after rotor has been turned 40 revolutions.

First Run

Ch. No.	Reading	Reading O.K.
1	719	
2	1003	
3	391	
4	53	
5	361	
6	0	

Second Run

Ch. No.	Reading	Reading O.K.
1	718	
2	1023	
3	39	
4	52	
5	869	
6	481	

Comments:
Rotor counter = 2

To decide whether a reading is O.K. compare with calibration sheet.

Duration of each measuring cycle ...15... O.K., if within ± 1 second of value stated in Test and Specification Sheet (Form No. 160) following each new instrument.

Clock function: Power switched on 22 hour 45 minutes.   Acoustic Oscillator O.K. ☐ none installed
First triggering 22 hour 45 minutes.
Second triggering 23 hour 00 minutes.

Date 4-7-92 Signature KAK

Deployment Preparations

Recording head, capstan shaft and tape guiding parts cleaned ☑
Fresh battery installed ☑ Type 9V No. 821 Open loop voltage 9.99 Voltage with 100Ω Load 9.50
Tape threaded according to instructions ☑   Tape demagnetized ☑
Lower tape spool labeled 718
Time of first measurement 7 day 4 month 92 year 22 hour 45 minutes ☐ GMT ☒ LT
O-ring inspected, cleaned and greased ☒
C-clamps tightened ☑

Date 4-8-92 Signature KAK

Retrieval Phase

Recording unit cleaned and rinsed in fresh water ☒
Time of last measurement 5 day 6 month 92 year 11 hour 59:40 minutes ☐ GMT ☒ LT
State of recording unit
looks good, no problems

Date 6-5-92 Signature Karl Kurus

Form No 176

Visual and Mechanical Checks

Epoxy coating intact (especially near conductivity cell) ☑
No corrosion, O-ring groove pressure case ☑
No corrosion, other parts ☑
No marine fouling (especially in bore of conductivity cell) ☑
Zinc anode installed ☑
Rotor end play (0.1 – 0.5 mm) ☑
Rotor threshold check ☑
Pressure sensor oil filled ☑
Upper spool brake, normal ☑
Pinch roller pressure, normal ☑

Comments.
Chips in epoxy coating

Date 4-7-92 Signature KAK

Performance Tests (to be carried out with test battery and *Printer 2152* connected)

First run, with 100Ω in sea water loop and orientation block facing east. *Second run,* with 1000Ω in sea water loop, orientation block facing west and after rotor has been turned 40 revolutions.

First Run

Ch. No.	Reading	Reading O.K.
1	458	
2	1023	
3	391	
4	70	
5	378	
6	0	

Second Run

Ch. No.	Reading	Reading O.K.
1	458	
2	1023	
3	39	
4	69	
5	905	
6	41	

Comments:
Rotor counter = 2

To decide whether a reading is O.K. compare with calibration sheet.

Duration of each measuring cycle ...15.... O.K., if within ± 1 second of value stated in Test and Specification Sheet (Form No. 160) following each new instrument.

Clock function: Power switched on 23 hour 15 minutes.   Acoustic Oscillator O.K. ☐ none installed
First triggering 23 hour 15 minutes.
Second triggering 23 hour 30 minutes.

Date 4/7/92 Signature KAK

Deployment Preparations

Recording head, capstan shaft and tape guiding parts cleaned ☑
Fresh battery installed ☑ Type 9V No. 621 Open loop voltage 9.97 Voltage with 100Ω Load 9.47
Tape threaded according to instructions ☑   Tape demagnetized ☑
Lower tape spool labeled 3180
Time of first measurement 7 day 4 month 92 year 23 hour 15 minutes ☐ GMT ☑ LT
O-ring inspected, cleaned and greased ☑
C-clamps tightened ☒

Date 4/8/92 Signature KAK

Retrieval Phase

Recording unit cleaned and rinsed in fresh water ☒
Time of last measurement 5 day 6 month 92 year 12 hour 01:01 minutes ☐ GMT ☒ LT
State of recording unit
No problems

Date 6-5-92 Signature Kirl Kumis

Form No 176

Visual and Mechanical Checks

Epoxy coating intact (especially near conductivity cell) ☑

No corrosion, O-ring groove pressure case ☑

No corrosion, other parts ☑

No marine fouling (especially in bore of conductivity cell) ☑

Zinc anode installed ☑

Rotor end play (0.1 – 0.5 mm) ☑

Rotor threshold check ☑

Pressure sensor oil filled ☑

Upper spool brake, normal ☑

Pinch roller pressure, normal ☑

Comments

...Chips in epoxy coating....

. . . .

. . . .

. . . .

. . . .

. . . .

. . . .

. . . .

Date 4-7-92 Signature .KAK..

Performance Tests (to be carried out with test battery and *Printer 2152* connected)

First run, with 100Ω in sea water loop and orientation block facing east. *Second run*, with 1000Ω in sea water loop, orientation block facing west and after rotor has been turned .40. revolutions.

First Run

Ch. No.	Reading	Reading O.K.
1	273	
2	1023	
3	391	
4	61	
5	368	
6	0	

Second Run

Ch. No.	Reading	Reading O.K.
1	273	
2	1023	
3	39	
4	60	
5	860	
6	40	

Comments:
..... Rotor counter = 2 ....

To decide whether a reading is O.K. compare with calibration sheet.

Duration of each measuring cycle .15 mm. O.K., if within ±1 second of value stated in Test and Specification Sheet (Form No. 160) following each new instrument.

Clock function: Power switched on .23. hour .45. minutes.

First triggering ....23. hour .45. minutes.

Second triggering ....0. hour ...0... minutes.

Acoustic Oscillator O.K. ☐ none installed

Date 4-7-92 Signature .KAK..

Deployment Preparations

Recording head, capstan shaft and tape guiding parts cleaned ☑

Fresh battery installed ☑ Type .9V. No.821. Open loop voltage 9.97. Voltage with 100Ω Load 9.47

Tape threaded according to instructions ☑   Tape demagnetized ☑

Lower tape spool labeled .7315....

Time of first measurement ..7. day .4. month .92 year .23. hour .45 minutes ☐ GMT ☒ LT

O-ring inspected, cleaned and greased ☒

C-clamps tightened ☒

Date 4-8-92 Signature .KAK..

Retrieval Phase

Recording unit cleaned and rinsed in fresh water ☒

Time of last measurement .5. day .6. month .92 year .17. hour 00:38 minutes ☐ GMT ☒ LT

State of recording unit . . . .

..... No problems . . . .

. . . .

Date 6-5-92 Signature Ken Kumus

Appendix D. Mathematical Basis for Numerical
Simulation Model for Akutan Harbor
(Koutitas 1988)

Description of main variables:

W   = number of wave episodes with corresponding H_s, T and annual frequencies, available
PEK = period of reappearance of the required wave
Hs(I) = significant wave heights available
T(I) = corresponding periods
F(I) = corresponding annual frequencies

The application is performed with the previously found data, HS, T, F (hindcast wave heights and periods and annual frequencies respectively). It gives as slope of the straight line found by least squares, -0.6878. It is found that for PER = 10 years, $H_{s,10} = 6.6$ m, $H_{max,10} = 12.9$ m and $T = 11.5$ s.

2

Mathematical models of coastal circulation

2.1 DEFINITION—THE GENERAL FORM OF THE MODEL

Coastal circulation is defined by the development of generally non steady velocity and surface elevation fields in a coastal geophysical domain where the depths are of the order of 10 or more metres, the horizontal dimensions are of the order of 10 or more kilometres and the geometry of the coastline is not simple. This geophysical domain is connected to the open sea through one or more openings (open sea boundaries). The circulation in these areas is generated and sustained by various generating factors such as the tide, the wind or atmospheric pressure acting on the water surface, the horizontal variation of wave momentum due to diffraction refraction and shoaling, and by the spatial variation of water density

The defined coastal domain extends from the coastline to the continental slope, so it comprises of marine areas where currently engineering developments are extensive.

The definition given for the circulation applies to the waves described in Chapter 1. Indeed, the long-wave mathematical model will reappear in the present chapter, but the phenomena to be investigated here are differentiated from those of the first chapter, so far as their time scale is concerned (hours or days compared to seconds or minutes in the first chapter)

In the following sections, the phenomena and the corresponding mathematical models will be presented according to the generating factors. This distinction has mathematical rather than physical meaning, as the various circulation generating factors coexist and are mingled in varying proportions. The general mathematical model will be formulated in the present section and specific forms of the general model in subsequent ones, derived under special simplifying assumptions.

The general model for coastal circulation is based on the following

physical assumptions:

(1) As the horizontal dimension of the flow domain L is several orders of magnitude larger than the vertical dimension (depth H), the assumption of nearly horizontal flow is realistic. The horizontal velocity components u, v, are several orders of magnitude larger than the vertical component, w. This observation is generally valid except for certain minor regions of the flow domain; such as areas of sharp bed slopes ($> 1:5$) or areas where upwelling or fronts occur. The assumption of nearly horizontal flow contributes to a considerable simplification of the model as it excludes the vertical velocity component w from the main unknown functions and leads to a hydrostatic pressure distribution. Mathematically speaking, this assumption simplifies the form of the vertical momentum conservation equation to

$$w \approx 0 \rightarrow \frac{\partial p}{\partial z} = -\rho g \qquad (2.1)$$

(2) The horizontal dimension of the flow domain is usually very large in comparison with the magnitude of the horizontal velocities developed within them and the time taken for circulation to develop may reach the order of some days. During that time, the effect on the flow domain of the earth's rotation is such that the contribution of the Coriolis force (at least of its horizontal components) cannot be neglected. The Coriolis mass force is expressed by the term $2\rho \Omega \times \mathbf{V}$ where Ω is the angular rotation of the earth vector and $\mathbf{V}$ the fluid velocity vector. The relation between the Coriolis and inertial forces can be expressed via the dimensionless number $T\Omega$ or $\Omega L/U$, where T is the time scale of evolution of the phenomenon, L the horizontal dimension of the flow domain, and U a characteristic velocity magnitude. The second number, known as the Rossby number, is an indicator of the importance of the Coriolis effect.

The horizontal components of the Coriolis force are given by the equations

$$f_{xc} = 2\Omega(\sin \varphi)v = fv \qquad (2.2)$$

$$f_{yc} = -2\Omega(\sin \varphi)u = -fu \qquad (2.3)$$

where f is the Coriolis coefficient and φ the geographic latitude of the domain. If the flow domain is of limited horizontal dimension, the mean φ value is used and the f coefficient is constant over the whole domain. Extension of the domain over several degrees of latitude shows the the β-effect (variation of f) has to be considered. Although the Coriolis effect is included in coastal circulation models the

curvature of the earth is not considered in most cases and the flow domain is approximated by its mercatorial projection (f plane).
(3) A flow domain of large dimension results in quite large Reynolds numbers, $O[\text{Re}] > 10^4$, even for minimal velocity values (order of 1 cm/s). The flows are always turbulent. For turbulent stresses, the Boussinesq approximation is made, approximating the Reynolds stresses by the turbulent mean velocity gradient. The eddy viscosity coefficient appearing in this approximation develops generally in an anisotropic way, depending on the nature of the turbulence. For the simplest possible realistic turbulence closure in applications of physical oceanographic scale, two final assumptions are made:

(i) The eddy viscosity coefficients are differentiated between the horizontal v_h and vertical v dimensions.
(ii) Constant or variable values of v_h and v_v (in general $v_h \neq v_v$) are adopted. In the second case the functional forms of $v_h, v_v(x, y, z)$ are the simplest possible. Prandtl mixing length theory is commonly used or in special cases, requiring the most detailed vertical current profile description, k or $k - \varepsilon$ models for turbulence closure are used. The mathematical expressions for v_v in ascending order of complexity are:

$$v_v = \text{constant}$$

$$v_v = \lambda u h \frac{z}{h}\left(1 + \frac{z}{h}\right)$$

$$v_v = l_m^2 \left|\frac{\partial u}{\partial z}\right|$$

$$v_v = L_0 \cdot k^{1/2} \qquad \text{where } k = \frac{1}{2}(\overline{u'^2 + v'^2 + w'^2}) \qquad (2.4)$$

and l_m, L_0 are the mixing and dissipation lengths respectively, functions of z. Figure 2.1 shows the most common morphologies for the v_v distribution.

Under the abovementioned assumptions, the coastal circulation model in its most general form is composed of the equations of equilibrium of forces in a horizontal dimension, and the mass continuity equation. According to the notation of Fig. 2.2 these have the form:
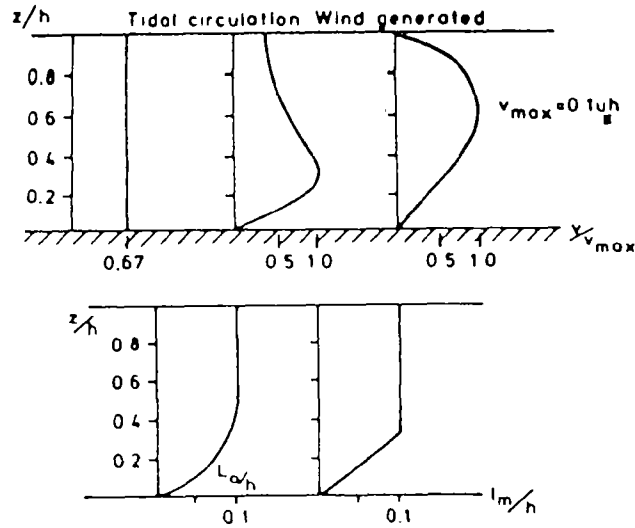
Fig 2 1   Eddy viscosity and mixing length distributions for tidal and wind generated flows
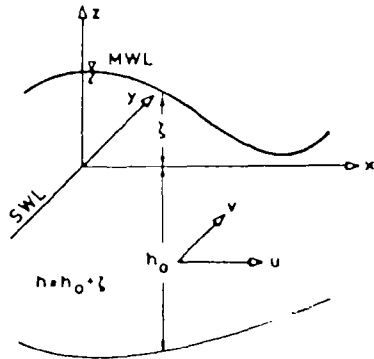
Fig 2 2   Coordinate axes and basic symbols in circulation models

(1) Equilibrium equations

$$\frac{\partial u}{\partial t} + u\frac{\partial u}{\partial x} + v\frac{\partial u}{\partial y} + w\frac{\partial u}{\partial z}$$

$$= -\frac{1}{\rho}\frac{\partial p}{\partial x} + a_x + \frac{\partial}{\partial x}\left(v_h\frac{\partial u}{\partial x}\right) + \frac{\partial}{\partial y}\left(v_h\frac{\partial u}{\partial y}\right) + \frac{\partial}{\partial z}\left(v_v\frac{\partial u}{\partial z}\right)$$

$$(2\ 5)$$

$$\frac{\partial v}{\partial t} + u\frac{\partial v}{\partial x} + v\frac{\partial v}{\partial y} + w\frac{\partial v}{\partial z}$$

$$= -\frac{1}{\rho}\frac{\partial p}{\partial y} + a_y + \frac{\partial}{\partial x}\left(v_h\frac{\partial v}{\partial x}\right) + \frac{\partial}{\partial y}\left(v_h\frac{\partial v}{\partial y}\right) + \frac{\partial}{\partial z}\left(v_v\frac{\partial v}{\partial z}\right)$$

$$(2\ 6)$$

where $u(x,y,z,t)$, $v(x,y,z,t)$, $w(x,y,z,t)$ and $p(x,y,z,t)$ are the velocity components and pressure functions and v_h, v_v the eddy viscosity functions.

(2) Equation of mass continuity (incompressible fluid)·

$$\frac{\partial u}{\partial x} + \frac{\partial v}{\partial y} + \frac{\partial w}{\partial z} = 0 \qquad (2.7)$$

A more useful form for free surface, nearly horizontal flows, derives from the integration of (2.7) over the depth

$$\frac{\partial}{\partial x}\int_{-h_0}^{\zeta} u\,dz + \frac{\partial}{\partial y}\int_{-h_0}^{\zeta} v\,dz + w\Big|_{\zeta} - w\Big|_{-h_0} = 0 \qquad (2\ 8)$$

where $\zeta(x,y,t)$ is the free surface elevation relative to the still water level (SWL). For $w(x,y,z=-h)=0$ and $w(x,y,z=\zeta) \approx \partial\zeta/\partial t$ Equation (2.8) takes the useful form

$$\frac{\partial\zeta}{\partial t} + \frac{\partial}{\partial x}\int u\,dz + \frac{\partial}{\partial y}\int v\,dz = \frac{\partial\zeta}{\partial t} + \frac{\partial Uh}{\partial x} + \frac{\partial Vh}{\partial y} = q \qquad (2\ 9)$$

where $U(x,y,t)$ and $V(x,y,t)$ are the depth mean horizontal velocity components and $q(x,y,t)$ ($[q] = L^3/L^2/T$) is the specific discharge of a source or sink that may exist in the flow domain, such as the effluence of a river, etc.

The variables a_x, a_y, describe distributed mass forces such as in our case the Coriolis horizontal components, or forces due to waves (gradients of radiation stresses that will be described in detail in Section 2 4 on wave generated circulation).

The vertical velocity component w appearing in the equilibrium equations may be either neglected or computed from the solution of the continuity equation (2 7).

The turbulence closure in coastal general circulation models is resolved via the approximation of v_v by one of the forms (2.4) A comparison of v_v and v_h and consequently of the horizontal and vertical momentum diffusion terms can be analysed as follows: As

$$[v] = L^2/T$$

then

$$O[v_h] \propto O[L] \quad O[U]$$

$$O[v_v] \propto O[H] \quad O[U]$$

giving

$$O[v_v] \ll O[v_h] \quad \text{since} \quad O[L] \gg O[H]$$

where L and H are the horizontal and vertical flow field dimensions. Expressions for the horizontal and vertical momentum diffusion are given by

$$O\left[\frac{\partial}{\partial x}\left(v_h \frac{\partial u}{\partial x}\right)\right] \propto \frac{O[L] \cdot O[U]^2}{O[L]^2} \propto \frac{O[U]^2}{O[L]}$$

and

$$O\left[\frac{\partial}{\partial z}\left(v_v \frac{\partial u}{\partial z}\right)\right] \propto \frac{O[H] \cdot O[U]^2}{O[H]^2} \propto \frac{O[U]^2}{O[H]}$$

The second expression dominates the first The horizontal momentum diffusion terms thus may be neglected before the vertical terms Their retention and use of constant v_h values is recommended for numerical stability reasons as the induced physical/numerical diffusion smooths out numerically produced perturbations in the velocity field

The field equations described are completed by appropriate boundary conditions. From the physical point of view these can be distinguished as:

(1) The coastal perimeter. The velocity component normal to this boundary is suppressed. The tangential component is left free to develop, simulating any longshore current. The suppression of the normal velocity does not permit flooding of low coastal areas. In the case of strong storm surges, special weir type conditions have to be applied to the boundary to describe lowland flooding

(2) The open sea. This boundary in itself has no strict character, no easily discernible features, but it is indispensable for reasons of computational economy It is a physical or fictitious line separating the investigated domain from the rest of the sea. It is easily fixed in the case of a semi-enclosed coastal basin connected via a fixed opening to a wide, deep water body. If on that boundary no in situ measurements of velocity or sea surface elevation are given some assumptions have to be made. A most convenient condition is one describing the free radiation to the open sea (without back reflection) of any perturbation reaching that boundary from inside. The mathematical expression quantifying this physical operation derives from the conservation principle for a moving surge and relates the depth mean velocity U_n, normal to the boundary, to the free surface elevation ζ

$$\mathbf{n} \cdot \mathbf{U}_n = \zeta \sqrt{(g/h)} \tag{2 10}$$

where $\mathbf{n}$ is the unit outward vector.

Equivalent to Equation (2.10), but deriving from the theory of linear long waves moving unidirectionally, the following relation describes, in differential form, the evolution of the radiated part of the ζ magnitude

$$\frac{\partial \zeta_r}{\partial t} + \frac{\partial \zeta_r}{\partial n} \cdot \sqrt{(gh)} = 0 \tag{2 11}$$

The total value of ζ is assumed as the superposition of ζ_i(incident) + ζ_r(radiated)

$$\zeta = \zeta_i + \zeta_r \tag{2 12}$$

(3) The free surface The wind, having near surface velocity components W_x, W_y (measured at a height of 10 m above the surface) exercises a frictional force on the surface of the water The x, y components of that force can be expressed by the quadratic forms:

$$\frac{\tau_{sx}}{\rho} = v_v \frac{\partial u}{\partial z}\bigg|_{z=\zeta} = kW_x\sqrt{(W_x^2 + W_y^2)} \tag{2 13}$$

$$\frac{\tau_{sy}}{\rho} = v_v \frac{\partial v}{\partial z}\bigg|_{z=\zeta} = kW_y\sqrt{(W_x^2 + W_y^2)} \tag{2 14}$$

where k is a friction coefficient (with values $O[k] = 10^{-6}$) and ρ is the water density.

(4) The sea bed. On the sea bed or at a height $\sim k_s/30$ above, where k_s is the absolute bed roughness, the velocity may be assumed equal to zero. The 'no slip' condition is the simplest one. The shear stress developed near the bed is defined by the relations

$$\frac{\tau_{bx}}{\rho} = v_v \frac{\partial u}{\partial z}\bigg|_{z=-h}, \quad \frac{\tau_{by}}{\rho} = v_v \frac{\partial v}{\partial z}\bigg|_{z=-h} \tag{2 15}$$

Instead of the 'no slip' condition the bed shear may be related to the velocity magnitude at a height Δz above the bed This relation is based on the assumption that over the distance Δz the velocity follows the logarithmic distribution for uniform turbulent flow,

$$u = \frac{u_*}{k} \ln \frac{z+h}{z_0} \tag{2 16}$$

where $k = 0.4$, $u_* = \sqrt{(\tau_{bx}/\rho)}$, $z_0 = k_s/30$. At a distance Δz

$$u\bigg|_{z=-h_0+\Delta z} = \frac{1}{k}\sqrt{\left(\frac{\tau_{bx}}{\rho}\right)} \ln \frac{\Delta z}{z_0} \tag{2 17}$$

Readers will recall that the velocity distribution for uniform flow (2.16) results in the following relation of τ_b/ρ to the depth mean velocity U:

$$\frac{\tau_b}{\rho} = U^2\left(\frac{k}{\ln(h/z_0) - 1}\right)^2 = \lambda U^2 = \frac{g}{C^2} U^2 \qquad (2.18)$$

where λ is a nondimensional friction coefficient and C the Chézy bed friction coefficient.

2.2 MATHEMATICAL MODELS OF LONG WAVE INDUCED CIRCULATION (TIDAL MODELS)

2.2.1 Formulation in terms of the depth mean velocities

The circulation generating factor is a periodic or non-periodic perturbation of the free surface elevation, arriving from the open sea and developing over a period of several hours (in the most common case of the M_2 tide component generated by the influence of the moon on the earth, it is periodic with period 12.8 h) The long waves arriving from the open sea enter through the open sea boundary, propagate to the coastal area and are reflected from the coastal boundaries. They are subject to various deformations due to diffraction, refraction shoaling and frictional losses of energy and part of their energy is radiated through the open sea boundary back to the sea.

The applicability of the long-wave mathematical theory can be verified by comparison with the wave length L and the depth h. For $O[h] = 100$ m $(L \gg h)$. For wave amplitudes $O[H] = 1$ m, the ratio HL/h^2 is much greater than 20–30. The flow develops as a boundary layer $(h = \delta)$. As this phenomenon evolves slowly with time the velocity profile develops uniformly in stages,

$$u = \frac{u_*}{k} \ln\frac{h + z}{z_0} \qquad (2\,16)$$

The wave celerity is $O[C] = 30$ m/s, resulting, in the case of an M_2 tide, in a wave length $O[L] = 1.3 \times 10^6$ m.

The current intensity is almost uniform over the depth, steep gradients developing only near the bed. The uniformity of velocity over the depth permits simplification of the general model (2 5)–(2 7) by integration over the depth and the introduction of the depth mean velocity values:

$$U = \frac{1}{h}\int_{-h_0}^{\zeta} u\,dz, \qquad V = \frac{1}{h}\int_{h_0}^{\zeta} v\,dz \qquad (2.19)$$

In the case of homogeneous fluid, the pressure terms become under the hydrostatic pressure approximation

$$-\frac{1}{\rho}\cdot\frac{\partial p}{\partial x} = -g\frac{\partial\zeta}{\partial x}, \qquad \frac{1}{\rho}\cdot\frac{\partial p}{\partial y} = -g\frac{\partial\zeta}{\partial y} \qquad (2\,20)$$

The Coriolis terms are retained. The integration of (2 5), (2.6) over the depth, the approximation of the non linear convective terms by their depth mean values and the expression of the bed friction using the quadratic forms (2 18) result in a simple model known as the 2DH (2-dimensional horizontal flow) model

$$\frac{\partial U}{\partial t} + U\frac{\partial U}{\partial x} + V\frac{\partial U}{\partial y} = -g\frac{\partial\zeta}{\partial x} + fV - \frac{gU\sqrt{(U^2 + V^2)}}{hC^2} + \nu_h\nabla_h^2 U$$

$$(2.21)$$

$$\frac{\partial V}{\partial t} + U\frac{\partial V}{\partial x} + V\frac{\partial V}{\partial y} = -g\frac{\partial\zeta}{\partial y} - fU - \frac{gV\sqrt{(U^2 + V^2)}}{hC^2} + \nu_h\nabla_h^2 V$$

$$(2\,22)$$

$$\frac{\partial\zeta}{\partial t} + \frac{\partial Uh}{\partial x} + \frac{\partial Vh}{\partial y} = 0 \qquad (2\,23)$$

where ∇_h^2 is the horizontal Laplacian, $\nabla_h^2 = \partial^2/\partial x^2 + \partial^2/\partial y^2$

2.2.2 Numerical solution of the 2-D horizontal flow model by explicit finite differences

Various numerical schemes for the solution of the long wave induced circulation models in coastal domains are still the subject of investigation by researchers. The models actually treated here consist of Equations (2.21) (2 23) in the given or slightly modified forms The schemes are based on the finite difference or finite element methods A finite difference scheme selected on the basis of its simplicity and efficiency is presented here

The flow domain is discretised by an orthogonal horizontal grid with mesh sides $\Delta x, \Delta y$. The lateral coastal boundaries are approximated by mesh sides $\|Ox$, or $\|Oy$ The open sea boundaries are also selected piecewise by $\|Ox$, or $\|Oy$ The unknown functions U, V, ζ are computed on characteristic locations in a staggered way The U, V values refer to the mesh sides $\|Oy$ and $\|Ox$ respectively and the ζ refer to the mesh centers. The coordinates of the computation points are characterised by the i, j, n indices, the first referring to the abscissa, the second to the ordinate and the third to the time. The
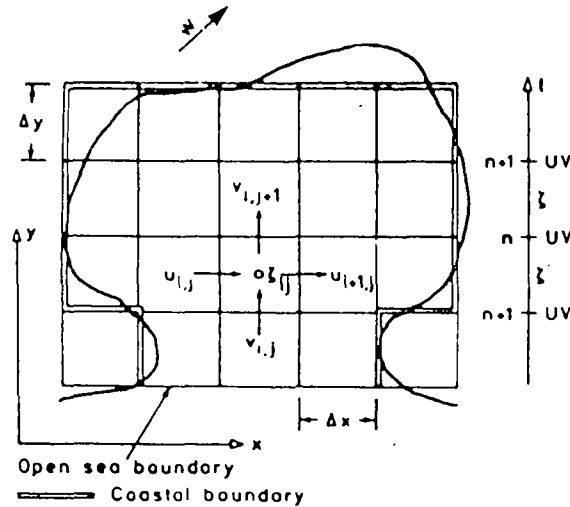
Fig 2 3 Orthogonal staggered grid for spatial and time discretisations

computation points and the indices i, j relevant to a typical mesh are illustrated in Fig 2 3

The terms of the Equations (2.21)-(2.23) are approximated by finite differences Forward differences are used for the time derivative and centered differences for the rest of the space derivatives, synthesising an explicit numerical scheme. The computation of U, V values at the $n + 1$ time level involves known values of U, V, ζ (n and $n + \frac{1}{2}$ level) and there is no algebraic system to be solved.

The functional forms

$$U_{ij}^{n+1} = f_1(U^n, V^n, \zeta^{n+\frac{1}{2}})$$ (2.24)

$$V_{ij}^{n+1} = f_2(U^n, V^n, \zeta^{n+\frac{1}{2}})$$ (2 25)

$$\zeta_{ij}^{n+\frac{1}{2}} = f_3(U^{n+1}, V^{n+1}, \zeta^{n+\frac{1}{2}})$$ (2 26)

facilitate the organisation of a simple integration algorithm subject to a numerical stability limit of the Δt value used That limit is given by the known CFL criterion

$$\frac{c\Delta t}{\sqrt{(2\Delta x)}} < 1 \qquad (c = \sqrt{(gh)})$$ (2 27)

From the physical aspect this inequality means that the Δt used must be less than the time needed for any perturbation to cover the extent of a mesh This limit results in greater computer time than that required by an implicit scheme The Δt used must of course be at least

one or two orders of magnitude less than the characteristic time scale for the long wave to develop, so that no information is lost during the integration in time. For example, in the case of a tidal wave with $T = 43,000$ s, the optimal Δt would be $\Delta t = 430/4300$ s. Although the advent of more powerful computers makes this problem of secondary importance, implicit schemes have been investigated also for the integration of that numerical model. The most economic ones are based on the ADI technique, solving successively along the Ox and Oy directions implicitly and thus involving a large number of small algebraic systems instead of one large system in all the field unknowns.

The finite difference forms according to the present explicit scheme are:

$$U_{ij}^{n+1} = U_{ij}^n - \frac{\Delta t}{8\Delta x} \left[(U_{i+1,j}^n + U_{ij}^n)^2 - (U_{ij}^n + U_{i-1,j}^n)^2 \right]$$

$$- \frac{\Delta t}{2\Delta y} \bar{V}_{ij}^n (U_{ij+1}^n - U_{ij-1}^n) - \frac{g\Delta t}{\Delta x} (\zeta_{ij}^{n+\frac{1}{2}}) - \zeta_{i-1}^{n+\frac{1}{2}})$$

$$- \frac{2g U_{ij}^n \sqrt{(U_{ij}^{n2} + \bar{V}_{ij}^{n2})}}{C^2(h_{ij} + h_{i-1,j})} + f\bar{V}_{ij}^n$$ (2.28)

$$V_{ij}^{n+1} = V_{ij}^n - \frac{\Delta t}{8\Delta y} \left[(V_{ij}^n + V_{ij+1}^n)^2 - (V_{ij}^n + V_{ij-1}^n)^2 \right]$$

$$- \frac{\Delta t}{2\Delta x} \bar{U}_{ij}^n (V_{i+1,j}^n - V_{i-1,j}^n) - \frac{g\Delta t}{\Delta y} (\zeta_{ij}^{n+\frac{1}{2}} - \zeta_{ij-1}^{n+\frac{1}{2}})$$

$$- \frac{2g V_{ij}^n \sqrt{(\bar{U}_{ij}^{n2} + V_{ij}^{n2})}}{C^2(h_{ij} + h_{ij-1})} - f\bar{U}_{ij}^n$$ (2 29)

$$\zeta_{ij}^{n+\frac{1}{2}} = \zeta_{ij}^{n+\frac{1}{2}} - \frac{\Delta t}{2\Delta x} (U_{i+1,j}^{n+1}(h_{ij} + h_{i+1,j}) - U_{ij}^{n+1}(h_{ij} + h_{i-1,j}))$$

$$- \frac{\Delta t}{2\Delta y} \left[V_{ij+1}^{n+1}(h_{ij} + h_{ij+1}) - V_{ij}^{n+1}(h_{ij} + h_{ij-1}) \right]$$

$$+ q_{ij}\Delta t$$ (2 30)

where

$$\bar{V}_{ij}^n = (V_{ij}^n + V_{i-1,j}^n + V_{ij+1}^n + V_{i-1,j+1}^n)/4$$

$$\bar{U}_{ij}^n = (U_{ij}^n + U_{ij-1}^n + U_{i+1,j}^n + U_{i+1,j-1}^n)/4$$

The boundary conditions are treated very easily with the assumed approximation for the coastal boundaries and the use of a staggered grid. On the $\|Ox$ boundaries, $V_{ij} = 0$ and on the $\|Oy$ boundaries,

$U_{ij}^n = 0$. On the open sea boundaries either the total ζ_{ij}^n time series is known ($n = 1, 2, \ldots$) or the incident part of it ζ_i ($\zeta = \zeta_i + \zeta_r$) is known; for the radiated part ζ_r, Equation (2.11) is applied. On the boundary, the necessary velocity values have to be given or computed via relations based on the method of characteristics. A simple efficient approximation is the assumption of quasi-uniformity of the velocity across it, i e. $\partial U/\partial n = 0$.

The synthesis of a computer program analysis, Program 7, is straightforward The most important points of the program are.

(1) The scanning of the field The field is swept in the x direction (index i) for successive values of the ordinate y (index j). The leftmost and rightmost limits of the field for various j's are defined by the integer arrays IS(J), IE(J) An illustration of the procedure is included in Fig 2 4.

(2) The special meshes are characterised by integer indices describing their properties. These are the meshes not belonging to the interior of the field but having one or more sides along a coastal or open sea boundary (dry meshes). This last type of mesh is used for the islands in multiply-connected flow domains The characterisation and enumeration of the special meshes is illustrated in Fig 2 4.

Numbering of boundary meshes

J	1	2	3	4	5	6	7	8	9	10
IS	2	3	3	3	3	3	3	3	3	5
IE	9	6	5	9	9	9	9	9	9	7
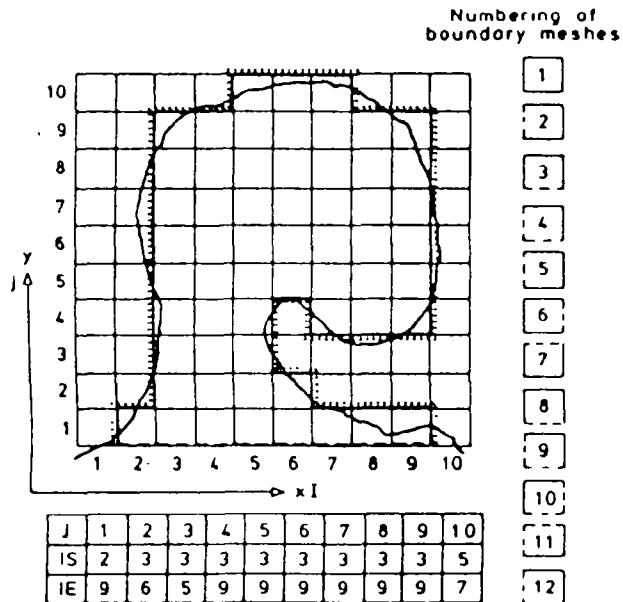
Fig 2 4   Morphology of coastal boundaries and typical boundary meshes

(3) The U_{ij}^n, V_{ij}^n values are described by the U(I, J), V(I, J) arrays and the U_{ij}^{n+1}, V_{ij}^{n+1} by the UN(I, J), VN(I, J) arrays. In each time step the computed UN, VN values are stored as U, V arrays after their computation.

(4) After the computation of the velocity components on the mesh sides their mean values referring to the mesh center $(U_{ij} + U_{i+1j})/2$, $(V_{ij} + V_{ij+1})/2$ are computed. These are the plotted velocity values

(5) The model computes a non-steady flow, evolving continuously in time due to a variable flow forcing factor (tidal flow) The same model can be used with a cold start (no flow) for the initial condition and can describe under a steady forcing factor the transient situation for a steady flow final state. It is a time-marching type technique In each time-step the total kinetic energy in the flow domain is computed from the sum

$$E_{kin}^n = \sum_i \sum_j ((U_{ij}^n + U_{i+1j}^n)^2 + (V_{ij}^n + V_{ij+1}^n)^2) h_{ij} \Delta x \Delta y / 8$$

$$(2.31)$$

The steady state is reached when the ratio $|E^{n+1} - E^n|/E^{n+1}$ becomes less than a test convergence value (10^{-3}).

PROGRAM 7: 2-D NON-LINEAR LONG-WAVE CIRCULATION MODEL

```
5REM 2-D NON LINEAR LONG WAVES MODEL
10DIMU(20,20),UN(20,20),V(20,20),VN(20,20),H(20
,20),Z(20,20),IS(20),IE(20),IB(50),JB(50),NB(50)
20READDT,DX,CF,F,IM,JM,KB,NM,AMPL,PER
30DATA...
40FORJ=1TOJM-1iREADIS(J),IE(J)iNEXTJ
50DATA....
60FORJ=1TOJM-1iFORI=IS(J)-1TOIE(J)+1iREADH(I,J)
iNEXTIiNEXTJ
70DATA...
80FORI=IS(J)-1TOIE(J)+1
90FORK=1TOKBiREADIB(K),JB(K),NB(K)iNEXTK
100DATA...
110N=0iT=0iEK=0
120N=N+1iT=T+DT
130FORJ=2TOJM-2iFORI=IS(J)TOIE(J)
140Z(I,J)=Z(I,J)-DT/2/DX*(U(I+1,J)*(H(I,J)+H(I+1
,J))-U(I,J)*(H(I,J)+H(I-1,J))+V(I,J+1)*(H(I,J+1)+H
(I,J))-V(I,J)*(H(I,J)+H(I,J-1)))
145NEXTIiNEXTJ
150FORJ=2TOJM-2 iFORI=IS(J)+1TOIE(J)
160VV=(V(I,J)+V(I-1,J)+V(I,J+1)+V(I-1,J+1))/4iHM
=(H(I,J)+H(I-1,J))/2
170UN(I,J)=U(I,J)-DT*(((U(I,J)+U(I+1,J))^2-(U(I,
```

```
J)+U(I-1,J))^2)/8/DX+VV*(U(I,J+1)-U(I,J-1))/2/DX+9
.81*(Z(I,J)-Z(I-1,J))/DX-F*VV+CF*U(I,J)*SQR(VV^2+U
(I,J)^2)/HM)
    180NEXTI;NEXTJ
    190FORJ=3TOJM-2;FORI=IS(J)TOIE(J)
    200UU=(U(I,J)+U(I+1,J)+U(I,J-1)+U(I+1,J-1))/4;HM
=(H(I,J)+H(I,J-1))/2
    210VN(I,J)=V(I,J)-DT*(((V(I,J+1)+V(I,J))^2-(V(I,
J)+V(I,J-1))^2)/8/DX+UU*(V(I+1,J)-V(I-1,J))/2/DX+9
.81*(Z(I,J)-Z(I,J-1))/DX+F*UU+CF*V(I,J)*SQR(UU^2+V
(I,J)^2)/HM)
    220NEXTI ;NEXTJ
    230FORK=1TOKB;I=IB(K);J=JB(K)
    340ON NB(K)-1 GOTO 350,360,370,380,390,400,410,4
20,430,440,450
    350UN(I,J)=0;GOTO465
    360VN(I,J)=0;GOTO465
    370UN(I,J)=0;VN(I,J)=0;GOTO465
    380UN(I,J)=UN(I+1,J);VN(I,J)=VN(I+1,J);GOTO460
    390UN(I+1,J)=UN(I,J);VN(I,J)=VN(I-1,J);GOTO460
    400VN(I,J+1)=VN(I,J);UN(I,J)=UN(I,J-1);GOTO460
    410UN(I,J)=UN(I,J+1);VN(I,J)=VN(I,J+1);GOTO460
    420UN(I,J)=UN(I+1,J);VN(I,J)=0;GOTO460
    430UN(I+1,J)=UN(I,J);VN(I,J)=0;GOTO460
    440VN(I,J+1)=VN(I,J);UN(I,J)=0;GOTO460
    450VN(I,J)=VN(I,J+1);UN(I,J)=0;GOTO460
    460Z(I,J)=AMPL*SIN(2*PI*T/PER)
    465NEXTK
    470FORJ=1TOJM;FORI=1TOIM;U(I,J)=UN(I,J);V(I,J)=V
N(I,J);NEXTI;NEXTJ
    480IFN/2<>INT(N/2) THEN GOTO120
    490EK=0;FORJ=2TOJM-2;FORI=IS(J)TOIE(J);EK=EK+((U
(I,J)+U(I+1,J))^2+(V(I,J)+V(I,J+1))^2)*H(I,J)/8 ;N
EXTI;NEXTJ
    500PRINTN,EK
    510PRINT"UU";FORJ=JM-2 TO 2 STEP-1;FORI=2TOIM-2;
PRINT(U(I,J)+U(I+1,J))/2;;NEXTI;PRINT;NEXTJ
    520PRINT"VV";FORJ=JM-2 TO 2 STEP-1;FORI=2TOIM-2;
PRINT(V(I,J)+V(I,J+1))/2;;NEXTI;PRINT;NEXTJ
    530PRINT"ZZ" ;FORJ=JM-2 TO 2 STEP-1;FORI=2TOIM-2
;PRINTZ(I,J);;NEXTI ;PRINT;NEXTJ
    540IFN<NM THEN GOTO120
    550END
```

Description of main variables:

DT, DX   = discretisation in time and space (square mesh) steps
CF   = bed friction coefficient (g/C^2)
F   = Coriolis coefficient
IM, JM, NM = max values of i, j, n indices in x, y, t directions

KB   = number of special meshes
AMPL   = long wave amplitude on the open sea boundary (in the program the ζ (total) values are prescribed)
PER   = period of long wave
IS(J), IE(J) = lateral domain boundaries
H(I,J)   = water depths at mesh centers
IB, JB, NB = abscissa, ordinate, and index characterising one of the KB special meshes (NB takes the value from 2 to 12)

The above program has a general validity It can describe the tidal 2-D horizontal flow in any coastal basin with one open-sea boundary on which the total free surface elevation ζ has a prescribed sinusoidal variation If on that boundary the incident component ζ_i is prescribed, then the open sea boundary is modified and the ζ_r component is computed via (2.11). An illustration of that procedure will be given in a subsequent program.

The present application refers to the circulation generated by a long wave in a semi-enclosed coastal basin of geometry given in Fig 2.5.

The main data are: DT = 240 s, DX = 4000 m, CF = 0.01, F = 0 0001, IM = 9, JM = 9, KB = 11, NM = 200, AMPL = 1 m, PER = 4800 s.

IS	2	2	2	2	2	2	2				
IE	7	7	7	7	7	7	7				
IB	2	3	4	5	6	7	2	2	2	2	2
JB	2	2	2	2	2	2	3	4	5	6	7
NB	12	8	8	8	8	8	2	2	2	2	2
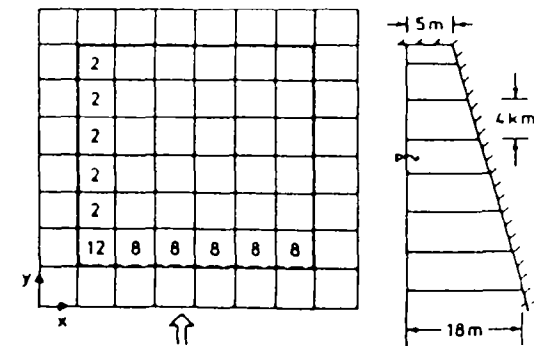
Fig 2 5   Flow domain and discretisation for long-wave generated 2-D non linear model

The evolution of the free surface during a wave period $(t - t + T)$ along two main directions of the flow domain is illustrated in Fig. 2.6 The influence of the Coriolis effect is shown from the surface slope along the section b–b. This slope produces the velocity component in the x direction.

The differences of the velocity hodographs (tidal velocity ellipses)
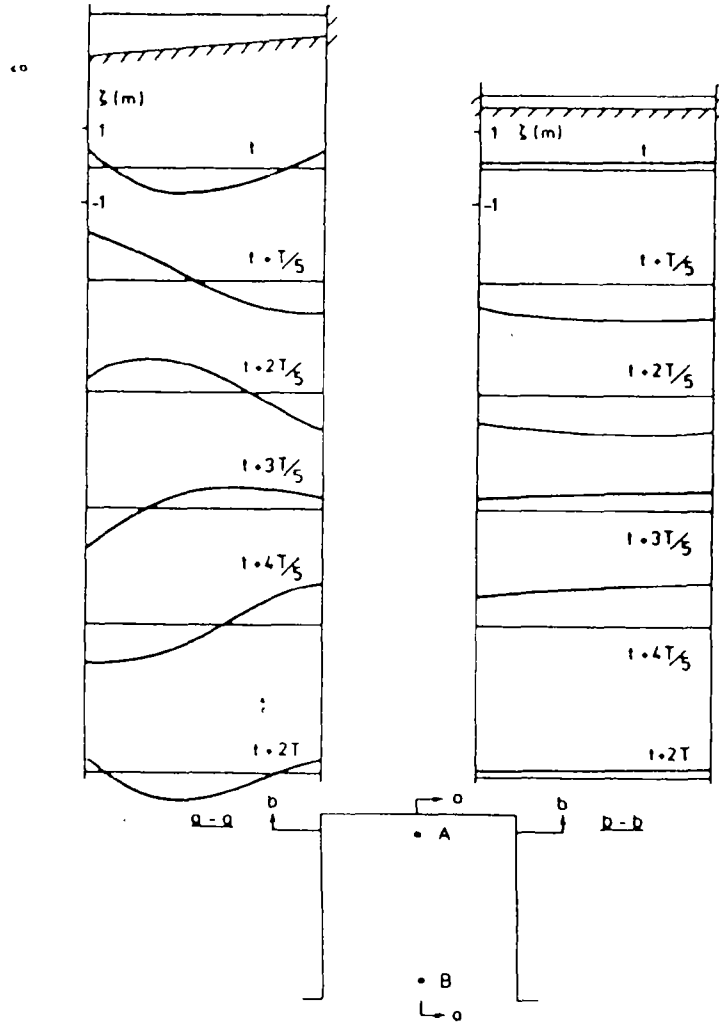
Fig 2.6 Evolution of free surface with time along sections a-a, b-b
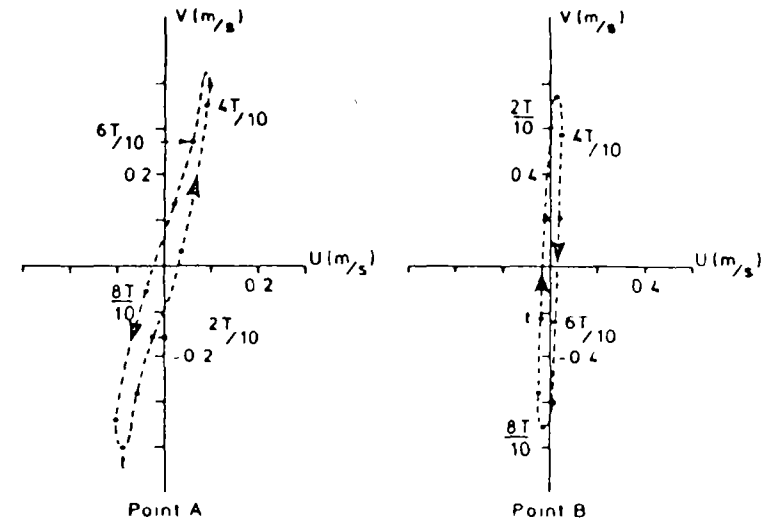
Fig 2.7 Velocity hodographs at points A and B

at the points A and B, shown in Fig 2.7, both with respect to the direction of rotation and the velocity magnitude, are due to the Coriolis effect and the depth difference.

2.2.3 1-D circulation model in a channel of varying cross-section

In some estuaries the flow domain has a length dimension much greater than the width. In that case the model can be further simplified by integration and averaging over the width dimension

The velocities developing mainly along the longitudinal dimension can refer to the whole cross-section of the channel The cross-section of the 1-D channel are approximated by orthogonal parallelograms in this version of the model These may be of varying depth and width along the longitudinal axis Ox. The long-wave model (actually the generalised St. Venant model) is written in terms of the unknown functions of discharge $Q(x, t)$ and the water surface elevation $\zeta(x, t)$ measured from the horizontal SWL. The equilibrium of force and mass continuity equations, according to the notation of Fig 2 8, are written.

$$\frac{\partial \zeta}{\partial t} + \frac{1}{B} \frac{\partial Q}{\partial x} = 0 \tag{2.32}$$

$$\frac{\partial Q}{\partial t} + \frac{\partial Q^2/A}{\partial x} = -gA \frac{\partial \zeta}{\partial x} - gAS_f \tag{2.33}$$

$$\frac{Q_i^{n+1} - Q_i^n}{\Delta t} = -\frac{(Q_{i+1}^n)^2/A_{i+1} - (Q_{i-1}^n)^2/A_{i-1}}{2\Delta x} - gA_i \frac{\zeta_{i+1}^{n+1} - \zeta_{i-1}^{n+1}}{\Delta x}$$

$$-gA_i\left[\frac{(U_i^n)^2}{C^2R_i} + \frac{(|U_{i+1}^n| - |U_{i-1}^n|)^2}{2g2\Delta x}\ \text{sign}\ U_i^n\right] \qquad (2\ 37)$$

The last term in (2.37) describing the local losses is valid if $U_{i+1} < U_{i-1}$

The boundary conditions on the first and last section of channel reaches depend on the physical processes there On the first upstream reach usually the ζ or ζ_i variation with time is prescribed In the first case that value is used directly in the equilibrium equation In the second case a numerical solution of (1.33) has to be done for the computation of updated ζ_i values and ζ is expressed as the sum of $\zeta_r + \zeta_i$. If the incident perturbation is known on the first and second sections, for example $\zeta_i = \zeta_{i_0} \sin[(2\pi t/T)]$, then

$$\zeta_{i_1}^n = \zeta_{0i} \sin[2\pi(n-1)\Delta t/T] \qquad (2\ 38)$$

$$\zeta_{i_2}^n = \zeta_{0i} \sin[2\pi(n-1)\Delta t/T - \Delta x/L] \qquad (2\ 39)$$

where $L - T\sqrt{(gh)}$. Equation (2.39) is a direct consequence of the long progressive wave theory. Based on (2.38) and (2.39) the ζ_{r_1}, ζ_{r_2} values are computed as the differences

$$\zeta_{r_1}^n = \zeta_1^n - \zeta_{i_1}^n \qquad (2\ 40)$$

$$\zeta_{r_2}^n = \zeta_2^n - \zeta_{i_2}^n \qquad (2\ 41)$$

These $\zeta_{r_1}^n, \zeta_{r_2}^n$ values, available at time level n, are used in an explicit backward difference scheme for the integration of (1 33) on the open sea boundary,

$$\zeta_{r_1}^{n+1} = \zeta_{r_1}^n + \frac{\Delta t}{\Delta x} C(\zeta_{r_2}^n - \zeta_{r_1}^n) \qquad (2\ 42)$$

The required ζ_1^{n+1} value on the boundary is the sum

$$\zeta_1^{n+1} = \zeta_{i_1}^{n+1} + \zeta_{r_1}^{n+1} = \zeta_0 \sin(2\pi n\Delta t)/T + \zeta_{r_1}^{n+1} \qquad (2.43)$$

At the downstream end if there is a coastal boundary the full reflection condition is expressed as $Q = 0$. If there is an open sea boundary the free transmission condition corresponding to (2 10) becomes,

$$Q_{i_{max}}^{n+1} = \zeta_{i_{max}-1}^{n+1} \sqrt{(9.81 B_{i_{max}} \cdot A_{i_{max}})} \qquad (2\ 44)$$

Any other form of end conditions can be investigated Program 8, in BASIC, refers to a flow domain with a given ζ upstream and downstream condition, either of full reflection or free transmission.

Fig 2.8   1-D long-wave model Flow domain discretisation and computation points in the x-t plane

where S_f the slope of the energy line, expressed according to the Chézy law, by the equation

$$S_f = \frac{U^2}{C^2 R} \qquad \left(R = \frac{A}{P} = \text{hydraulic radius}\right) \qquad (2\ 34)$$

In (2 34) a local energy loss term, in abrupt channel enlargements, can be included, expressed as

$$\Delta h = (\Delta U)^2/2g \qquad (2\ 35)$$

The numerical solution scheme to be presented is based on finite differences. An explicit scheme on a staggered grid is used. Figure 2.8 illustrates the location of the computation of Q, ζ functions on the x, t plane.

The finite difference form of Equations (2.32), (2.33), is

$$\frac{\zeta_i^{n+1} - \zeta_i^{n-1}}{\Delta t} = \frac{-2}{B_i + B_{i+1}} \cdot \frac{Q_{i+1}^n - Q_i^n}{\Delta x} \qquad (2.36)$$

PROGRAM 8. 1-D NON-LINEAR TIDAL CIRCULATION MODEL

```
      5REM 1-D NONLINEAR TIDAL CIRCULATION MODEL
      10DIM Q(50),QN(50),H(50),Z(50),R(50),B(50),A(5(
)),H0(50)
      20READ IM,DT,DX,C,PR,Z0,NM,BK
      25DATA...
      30FORI=1TOIM:READB(I):NEXTI
      35DATA...
      40FORI=1TOIM:READH0(I):H(I)=H0(I):NEXTI
      45DATA...
      50N=0:T=0
      60N=N+1:T=T+DT
      70FORI=2TOIM-1:H(I)=H0(I)+(Z(I)+Z(I-1))/2:NEXTI
      :H(1)=H0(1)+Z(1):H(IM)=H0(IM)+Z(IM-1)
      80FORI=1TOIM:A(I)=B(I)*H(I):R(I)=A(I)/(B(I)+2*H
(I)):NEXTI
      90FORI=2TOIM-1:Z(I)-Z(I)  DT/DX*(Q(I+1)-Q(I))/(B
(I)+B(I+1))*2:NEXTI
      100Z(1)=Z0*SIN(2*PI*T/PR)
      110FORI=2TOIM-1:VV=0
      120IFB(I+1)>B(I-1)ANDQ(I)>0 THEN GOTO150
      130IFB(I+1)<B(I-1) ANDQ(I)<0 THEN GOTO150
      140GOTO160
      150VV=(ABS(Q(I+1)/A(I+1))-ABS(Q(I-1)/A(I-1)))^2/
4./9.8/DX
      160QN(I)=Q(I)-DT*(Q(I+1)^2/A(I+1)-Q(I-1)^2/A(I-1
))/2/DX-DT*9.8*A(I)*(Z(I)-Z(I-1))/DX-DT*9.8*A(I)*(
(Q(I)/A(I))^2/C^2/R(I)+VV)*SGN(Q(I)):NEXTI
      170QN(1)=QN(2)
      180ON BK GOTO190,200
      190QN(IM)=Z(IM-1)*SQR(9.8*B(IM)*A(IM)):GOTO210
      200QN(IM)=0
      210FORI=1TOIM:Q(I)=QN(I):NEXTI
      220IFN/20<>INT(N/20) THEN GOTO60
      230PRINT:PRINTN:FORI=1TOIM:PRINTZ(I)::NEXTI:PRIN
T:FORI=1TOIM:PRINTQ(I)/A(I)::NEXTI:PRINT
      240IFN<NM THEN GOTO60
      250END
>
```

Description of main variables

DT, DX = time and space discretisation steps
IM = number of cross-sections in the field discretisation
C = Chézy bed friction coefficient
PR = long-wave period
Z0 = long-wave amplitude
NM = number of time steps for the numerical solution

BK = parameter defining the type of downstream boundary condition (BK = 1 → free transmission   BK = 2 → full reflection)
B(I) = width of cross-section #i
H0(I) = initial depth at section #i.

The application refers to a flow domain illustrated in Fig 2 9 It is a long channel of length = 2 km, of depth = 10 m and width varying from 30 to 10 m. At the upstream end the free surface varies sinusoidally with period $T = 500$ s and amplitude 1 m

The evolution of a free surface and the velocity along the channel is required. A free transmission downstream boundary condition (connection of the channel end to a large water body) is assumed The data are: IM = 21, DT = 5 s, DX = 100 m, C = 50 m^{1}/s, PR = 500 s, Z0 = 1 m, NM = 1000, BK = 1, H0(I) = 10 m, B(I) varying linearly from 30 to 10 m Figure 2.10 contains the free surface profiles along the channel during one wave cycle after the establishment of periodic conditions in the channel. Due to the type of downstream boundary condition, this is achieved only after the 2nd wave cycle, starting with no flow initial conditions ($Q_i = 0$, $\zeta_i = 0$, for $t = 0$).

2.2.4 Linearised model for long-wave induced circulation

A realistic simplification of the mathematical model for long-wave induced circulation is introduced by linearisation (disregarding non-linear convective and friction terms) and leads to a practical and efficient form. The formulation starts from Equations (2 21) and (2 22), dropping the convective terms. Solving successively the two equations for the ζ function in one dimension, it is found.

$$\frac{\partial U}{\partial t} = -g\frac{\partial \zeta}{\partial x} - g\frac{U|U|}{hC^2} \qquad (2\ 45)$$
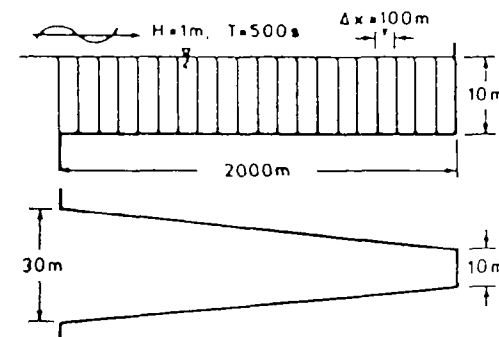
Fig 2 9   Flow domain discretisation for 1-D long-wave model
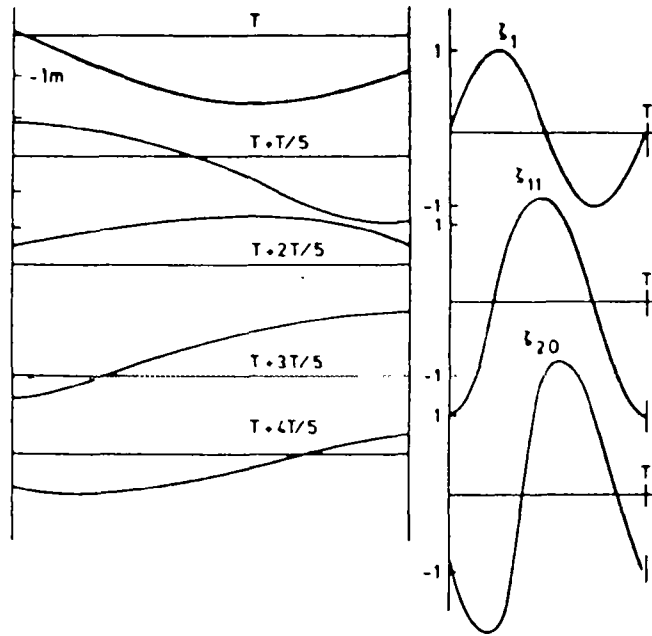
Fig 2 10   Surface time history during a wave period

$$\frac{\partial \zeta}{\partial t} + \frac{\partial h U}{\partial x} = 0 \tag{2.46}$$

$$\frac{\partial^2 \zeta}{\partial t^2} = \frac{\partial}{\partial x}\left(gh \frac{\partial \zeta}{\partial x}\right) - \frac{2g|U|}{hC^2} \cdot \frac{\partial \zeta}{\partial t} \tag{2.47}$$

The bed friction term in (2 47) has the form of the product of the time derivative by a term that can be considered as a friction coefficient

$$k = \frac{2g|U|}{hC^2} \quad \text{where } C = 18 \log\left(\frac{12h}{k_N}\right) \tag{2.48}$$

and $|U|$ is a measure of the velocity The application of long-wave theory permits the correlation of $|U|$ to the wave and the depth $(u = u_0 \sin(2pt/T)$ where $u_0 = H/2 \sqrt{(g/h)})$. The approximation of $|U|$ with its root mean value $\sqrt{(\bar{u}^2)}$ leads to an expression for k,

$$k = \frac{2g^{3/2}H}{3C^2h^{3/2}} \tag{2.49}$$

Equation (2.47) generalised in two dimensions is written

$$\frac{\partial^2 \zeta}{\partial t^2} = \frac{\partial}{\partial x}\left(gh \frac{\partial \zeta}{\partial x}\right) + \frac{\partial}{\partial y}\left(gh \frac{\partial \zeta}{\partial y}\right) - k\frac{\partial \zeta}{\partial t} \tag{2 50}$$

This is a 2nd order hyperbolic equation completed by a friction term (generalised telegraphy equation). It describes the variation only of ζ in time and space. If the velocity magnitudes are necessary at various locations of the flow domain those can be computed from the known ζ and grad ζ values by time integration of equations having the form of (2 45). Equation (2.50) does not contain the Coriolis term. Simple mathematical manipulation shows that when that term is important the right hand side of (2 50) has to be completed by a term $-f^2 \cdot \zeta$ where $f = 2\Omega \sin \varphi$

The field Equation (2 50) is completed by boundary conditions of two types:

(1) At the perimeter of the coastal boundary where full reflection of the long wave takes place

$$\frac{\partial \zeta}{\partial n} = 0 \tag{2 51}$$

(2) At the open sea boundary, the condition of free radiation of the ζ_r part is

$$\frac{\partial \zeta_r}{\partial t} + \sqrt{(gh)}\frac{\partial \zeta_r}{\partial n} = 0 \tag{2 52}$$

where n is the unit outward vector normal to that boundary The incident component ζ_i is known The numerical solution of (2 50) is based on an explicit centered finite difference scheme On the i, j nodes of the orthogonal mesh discretising the flow domain, the $\zeta_{i,j}^n$ values are computed at each time level n $(t_n = n Dt)$ The $h_{i,j}$ values referring to the node i, j are used Equation (2 50) takes the form,

$$\zeta_{i,j}^{n+1} = 2\zeta_{i,j}^n - \zeta_{i,j}^{n-1} + \frac{\Delta t^2}{2\Delta x^2} g[(h_{i+1,j} + h_{i,j})(\zeta_{i+1,j}^n - \zeta_{i,j}^n)$$
$$- (h_{i,j} + h_{i-1,j})(\zeta_{i,j}^n - \zeta_{i-1,j}^n) + (h_{i,j+1} + h_{i,j})(\zeta_{i,j+1}^n - \zeta_{i,j}^n)$$
$$- (h_{i,j} + h_{i,j-1})(\zeta_{i,j}^n - \zeta_{i,j-1}^n)] - k\Delta t(\zeta_{i,j}^n - \zeta_{i,j}^{n-1}) \tag{2 53}$$

On the coastal boundary not parallel to the Ox, Oy axes and not coinciding with mesh sides, the approximation of the $\partial\zeta/\partial n$ derivative introduces an external node to the computations where the ζ value,
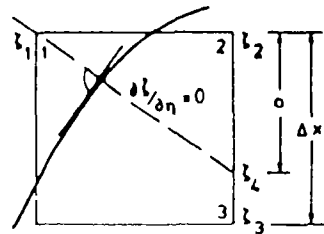
Fig 2 11   Coastal boundary node notations for 2-D linear long-wave model

according to the notation of Fig 2.11, is approximated by

$$\zeta_1 = \zeta_4, \qquad \zeta_4 = \zeta_2 + (\zeta_3 - \zeta_2)u/\Delta x \qquad (2.54)$$

where the ζ_2, ζ_3 are known internal values and u is a known line segment.

A linear long-wave model based on the forgoing numerical analysis is programmed in BASIC, Program 9. The program refers to a flow domain bounded laterally by a coast of arbitrary geometry and presenting a lower open-sea boundary parallel to Ox. The bathymetry is also variable

PROGRAM 9. 2-D LINEAR TIDAL CIRCULATION MODEL

```
>L.
    5REM 2-D LINEAR TIDAL CIRCULATION MODEL
    10DIMH(20,20),Z1(20,20),Z(20,20),ZO(20,20),IS(2
0),IE(20),I1(50),I2(50),I3(50),J1(50),J2(50),J3(50
),EL(50)
    20READ DT,DX,PR,AO,CF,IM,JM,NM,BR
    30DATA...
    40FORJ=1TOJM-1:READIS(J),IE(J):NEXTJ
    50DATA...
    60FORK=1TOBR:READI1(K),J1(K),I2(K),J2(K),I3(K),
J3(K),EL(K):NEXTK
    70DATA...
    80FORJ=1TOJM-1:FORI=IS(J)TOIE(J):H(I,J)=30:NEXT
I:NEXTJ
    110T=0:N=0
    120T=T+DT:N=N+1
    130FORJ=2TOJM-1:FORI=IS(J)TOIE(J):Z1(I,J)=2*Z(I,
J)-ZO(I,J)+DT^2/DX^2/2*9.81*((H(I+1,J)+H(I,J))*(Z(
I+1,J)-Z(I,J))-(H(I,J)+H(I-1,J))*(Z(I,J)-Z(I-1,J))
+(H(I,J)+H(I,J+1))*(Z(I,J+1)-Z(I,J))-(H(I,J)+H(I,J
-1))*(Z(I,J)-Z(I,J-1)))
    140ZZ1(I,J)=Z1(I,J)-CF*DT*(Z(I,J)-ZO(I,J)):NEXTI:
```

No .TJ
```
    160FORK=1TOBR:I1=I1(K):I2=I2(K):I3=I3(K):J1=J1(K
):J2=J2(K):J3=J3(K)
    170Z1(I1,J1)=Z1(I2,J2)+(Z1(I3,J3)-Z1(I2,J2))*EL(
K):NEXTK
    180FORI=IS(1)TOIE(1):C=SQR(9.81*H(I,1)):L=C*PR
    190IF(T-DT)>DX/C THEN GOTO210
    200Z1=0:GOTO220
    210Z1=Z(I,1)-AO*SIN(2*PI*(T-DT)/PR):Z2=Z(1,2)-AO
*SIN(2*PI*(T-DT)/PR-DX/L):Z1=Z1+DT/DX*C*(Z2-Z1)
    220Z1(I,1)=Z1+AO*SIN(2*PI*T/PR):NEXTI :JV
    230FORJ=1TOJM:FORI=1TOIM:ZO(I,J)=Z(I,J):Z(I,J)=Z
1(I,J):NEXTI:NEXTJ
    240IFN/10<>INT(N/10) THEN GOTO120
    250PRINT:PRINT:FORJ=JM TO 1 STEP-1:FORI=1TOIM:P
RINTZ(I,J)::NEXTI:PRINT:NEXTJ
    260IFN<NM THEN GOTO120
    270END
```

Description of main variables:

DT, DX = time and space discretisation steps
PR   = period of incident wave
A0   = amplitude of incident wave
CF   = bed friction coefficient (k)
IM, JM = maximum values of i, j indices along Ox, Oy
NM   = time steps of computation
BK   = number of coastal nodes on exterior and interior (islands) coastal boundaries. The indices I_1, J_1 (coordinates of the node) and I_2, J_2, I_3, J_3 (coordinates of related internal nodes) according to Fig. 2.11 and Equation (2.54)
EL   = the corresponding ratio a/Dx in (2.54)
IS, IE = coupled values of i index for each j, indicating lateral limits (leftmost and rightmost limits respectively) of the flow domain.

The application described below is intended to demonstrate the variation of wave height between the entrance and innermost boundary of a coastal basin. The flow domain and its discretisation are given in Fig. 2.12. The data for that application is DT = 30 s, DX = 1000 m, PR = 2000 s, CF = 3 10⁻⁴ (corresponding to Chézy $C = 20 \text{ m}^{1/2}/\text{s}$), IM = 9, JM = 9, NM = 300, BK = 15, A0 = 1 m, H(I, J) = 30 m The rest of the data are given in Tables 2 1 and 2.2 Figure 2.13 contains the free surface tide curves at the bay entrance and the inner coastal boundary.
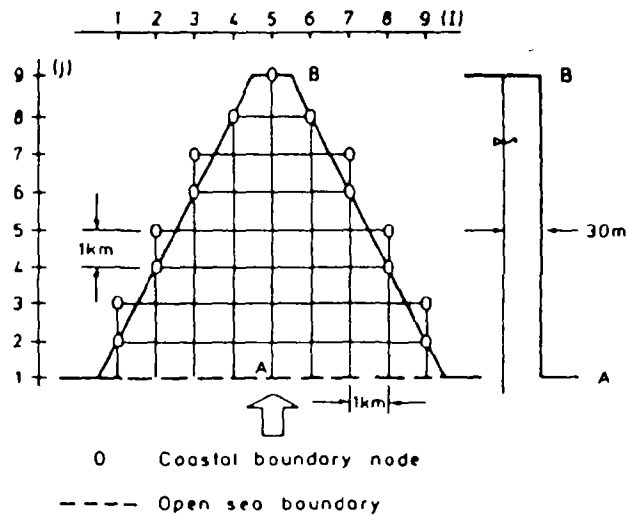
Fig 2 12 Coastal domain of 2-D linear long-wave model application

O Coastal boundary node

— — — Open sea boundary

Table 2.1

J	IS	IE
1	2	8
2	2	8
3	2	8
4	3	7
5	3	7
6	4	6
7	4	6
8	5	5

Table 2.2

K	I_1	J_1	I_2	J_2	I_3	J_3	H
1	1	2	2	2	2	1	0 5
2	1	3	2	3	2	2	0 5
3	2	4	3	4	3	3	0 5
4	2	5	3	5	3	4	0 5
5	3	6	4	6	4	5	0 5
6	3	7	4	7	4	6	0 5
7	4	8	5	8	5	7	0 5
8	5	9	5	8	5	8	0
9	6	8	5	8	5	7	0 5
10	7	7	6	7	6	6	0 5
11	7	6	6	6	6	5	0 5
12	8	5	7	5	7	4	0 5
13	8	4	7	4	7	3	0 5
14	9	3	8	3	8	2	0 5
15	9	2	8	2	8	1	0 5
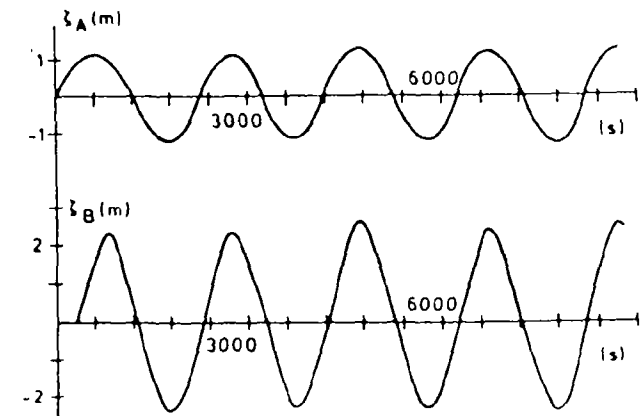
Fig 2 13 Evolution of free surface at points A, B

2.3 WIND GENERATED CIRCULATION

The wind generated circulation model describes the phenomenon under the same assumptions made in Section 2.1. So the general circulation equations (2.5) to (2 7) are valid in this case, too.

The circulation is forced by the shear stresses on the water surface exercised by the wind. They appear in the model in the form of free surface boundary conditions (2.13), (2 14) For small scale geophysical domains $(O[L] = 10^4 \, m)$ the wind velocity may be assumed uniform and thus the components τ_{sx}, τ_{sy} are constant in space but variable in time For larger geophysical domains this assumption is not realistic and the influence of wind nonuniformity has to be checked.

The wind generated waves are not incorporated in the model. Only the wind induced shear The free surface is approximated by the mean level (with respect to the waves). The inclusion of the influence of waves in the wind generated circulation can be done implicitly in a parametric manner during the model calibration (determination of

the surface friction coefficient and eddy viscosity distribution by comparison with the in situ measurements).

A solution of the general circulation model is not given in this book—only a comment on the eddy viscosity distribution over the vertical is considered worth mentioning. As the stronger velocity gradients appear near both the bed and the surface, the turbulence intensity and vertical momentum diffusion are related to both u_b and $u_* = \sqrt{(\tau_s/\rho)}$ The eddy viscosity distribution, deriving from higher order turbulence closure, simulates in an optimal way the wind generated profile (see Fig. 2.14). The maximum is at a distance $1/3h$ from the surface and its value is proportional to

$$v_{max} \propto \lambda u_* h, \qquad O[\lambda] = 0 \ 1 \qquad (2\ 55)$$

Figure 2 14 contains morphologies of current profiles in domains confined laterally by coastal boundaries. In such domains the current direction and intensity vary considerably along the depth. At the surface the current follows the wind direction (with declination to the right in the Northern hemisphere). Some distance below the surface, the direction is reversed due to return flows imposed by coastal boundaries.

These comments on the general morphology of the wind generated current profiles show that simple depth averaging of the general model (analogous to that for the long-wave induced circulation) has
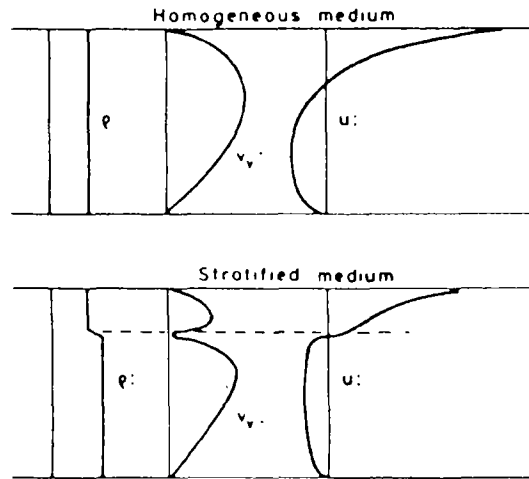
Fig 2 14 Distribution of wind generated current in 1-D enclosed basin for homogeneous and stratified medium

to be done very carefully. The simple 2-D horizontal model used operationally in the past for wind generated circulation has the form:

$$\frac{\partial U}{\partial t} + U\frac{\partial U}{\partial x} + V\frac{\partial U}{\partial y} = -g\frac{\partial \zeta}{\partial x} + fV + \frac{\tau_{sx}}{\rho h} - \frac{\tau_{bx}}{\rho h} \qquad (2\ 56)$$

$$\frac{\partial V}{\partial t} + U\frac{\partial V}{\partial x} + V\frac{\partial V}{\partial y} = -g\frac{\partial \zeta}{\partial y} - fU + \frac{\tau_{sy}}{\rho h} - \frac{\tau_{by}}{\rho h} \qquad (2\ 57)$$

$$\frac{\partial \zeta}{\partial t} + \frac{\partial (Uh)}{\partial x} + \frac{\partial (Vh)}{\partial y} = 0 \qquad (2\ 58)$$

where the bed friction terms are expressed by quadratic forms

$$\frac{\tau_{bx}}{\rho} = kU\sqrt{(U^2 + V^2)}, \qquad \frac{\tau_{by}}{\rho} = kV\sqrt{(U^2 + V^2)} \qquad (2\ 59)$$

The criticism that can be made of that model refers to

(1) The depth average approximation of the convective terms:

$$\frac{1}{h}\int_{-h}^{0} u\frac{\partial u}{\partial x}\,dz \simeq U\frac{\partial U}{\partial x} \qquad (2\ 60)$$

As the $u(z), v(z)$ distributions are highly non-uniform (2.60) is inaccurate. The correction that can be made to (2 60) can take the form of an additional term known as horizontal momentum dispersion term.

(2) Equation (2.59) implies that when the depth-mean velocity components are zero, the friction terms are suppressed From the typical morphology of wind generated current profile it can be concluded that even in the case of zero depth-mean velocities the near bed shear is not negligible and acts in the same direction as the surface shear. This means that a better approximation to τ_{bx}, τ_{by} than (2 59) has to be used

A first upgrading of the model (2.56),(2 57) without solving in three-dimensional space can be made by adopting a certain distribution of current over the depth. Let us assume that the $u(z)$ form is:

$$u(z) = \alpha z^2 + \beta z + \gamma \qquad (2\ 61)$$

The following conditions are used for computation of the undetermined coefficients α, β, γ:

(1) Free surface condition

$$\frac{\partial u}{\partial z}\bigg|_{z=0} = \frac{\tau_s}{\rho \nu} \qquad (2.62)$$

(2) Bed condition

$$u\bigg|_{z=-h} = 0 \qquad (2.63)$$

(3) Depth mean velocity definition

$$U = \frac{1}{h}\int_{-h}^{0} u\, dz \qquad (2.64)$$

The application of Equations (2 62) to (2 64) in (2.61) gives

$$u(z) = (\tfrac{3}{4}a - \tfrac{3}{2}U)\left[\left(\frac{z}{h}\right)^2 - 1\right] + a\left(\frac{z}{h} + 1\right) \qquad (2.65)$$

where

$$a = \frac{\tau_s h}{\rho \nu}$$

The problem is transposed to the determination of the eddy viscosity ν (at the surface). In order to be consistent with the parabolic velocity distribution a constant eddy viscosity is assumed with mean value

$$\bar{\nu} = \lambda h \sqrt{\left(\frac{\tau_s}{\rho}\right)} \qquad (2.66)$$

Turbulence models and laboratory measurements indicate that $O[\lambda] = 0.1$. For $\bar{\lambda} = 0\,066$, it is found that

$$a = \frac{h\tau_s}{\rho\nu} = 16.6 \sqrt{\left(\frac{\tau_s}{\rho}\right)}$$

and the velocity distribution (2 65) is expressed in terms of known magnitudes and the mean depth $U(x, y)$. The substitution of (2.65) and (2.66) in the bed shear expression $\tau_b/\rho = \nu\, \partial u/\partial z$ gives for τ_b/ρ:

$$\frac{\tau_b}{\rho} = 0\,18 \sqrt{\left(\frac{\tau_s}{\rho}\right)} U - 0.5\frac{\tau_s}{\rho} \qquad (2.67)$$

Finally, the use of (2.65) in the integral of the convective term $u\, \partial u/\partial x$ along the depth gives

$$\frac{1}{h}\int_{-h}^{0} u\frac{\partial u}{\partial x}\, dz = U\frac{\partial U}{\partial x} + \left(0.2U + \frac{a}{40}\right)\frac{\partial U}{\partial x} \qquad (2.68)$$

The 2DH model, improved with respect to the horizontal momentum

dispersion and the bed friction for wind generated circulation, becomes on the basis of (2.67) and (2.68):

$$\frac{\partial U}{\partial t} + U\frac{\partial U}{\partial x} + V\frac{\partial U}{\partial y} + \left(0.2U + \frac{a_x}{40}\right)\frac{\partial U}{\partial x} + \left(0.2V + \frac{a_y}{40}\right)\frac{\partial U}{\partial y}$$

$$= -g\frac{\partial \zeta}{\partial x} + fV + \frac{\tau_{sx}}{\rho h} - \left(0\,18\frac{U}{h}\sqrt{\left(\frac{\tau_s}{\rho}\right)} - 0\,5\frac{\tau_{sx}}{\rho h}\right) \qquad (2\,69)$$

$$\frac{\partial V}{\partial t} + U\frac{\partial V}{\partial x} + V\frac{\partial V}{\partial y} + \left(0.2U + \frac{a_x}{40}\right)\frac{\partial V}{\partial x} + \left(0\,2V + \frac{a_y}{40}\right)\frac{\partial V}{\partial y}$$

$$= -g\frac{\partial \zeta}{\partial y} - fU + \frac{\tau_{sy}}{\rho h} - \left(0.18\frac{V}{h}\sqrt{\left(\frac{\tau_s}{\rho}\right)} - 0\,5\frac{\tau_{sy}}{\rho h}\right) \qquad (2\,70)$$

The continuity equation keeps its form (2.58)

The coastal boundary conditions are the same as those for long-wave circulation. On the open sea boundary where there is no incidence perturbation waves coming from inside are freely radiated by application of condition (2.10).

Based on the same explicit finite difference scheme on a staggered grid as that used for the long-wave induced circulation, the computer program synthesized for the wind generated model is little different from the previous one. The only variation appears in the statements for the computation of UN, VN (the velocity components) and in the application of the open-sea boundary condition. By way of repetition a BASIC program is presented which refers to a flow domain with arbitrary coastal geometry, Program 10. The wind influence is assumed constant over the flow field. A time series of wind velocity components could be introduced in the case of wind varying with time. The initial condition is one of a cold start and the transient development of the hydrodynamic conditions to steady flow is followed. The printed results display U, V and ζ values at the mesh centers. Equation (2.65) permits the computation of the current pattern at any depth. If, for example, the free surface velocity components are required (for subsequent use in a surface advective diffusive pollutant transport model) they can be computed from (2.65)

$$u_{surf} = 1\,5U + a_x/4 \qquad (2.71)$$

$$v_{surf} = 1.5V + a_y/4 \qquad (2.72)$$

PROGRAM 10: 2-D MODIFIED WIND GENERATED CIRCULATION MODEL

```
    5REM 2-D MODIFIED WIND GENERATED CIRCULATION M
ODEL
    10DIMU(20,20),UN(20,20),V(20,20),VN(20,20),H(20
,20),Z(20,20),IS(20),IE(20),IB(50),JB(50),NB(50)
    20READDT,DX,CS,WX,WY,F,IM,JM,KB,NM
    30DATA...
    40FORJ=1TOJM-1:READIS(J),IE(J):NEXTJ
    50DATA...
    60FORJ=1TOJM-1 :FORI=IS(J)-1TOIE(J)+1:READH(I,J
):NEXTI:NEXTJ
    70DATA...
    80TX=CS*WX*SQR(WX^2+WY^2):TY=CS*WY*SQR(WX^2+WY
2):TS=SQR(TX^2+TY^2)
    90FORK=1 TO KB:READIB(K),JB(K),NB(K):NEXTK
    100DATA...
    110N=0:T=0:EK=0
    120N=N+1:T=T+DT
    130FORJ=2TOJM-2:FORI=IS(J)TOIE(J):Z(I,J)=Z(I,J)-
DT/2/DX*(U(I+1,J)*(H(I,J)+H(I+1,J))-U(I,J)*(H(I,J)
+H(I-1,J))+V(I,J+1)*(H(I,J+1)+H(I,J))-V(I,J)*(H(I,
J)+H(I,J-1))):NEXTI:NEXTJ
    140FORJ=2TOJM-2:FORI=IS(J)+1TOIE(J):VV=(V(I,J)+V
(I-1,J)+V(I,J+1)+V(I-1,J+1))/4:HM=(H(I,J)+H(I-1,J)
)/2
    150AD=(1.2*U(I,J)+.4*SGN(TX)*SQR(ABS(TX)))*(U(I+
1,J)-U(I-1,J))/2/DX+(1.2*VV+.4*SGN(TY)*SQR(ABS(TY)
))*(U(I,J+1)-U(I,J-1))/2/DX:BF=.18*U(I,J)/HM*SQR(T
S)-.5*TX/HM:UN(I,J)=U(I,J)-DT*(AD+9.81*(Z(I,J)-Z(I
-1,J))/DX-F*VV+BF-TX/HM):NEXTI:NEXTJ
    160FORJ=3TOJM-2:FORI=IS(J)TOIE(J):UU=(U(I,J)+U(I
+1,J)+U(I,J-1)+U(I+1,J-1))/4:HM=(H(I,J)+H(I,J-1))/
2
    170AD=(1.2*V(I,J)+.4*SGN(TY)*SQR(ABS(TY)))*(V(I,
J+1)-V(I,J-1))/2/DX+(1.2*UU+.4*SGN(TX)*SQR(ABS(TY)
))*(V(I+1,J)-V(I-1,J))/2/DX:BF=.18*V(I,J)/HM*SQR(T
S)-.5*TY/HM:VN(I,J)=V(I,J)-DT*(AD+9.81*(Z(I,J)-Z(I
,J-1))/DX+F*UU+BF-TY/HM):NEXTI:NEXTJ
    180FORK=1TOKB:I=IB(K):J=JB(K):ON NB(K)-1 GOTO 19
0,200,210,220,230,240,250,260,270,280,290
    190UN(I,J)=0:GOTO310
    200VN(I,J)=0:GOTO310
    210UN(I,J)=0:VN(I,J)=0:GOTO310
    220UN(I,J)=-Z(I,J)*SQR(9.81/H(I,J)):VN(I-1,J)=VN
(I,J):GOTO310
    230UN(I+1,J)=Z(I,J)*SQR(9.81/H(I,J)):VN(I+1,J)=V
N(I,J):GOTO310
    240VN(I,J+1)=Z(I,J)*SQR(9.81/H(I,J)):UN(I,J+1)=U
    250VN(I,J)=-Z(I,J)*SQR(9.81/H(I,J)):UN(I,J-1)=UN
(I,J):GOTO310
    260UN(I,J)=-Z(I,J)*SQR(9.81/H(I,J)):VN(I,J)=0:GO
TO310
    270UN(I+1,J)=Z(I,J)*SQR(9.81/H(I,J)):VN(I,J)=0:G
OTO310
    280UN(I,J)=0:VN(I,J+1)=Z(I,J)*SQR(9.81/H(I,J)):G
OTO310
    290UN(I,J)=0:VN(I,J)=-Z(I,J)*SQR(9.81/H(I,J))
    310NEXTK
    320FORJ=1TOJM:FORI=1TOIM:U(I,J)=UN(I,J):V(I,J)=V
N(I,J):NEXTI:NEXTJ
    330IFN/50<>INT(N/50) THEN GOTO120
    340KK=EK:EK=0:FORJ=2TOJM-2:FORI=IS(J)TOIE(J):EK=
EK+((U(I,J)+U(I+1,J))^2+(V(I,J)+V(I,J+1))^2)*H(I,J
)/8:NEXTI:NEXTJ
    350PRINTN,EK
    360IFABS(EK-KK)/EK>.0001 OR N<NM THEN GOTO120
    370PRINT"UU":FORJ=JM-2 TO 2 STEP-1:FORI=2TOIM-2:
PRINT(U(I,J)+U(I+1,J))/2:NEXTI:PRINT:NEXTJ
    380PRINT"VV":FORJ=JM-2 TO 2 STEP-1:FORI=2TOIM-2:
PRINT(V(I,J)+V(I,J+1))/2:NEXTI:PRINT:NEXTJ
    390PRINT"ZZ":FORJ=JM-2 TO 2 STEP-1:FORI=2TOIM-2:
PRINTZ(I,J):NEXTI:PRINT:NEXTJ
    400END
```

Description of main variables:

DX, DT	= space and time discretisation steps
CS	= wind friction coefficient K
WX, WY	= wind velocity components along Ox, Oy
F	= Coriolis coefficient
IM, JM	= maximum values of I, J grid indices
KB	= number of boundary (coastal + open sea) meshes to be specially treated
NM	= maximum number of time steps
IS(J), IE(J)	= leftmost and rightmost values of mesh index i for various ordinates j
H(I, J)	= water depths at mesh centers
IB, JB, NB	= coordinate indices for boundary meshes and index denoting the type of boundary For NB, the numbering as shown in Fig. 2.4 is used

The application is a comparative presentation of the numerical solutions of the two 2DH models of wind generated circulation, the modified one and the classical one without correction of the $u(\partial u/\partial x)$, τ_b/ρ terms. The flow domain morphology and its discretisation by a
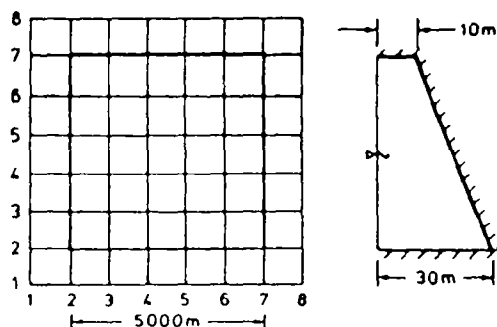
Fig 2.15   Flow domain and discretisation for wind generated circulation model

square grid is given in Fig 2.15. Program data: $DT = 30\,s$, $DX = 1000\,m$, $CS = 0.000\,005$ (an exaggerated value as $O[k] = 1 - 3 \times 10^{-6}$), $WX = 10\,m/s$, $WY = 10\,m/s$, $IM = 8$, $JM = 8$, $KB = 9$, $NM = 2000$

IS	2	2	2	2	2	2	2	
IE	6	6	6	6	6	6	6	
IB	2	2	2	2	2	3	4	5	6
JB	2	3	4	5	6	2	2	2	2
NB	4	2	2	2	2	3	3	3	3

Figure 2.16 illustrates the development of the kinetic energy up to the establishment of steady flow conditions, the steady flow U, V fields and the surface profile along the diagonal oriented parallel to the wind. The difference between the two models in the kinetic energy development and the storm surge is obvious. Regarding the latter, it has to be said that the corrected model in the case of wind blowing normal to a coast (with small depth mean velocities) results in higher free surface gradients balancing both the free surface shear and the bed shear (in the same direction) and consequently to higher storm surges along the coast

2.4 WAVE GENERATED CIRCULATION

Wave generated circulation describes the mean motion that is generated in coastal areas where wind-generated short waves refract,
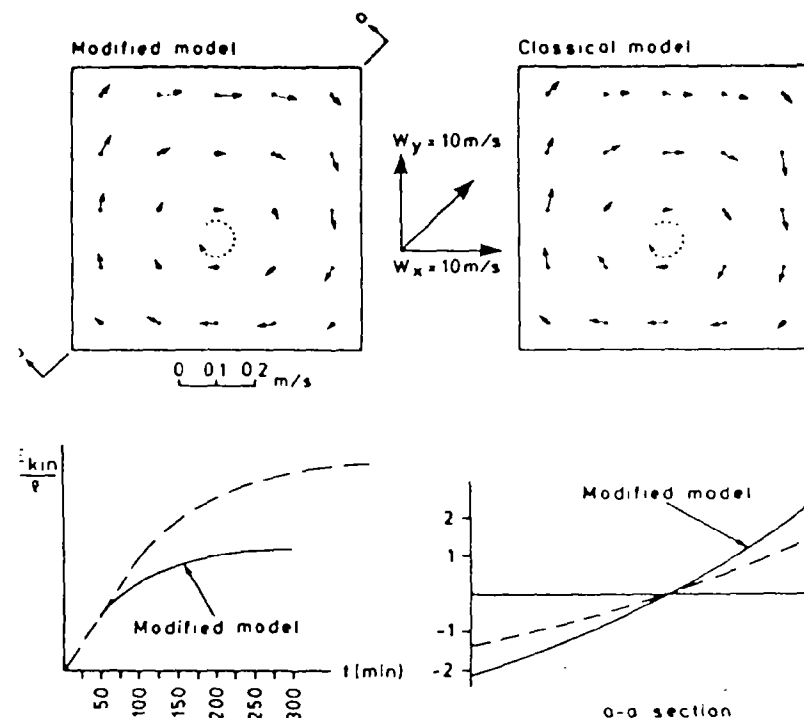
Fig 2.16   Circulation patterns, energy evolution and surface profile for the classical and modified wind generated circulation model

shoal, diffract or break. This circulation is due to the spatial variation in the momentum contained by the waves. As was mentioned in Chapter 1, the radiation stresses describe the depth mean wave momentum integrated over a wave period T It was shown in Section 1.7 (Equations (1.76)–(1.78)) that the radiation stress components $\sigma_{xx}, \sigma_{xy}, \sigma_{yx}, \sigma_{yy}$ form a symmetric second order tensor and their action is completely analogous to the stress tensor As they describe the depth mean components of momentum along the sides of an infinitesimal column of water (base dx, dy, height h), their inclusion in the mathematical model for the 2DH flows is straightforward. Their spatial gradients appear on the right hand side of the equilibrium equations The wave generated circulation model containing the radiation stresses as flow forcing factor has the form:

$$\frac{dU}{dt} = -g\frac{\partial \zeta}{\partial x} - \frac{\tau_{bx}}{\rho h} - \frac{1}{\rho h}\left(\frac{\partial \sigma_{xx}}{\partial x} + \frac{\partial \sigma_{xy}}{\partial y}\right) \qquad (2.73)$$

$$\frac{dV}{dt} = -g\frac{\partial\zeta}{\partial y} - \frac{\tau_{by}}{\rho h} - \frac{1}{\rho h}\left(\frac{\partial\sigma_{xy}}{\partial x} + \frac{\partial\sigma_{yy}}{\partial y}\right) \qquad (2.74)$$

$$\frac{\partial\zeta}{\partial t} + \frac{\partial(Uh)}{\partial x} + \frac{\partial(Vh)}{\partial y} = 0 \qquad (2.75)$$

The $\zeta(x, y, t)$ function describes the difference between the mean surface level (with respect to waves) and the still water level (difference between MWL and SWL). Its time variation does not refer to the rapid variation of the surface during the passage of the waves (with period of some seconds) but to the long term variations of the MWL. The Coriolis term can be dropped from (2.73), and (2.74) when the model is applied over small geophysical domains such as narrow coastal strips where the refraction or diffraction of waves takes place

A criticism that can be made of the form of the model presented refers to the depth averaging of the momentum. Unlike long-wave generated barotropic flows and wind generated circulation, the velocity variation over the depth is considerable (as analysis in the x, y, z, t space and measurements in the surf zone indicate) and the depth varying model should be used It is beyond the scope of this book and most of the operational models used today. The bed shear is expressed also by quadratic relations of the form (2.59).

The remaining boundary conditions and the numerical solution follow the same path as the described wind or tidal circulation. The difference appears in the statements for the composition of UN, VN values, where the radiation stress gradients appear. This means that a subprogram for the computation of the SXX(I,J), SYY(I,J) and SXY(I,J) components from the wave characteristics should precede the computation of velocities First, the value of the wave parameter n, the wave angle θ (angle measured from the positive Ox axis to the wave orthogonal according to the notation of Fig 2 17) and the wave height H (the H_{rms} value in case of random waves) have to be computed. The radiation stress components computed refer to the mesh centers.

Program 11 is adapted to a flow domain of variable depth bounded by an upper coastal boundary, a lower open sea boundary and lateral uniform flow boundaries ($\partial/\partial x = 0$). It may also contain several coastal structures, such as moles, a breakwater, etc around which the wave generated circulation has to be computed A typical morphology of the flow domain is given in Fig. 2.17.

The order of magnitude of the Δx step in such a situation (circulation around a coastal structure) is smaller than that for a model of general circulation in a bay $O[\Delta x] = 10^2$ m. It is preferable
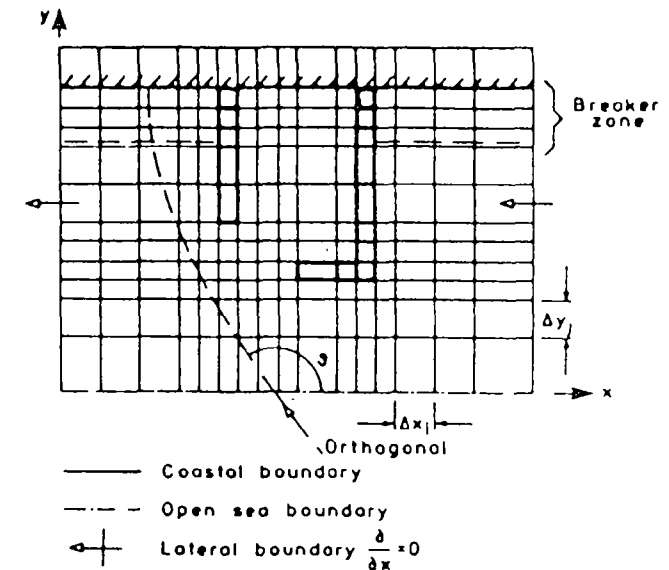
Fig 2 17 Wave induced circulation in refraction-diffraction and breaking areas Morphology of domain

for the $\Delta x, \Delta y$ steps to be variable, so that the resolution is higher in desired areas of the flow domain.

PROGRAM 11: 2-D WIND AND WAVE GENERATED CIRCULATION MODEL

```
5REM 2-D WIND AND WAVE GENERATED CIRCULATION M
ODEL
10DIMU(20,20),UN(20,20),V(20,20),VN(22,20),Z(20
,20),H(20,20),XX(20,20),XY(20,20),YY(20,20),DX(20)
,DY(20),IB(80),JB(80),NB(80)
20READDT,IM,JM,NM,CF,WX,WY,CB,TH,KB
22DATA...
30FORI=1TOIM-1:READDX(I):NEXTI
40DATA...
50FORJ=1TOJM-1:READDY(J):NEXTJ
60DATA...
70FORI=1TOIM-1:FORJ=1TOJM-1:READH(I,J),XX(I,J),
XY(I,J),YY(I,J) :NEXTJ:NEXTI
75DATA...
80SX=CS*WX*SQR(WX^2+WY^2):SY=CS*WY*SQR(WX^2+WY^
2)
90FORK=1TOKB:READIB(K),JB(K),NB(K):NEXTK
100DATA....
110FORI=1TOIM-1:H(I,0)=H(I,1):XX(I,0)=XX(I,1):YY
```

```
(I,0)=YY(I,1);XY(I,0)=XY(I,1);DY(0)=DY(1);NEXTI
120FORJ=1TOJM-1;H(0,J)=H(1,J);XX(0,J)=XX(1,J);XY
(0,J)=XY(1,J);YY(0,J)=YY(1,J);DX(0)=DX(1);H(IM,J)=
H(IM-1,J);XX(IM,J)=XX(IM-1,J);YY(IM,J)=YY(IM-1,J);
XY(IM,J)=XY(IM-1,J);DX(IM)=DX(IM-1);NEXTJ
130FORK=1TOKB;IF NB(K)<>4 THEN GOTO150
140I=IB(K);J=JB(K);H(I,J)=1
150NEXTK;N=0;T=0
160N=N+1;T=T+DT
170FORJ=1TOJM-2;FORI=1TOIM-1;Z(I,J)=Z(I,J)-DT*((
U(I+1,J)*(H(I+1,J)+H(I,J))-U(I,J)*(H(I,J)+H(I-1,J)
))/DX(I)+(V(I,J+1)*(H(I,J+1)+H(I,J))-V(I,J)*(H(I,J
)+H(I,J-1)))/DY(J))/2  ;NEXTI;NEXTJ
180FORJ=1TOJM-2;FORI=2TOIM-1;HM=(H(I,J)+H(I-1,J)
)/2;VV=(V(I,J)+V(I,J+1)+V(I-1,J)+V(I-1,J+1))/4;XM=
(DX(I)+DX(I-1))/2;YM=(DY(J)+(DY(J-1)+DY(J+1))*.5)

190UN(I,J)=U(I,J)*TH+(1-TH)/4*(U(I+1,J)+U(I-1,J)
+U(I,J+1)+U(I,J-1))-DT*(U(I,J)*(U(I+1,J)-U(I-1,J))
/XM/2+VV*(U(I,J+1)-U(I,J-1))/YM+9.81*(Z(I,J)-Z(I-1
,J))/XM+((XX(I,J)-XX(I-1,J))/XM+(XY(I,J+1)+XY(I-1,
J+1)-XY(I,J-1)-XY(I-1,J-1))/YM/2)/HM)
200UN(I,J)=UN(I,J)-DT*CF*U(I,J)*SQR(U(I,J)^2+VV^
2)/HM+DT*8X/HM;NEXTI;NEXTJ
210FORJ=2TOJM-2;FORI=1TOIM-1;UU=(U(I,J)+U(I+1,J)
+U(I,J-1)+U(I+1,J-1))/4;HM=(H(I,J)+H(I,J-1))/2;XM=
DX(I)+(DX(I+1)+DX(I-1))*.5;YM=(DY(J)+DY(J-1))/2
220VN(I,J)=V(I,J)*TH+(1-TH)/4*(V(I,J+1)+V(I,J-1)
+V(I+1,J)+V(I-1,J))-DT*(V(I,J)*(V(I,J+1)-V(I,J-1))
/YM/2+UU*(V(I+1,J)-V(I-1,J))/XM+9.81*(Z(I,J)-Z(I,J
-1))/YM+((YY(I,J+1)-YY(I,J-1))/YM+(XY(I+1,J)+XY(I+
1,J-1)-XY(I-1,J)-XY(I-1,J-1))/2/XM)/HM)
230VN(I,J)=VN(I,J)-DT*CF*V(I,J)*SQR(V(I,J)^2+UU^
2)/HM+DT*8Y/HM;NEXTI;NEXTJ
240FORK=1TOKB;I=IB(K);J=JB(K)    ;ONNB(K)-1 GOTO25
0,260,270
250UN(I,J)=0;GOTO280
260VN(I,J)=0;GOTO280
270VN(I,J)=0;UN(I,J)=0
280NEXTK
290FORJ=1TOJM-1;UN(1,J)=UN(2,J);VN(0,J)=VN(1,J);
UN(IM,J)=UN(IM-1,J);VN(IM,J)=VN(IM-1,J);NEXTJ
300FORI=1TOIM-1;UN(I,0)=UN(I,1);VN(I,1)=-Z(I,1)*
SQR(9.8/H(I,1));NEXTI
310FORJ=1TOJM;FORI=1TOIM;U(I,J)=UN(I,J);V(I,J)=V
N(I,J);NEXTI;NEXTJ
320IF N/20<>INT(N/20) THEN GOTO160
330EKK=EK;EK=0;FORJ=1TOJM-2;FORI=1TOIM-1;EK=EK+(
(U(I,J)+U(I+1,J))^2+(V(I,J)+V(I,J+1))^2)/8/DX(I)*D
Y(J)*H(I,J)  ;NEXTI;NEXTJ
```

```
340P    'N,EK
3501    .NM OR ABB(EKK-EK)/EK>.001 THEN GOTO 160
360F.   -JM-2 TO 2 STEP-1;FORI=1TOIM-1;PRINT(U(I,
J)+U(I+1,J))/2;;NEXTI;PRINT;NEXTJ;PRINT
370FORJ=JM-2 TO 2 STEP-1;FORI=1TOIM-1;PRINT(V(I,
J)+V(I,J+1))/2;;NEXTI;PRINT;NEXTJ;PRINT
380FORJ=JM-2 TO 2 STEP-1;FORI=1TOIM-1;PRINTZ(I,J
);;NEXTI;PRINT;NEXTJ;PRINT
400END
```

In the description of variables the only new ones, compared with the previous models, are the data arrays for the radiation stresses $\sigma_{xx}/\rho = XX$, $\sigma_{xy}/\rho = XY$, $\sigma_{yy}/\rho = YY$ and the parameter θ in the recommended diffusive Lax type finite difference for the time derivative.

$$\frac{\partial U}{\partial t} = [U_{i,j}^{n+1} - U_{i,j}^{n} \; \theta + \{(1-\theta)/4\} \times (U_{i+1,j}^{n} + U_{i-1,j}^{n} + U_{i,j+1}^{n} + U_{i,j-1}^{n})]/\Delta t \qquad (2.76)$$

This type of finite difference approximation entails horizontal momentum diffusion with a diffusion coefficient equal to $\{(1-\theta)\Delta x^2\}/\Delta t/4$. Care should be taken in the determination of θ that the introduced diffusion is realistic.

The application is concerned with the wave generated circulation in a coastal area of simple geometry (i.e. straight coastline, constant bed slope and parallel bed contours). An L-shaped mole is constructed to face the prevailing waves. The flow domain and its discretisation are shown in Fig 2.18. The waves approaching the coast have $H_0 = 2$ m, $T = 7$ s and direction SW.

The main program data are: DT = 5 s, IM = 20, VM = 16, MN = 300, CF = 0.01, TH = 0.95, KB = 26

DX(I).   40, 40, 40, 40, 20, 10, 10, 10, 10, 10, 20, 20, 20, 20, 20, 40, 40, 40, 40, 40

DY(J):   40, 40, 20, 20, 20, 10, 10, 10, 10, 10, 10, 10, 10, 10, 10

The water depth refers to the mesh centers. In the modelled port basin the depth is considered constant, equal to 6 m. The radiation stresses are computed via the refraction and diffraction of waves in the area. The B's (orthogonal spacing) giving k, and the θ's (wave angles) are computed in the flow domain. In the basin interior k_D and θ are computed by the Wiegel tables (diffraction around an infinite breakwater). The above refraction and diffraction computations give the wave heights and θ at the mesh centers. The σ_{xx}/ρ, σ_{xy}/ρ, σ_{yy}/ρ values are computed by means of a sub-routine for radiation stress
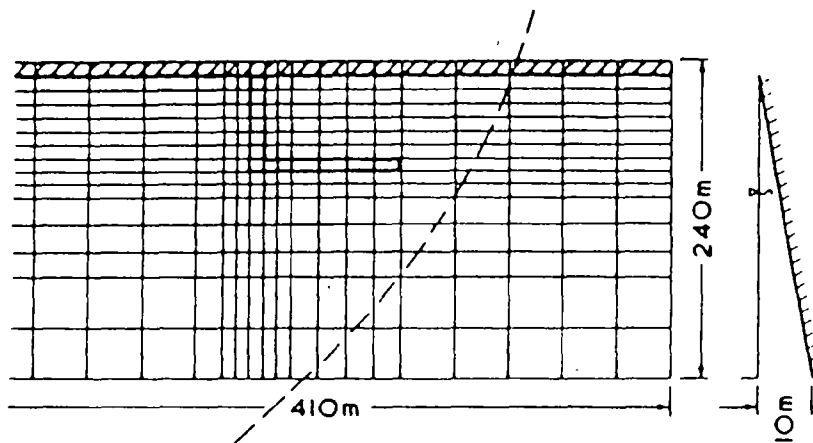
Fig 2 18 Flow domain, its discretisation and typical refracted orthogonal

PROGRAM 12: RADIATION STRESS COMPUTATION FROM WAVE ANGLE AND ORTHOGONALS DISTANCE

```
5REM RADIATION STRESSES COMPUTATION FROM WAVE
ANGLE AND ORTHOGONALS DISTANCE
   10DIMH(20,20),HH(20,20),SXX(20,20),SXY(20,20),S
YY(20,20),TH(20,20),DX(20),DY(20),B(20,20),LL(50)
   20READIM,JM,H0,T,DM,B0
   30DATA...
   40FORJ=1TOJM-1:FORI=1TOIM-1:READH(I,J):NEXTI:NE
XTJ
   50DATA...
   60FORJ=1TOJM-1:FORI=1TOIM-1:READTH(I,J):NEXTI:N
EXTJ
   70DATA...
   80FORJ=1TOJM-1:FORI=1TOIM-1:READB(I,J):NEXTI :N
EXTJ
   90DATA...
   100L0=9.81*T^2/2/PI
   105FORK=1TODM:L=L0:TM=L
   110MN=(L+TM)/2:TM=L:A=2*PI*K/MN:L=L0*(EXP(A)-EXP
(-A))/(EXP(A)+EXP(-A))
   120IF(ABS(L-TM)>.1)THEN GOTO110
   130LL(K)=L:NEXTK
   140FORJ=1TOJM:FORI=1TOIM :IF(H(I,J)=0)THEN GOTO1
95
   150FORK=1TODM :IF(H(I,J)<K)THEN GOTO170
   160NEXTK
   170L=LL(K-1)+(LL(K)-LL(K-1))*(K-H(I,J)):A=2*2*PI
```

```
*H(I,J)/L   -NH=(EXP(A)-EXP(-A))/2:N=.5*(1+A/SANH):
KS=SQR(L0,  /N/L):KR=SQR(B0/b(I,J)):HH(I,J)=H0*KS*K
R
   180IF(HH(I,J)>.7*H(I,J))THEN HH(I,J)=.7*H(I,J)
   190SXX(I,J)=9.81*HH(I,J)^2/16*(2*N-1+N*(COS(RAD(T
H(I,J))))^2):SXY(I,J)=9.81*HH(I,J)^2/16*N*SIN(2*RA
D(TH(I,J))):SYY(I,J)=9.81*HH(I,J)^2/16*(2*N-1+N*(S
IN(RAD(TH(I,J))))^2)
   195NEXTI:NEXTJ
   200FORJ=1TOJM-1:FORI=1TOIM-1:PRINTH(I,J),HH(I,J)
,SXX(I,J),SXY(I,J),SYY(I,J):NEXTI:NEXTJ
   210END
```

Description of variables:

IM,JM = maximum values of indices along Ox, Oy
H0 = wave height in the open sea
T = wave period
DM = maximum water depth in the flow area in m
B0 = wave orthogonals distance in the open sea
H(I,J) = water depth values in mesh center
TH(I,J) = corresponding wave approach angle measured counter-clockwise from the x^* axis in degrees
B(I,J) = corresponding wave orthogonals distance.

In this routine first the wave characteristics L, H, n are computed at the mesh centers and then the radiation stress components. Near the coast, the wave breaking is checked and the wave height is estimated with a breaking factor $\gamma = 0.7$ ($H = \gamma h$). The radiation stress components are introduced as data to the circulation program. The current is computed up to the stabilisation of the flow. The steady current pattern is illustrated in Fig 2 19. Some easily discernible eddies are shown. The strong longshore current is present in the surf zone-before the mole and is re-established some distance after it.

The wave generated current field diminishes rapidly away from the coast. This type of circulation, as stated a priori, is important in limited areas where the water depth is much smaller than the wavelength and intensive wave deformation is taking place. Nevertheless, it is an important feature in the design and operation of coastal structures.

2.5 DENSITY CURRENTS. STRATIFIED FLOWS

2.5.1 General notions, definitions

In all the. previous circulation models the water was assumed
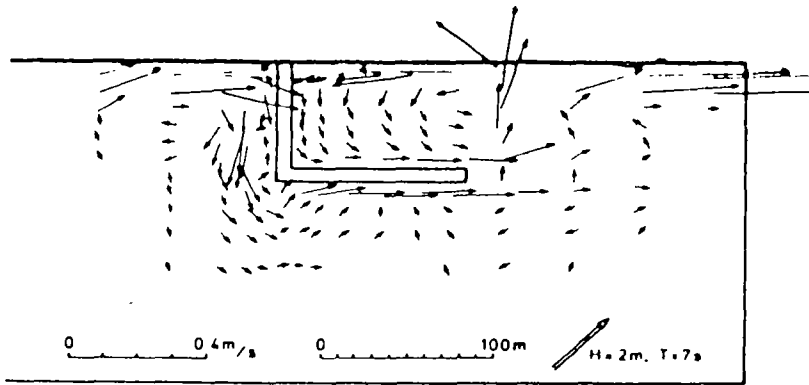
Fig. 2 19   Wave-induced circulation around the mole

homogeneous (of constant density) and the gravity force distributed uniformly throughout the mass of the fluid. The resulting hydrostatic pressure distribution in the case of quasi-horizontal flows was assumed linear and the horizontal pressure gradient was expressed by means of the free surface elevation gradient

$$-\frac{1}{\rho}\cdot\frac{\partial p}{\partial x} = -g\frac{\partial \zeta}{\partial x} \qquad (2.77)$$

In the case of nonhomogeneous fluid, however, the density varies in three-dimensional space $\rho(x, y, z, t)$. The variation is due to:

(1) salinity variation, as in the case where fresh land-based water is mixed with sea water, and
(2) horizontal or vertical temperature differences

The resulting density field $(\rho = \rho(S, T))$ implies a hydrostatic pressure distribution of a more complicated form·

$$p(z) = \int_{z}^{\zeta} \rho g \, dz + p_0 \qquad (2.78)$$

where p_0 is the atmospheric pressure. The general form of the horizontal pressure gradient becomes

$$-\frac{1}{\rho}\cdot\frac{\partial p}{\partial x} = -\frac{g}{\rho}\int_{z}^{\zeta}\frac{\partial \rho}{\partial x}\,dz - \frac{g}{\rho}\cdot\frac{\partial \zeta}{\partial x}\rho\Big|_{z=\zeta} - \frac{1}{\rho}\cdot\frac{\partial p_{atm}}{\partial x} \qquad (2.79)$$

In the case where depth averaging provides a realistic approximation (intensive vertical mixing due to turbulence) and

$\rho = \rho(x, y, t)$ then (2.79) becomes

$$\frac{1}{\rho}\cdot\frac{\partial p}{\partial x} = -\frac{g}{\rho}\cdot\frac{\partial \rho}{\partial x}(\zeta - z) - \frac{1}{\rho}\cdot\frac{\partial p_{atm}}{\partial x} - g\frac{\partial \zeta}{\partial x} \qquad (2.80)$$

When $\rho = $ constant we return to the form of Equation (2 77)

In a nonhomogeneous fluid either the nonhomogeneity is itself the flow generating factor (density currents) or it influences the hydrodynamic conditions in the flow domain Two limiting cases can be distinguished in nonhomogeneous flow domains·

(1) Well-mixed domains in which water is homogeneous over the depth. Horizontal density gradients may exist resulting in horizontal flow, a form of density currents
(2) Fully stratified domains. Two or more distinct layers are formed along the vertical, separated by a thin interface (pycnocline). The layers communicate only through their interface where mixing phenomena are considered weak In a two-layers environment when the more dense layer is above the less dense, the case is hydrodynamically unstable and vertical convection may take place resulting in mixing of the two layers

When the less dense layer is on top, the situation is hydrodynamically stable and a relatively large energy supply is required to achieve the mixing of the two layers (storm waves for example).

When the surface and the interface are horizontal the two layers may be stagnant. Horizontal gradients in the elevation of the two surfaces (free and interface) result in fluid motion known as baroclinic motion.

A mathematical model of coastal circulation in the general form consisting of Equations (2 5) and (2 6) can describe the circulation of a nonhomogeneous fluid The differences concern the horizontal pressure gradients and are expressed by Equation (2 79) This means that the density magnitude must be known over the whole extent of the flow domain. The density may be considered variable in space and constant in time during the development of the circulation phenomenon or may be considered as an evolving magnitude In the later case, as the density is basically a function of temperature T and salinity S, two equations formulated on the principle of heat and salt conservation are required to complete the model, their form is the same. For $c = T$ or $c = S$, the conservation equation is

$$\frac{\partial c}{\partial t} + \frac{\partial (cu)}{\partial x} + \frac{\partial (cv)}{\partial y} + \frac{\partial (cw)}{\partial z} = \frac{\partial}{\partial x}\left(D_h\frac{\partial c}{\partial x}\right) + \frac{\partial}{\partial y}\left(D_h\frac{\partial c}{\partial y}\right) + \frac{\partial}{\partial z}\left(D_v\frac{\partial c}{\partial z}\right)$$

$$(2 81)$$

Equation (2.81) is the advective turbulent diffusion equation for a conservative substance with different horizontal and vertical diffusion coefficients D_x, D_z. The state equation relating ρ to S and T can be approximated by a linear one

$$\rho = \rho_0(1 + ac) \tag{2.82}$$

where a in the case of the $\rho(T)$ function is a volume expansion coefficient. A final difference between the homogeneous and nonhomogeneous fluid circulation model concerns the eddy viscosity magnitude distribution. This magnitude describes the rate of diffusion of momentum over the depth. In the case of a steep density gradient along the interface the momentum cannot be diffused through the pycnocline. The parametrisation of that physical process, i.e. the tapering of momentum in one layer is done through the eddy viscosity distribution. A nondimensional parameter called the Richardson number is the parameter involved, defined as the ratio

$$R_i = \frac{g \dfrac{\partial \rho}{\partial z}}{\rho \left(\dfrac{\partial u}{\partial z}\right)^2} \tag{2.83}$$

The large density gradients on the pycnocline results in high R_i. The quantification of the influence of R_i on the eddy viscosity is done usually by means of the relation

$$v_v = v_{v_{homog}} \cdot (1 + aR_i)^{-b} \tag{2.84}$$

where $v_{v_{homog}}$ is the eddy viscosity for the homogeneous fluid and a and b coefficients fixed by in situ measurements, $O[a] = 10$, $O[b] = 0.5$.

The density distribution, eddy viscosity and velocity in the case of steady uniform barotropic flow in a stratified fluid is shown schematically in Fig. 2.20. It is obvious that the two flow regions (the
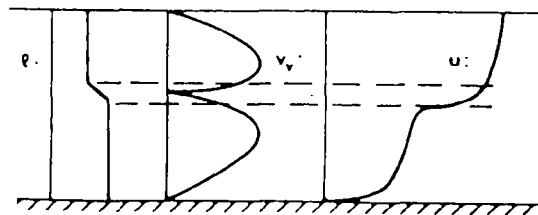
Fig. 2.20   Eddy viscosity and velocity distribution for barotropic flow in stratified medium

upper and lower) behave differently under the same flow generating factor. The momentum diffusion is minimised across the interface and as a result sharp velocity gradients develop there. The flow profile in each layer is almost uniformly distributed over the depth of the respective layer, but the velocity in the upper layer is higher than that in the lower layer due to the greater friction at the bed than at the interface.

From the above observations it becomes clear that the first simplifying approximation for the description of the phenomenon of a 2-layered flow is to assume two distinct layers and apply the depth averaged model for each one separately.

As the solution of the depth-varying model for such types of barotropic–baroclinic flow is beyond the scope of this book we will limit our modelling to the 2DH methodology applied to the two limiting cases of horizontal and vertical density variability. First, the case of fluid fully mixed over the depth, with horizontal density variation, second, the case of vertically layered fluid (2-layer model).

2.5.2 A model for horizontal flow of a nonhomogeneous fluid vertically well mixed

This model is the crudest approximation for the description of circulation with density variations due to advection and diffusion in a coastal domain of very shallow water connected to the open sea (an infinite domain of constant density) and receiving fresh water outflow from a land based source. It is assumed that due to several physical reasons vertical mixing is complete and that only horizontal density differences drive or regulate the circulation.

Let us confine our investigation for simplicity to the one-dimensional case. The general form of the mathematical model for the depth varying circulation is written in the unknowns $u(x, z, t)$, $\zeta(x, t)$, $\rho(x, t)$, $S(x, t)$

$$\frac{\partial u}{\partial t} + u \frac{\partial u}{\partial x} = -g \frac{\partial \zeta}{\partial x} + q \frac{z}{\rho} \frac{\partial \rho}{\partial x} + \frac{\partial}{\partial z}\left(v \frac{\partial u}{\partial z}\right) \tag{2.85}$$

$$\frac{\partial \zeta}{\partial t} + \frac{\partial(Uh)}{\partial x} = q \qquad \left(U = \frac{1}{h}\int_{-h}^{0} u\,dz\right) \tag{2.86}$$

where q is the inflowing discharge of fresh water of density ρ_0,

$$\rho = \rho_0(1 + aS) \tag{2.87}$$

$$\frac{\partial S}{\partial t} + \frac{\partial(SU)}{\partial x} = \frac{\partial}{\partial x}\left(R \frac{\partial S}{\partial x}\right) \tag{2.88}$$

The boundary conditions completing (2.85)–(2.87) are $u|_{\ldots-\Lambda} = 0$, $\partial u/\partial z|_{\ldots-0} = 0$ with respect to velocity and $\partial S/\partial x = 0$ on no-flow coastal boundaries, S = given constant on an open sea or river boundary with respect to salinity. The parameters v_v and R (vertical eddy viscosity and horizontal mass dispersivity) are also unknown magnitudes. A sensitivity analysis shows that their values influence the solutions substantially. An order of magnitude analysis for them indicate that

$$O[v_v] = O[U] \cdot O[h] \cdot 0.1 \tag{2.89}$$

$$O[R] = O[U] \cdot O[S] \cdot O[\Delta x/\Delta s] \tag{2.90}$$

where $\Delta s/\Delta x$ a measure of the horizontal salinity gradient

A substantial simplification is introduced by integration of Equation (2.85) over the depth and its expression in terms of the depth mean velocity

$$\frac{\partial U}{\partial t} + U\frac{\partial U}{\partial x} = -g\frac{\partial \zeta}{\partial x} - \frac{gh}{2}\cdot\frac{\partial \ln\rho}{\partial x} - \frac{kU}{h} \tag{2.91}$$

The bed friction term can have this linear form or a classical quadratic one

The model consisting of Equations (2.91), (2.86), (2.88) and the state Equation (2.87) is capable of describing the formation of density induced currents and the density field and their continuous interaction in the case of horizontal density variations only. These density currents can be induced by the inflow of fresh water into initially stagnant salt water or by the joining of a fresh water body with the sea.

The problem of the difference in the order of magnitude of the time scales in the formation of the hydrodynamic and density magnitudes can be resolved by the use of implicit finite differences for (2.91) permitting the increase in a common Δt step used for both (2.91) and (2.88).

The numerical solution of the depth averaged horizontally stratified fluid model presented here is based on the explicit finite difference scheme using the staggered grid illustrated in Fig. 2.21. The velocity values are computed at the cross-sections (nodes) while the water depth, surface elevation and salinity-density values refer to the reaches between successive nodes. The finite difference approximation of the model's equations are:

(1) Continuity equation:

$$\frac{\zeta_i^{n+1} - \zeta_i^n}{\Delta t} = \frac{1}{2\Delta x}((h_{i+1} + h_i)U_{i+1}^n - (h_i + h_{i-1})U_i^n) \tag{2.92}$$
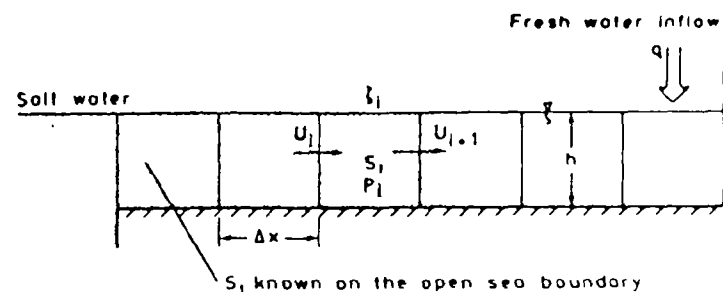
Fig 2.21   1-D density current due to horizontal density gradients. Domain morphology and discretisation

(2) Equilibrium equation:

$$\frac{U_i^{n+1} - U_i^n}{\Delta t} = -\frac{U_i^n}{2\Delta x}(U_{i+1}^n - U_{i-1}^n) - \frac{g}{\Delta x}(\zeta_i^n - \zeta_{i-1}^n) - \frac{g(h_i + h_{i-1})}{4\Delta x}$$
$$\times (\ln\rho_i^n - \ln\rho_{i-1}^n) - 2kU_i^n/(h_i + h_{i-1}) \tag{2.93}$$

(3) Salt conservation:

$$\frac{S_i^{n+1} - S_i^n}{\Delta t} = -\frac{1}{g\Delta x}[(S_{i+1}^n + S_i^n)U_{i+1}^n - (S_i^n + S_{i-1}^n)U_i^n]$$
$$+ \frac{R}{\Delta x^2}(S_{i+1}^n - 2S_i^n + S_{i-1}^n) \tag{2.94}$$

(4) State equation:

$$\rho_i^{n+1} = \rho_0(1 + \alpha S_i^{n+1}) \tag{2.95}$$

The procedure is organised in a BASIC program (Program 13) referring to the case of an enclosed domain (upstream and downstream no-flow conditions $\partial S/\partial x = 0$, $U = 0$) where an initial density distribution induces circulation that, after the completion of mixing, leads asymptotically to a new equilibrium after the homogenisation of the fluid and the frictional decay of the initial motion. Different boundary conditions can be used with a slight modification to the program to simulate other types of density induced flow.

PROGRAM 13: 1-D CURRENT WITH HORIZONTAL DENSITY GRADIENT

```
5REM 1-D DENSITY CURRENT HORIZONTAL DENSITY GR
ADIENT
10DIMU(21),UN(21),Z(21),S(21),SN(21),R(21),H(21
```

```
20READ DT,DX,IM,NM,K,E,HO,A
30DATA...
40FORI=0TOIM:READB(I):R(I)=100*(1+A*B(I)):NEXTI

42DATA...
45FORI=0TOIM:READH(I):NEXTI
47DATA...
50N=0:T=0
60N=N+1:T=T+DT
70FORI=1TOIM-1:Z(I)=Z(I)-DT/2/DX*((H(I)+H(I+1))
*U(I+1)-(H(I)+H(I-1))*U(I)):NEXTI
80FORI=2TOIM-1:UN(I)=U(I)-DT/2/DX*U(I)*(U(I+1)-
U(I-1))-DT*9.81/DX*(Z(I)-Z(I-1))-DT*9.81*(H(I)+H(I
-1))/4*(LOG(R(I))-LOG(R(I-1)))/DX-DT*K*U(I)*ABS(U(
I))*2/(H(I)+H(I-1)):NEXTI
90FORI=1TOIM-1:SN(I)=S(I)-DT/2/DX*((S(I+1)+S(I)
)*U(I+1)-(S(I)+S(I-1))*U(I))+DT/DX^2*E*(S(I+1)-2*S
(I)+S(I-1)):NEXTI:SN(0)=SN(1):SN(IM)=SN(IM-1)
100FORI=0TOIM:U(I)=UN(I):S(I)=SN(I):R(I)=100*(1+
A*S(I)):NEXTI
110IFN/20<>INT(N/20) THEN GOTO 60
120PRINTN
130FORI=1TOIM:PRINTZ(I)::NEXTI:PRINT
140FORI=1TOIM:PRINTU(I)::NEXTI:PRINT
150FORI=1TOIM:PRINTS(I)::NEXTI:PRINT
160IFN<NM THEN GOTO 60
170END
```

Description of main variables:

DT, DX = time and space discretisation steps

IM, NM = number of cross-sections in the flow domain discretisation and maximum number of time steps

K   = bed friction coefficient (m/s)

E   = salt dispersion coefficient (m²/s)

HO   = common water depth (in this case $h = cte$, variable in general)

A   = linear $\rho - S$ relation coefficient

SO   = salinity at (seaward) boundary (kg/m³).

The application refers to a flow domain of constant depth $HO = 3.67$ m. length 20 km, bounded by coastal boundaries where the density has an initial linear variation; on the left boundary the water is fresh, $\rho = 1000$ kg/m³, and on the right it is salt sea water, $\rho = 1020$ kg/m³. The horizontal density variation induces density currents and free surface variations that result in the seiching of the flow domain at the lowest natural frequency. The phenomenon proceeds up to the homogenisation of the fluid after $\approx 10,000$ s.

The application data are $DT = 10$ s, $DX = 100$ m. $IM = 21$. $NM = 1000$, $K = 0.001$ m/s, $E = 100$ m²/s, $HO = 3.67$ m, $A = 0.0007$. $SO = 30$ ppt. The flow domain, its discretisation, the velocity evolution in the middle $U_B(t)$ and the $\zeta_A(t)$ evolution at the boundary are depicted in Fig. 2.22(a). Figure 2.22(b) shows the change in salinity along the flow domain up to homogenisation

2.5.3 Stratified flow model (2-layer model)

In the case of vertically stratified fluid the model describing the depth averaged magnitudes is not realistic. Either the depth-varying model describing the continuous evolution of the hydrodynamic magnitudes $u(x, y, z, t)$ along the depth, or a series of superimposed depth-averaged models corresponding to each layer have to be used The second approach is common operational practice and its 2-layer version will be presented here

In the case of the existence of a discrete pycnocline, the fluid can be considered as consisting of two quasi-horizontal layers and, according to the notation of Fig 2.23, the equations of equilibrium of forces and mass continuity can be written for the two layers separately. For the pressure in the upper layer,

$$p = \lambda\rho_0 g(\zeta - z) \rightarrow \frac{1}{\lambda\rho_0} \cdot \frac{\partial p}{\partial x} = g\frac{\partial \zeta}{\partial x} \qquad (2.96)$$

while for the lower layer it can be easily proved that

$$p_0 = \lambda\rho_0 g(\zeta + h - \zeta_0) + \rho_0 g(-z - h + \zeta_0) \qquad (2.97)$$

giving

$$\frac{1}{\rho_0}\frac{\partial p_0}{\partial x} = \lambda g\frac{\partial \zeta}{\partial x} - \lambda g\frac{\partial \zeta_0}{\partial x} + g\frac{\partial \zeta_0}{\partial x}$$

$$= \lambda g\frac{\partial \zeta}{\partial x} + (1 - \lambda)g\frac{\partial \zeta_0}{\partial x} \qquad (2.98)$$

where λ is the ratio of the densities of the two layers

$$\lambda = \frac{\rho}{\rho_0} < 1 \qquad (1 \geqslant \lambda \geqslant 0.98) \qquad (2.99)$$

From Equation (2.98) it is obvious that the free surface gradients multiplied by λ (≈ 1) and the interface gradients multiplied by $(1 - \lambda)$ (≈ 0), are involved in the determination of the velocity field in the lower layer. This indicates a priori that the orders of magnitude of the ζ and ζ_0 values have to be different so that the two pressure terms keep the same order, i.e. $O[\zeta] < O[\zeta_0]$

A second important concern in a stratified fluid model is the
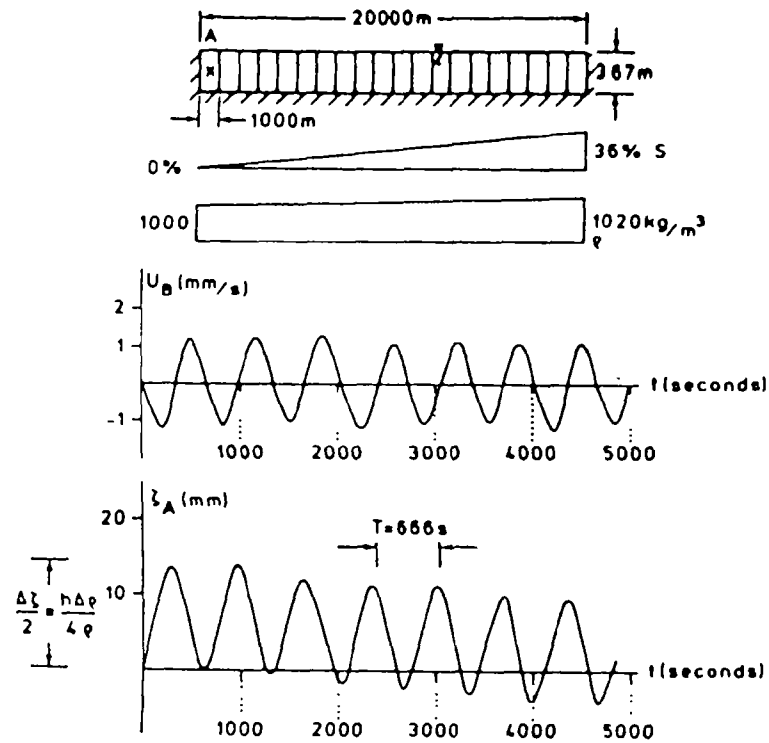
Fig 2 22(a)   1-D density current flow domain, its discretisation and evolution of velocity and surface elevation at two locations
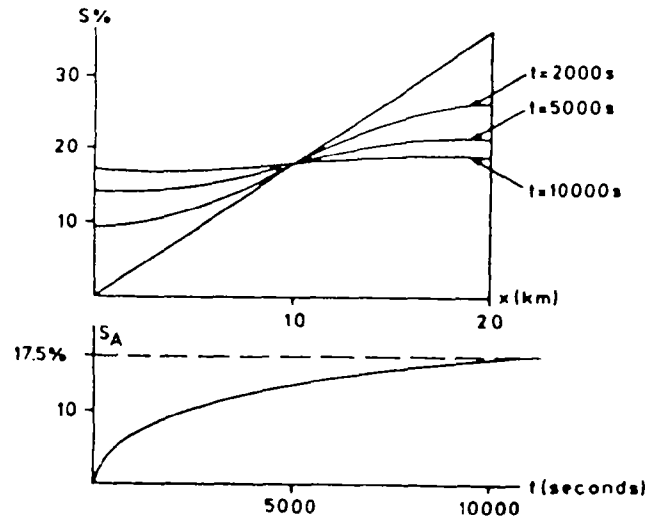
Fig 2 22(b)   Evolution of salinity with time
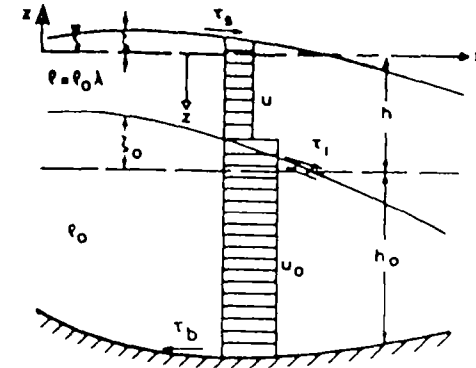
Fig 2 23   Stratified flow model Basic notations

development of interfacial stresses Their magnitude can be simply approximated by a quadratic form containing the difference of the mean velocities of the two layers. The form of the 2DH, 2-layer, model is

(1) Continuity equations in the two layers:

$$\frac{\partial \zeta_0}{\partial t} + \frac{\partial}{\partial x}(U_0 h_0) + \frac{\partial}{\partial y}(V_0 h_0) = 0 \qquad (2\ 100)$$

$$\frac{\partial(\zeta - \zeta_0)}{\partial t} + \frac{\partial}{\partial x}(Uh) + \frac{\partial}{\partial y}(Vh) = 0 \qquad (2\ 101)$$

(2) Equilibrium of forces equations along x, y in the two layers

$$\frac{\partial U}{\partial t} + U\frac{\partial U}{\partial x} + V\frac{\partial U}{\partial y} = -g\frac{\partial \zeta}{\partial x} + \frac{\tau_{sx} - \tau_{ix}}{\lambda \rho_0 h} + fV \qquad (2\ 102)$$

$$\frac{\partial V}{\partial t} + U\frac{\partial V}{\partial x} + V\frac{\partial V}{\partial y} = -g\frac{\partial \zeta}{\partial y} + \frac{\tau_{sy} - \tau_{iy}}{\lambda \rho_0 h} - fU \qquad (2\ 103)$$

$$\frac{\partial U_0}{\partial t} + U_0\frac{\partial U_0}{\partial x} + V_0\frac{\partial U_0}{\partial y} = -\lambda g\frac{\partial \zeta}{\partial x} - (1-\lambda)g\frac{\partial \zeta_0}{\partial x} + \frac{\tau_{ix} - \tau_{bx}}{\rho_0 h_0} + fV_0$$

$$(2\ 104)$$

$$\frac{\partial V_0}{\partial t} + U_0\frac{\partial V_0}{\partial x} + V_0\frac{\partial V_0}{\partial y} = -\lambda g\frac{\partial \zeta}{\partial y} - (1-\lambda)g\frac{\partial \zeta_0}{\partial y} + \frac{\tau_{iy} - \tau_{by}}{\rho_0 h_0} - fU_0$$

$$(2\ 105)$$

where

$$\frac{\tau_{sx}}{\rho_0} = k_w W_x \sqrt{(W_x^2 + W_y^2)}$$

$$\frac{\tau_{sy}}{\rho_0} = k_w W_y \sqrt{(W_x^2 + W_y^2)}$$

(2.106)

$$\frac{\tau_{ix}}{\rho_0} = (U - U_0)k_i \sqrt{[(U - U_0)^2 + (V - V_0)^2]}$$

$$\frac{\tau_{iy}}{\rho_0} = (V - V_0)k_i \sqrt{[(U - U_0)^2 + (V - V_0)^2]}$$

(2.107)

$$\frac{\tau_{bx}}{\rho_0} = k_b U_0 \sqrt{(U_0^2 + V_0^2)}$$

$$\frac{\tau_{by}}{\rho_0} = k_b V_0 \sqrt{(U_0^2 + V_0^2)}$$

(2.108)

The coefficients k_w (wind friction), k_i (interface friction), k_b (bed friction) have values depending on the wind, flow, fluid and bed morphology. An approximation to their orders of magnitude is, $O[k_w] = 10^{-6}$, $O[k_i] = 10^{-3}$, $O[k_b] = 10^{-2}$.

The above 2-layer model can describe the circulation in a stratified medium due

(1) to the wind influence on the free surface
(2) to incident long waves through the open sea boundary or induced from barometric pressure fluctuations
(3) to primary or secondary interface gradients (baroclinic flows, internal waves). It is completed by appropriate boundary conditions completely analogous to those for the homogeneous medium. At the open sea boundary the free radiation conditions for the two layers take the form:

Lower layer: $\quad U_{n_0} h_0 = -\zeta_0 \sqrt{\left[\dfrac{ghh_0(1-\lambda)}{(h+h_0)}\right]}$ (2.109)

Upper layer: $\quad U_n h = -\zeta \sqrt{[g(h+h_0)]}$ (2.110)

The numerical solution of the 2-layer model follows the same methodology as the 2DH model for a homogeneous fluid, i.e. an explicit finite difference scheme on a staggered grid. Program 14 gives the structure for the one-dimensional case.

PROGRAM 14: 1-D STRATIFIED FLOW MODEL, TWO-LAYER

```
5REM 1-D STRATIFIED FLOW MODEL 2LAYER5
10DIMU(20),UN(20),UO(20),UON(20),H(20),Z(20),HO
(20),ZO(20),DX(20)
20READ DT,CF,CI,IM,EL,NM,PER,EDH,W,CS
25DATA...
30FORI=0TOIM:READH(I),HO(I),DX(I):NEXTI
40DATA...
50FORI=1TOIM:U(I)=0:UN(I)=0:UO(I)=0:UON(I)=0:NE
XTI
60TSX0=CS*W*ABS(W):N=0:T=0
70N=N+1:T=T+DT
80IFN<PER/4 THENTSX=TSX0*SIN(2*PI*N/PER) ELSE T
SX=TSX0
90FORI=1TOIM-1:FT=ZO(I):ZO(I)=ZO(I)-DT/DX(I)/2*
((HO(I+1)+HO(I))*UO(I+1)-(HO(I)+HO(I-1))*UO(I)):Z(
I)=Z(I)+ZO(I)-FT-DT/DX(I)/2*((H(I)+H(I+1))*U(I+1)-
(H(I)+H(I-1))*U(I)):NEXTI
100FORI=2TOIM-1:HM=(H(I)+H(I-1))/2:HMO=(HO(I)+HO
(I-1))/2:TBX=UO(I)*ABS(UO(I))*CF:DXM=(DX(I)+DX(I-1
))/2:TIX=CI*(U(I)-UO(I))*ABS(U(I)-UO(I))
110UN(I)=U(I)*EDH+(U(I+1)+U(I-1))*(1-EDH)/2+DT*(
-((U(I+1)+U(I))^2-(U(I)+U(I-1))^2)/8/DXM-9.81*(Z(I
)-Z(I-1))/DXM-(TIX-TSX)/EL/HM)
120UON(I)=UO(I)*EDH+(UO(I+1)+UO(I-1))*(1-EDH)/2*
DT*(-((UO(I+1)+UO(I))^2-(UO(I)+UO(I-1))^2)/8/DXM-9
.81*(ZO(I)-ZO(I-1))/DXM*(1-EL)-9.81*EL*(Z(I)-Z(I-1
))/DXM-(TBX-TIX)/HMO) :NEXTI
130UN(1)=-Z(1)*SQR(9.81*(H(1)+HO(1)))/H(1):UON(1
)=-ZO(1)*SQR(9.81*H(1)*HO(1)/(H(1)+HO(1))*(1-EL))/
HO(1)
140FORI=1TOIM:U(I)=UN(I):UO(I)=UON(I):NEXTI
150IFN/50<>INT(N/50)THEN GOTO70
160EK=0:EKO=0:FORI=1TOIM-1:EK=EK+((U(I)+U(I+1))/
2)^2*H(I):EKO=EKO+((UO(I)+UO(I+1))/2)^2*HO(I):NEXT
I
170PRINTT,EK,EKO,Z(6),ZO(6),U(4),UO(4):IF(N<NM)
THEN GOTO70
180PRINT"Z":PRINT:FORI=1TOIM :PRINTZ(I)::NEXTI:P
RINT:PRINT"ZO":FORI=1TOIM:PRINTZO(I)::NEXTI:PRINT:
PRINT"U":FORI=1TOIM:PRINTU(I)::NEXTI
190PRINT:PRINT"UO":FORI=1TOIM:PRINTUO(I)::NEXTI
:IF(N<NM) THEN GOTO70
200END
```

Description of variables:

DT, DX = time and space discretisation steps
CF   = bed friction coefficient
CI   = interface friction coefficient

CS   — surface wind friction coefficient
IM   — number of cross-sections for the discretisation of the flow field
NM   = number of time steps in the numerical solution
EL   = density ratio λ
EDH   = weight factor in the Lax type time difference
PER   = time for the sinusoidal increase of wind intensity from a cold start to steady blow
W   = wind velocity
H, H0 = initial depths in no-flow conditions for the two layers (horizontal interface and surface).

The program refers to a linear basin (the left and right boundaries
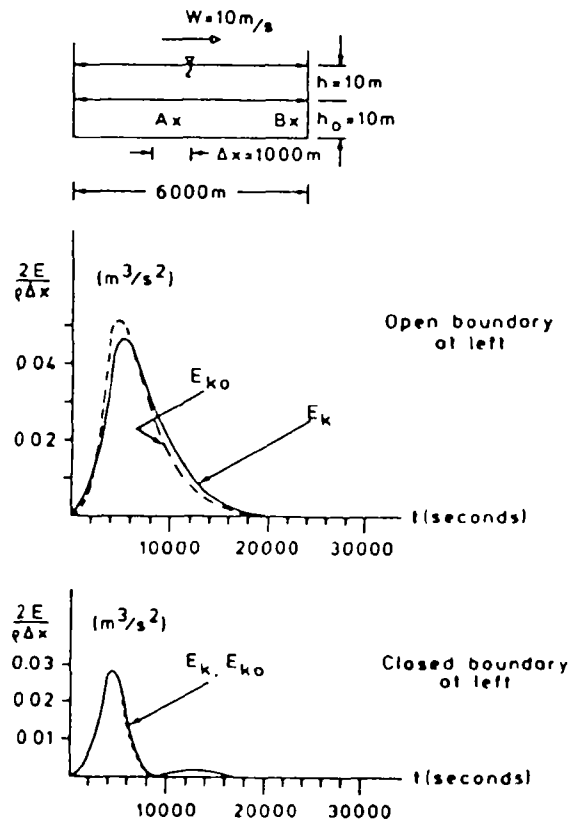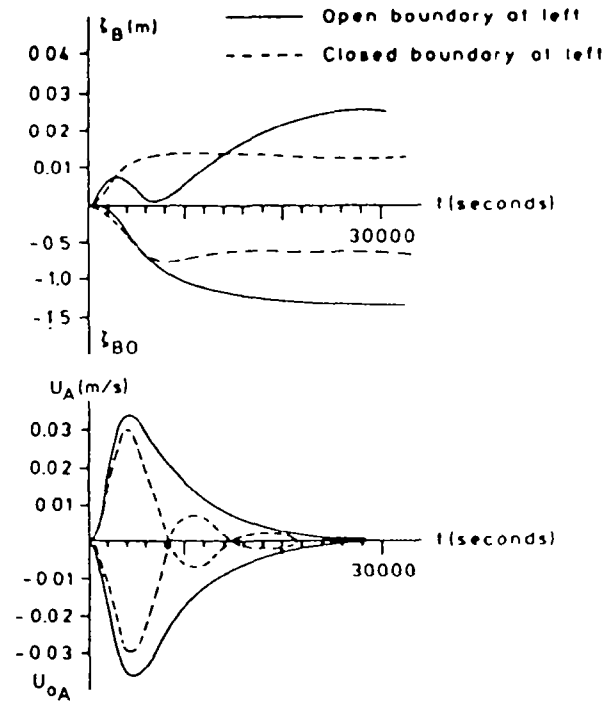
Fig 2 25   Evolution of free surface and velocity at 2 locations in previous model

may be open or closed). The open sea boundary condition can be incorporated by introduction of a statement of the form

130    $UN(1) = -Z(1) * SQR(9.8 * (H(1) + HO(1)))/H(1)$
       $U0N(1) = -Z0(1) * SQR(9.8 * H(1) * HO(1)/(H(1) + HO(1))$
       $* (1 - EL))/HO(1)$

The application refers to the description of the transient flow in a flow domain extending over 6 km with two layers of equal depth. $h = h_0 = 10$ m, under the influence of a wind of 10 m/s Two cases are examined, a laterally closed channel and a channel with an open sea boundary at left The program data are DT = 20 s, CF = 0.05, CI = 0.005, IM = 7, EL = 0.98, (fresh water above sea water), NM = 3000, PR = 800 s, EDH = 0.98, W = 10 m/s, CS = 0.000.005, H(1) = 10 m, HO(1) = 10 m (1 = 1-7), DX(1) = 1000 m

Figure 2 24 shows the evolution of the kinetic energies of the two layers for closed and open flow fields Figure 2 25 shows the transient evolution up to steady conditions of the ζ, ζ_0 on the right closed boundary and the u, u_0 in the middle of the flow field

Appendix E.   Program Code for Akutan Harbor Model

```
        PROGRAM WINDDRVN
C
C       MODIFIED FOR AKUTAN BATHYMETRY FILE
C
C       PROGRAM 2 1/2-D WIND DRIVEN CIRCULATION MODEL 1
C
C       KOUTITAS 1988 PG 61-62
C
        real sqh1(40,60)
        real*4 u(40,60),un(40,60),v(40,60),vn(40,60),z(40,60)
        real*4 px(40,60),py(40,60),pp(40,60)
        real*4 af(7)
        integer jf(7),iss(60),iee(60)
        COMMON/BATH/ H(40,60),IS(60),IE(60)
        COMMON/BDRY/ IB(250),JB(250),NB(250),QQ(250)
        COMMON/CUR/  U,UN,V,VN,Z
        COMMON/HH/ HIP(40,60),HIM(40,60),HJP(40,60),HJM(40,60)
        CHARACTER IFILE*20,OFILE*20,B1FILE*20,B2FILE*20,tsfile*20
        REAL KK
C
        G=9.81
        g2=sqrt(g)
        PI=3.14159
        W1=2.*PI/(24.8*3600.)
        W2=2.*W1
        jf(1)=20
        jf(2)=30
        jf(3)=40
        jf(4)=45
        jf(5)=52
        jf(6)=58
        do i=1,40
        do j=1,60
        px(i,j)=0
        py(i,j)=0
        pp(i,j)=0
        h(i,j)=1.0
        u(i,j)=0
        v(i,j)=0
        un(i,j)=0
        vn(i,j)=0
        z(i,j)=0
        hip(i,j)=0
        him(i,j)=0
        hjp(i,j)=0
        hjm(i,j)=0
        enddo
        enddo
C       depths are in meters, units are mks
C       READ INPUT DATA
C
        WRITE(*,*) 'INPUT DATA FILE NAME ?'
        READ(*,100) IFILE
  100   FORMAT(A)
        OPEN(10,FILE=IFILE,STATUS='OLD')
        READ(10,*)
        READ(10,100) B1FILE
        READ(10,100) B2FILE
        READ(10,*) ICHK,DT,DX,F,NM
        CF=.01
```

```
      READ(10,*) CS,WX,WY,tsave,nsave
      READ(10,100) OFILE
      read(10,100) tsfile
      CLOSE(10)
C
      IF(ICHK .NE. 99) WRITE(*,*) 'FATAL ERROR ... IMPROPER DATA FILE'
      IF(ICHK .NE. 99) GOTO 99
C
      CALL RBDF(B1FILE,B2FILE,AVGH,I1M,I2X,JM,KB)
      WRITE(*,*) 'DT,KB',DT,KB
C
      TXX=CS*WX*SQRT(WX**2+WY**2)
      TYY=CS*WY*SQRT(WX**2+WY**2)
      TS=SQRT(TXX**2+TYY**2)
      do i=1,40
      do j=1,60
C     if(h(i,j).le.0.0) h(i,j)=1.0
      sqh1(i,j)=sqrt(h(i,j))
      enddo
      enddo
C
      TWODX=2*DX
      TWODXI=1./TWODX
C
      write(*,*) 'dx', dx
      DO J=2,JM
      do i=is(j),ie(j)
      HIP(I,J)=0.5*(H(I,J)+H(I+1,J))
      HIM(I,J)=0.5*(H(I,J)+H(I-1,J))
      HJP(I,J)=0.5*(H(I,J)+H(I,J+1))
      HJM(I,J)=0.5*(H(I,J)+H(I,J-1))
        enddo
        enddo
      OPEN(15,FILE=OFILE,STATUS='NEW')
      WRITE(15,240) OFILE
  240 FORMAT(' FILE: ',A,/)
        write(*,*) 'opened ',ofile
      WRITE(15,241) IFILE,B1FILE,B2FILE
  241 FORMAT(1X,A,5X,A,5X,A,/)
      WRITE(15,242) AX,AY,JM
  242 FORMAT(2E15.5,I5)
C
C     MAIN COMPUTATION SCHEME
C
      write(*,*) 'entering main'
      TINIT=24.8*3600.
      ISAVE=0
C      TNEXT=TINIT
       TNEXT=TSAVE
      do i=1,60
      iss(i)=is(i)
      iee(i)=ie(i)
      enddo
      iss(11)=13
      iss(12)=12
      iss(13)=8
      iss(15)=7
      iss(16)=6
      iss(29)=10
      iss(53)=is(53)+1
```

```fortran
      iee(33)=ie(33)-1
      iee(37)=ie(37)-1
      iee(43)=ie(43)-1
      iee(46)=ie(46)-1
      N=0
      T=0.
      EK=0.
      tx=txx
      ty=tyy
      anu=0.66*sqrt(ts)
      stx=tx/anu
      sty=ty/anu
    1 N=N+1
      T=T+DT
      do 2000 j=2,jm
      do 2000 i=is(j),ie(j)
 2000 z(i,j)=z(i,j)-(dt/dx)*(u(i+1,j)*hip(i,j)-u(i,j)*
     c him(i,j)+v(i,j+1)*hjp(i,j)-v(i,j)*hjm(i,j))
      DO 2001 J=2,JM
      DO 2001 I=IS(J)+1,IE(J)
      VV=(V(I,J)+V(I-1,J)+V(I,J+1)+V(I-1,J+1))/4.
      HM=Him(I,J)
      AD=(1.2*U(I,J)+STX/40.0)*(U(I+1,J)-U(I-1,J))/TWODX
      AD=AD+(1.2*VV+Sty/40.0)*(U(I,J+1)-U(I,J-1))/TWODX
      BF=.18*U(I,J)/HM*SQRT(TS)-.5*TX/HM
      UN(I,J)=U(I,J)-DT*(AD+g*(z(i,j)-z(i-1,j))/dx-F*VV
     * +BF-TX/HM)
 2001 CONTINUE
      DO 2002 J=3,JM
      DO 2002 I=iss(j),IEe(J)
      UU=0.25*(U(I,J)+U(I+1,J)+U(I,J-1)+U(I+1,J-1))
      HM=hjm(I,J)
      AD=(1.2*V(I,J)+STY/40.0)*(V(I,J+1)-V(I,J-1))/TWODX
      AD=AD+(1.2*UU+STX/40.0)*(V(I+1,J)-V(I-1,J))/TWODX
      BF=.18*V(I,J)/HM*SQRT(TS)-.5*TY/HM
      VN(I,J)=V(I,J)-DT*(AD+g*(z(i,j)-z(i,j-1))/dx
     * +F*UU+BF -TY/HM)
 2002 CONTINUE
      DO 2003 K=1,KB
      I=IB(K)
      J=JB(K)
      GOTO(11,12,13,14,15,16,17,18,19,20,21) NB(K)
   11 UN(I,J)=0.
      vn(i-1,j)=vn(i,j)
      GOTO 2003
   12 VN(I,J)=0.
      un(i,j)=un(i,j+1)
c        vn(i,j-1)=0
      un(i,j-1)=un(i,j)
c        UU=0.5*(Un(I,J)+Un(I+1,J))
c        HM=hjm(I,J)
c        AD=(STY/40.0)*(Vn(I,J+1))/TWODX
c        AD=AD+(1.2*UU+STX/40.0)*(Vn(I+1,J)-Vn(I-1,J))/TWODX
c        BF=-.5*TY/HM
c        z(i,j-1)=z(i,j)+dx*(ad+f*uu+bf-ty/hm)/g
      GOTO 2003
   13 UN(I,J+1)=0.
      vn(i+1,j)=vn(i,j)
      GOTO 2003
   14 vn(i,j)=0.
```

```
        un(i,j+1)=un(i,j)
        GOTO 2003
   15 UN(I,J)=0.
        vn(i,j)=0.0
c      vn(i,j-1)=0
        un(i,j-1)=un(i,j)
c      UU=0.5*(Un(I,J)+Un(I+1,J))
c      HM=hjm(I,J)
c      AD=(STY/40.0)*(Vn(I,J+1))/TWODX
c      AD=AD+(1.2*UU+STX/40.0)*(Vn(I+1,J))/TWODX
c      BF=-.5*TY/HM
c      z(i,j-1)=z(i,j)+dx*(ad+f*uu+bf-ty/hm)/g
        GOTO 2003
   16 VN(I,J)=0.0
        UN(I+1,J)=0.
        vn(i,j+1)=0
        un(i+1,j-1)=0
        vn(i+1,j)=vn(i,j)
c      UU=Un(I,J)
c      HM=hjm(I,J)
c      AD=(1.2*UU+STX/40.0)*(-Vn(I-1,J))/TWODX
c      BF=-.5*TY/HM
c      z(i,j-1)=z(i,j)+dx*(ad+f*uu+bf-ty/hm)/g
        GOTO 2003
   17 VN(I,J+1)=0.0
        UN(I+1,J)=0.0
        un(i,j+1)=un(i,j)
        vn(i+1,j)=vn(i,j)
        GOTO 2003
   18 vN(I,J+1)=0.0
        uN(I,J)=0.
        vn(i-1,j)=vn(i,j)
        vn(i-1,j+1)=vn(i,j+1)
        GOTO 2003
   19 UN(I,J-1)=un(I,j)
        vn(i,j)=-z(i,j)*sqrt(g/h(i,j))
        GOTO 2003
   20 uN(I+1,J)=0.0
        un(i,j-1)=un(i,j)
        vn(i,j)=-z(i,j)*sqrt(g/h(i,j))
        GOTO 2003
   21 uN(I,J)=0.0
        un(i,j-1)=0.0
        vn(i,j)=-z(i,j)*sqrt(g/h(i,j))
 2003 CONTINUE
        pp(10,14)=pp(10,14)+1
        pp(19,54)=pp(19,54)+1
        pp(18,46)=pp(18,46)+1
        pp(21,30)=pp(21,30)+1
        pp(20,42)=pp(20,42)+1
        pp(22,56)=pp(22,56)+1
        pp(20,10)=pp(20,10)+1
        pp(20,20)=pp(20,20)+1
        pp(18,30)=pp(18,30)+1
        pp(28,10)=pp(28,10)+1
        DO 2004 J=1,JM
        DO 2004 I=is(j),ie(j)
        U(I,J)=UN(I,J)
        V(I,J)=VN(I,J)
        if(pp(i,j).gt.0.00001) then
```

```fortran
      uu=0.5*(u(i,j)+u(i+1,j))
      vv=0.5*(v(i,j)+v(i,j+1))
      uu=(0.75*stx-1.5*uu)*(0.8*0.8-1)+stx*(1-.8)
      vv=(0.75*sty-1.5*vv)*(0.8*0.8-1)+sty*(1-.8)
      px(i,j)=px(i,j)+uu*dt
      py(i,j)=py(i,j)+vv*dt
      endif
      if(pp(i,j).lt.0.00001) goto 2004
      rr=sqrt(px(i,j)*px(i,j)+py(i,j)*py(i,j))
      if(rr.gt.70.0) then
      q1=abs(px(i,j))
      q2=abs(py(i,j))
      if(q1.gt.q2.and.px(i,j).gt.0.0) then
      pp(i+1,j)=pp(i+1,j)+0.4*pp(i,j)
      if(py(i,j).gt.0) pp(i+1,j+1)=pp(i+1,j+1)+0.1*pp(i,j)
      if(py(i,j).lt.0) pp(i+1,j-1)=pp(i+1,j-1)+0.1*pp(i,j)
      endif
      if(q1.gt.q2.and.px(i,j).lt.0.0) then
      pp(i-1,j)=pp(i-1,j)+0.4*pp(i,j)
      if(py(i,j).gt.0) pp(i-1,j+1)=pp(i-1,j+1)+0.1*pp(i,j)
      if(py(i,j).lt.0) pp(i-1,j-1)=pp(i-1,j-1)+0.1*pp(i,j)
      endif
      if(q2.gt.q1.and.py(i,j).gt.0.0) then
      pp(i,j+1)=pp(i,j+1)+0.4*pp(i,j)
      if(px(i,j).gt.0) pp(i+1,j+1)=pp(i+1,j+1)+0.1*pp(i,j)
      if(px(i,j).lt.0) pp(i-1,j+1)=pp(i-1,j+1)+0.1*pp(i,j)
      endif
      if(q2.gt.q1.and.py(i,j).lt.0.0) then
      pp(i,j-1)=pp(i,j-1)+0.4*pp(i,j)
      if(px(i,j).gt.0) pp(i+1,j-1)=pp(i+1,j-1)+0.1*pp(i,j)
      if(px(i,j).lt.0) pp(i-1,j-1)=pp(i-1,j-1)+0.1*pp(i,j)
      endif
      px(i,j)=0
      py(i,j)=0
          pp(i,j)=pp(i,j)*0.5
      endif
 2004 CONTINUE

C
C     SAVE RESULTS
C
      IF(N/50. .NE. N/50) GOTO 1
C
  700 continue
      EK=0
      DO 2005 J=2,JM
      DO 2005 I=IS(J),IE(J)
      EK=EK+((U(I,J)+U(I+1,J))**2+(V(I,J)+V(I,J+1))**2)*H(I,J)/8.
 2005 CONTINUE
         ttt=t/60.0
      do ii=1,6
      af(ii)=0
      j=jf(ii)
      do i=is(j),ie(j)
      af(ii)=af(ii)+v(i,j)*h(i,j)
      enddo
      enddo
   32 format(f7.2,1x,6(i4,1x,f8.4))
      WRITE(*,555) ttt,EK,jm,i1m,i2x
  555 FORMAT(' N,EK=',f10.4,F10.4,1x,3(i4,1x))
```

```fortran
      if(ek.gt.1000000.0) then
      write(*,*) 'numerical instability',n,ek
      goto 99
      endif
      imax=0
      jmax=0
      UVMAX=0
      DO 2006 J=2,JM-1
      DO 2006 I=is(j),ie(j)
      UV2=U(I,J)*U(I,J)+V(I,J)*V(I,J)
      IF(UV2 .LT. UVMAX) GOTO 2006
      IMAX=I
      JMAX=J
      UVMAX=UV2
 2006 CONTINUE
      WRITE(*,*) 'N,IMAX,JMAX,MAGUMAX',N,IMAX,JMAX,SQRT(UVMAX)
      IF(T .LT. TNEXT ) GOTO 1
      WRITE(*,*) 'SAVED T(HR) =',T/3600.
      WRITE(15,250) T,T/3600.
  250 FORMAT(' T= ',F10.0,' SEC =',F10.4,' HRS')
      DO 2100 J=1,JM-1
      WRITE(15,251) J,IS(J),IE(J)
  251 FORMAT(3I3)
      WRITE(15,252) (U(I,J),I=IS(J),IE(J))
  252 FORMAT(10(F10.6,1X))
  253 format(10(f10.1,1x))
      WRITE(15,252) (V(I,J),I=IS(J),IE(J))
      WRITE(15,252) (Z(I,J),I=IS(J),IE(J))
      write(15,253) (pp(i,j),i=is(j),ie(j))
 2100 CONTINUE
      ISAVE=ISAVE+1
      IF(ISAVE .Ge. NSAVE) GOTO 99
      TNEXT=TNEXT+TSAVE
      GOTO 1
C
   99 CLOSE(15)
      END
      SUBROUTINE RBDF(B1FILE,B2FILE,AVGH,I1M,I2X,JM,KB)
C
C     ROUTINE TO READ BATHYMETRIC AND BOUNDARY DATA FILES
C
      real*4 u(40,60),un(40,60),v(40,60),vn(40,60),z(40,60)

      COMMON/BATH/ H(40,60),IS(60),IE(60)
      COMMON/BDRY/ IB(250),JB(250),NB(250),QQ(250)
      COMMON/CUR/   U,UN,V,VN,Z
      COMMON/HH/ HIP(40,60),HIM(40,60),HJP(40,60),HJM(40,60)
      DIMENSION IJB(40,60)
      CHARACTER*20 B1FILE*20,B2FILE*20
C
      DO 1000 I=1,40
      DO 1000 J=1,60
 1000 H(I,J)=0.
C
      OPEN(10,FILE=B1FILE,STATUS='OLD')
C
      J=0
      i1m=39
      i2x=1
    1 J=J+1
```

```fortran
      READ(10,*,END=10) Is(j),ie(j)
      if(is(j).lt.i1m) i1m=is(j)
      if(ie(j).gt.i2x) i2x=ie(j)
      READ(10,*,END=10) (H(I,J),I=1,39)
      if(j.ge.60) goto 10
      goto 1
   10 CLOSE(10)
      JM=J-1
C
C     READ BOUNDARY DATA FILE
C
      OPEN(10,FILE=B2FILE,STATUS='OLD')
      READ(10,*) KB
      DO K=1,KB
         READ(10,*) IBB,IB(K),JB(K),NB(K)
      enddo
      CLOSE(10)
C
      fattom=6.0*.3048
      do j=1,60
      do i=1,40
      if(h(i,j).le.0.0) h(i,j)=1
      h(i,j)=h(i,j)*fattom
      enddo
      enddo
      RETURN
      END
```

Appendix F.   **Quantity of Crab Processed in Akutan
Harbor (Griffin pers. comm.)**

CRAB PROCESSED IN AKUTAN HARBOR-JANUARY 1, 1991-FEBRUARY 16, 1992

WEEK ENDING:	POUNDS PROCESSED
1/6/91	112,747
1/13/91	172,644
1/20/91	456,144
1/27/91	995,927
2/3/91	2,095,910
2/10/91	1,338,306
2/17/91	3,965,635
2/24/91	4,299,224
3/3/91	3,370,794
3/10/91	3,547,323
3/17/91	4,145,254
3/24/91	3,101,422
3/31/91	3,594,238
4/7/91	2,382,637
4/14/91	3,762,069
4/21/91	2,259,928
4/28/91	1,310,679
5/5/91	1,283,177
5/12/91	223,047
5/19/91	540,010
5/26/91	153,860
6/2/91	528,413
6/9/91	198,693
6/16/91	312,480
6/23/91	581,029
6/30/91	602,210
11/17/91 (KING CRAB)	1,149,877
12/1/91	37,412
12/8/91	956,077
12/15/91	1,463,369
12/22/91	623,150
12/29/91	37,188
1/5/92	48,441
1/12/92	252,485
1/19/92	196,205
1/26/92	286,363
2/2/92	48,441
2/9/92	6,666,736
2/16/92	7,413,328
TOTAL 1991	49,600,873
TOTAL 1/5/92 - 2/16/92	21,835,616
GRAND TOTAL	71,436,489

CRAB PROCESSED IN AKUTAN HARBOR - FEBRUARY 23, 1992 - APRIL 1992

WEEK ENDING	POUNDS	PROCESSORS
2/23	7,912,619	9
3/1	7,592,226	9
3/8	7,010,523	9
3/15	4,649,571	9
3/22	3,631,449	9
3/29	3,464,153	9
4/5	4,461,085	9
4/12	1,254,745	6
4/19	270,003	5
4/26[1]	1,980,932	6

[1] Season closed 4/22.

Appendix G.   Side-Scan Sonar Survey

SIDE SCAN SONAR SURVEY
TO DETECT
SEAFOOD PROCESSOR WASTE PILES
IN
AKUTAN HARBOR, ALASKA

Prepared for:

U.S. Environmental Protection Agency
Office of Wastewater Enforcement and Compliance
401 M Street, Southwest
Washington, DC 20460

U.S. Environmental Protection Agency
Region X Water Compliance Section
1200 Sixth Avenue WD-135
Seattle, Washington 98101

Prepared by:

Science Applications International Corporation
10260 Campus Point Drive, M/S C2
San Diego, California 92121

Cover Photograph Courtesy of Jones & Stokes Associates, Inc.
Bellevue, Washington

EPA Contract No. 68-C8-0066
OWEC Work Assignment No. C-3-2(E)
SAIC Project No. 01-0895-03-2152-037

August 1992

TABLE OF CONTENTS

LIST OF TABLES

LIST OF FIGURES

EXECUTIVE SUMMARY

This report presents results of side scan sonar (SSS) investigations of Akutan Harbor, Akutan, Alaska. Akutan Harbor was surveyed to determine the extent of seafood processor waste discharged within the harbor by floating seafood processors and a shore-based processing facility. The SSS surveys[1] were conducted from April 9 to 11, 1992 and included two phases: a general reconnaissance survey and site-specific surveys of areas believed to exhibit significant accumulations of seafood processing wastes. Following the first survey phase, it was determined that three areas potentially had significant seafood waste accumulations: The DEEP SEA and CLIPPERTON floating processors and the Trident Seafood outfall site. Of these three sites, only the DEEP SEA and Trident sites showed evidence of significant seafood processing waste accumulation. Estimates of areal waste coverage at the DEEP SEA site was 2.5 acres ±25% while areal coverage of waste at the Trident site was greater, 11.2 acres ±15%.

Additional studies to estimate the volume of seafood waste accumulations are recommended. Such studies would require a precision depth sounder used in conjunction with navigation and side scan sonar systems.

---

[1]Side scan sonar and associated navigation records are available through Florence K. Carroll, Compliance Officer, Water Compliance Section, 1200 Sixth Avenue WD-135, Seattle, WA 98101.

1.0   INTRODUCTION

Akutan Harbor, Akutan Island—located on the Aleutian Island chain in Alaska (Figure 1-1)—has become a major center for both mobile and shore-based seafood processors. Akutan Harbor offers protected waters for floating processors and off-loading vessels and is also near major crab, cod, sole, and pollock harvesting areas.

In the past, substantial amounts of ground crab and finfish wastes have been discharged by the shore-based facility, permanently moored vessels, and floating processors. The large, shore-based, Trident plant now uses a fish meal plant to dispose of finfish wastes. However, ground crab wastes are still discharged in the receiving water. The National Pollutant Discharge Elimination System (NPDES) Seafood General Permit limits discharges to 310,000 pounds of seafood waste per month in Akutan Harbor.

The cumulative impact of the discharges to the subtidal benthic habitats is uncertain. In addition, there is no indication that currents are sufficient to disperse the waste piles. Microbial decomposition of the organic wastes is expected to be relatively slow due to the effects of low water temperatures on biodegradation rates (e.g., Atlas 1975).

A study conducted by EPA (1984) of Akutan Harbor indicated that there was some environmental stress related to seafood processing activities in Akutan Harbor, but the study did not suggest that serious environmental or water quality problems existed at that time. The study was very short in duration and did not include locations of waste accumulations, extensive water quality monitoring, sediment sampling, and current studies beyond what was influenced by immediate weather/wind conditions.

A Side Scan Sonar Investigation was conducted by Watson (1989) of Akutan Harbor (and Unalaska Island). The Akutan Harbor portion of the investigation concentrated on the waste pile at the Trident Seafoods site. The findings indicated that wastes covered an area of 23,000 square meters with a estimated volume of 100,000 cubic meters.

With increased fish waste discharges since 1983 and a potential increase in the Bering Sea pollock allocation for shore-based plants, present conditions need to be assessed in order for EPA to issue and enforce both individual permits and the Seafood General Permit. One of the ways to assess the conditions is to determine the area of seafood waste accumulations

1

Akutan, Alaska
Vicinity Map

Fairbanks

Alaska

Anchorage

Akutan

Kodiak

Unimak Island

A L E U T I A N   I S L A N D S

Akun Island

Akutan Island

Dutch Harbor

Tigalda Island

Rootok Island   Avatanak Island

Unalaska   KRENITZEN ISLANDS

Chemofski   Unalaska Island   North Head

Unmak Island

Open Bight

Hot Springs Bay

FOX ISLANDS

Lava Point

Hot Springs

Akutan Peak 4,275
+

Akutan Island

Akutan Village   Akutan Point

Akutan Harbor

Reef Bight

Reef Point

+
Flat Top Peak 3,445

Green Bight

City of Akutan Boundary

Cascade Bight

Broad Bight

Sarana Bay   Talus Point

Source City of Akutan 1982

Figure 1-1.   Overview of Study Area Location.

2

in Akutan harbor using a side scan sonar survey Once the areas of accumulation are plotted, another environmental assessment survey will evaluate the sediments near the accumulations for chemistry and benthos effects and provide the locations for water quality monitoring over the accumulations.

This report presents the results and conclusions from a side scan sonar (SSS) survey of Akutan Harbor conducted by Science Applications International Corporation (SAIC) for the U.S. Environmental Protection Agency (EPA). The purpose of the survey was to determine the areal extent of significant seafood waste piles located on the harbor floor which have been discharged from land-based and floating seafood processor facilities. The area surveyed (Figure 1-2) included a general SSS reconnaissance survey of the inner harbor west of Longitude 165° 46'W as well as site specific investigations of :

- The Trident Seafood outfall area,
- The DEEP SEA Fisheries permanently moored floating processor area, and
- A temporarily moored floating processor.

The survey was conducted from April 9 to 11, 1992, using a digital SSS system. Based on recommendations from an earlier survey (Watson 1989), a precise navigation system was used to provide accurate positioning during the survey. Following the survey, grab samples were collected near the edges of the waste piles to confirm their areal extent.

The sections of the report are: Survey Methodology (2.0); Field Operations (3.0); Results and Discussion (4.0); and Summary and Conclusions (5.0).
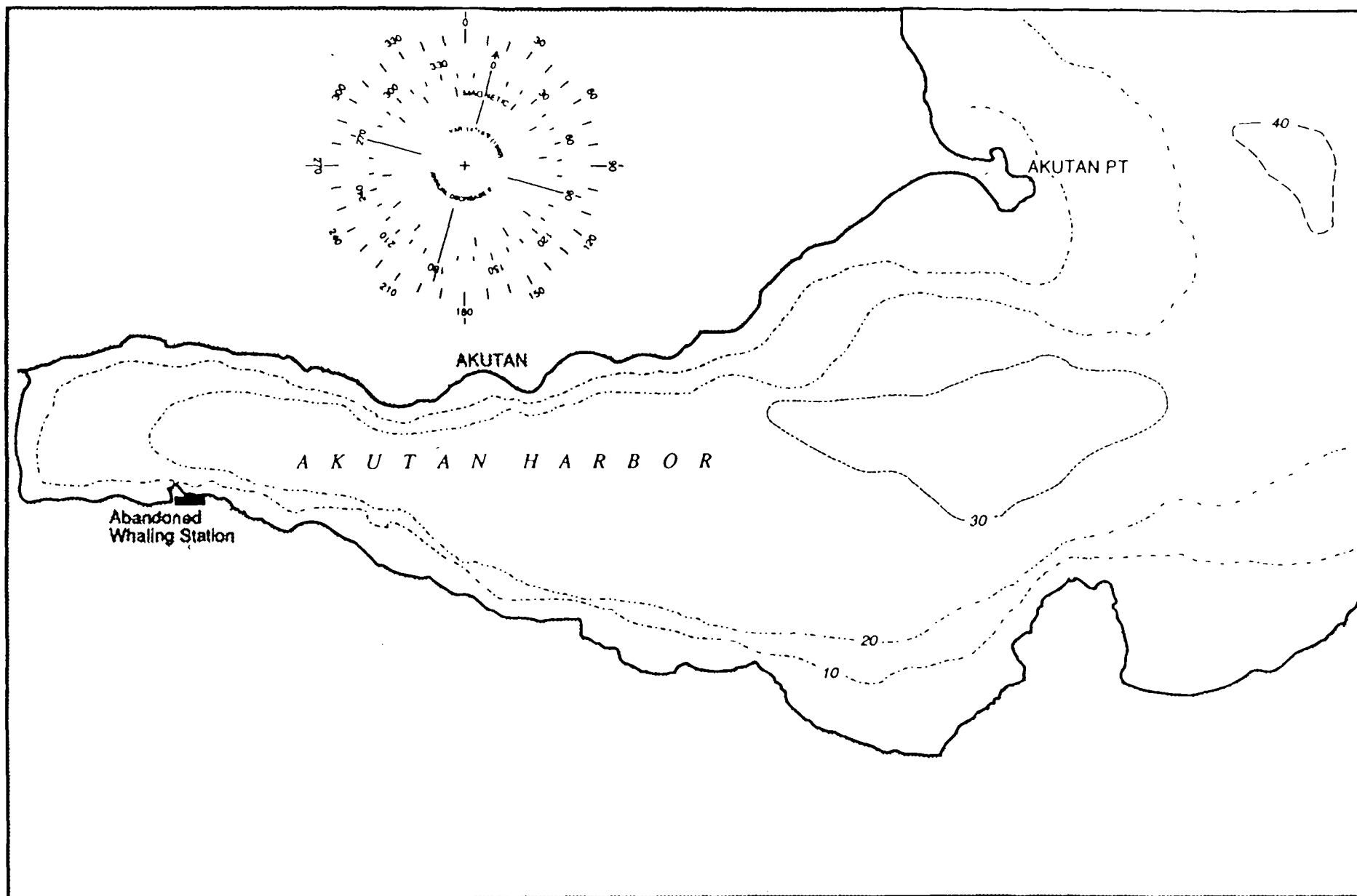
Figure 1-2.   Akutan Harbor.
Depths in fathoms

2.0   SURVEY METHODOLOGY

To accurately map the areal extent of crab waste piles from a survey vessel, it was essential that the SSS system be used in conjunction with an accurate positioning system On April 6 to 8, 1992, land surveyors from DOWL Engineers, an Anchorage engineering and surveying company, set up a rectilinear coordinate system within the harbor for use during the SSS survey. An arbitrary coordinate system was used because survey monuments for the Alaska state plane coordinate system were either unknown or did not exist in the Akutan Harbor area. The land survey was to provided coordinates for the shore-based navigation stations which were needed for proper operation of the positioning system while surveying. Coordinates for nine stations along the shore of the harbor as well as dock and GPS positions were provided by the surveyors, and are listed in Table 2-1. A map of the stations surveyed is shown in Figure 2-1. Five of the nine shore-based navigation stations were used during the survey. Detailed survey notes from the land survey were obtained from DOWL Engineers in Anchorage.

A Motorola Miniranger IV (MR4) positioning system was used for the survey. This system determines position by ranging from the survey vessel, via microwave frequency signal, to shore stations located at known coordinates. Using the ranges acquired by the system and the known coordinates of the survey stations, the system can determine the survey vessel position through a trigonometric software application. The system included a data processor with keyboard, printer, trackline plotter, digital tape recorder, and trackline indicator.

The SSS survey was conducted using an EG&G Model 260 Digital Image Correcting Side Scan Sonar system. The system consisted of a graphic recorder, tow cable, and towfish fitted with side-looking transducers. The system provides sonograms of the seabed analogous to a plan-view photograph and indicates distinguishing features of interest. The image-correcting properties of the system ensure that distances of seabed features found to either side of the survey trackline are accurate. However, because the navigation system was not interfaced directly with the side scan recorder, distances along the survey centerline were calculated from the navigation records. The recording paper feed rate is a function of survey

Table 2-1. Miniranger Station Positions From Side-Scan Sonar Survey in Akutan Harbor, AK.

Station	Northing (Y) (ft)	Easting (X) (ft)	Elevation (ft)	Used During Survey
Dock	5664.46	9089.23	9.9	
GPS	6566.65	5845.65	7.8	
MR-1	5264.78	6433.74	49.0	✓
MR-2	5594.89	9557.93	16.5	
MR-3	5506.80	10240.27	49.0	
MR-4	4785.28	12716.19	59.0	✓
MR-5	3290.84	17298.17	21.4	✓
MR-6	8866.49	17448.22	20.0	✓
MR-7	8257.15	12449.38	29.0	
MR-8	8777.27	9154.95	48.5	
MR-9	8143.50	6589.31	33.5	✓

NOTE: Miniranger positions surveyed by DOWL Engineers of Anchorage, AK on April 6-8, 1992. All units are in feet. Coordinates are based on a local grid system established by the surveyors.

6

Figure 2-1. Akutan Harbor Navigation Stations.

vessel speed; because the navigation system was not interfaced directly with the side scan recorder, the feed rate was arbitrarily set at 2 nautical miles per hour (kts). Details of theory and operation of the SSS system are presented in the operators' manual (EG&G 1987)

The boat originally proposed for use during the survey (THE FLYING D, a 90 ft converted landing craft with pilot house on the second deck), was found to be inappropriate due to its pilot house/deck layout, high windage, and lack of maneuverability. An alternate vessel, a 24 ft flat bottom fishing boat with a small cabin, was located in Akutan village and mobilized for the SSS survey. This vessel was too small to acquire the grab samples required for the SSS survey verification. Thus, after completion of the SSS survey, the MR4 navigation system was transferred to the FLYING D for grab sample collection.

3.0   FIELD OPERATIONS

The SSS survey was conducted in two segments and included 19 survey tracklines. The first segment was a reconnaissance survey of the harbor, that included nine tracklines (Figure 3-1). The purpose of this survey was to gather sufficient SSS data to determine potential impact sites due to floating processor, as well as shore-based, seafood processing plant activities. All survey lines were run at approximately 183 m (600 ft) line spacing except when lines intersected the shoreline. When this occurred, the survey vessel "contoured" around promontories at constant water depth. Except for the first line run at the 200 m scale (swath width) on the SSS recorder, the other lines were run at the 150 m scale. Thus, each trackline covered a 300 m swath width (150 m per channel, port and starboard). This resulted in a 117 m (or 64%) overlap per transect line, ensuring complete survey coverage. It was planned that preliminary analysis of these data in the field would provide sufficient information to develop a target list of seafood processor waste impact areas which could be surveyed in greater detail. The nearshore area on the north side of the harbor west of the Trident facility was not surveyed due to the presence of a floating water supply hose.

Preliminary assessment of the reconnaissance survey data indicated that three areas warranted more detailed survey. They included:

- Trident Seafoods, a shore-based processor with an offshore outfall for discharge of seafood processing waste,

- DEEP SEA, a permanently moored floating crab processor, and

- CLIPPERTON, a temporarily moored floating crab processor, on site since January 1992.

Also, following preliminary assessment of the side scan data, approximate positions for 12 grab sample sites (Figure 3-1) were determined. Collection and analysis of these samples provided additional ground-truth information on seabed conditions and assisted in assessment of side scan data.

The second survey segment was designed to examine seafood processing waste impact areas identified during the reconnaissance survey. It included ten tracklines run at the
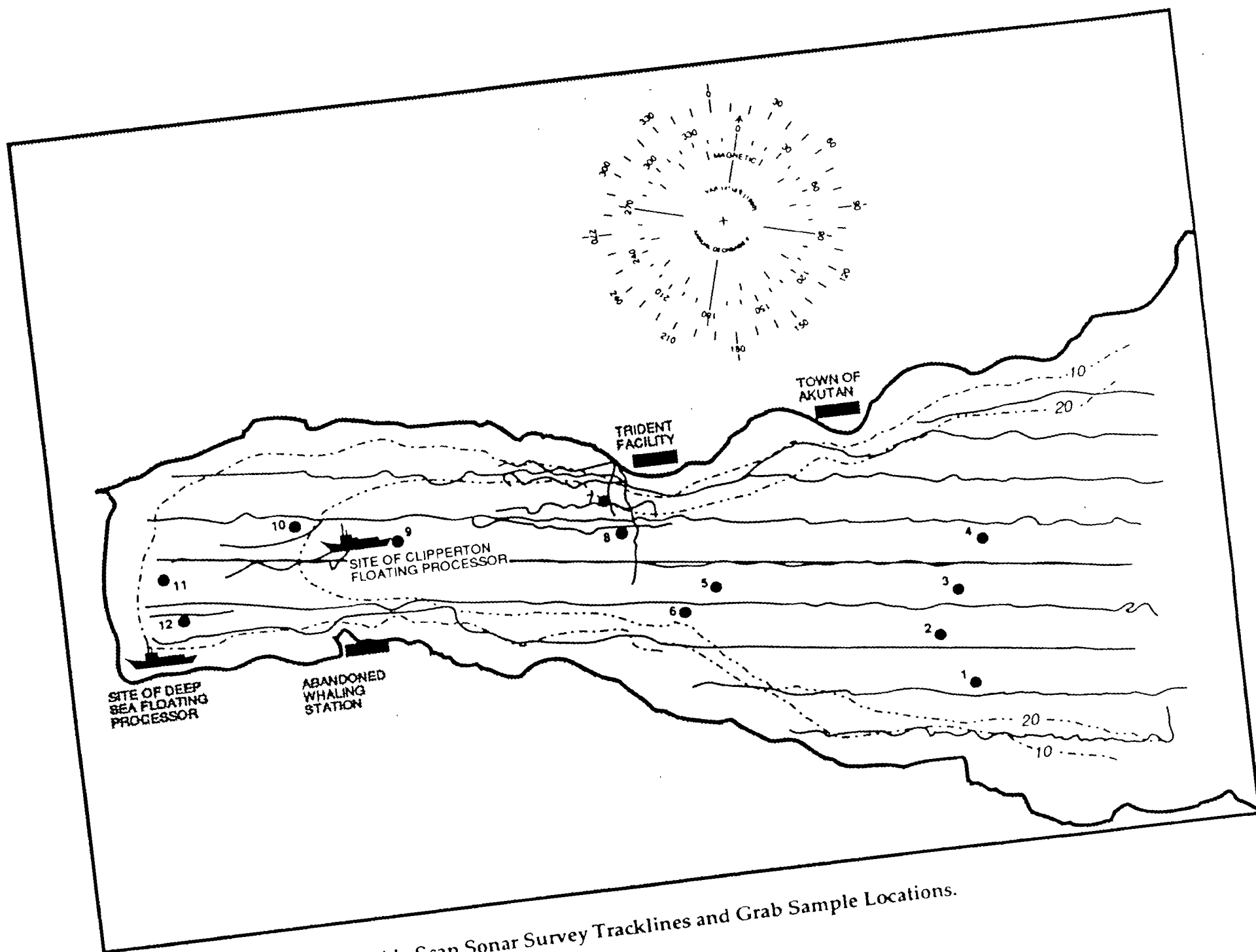
Figure 3-1. Akutan Harbor Side Scan Sonar Survey Tracklines and Grab Sample Locations.
Depths in fathoms

75 m (~250 ft) scale with 150 m (~500 ft) swath widths per transect. The line spacing for these site specific survey tracks was variable due to operational considerations such as obstruction by floating processor mooring lines, moored buoys, submerged fresh water lines, dock faces, and shoal (i.e., shallow depth) waters.

The first site examined was the permanently moored DEEP SEA floating processor. Two transects were run from east to west: one on the north side of the processor and one on the south side. The second site surveyed was the temporarily moored CLIPPERTON floating processor. Again, two lines were run from east to west on the north and south sides of the processor.

Six SSS transects were completed at the Trident shore-based facility. Two of these transects were run across the bathymetric contours. The final four lines were run from west to east at approximately 90 m (300 ft) line spacing. These lines provided more complete coverage of the Trident seafood waste pile. Details of the survey tracklines are listed in Table 3-1.

Twelve grab samples were obtained to substantiate the findings of the side scan survey. A listing of positioning and other ancillary data for the grab samples is shown in Table 3-2, a summary of the descriptions of each grab sample is contained in Table 3-3, and the positions of the grab samples relative to the tracklines are provided in Figure 3-1.

11

Table 3-1. Akutan Side Scan Sonar Survey Transect Data.
Survey conducted on April 9 through 11, 1992 at Akutan, AK.

Line No	Date	Start Time (hhmm)	End Time (hhmm)	Plot Refer Line	Offset (ft)	Heading	Side Scan Scale (m)	Fix Start	Fix End	No of Pages of Data	Comments
1	4/9/92	1646	1812	1	0	E->W	200	6	47	7	Reconnaissance
2	4/9/92	1928	2050	1	600 S	E->W	150	49	89	8	Reconnaissance
3	4/9/92	2106	2224	1	1200 S	E->W	150	90	126	8	Reconnaissance
4	4/10/92	853	941	1	1800 S	E->W	150	128	149	5	Reconnaissance
5	4/10/92	954	1035	1	2400 S	E->W	150	150	170	5	Reconnaissance
6	4/10/92	1128	1311	1	600 N	E->W	150	171	224	11	Reconnaissance
7	4/10/92	1409	1547	1	1200 N	E->W	150	225	275	10	Reconnaissance
8	4/10/92	1608	1638	1	1800 N	E->W	150	277	292	3	Reconnaissance
9	4/10/92	1650	1706	1	2400 N	E->W	150	293	302	2	Reconnaissance
10	4/10/92	1820	1831	1	~900 S	E->W	75	304	309	3	Deep Sea site S
11	4/10/92	1843	1848	1	~500 S	E->W	75	310	314	2	Deep Sea site N
12	4/10/92	1857	1906	1	~0	E->W	75	315	320	2	Clipperton site S
13	4/10/92	1913	1918	1	~200 N	E->W	75	321	324	2	Clipperton site N
14	4/10/92	1943	1954	4	3100 E	S->N	75	325	332	3	Trident site
15	4/10/92	2001	2005	4	2800 E	N->S	75	333	335	2	Abort line
16	4/11/92	907	928	1	500 N	W->E	75	401	412	5	Trident site
17	4/11/92	940	957	1	800 N	W->E	75	413	423	4	Trident site
18	4/11/92	1008	1020	1	1100 N	W->E	75	424	431	5	Trident site
19	4/11/92	1030	1045	1	1300 N	W->E	75	432	440	4	Trident site

Table 3-2. Grab Sample Locations and Ancillary Data. Grab samples were taken on 12 April 1992 in Akutan Harbor, AK.

Sample Number	Location Chainage (ft)	Location Offset (ft)	Uncor. Depth (ft)	Magnetic Heading (deg)	Local Time (hhmm)
1	2128	1665	---	073	1045
2	2573	1006	163	122	1100 (est)
3	2334	363	---	351	1127
4	2034	-321	150	106	1143
5	5605	364	159	140	1214
6	6038	692	156	324	1230 (est)
7	7133	-811	138	079	1258
8	6900	-375	---	348	1317
9	9941	-268	142	057	1350
10	11361	-480	112	334	1407
11	13142	267	84	284	1418
12	12841	842	88	074	1430 (est)

Note: The Mini-Ranger IV antenna was located above the pilot house. The grab sample boom was located at a position 28 6° clockwise from the ship's head at a distance of 25 ft relative to the antenna.

Chainage and offsets were calculated based on a survey centerline defined by the following parameters.

Line	Easting(x) (ft)	Northing(y) (ft)	Chainage (ft)	Offset (ft)
Start	19800	6200	0	0
End	6625	6800	13181	0

Coordinates were based on a local coordinate system established by DOWL Engineers of Anchorage, AK. Positive offsets were to the left (or south) of the centerline and negative offsets were to the right (or north) of the centerline.

Table 3-3.   Description of Grab Samples Taken in Akutan Harbor on 12 April 1992.

Sample Number	Description
1	Fine silt with some clam shells. No hydrogen sulfide odor.
2	Coarse silt with clam shell fragments. Strong hydrogen sulfide odor
3	Coarse silt with fine sand and clam shell fragments. Strong hydrogen sulfide odor.
4	Silt with no sand. Fish bones evident. No odor.
5	Brown muddy silt. No odor.
6	Silt with some clam shells. No odor.
7	Fish waste odor. No natural sediments. Very strong hydrogen sulfide odor.
8	Silt with clam shells. Hydrogen sulfide odor. White ooze evident.
9	Silt with clam shells and numerous worm tubes. No odor.
10	Coarse brown silt with some shells and rocks
11	Silt with clam shells and numerous polychaetes.
12	Coarse silt with crab shell. Hydrogen sulfide odor.

This section presents the results and discussion from the side scan sonar survey including grab sample analyses. The reconnaissance survey is presented in Section 4 1, Site-specific survey information is presented in Section 4 2.

4.1   Reconnaissance Survey

Analysis of the reconnaissance survey data indicated two significant areas of accumulated seafood waste. These areas included regions in proximity to the Trident shore-based seafood processing facility's discharge and the DEEP SEA floating processor (Figure 4-1). These areas were characterized on the side scan records by distinct differences in the acoustic reflectivity of the seabed in the vicinity of the waste piles when compared to reflectivity of the natural bottom. Except in the nearshore area, and for occasional man-made and natural features, the natural bottom was composed of silts which generally appeared on the side scan records as a light gray tone indicating a relatively soft, smooth reflector. In the nearshore area, steep slopes and coarser bottom materials acted as strong reflectors and appeared as a dark gray or nearly black tone that was significantly different from the acoustic properties of the main harbor basin. The presence of silt throughout the natural harbor bottom was confirmed by the acquired grab samples (Table 3-3).

Other than the two sites discussed above, the side scan records indicated a significant number of anchor drag marks throughout the harbor. These evidently were the result of moorings made by transient, floating seafood processors and other vessels. It was expected that some seafood waste piles would be evident on the seabed in the outer harbor. However, because most processors are single-point moored, shift position with the wind, and are only in the harbor for short durations, seafood waste concentrations were too diffuse to detect using side scan sonar alone. However, grab samples 2 and 3 from the outer harbor (see Figure 3-1) had a strong odor of hydrogen sulfide although no crab or fish parts were evident in the sample. The stronger acoustic reflectivity, evident on the side scan records, the presence of
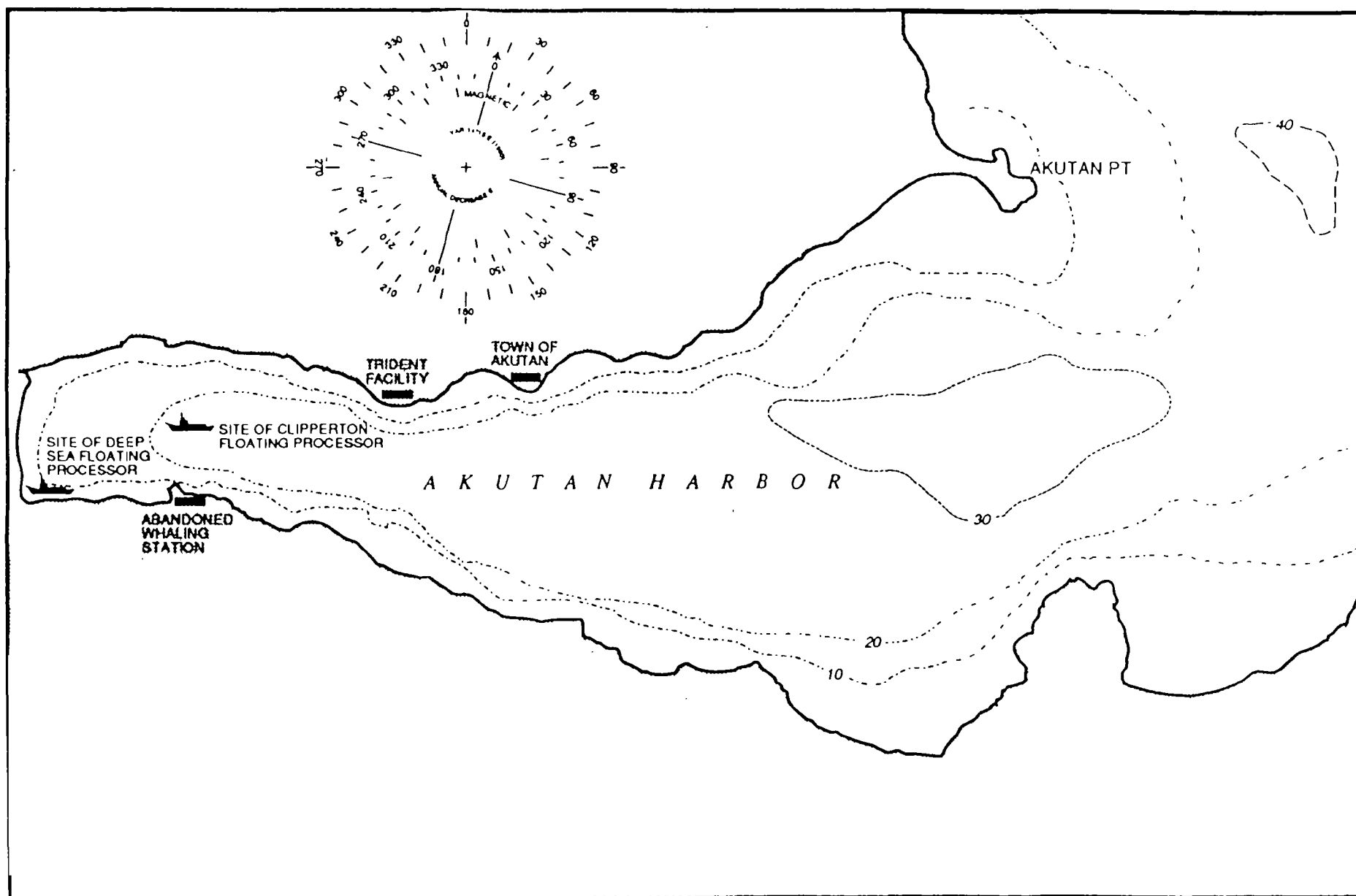
Figure 4-1.   Site Survey Locations: (DEEP SEA, CLIPPERTON Floating Processors and Trident Facility).

anchor drag marks, and the hydrogen sulfide smell of grab samples collected in the vicinity suggest that these locations may have been historical crab or fish waste disposal sites.

4.2   Site Specific Surveys

The following sections present results from detailed surveys of the DEEP SEA and CLIPPERTON floating processor sites and the shore-based Trident processing facility.

4.2.1   The DEEP SEA Site

The seabed beneath the DEEP SEA floating processor was analyzed using data taken from transects 2, 3, 10, and 11. The first two lines were completed as part of the reconnaissance survey while the second two lines were run specifically to examine seabed conditions beneath the DEEP SEA. The survey in this area was complicated by the presence of water supply lines which ran from shore to the processor, permanent mooring lines, the steep bathymetric slope running up to the beach at the end of the harbor, the presence of a seasonal stream depositing sediments in the southwest corner of the site, and the location of the processor in the corner of the harbor.

Based on the side scan data it appeared that the distribution of seafood waste on the seabed was quite patchy. This patchiness was confirmed by grab samples taken by others during the same survey period (Oestman, pers. comm. 1992). Six patches were identified from the side scan records as potentially representing seafood waste disposal accumulations. The area of the seabed covered by these six patches is approximately 2.5 acres or 10,000 sq. m (109,000 sq. ft). A seventh patch was identified just to the west of the surveyed area but was considered too close to shore to be a waste pile. Unfortunately, there were insufficient resources to allow grab samples to be taken at the center and edges of each of the patch sites. Thus, confirmation of each patch as a waste pile was not possible. The estimated error for patch area is +/- 25%. This areal measurement does not include areas that may be covered only by a thin veneer of seafood waste.

4.2.2   The CLIPPERTON Site

Analysis of the CLIPPERTON site data was based on side scan data collected from transects 1, 6, 12, and 13. Tracklines 12 and 13 were run on the south and north sides of the CLIPPERTON. The CLIPPERTON site was chosen because it was moored fore and aft and could not swing freely at anchor like most temporarily moored seafood processors. Because it was anchored in a semi-fixed position, the CLIPPERTON was assumed to have the greatest likelihood of accumulated seafood waste beneath it. There was evidence of crab shell and hydrogen sulfide odor in a sediment grab sample acquired on the north side of the CLIPPERTON (Larsen, pers. comm. 1992). However, analysis of the side scan data indicated little evidence of accumulated seabed waste in the vicinity of the CLIPPERTON except for slightly higher acoustic reflectivity of the seabed on the north side of the processor.

4.2.3   Trident Site

The Trident site was analyzed using side scan data collected from transects 6, 7, and 14 through 19. The first two transects were run as part of the reconnaissance survey. The last six lines were part of a site specific survey in the vicinity of the Trident outfall. Based on analysis of the side scan data, several seafood waste features were identified at the outfall site (Figure 4-2). The first feature is the boundary limit of the seafood waste coverage of the seabed. This was clearly evident from the side scan records as denoted by the difference in acoustic reflectivity between the natural seabed and the seafood waste pile near the outfall. The boundary was not as clear in the region adjacent to the Trident dock. The area covered by seafood waste was estimated to be approximately 11.2 acres or 45,500 sq. m (490,000 sq. ft).

The second feature identified was the primary waste pile. The pile appeared to be approximately 75 m in diameter, resulting in an area of about 1.2 acres or 4850 sq. m (52,200 sq. ft).
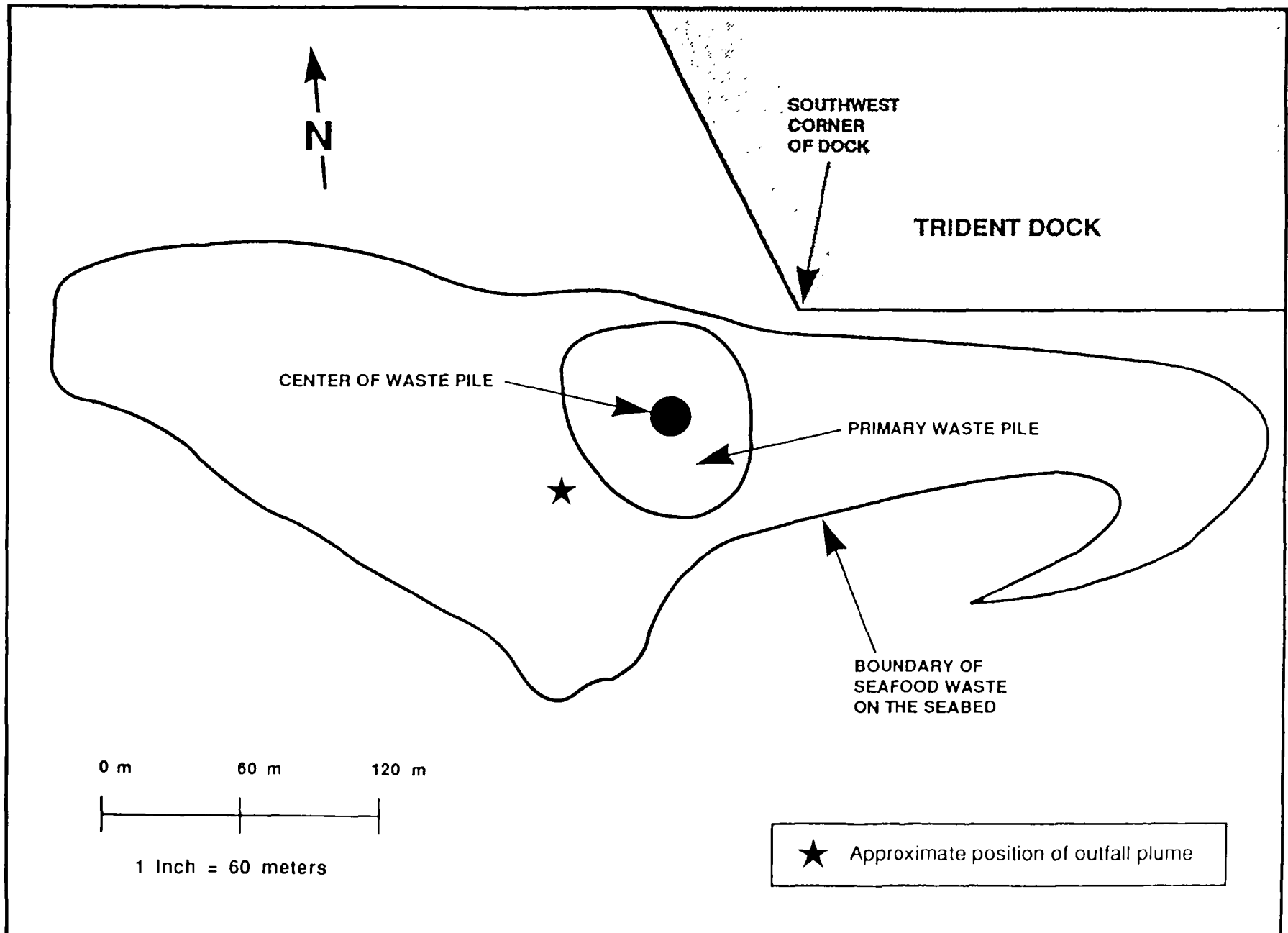
Figure 4-2.   Seafood Waste Accumulations at the Trident Outfall Site.

Based on the waste boundary shape, it appeared that seafood waste may have spread downslope in a southerly direction, and along the bathymetric contour in both easterly and westerly directions

5.0 SUMMARY AND CONCLUSIONS

Akutan Harbor was surveyed to determine the extent of seafood processor waste on the seabed within the harbor. A reconnaissance survey of the harbor was conducted to determine probable sites of seafood processor waste piles. Through preliminary assessment of data in the field it was determined that the only sites which were important to consider further—based on the scope of this project—were the DEEP SEA site at the southwest corner of the harbor, the CLIPPERTON site at the west central edge of the harbor, and the Trident site located at the north central shore of the harbor, just west of the town of Akutan.

Of the three sites, only the DEEP SEA and Trident sites showed evidence of significant seafood processing waste accumulation. At the DEEP SEA site, the areal extent of seafood accumulation was estimated to be 2.5 acres (10,000 sq. m) +/-25%. At the Trident site the areal extent of seafood processor waste was estimated to be 11.2 acres (45,500 sq m) +/ 15%.

Subbottom profiling has been suggested by Watson (1989) as a method of determining the depth of crab waste in the harbor; however, there is evidence that this method would not be entirely successful. Based on the experience of flying a remotely operated vehicle (ROV) over the crab and fish waste piles, it was evident that there was a significant quantity of biogenic gas bubbling up from the piles. This may be observed on the video tapes acquired by Jones and Stokes Associates during this field effort. Because biogenic gas in sediments makes them acoustically opaque, it would probably not be possible to "see" through the waste material to natural bottom and subsequently determine the thickness of seafood waste. Only in areas where the sediments and the seafood waste were degassed would it be possible to conduct this type of survey.

6 0   REFERENCES

Atlas, R.M. 1975. Effects of temperature and crude oil composition on petroleum biodegradation. Applied Microbiology 30.396-403.

EG&G 1987. Model 260 Image Correcting Side Scan Sonar Instruction Manual. EG&G Environmental Equipment, 216 Middlesex Turnpike, Burlington, MA 01803

Larsen, L. 1992. Personal communication. Field notes taken during grab sampling in Akutan during April 1992. Jones and Stokes Associates, Bellevue, WA.

Motorola Corporation. (Date unspecified). Motorola Miniranger IV Operators Manual. Motorola Corporation, Tempe, AZ.

Oestman, R. 1992. Personal communication. Telephone call from T. Petrillo to R. Oestman, Jones and Stokes Associates, Bellevue, WA, on 10 June 1992.

U.S. EPA. 1984. Effects of Seafood Waste Deposits on Water Quality and Benthos, Akutan Harbor, Alaska. EPA Report No. 910/9-83-114. 81 pp.

Watson, W.D. 1989. Akutan Harbor - Unalaska Island Side Scan Sonar Investigation, Report No. WOI-5689601. Prepared for U.S. EPA, Anchorage, AK. Prepared by Watson Co., Anchorage, AK.

Chronology of Events

Tuesday, April 7th

The survey team and equipment arrived in Akutan via amphibious plane on four separate flights due to the excessive weight of the equipment. Most of the equipment was moved into a storage shed near the town dock which served as the staging area for the field effort.

After inspecting the FLYING D, a 90 ft converted landing craft, it was determined that it would not serve well as a survey vessel. A 24' fishing boat, on shore for the winter, was available and was chosen for conducting the survey.

The marine survey team met with the land survey team to coordinate details of the locations of the shore stations.

Wednesday, April 8th

Due to a problem with the starboard engine, the survey boat could not be launched before low tide. In addition, because the navigation system needed A/C power, a portable generator was flown in from Anchorage, and arrived on Thursday, April 9th.

Most of the day was spent mobilizing and testing the SSS and MR4 equipment on the survey vessel and setting up five positioning shore stations around the harbor. After the MR4 equipment was set up, it was tested using shore power; because of its proximity to the navigation stations, it was determined to be capable of receiving signals from four of the five stations.

Thursday, April 9th

The boat was launched at high tide around 1100 and brought to the city pier. The SSS was tested in the water and was found to function properly. The portable generator which arrived at approximately 1500.

Three side scan survey lines (numbers 1 through 3) were run in the late afternoon and early evening. The first line, set at the 200 m scale on the SSS, was run along the centerline

of the survey. The centerline was an arbitrary line, set approximately east-west, which ran along the approximate centerline of the harbor. This allowed most of the survey lines to be run as offsets of this centerline, approximately parallel with the bathymetric contours of the harbor.

The second and third lines were run parallel with the centerline at approximately 200 meter offsets to the south.

Friday, April 10th

Twelve SSS lines (numbers 4 through 15) were run. Lines 4 through 9 were run at the 150 meter scale on the SSS. This completed the reconnaissance survey of the harbor. From preliminary assessment of the data it was determined that three sites would be examined in more detail. They included:

- Trident Seafoods site, a shore-based processor with an offshore outfall for seafood processing waste,

- Deep Sea Fisheries site, a permanently moored crab processor, and

- CLIPPERTON site, a temporarily moored crab processor, on site since January 1992.

The last six survey transects of the day were run at the 75 m scale on the SSS. The first two lines were run from east to west on the south and north sides of the DEEP SEA site. The second two lines were run from east to west on the south and north sides of the CLIPPERTON site. The last two lines were run at the Trident site in a north-south direction. These lines were not as successful as the east-west lines because the SSS towfish had to be raised and lowered as the survey vessel crossed the bathymetric contours of the harbor. It was determined that additional lines should be run on April 11 to achieve the detailed coverage needed.

Saturday, April 11th

Four SSS lines (numbers 16 through 19) were run at the 75 m scale at the Trident Seafood outfall site. Following this, the SSS was demobilized and the ROV was set up for operations.

To determine the positions of grab samples taken for SSS data verification, all of the SSS and MR4 data were examined in Akutan. Due to time limitations, twelve sites were chosen to provide baseline information for SSS data analysis Following this, compiling navigation data for the twelve stations, survey personnel and Jones and Stokes Associates personnel collected the grab samples from the survey vessel FLYING D.

The remainder of the day was spent conducting ROV surveys.

Sunday, April 12th

ROV Surveys and sediment grab sampling were conducted.

Monday, April 13th

Several ROV lines were run in the morning. Because the weather had been marginal, it was decided that all of the equipment should be transferred to Dutch Harbor on the FLYING D instead of by aircraft. All equipment was loaded onto the boat and either tied down under the pilot house or packed into the forward hold.

The survey team flew to Dutch Harbor in the late afternoon but could not connect with a flight to Anchorage and thus remained in Dutch Harbor for the night. At approximately 2200, the FLYING D arrived from Akutan. The equipment was offloaded to a truck and transferred to a shipping container for transfer to Seattle.

Tuesday, April 14th

The survey team flew from Dutch Harbor, Alaska, to Seattle, Washington.

Appendix H.   Qualitative Characterization of Sediments in Akutan Harbor

Table H-1. Fractional Distribution by Weight of the Three Dominant Sediment Grain Sizes
from Stations Sampled in 1983 and 1992, Akutan Harbor, Alaska

Station #	1983 Sediments			1992 Sediments				
	Dominant (%)	1st Sub-dominant (%)	2nd Sub-dominant (%)	Dominant (%)	1st Sub-dominant (%)	2nd Sub-dominant (%)	Depth (ft)	Comments
1	38.9[k]	31.8[j]	19.1[i]	65.9[k]	11.2[j]	9.9[i]	101	hydrogen sulfide smell
2	41.7[d]	21.9[k]	12.0[i]	55.9[k]	14.9[j]	14.4[i]	54	course sediments, oily sheen in sediments, two large anenomes, benthic algae, few worms, propuloids
3	44.6[k]	26.0[i]	12.8[j]	49.5[i]	24.0[k]	10.5[b]	89	course sediments, a large amount of clamshell debris, some crab waste
5	61.3[k]	21.9[j]	7.3[i]	61.1[k]	18.8[j]	11.6[i]	128	moderately anoxic, numerous polychaetes, clamshell debris, several unidentified clams
6	70.9[k]	18.4[j]	5.5[i]	64.6[k]	18.1[j]	4.6[i]	143	strong hydrogen sulfide smell, some *Ulva*, some crab waste
7	63.6[k]	23.7[j]	9.2[i]	38.4[k]	23.4[j]	18.6[i]	157	small amount of shell debris
7A	--	--	--	57.4[k]	16.4[i]	15.3[j]	124	very anoxic, strong hydrogen sulfide smell, a large number of fish bones
8	50.0[k]	25.7[j]	14.6[i]	39.8[k]	25.8[i]	25.6[j]	118	course sediments, large amount of clamshell debris
8A	--	--	--	54.2[k]	16.9[i]	14.0[j]	154	hydrogen sulfide smell, some crab waste
9	68.6[k]	21.1[j]	4.4[i]	61.6[k]	24.2[j]	4.6[i]	156	fairly anoxic, some crab chelipeds
10	27.0[k]	24.1[f]	18.6[i]	58.0[k]	20.5[j]	12.1[i]	140	very silty
10A	--	--	--	48.8[k]	25.5[i]	20.3[j]	113	strong hydrogen sulfide smell, larger bivalve debris and fragments
11	65.4[k]	25.1[j]	5.6[i]	64.4[k]	27.9[j]	5.8[i]	170	few polychaetes

Table H-1. Continued

Station #	1983 Sediments			1992 Sediments				
	Dominant (%)	1st Sub-dominant (%)	2nd Sub-dominant (%)	Dominant (%)	1st Sub-dominant (%)	2nd Sub-dominant (%)	Depth (ft)	Comments
12	42.6[j]	39.6[k]	14.5[l]	39.5[h]	32.0[i]	21.6[j]	126	slight hydrogen sulfide smell, some crab shell debris
13	.82.5[g]	10.0[h]	3.0[j]	37.0[k]	30.6[j]	25.3[i]	160	few bivalve shells
PO3	--	--	--	56.2[k]	22.5[j]	15.0[i]	--	some clamshell debris
BPO	--	--	--	24.6[j]	24.0[j]	18.2[i]	--	large amount of clamshell debris, one unidentified clam, numerous polychaetes

Note: Samples taken in 1992 were not sorted for substrates larger than fine gravel.
   -- indicates no data

[a] Cobbles or Larger . . . . >50 mm
[b] Coarse Gravel . . . . 31.5 to 50 mm
[c] Medium Gravel . . . . 19 to 31.5 mm
[d] Fine Gravel . . . . 0.75 to 19 mm

[e] Very Fine Gravel . . . . 2 to 4.75 mm
[f] Very Coarse Sand . . . . 1 to 2 mm
[g] Coarse Sand . . . . 0.5 to 1 mm
[h] Medium Sand . . . . 0.25 to 0.5 mm

[i] Fine Sand . . . . 0.125 to 0.25 mm
[j] Very Fine Sand . . . . . . 0.063 to 0.125 mm
[k] Silts and Clays . . . . <0.063 mm
[l] Fine Gravel and Larger . . . . . >4.75 mm

Source of 1983 data: EPA 1984b.

Table H-2. Qualitative Description of Physical and Biological Conditions in Gravity Core and Van Veen Sediment Samples
Taken in April 1992, Akutan Harbor, Alaska

Sample #	Depth (ft)	Physical Observations	Biological Observations
Core Samples			
Sample Stations			
C1	91	4-inch penetration; 2 inches of soft silt overlaying compacted silt; sediment is gray	scattered shell debris and large tubeworm casings found
C3	109	8-inch penetration, uniform texture, gray sediments	clamshell fragments
C5	131	8-inch penetration, 4 inches of soft, gelatinous silt overlaying compacted silt, gray sediments	tubeworms in upper 3 inches, some shell debris
C6	149	6-inch penetration, some sediments have a brown color	tubeworms in upper 3 inches
C7	121	6- to 8-inch penetration, coarse sediments (sand and gravel) on surface overlaying fine sediments	tubeworms in upper 2 inches, 10% to 20% shell debris
C7A	122	sediments too soft to collect core sample	
C9	158	2-inch penetration, very consolidated	few shell fragments
C14	200	4-inch penetration, 2 inches of soft silt overlaying a loose, fine, silty mud	a few tubeworms and a small amount of shell debris
C15	167	6-inch penetration, top 1.5 inches composed of soft silt over a slightly more compacted layer	a few tubeworms
Other Stations			
CO1 (halfway between Core Stations 1 and 2)	86	8-inch penetration, 2 inches of fine, soft, silty mud overlaying semi-consolidated silt	some shell debris
CO2 (40'N of proposed Deep Sea outfall)	80*	too loose to get a sample, took a Van Veen grab sample at site, little silt	Van Veen sample contained all crab waste with a lot of unground shell; 8 to 10 full carapaces and approximately 20 leg exoskeletons

Sample #	Depth (ft)	Physical Observations	Biological Observations
Other Stations, continued			
CO3 (60'N of proposed Deep Sea outfall)	100*	4-inch penetration, sand/gravel with some surface silt	some clamshell debris, no hydrogen sulfide smell
CO4 (120'N of proposed Deep Sea outfall)	100*	6-inch penetration, very consolidated at depth, some gravel	some tubeworms, clamshell debris, and pieces of crab waste, no hydrogen sulfide odor
CO5 (180'N of proposed Deep Sea outfall)	100*	2-inch penetration, silt substrate	hydrogen sulfide odor
COP1 (Deep Sea crab waste)	80*	too loose to retrieve a core sample	
COP2 (Deep Sea crab waste)	80*	too loose to retrieve a core sample	hydrogen sulfide odor emanating from the empty sampler
Van Veen Grab Samples			
Deep Sea Outfall			
VT1	80*	consolidated dark silts	hydrogen sulfide odor, a few polychaetes
VT2	80*	1/8- to 1/4-inch gravel, very dark in color with very little fine sediments	moderate hydrogen sulfide odor, small amount of shell debris
VT3	80*	coarse sediments	strong hydrogen sulfide odor, a lot of decomposed crab waste, some exoskeletal remains
VT4	80*	piece of plastic buoy in sample, coarse sediments	a slight hydrogen sulfide odor, two anenomes attached to buoy, several brittle stars and many larger tubeworm casings
VT5	80*	coarse sediments with some gravel, a trace of oil was also found	crab debris, a scaphopod, and clamshell debris

Sample #	Depth (ft)	Physical Observations	Biological Observations
Clipperton Outfall			
VCL1	120*	black silt	tubeworms
VCL2	120*	silt	hydrogen sulfide odor, crab debris
Trident Dock			
VO1 (Trident Dock)	130*	too soft, winnowing as sample was retrieved	fish bones
Proposed Outfall			
VPO1	100*	sediments composed primarily of silt sediments	a small amount of crab waste, many polychaetes, clams, some algae, and a brittle star
VPO2	60*	gravel with fine sediments	*Ulva*, two 1-inch diameter unidentified clams, shell debris
VPO3	60*	silt and sand	*Ulva*, 1-inch diameter unidentified clams, shell debris
VPO4	60*	gray silt with some brown fine sediments	butter clams (*Saxidomus giganteus*), tubeworms
VBPO1	60*	scattered cobbles with silt	barnacles on cobbles, one 1-inch unidentified clam, a variety of polychaetes, clamshell debris
Side-Scan Samples			
VSSS1	160*	fine silt	some shell debris
VSSS2	163	coarse silt	strong hydrogen sulfide odor, some clamshell debris
VSSS3	155*	coarse silt, sand	strong hydrogen sulfide odor, some shell debris
VSSS4	150	silt, no sand	fish bones, no hydrogen sulfide odor
VSSS5	159	muddy, brown silt	no hydrogen sulfide odor

Sample #	Depth (ft)	Physical Observations	Biological Observations
Side-Scan Samples, continued			
VSSS6	156	silt	clamshell debris
VSSS7	128		solid fish waste, strong hydrogen sulfide odor
VSSS8	138	silt	hydrogen sulfide odor, unidentified organic white viscous liquid, shell debris
VSSS9	142	silt	a large quantity of tubeworms and a medium amount of shell debris
VSSS10	112	coarse brown silt with cobble sized rocks	shell debris
VSSS11	84	silt	lots of polychaetes, little shell debris
VSSS12	88	coarse silt	crab waste, hydrogen sulfide odor
Sample Stations			
1	100	granular silt	hydrogen sulfide smell, anoxic
2	39	coarse sediments, contains 1/4- to 1/2-inch gravel, oily sheen on gravel	two large anenomes, benthic algae, prapuloids? - 20, a few polychaetes
3	79	coarse sediments, contains 1/2- to 1-inch rock	some crab waste, large quantities of clamshell debris
5	126	sand and silt	moderately anoxic, numerous polychaetes, unidentified clams, clamshell debris
6	143	sediments composed of silt	anoxic, strong hydrogen sulfide odor, a small amount of crab waste, a small amount of *Ulva*
7	158	sediments composed primarily of silt	a minor amount of shell debris
7A	108	sediments composed of silt	very anoxic, strong hydrogen sulfide odor, a large amount of fish bones

Table H-2. Continued

Sample #	Depth (ft)	Physical Observations	Biological Observations
Sample Stations, continued			
8	136	very coarse sediments, high gravel and cobble component	a larger amount of shell debris and fewer polychaetes than other samples from unimpacted areas
8A	130	sediments composed of silt	hydrogen sulfide odor present with some crab waste
9	157	silt and clay	fairly anoxic, some pieces of crab chelipeds
10	145	sediments composed of silt	
10A	104	sediments composed primarily of silt	strong hydrogen sulfide odor, a large amount of clamshell debris with larger shell fragments
11	167	sediments composed primarily of silt	fewer polychaetes than other samples
12	115	sediments composed primarily of silt	slight hydrogen sulfide smell, a small amount of ground crab shell
13	152	sediments composed primarily of silt	a moderate amount of shell debris

* Depths are estimated at these stations.
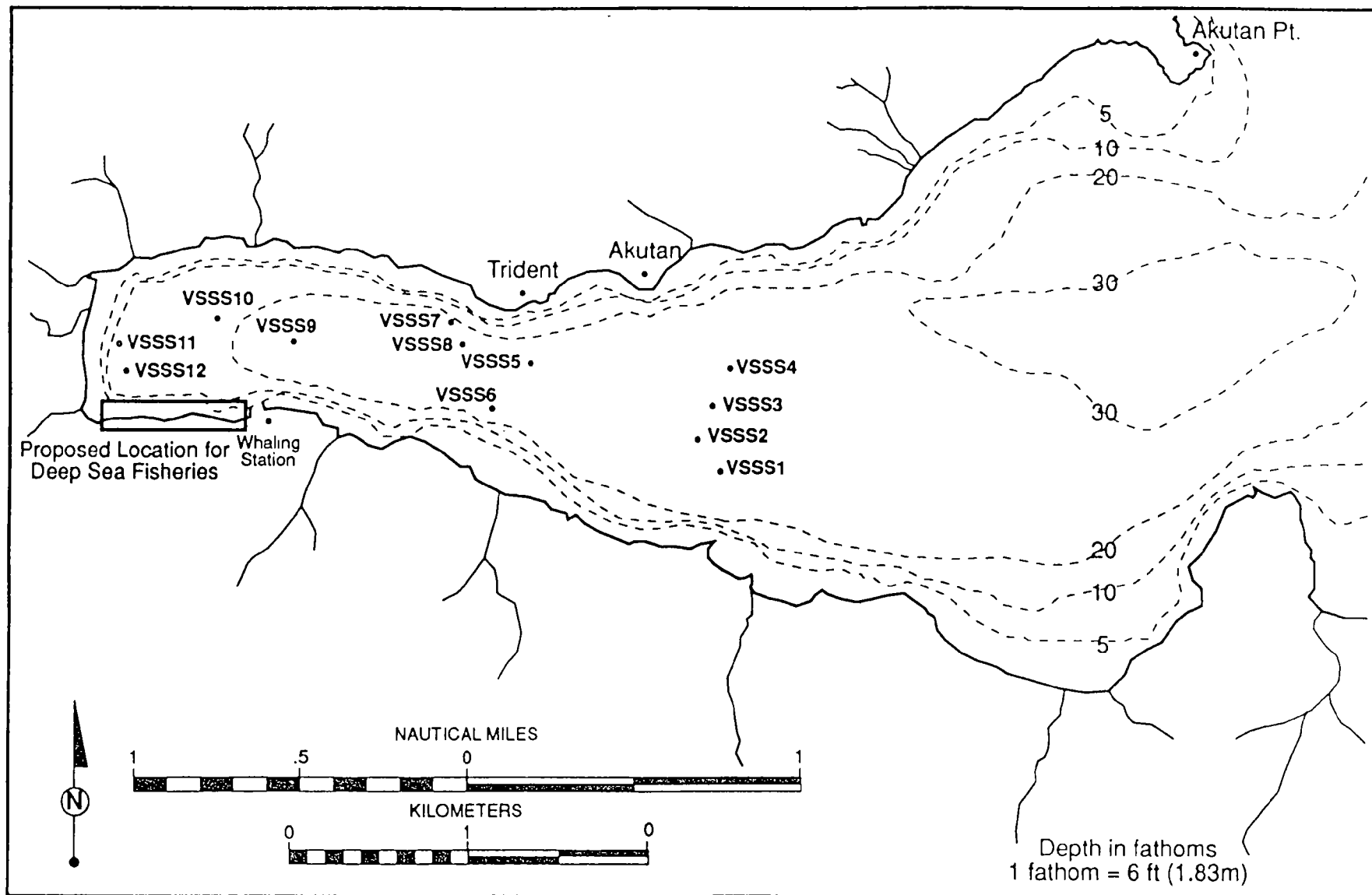
Figure H-1. Locations of Benthic Samples Collected to Evaluate Side-Scan Sonar Surveys in 1992, Akutan Harbor, Alaska
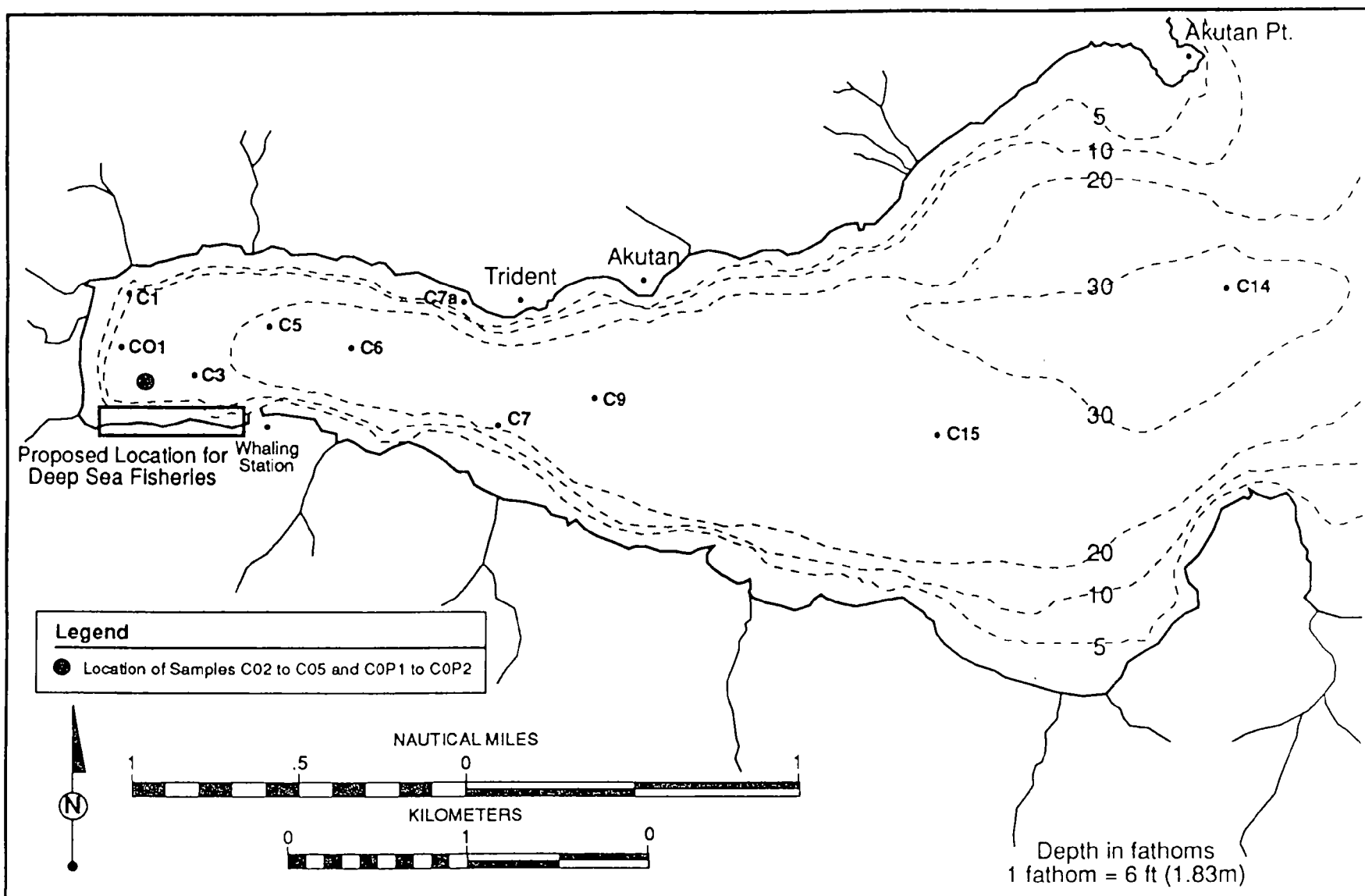
Figure H-2. Locations of Additional Core Sampling Sites in 1992, Akutan Harbor, Alaska
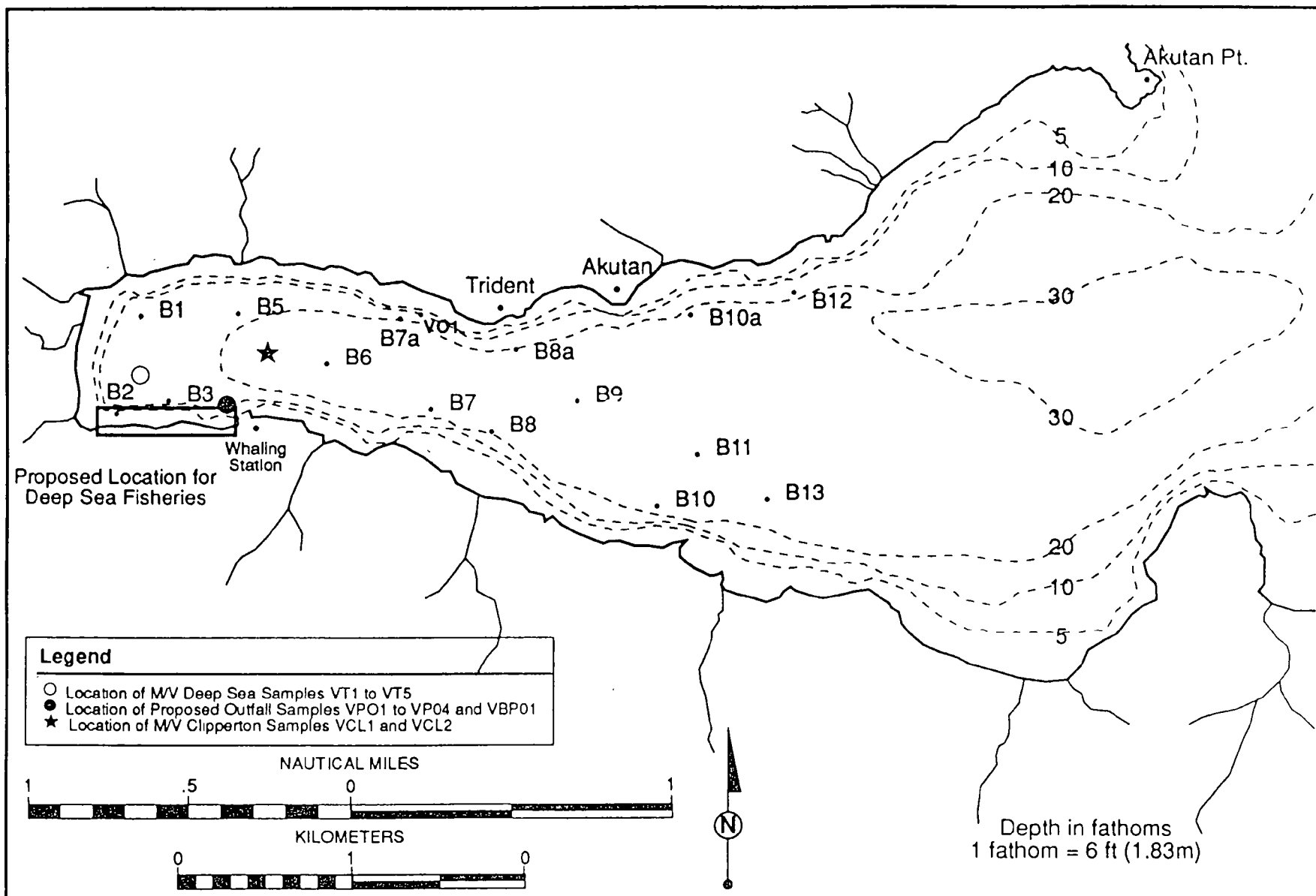
Figure H-3. Locations of Sites Sampled with Van Veen Grab for Qualitative Analysis of Harbor Sediments

Appendix I.   Species Checklist and Individual Counts of
               Benthic Species Found in Akutan Harbor,
               April 1992

Phylum Protozoa
    Order Foraminiferida
        Foraminifera sp. Indeterminate

Phylum Nemertea
    Nemertea sp. Indeterminate

Phylum Nematoda
    Nematoda sp. Indeterminate

Phylum Priapulida
    Order Priapulomorpha
        Family Priapulidae
            Priapulus caudatus (Lamarck, 1816)

Phylum Annelida
    Class Polychaeta
        Order Orbiniida
            Family Orbiniidae
                Leitoscoloplos pugettensis (Johnson, 1901)
            Family Paraonidae
                Paraonidae sp. Indeterminate
        Order Cossurida
            Family Cossuridae
                Cossura sp. Indeterminate
        Order Spionida
            Family Apistobranchidae
                Apistobranchus tullbergi (Theel, 1879)
            Family Spionidae
                Boccardia nr. polybranchia (Haswell, 1885)
                Polydora brachycephala (Hartman, 1936)
                Polydora socialis (Schmarda, 1861)
                Polydora sp. A
                Prionospio sp. Indeterminate
                Prionospio (Prionospio) steenstrupi (Malmgren, 1867)
                Spio cirrifera (Banse and Hobson, 1968)
                Spionidae sp. Indeterminate
                Spiophanes berkeleyorum (Pettibone, 1962)
            Family Magelonidae
                Magelona longicornis (Johnson, 1901)

Table I-1. Continued

Family Cirratulidae
    Chaetozone setosa (Malmgren, 1867)
    Cirratulidae sp. Indeterminate
Order Capitellida
    Family Capitellidae
        Barantolla sp. A
        Capitella capitata complex (Fabricius, 1780)
        Capitellidae sp. Indeterminate
        Decamastus gracilis (Hartman, 1963)
        Heteromastus filobranchus (Berkeley & Berkeley, 1932)
        Mediomastus sp. Indeterminate
        Notomastus (Clistomastus) lineatus (Claparede, 1870)
    Family Maldanidae
        Euclymene reticulata (Moore, 1923)
        Euclymeninae sp. Indeterminate
        Maldanidae sp. Indeterminate
        Praxillella gracilis (M. Sars, 1861)
        Rhodine bitorquata (Moore, 1923)
Order Opheliida
    Family Opheliidae
        Armandia brevis (Moore, 1906)
        Ophelina acuminata (Oersted, 1843)
        Travisia forbesii (Johnston, 1840)
    Family Scalibregmidae
        Scalibregma inflatum (Rathke, 1843)
Order Phyllodocida
    · Family Phyllodocidae
        Eteone californica (Hartman, 1936)
        Phyllodoce citrina (Malmgren, 1865)
        Phyllodoce (Anaitides) groenlandica (Oersted, 1843)
        Phyllodoce sp. Indeterminate
    Family Polynoidae
        Harmothoe imbricata (Linnaeus, 1767)
        Polynoidae sp. Indeterminate
        Polynoidae sp. A
    Family Sigalionidae
        Pholoe minuta (Fabricius, 1780)
    Family Syllidae
        Syllidae sp. Indeterminate
        Syllis (Ehlersia) heterochaeta (Moore, 1909)
        Syllis sp. Indeterminate
        Syllis (Syllis) elongata (Johnson, 1901)

Table I-1. Continued

Family Nereidae
    Nereis zonata (Malmgren, 1867)
Family Goniadidae
    Glycinde picta (Berkeley, 1927)
    Goniada maculata (Oersted, 1843)
Family Nephtyidae
    Nephtys caeca (Fabricius, 1780)
    Nephtys ferruginea (Hartman, 1940)
    Nephtys punctata (Hartman, 1938)
    Nephtys sp. Indeterminate
    Nephtys sp. Juvenile
Family Sphaerodoridae
    Sphaerodoropsis sphaerulifer (Moore, 1909)
Order Eunicida
    Family Onuphidae
        Onuphis sp. Juvenile
    Family Lumbrineridae
        Lumbrineris bicirrata (Treadwell, 1929)
        Lumbrineris luti (Berkeley & Berkeley, 1945)
        Lumbrineris sp. Indeterminate
    Family Dorvilleidae
        Dorvillea annulata (Moore, 1906)
        Dorvilleidae sp. Juvenile
Order Oweniidae
    Family Oweniidae
        Galathowenia oculata (Zachs, 1923)
Order Flabelligerida
    Family Flabelligeridae
Order Terebellida
    Family Pectinariidae
        Pectinaria granulata (Linnaeus, 1767)
    Family Ampharetidae
        Ampharete acutifrons (Grube, 1860)
        Ampharete finmarchica (Sars, 1865)
        Ampharetidae sp. Indeterminate
        Ampharetidae sp. Juvenile
        Amphicteis glabra (Moore, 1905)
        Amphicteis mucronata (Moore, 1923)
        Asabellides sibirica (Wiren, 1883)
        Glyphanostomum nr. pallescens (Theel, 1878)
        Lysippe labiata (Malmgren, 1866)
        Melinna elisabethae (McIntosh, 1922)

Table I-1. Continued

Family Terebellidae
    Lanassa sp. A
    Neoamphitrite edwardsi (Quatrefages, 1865)
    Pista cristata (Muller, 1776)
    Terebellidae sp. Indeterminate
Family Trichobranchidae
    Terebellides stroemi (Sars, 1835)
Order Sabellida
  Family Sabellidae
    Chone duneri (Malmgren, 1867)
Class Oligochaeta
    Oligochaeta sp. Indeterminate

Phylum Mollusca
Class Gastropoda
  Order Archaeogastropoda
    Family Lepetidae
      Lepeta concentrica (Middendorff, 1851)
  Order Mesogastropoda
    Family Lacunidae
      Lacuna vincta (Montagu, 1803)
    Family Littorinidae
      Littorina saxitilis (Olivi, 1792)
    Family Rissoidae
      Alvania compacta (Carpenter, 1864)
    Family Naticidae
      Natica clausa (Broderip & Sowerby, 1829)
  Order Neogastropoda
    Family Columbellidae
      . Nitidella gouldi (Carpenter, 1857)
    Family Turridae
      Oenopota harpularia (Couthouy, 1838)
      Oenopota elegans
Subclass Opistobranchia
    Family Pyramidellidae
      Odostomia sp. Indeterminate
      Turbonilla sp. Indeterminate
  Order Cephalaspidea
    Family Retusidae
      Retusa sp. Indeterminate
    Family Cylichnidae
      Cylichna attonsa (Carpenter, 1865)

Table I-1. Continued

Class Bivalvia
        Bivalvia sp. Juvenile
    Order Nuculoida
        Family Nuculidae
            Nucula tenuis (Montagu, 1808)
        Family Nuculanidae
            Malletia sp. Indeterminate
            Nuculana minuta (Fabricius, 1776)
            Yoldia hyperboria (Torrell, 1859)
            Yoldia scissurata (Dall, 1897)
        Family Mytilidae
            Musculus niger (J. E. Gray, 1824)
            Mytilidae sp. Juvenile
        Family Anomiidae
            Pododesmus macroschisma (Deshayes, 1839)
    Order Veneroida
        Family Thyasiridae
            Adontorhina cyclia (Berry, 1947)
            Axinopsida serricata (Carpenter, 1864)
            Thyasira flexuosa (Montagu, 1803)
        Family Montacutidae
            Mysella tumida (Carpenter, 1864)
        Family Cardiidae
            Clinocardium ciliatum (Fabricius, 1780)
            Serripes groenlandicus (Bruguiere, 1789)
        Family Tellinidae
            Macoma calcarea (Gmelin, 1791)
            Macoma carlottensis (Whiteaves, 1880)
            Macoma moesta alaskana (Deshayes, 1855)
            Macoma sp. Juvenile
        Family Veneridae
            Saxidomus giganteus (Deshayes, 1839)
    Order Myoida
        Family Myidae
            Cryptomya californica (Conrad, 1837)
            Mya pseudoarenaria (Schlesch, 1931)
            Mya sp. Juvenile
            Mya uzensis (Nomura & Zinbo, 1937)
        Family Hiatellidae
            Hiatella arctica (Linnaeus, 1767)

Table I-1. Continued

Phylum Arthropoda
    Subphylum Crustacea
        Class Ostracoda
            Order Myodocopida
                Family Philomedidae
                    Philomedidae sp. Indeterminate
                Family Cylindroleberididae
                    Bathyleberis garthi (Baker, 1979)
                    Cylindroleberididae sp. Indeterminate
        Class Copepoda
            Order Calanoida
                Calanoida sp. Indeterminate
            Order Cyclopoida
                Cyclopoida sp. Indeterminate
        Class Cirripedia
                Cirripedia sp. Indeterminate
            Order Cumacea
                Family Leuconidae
                    Eudorella emarginata (Kroyer, 1846)
                    Leucon sp. Indeterminate
            Order Isopoda
                Family Limnoriidae
                    Limnoria lignorum (Rathke, 1799)
            Order Amphipoda
                Amphipoda sp. Indeterminate
                Family Oedicerotidae
                    Monoculodes sp. Indeterminate
                    Monoculodes zernovi (Gurjanova, 1936)
                Family Stenothoidae
                    Proboloides holmesi (Bousfield, 1982)
                Family Phoxocephalidae
                    Eyakia robustus (Holmes, 1908)
                Family Lysianassidae
                    Anonyx lilljeborgi (Boeck, 1871)
                Family Uristidae
                    Uristidae sp. Indeterminate
                Family Ampeliscidae
                    Ampelisca agassizi (Judd, 1896)
                    Ampelisca sp. Indeterminate
                Family Aoroidae
                    Aoroides sp. Indeterminate
                Family Hippolytidae
                    Eualus sp. Indeterminate

Table I-1. Continued

Family Majidae
    Hyas lyratus (Dana, 1851)
    Majidae sp. Indeterminate
Family Pinnotheridae
    Pinnixa sp. Indeterminate

Phylum Echiura
    Order Echiuroinea
        Family Echiuridae
            Echiuris echiuris (Pallas, 1767)

Phylum Phoronida
    Family Phoronidae
        Phoronida sp. Indeterminate

Phylum Echinodermata
    Class Asteroidea
        Order Spinulosida
            Family Solasteridae
                Crossaster papposus (Linnaeus, 1767)
    Class Ophiuroidea
            Ophiuroidea sp. Indeterminate
        Order Dendrochirotida
            Family Cucumariidae
                Cucumaria sp. Indeterminate

Table I-2. Number of Individual Organisms Found in Sampled Collected from
Akutan Harbor in April 1992 (Stations 1 through 8A)

TAXON	Station								
	1	2	3	5	6	7	7A	8	8A
Polychaetes									
Ampharete acutifrons	0	0	0	0	0	0	0	0	0
Ampharete finmarchica	0	0	0	7	0	0	0	13	1
Ampharetidae sp. Indet.	2	2	1	4	0	0	0	1	0
Ampharetidae sp. Juv.	0	0	0	0	0	0	0	0	0
Amphicteis glabra	0	0	0	0	0	0	0	0	0
Apistobranchus tullbergi	0	0	0	0	0	0	0	0	0
Armandia brevis	0	2	0	0	0	0	0	0	0
Asabellides sibirica	2	0	0	0	0	0	0	0	1
Barantolla sp. A	0	0	0	0	0	0	0	0	1
Boccardia nr. polybranchia	22	0	0	49	4	3	0	4	1
Campesyllis sp.	0	0	0	0	0	0	0	0	0
Capitella capitata complex	27	32	8	32	33	4	0	7	69
Capitellidae sp. Indet.	0	0	0	0	0	0	0	0	0
Chaetozone setosa	0	0	0	1	0	0	0	0	0
Chone duneri	0	0	0	0	0	0	0	0	0
Cirratulidae sp. Indet.	0	2	0	0	0	0	0	3	0
Cossura sp. Indet.	1	0	0	0	1	0	0	0	0
Decamastus gracilis	0	0	0	0	0	0	0	0	0

Table I-2. Continued

TAXON	Station								
	1	2	3	5	6	7	7A	8	8A
Polychaetes, continued									
Dorvillea annulata	0	0	0	0	0	0	0	0	0
Dorvilleidae sp. Juv.	1	0	0	0	0	0	0	0	0
Ehlersia heterochaeta	0	0	0	0	0	0	0	0	7
Eteone californica	2	1	5	1	0	0	0	3	3
Euclymene reticulata	0	0	0	0	0	0	0	0	0
Euclymeninae sp. Indet.	6	0	0	9	0	0	0	7	0
Galathowenia oculata	0	0	0	0	0	0	0	2	0
Glycinde picta	8	0	0	2	0	3	0	4	5
Glyphanostomum nr. pallescens	59	0	74	38	1	0	0	20	20
Goniada maculata	0	0	0	0	0	0	0	0	0
Harmothoe imbricata	2	16	0	12	0	0	0	0	0
Heteromastus filobranchus	6	1	2	4	16	5	0	0	11
Lanassa sp. A	0	0	0	0	0	0	0	0	0
Leitoscoloplos pugettensis	3	0	0	2	2	1	3	41	2
Lumbrineris bicirrata	0	0	0	0	0	0	0	0	0
Lumbrineris luti	0	0	0	0	15	2	0	0	4
Lumbrineris sp. Indet.	95	6	10	141	41	20	0	116	37
Lysippe labiata	11	0	0	0	0	0	0	12	0

Table I-2. Continued

TAXON	Station								
	1	2	3	5	6	· 7	7A	8	8A
Polychaetes, continued									
Magelona longicornis	0	1	0	2	0	0	0	5	5
Maldanidae sp. Indet.	0	0	0	0	0	0	0	0	0
Mediomastus sp. Indet.	2	0	7	3	5	1	0	0	0
Melinna elisabethae	10	0	0	0	0	0	0	1	0
Neoamphitrite edwardsi	3	0	0	0	0	0	0	0	0
Nephtys caeca	0	0	0	1	0	0	0	0	0
Nephtys ferruginea	0	1	0	0	0	0	0	0	0
Nephtys punctata	0	0	0	0	0	0	0	0	0
Nephtys sp. Indet.	0	0	0	0	0	0	0	0	0
Nephtys sp. Juv.	0	0	0	0	1	0	0	0	0
Nereis nr. zonata	1	1	0	3	2	1	0	0	1
Notomastus lineatus	0	0	0	0	0	0	0	0	0
Onuphis sp. Juv.	0	0	0	0	0	0	0	0	0
Ophelina acuminata	0	0	0	0	0	0	0	0	0
Paraonidae sp. Indet.	0	0	0	0	0	0	0	0	0
Pectinaria granulata	0	0	0	0	0	0	0	8	0
Pholoe minuta	25	108	12	35	24	16	0	19	6
Phyllodoce citrina	1	0	1	0	0	0	0	1	2

Table I-2. Continued

TAXON	Station								
	1	2	3	5	6	7	7A	8	8A
Polychaetes, continued									
Phyllodoce groenlandica	8	0	2	5	0	4	0	20	1
Phyllodoce sp. Indet.	0	0	0	0	0	0	0	0	0
Pista cristata	0	0	0	0	0	0	0	0	0
Polydora brachycephala	15	6	1	0	0	0	0	0	0
Polydora socialis	0	0	0	0	0	0	0	0	0
Polydora sp. A	15	0	0	1	0	0	0	0	0
Polynoidae sp. A	1	0	0	0	0	0	0	0	0
Polynoidae sp. Indet.	0	0	0	1	0	0	0	0	0
Praxillella gracilis	0	0	0	0	0	0	0	0	0
Prionospio sp. Indet.	1	0	0	0	1	0	0	0	0
Prionospio steenstrupi	36	7	1	0	0	0	0	16	0
Rhodine bitorquata	0	0	0	0	0	0	0	0	0
Scalibregma inflatum	1	0	0	7	0	1	0	1	0
Sphaerodoropsis sphaerulifer	0	0	0	0	0	0	0	0	0
Spio cirrifera	1	0	0	6	7	0	0	0	0
Spionidae sp. Indet.	6	13	3	1	2	0	0	3	0
Spiophanes berkeleyorum	2	0	0	0	0	0	0	0	0
Syllis elongata	15	0	0	1	0	0	0	2	0

Table I-2. Continued

TAXON	Station								
	1	2	3	5	6	7	7A	8	8A
Polychaetes, continued									
Syllis sp. Indet.	0	0	0	0	7	1	0	0	2
Terebellidae sp. Indet.	1	0	2	0	0	0	0	0	0
Terebellides stroemi	0	0	0	0	0	0	0	0	0
Travisia forbesii	0	0	0	0	0	0	0	0	0
Bivalves									
Adontorhina cyclia	1	0	0	0	0	0	0	0	0
Alvania compacta	0	173	0	0	0	0	0	0	0
Axinopsida serricata	100	0	3	43	9	27	0	35	14
Bivalvia sp. Juv.	0	0	0	0	0	0	0	0	0
Clinocardium ciliatum	1	0	0	0	0	0	0	1	0
Cylichna attonsa	0	0	0	1	0	0	0	1	0
Hiatella arctica	0	2	0	0	0	0	0	0	0
Lacuna vincta	1	93	0	0	0	0	0	0	0
Lepeta concentrica	0	0	0	0	0	0	0	1	0
Littorina saxitilis	0	0	0	0	0	0	0	0	0
Macoma calcarea	35	7	2	26	2	3	0	13	3
Macoma carlottensis	0	0	0	0	0	0	0	0	0
Macoma moesta alaskana	0	0	0	0	0	0	0	0	1

Table I-2. Continued

TAXON	Station								
	1	2	3	5	6	7	7A	8	8A
Bivalves, continued									
Macoma sp. Juv.	3	0	0	2	0	0	0	0	0
Mallettia sp. Indet.	0	0	0	0	0	0	0	0	0
Musculus niger	0	0	0	0	0	0	0	0	0
Mya pseudoarenaria	0	1	0	0	0	0	0	0	0
Mya sp. Juv.	3	0	0	1	0	0	0	1	0
Mya uzensis	1	0	0	0	0	0	0	0	0
Mysella tumida	1	12	0	0	0	0	0	0	0
Mytilidae sp. Juv.	0	0	0	1	0	0	0	0	0
Natica clausa	0	0	0	0	0	0	0	0	0
Nitidella gouldi	2	0	0	4	0	0	0	1	0
Nucula tenuis	21	2	1	19	5	5	0	18	3
Nuculana minuta	0	0	0	1	0	0	0	0	1
Odostomia sp. Indet.	0	1	0	0	0	0	0	0	0
Oenopota harpularia	0	0	0	1	0	0	0	0	0
Oenopota elegans	0	0	0	0	0	0	0	2	0
Pododesmus macroschisma	0	1	0	0	0	0	0	0	0
Retusa sp. Indet.	0	0	0	0	0	0	0	0	0
Saxidomus giganteus	0	0	0	0	0	0	0	0	0

Table I-2. Continued

TAXON	Station								
	1	2	3	5	6	7	7A	8	8A
Bivalves, continued									
Serripes groenlandicus	1	0	0	0	0	0	0	3	0
Thyasira flexuosa	0	0	0	0	0	0	0	0	0
Turbonilla sp. Indet.	0	0	0	0	0	0	0	4	0
Yoldia hyperborea	0	0	0	0	0	1	0	0	0
Yoldia scissurata	0	0	0	0	0	0	0	0	0
Others									
Ampelisca agassizi	0	0	0	0	0	0	0	0	0
Ampelisca sp Indeterminate	0	0	0	0	0	0	0	0	0
Amphipoda sp. Indeterminate	0	0	0	0	0	0	1	0	0
Anonyx lilljeborgi	0	0	0	0	0	0	0	2	0
Aoridae sp. Indeterminate	0	0	0	0	0	0	0	0	0
Bathyleberis garthi	0	0	0	0	0	0	0	0	0
Calanoida sp. Indet.	2	0	0	0	0	0	0	0	0
Cirripedia sp. Indet.	0	1	0	0	1	0	0	0	0
Crossaster papposus	0	0	0	0	0	0	0	0	0
Cucumaria sp. Indet.	0	0	0	0	0	0	0	0	0
Cyclopoida sp. Indeterminate	0	0	0	0	0	0	0	0	0
Cylindroleberididae sp. Indet.	0	0	0	0	0	0	0	0	0

Table I-2. Continued

TAXON	Station								
	1	2	3	5	6	7	7A	8	8A
Others, continued									
Echiuris echiuris	0	10	0	0	0	0	0	0	0
Eualus sp. Indet.	0	2	0	0	0	0	0	0	0
Eudorella emarginata	0	0	0	1	0	0	0	2	0
Eyakia robusta	0	0	0	0	1	0	0	9	0
Foraminifera sp. Indet.	22	5	84	0	0	0	0	15	8
Hyas lyratus	0	0	0	1	0	0	0	1	0
Leucon sp. Indet.	0	1	0	0	0	0	0	0	0
Limnoria lignorum	0	1	0	0	0	0	0	0	0
Majidae sp. Indeterminate	0	0	0	0	0	0	0	1	0
Monoculodes sp. Indeterminate	0	0	0	0	1	0	0	1	0
Monoculodes zernovi	0	0	0	0	0	0	0	0	0
Nematoda sp. Indet.	73	454	3	3	58	0	0	3	62
Nemertinea sp. Indet.	23	0	3	11	9	6	1	24	8
Oligochaeta sp. Indet.	0	0	0	0	0	0	0	0	0
Ophiuroidea sp. Indet.	2	1	0	2	0	0	0	15	1
Philomedidae sp. Indeterminate	0	0	0	0	0	0	0	1	0
Phoronida sp. Indet.	0	0	0	0	0	0	0	0	0
Pinnixa sp. Indeterminate	0	0	0	0	0	0	0	0	0

Table I-2. Continued

TAXON	Station								
	1	2	3	5	6	7	7A	8	8A
Others, continued									
Priapulus caudatus	1	0	0	0	2	1	0	3	0
Proboloides holmesi	0	0	0	0	0	0	0	0	0
Uristidae sp. Indeterminate	0	0	0	0	0	0	0	0	1

Table I-3. Number of Individual Organisms Found in Sampled Collected from
Akutan Harbor in April 1992 (Stations 9 through PO2)

Taxon	Station								
	9	10	10A	11	12	13	BPO	PO1	PO2
Polychaetes									
Ampharete acutifrons	1	0	0	0	0	0	0	0	0
Ampharete finmarchica	1	3	5	0	14	8	2	0	0
Ampharetidae sp. Indet.	5	2	1	0	0	1	0	0	0
Ampharetidae sp. Juv.	0	0	0	1	0	0	0	0	0
Amphicteis glabra	1	3	1	0	0	0	0	0	0
Apistobranchus tullbergi	0	0	1	0	2	0	0	0	0
Armandia brevis	0	0	1	1	0	0	1	0	0
Asabellides sibirica	0	0	0	0	0	0	1	5	0
Barantolla sp. A	0	0	0	0	0	0	0	0	0
Boccardia nr. polybranchia	0	6	29	1	16	6	12	0	0
Campesyllis sp.	0	0	0	0	0	0	0	1	0
Capitella capitata complex	12	0	3	0	1	0	4	5	0
Capitellidae sp. Indet.	0	0	0	0	0	1	0	1	0
Chaetozone setosa	0	0	0	3	0	0	3	0	0
Chone duneri	0	0	0	0	0	0	1	0	0
Cirratulidae sp. Indet.	4	1	0	0	0	3	0	1	0
Cossura sp. Indet.	0	0	0	0	0	0	0	0	0
Decamastus gracilis	0	0	0	0	0	0	1	0	0

Table I-3. Continued

Taxon	Station								
	9	10	10A	11	12	13	BPO	PO1	PO2
Polychaetes, continued									
Dorvillea annulata	0	0	0	0	0	0	0	1	0
Dorvilleidae sp. Juv.	0	0	0	0	0	0	0	0	0
Ehlersia heterochaeta	0	2	0	0	0	0	1	3	0
Eteone californica	0	0	2	0	1	1	0	3	0
Euclymene reticulata	0	5	0	0	0	0	0	0	0
Euclymeninae sp. Indet.	0	0	13	2	12	10	0	9	0
Galathowenia oculata	0	0	1	0	0	0	0	0	0
Glycinde picta	24	3	8	11	21	13	13	8	0
Glyphanostomum nr. pallescens	2	6	14	1	11	17	1	105	0
Goniada maculata	0	0	0	0	2	0	0	0	0
Harmothoe imbricata	0	1	0	2	1	0	6	4	3
Heteromastus filobranchus	2	1	0	6	0	6	0	12	0
Lanassa sp. A	0	2	1	0	4	0	1	1	0
Leitoscoloplos pugettensis	10	14	12	6	16	0	16	2	0
Lumbrineris bicirrata	0	0	0	0	0	0	1	0	0
Lumbrineris luti	20	0	0	0	21	0	9	0	0
Lumbrineris sp. Indet.	0	159	80	54	118	156	28	91	0
Lysippe labiata	0	0	7	3	22	0	0	3	0

Table I-3. Continued

Taxon	Station								
	9	10	10A	11	12	13	BPO	PO1	PO2
Polychaetes, continued									
Magelona longicornis	2	3	20	4	15	5	2	0	0
Maldanidae sp. Indet.	2	3	0	0	0	0	0	1	0
Mediomastus sp. Indet.	1	0	0	0	0	0	1	1	0
Melinna elisabethae	0	0	0	0	1	0	1	1	0
Neoamphitrite edwardsi	0	0	0	0	0	0	2	0	0
Nephtys caeca	0	0	0	1	0	0	0	0	0
Nephtys ferruginea	1	0	0	0	1	0	0	0	0
Nephtys punctata	0	0	0	0	0	1	0	0	0
Nephtys sp. Indet.	0	0	0	0	0	1	0	0	0
Nephtys sp. Juv.	0	0	0	0	0	0	0	0	0
Nereis nr. zonata	2	11	3	5	5	10	0	0	0
Notomastus lineatus	0	0	5	0	8	0	0	0	0
Onuphis sp. Juv.	0	0	0	0	1	0	0	0	0
Ophelina acuminata	1	0	0	0	2	0	0	0	0
Paraonidae sp. Indet.	0	0	1	1	0	0	0	0	0
Pectinaria granulata	0	0	0	0	0	0	0	0	0
Pholoe minuta	14	14	12	24	47	37	17	48	0
Phyllodoce citrina	4	1	1	1	0	0	0	3	0

Table I-3. Continued

Taxon	Station								
	9	10	10A	11	12	13	BPO	PO1	PO2
Polychaetes, continued									
Phyllodoce groenlandica	11	1	5	9	24	5	0	13	0
Phyllodoce sp. Indet.	0	0	0	2	0	0	0	0	0
Pista cristata	0	0	0	0	2	0	0	0	0
Polydora brachycephala	1	6	2	0	1	0	0	0	0
Polydora socialis	0	0	0	0	2	0	0	2	0
Polydora sp. A	0	0	0	0	0	0	1	0	0
Polynoidae sp. A	0	0	0	0	0	0	0	0	0
Polynoidae sp. Indet.	2	0	1	0	0	0	0	4	0
Praxillella gracilis	0	1	1	0	4	0	0	0	0
Prionospio sp. Indet.	0	0	0	0	0	0	2	0	0
Prionospio steenstrupi	0	0	0	0	12	0	93	1	0
Rhodine bitorquata	0	0	1	0	5	0	0	0	0
Scalibregma inflatum	7	4	0	6	1	2	2	0	0
Sphaerodoropsis sphaerulifer	0	4	0	0	2	7	0	4	0
Spio cirrifera	3	0	2	1	2	0	1	0	0
Spionidae sp. Indet.	1	0	1	2	0	4	0	0	0
Spiophanes berkeleyorum	0	0	2	2	0	0	0	2	0
Syllis elongata	0	0	13	0	8	3	1	3	0

Table I-3. Continued

Taxon	Station								
	9	10	10A	11	12	13	BPO	PO1	PO2
Polychaetes, continued									
Syllis sp. Indet.	0	0	0	0	0	0	0	1	0
Terebellidae sp. Indet.	0	0	0	0	1	0	0	0	0
Terebellides stroemi	0	2	0	0	0	4	0	0	0
Travisia forbesii	0	0	2	0	6	0	0	0	0
Bivalves									
Adontorhina cyclia	0	0	2	0	38	1	0	0	0
Alvania compacta	0	0	0	0	1	2	0	0	0
Axinopsida serricata	27	55	136	73	276	113	13	102	0
Bivalvia sp. Juv.	0	0	0	0	0	8	0	0	0
Clinocardium ciliatum	1	0	0	1	2	0	0	1	0
Cylichna attonsa	1	0	0	0	0	0	0	8	0
Hiatella arctica	0	0	1	1	2	2	0	0	0
Lacuna vincta	0	0	0	0	0	0	0	0	0
Lepeta concentrica	0	0	0	0	0	0	0	0	0
Littorina saxitilis	0	0	1	0	0	0	0	0	0
Macoma calcarea	1	4	3	3	6	4	6	21	0
Macoma carlottensis	1	0	1	0	0	0	0	0	0
Macoma moesta alaskana	0	0	1	0	1	1	0	0	0

Table I-3. Continued

Taxon	Station								
	9	10	10A	11	12	13	BPO	PO1	PO2
Bivalves, continued									
Macoma sp. Juv.	5	0	3	8	0	3	0	2	0
Mallettia sp. Indet.	0	0	0	0	0	0	0	1	0
Musculus niger	0	0	0	0	1	0	0	0	0
Mya pseudoarenaria	0	0	0	0	0	0	0	0	0
Mya sp. Juv.	0	0	0	0	0	0	1	1	0
Mya uzensis	0	0	0	0	2	0	0	0	0
Mysella tumida	0	0	0	0	0	0	3	0	0
Mytilidae sp. Juv.	0	0	0	0	0	0	0	0	0
Natica clausa	0	0	0	0	0	0	0	0	1
Nitidella gouldi	0	0	0	0	0	0	0	0	0
Nucula tenuis	18	24	19	10	35	95	0	15	1
Nuculana minuta	1	18	2	3	6	38	0	1	0
Odostomia sp. Indet.	0	0	0	0	1	5	0	0	0
Oenopota harpularia	0	0	1	0	1	0	0	0	0
Oenopota elegans	0	0	0	0	0	0	0	0	0
Pododesmus macroschisma	0	0	0	0	0	0	0	0	0
Retusa sp. Indet.	0	0	0	2	1	4	0	0	0
Saxidomus giganteus	0	0	0	0	4	0	0	0	0

Table I-3. Continued

Taxon	Station								
	9	10	10A	11	12	13	BPO	PO1	PO2
Bivalves, continued									
Serripes groenlandicus	0	1	0	1	0	3	3	1	0
Thyasira flexuosa	0	0	1	0	1	0	0	0	0
Turbonilla sp. Indet.	0	0	3	0	1	3	0	0	0
Yoldia hyperborea	1	0	1	0	1	6	0	2	0
Yoldia scissurata	0	0	0	0	0	2	0	0	0
Others									
Ampelisca agassizi	0	0	0	0	3	0	0	0	0
Ampelisca sp Indeterminate	0	0	0	0	3	0	0	0	0
Amphipoda sp. Indeterminate	0	0	0	0	0	0	0	0	0
Anonyx lilljeborgi	0	0	1	0	1	0	0	0	0
Aoridae sp. Indeterminate	0	0	1	0	2	2	0	0	0
Bathyleberis garthi	0	0	0	0	4	0	0	0	0
Calanoida sp. Indet.	0	0	0	0	0	0	0	0	0
Cirripedia sp. Indet.	0	0	0	0	0	0	0	0	0
Crossaster papposus	0	0	0	0	1	0	0	0	0
Cucumaria sp. Indet.	0	0	0	2	0	0	0	0	0
Cyclopoida sp. Indeterminate	0	2	0	0	0	0	0	0	0
Cylindroleberididae sp. Indet.	0	0	0	1	0	2	0	0	0

I-23

Table I-3. Continued

Taxon	Station								
	9	10	10A	11	12	13	BPO	PO1	PO2
Other, continued									
Echiuris echiuris	0	0	0	0	0	0	0	0	0
Eualus sp. Indet.	0	0	0	0	0	0	0	0	0
Eudorella emarginata	0	0	2	2	3	2	0	0	0
Eyakia robusta	0	0	0	1	3	1	1	0	0
Foraminifera sp. Indet.	0	2	12	11	6	5	67	12	0
Hyas lyratus	0	0	0	0	0	0	0	0	0
Leucon sp. Indet.	0	0	0	0	0	0	0	0	0
Limnoria lignorum	0	0	0	0	0	0	0	0	0
Majidae sp. Indeterminate	0	0	0	0	0	0	0	0	0
Monoculodes sp. Indeterminate	0	0	0	2	0	0	0	1	0
Monoculodes zernovi	3	1	0	2	0	4	0	0	0
Nematoda sp. Indet.	2	7	20	8	37	47	8	10	0
Nemertinea sp. Indet.	3	10	18	1	6	1	19	33	0
Oligochaeta sp. Indet.	0	0	0	0	0	0	1	0	0
Ophiuroidea sp. Indet.	0	4	0	0	0	4	2	1	0
Philomedidae sp. Indeterminate	0	0	0	0	0	0	0	0	0
Phoronida sp. Indet.	0	0	0	0	1	0	0	1	0
Pinnixa sp. Indeterminate	0	1	0	0	0	0	0	0	0

Table I-3. Continued

Taxon	Station								
	9	10	10A	11	12	13	BPO	PO1	PO2
Other, continued									
Priapulus caudatus	1	1	0	0	0	0	0	4	0
Proboloides holmesi	0	0	1	0	0	0	0	0	0
Uristidae sp. Indeterminate	0	0	0	0	0	0	0	0	0

Appendix J. Underwater Video Information

LOG OF REMOTELY OPERATED VEHICLE
VIDEOTAPED OBSERVATIONS

The following is a summary log of videotaped observations made during ROV surveys of Akutan Harbor, April 11 to 13, 1992. It describes transect locations, timing, and depths. This log is intended to be used with a VHS format videotape, 140 min long. The tape was prepared from 340 min of raw 8 mm tape by editing and removing elements not directly related to the bottom survey, such as clear water views of descents and ascents, or footage obscured by thruster propeller turbulence.

ROV-1

- Location: Outer Harbor, south shore. Suspected site of crab or fish waste piles. Depth, 160 ft.

- Coordinates: Miniranger - chain: 2,381; offset: 1,677.

- April 11, 1651 hrs (ADT) at beginning of transect.

- Start of tape, 17 min long.

This transect was located near the outside of the harbor, near the south shore, at a depth ranging from 159 to 161 ft. A preliminary analysis of the SSS printouts showed this site had an uneven topography, indicating possible deposition of crab or fish processing wastes.

The bottom terrain was hummocky, sometimes with rolling features, 6 in to 2 ft high. Sediments were fine, silty sand. A layer of suspended particles hung 2 to 4 ft over the bottom. This turbid layer appeared to be due to bottom currents in the area, because particles were swept by the stationary ROV. There was a small amount of litter along this transect including aluminum cans and a cardboard box. Crab processing debris was either absent or very sparse, with occasional scattered whole dead crabs (or crab molts).

The parchment or paper-like burrows of tube worms (probably *Glyphanostomum*) were moderately abundant. Densities ranged from 20 to 50 burrows per square foot. An aeolid nudibranch was also common, mainly in association with tube worms, with densities of up to 5 per square foot.

Larger invertebrate and fish fauna were uncommon. They included sea anemones (*Metridium* and possibly *Anthopleura*), one flatfish, a small greenling, and the large *Pycnopodia* starfish (about 10 in wide).

Aside from widely scattered debris, there was no evidence of crab and fish waste. This site shows little or no impact due to fish processing in the harbor.

ROV-2

● Location: Inner Harbor, north shore. At the old Trident Seafoods outfall. Depth, 150 ft.

● Coordinates: Miniranger - chain: 7,222; offset: -534.

● April 11, 1844 hrs at beginning of transect.

● 17 min into tape, 9-1/2 min long.

This transect was located near the old Trident Seafoods outfall on the north shore of the inner harbor at a depth of 150 ft.

There was no mounding or topographic relief and the entire bottom appeared to be covered with fish waste. The surface layer was very soft, and a leadline placed on the bottom to guide the ROV was buried about 1 in into the fish waste. The waste had a jelly-like to stringy consistency and appeared to be covered with a thin layer of bacteria (probably *Beggiatoa*). The bottom was easily disturbed and bubbles of gas (probably methane and/or hydrogen sulfide) rose from the surface when it was disturbed by the ROV. There was little near bottom turbidity, and no current-induced motion of suspended particles was seen in relation to the ROV.

No benthic infauna was visible. Animal life only occurred on rocks or debris that rose above bottom. For example, large debris (i.e., a 5 gal can, anchor, and crab pot) were colonized with the large white anemone *Metridium senile*. No fish waste had collected on the cans, rocks, etc., possibly indicating a low rate of deposition or consistent sweeping of this area by water currents.

The benthic community in this area has been eliminated by the deposition of fish processing wastes. Water quality (at least dissolved oxygen), however, immediately above the intact waste pile does not appear to be significantly impacted.

ROV-3

● Location: Inner Harbor, south shore. Deep Sea Fisheries anchorage area, bottom and crab waste north of vessel. Depth, 83 ft.

● April 12, 1107 hrs at beginning of transect.

● 27-1/2 min into tape, 13 min long.

This station was located on the south shore of the inner harbor in the M/V Deep Sea anchorage area at a depth of 80 to 90 ft. The bottom and crab waste pile immediately north of the M/V Deep Sea and TNT barge were surveyed.

The bottom north of the TNT barge was very uneven and composed of a mix of fine sediments and miscellaneous fishing-related debris, such as tires, old traps, cable, etc. Huge numbers of the sea anemone *Metridium senile* were attached to the bottom or onto any of the available hard surfaces. These grew in a wide range of sizes and formed up to a 25 to 50% cover in some areas near the barge. Colonies of finely branching hydroids and bryozoans were also common here.

Farther to the east, north of the M/V Deep Sea, and at a depth of 80 ft, the ROV was over the crab pile. Crab waste was coarsely ground and formed a mounded layer. Anemones grew on the surface of the crab waste pile, but were not as abundant as seen off the TNT. Anemone coverage was 1 to 5% of the total bottom cover.

Crab waste and debris disposal have eliminated most of the soft-bottom benthic community. Opportunistic filter-feeding organisms (such as anemones) have been enhanced, particularly in areas set off from the main areas of crab waste deposition.

ROV-4

- Location: Inner Harbor, south shore. Deep Sea Fisheries anchorage area, bottom on south side of vessel. Depth, 80 to 90 ft.

- April 12, 1246 hrs at beginning of transect.

- 40-1/2 min into tape, 13-1/2 min long.

This transect was in the same general location as ROV-3, surveying the bottom beneath and south of the M/V Deep Sea. There was a high turbidity layer 2 to 4 ft above the bottom, and bubbles were seen rising from the crab waste pile. The water depth at the crab pile was 90 ft.

The survey continued at a water depth of 79 ft south of the M/V Deep Sea. The bottom was smooth and anemones (*Metridium*) were growing on any solid surfaces that rose above the bottom. Mysid shrimp (molts or dead animals) formed a 1 to 2 in layer over much of the bottom. Only larger sections of crab carapaces and legs were seen.

Shrimp and crab waste cover was largely absent south of the M/V Deep Sea's freshwater pipeline (at 84 ft deep). At a water depth of 73 ft, bottom sediments shifted from predominantly fine grained materials to a mix of fines and small cobbles. There was a dense, but patchy, cover by tubes of the polychaete *Glyphanostomum* (hundreds per square foot). *Metridium* and the starfish *Pycnopodia* were also common.

Site conditions varied widely on this transect. The area near the M/V Deep Sea was a settling environment as suggested by large numbers of mysid shrimp molts. This area was also heavily impacted by crab waste. Habitat conditions near shore were unaffected by waste deposition, but high densities of polychaete worms indicated nutrient enrichment was occurring.

ROV-5

- Location: Inner Harbor, south shore. Proposed site of Deep Sea Fisheries outfall. Depth, 110 to 20 ft.

- Coordinates: Satellite - 54° 7.01' N, 165° 48.57' W; Miniranger - chain: 10,846; offset: 1,115.

- April 12, 1414 hrs at beginning of transect.

- 54 min into tape, 21 min long.

Located on the south shore of the inner harbor, this transect surveyed the proposed site of the Deep Sea Fisheries outfall and areas near the abandoned whaling station.

The transect began at a water depth of 110 ft, 400 to 500 ft offshore from the whaling station, and continued toward the southern shore of the harbor.

Fine silty sediments dominated the bottom cover, along with a great deal of shell debris and drift algae. There were thick patches of tube worms, bryozoans, and occasional live mysid shrimp and starfish. Tube worm density was slightly lower than the coverage seen south of the M/V Deep Sea. Anemones (densities about 1 per m^2) were attached directly to the bottom or to rocks on the bottom.

Large rocks and debris cover (i.e., cable, pipe, old pots) increased toward the south at depths above 100 ft. Shell debris also became more common. At a water depth of 57 ft the bottom had become very rocky with anemones, bryozoans, and hydroids attached to anything elevated above the bottom. *Alaria* and other algae were common. Some were probably attached, but most seemed to be drift algae.

The bottom was very irregular and massive amounts of large debris (crab pots, large pipe, etc.) were seen at a water depth of 40 ft. This material was colonized with anemones, but at much lower densities than on ROV-3 and ROV-4. The sunflower seastar *Pycnopodia helianthoides* was also common.

Above 40 ft to a depth of 10 ft (the shallowest depth surveyed), bottom sediments appeared to consist of mixed sand, gravel, and large cobble, along with occasional metal debris. Clam and mussel shell debris and large gravel dominated the sediment mix in some areas, while other locations on the transect had more large rock and cobble cover.

Attached algae were common and in some areas covered up to 25% of the bottom. They were dominated by *Ulva, Alaria*, and *Laminaria*. Also seen were starfish, blennies or pricklebacks, and sculpins. Anemones were much less abundant than at lower elevations.

This transect offered a good cross section of the biological communities in the harbor, from deeper bottoms to the shallow subtidal. With the exception of the metal waste and other remnants of the whaling station, this area appeared to show no effects from fish and crab processing.

ROV-6

- Location: Inner Harbor, north shore. Trident Seafoods old outfall. Depth, 150 ft. Repeat of transect 2.

- April 12, 1515 hrs at beginning of transect.

- 1 hr 15 min into tape, 16 min long.

This transect began immediately north of ROV-2 in about 150 ft of water. Conditions at the beginning of the transect were similar to ROV-2; however, the waste layer changed dramatically as the machine swam north. The rather uniform bacteria-covered surface of the waste pile began to take on a pockmarked or mottled appearance. The leadline was never located, and it was apparently buried and covered by the waste material. Pools of a grayish liquid or semi-liquid substance filled the depressions. These pools were 6 in to a foot in diameter, and some were interconnected. When one of the pools was disturbed by the ROV, a density difference could be observed between the material in the pool and surrounding water. The water above the waste pile was clear, with none of the particle motion such as seen on ROV-1. The surface was more compact and less easily disturbed by the ROV, and the material raised from the bottom was stringy and plastic. No large invertebrate or fish organisms were seen.

This portion of the harbor floor is highly altered from natural conditions and supports no benthic fauna. The waste pile appears to be a slowly decomposing but long-term feature of the bottom landscape.

ROV-7

- Location: Inner Harbor, north shore. M/V Clipperton crab pile on north side of vessel and bottom areas on south side of vessel. Depth, 118 ft.

- Coordinates: Satellite - 54° 7.80' N, 165° 48.79' W; Miniranger - chain: 11,647; offset: 61.

- April 12, 1755 hrs at beginning of transect.

- 1 hr 31 min into tape, 22 min long.

Two separate transect lines were run in the middle of the inner harbor north and south of the M/V Clipperton at a water depth of 118 ft. North of the M/V Clipperton the bottom was covered with ground crab waste (and a surprising number of rubber bands). The bottom was easily disturbed by the ROV, but there was very little turbidity and the water was clear. All the crab waste was well ground.

There were no tube worms or other similar bottom fauna, and no anemones. Amphipods were abundant; up to 20 were seen in some scenes. This condition continued farther east on the crab pile, where some larger waste (whole carapaces and legs) was seen.

South of the M/V Clipperton, there was a scattered and light cover of crab waste, mostly consisting of carapace and leg portions (along with more rubber bands). Crab waste made up less than 5% of the total bottom cover, and there was no evidence of ground crab shell. Sediments were fine grained and silty, and formed into low hummocks. Patches of the bacteria *Beggiatoa* occurred infrequently. Tube worm density (probably *Glyphanostomum*) was high, although the density was less than half that seen at the M/V Deep Sea transect (ROV-4). Farther from the M/V Clipperton, tube worm burrow height and density increased; however, coverage was patchy. Amphipods were common, and in some instances densities were similar to those seen on the crab waste pile north of the M/V Clipperton. Other animal life included a small nudibranch (probably an aeolid), seen on many of the worm tubes, and anemones.

The M/V Clipperton crab waste discharge has had a substantial impact on the bottom fauna north of the vessel, but little obvious effect to the south.

ROV-8

- Location: Outer Harbor, midchannel. Open water area, lightly impacted by crab or fish waste. Depth, 150 ft.

- Coordinates: Satellite - 54° 7.65' N, 165° 46.34' W.

- April 13, 0950 hrs at beginning of transect.

- 1 hr 53 min into tape, 8-1/2 min long.

This transect was located in a central harbor area due south of the Akutan community center at a depth of 150 to 158 ft. It was intended to survey the bottom outside the major zone of influence of the shore-based processors, but in an area used by ship-based processors.

Many features of this transect were similar to ROV-1. Bottom sediments appeared to be fine silts with mounds up to 1 ft in height dominating the topography. Wave-like patterns were also visible. These waves were 2 to 6 in high, and paralleled a line angled at approximately 330° north (magnetic). There was a slight to moderate quantity of unground whole crab waste. Much of this waste was surrounded by patches of the surface-dwelling bacterium *Beggiatoa*, with bacterial coverage generally less than 1% of the total bottom cover.

Tube worm burrows were very common, although the tubes were shorter than at the Deep Sea outfall. The distribution was patchy and similar to that at ROV-1 and ROV-5. Thick patches of tube worms were encountered, colonized with numerous nudibranchs. Other macrofauna included amphipods, unidentified smaller zooplankton, and the anemone *Metridium*.

Approximately half of the bottom area covered by the ROV appeared to be directly impacted by bacteria and shell waste.

ROV-9

- Location: Inner Harbor, north shore. Moving from dock toward Trident Seafoods' new outfall. Depth, 72 to 110 ft.

- April 13, 1026 hrs at beginning of transect.

- 2 hr 1-1/2 min into tape, 14-1/2 min long.

This transect began in 72 ft of water and 150 ft west of the Trident Seafoods dock. It followed the new outfall line to the discharge port at 110 ft. The line was not discharging during the survey. A layer of screened fish or crab waste covered 100% of the bottom except where large debris or the pipeline was elevated above the surface. The waste was piled up level with the outfall pipe (8 to 10 in deep). All of the waste appeared to be lighter and more easily disturbed than the material seen in ROV-2 and ROV-6, and fine particles were suspended in the water. Great numbers of red oligochaete worms occurred in loose aggregations 2 to 8 inches in diameter, and small numbers of amphipods were also seen.

Trident Seafoods' crab and fish waste deposits have eliminated the soft-bottom benthos; however, this area still supports some biota in the form of oligochaete worms.

ROV-10

- Location: Inner Harbor, north shore. Trident Seafoods old outfall. 200 ft south of transect 9. Depth, 133 ft.

- April 13, 1046 hrs at beginning of transect.

- 2 hr 16 min into tape, 4 min long.

This transect began about 200 ft south of ROV-9 at a depth of 133 ft. Waste deposits covered 100% of the bottom and appeared to be older and thicker than the material seen in ROV-9. The bottom features ranged from the conditions seen in ROV-9 to the decomposed conditions of ROV-6. There were occasional oligochaete worm masses, grading to entirely abiotic materials on the southern extent of this transect.

Appendix K.   Results of Plume Modeling

Table K-1. UM Model Input and Output for the Maximum-Rated Capacity,
Winter Discharge Scenario

Model Parameters

tot flow	# ports	port flow	spacing	effl sal	effl temp	far inc	far dis
0.4294	1	0.4294	1000	37.32	0	50	1000
port dep	port dia	plume dia	total vel	horiz vel	vertl vel	asp coeff	print frq
24.4	0.3048	0.3048	5.885	0.000	5.885	0.10	50
port elev	ver angle	cont coef	effl den	poll conc	decay	Froude #	Roberts F
6.1	90	1	30.00	439	0	-40.35	0.001365
hor angle	red space	p amb den	p current	far dif	far vel	K:vel/cur	Stratif #
90	1000.0	22.67	0.05120	0.000453	0.05	114.9	-0.0003707
depth	current	density	salinity	temp	amb conc	N (freq)	red grav.
0	0.1	22.45	28.85	8.2	0	0.009245	-0.06978
25	0.05	22.68	29.1	8	0	buoy flux	puff-ther
30	0.05	22.68	29.1	8	0	-0.02996	16.09
30						jet-plume	jet-cross
						11.58	31.05
						plu-cross	jet-strat
						223.3	13.11
						plu-strat	
						13.95	
						hor dis>=	

Initial Dilution Calculations

plume dep	plume dia	effl sal	poll conc	dilution	hor dis
m	m	o/oo			m
24.40	0.3048	37.32	439.0	1.000	0.000
24.08	0.4302	34.91	310.4	1.417	0.0005847
23.64	0.6092	33.21	219.5	2.007	0.003397
23.00	0.8634	32.00	155.2	2.841	0.01144
22.11	1.225	31.14	109.8	4.021	0.03124
20.83	1.744	30.53	77.61	5.690	0.07713
19.02	2.500	30.10	54.88	8.050	0.1816
16.48	3.640	29.79	38.80	11.39	0.4178
13.37	5.473	29.55	27.44	16.11	0.9075
10.48	8.654	29.38	19.40	22.78	1.753
9.745	10.39	29.33	16.89	26.17	2.116

< plume element overlap.

Farfield Calculations

Farfield dispersion based on wastefield width of   10.39m

conc	dilution	conc	dilution	distance m	sec	hrs
10.17	43.4	12.79	34.5	50.00	957.7	0.3
5.909	74.5	9.890	44.6	100.0	1958	0.5
3.960	111.0	8.329	52.9	150.0	2958	0.8
2.887	152.2	7.327	60.1	200.0	3958	1.1
2.225	197.5	6.614	66.6	250.0	4958	1.4
1.782	246.5	6.075	72.4	300.0	5958	1.7
1.469	299.1	5.650	77.9	350.0	6958	1.9
1.238	354.9	5.303	83.0	400.0	7958	2.2
1.061	413.8	5.012	87.8	450.0	8958	2.5
0.9227	476.0	4.765	92.3	500.0	9958	2.8
0.8122	540.7	4.551	96.6	550.0	10960	3.0
0.7221	608.1	4.364	100.8	600.0	11960	3.3
0.6476	678.1	4.198	104.8	650.0	12960	3.6
0.5850	750.6	4.049	108.6	700.0	13960	3.9
0.5319	825.5	3.915	112.3	750.0	14960	4.2
0.4864	902.8	3.794	115.9	800.0	15960	4.4
0.4470	982.3	3.683	119.4	850.0	16960	4.7
0.4126	1064.1	3.581	122.8	900.0	17960	5.0
0.3825	1148.0	3.488	126.1	950.0	18960	5.3
0.3558	1233.9	3.401	129.3	1000	19960	5.5

Column group headers: --4/3 Power Law-- (conc, dilution); -Const Eddy Diff- (conc, dilution); distance; Time (sec, hrs)

Table K-2. UM Model Input and Output for the Maximum Estimated Production, Winter Discharge Scenario

Model Parameters

tot flow	# ports	port flow	spacing	effl sal	effl temp	far inc	far dis
0.4677	1	0.4677	1000	37.32	0	50	1000
port dep	port dia	plume dia	total vel	horiz vel	vertl vel	asp coeff	print frq
24.4	0.3048	0.3048	6.410	0.000	6.410	0.10	50
port elev	ver angle	cont coef	effl den	poll conc	decay	Froude #	Roberts F
6.1	90	1	30.00	439	0	-43.95	0.001253
hor angle	red space	p amb den	p current	far dif	far vel	K:vel/cur	Stratif #
90	1000.0	22.67	0.05120	0.000453	0.05	125.2	-0.0003707
depth	current	density	salinity	temp	amb conc	N (freq)	red grav.
0	0.1	22.45	28.85	8.2	0	0.009245	-0.06978
25	0.05	22.68	29.1	8	0	buoy flux	puff-ther
30	0.05	22.68	29.1	8	0	-0.03264	17.52
30						jet-plume	jet-cross
						12.61	33.82
						plu-cross	jet-strat.
						243.2	13.68
						plu-strat	
						14.26	
						hor dis>=	

Initial Dilution Calculations

plume dep	plume dia	effl sal	poll conc	dilution	hor dis
m	m	o/oo			m
24.40	0.3048	37.32	439.0	1.000	0.000
24.08	0.4301	34.91	310.4	1.417	0.0005367
23.64	0.6091	33.21	219.5	2.007	0.003118
23.00	0.8630	32.00	155.2	2.841	0.01049
22.11	1.224	31.14	109.8	4.021	0.02864
20.84	1.741	30.53	77.61	5.690	0.07060
19.03	2.490	30.10	54.88	8.050	0.1657
16.47	3.607	29.79	38.80	11.39	0.3812
13.22	5.369	29.55	27.44	16.11	0.8364
9.948	8.380	29.38	19.40	22.78	1.668
8.590	11.13	29.30	15.65	28.25	2.281

< plume element overlap.

Farfield Calculations

Farfield dispersion based on wastefield width of   11.13m

	--4/3 Power Law--		-Const Eddy Diff-			
conc	dilution	conc	dilution	distance	Time	
				m	sec	hrs
9.708	45.4	12.03	36.7	50.00	954.4	0.3
5.711	77.1	9.339	47.2	100.0	1954	0.5
3.851	114.2	7.875	55.9	150.0	2954	0.8
2.819	155.9	6.932	63.5	200.0	3954	1.1
2.178	201.7	6.261	70.3	250.0	4954	1.4
1.748	251.4	5.752	76.5	300.0	5954	1.7
1.443	304.5	5.351	82.2	350.0	6954	1.9
1.217	360.9	5.023	87.6	400.0	7954	2.2
1.045	420.5	4.748	92.7	450.0	8954	2.5
0.9093	483.0	4.514	97.5	500.0	9954	2.8
0.8005	548.6	4.311	102.0	550.0	10950	3.0
0.7121	616.7	4.134	106.4	600.0	11950	3.3
0.6389	687.3	3.977	110.6	650.0	12950	3.6
0.5774	760.5	3.837	114.6	700.0	13950	3.9
0.5252	836.1	3.710	118.5	750.0	14950	4.2
0.4804	914.1	3.595	122.3	800.0	15950	4.4
0.4416	994.3	3.490	126.0	850.0	16950	4.7
0.4078	1076.8	3.394	129.5	900.0	17950	5.0
0.3780	1161.4	3.305	133.0	950.0	18950	5.3
0.3518	1248.2	3.223	136.4	1000	19950	5.5

Table K-3. UM Model Input and Output for the Maximum Rated Capacity,
Summer Discharge Scenario

Model Parameters

tot flow	# ports	port flow	spacing	effl sal	effl temp	far inc	far dis
0.2085	1	0.2085	1000	37.32	0	50	1000
port dep	port dia	plume dia	total vel	horiz vel	vertl vel	asp coeff	print frq
24.4	0.3048	0.3048	2.858	0.000	2.858	0.10	50
port elev	ver angle	cont coef	effl den	poll conc	decay	Froude #	Roberts F
6.1	90	1	30.00	814	0	-19.59	0.002812
hor angle	red space	p amb den	p current	far dif	far vel	K:vel/cur	Stratif #
90	1000.0	22.67	0.05120	0.000453	0.05	55.81	-0.0003707
depth	current	density	salinity	temp	amb conc	N (freq)	red grav.
0	0.1	22.45	28.85	8.2	0	0.009245	-0.06978
25	0.05	22.68	29.1	8	0	buoy flux	puff-ther
30	0.05	22.68	29.1	8	0	-0.01455	7.811
30						jet-plume	jet-cross
						5.622	15.08
						plu-cross	jet-strat
						108.4	9.137
						plu-strat	
						11.65	
						hor dis>=	

Initial Dilution Calculations

plume dep	plume dia	effl sal	poll conc	dilution	hor dis
m	m	o/oo			m
24.40	0.3048	37.32	814.0	1.000	0.000
24.08	0.4307	34.91	575.6	1.417	0.001207
23.63	0.6115	33.21	407.0	2.007	0.007042
23.00	0.8711	32.00	287.8	2.841	0.02391
22.09	1.250	31.14	203.5	4.021	0.06642
20.80	1.823	30.53	143.9	5.690	0.1689
19.15	2.760	30.10	101.8	8.050	0.3967
17.51	4.485	29.79	71.95	11.39	0.8273
17.11	5.434	29.69	63.07	12.99	1.011

< plume element overlap.

Farfield Calculations

Farfield dispersion based on wastefield width of .   5.434m

conc	dilution	conc	dilution	distance	Time	
		--4/3 Power Law--		-Const Eddy Diff-		
				m	sec	hrs
27.52	29.7	40.85	20.0	50.00	979.8	0.3
14.32	56.9	30.70	26.6	100.0	1980	0.5
9.100,	89.5	25.59	31.9	150.0	2980	0.8
6.426	126.8	22.39	36.4	200.0	3980	1.1
4.846	168.1	20.15	40.5	250.0	4980	1.4
3.822	213.1	18.47	44.1	300.0	5980	1.7
3.112	261.7	17.15	47.5	350.0	6980	1.9
2.599	313.3	16.08	50.7	400.0	7980	2.2
2.212	368.0	15.19	53.7	450.0	8980	2.5
1.913	425.6	14.43	56.5	500.0	9980	2.8
1.676	485.8	13.77	59.2	550.0	10980	3.0
1.484	548.7	13.20	61.8	600.0	11980	3.3
1.326	614.1	12.69	64.2	650.0	12980	3.6
1.194	681.8	12.24	66.6	700.0	13980	3.9
1.083	751.9	11.83	68.9	750.0	14980	4.2
0.9876	824.3	11.46	71.1	800.0	15980	4.4
0.9057	898.8	11.12	73.3	850.0	16980	4.7
0.8345	975.5	10.81	75.4	900.0	17980	5.0
0.7722	1054.2	10.53	77.4	950.0	18980	5.3
0.7173	1134.9	10.27	79.4	1000	19980	5.5

Table K-4. UM Model Input and Output for the Maximum Estimated Production,
Summer Discharge Scenario

Model Parameters

tot flow	# ports	port flow	spacing	effl sal	effl temp	far inc	far dis
0.2615	1	0.2615	1000	37.32	0	50	1000
port dep	port dia	plume dia	total vel	horiz vel	vertl vel	asp coeff	print frq
24.4	0.3048	0.3048	3.584	0.000	3.584	0.10	50
port elev	ver angle	cont coef	effl den	poll conc	decay	Froude #	Roberts F
6.1	90	1	30.00	814	0	-24.57	0.002242
hor angle	red space	p amb den	p current	far dif	far vel	K:vel/cur	Stratif #
90	1000.0	22.67	0.05120	0.000453	0.05	70.00	-0.0003707
depth	current	density	salinity	temp	amb conc	N (freq)	red grav.
0	0.1	22.45	28.85	8.2	0	0.009245	-0.06978
25	0.05	22.68	29.1	8	0	buoy flux	puff-ther
30	0.05	22.68	29.1	8	0	-0.01825	9.796
30						jet-plume	jet-cross
						7.051	18.91
						plu-cross	jet-strat
						136.0	10.23
						plu-strat	
						12.33	
						hor dis>=	

Initial Dilution Calculations

plume dep	plume dia	effl sal	poll conc	dilution	hor dis
m	m	o/oo			m
24.40	0.3048	37.32	814.0	1.000	0.000
24.08	0.4304	34.91	575.6	1.417	0.0009612
23.64	0.6104	33.21	407.0	2.007	0.005597
23.00	0.8673	32.00	287.8	2.841	0.01893
22.10	1.238	31.14	203.5	4.021	0.05215
20.81	1.783	30.53	143.9	5.690	0.1311
19.03	2.626	30.10	101.8	8.050	0.3125
16.93	4.052	29.79	71.95	11.39	0.6904
15.27	6.615	29.56	50.88	16.11	1.279
15.25	6.678	29.55	50.52	16.22	1.290

< plume element overlap.

Farfield Calculations

Farfield dispersion based on wastefield width of   6.678m

	--4/3 Power Law--		-Const	Eddy Diff-		
conc	dilution	conc	dilution	distance	Time	
				m	sec	hrs
24.61	33.2	34.47	23.7	50.00	974.2	0.3
13.25	61.5	26.12	31.3	100.0	1974	0.5
8.551	95.3	21.83	37.4	150.0	2974	0.8
6.097	133.6	19.13	42.7	200.0	3974	1.1
4.627	176.0	17.23	47.3	250.0	4974	1.4
3.665	222.2	15.81	51.6	300.0	5974	1.7
2.996	271.8	14.68	55.6	350.0	6974	1.9
2.507	324.8	13.77	59.2	400.0	7974	2.2
2.139	380.7	13.01	62.7	450.0	8974	2.5
1.852	439.5	12.36	66.0	500.0	9974	2.8
1.625	501.1	11.80	69.1	550.0	10970	3.0
1.440	565.3	11.31	72.1	600.0	11970	3.3
1.288	632.0	10.88	75.0	650.0	12970	3.6
1.161	701.1	10.49	77.7	700.0	13970	3.9
1.054	772.6	10.14	80.4	750.0	14970	4.2
0.9619	846.4	9.823	83.0	800.0	15970	4.4
0.8826	922.4	9.534	85.5	850.0	16970	4.7
0.8137	1000.5	9.269	87.9	900.0	17970	5.0
0.7533	1080.7	9.026	90.3	950.0	18970	5.3
0.7000	1163.0	8.800	92.6	1000	19970	5.5

Appendix L.   Results of Dispersion Modeling
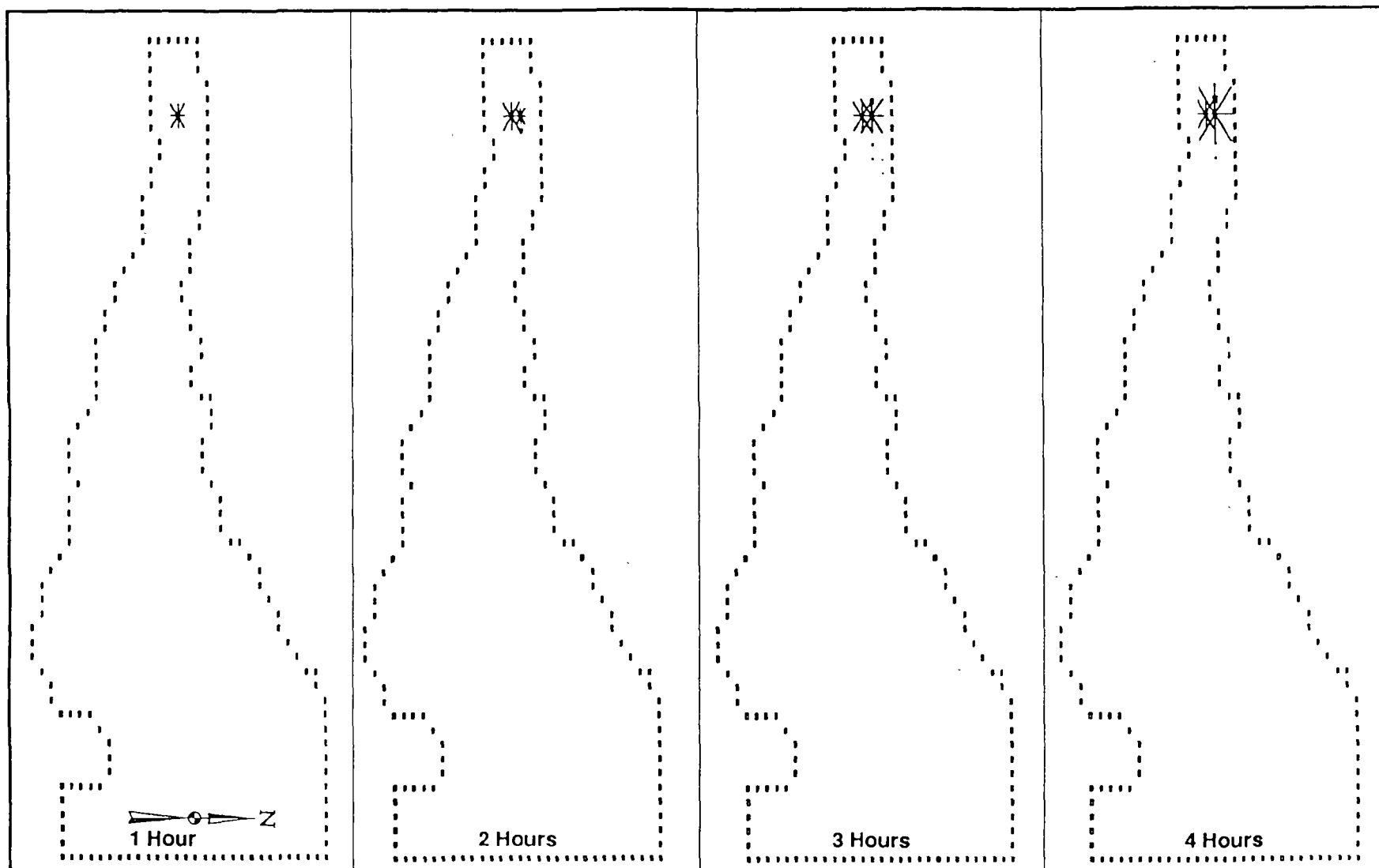
1 Hour   2 Hours   3 Hours   4 Hours
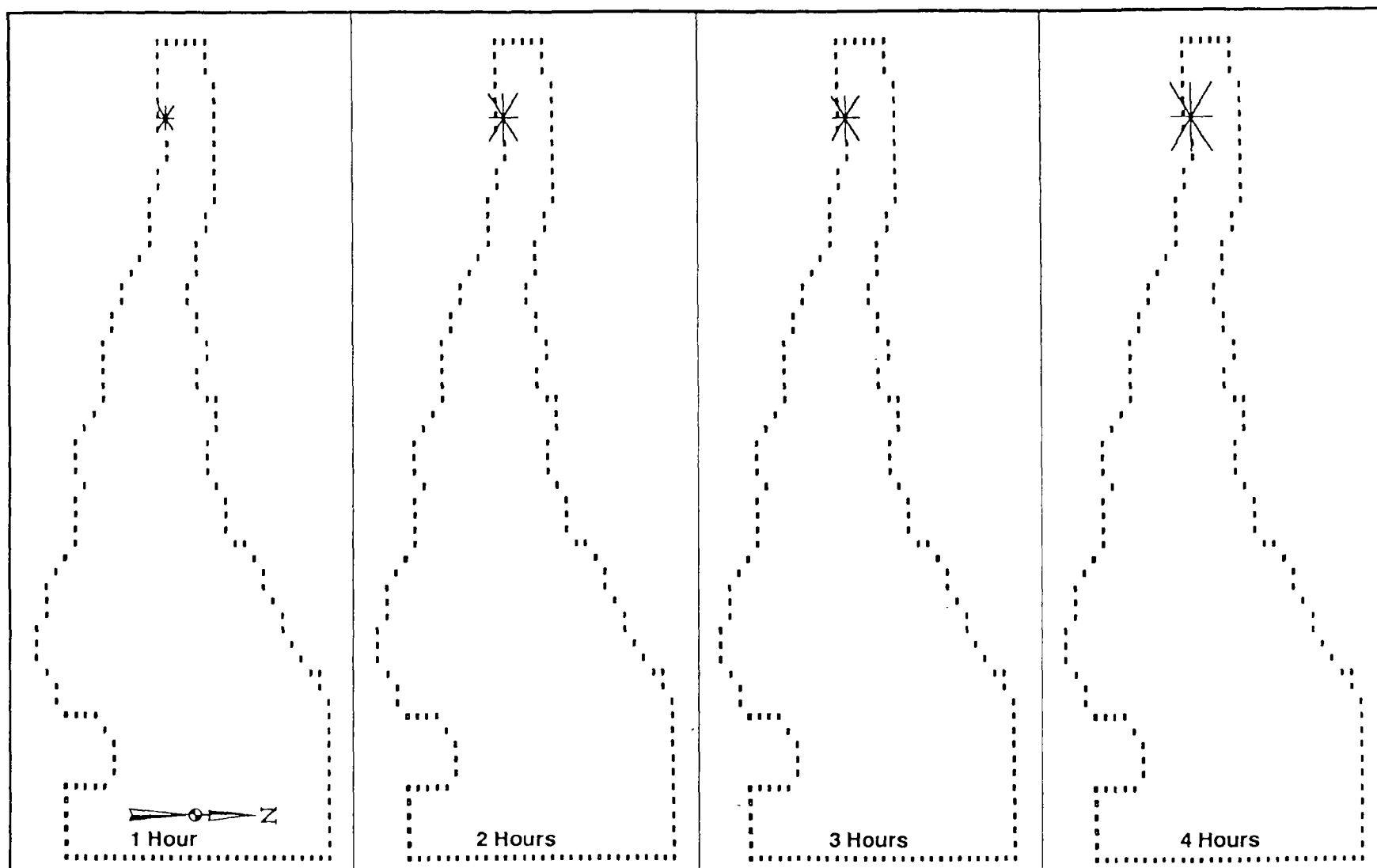
Note: 0.5 inch = 40,000 trace units

Figure L-1. Simulated Dispersion of Effluent from the Proposed Outfall Site During a 4-Hour, 20 m/s West Wind Event
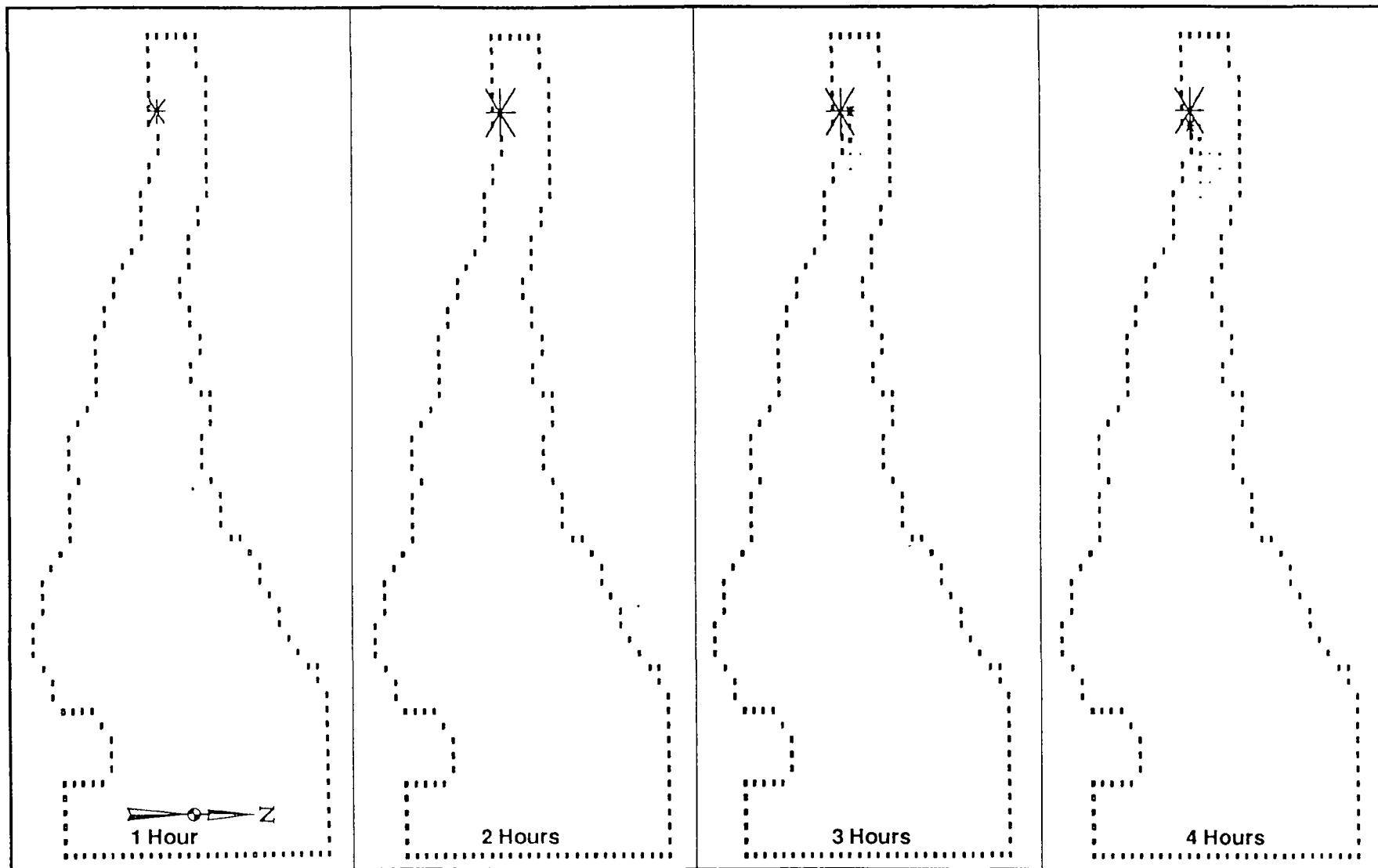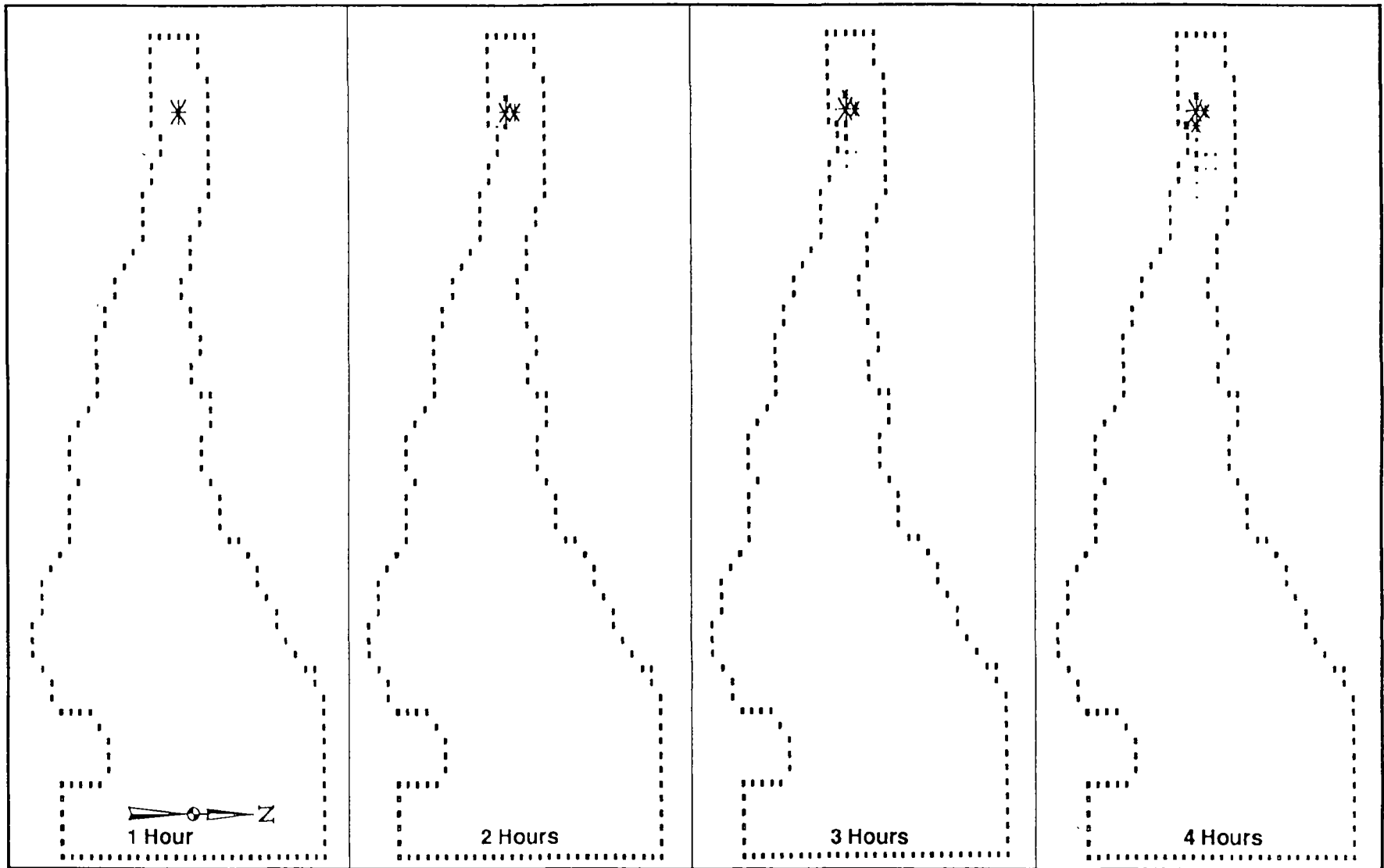
Note: 0.5 Inch = 40,000 trace units

Figure L-2. Simulated Dispersion of Effluent from the Proposed Outfall Site During a 4-Hour, 20 m/s East Wind Event

Note: 0.5 Inch = 40,000 trace units

Figure L-3. Simulated Dispersion of Effluent from Alternative Outfall Site 1 During a 4-Hour, 20 m/s West Wind Event

Note: 0.5 inch = 40,000 trace units

Figure L-4. Simulated Dispersion of Effluent from Alternative Outfall Site 1 During a 4-Hour, 20 m/s East Wind Event
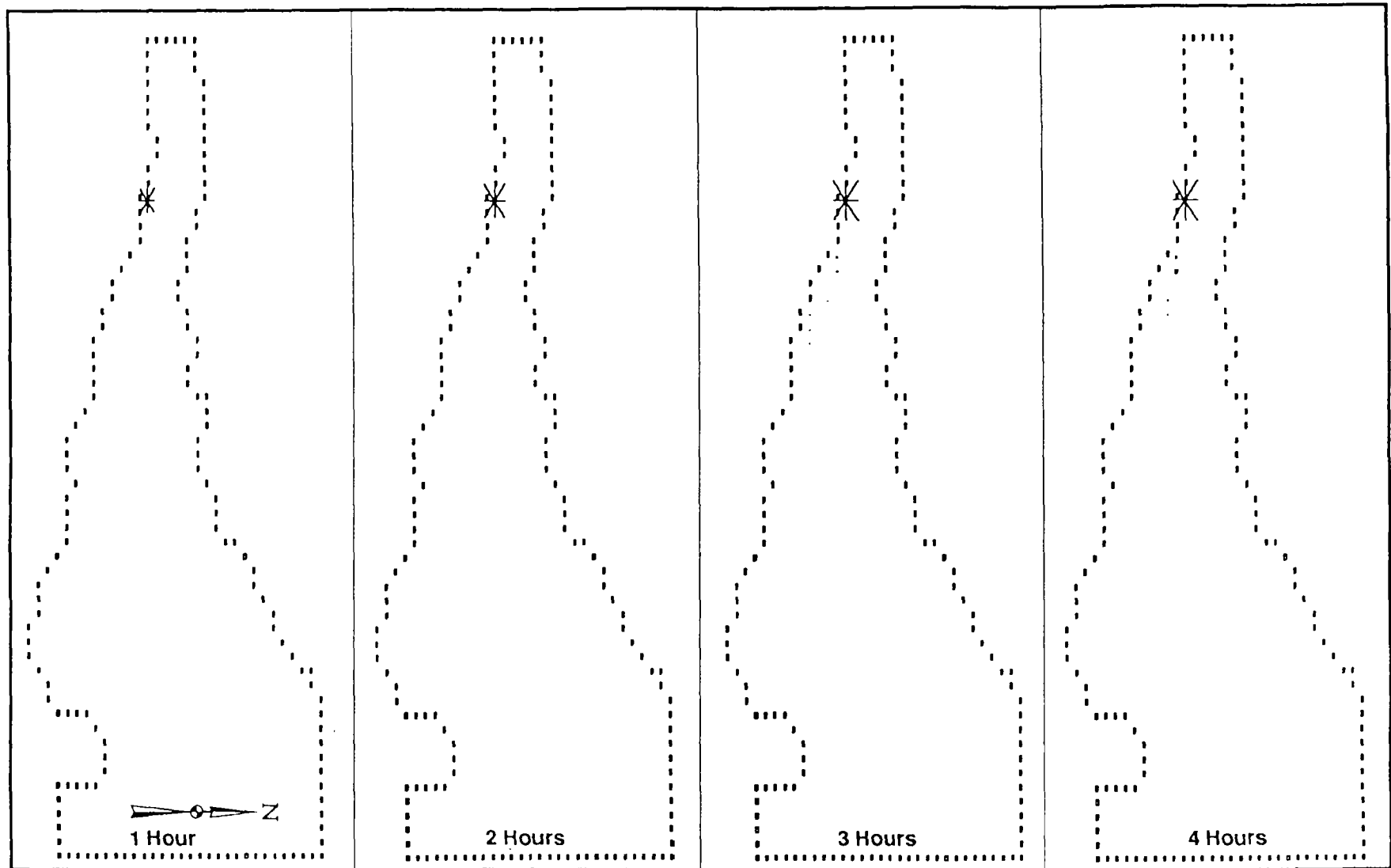
Note: 0.5 inch = 40,000 trace units

Figure L-5. Simulated Dispersion of Effluent from Alternative Outfall Site 2 During a 4-Hour, 20 m/s West Wind Event

Note: 0.5 Inch = 40,000 trace units

Figure L-6. Simulated Dispersion of Effluent from Alternative Outfall Site 2 During a 4-Hour, 20 m/s East Wind Event

Note: 0.5 Inch = 40,000 trace units

Figure L-7. Simulated Dispersion of Effluent from Alternative Outfall Site 3 During a 4-Hour, 20 m/s West Wind Event
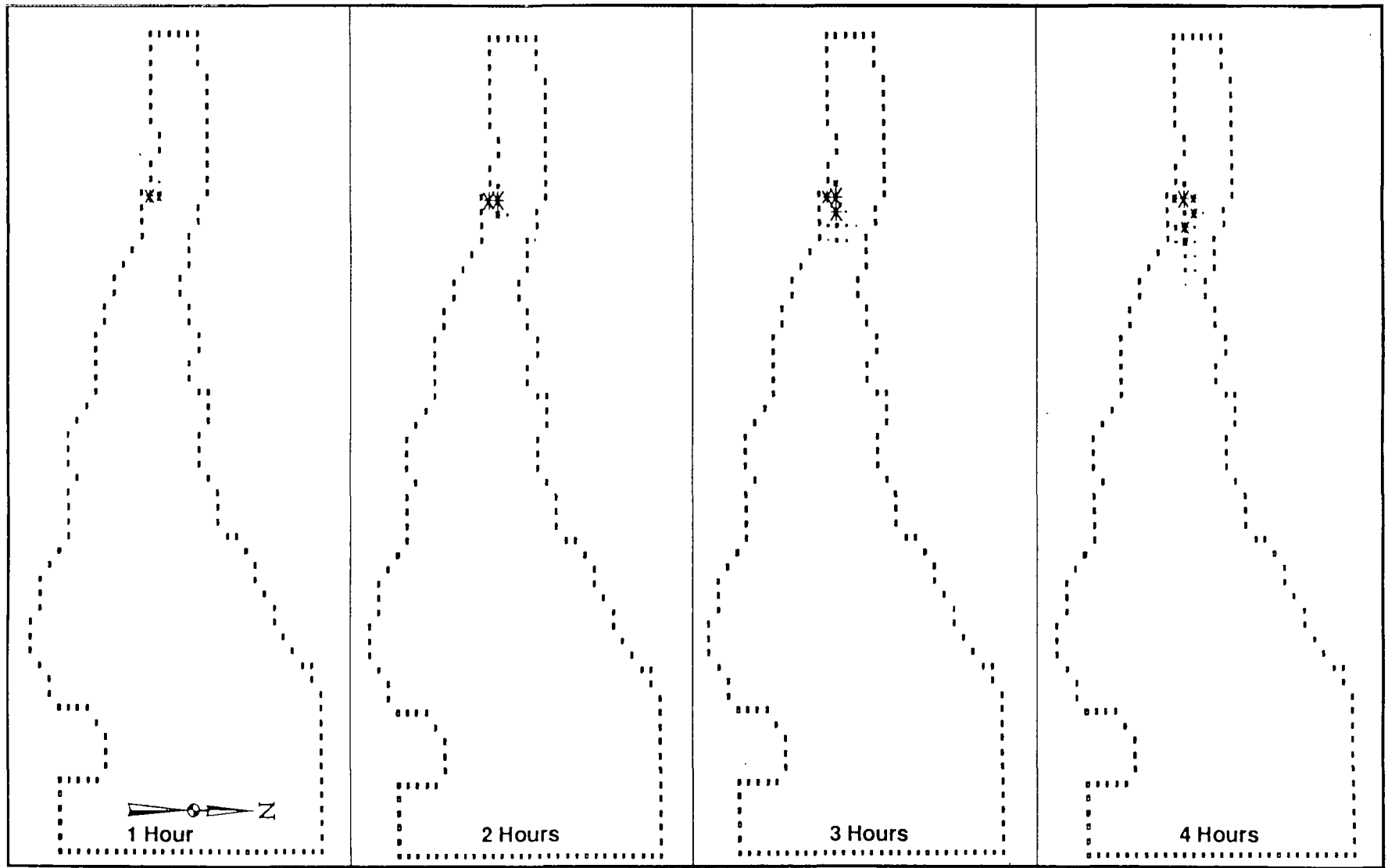
L-8
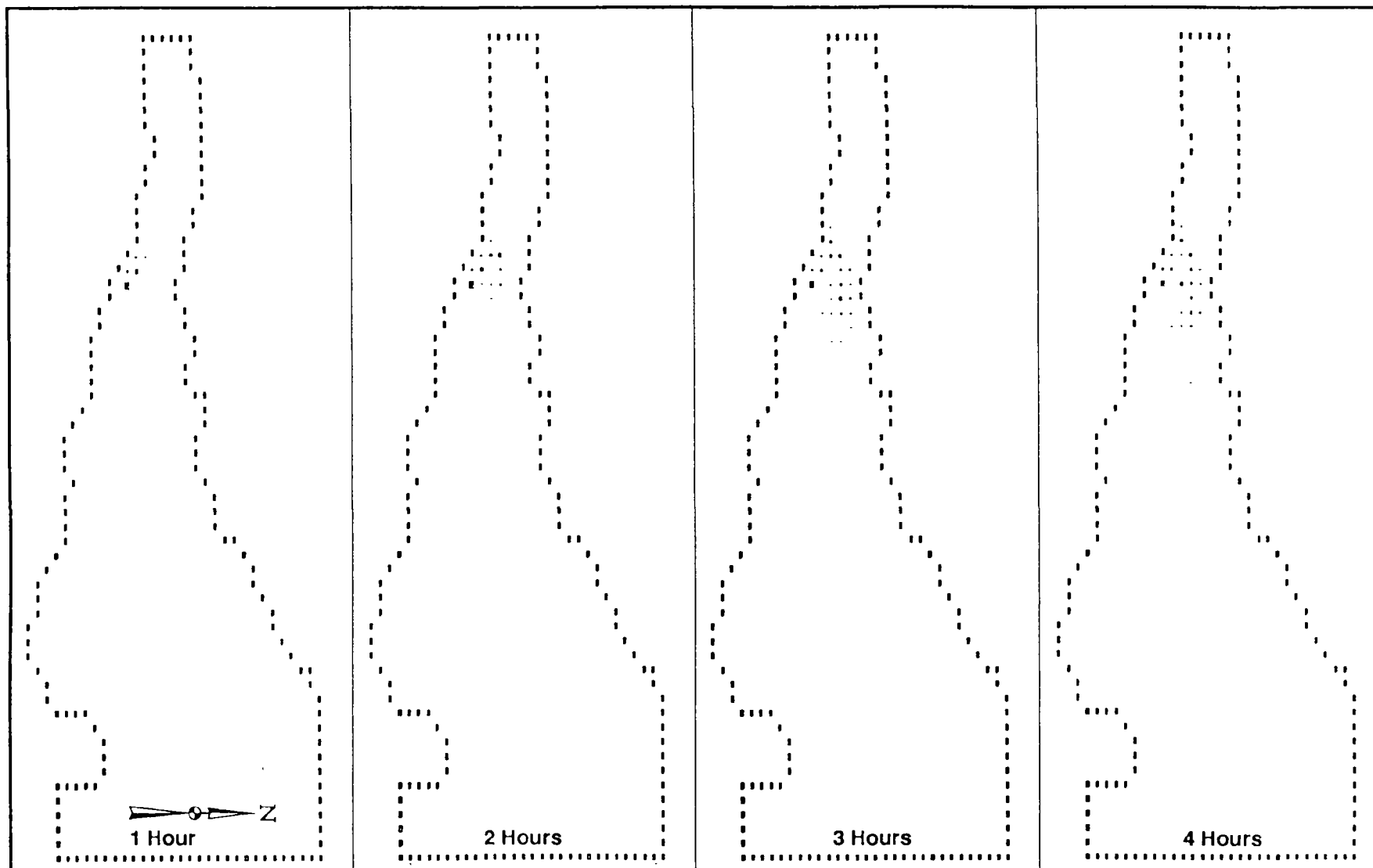
Note: 0.5 inch = 40,000 trace units

Figure L-8. Simulated Dispersion of Effluent from Alternative Outfall Site 3 During a 4-Hour, 20 m/s East Wind Event
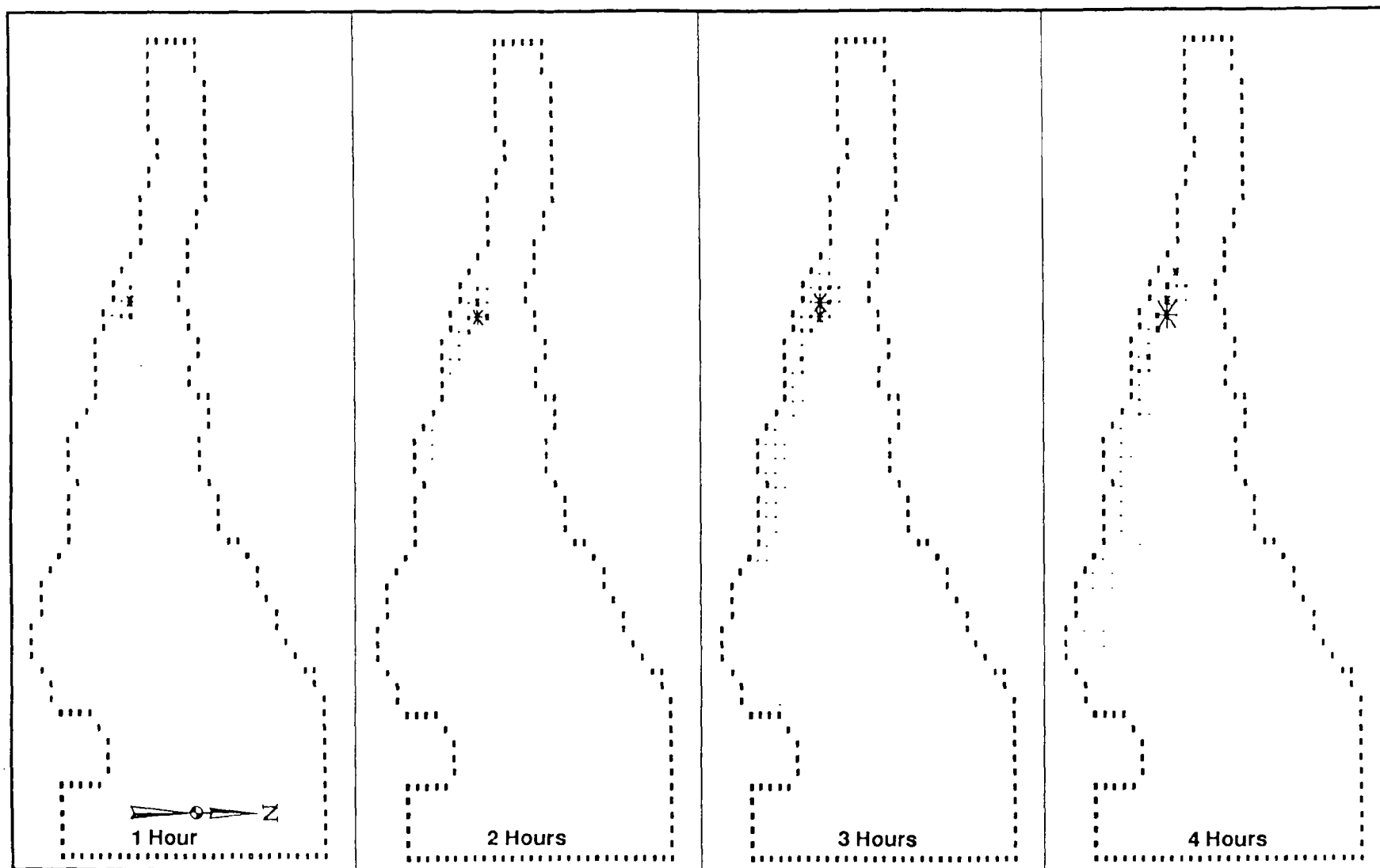
Figure L-9. Simulated Dispersion of Effluent from the Proposed Outfall Site during a 32-Hour, 5 m/s West Wind

Figure L-10. Simulated Dispersion of Effluent from the Proposed Outfall Site during a 32-Hour, 5 m/s East Wind
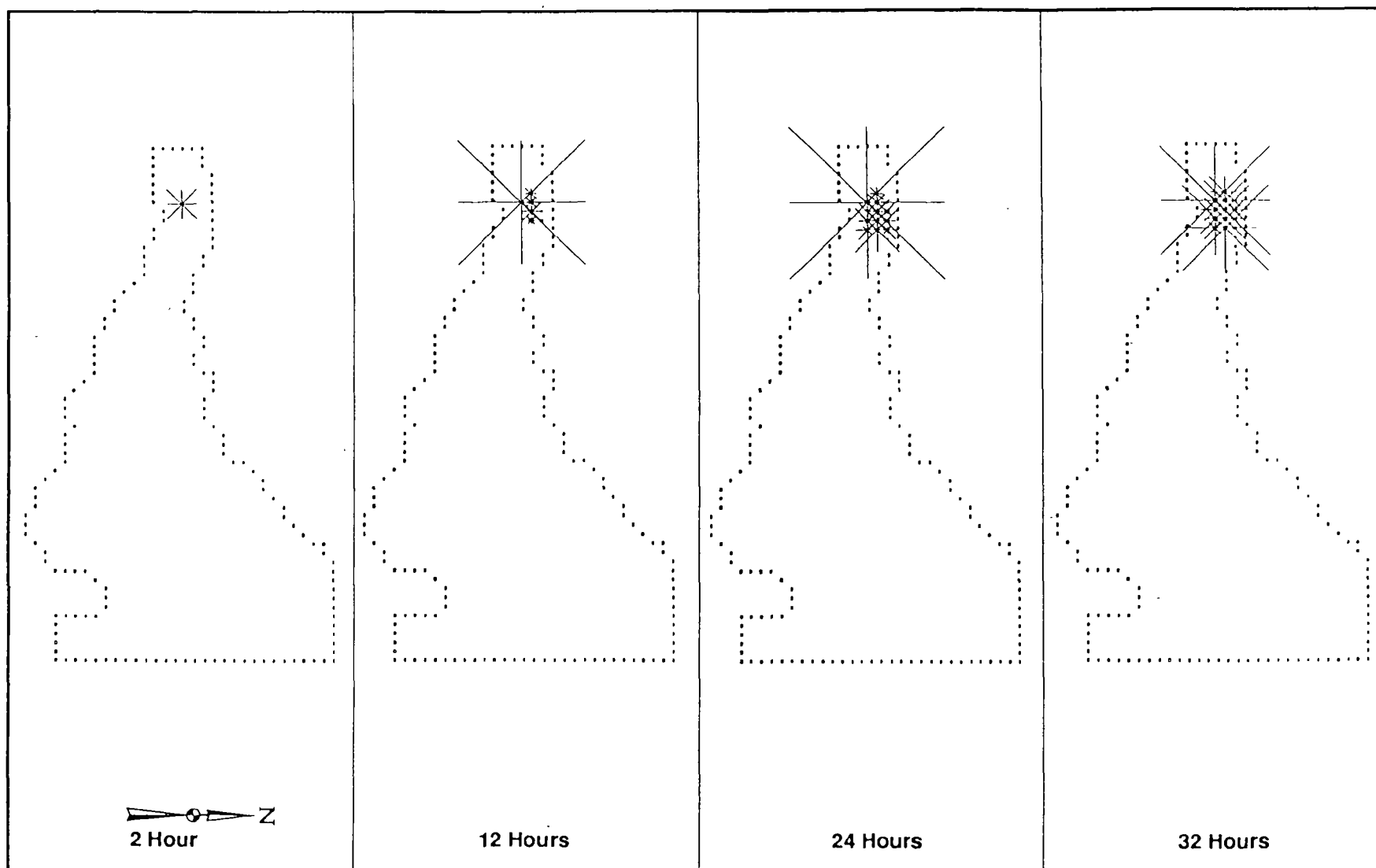
Figure L-11. Simulated Dispersion of Effluent from Alternative Outfall Site A-1 during a 32-Hour, 5 m/s West Wind
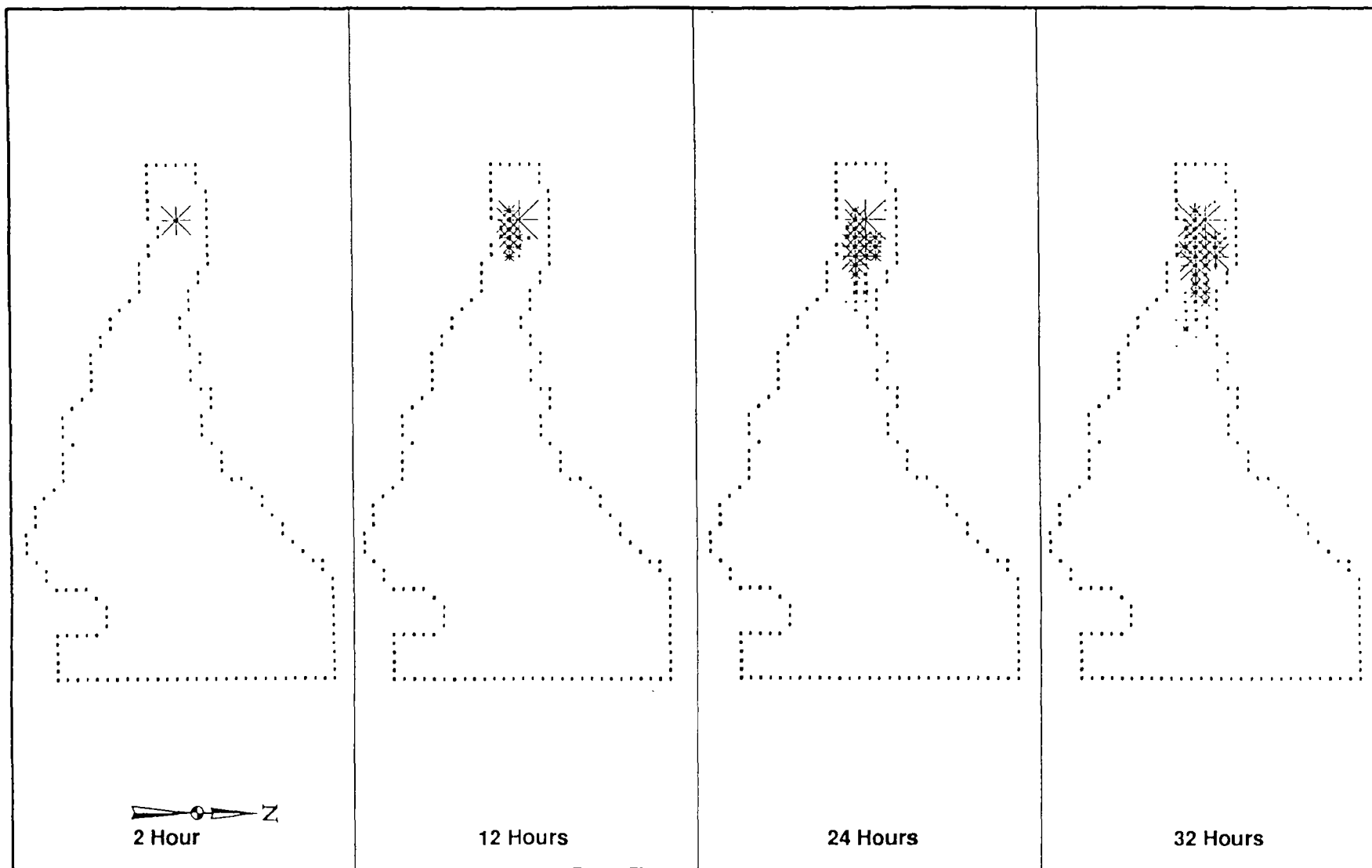
Figure L-12. Simulated Dispersion of Effluent from Alternative Outfall Site A-1 during a 32-Hour, 5 m/s East Wind

2 Hour

12 Hours

24 Hours

32 Hours

Figure L-13. Simulated Dispersion of Effluent from Alternative Outfall Site A-2 during a 32-Hour, 5 m/s West Wind

Figure L-14. Simulated Dispersion of Effluent from Alternative Outfall Site A-2 during a 32-Hour, 5 m/s East Wind
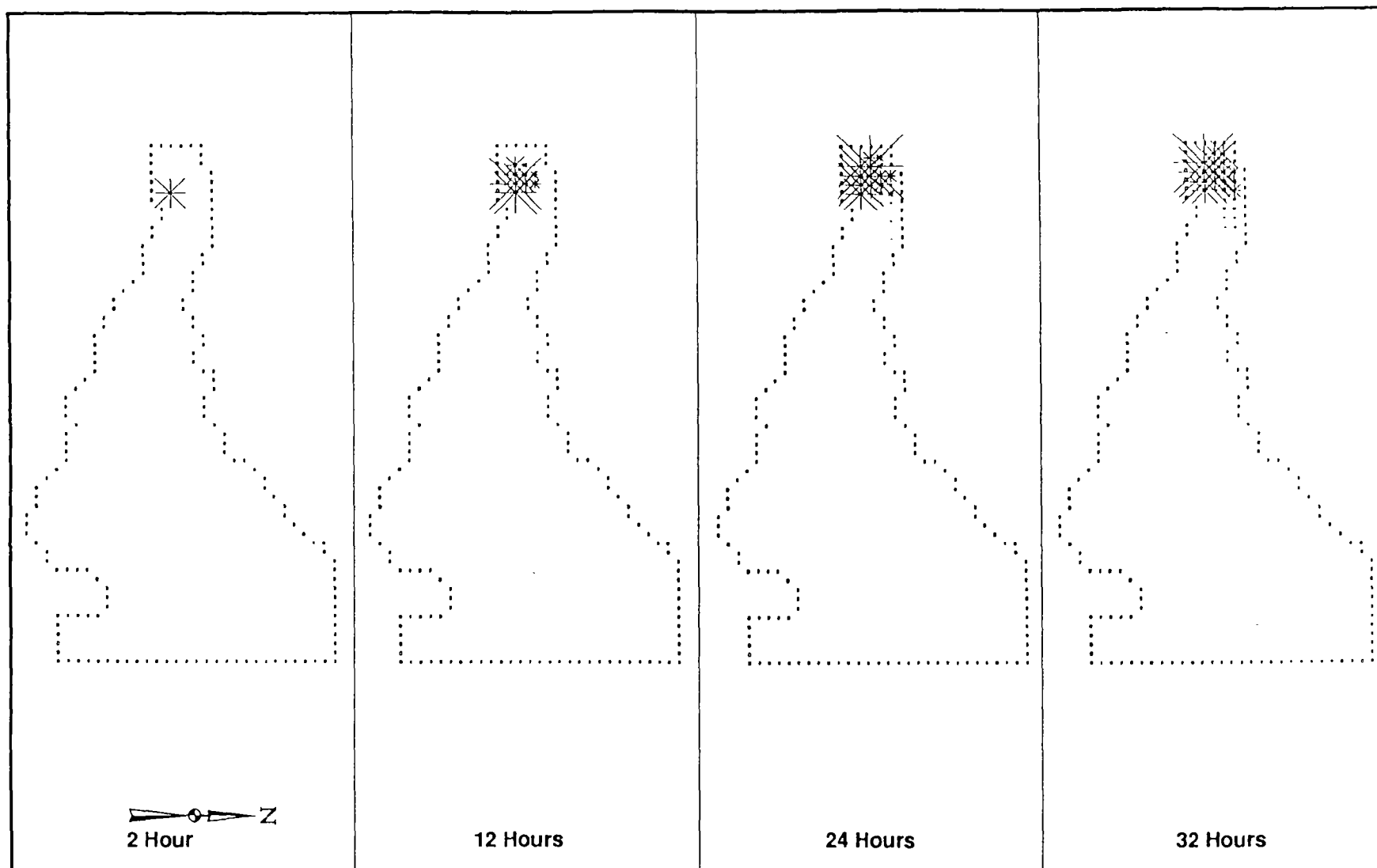
2 Hour

12 Hours

24 Hours

32 Hours

Figure L-15. Simulated Dispersion of Effluent from Alternative Outfall Site A-3 during a 32-Hour, 5 m/s West Wind
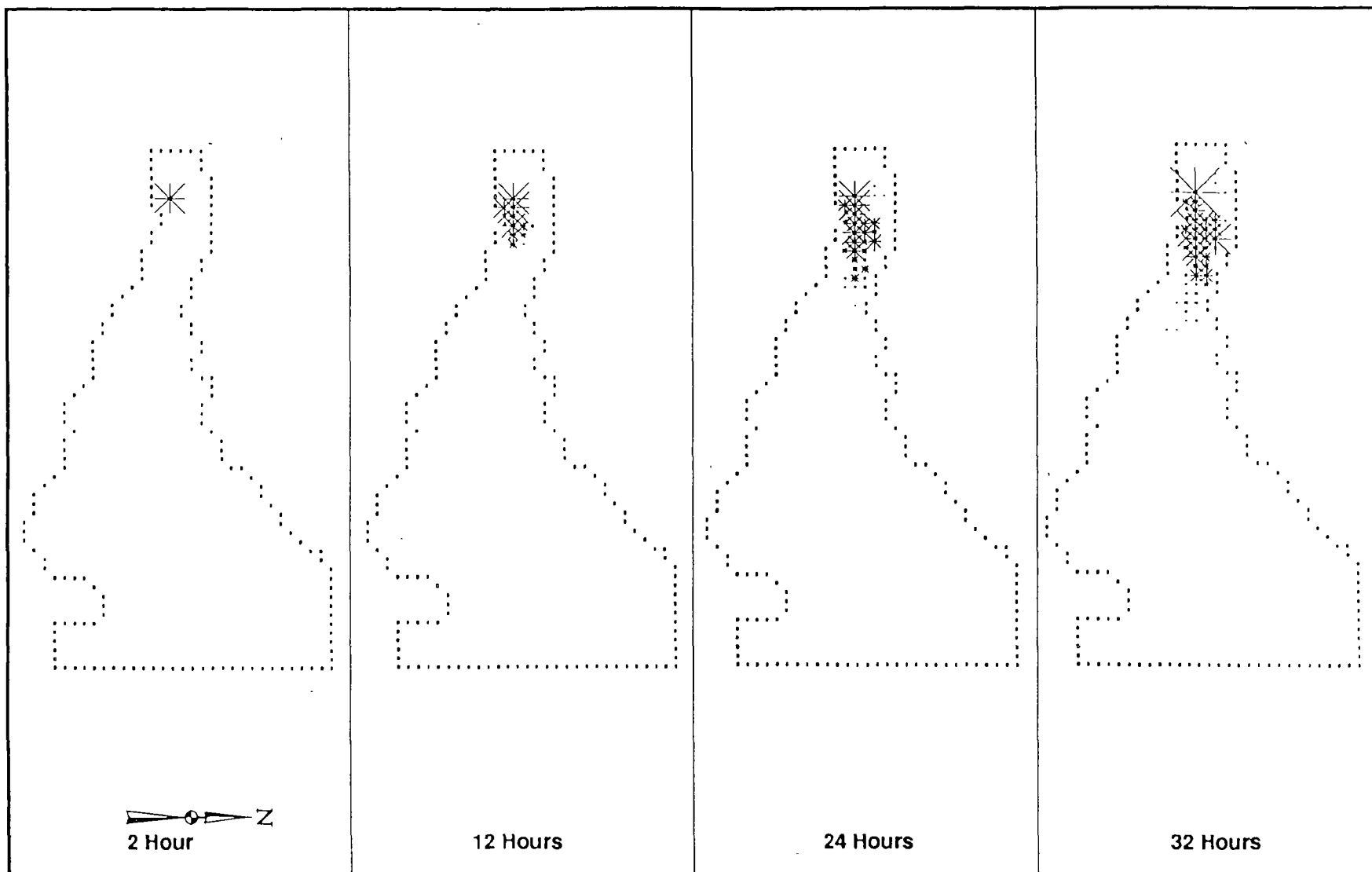
Figure L-16. Simulated Dispersion of Effluent from Alternative Outfall Site A-3 during a 32-Hour, 5 m/s East Wind
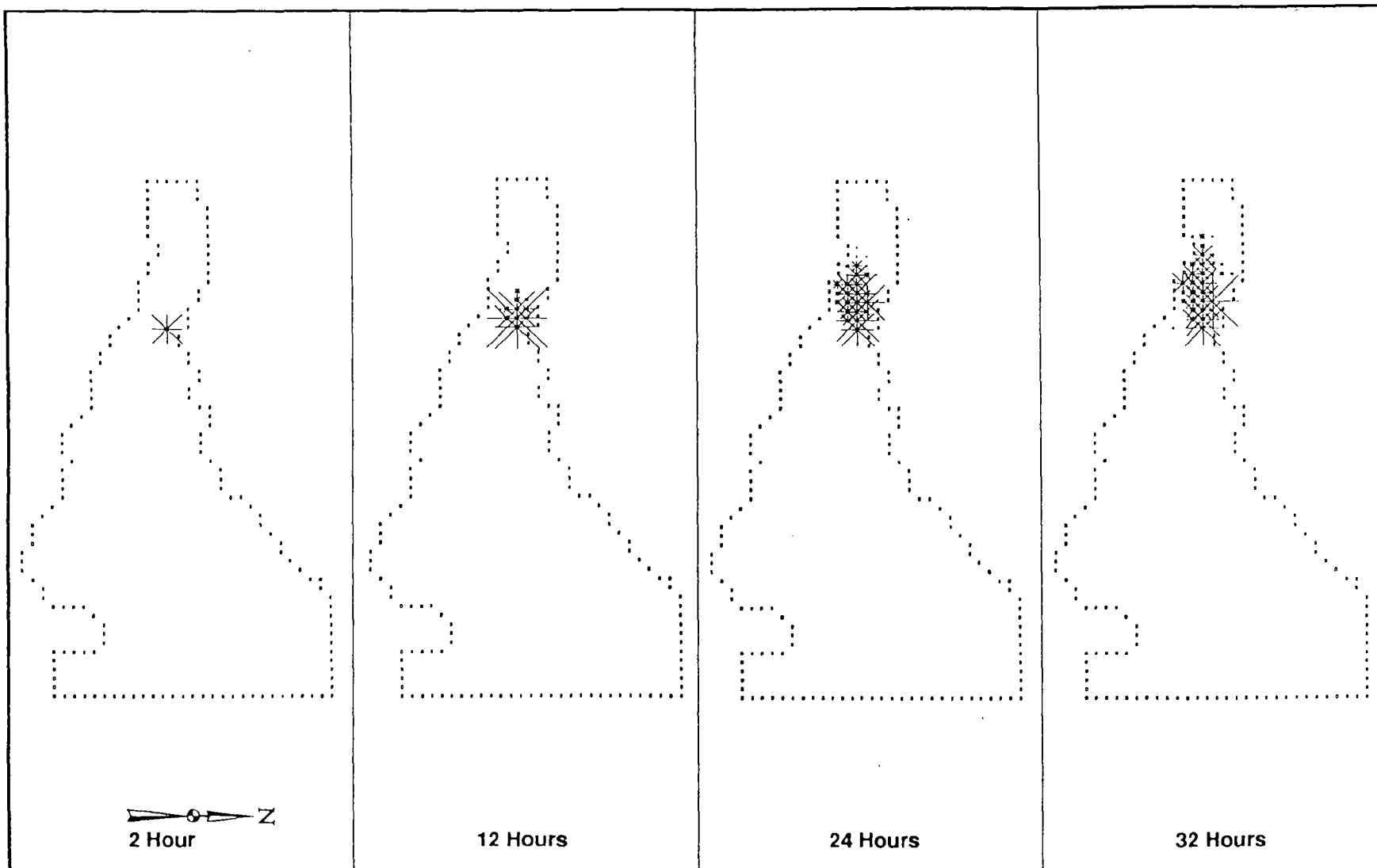
Figure L-17. Simulated Dispersion of Effluent from Trident Seafoods during a 32-Hour, 5 m/s West Wind

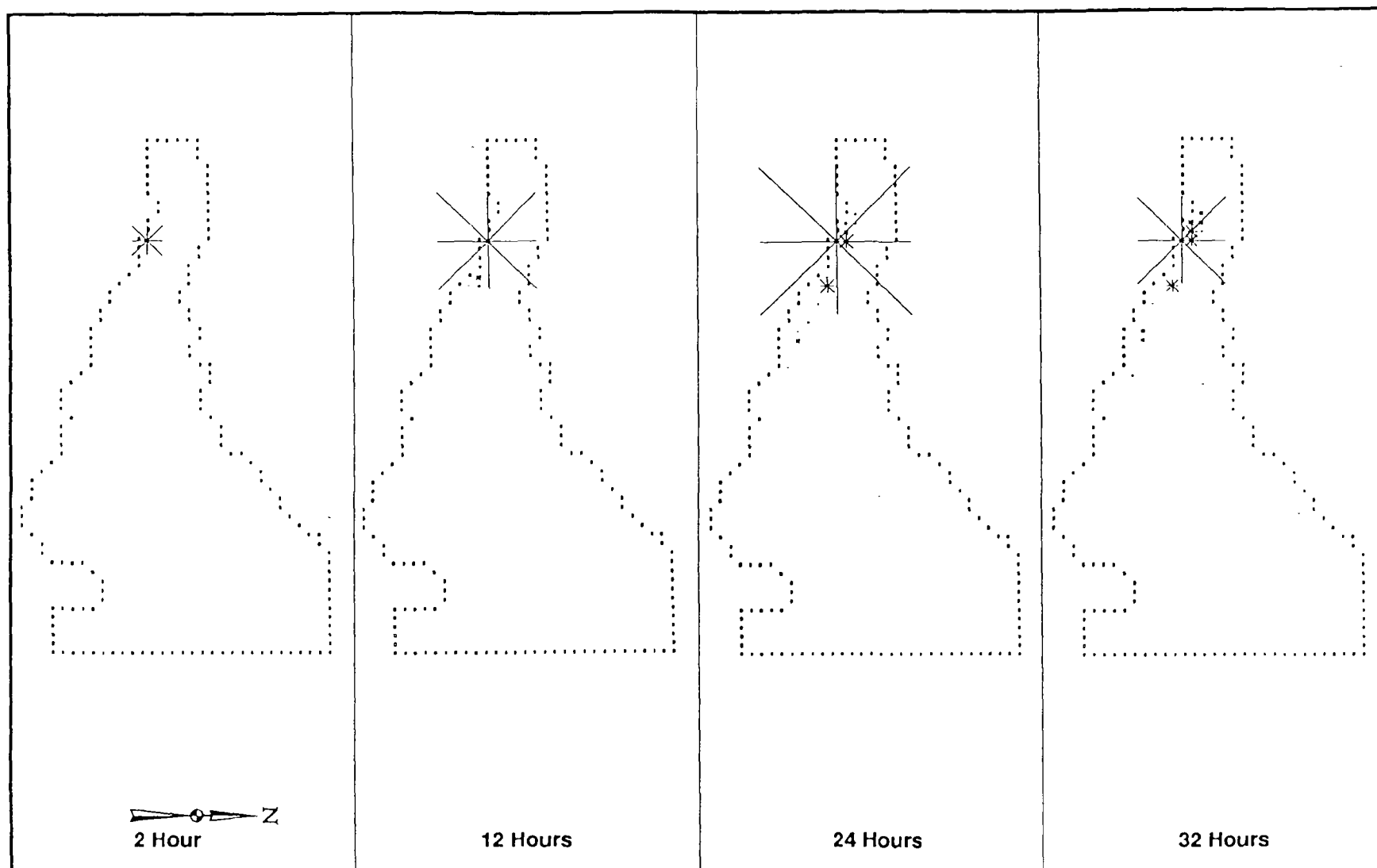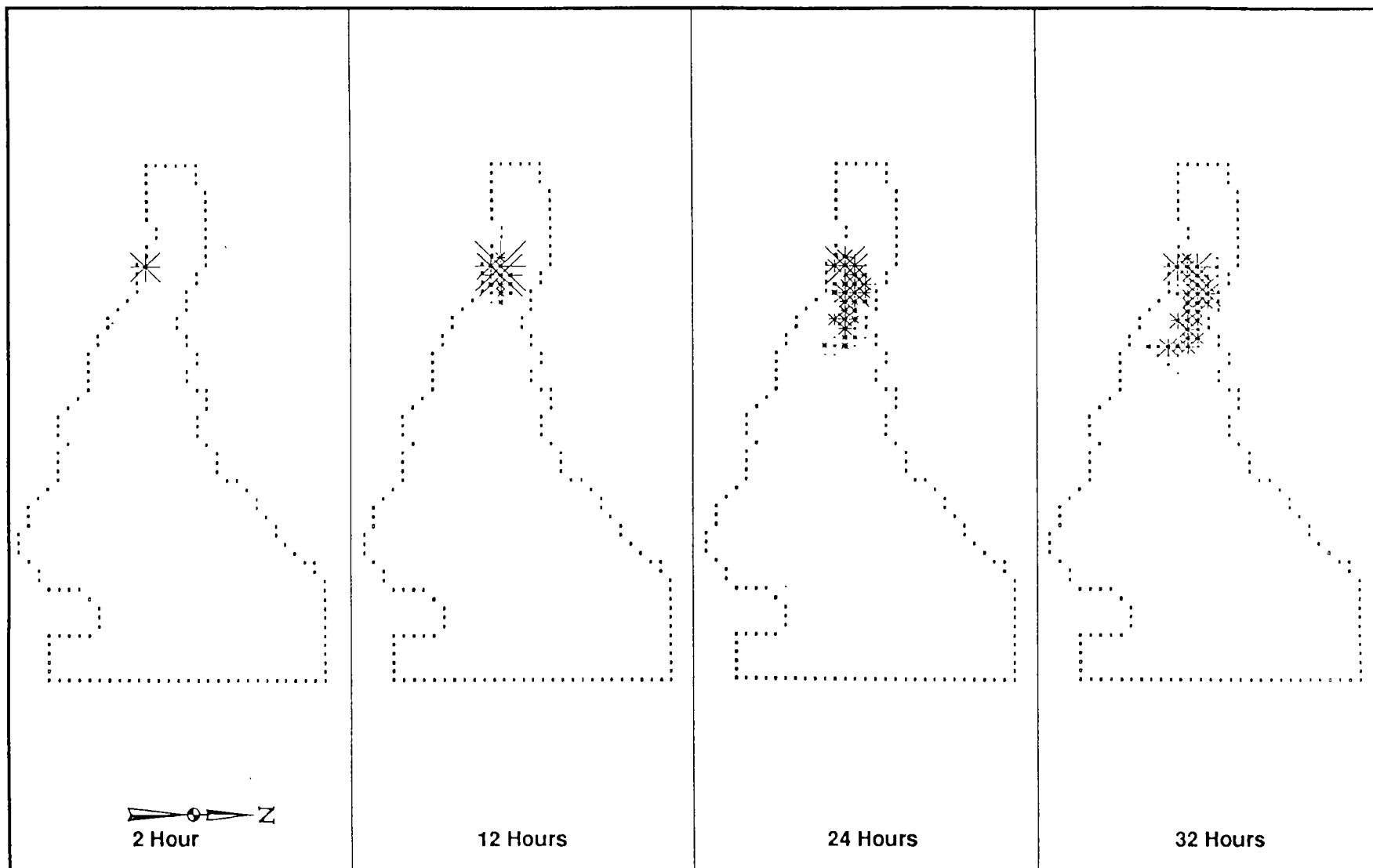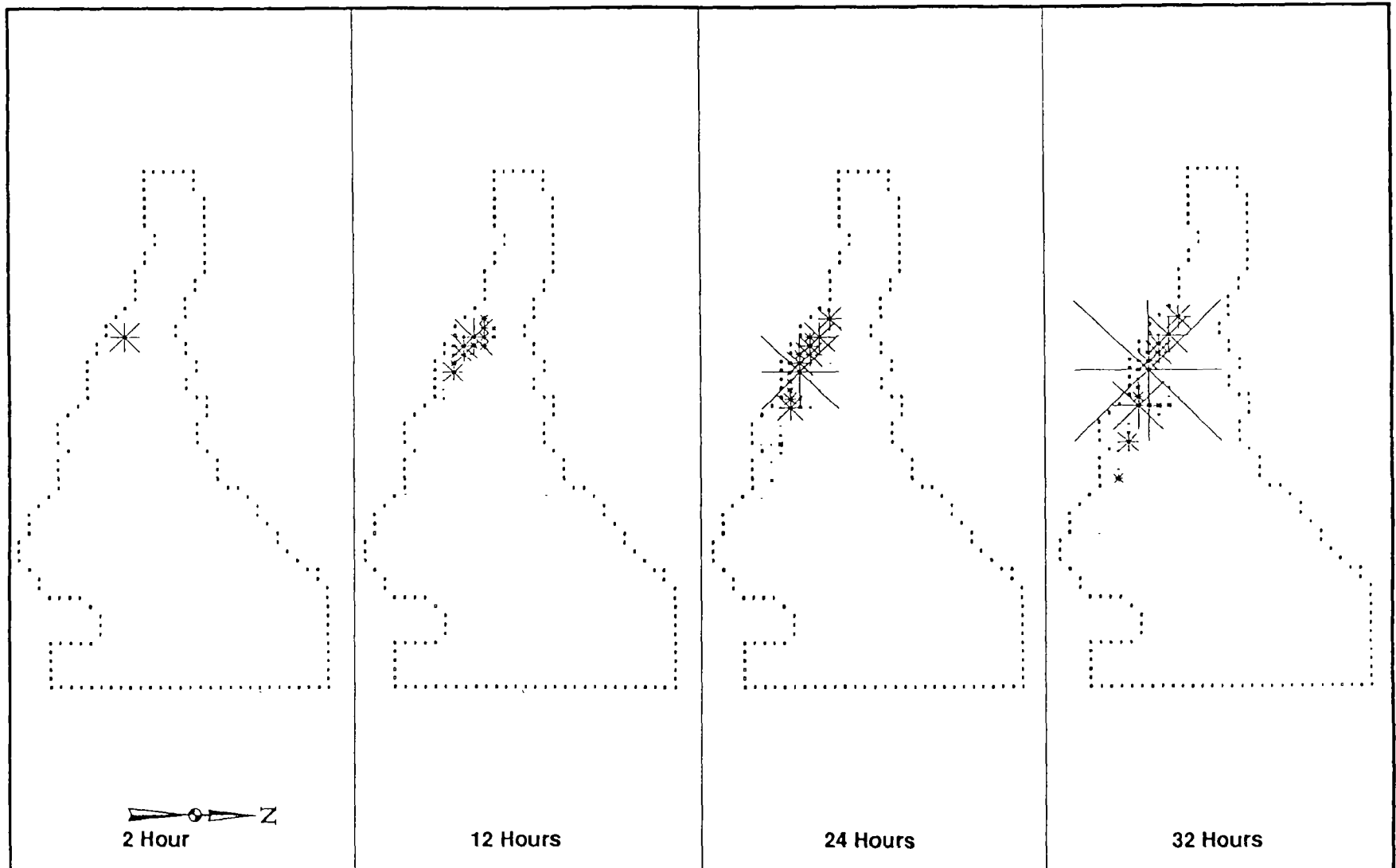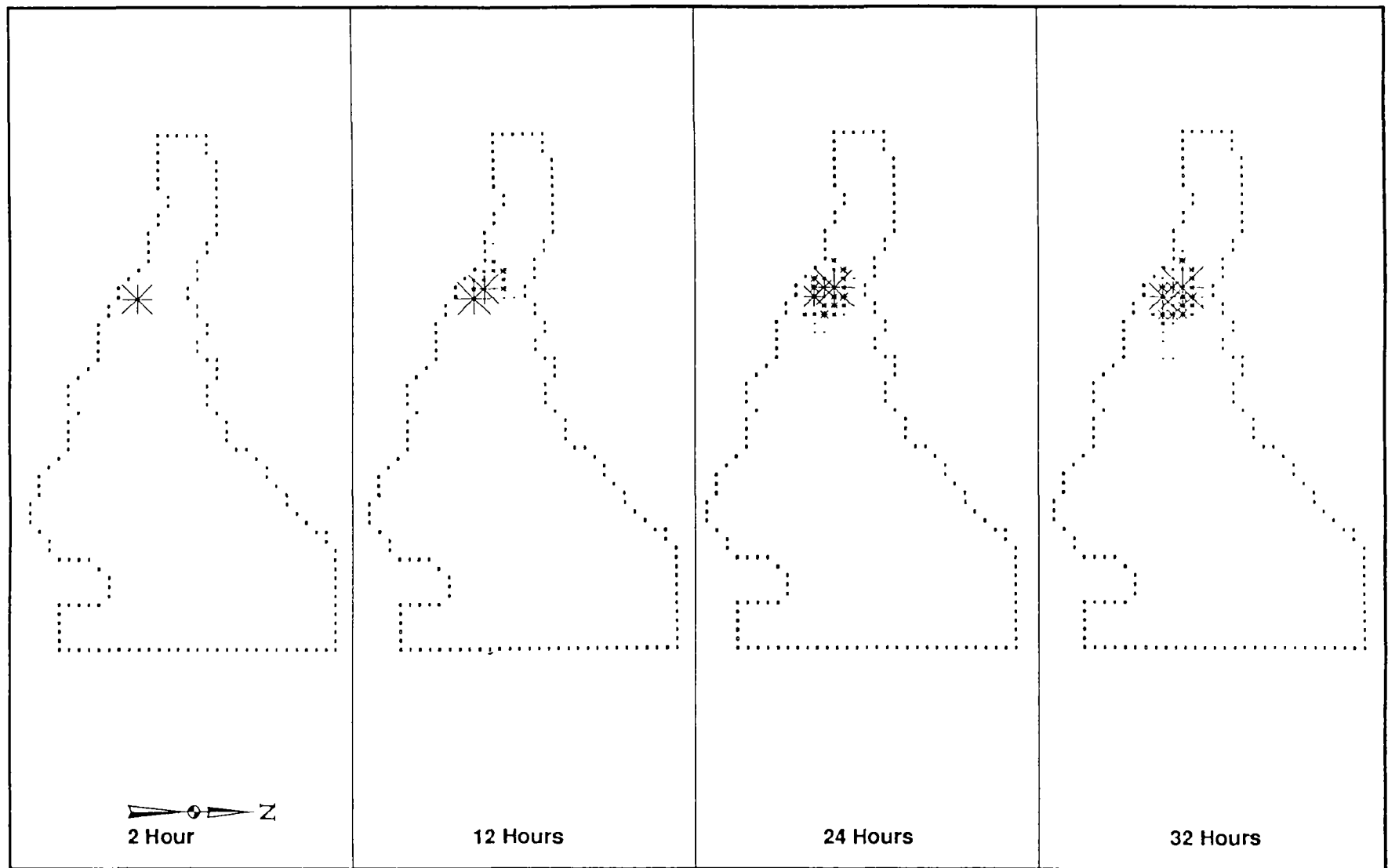2 Hour   12 Hours   24 Hours   32 Hours
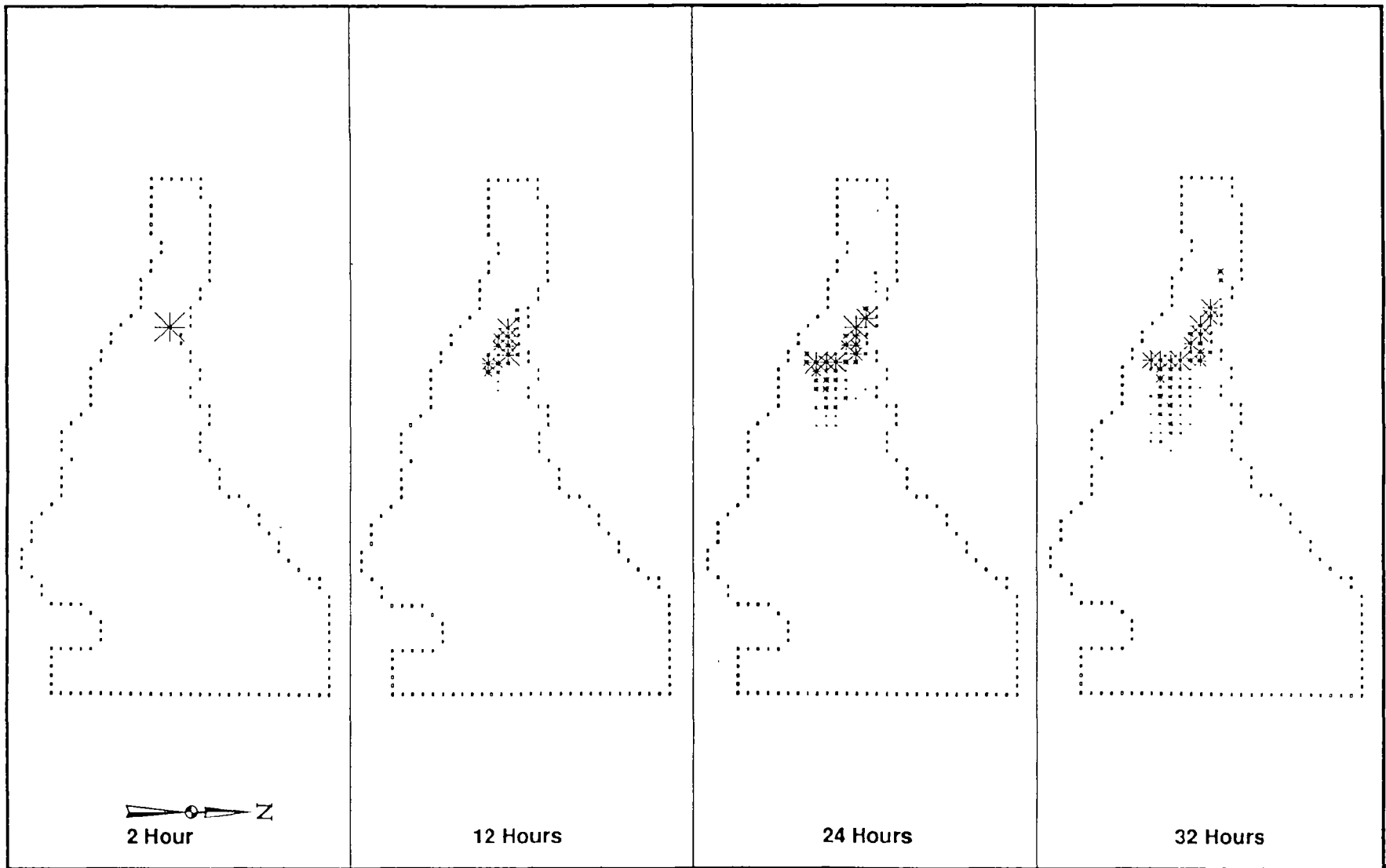
Figure L-18. Simulated Dispersion of Effluent from Trident Seafoods during a 32-Hour, 5 m/s East Wind

Appendix M.   Cumulative Impacts of Seafood Processing on Dissolved Oxygen in Akutan Harbor, Alaska

Appendix M. Cumulative Impacts of Seafood Processing on Dissolved Oxygen in Akutan Harbor, Alaska

Introduction

Deep Sea Fisheries' proposed shore-based seafood processing plant in Akutan Harbor, Alaska, will contribute a significant organic loading to the harbor. In view of the fact that existing seafood processors, including the shore-based Trident Seafoods facility and several floating processors, discharge large quantities of fish wastes under present conditions, it is necessary to characterize the cumulative impacts of existing and proposed discharges on the beneficial uses in the harbor. Given the oxygen-demanding nature of these discharges, there is particular concern about the cumulative impacts of seafood processors on dissolved oxygen (DO) in Akutan Harbor. For Akutan Harbor, the State of Alaska's water quality standard regulations (Alaska Department of Environmental Conservation 1989) require:

> Surface dissolved oxygen (DO) concentrations in coastal water shall not be less than 6.0 mg/l for a depth of one meter except when natural conditions cause this value to be depressed. DO shall not be reduced below 4 mg/l at any point beneath the surface.

Recognizing the need to maintain this standard, this report estimates the cumulative impacts of various scenarios of seafood processor discharges on the DO resources of Akutan Harbor.

Conceptual Model

The conceptual model for estimating cumulative impacts of seafood processing on the DO in Akutan Harbor is derived from the equations of mass balance for dissolved constituents as described in the manual for WASP4 (Ambrose et al. 1991). More specifically, it assumes that the oxygen-demanding properties of the seafood waste can be described in terms of biological oxygen demand (BOD) and that the important processes in the mass balance for BOD and DO are:

- Horizontal and vertical advection

- Horizontal and vertical diffusion

- Consumption of DO as microorganisms metabolize BOD in the water column

- Transfer of DO across the air-water interface (reaeration) by various processes including mixing due to wind stress

- Introduction of BOD from external sources such as seafood discharges

- Introduction of DO and BOD across boundaries between the harbor and the open ocean

Invoking standard assumptions regarding turbulent fluxes and kinetics of BOD stabilization and DO reaeration, as described in the WASP4 manual, the appropriate equations for the mass balance of BOD and DO in Akutan Harbor are:

$$\frac{\partial L}{\partial t} = -\frac{\partial}{\partial x}(U_x L) - \frac{\partial}{\partial y}(U_y L) - \frac{\partial}{\partial z}(U_z L)$$
$$+ \frac{\partial}{\partial x}\left(E_x\frac{\partial L}{\partial x}\right) + \frac{\partial}{\partial y}\left(E_y\frac{\partial L}{\partial y}\right) + \frac{\partial}{\partial z}\left(E_z\frac{\partial L}{\partial z}\right) \qquad (1)$$
$$- k_1 L + S_L$$

$$\frac{\partial C}{\partial t} = -\frac{\partial}{\partial x}(U_x C) - \frac{\partial}{\partial y}(U_y C) - \frac{\partial}{\partial z}(U_z C)$$
$$+ \frac{\partial}{\partial x}\left(E_x\frac{\partial C}{\partial x}\right) + \frac{\partial}{\partial y}\left(E_y\frac{\partial C}{\partial y}\right) + \frac{\partial}{\partial z}\left(E_z\frac{\partial C}{\partial z}\right) \qquad (2)$$
$$- k_1 L + S_C + k_2 (C_{sat}-C)$$

where

L	=	concentration of BOD, mg/l
C	=	concentration of DO, mg/l
C_{sat}	=	saturation level of DO, mg/l
t	=	time, seconds
x,y,z	=	spatial coordinates, meters

E_x, E_y, E_z = longitudinal, lateral, and vertical coefficients of eddy diffusivity, meters^2/second

U_x, U_y, U_z = longitudinal, lateral, and vertical velocities, meters/second

S_L = source of BOD, mg/l/second

S_C = source of DO, mg/l/second

k_1 = deoxygenation rate, seconds^{-1}

k_2 = reaeration rate, seconds^{-1}

Equations (1) and (2) are solved numerically using a finite difference method in which Akutan Harbor is idealized by a number of parallelepipeds (called control volumes or segments in WASP4), all of the same size. The plan of the grid used to define the horizontal extent of these segments is shown in Figure M-1. The vertical extent of the segmentation varies from location to location depending on the average water depth associated with the horizontal segmentation. Mass balances for BOD and DO are performed on these segments, using the explicit, finite difference formulation of Equations (1) and (2). It is the nature of the finite difference methods that at each time step in the solution of these equations, the simulated concentrations of BOD and DO are constant throughout each segment.

The elements of the conceptual model described above apply to applications of the WASP4 methodology to simulate BOD and DO. Elements of the conceptual model that are specific to the implementation of the methodology in Akutan Harbor include:

- Oxygen-demanding wastes associated with the various seafood processing streams from each source are aggregated into a single category with uniform oxygen-demanding characteristics.

- The discharges from all sources have come to equilibrium in the surface water whether they are discharged at depth or at the surface.

- Transfer of oxygen across the air-water interface is due to wind stress only.

Design Conditions

For purposes of estimating waste loads to Akutan Harbor that will not impair beneficial uses associated with levels of DO greater than 6.0 mg/l, it is necessary to choose appropriate design conditions. Since data from Akutan Harbor are limited, the approach adopted for this analysis is to choose two seasons, summer and winter, based on production
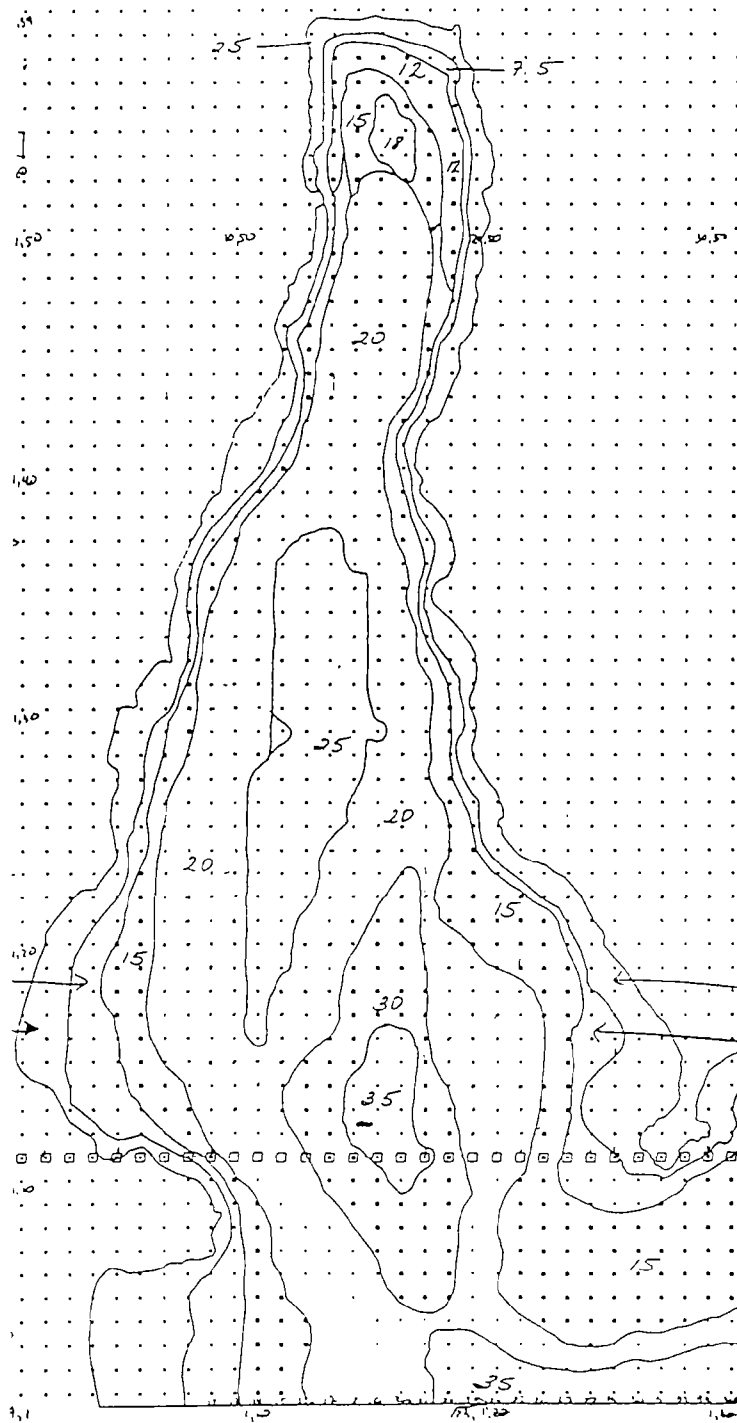
Figure M-1. WASP Model Grid Plan for Akutan Harbor

characteristics, as described in the Environmental Assessment (EA). Data from the EA are also used to characterize hydrographic conditions for the summer and winter seasons. In addition, the following assumptions are used:

- The critical design conditions for both summer and winter discharge are ones of average wind speeds and zero mean current.

- In the design conditions, advection processes are small and random and can be incorporated into the coefficients of eddy diffusivity.

- The Akutan Harbor DO/BOD system reaches a steady state during the design condition.

Parameter Estimation

In the absence of data from Akutan Harbor, it was necessary to obtain parameter estimates from other studies. Data from a study of seafood processing wastes in Captains Bay, Alaska (Cope 1993) were used to estimate coefficients of horizontal and vertical eddy diffusivity and deoxygenation rates associated with seafood wastes. Current measurements in Akutan Harbor, reported by Evans-Hamilton (Appendix C of EA), were used to determine if the estimates for Captains Bay used by Cope (1993) were reasonable ones for Akutan Harbor. This was done by assuming the length scale associated with turbulent diffusion is related to the asymptotic form of variance in an homogeneous, isotropic, stationary field of turbulence for large dispersion times. This variance, $\overline{\sigma}_T^2$, is given by Frenkiel (1953):

$$\overline{\sigma}_T^2 \approx 2 \, \kappa^* \, t$$

where,

κ^* =   the coefficient of eddy diffusivity,

t =   time.

For purposes of comparison, it was assumed the length scale associated with turbulent diffusion was twice the square root of the variance. In an infinite ocean this would correspond to 95% of the total surface area affected by diffusion. Length scales associated with currents in the harbor were estimated by computing the daily displacement in the progressive vector diagram for each of the three current meters. The daily displacement was

chosen based on the results of time-dependent simulations (Figure M-2), showing the response time of a typical location in the harbor is between one and two days. The cumulative distribution functions for daily displacement at each of the three current meter stations are given in Figures M-3 through M-5. Estimates of the coefficient of eddy diffusivity using this methodology range from .03 m^2/s to 89 m^2/s, with lowest estimates at the deep station near Deep Sea's proposed outfall and the highest estimates at the station in the central harbor. For an eddy diffusivity of 0.5 m^2/s, approximately that used by Cope (1993), the cumulative probabilities are 0.14, 0.32, and 0.85, respectively, for the current meter located in the central harbor near Trident, the shallow current meter at the proposed Deep Sea outfall, and the deep current meters at the proposed Deep Sea outfall. The variability in the cumulative probabilities supports the hypothesis that mixing in Akutan Harbor decreases with increasing distance from the harbor entrance. However, in light of the limited data, the horizontal coefficient of eddy diffusivity was assumed to be homogeneous, isotropic, and stationary.

Reaeration rates were estimated with the methodology used in WASP4 (Ambrose et al. 1991) using average wind speeds for the appropriate season.

Parameter values used in the base simulations are given in Table M-1.

Method of Analysis

The first step in the analysis was to develop a finite difference grid of Akutan Harbor. This grid was based on a bathymetric coverage developed by Jones & Stokes Associates and is shown in Figure M-6. Each grid is 261 by 261 meters in the horizontal and 5 meters thick. Primary considerations in choosing the grid size were (1) ability to resolve important water quality features associated with the various discharges, and (2) the need to keep required computer resources at a reasonable level.

With the finite difference grid, estimates of the impacts of seafood processing on DO in Akutan Harbor under the environmental design conditions described above were obtained using a simplified version of the WASP4 simulation methodology. The simplified version uses an explicit finite difference scheme to obtain a numerical solution to Equations (1) and (2) and has been used previously to develop mixing zones and NPDES Permit conditions in Silver Bay, Alaska (Yearsley 1991) and Ward Cove, Alaska (Yearsley 1990). The simplified methodology uses the same basic approach as WASP4 when the EUTRO4 module of WASP4 is applied at Complexity Level 1 (Table 2.4.1 in Ambrose et al. 1991). However, the simplified methodology does not have the administrative overhead that WASP4 does, so it is much easier to apply to problems such as Akutan Harbor for which there are a large number of elements and a potentially large number of discharge scenarios.
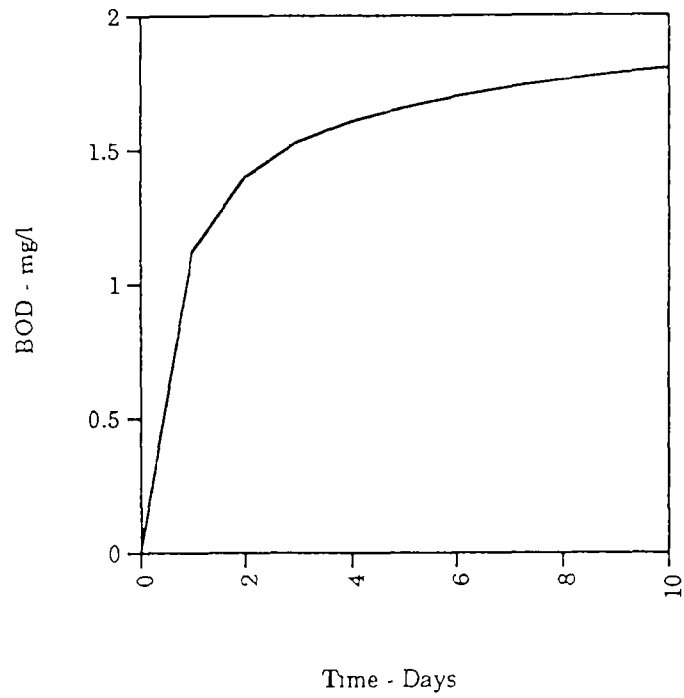
Figure M-2. Transient Response of BOD in Akutan Harbor for Parameter Set Given in Table 1
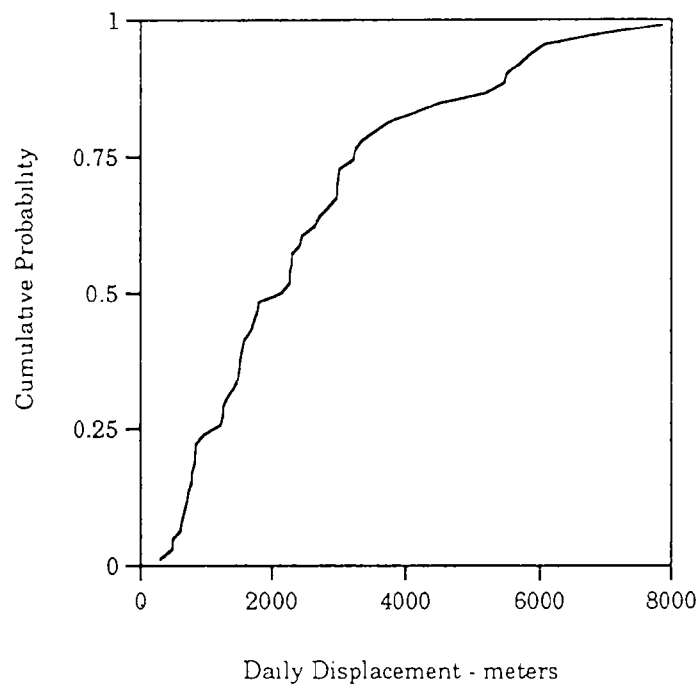
Figure M-3. Cumulative Distribution Function for Daily Displacement Estimated from Current Meter Station 718 (Mooring No. 1 near Trident)
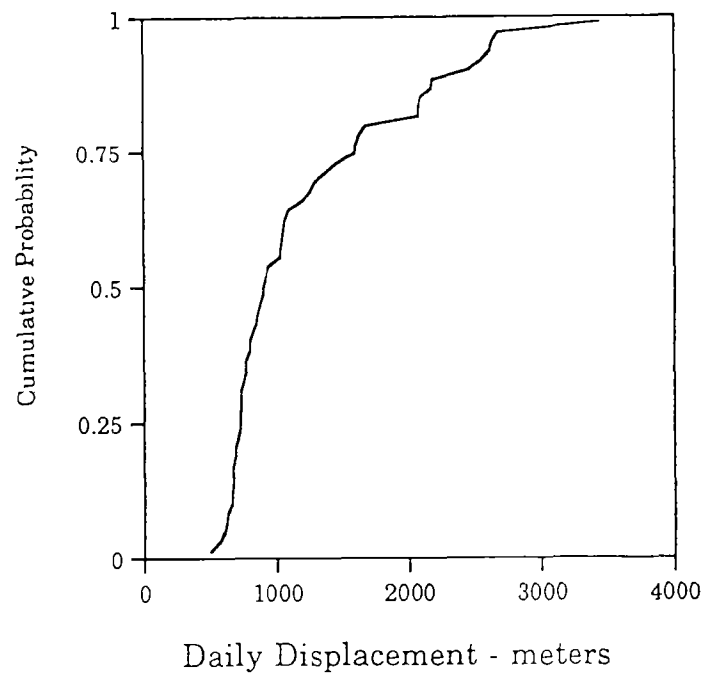
Figure M-4. Cumulative Distribution Function for Daily Displacement
Estimated from Current Meter Station 3180 (Mooring No. 2
near Deep Sea Fisheries)
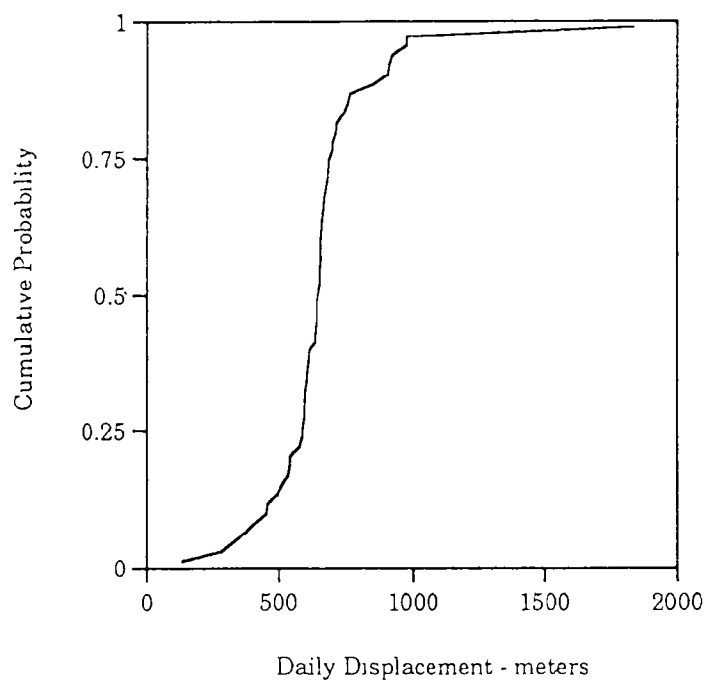
Figure M-5. Cumulative Distribution Function for Daily Displacement Estimated from Current Meter Station 7315 (Mooring No. 2 near Deep Sea Fisheries)

Table M-1. Estimates for Parameters Used to Assess Impacts
of Seafood Processors on DO in Akutan Harbor, Alaska

Parameter	Value	Unit
E_x, coefficient of eddy diffusivity, x-direction	0.5	m²/s
E_y, coefficient of eddy diffusivity, y-direction	0.5	m²/s
E_z, coefficient of eddy diffusivity, z-direction	1.0×10^{-4}	m²/s
k_1, deoxygenation rate	0.1	days⁻¹
W_s, average wind speed (summer)	5.0	m/s
W_w, average wind speed (winter)	5.0	m/s
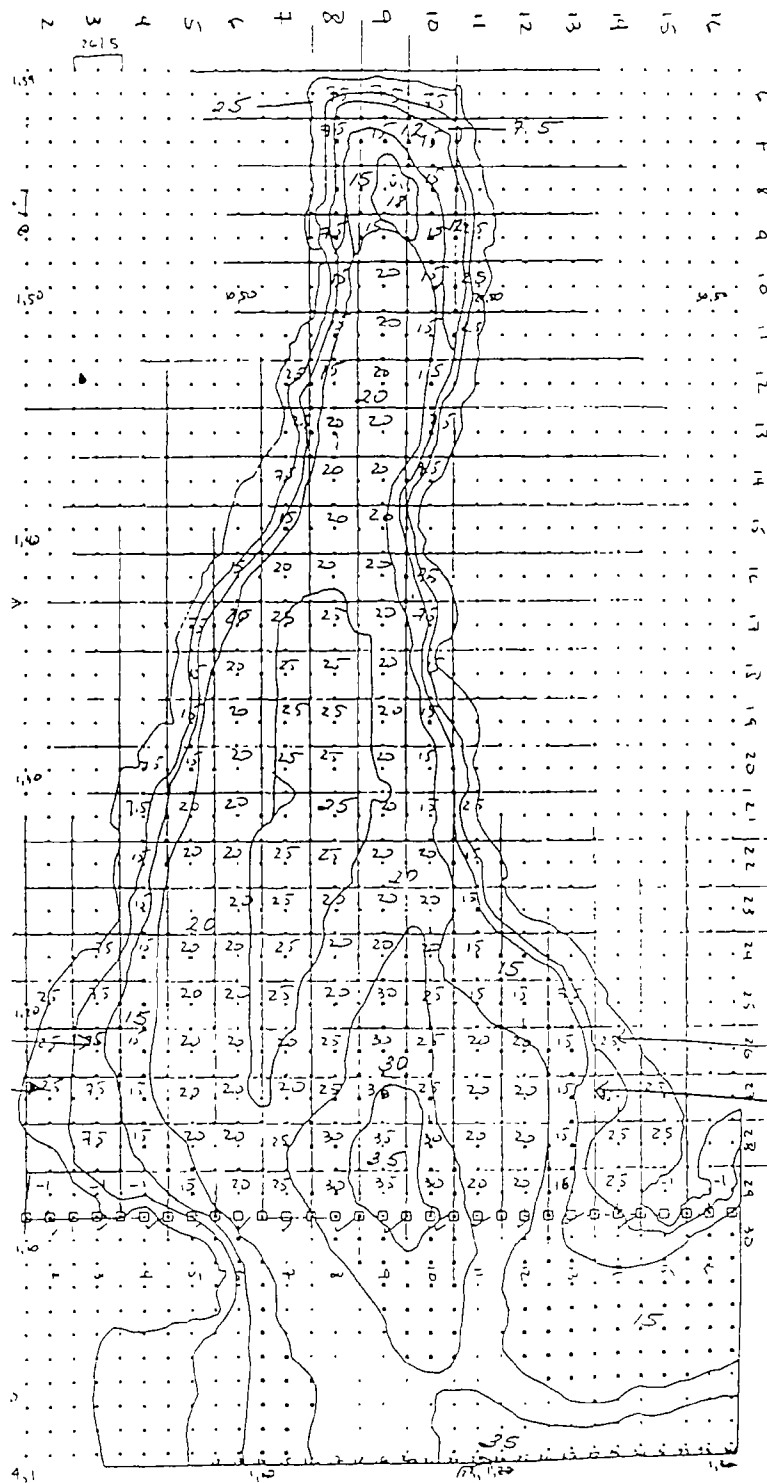
Figure M-6. WASP Model Grid Coordinate System for Akutan Harbor

The simplified finite difference model was used to develop a BOD influence matrix for each of the surface cells shown in Figure M-1 for both summer and winter. The BOD influence matrix for each cell was determined for each design condition (winter and summer) by obtaining a steady-state solution to Equations (1) and (2) when a reference loading was introduced, one cell at a time, into each cell. The impact on DO in the i, j^{th} cell of a reference loading, L_{ref}, into the l,m^{th} cell, defines the elements, $b(l,m)_{i,j}$, of the BOD influence matrix, $B(l,m)$. The elements for each cell are computed from

$$b(l,m)_{i,j} = \frac{C_{sat} - C(l,m)_{i,j}}{L_{ref}}$$

where,

C_{sat} =. the saturation level of dissolved oxygen, mg/l

$C(l,m)_{i,j}$ = the level of DO in the i,j^{th} cell estimated from Equations (1) and (2) when the reference load, L_{ref}, is discharged in the l,m^{th} cell , mg/l

l = the cell index in the x-direction for the cell receiving the reference discharge

m = the cell index in the y-direction for the cell receiving the reference discharge

i = the cell index in the x-direction for the cell at which the DO impact occurs

j = the cell index in the y-direction for the cell at which the DO impact occurs

Since the model is a linear model, the total DO impact of a given discharge scenario, where a scenario is a configuration of sources of various strengths at various locations during one of the two design conditions (summer or winter), is:

$$\Delta DO\big|_{i,j} = \sum_{l} \sum_{m} L_{ref} b(l,m)_{i,j}$$

Scenarios were judged to be satisfactory if:

$$C_{sat} - \Delta DO|_{i,j} \geq C_{Alaska_{wqs}} = 6.0 \text{ mg/l}$$

Scenarios

To evaluate the cumulative impact of Deep Sea, Trident, and various floating processors on DO in Akutan Harbor, 30 scenarios were tested with the methodology described above. The scenarios were developed by considering several configurations for discharges from the various processors. For those waste streams other than the proposed shore-based Deep Sea facility, monthly BOD_5 loadings for the various waste streams were based on values estimated by Jones & Stokes Associates (Tables M-2 and M-3). Jones & Stokes Associates used similar methodology to estimate the projected weekly average BOD_5 loading for the proposed Deep Sea facility. Projected values of weekly averaged BOD_5 loading for the Deep Sea facility for each month of the year are given in Table M-4.

The 30 scenarios were assembled by considering two dimensions of seafood waste discharge to Akutan Harbor. The two dimensions were loading rate and discharge location. The loading component of the 30 scenarios was obtained from these tables by choosing the maximum weekly average BOD_5 loading for each source during the summer and the winter. The discharge location of the 30 scenarios was defined by recommendations from Seaborne (1993). In each case, Deep Sea Fisheries' bailwater discharges enter the model in the grid cell nearest the facility. Deep Sea Fisheries' primary discharge enters the model at the grid cell corresponding to the location of the proposed or alternative outfall sites.

A. "No Action": No discharge from the shore plant, but continuing discharge from existing permitted Deep Sea Fisheries floating operations at the head of the harbor

   Summer BOD_5 = 0 lbs/day
   Winter BOD_5 = 671 lbs/day

B. Deep Sea Fisheries shore plant discharges:

   1. Proposed outfall location
   2. Alternative outfall location A-1
   3. Alternative outfall location A-2
   4. Alternative outfall location A-3

   Summer BOD_5 = 51,951 lbs/day
   Winter BOD_5 = 48,179 lbs/day

Table M-2. Estimated Monthly Loading of BOD$_5$ to the Waters
of Akutan Harbor from Seafood Processing during 1991
(includes finfish and crab wastes)

Month	Estimated Monthly BOD$_5$ Loading (pounds/day)		
	Trident	Deep Sea	Floating Processors
January	49,212	61	1,263
February	54,689	255	4,500
March	11,274	416	5,070
April	8,957	255	1,950
May	1,556	113	257
June	41,394	0	783
July	48,674	0	680
August	55,929	0	769
September	6,831	0	95
October	71	0	1
November	611	71	14
December	1,044	68	278

Table M-3. Estimated Monthly Loading of BOD_5 to the Waters
of Akutan Harbor from Seafood Processing during 1992
(includes finfish and crab wastes)

Month	Estimated Monthly BOD_5 Loading (pounds/day)		
	Trident	Deep Sea	Floating Processors
January	19,391	293	2,623
February	59,428	671	11,864
March	19,799	362	5,387
April	4,360	186	2,075
May	1,394	0	21
June	8,147	0	606
July	36,495	0	711
August	65,489	0	804
September	50,226	0	100
October	0	0	7
November	809	105	5
December	32,543	68	699

Table M-4. Projected Monthly Loading of BOD_5
to the Waters of Akutan Harbor from the
Proposed Deep Sea Shore-Based Facility

Month	Estimated Monthly BOD_5 Loading (pounds/day)
January	14,814
February	48,179
March	15,174
April	2,429
May	690
June	6,194
July	28,635
August	51,951
September	39,971
October	0
November	418
December	25,901

C. Trident shore plant discharge (existing outfall)

$$\text{Summer BOD}_5 \quad = \quad 65,489 \text{ lbs/day}$$
$$\text{Winter BOD}_5 \quad = \quad 59,428 \text{ lbs/day}$$

D. Floating processors discharge:

1. Located throughout harbor without restriction
2. Located only east of longitude 165° 46'
3. No floaters in harbor

$$\text{Summer BOD}_5 \quad = \quad 804 \text{ lbs/day}$$
$$\text{Winter BOD}_5 \quad = \quad 11,864 \text{ lbs/day}$$

The 30 scenarios were developed by examining combinations of these loadings and loadings during both summer and winter design conditions. The 30 scenarios are shown in Table M-5.

Uncertainty in Estimates

Due to the limited availability of data, it was necessary to make estimates of certain critical parameters including loading rates, deoxygenation rate, reaeration rate, and coefficient of eddy diffusivity. In addition, the density characteristics of the effluent are not well known. The density of the effluent determines where the waste comes to equilibrium in the water column. This is important for estimating impacts on DO for two reasons. First, reaeration is a surface phenomenon, and demand from organic matter which reaches the water surface will be mitigated by the transfer of DO from the air to the water. Second, the State of Alaska's criterion for DO is different in the surface layer than at depth (see above).

These factors lead to uncertainty in the estimated cumulative impacts of the discharges on water quality. The magnitude of this uncertainty was evaluated for two aspects of the problem: uncertainty in the coefficient of eddy diffusivity and uncertainty in the fate of the effluent. The uncertainty in the coefficient of eddy diffusivity was evaluated by estimating DO impacts on Akutan Harbor for the summer and winter conditions using loadings from Scenarios No. 4 and 19, respectively, and for values of the eddy diffusivity representing the lowest estimate (0.03 m²/s) and the highest (89 m²/s).

Table M-5. Combinations of Loadings and Locations Used to Estimate Cumulative Impacts of Seafood Processors in Akutan Harbor

| # | | Scenario | # | | Scenario | # | | Scenario |
Summer	Winter		Summer	Winter		Summer	Winter	
1.	16.	A,C,D.1	2.	17.	A,C,D.2	3.	18.	A,C,D.3
4.	19.	B.1,C,D.1	5.	20.	B.1,C,D.2	6.	21.	B.1,C,D.3
7.	22.	B.2,C,D.1	8.	23.	B.2,C,D.2	9.	24.	B.2,C,D.3
10.	25.	B.3,C,D.1	11.	26	B.3,C,D.2	12.	27.	B.3,C,D.3
13.	28.	B.4,C,D.1	14.	29	B.4,C,D.2	15.	30.	B.4,C,D.3

Results

Base Condition

The estimated cumulative impacts of the 30 scenarios under the base conditions are shown in Figures M-7 through M-36. Estimated DO levels in the surface waters are less than the State of Alaska's water quality standard of 6.0 mg/l for all summer scenarios. For existing conditions (Scenarios No. 1 through 3), the only source whose estimated impacts violate water quality standards for DO is the Trident shore-based facility. For all other summer scenarios (Scenarios No. 4 to 6, 10 to 12, and 12 to 15), except the one in which Deep Sea's proposed discharge is at Alternative Outfall Site A-1 (Scenarios No. 7 through 9), both Trident and Deep Sea's discharges are the sources of the unacceptable DO levels. The floating processors, under design conditions used in this analysis for summer, do not contribute significantly to water quality standards violations for DO so long as the floating processors are more than 400 meters from the shore-based sources. Reduction of Trident's BOD$_5$ loading to 36,800 lbs/day results in acceptable estimated levels of DO in Akutan Harbor under existing conditions. Limiting the proposed Deep Sea discharge to 31,500 lbs/day and reducing Trident's discharge to 36,800 lbs/day results in acceptable estimated levels of DO except discharge of Deep Sea waste at Alternative Outfall Site A-3.

For winter conditions, estimated cumulative impacts on DO from seafood processors do not result in water quality violations for the base conditions except for the scenario in which Deep Sea discharges at Alternative Outfall Site A-3 (Scenarios No. 27 through 30).

Uncertainty in Eddy Diffusivity

Levels of DO in the surface waters of Akutan Harbor for summer and winter conditions were estimated using coefficients of eddy diffusivity of 0.03 m^2/s and 89 m^2/s. As discussed above, these values represent a range of mixing levels inferred from observed currents in Akutan Harbor and the theory of turbulent diffusion. Loading Scenarios No. 4 and 19 were used for the summer and winter conditions, respectively. For the case of minimum turbulent diffusion (Figures M-37 and M-38), estimated DO levels for the preferred alternative are below the State of Alaska's water quality criterion during both winter and summer. Estimated levels of DO exceed the criterion for the preferred alternative when the coefficient of eddy diffusivity has the maximum estimated value (Figures M-39 and M-40).

Figure M-7. Scenario No.1 (Summer) -
Existing outfall, no restriction
on location of floating processors
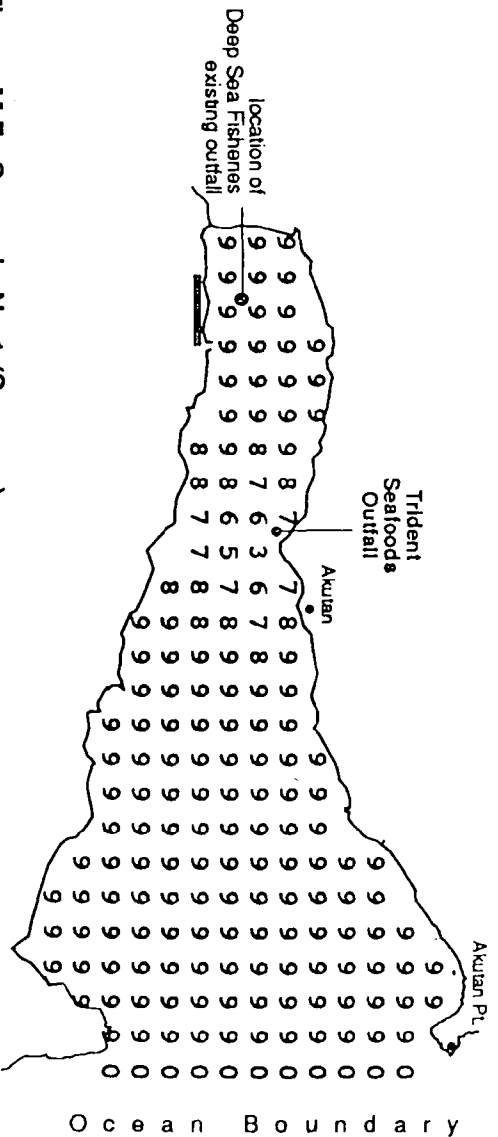
Figure M-8. Scenario No.2 (Summer) -
Existing outfall, floating processors
east of 165° 46' only

Scale Approximate

Note: Numbers represent predicted dissolved oxygen
concentration (mg/l) in surface layer.

M-21

Akutan Pt.

Trident
Seafoods
Outfall

Akutan

```
                                                  9 9
                                              9 9 9 9 0
                                          9 9 9 9 9 9 0
                                          9 9 9 9 9 9 0
        9 9 9               9 9 9 9 9 9 9 9 9 9 9 9 9 0
location of  9 9 9 9 9 9 9 9 8 7   7 8 9 9 9 9 9 9 9 9 9 9 9 9 0
Deep Sea Fisheries  9 9 9 9 9 9 8 7 6 3 6 7 8 9 9 9 9 9 9 9 9 9 9 9 0
existing outfall  9 9 9 9 9 9 9 8 6 5 7 8 9 9 9 9 9 9 9 9 9 9 9 9 0
              8 8 7 7 8 8 9 9 9 9 9 9 9 9 9 9 9 9 9 0
                  8 9 9 9 9 9 9 9 9 9 9 9 9 9 9 9 0
                    9 9 9 9 9 9 9 9 9 9 9 9 9 9 0
                      9 9 9 9 9 9 9 9 9 9 9 9 0 0
                        9 9 9 9 9
                          9 9 9
```

Ocean Boundary

**Figure M-9. Scenario No.3 (Summer) -
Existing outfall, no floating
processors in harbor**

Akutan Pt.

Trident
Seafoods
Outfall

Akutan

```
                                                  9 9
                                              9 9 9 9 0
                                          9 9 9 9 9 9 0
                                          9 9 9 9 9 9 0
        8 8 8               9 9 9 9 9 9 9 9 9 9 9 9 9 0
    8 8 7 7 8 8 8 7 7   7 8 9 9 9 9 9 9 9 9 9 9 9 9 0
    8 8 7 6 7 8 8 7 5 3 6 7 8 9 9 9 9 9 9 9 9 9 9 9 0
    8 7 5 3 5 7 8 7 6 5 7 8 9 9 9 9 9 9 9 9 9 9 9 9 0
              8 8 7 7 8 8 9 9 9 9 9 9 9 9 9 9 9 9 9 0
                  8 9 9 9 9 9 9 9 9 9 9 9 9 9 9 9 0
                    9 9 9 9 9 9 9 9 9 9 9 9 9 9 0
                      9 9 9 9 9 9 9 9 9 9 9 9 0 0
                        9 9 9 9 9
                          9 9 9
```

location for
Deep Sea Fisheries
proposed outfall site

Ocean Boundary

**Figure M-10. Scenario No.4 (Summer) -
Proposed outfall, no restriction
on location of floating processors**

NAUTICAL MILES

KILOMETERS

Scale Approximate

N

Note: Numbers represent predicted dissolved oxygen
concentration (mg/l) in surface layer.

Figure M-11. Scenario No.5 (Summer) - Proposed outfall, floating processors east of 165° 46' only

Figure M-12. Scenario No.6 (Summer) - Proposed outfall, no floating processors in harbor

Note: Numbers represent predicted dissolved oxygen concentration (mg/l) in surface layer.

Scale Approximate

Figure M-13. Scenario No.7 (Summer) -
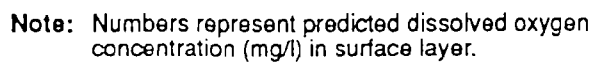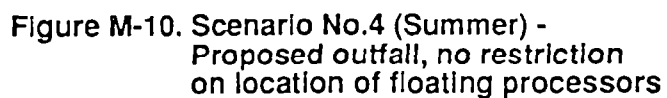Outfall A-1, no restriction
on location of floating processors
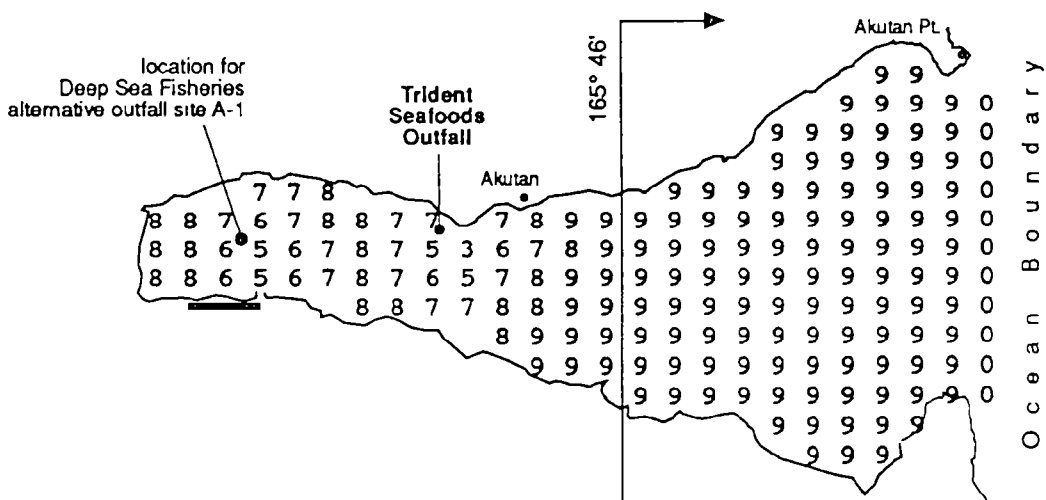
Figure M-14. Scenario No.8 (Summer) -
Outfall A-1, floating processors
east of 165° 46' only

Note: Numbers represent predicted dissolved oxygen
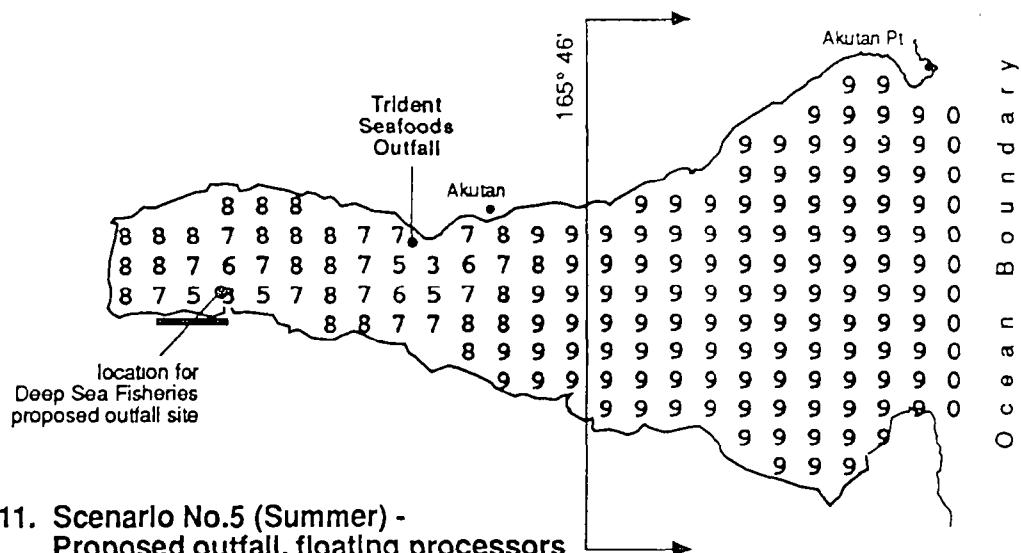concentration (mg/l) in surface layer.

location for
Deep Sea Fishenes
alternative outfall site A-1

Trident
Seafoods
Outfall

Akutan

Akutan Pt.

Ocean Boundary

```
                                          9  9
                                    9  9  9  9  0
                              9  9  9  9  9  9  0
                              9  9  9  9  9  9  0
        7  7  8          9  9  9  9  9  9  9  9  0
8  8  7  6  7  8  8  7  7  7  8  9  9  9  9  9  9  9  9  9  9  9  0
8  8  6  5  6  7  8  7  5  3  6  7  8  9  9  9  9  9  9  9  9  9  9  9  0
8  8  6  5  6  7  8  7  6  5  7  8  9  9  9  9  9  9  9  9  9  9  9  0
              8  8  7  7  8  8  9  9  9  9  9  9  9  9  9  9  9  9  0
                 8  9  9  9  9  9  9  9  9  9  9  9  9  9  9  0
                 9  9  9  9  9  9  9  9  9  9  9  9  9  9  0
                    9  9  9  9  9  9  9  9  9  9  0  0
                       9  9  9  9  9  0
                       9  9  9
```

**Figure M-15. Scenario No.9 (Summer) -
Outfall A-1, no floating processors
in harbor**

Trident
Seafoods
Outfall

Akutan

Akutan Pt.

Ocean Boundary

```
                                          9  9
                                    9  9  9  9  0
                              9  9  9  9  9  9  0
                              9  9  9  9  9  9  0
     8  8  8             9  9  9  9  9  9  9  9  0
9  9  8  8  7  7  7  6     7  8  9  9  9  9  9  9  9  9  9  9  9  0
9  9  8  7  7  6  6  6  5  3  6  7  8  9  9  9  9  9  9  9  9  9  9  9  0
9  9  8  7  5  4  6  6  6  5  7  8  9  9  9  9  9  9  9  9  9  9  9  0
              6  7  7  8  8  9  9  9  9  9  9  9  9  9  9  9  9  0
                 8  9  9  9  9  9  9  9  9  9  9  9  9  9  0
                 9  9  9  9  9  9  9  9  9  9  9  9  9  0
                    9  9  9  9  9  9  9  9  9  9  0  0
                       9  9  9  9  9  9
                       9  9  9
```

location for
Deep Sea Fishenes
alternative outfall site A-2

**Figure M-16. Scenario No.10 (Summer) -
Outfall A-2, no restriction on
location of floating processors**

NAUTICAL MILES
1   5   0   5   1

KILOMETERS
0   1   0

Scale Approximate

N

Note: Numbers represent predicted dissolved oxygen
concentration (mg/l) in surface layer.

**Figure M-17. Scenario No.11 (Summer) -
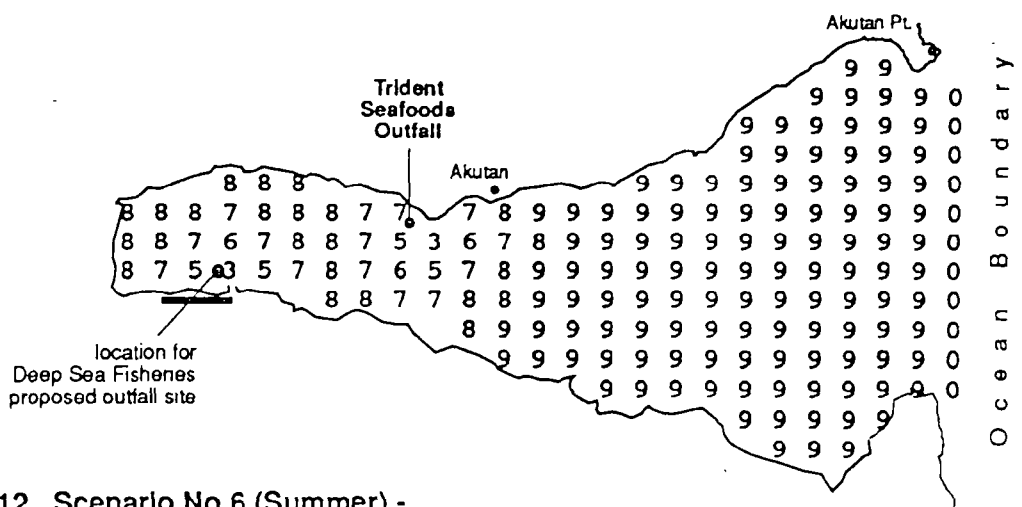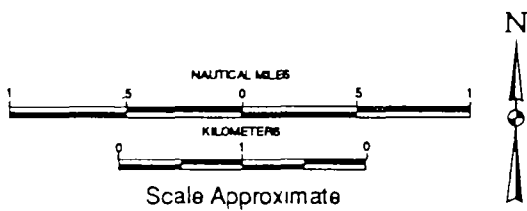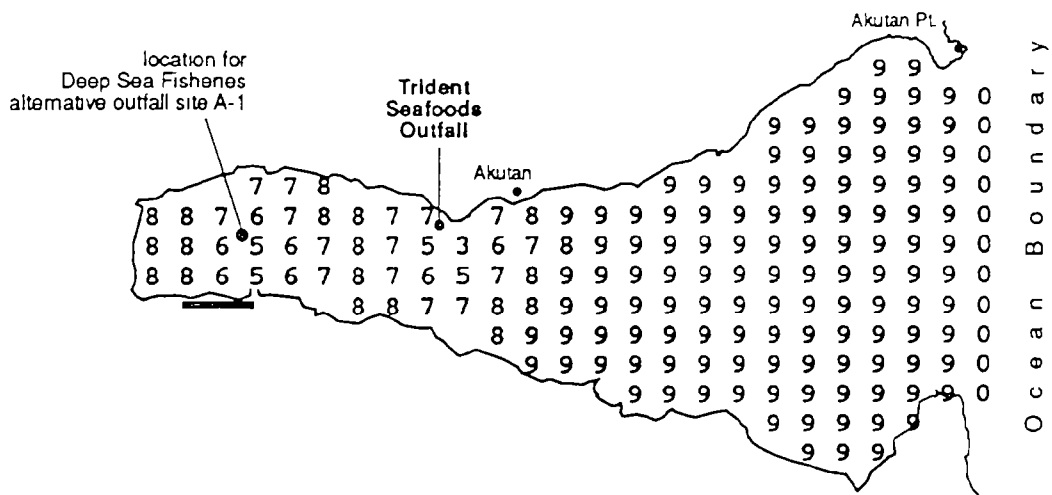Outfall A-2, floating processors
east of 165° 46' only**

**Figure M-18. Scenario No.12 (Summer) -
Outfall A-2, no floating
processors in harbor**

Note: Numbers represent predicted dissolved oxygen concentration (mg/l) in surface layer.

Scale Approximate

Figure M-19. Scenario No.13 (Summer) -
Outfall A-3, no restriction on
location of floating processors
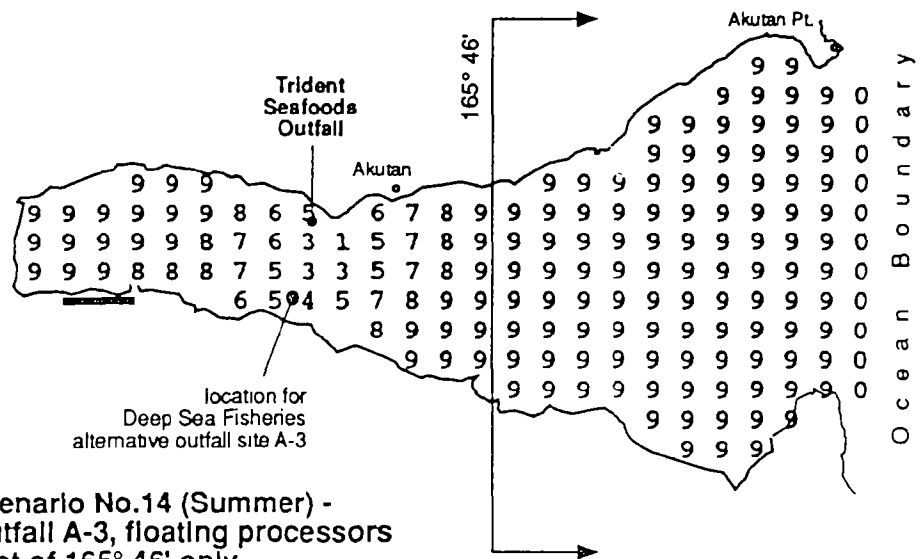
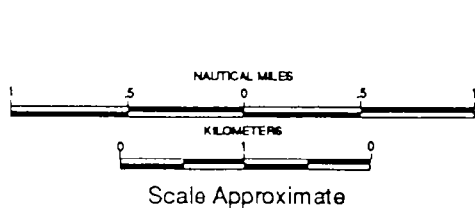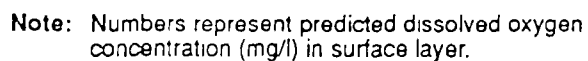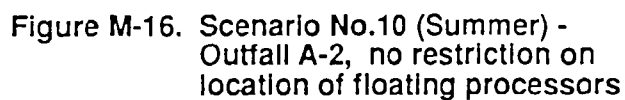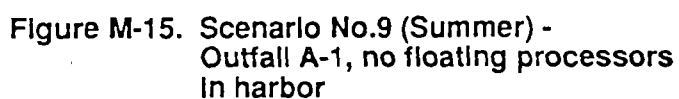**Figure M-20.** Scenario No.14 (Summer) -
Outfall A-3, floating processors
east of 165° 46' only

Note: Numbers represent predicted dissolved oxygen
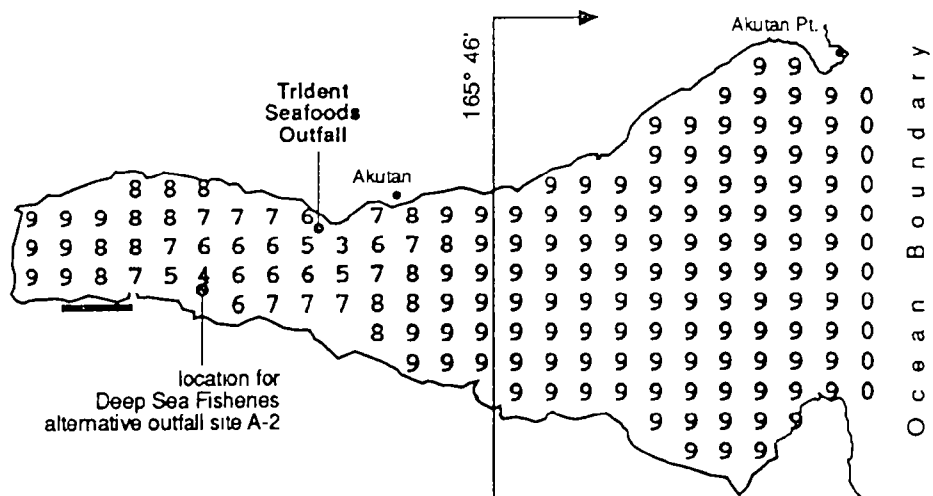concentration (mg/l) in surface layer.

Akutan Pt.
9 9
9 9 9 9 0
9 9 9 9 9 9 0
9 9 9 9 9 9 0

Trident
Seafoods
Outfall

Akutan
9 9 9 9 9 9 9 9 9 0
9 9 9 9 9 8 6 5   6 7 8 9 9 9 9 9 9 9 9 9 9 9 0
9 9 9 9 9 8 7 6 3 1 5 7 8 9 9 9 9 9 9 9 9 9 9 9 0
9 9 9 8 8 8 7 5 3 3 5 7 8 9 9 9 9 9 9 9 9 9 9 9 0
6 5 4 5 7 8 9 9 9 9 9 9 9 9 9 9 9 9 9 0
8 9 9 9 9 9 9 9 9 9 9 9 9 9 9 9 0
9 9 9 9 9 9 9 9 9 9 9 9 9 9 9 0
9 9 9 9 9 9 9 9 9 9 9 9 0
9 9 9 9 9 0
9 9 9

Ocean Boundary

location for
Deep Sea Fishenes
alternative outfall site A-3

Figure M-21. Scenario No.15 (Summer) -
Outfall A-3, no floating processors in harbor

Akutan Pt.
1 1 1 1
1 1 1 1 1 1 1 0
1 1 1 1 1 1 1 1 1 1 1 0
1 1 1 1 1 1 1 1 1 1 1 0

Trident
Seafoods
Outfall

Akutan
1 1 1 1 1 1 1 1 1 1 1 1 1 1 1 1 0
1 1 1 0 1 0   9 9 9 1 0 1 0 1 0 1 1 1 1 1 1 1 1 1 1 1 1 1 1 1 0
1 0 1 1 1 1 1 1 0 1 0 1 0 9 9 9 9 1 0 1 0 1 0 1 1 1 1 1 1 1 1 1 1 1 1 1 1 1 1 0
1 0 1 0 1 1 1 0 1 0 1 0 1 0 9 8 6 8 9 1 0 1 0 1 0 1 1 1 1 1 1 1 1 1 1 1 1 1 1 1 1 0
1 0 1 0 1 0 1 0 1 0 1 0 9 8 8 8 9 1 0 1 0 1 0 1 1 1 1 1 1 1 1 1 1 1 1 1 1 1 0
1 0 9 9 9 9 1 0 1 0 1 0 1 0 1 1 1 1 1 1 1 1 1 1 1 1 1 1 1 0
1 0 1 0 1 0 1 0 1 1 1 1 1 1 1 1 1 1 1 1 1 1 1 1 1 0
1 0 1 0 1 0 1 1 1 1 1 1 1 1 1 1 1 1 1 1 1 1 0
1 1 1 1 1 1 1 1 1 1 1 1 1 1 1 1 1 1 0
1 1 1 1 1 1 1 1 1
1 1 1 1 1 1

Ocean Boundary

location of
Deep Sea Fishenes
existing outfall

Figure M-22. Scenario No.16 (Winter) -
Existing outfall, no restriction
on location of floating processors

N

NAUTICAL MILES
1   .5   0   .5   1

KILOMETERS
0   1   0

Scale Approximate

Note: Numbers represent predicted dissolved oxygen
concentration (mg/l) in surface layer.

Figure M-23. Scenario No.17 (Winter) - Existing outfall, floating processors east of 165° 46' only
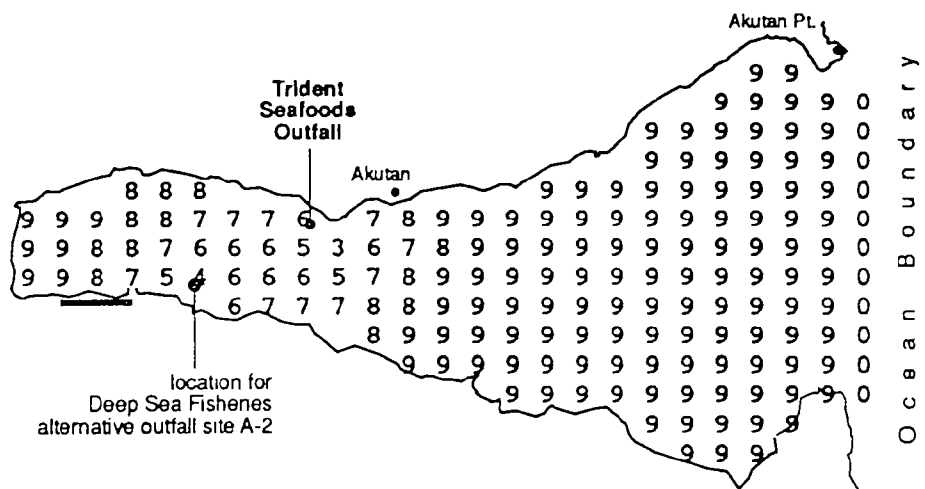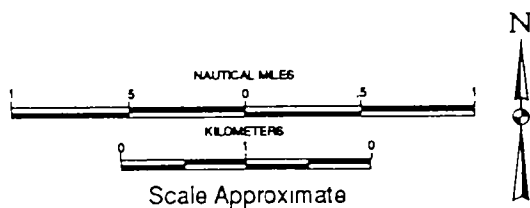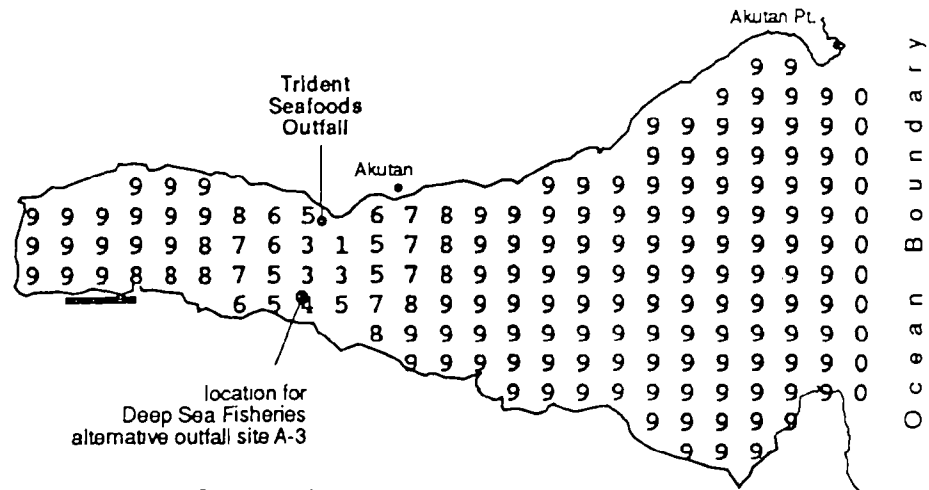

Figure M-24. Scenario No.18 (Winter) - Existing outfall, no floating processors in harbor
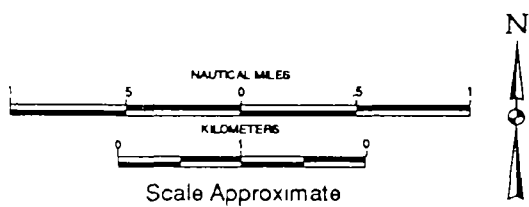
Note: Numbers represent predicted dissolved oxygen concentration (mg/l) in surface layer.

M-29

**Figure M-25. Scenario No.19 (Winter) -
Proposed outfall, no restriction
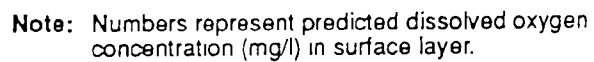on location of floating processors**

**Figure M-26. Scenario No.20 (Winter) -
Proposed outfall, floating processors
east of 165° 46' only**
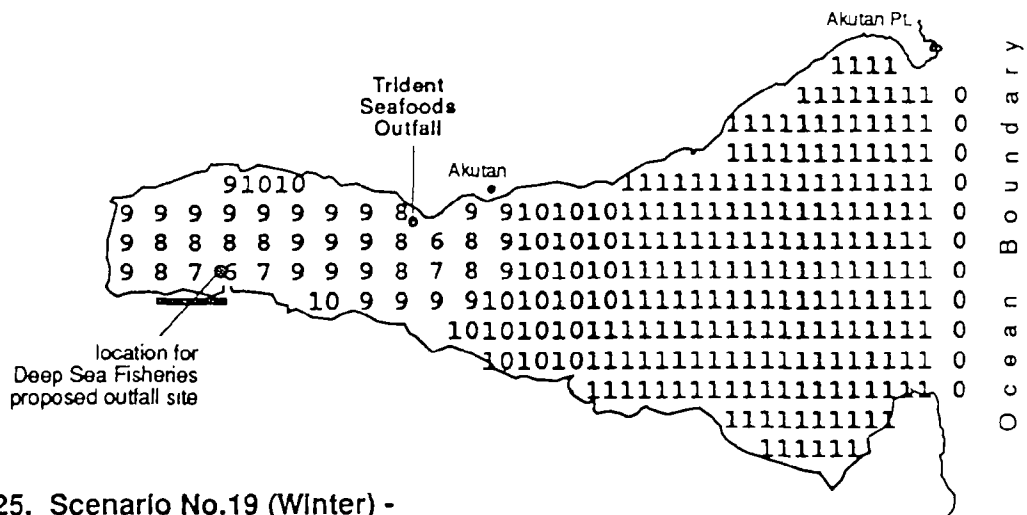
Note: Numbers represent predicted dissolved oxygen
concentration (mg/l) in surface layer.
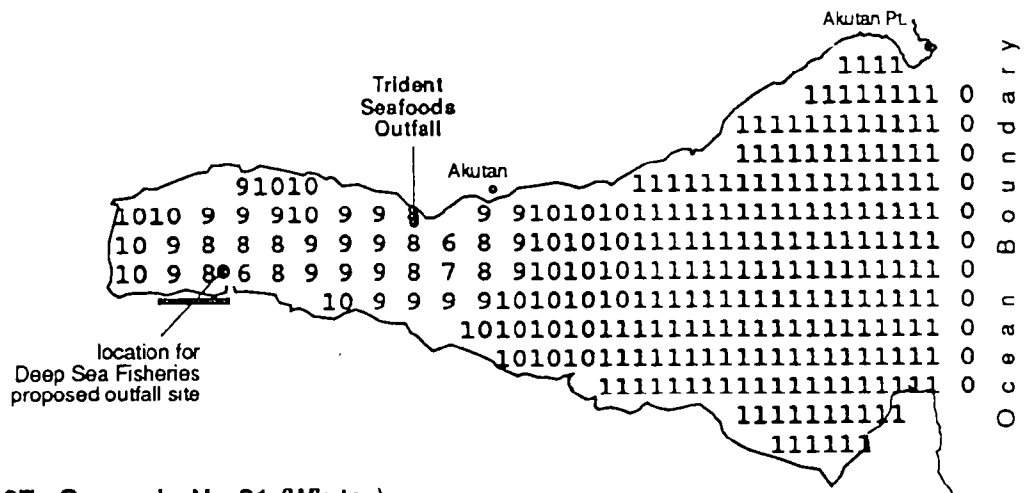
Figure M-27. Scenario No.21 (Winter) -
Proposed outfall, no floating
processors in harbor
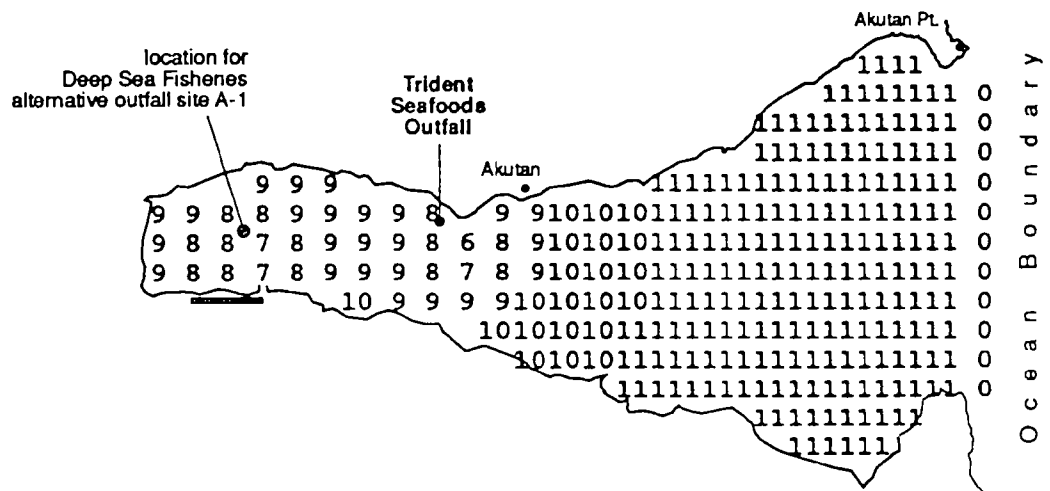
Figure M-28. Scenario No.22 (Winter) -
Outfall A-1, no restriction
on location of floating processors
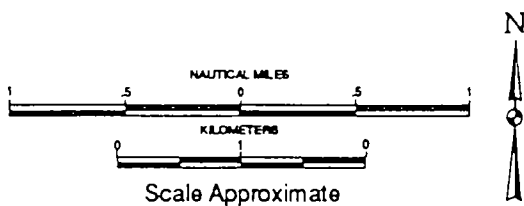
Note: Numbers represent predicted dissolved oxygen
concentration (mg/l) in surface layer.
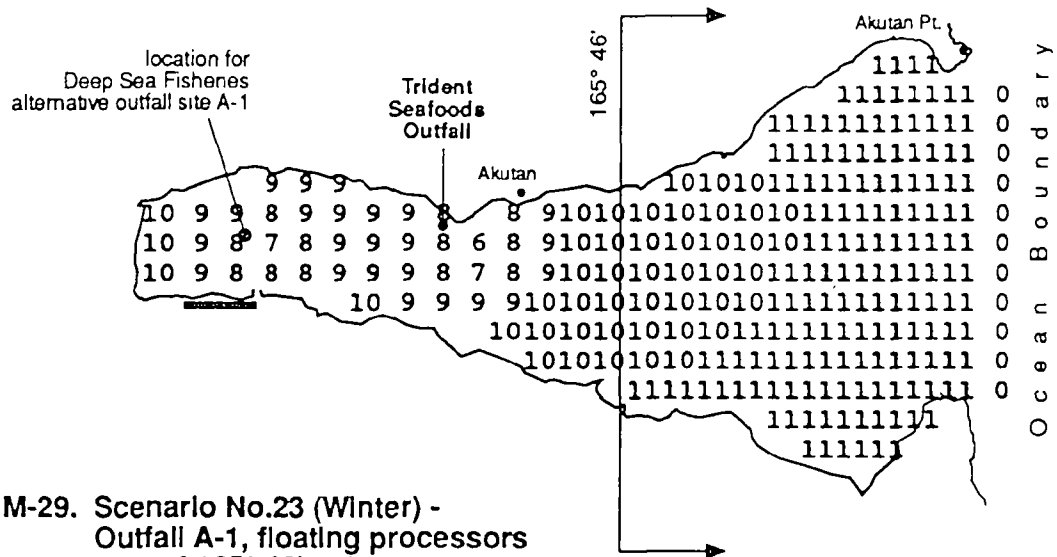
Figure M-29. Scenario No.23 (Winter) -
Outfall A-1, floating processors
east of 165° 46' only

Figure M-30. Scenario No.24 (Winter) -
Outfall A-1, no floating
processors in harbor

Scale Approximate

NAUTICAL MILES

KILOMETERS

N

Note: Numbers represent predicted dissolved oxygen
concentration (mg/l) in surface layer.

Figure M-31. Scenario No.25 (Winter) -
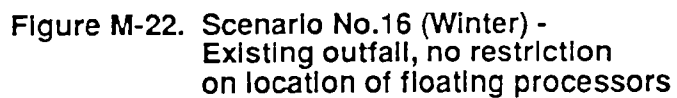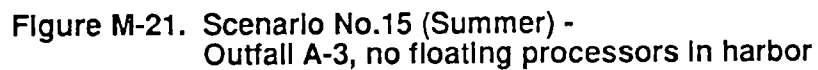Outfall A-2, no restriction on
location of floating processors

Figure M-32. Scenario No.26 (Winter) -
Outfall A-2, floating processors
east of 165° 46' only

Note: Numbers represent predicted dissolved oxygen
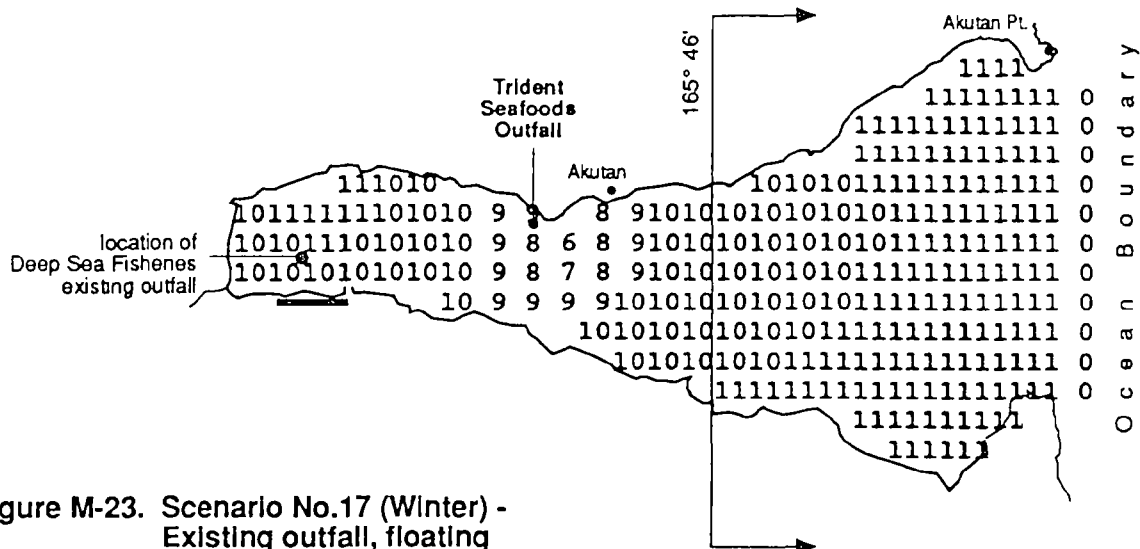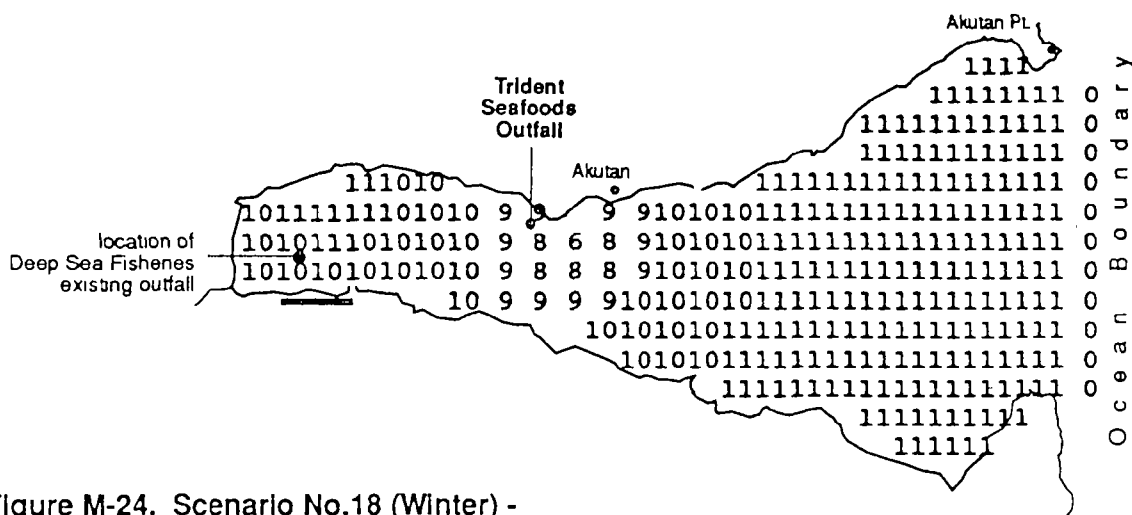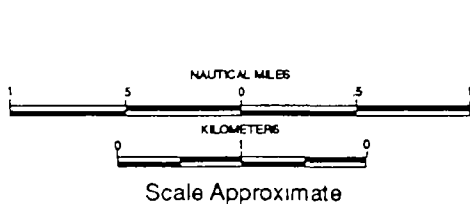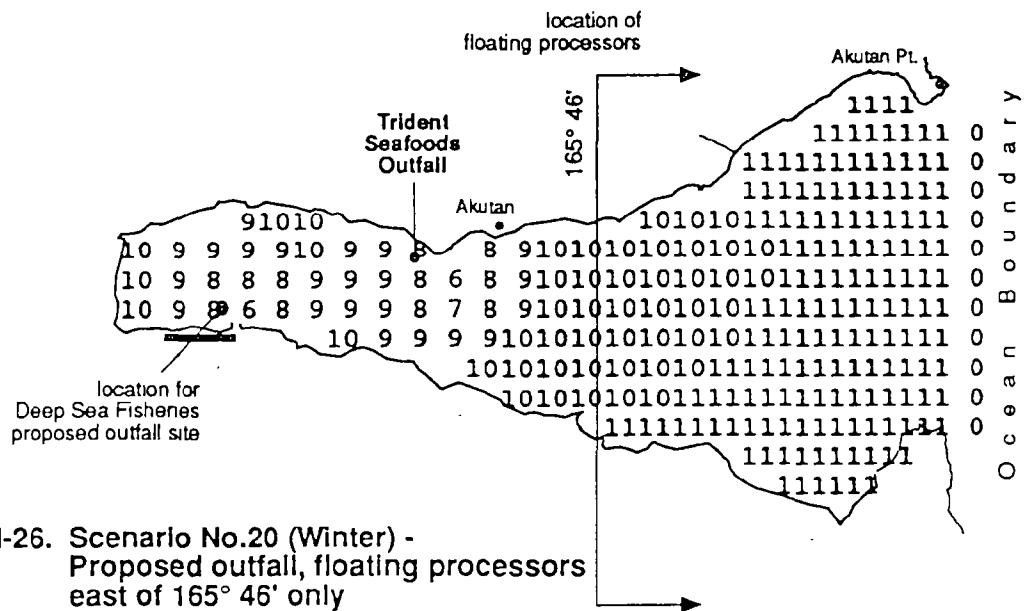concentration (mg/l) in surface layer.

Akutan Pt.

Trident
Seafoods
Outfall

Akutan

```
                                                              1111
                                                            11111111     0
                                                          111111111111   0
                                                          111111111111   0
             9  9  9                     Akutan       1111111111111111   0
   0  9  9  8  9  9  9  9  8        9   91010101111111111111111111   0
   0  9  8  7  8  9  9  9  8  6  8   910101011111111111111111111   0
   0  9  8  8  8  9  9  9  8  7  8   910101011111111111111111111   0
                    10  9  9  9   910101010111111111111111111111   0
                        10101010111111111111111111111   0
                      1010101111111111111111111111   0
                    111111111111111111111111   0
                      11111111111
```

location for
Deep Sea Fishenes
alternative outfall site A-2

Ocean Boundary

**Figure M-33. Scenario No.27 (Winter) -
Outfall A-2, no floating processors
in harbor**

Akutan Pt.

Trident
Seafoods
Outfall

Akutan

```
                                                              1111
                                                            11111111     0
                                                          111111111111   0
                                                          111111111111   0
          101010                          Akutan      1111111111111111   0
 101010101010   9  8  7        8   910101011111111111111111111   0
   9  910101010   9  8  6  4  7   910101011111111111111111111   0
  10  9  9  910  9  9  7  6  6  8   910101011111111111111111111   0
                    8  7  7  7  8   910101011111111111111111111   0
                        910101010111111111111111111   0
                      1010101111111111111111111111   0
                    1111111111111111111111   0
                      111111111
                      111111
```

location for
Deep Sea Fisheries
alternative outfall site A-3

Ocean Boundary

**Figure M-34. Scenario No.28 (Winter) -
Outfall A-3, no restriction on
location of floating processors**

N

NAUTICAL MILES
1   5   0   5   1

KILOMETERS
0   1   0

Scale Approximate

Note: Numbers represent predicted dissolved oxygen
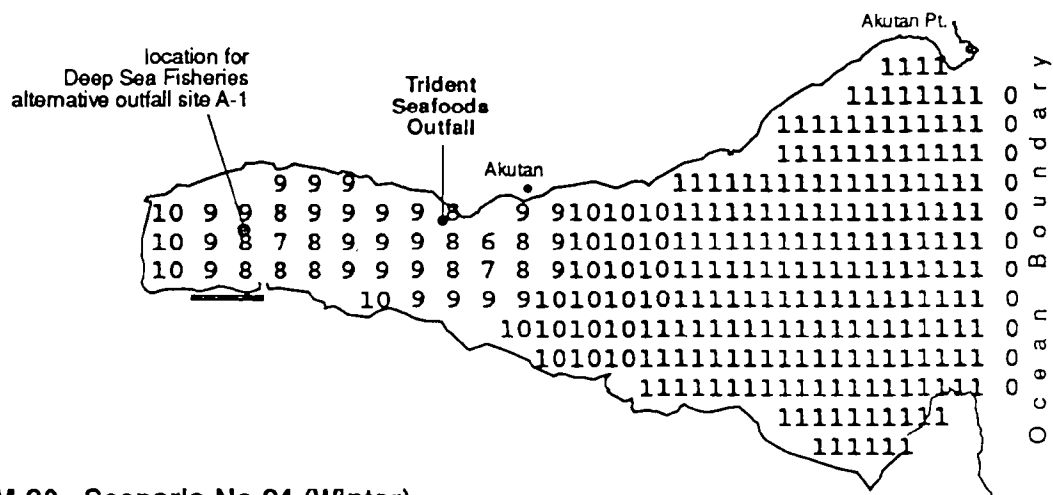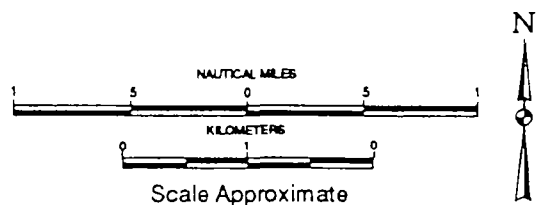concentration (mg/l) in surface layer.

165° 46'

Akutan Pt.

1111
11111111 0
111111111111 0
111111111111 0

Trident
Seafoods
Outfall

Akutan

101010
101010101010 9 8 7 8 91010101010101011111111111 0
101010101010 9 8 6 4 7 9 91010101010101011111111111 0
101010101010 9 7 6 6 8 91010101010101011111111111 0
8 7 7 7 8 91010101010101011111111111 0
91010101010101011111111111111 0
1010101010101111111111111111 0
11111111111111111111 0
1111111111
111111

Ocean Boundary

location for
Deep Sea Fisheries
alternative outfall site A-3

Figure M-35. Scenario No.29 (Winter) - Outfall A-3, floating processors east of 165° 46' only

Akutan Pt.

1111
11111111 0
111111111111 0
111111111111 0

Trident
Seafoods
Outfall

Akutan

101010
101010101010 9 8 7 8 910101011111111111111111111 0
101010101010 9 8 6 4 7 910101011111111111111111111 0
101010101010 9 7 6 6 8 910101011111111111111111111 0
8 7 7 7 8 910101011111111111111111111 0
910101010111111111111111111 0
1010101111111111111111111 0
1111111111111111111111 0
111111111
111111

Ocean Boundary

location for
Deep Sea Fisheries
alternative outfall site A-3

Figure M-36. Scenario No.30 (Winter) - Outfall A-3, no floating processors in harbor

N

NAUTICAL MILES
1   5   0   5   1

KILOMETERS
0   1   0

Scale Approximate

Note: Numbers represent predicted dissolved oxygen concentration (mg/l) in surface layer.

Akutan Pt

Trident
Seafoods
Outfall

Akutan

```
                                        111 1              
                               11111111    0
                             111111111111   0
                             111111111111   0
    11111                111111111111111111  0
101010101111111111    101111111111111111111111111  0
10 410 810111110 8 0 810111111111111111111111111111  0
11010 8 0 810111110 810111111111111111111111111111111  0
            111111101111111111111111111111111111111  0
            11111111111111111111111111111111  0
           11111111111111111111111111111111  0
            111111111111111111111  0
              1111111111
              11111
```

location for
Deep Sea Fisheries
proposed outfall site

**Figure M-37. Results of Scenario No.4 using
low (0.03 m²/s) coefficient of eddy diffusivity**

Akutan Pt

Trident
Seafoods
Outfall

Akutan

```
                                    9  9
                                  9 9 9 9  0
                                9 9 9 9 9 9  0
                                 9 9 9 9 9 9 0
      9  9  9          9 9 9 9 9 9 9 9 9 9 9 9  0
9 9 9 9 9 9 9 9 9    9 9 9 9 9 9 9 9 9 9 9 9 9 9 9 0
9 9 9 6 9 9 9 9 6 0 6 9 9 9 9 9 9 9 9 9 9 9 9 9 9 9 9 0
9 9 6 0 6 9 9 9 9 6 9 9 9 9 9 9 9 9 9 9 9 9 9 9 9 9 0
         9 9 9 9 9 9 9 9 9 9 9 9 9 9 9 9 9 9 9 9 0
          9 9 9 9 9 9 9 9 9 9 9 9 9 9 9 9 9 9 9 0
           9 9 9 9 9 9 9 9 9 9 9 9 9 9 9 9 9 0
             9 9 9 9 9 9 9 9 9 9
              9 9 9
```

location for
Deep Sea Fisheries
proposed outfall site

**Figure M-38. Results of Scenario No. 19
using low (0.03 m²/s) coefficient of eddy diffusivity**

N

NAUTICAL MILES
1   .5   0   .5   1

KILOMETERS
0   1   0

Scale Approximate

Note: Numbers represent predicted dissolved oxygen
concentration (mg/l) in surface layer.

Figure M-39. Results of Scenario No. 4 using high (89 m²/s) Coefficient of eddy diffusivity

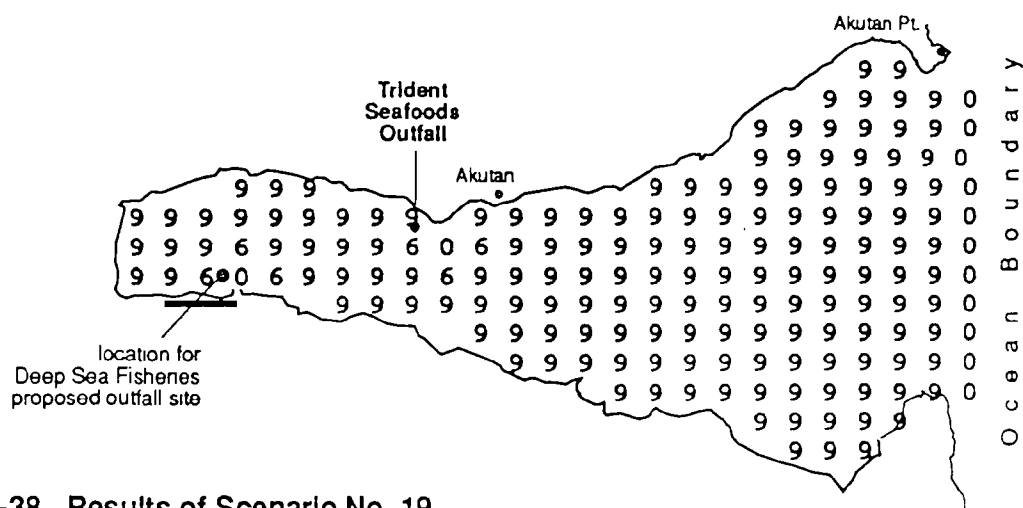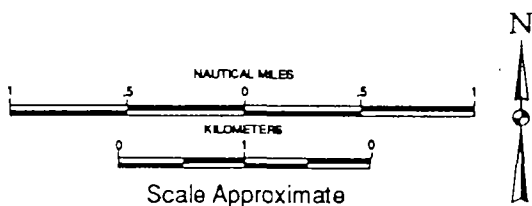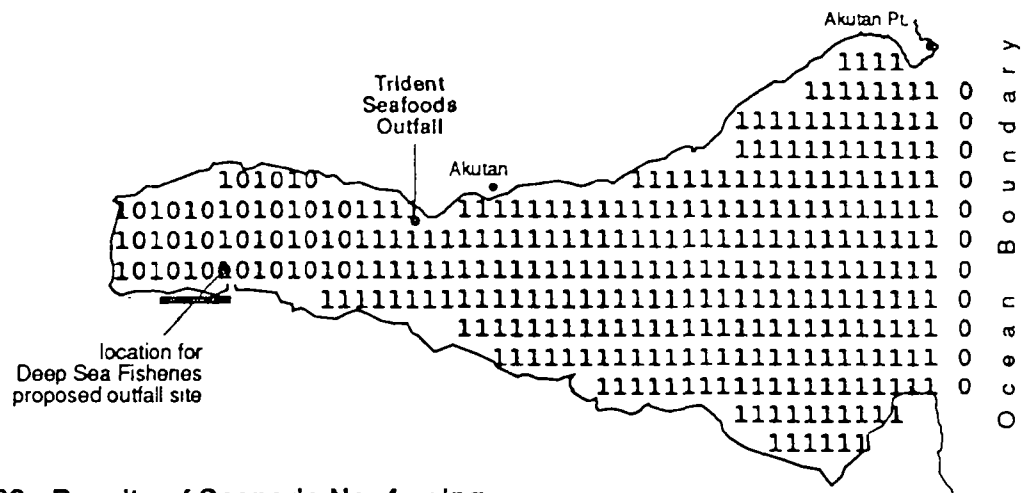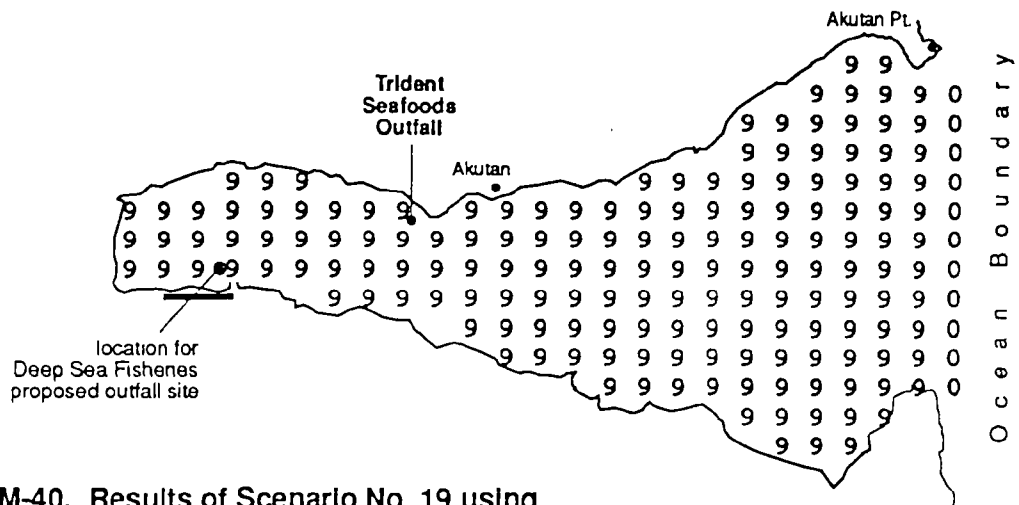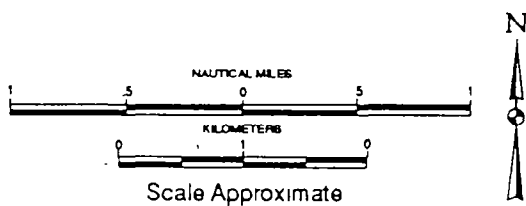**Figure M-40.** Results of Scenario No. 19 using high (89 m ²/s) coefficient of eddy diffusivity

Note: Numbers represent predicted dissolved oxygen concentration (mg/l) in surface layer.

Scale Approximate

References

Alaska Department of Environmental Conservation. 1989. Water quality standard regulations 18 AAC 70. 30 pp.

Ambrose, R. B., T. A. Wool, J. L. Martin, J. P. Connolly, and R. W. Schanz. 1991. WASP4, a hydrodynamic and water quality model--model theory, user's manual, and programmer's guide. Environmental Research Laboratory, ORD, EPA, Athens, Georgia. 324 pp.

Baumgartner, D. J., W. E. Frick, P. J. W. Roberts, and C. A. Bodeen. 1993. Dilution models for effluent discharges. U.S. Environmental Protection Agency, Pacific Ecosystems Branch, Newport Oregon, 176 pp.

Cope, B. 1993. Impacts of Westward Seafoods on DO in Captain's Bay, Alaska. EPA Region 10 draft.

Frenkiel, F. N. 1953. Turbulent diffusion: Mean concentration distribution in a flow field of homogeneous turbulence. *In* Advances in Applied Mechanics, edited by R. von Mises and T. von Karman, Academic Press Inc., New York, N.Y. pp. 61-107.

Seaborne, F. 1993. Deep Sea Fisheries/Akutan Harbor EA alternatives assessment. Memorandum to John Yearsley dated February 12, 1993. EPA Region 10, Seattle, Washington.

Yearsley, J. R. 1990. Estimating the impacts of discharges from Ketchikan Pulp Co. on the surface waters of Ward Cove, Alaska. EPA 910/R-93-004. EPA Region 10, Seattle, Washington.

_____. 1991. Estimates of dilution in the vicinity of ALP's discharge to Sawmill Cove near Sitka, Alaska. Memorandum to Carla Fisher, EPA Region 10, Water Division, dated April 23, 1991.